State of the Art Report on Performance Prediction and Evaluation of Steel Moment-Frame Buildings

Program to Reduce the Earthquake Hazards of Steel Moment-Frame Structures

DISCLAIMER

This document provides practicing engineers and building officials with a resource document for understanding the behavior of steel moment-frame buildings in earthquakes. It is one of the set of six State of the Art Reports containing detailed derivations and explanations of the basis for the design and evaluation recommendations prepared by the SAC Joint Venture. The recommendations and state of the art reports, developed by practicing engineers and researchers, are based on professional judgment and experience and supported by a large program of laboratory, field, and analytical research. **No warranty is offered with regard to the recommendations contained herein, by the Federal Emergency Management Agency, the SAC Joint Venture, the individual joint venture partners, or the partner's directors, members or employees. These organizations and their employees do not assume any legal liability or responsibility for the accuracy, completeness, or usefulness of any of the information, products or processes included in this publication. The reader is cautioned to review carefully the material presented herein and exercise independent judgment as to its suitability for application to specific engineering projects.** This publication has been prepared by the SAC Joint Venture with funding provided by the Federal Emergency Management Agency, under contract number EMW-95-C-4770.

Cover Art. The beam-column connection assembly shown on the cover depicts the standard detailing used in welded steel moment-frame construction prior to the 1994 Northridge earthquake. This connection detail was routinely specified by designers in the period 1970-1994 and was prescribed by the *Uniform Building Code* for seismic applications during the period 1985-1994. It is no longer considered to be an acceptable design for seismic applications. Following the Northridge earthquake, it was discovered that many of these beam-column connections had experienced brittle fractures at the joints between the beam flanges and column flanges.

State of the Art Report on Performance Prediction and Evaluation of Steel Moment-Frame Buildings

SAC Joint Venture

A partnership of
Structural Engineers Association of California (SEAOC)
Applied Technology Council (ATC)
California Universities for Research in Earthquake Engineering (CUREe)

Prepared for the SAC Joint Venture Partnership by
Douglas A. Foutch
Department of Civil and Environmental Engineering
University of Illinois at Urbana-Champaign

SAC Joint Venture
SEAOC: www.seaoc.org
ATC: www.atcouncil.org
CUREe: www.curee.org

September 2000

THE SAC JOINT VENTURE

SAC is a joint venture of the Structural Engineers Association of California (SEAOC), the Applied Technology Council (ATC), and California Universities for Research in Earthquake Engineering (CUREe), formed specifically to address both immediate and long-term needs related to solving performance problems with welded, steel moment-frame connections discovered following the 1994 Northridge earthquake. SEAOC is a professional organization composed of more than 3,000 practicing structural engineers in California. The volunteer efforts of SEAOC's members on various technical committees have been instrumental in the development of the earthquake design provisions contained in the *Uniform Building Code* and the 1997 *National Earthquake Hazards Reduction Program (NEHRP) Recommended Provisions for Seismic Regulations for New Buildings and other Structures*. ATC is a nonprofit corporation founded to develop structural engineering resources and applications to mitigate the effects of natural and other hazards on the built environment. Since its inception in the early 1970s, ATC has developed the technical basis for the current model national seismic design codes for buildings; the *de facto* national standard for postearthquake safety evaluation of buildings; nationally applicable guidelines and procedures for the identification, evaluation, and rehabilitation of seismically hazardous buildings; and other widely used procedures and data to improve structural engineering practice. CUREe is a nonprofit organization formed to promote and conduct research and educational activities related to earthquake hazard mitigation. CUREe's eight institutional members are the California Institute of Technology, Stanford University, the University of California at Berkeley, the University of California at Davis, the University of California at Irvine, the University of California at Los Angeles, the University of California at San Diego, and the University of Southern California. These laboratory, library, computer and faculty resources are among the most extensive in the United States. The SAC Joint Venture allows these three organizations to combine their extensive and unique resources, augmented by subcontractor universities and organizations from across the nation, into an integrated team of practitioners and researchers, uniquely qualified to solve problems related to the seismic performance of steel moment-frame buildings.

ACKNOWLEDGEMENTS

Funding for Phases I and II of the SAC Steel Program to Reduce the Earthquake Hazards of Steel Moment-Frame Structures was principally provided by the Federal Emergency Management Agency, with ten percent of the Phase I program funded by the State of California, Office of Emergency Services. Substantial additional support, in the form of donated materials, services, and data has been provided by a number of individual consulting engineers, inspectors, researchers, fabricators, materials suppliers and industry groups. Special efforts have been made to maintain a liaison with the engineering profession, researchers, the steel industry, fabricators, code-writing organizations and model code groups, building officials, insurance and risk-management groups, and federal and state agencies active in earthquake hazard mitigation efforts. SAC wishes to acknowledge the support and participation of each of the above groups, organizations and individuals. In particular, we wish to acknowledge the contributions provided by the American Institute of Steel Construction, the Lincoln Electric Company, the National Institute of Standards and Technology, the National Science Foundation, and the Structural Shape Producers Council. SAC also takes this opportunity to acknowledge the efforts of the project participants – the managers, investigators, writers, and editorial and production staff – whose work has contributed to the development of these documents. Finally, SAC extends special acknowledgement to Mr. Michael Mahoney, FEMA Project Officer, and Dr. Robert Hanson, FEMA Technical Advisor, for their continued support and contribution to the success of this effort.

In Memory of Egor Popov, Professor Emeritus, University of California at Berkeley

TABLE OF CONTENTS

LIST OF FIGURES

LIST OF TABLES

1. INTRODUCTION

1.1 Purpose

This report, FEMA-355F – *State of the Art Report on Performance Prediction and Evaluation of Steel Moment-Frame Buildings*, presents an overview of the current state of knowledge with regard to the prediction of the performance of moment-resisting steel frame buildings in future earthquakes. This state of the art report was prepared in support of the development of a series of Recommended Design Criteria documents, which were prepared by the SAC Joint Venture on behalf of the Federal Emergency Management Agency and which address the issue of the seismic performance of moment-resisting steel frame structures. These publications include:

- *FEMA-350 – Recommended Seismic Design Criteria for New Steel Moment-Frame Buildings.* This publication provides recommended criteria, supplemental to *FEMA-302 – 1997 NEHRP Recommended Provisions for Seismic Regulations for New Buildings and Other Structures,* for the design and construction of steel moment-frame buildings and provides alternative performance-based design criteria.
- *FEMA-351 – Recommended Seismic Evaluation and Upgrade Criteria for Existing Welded Steel Moment-Frame Buildings.* This publication provides recommended methods to evaluate the probable performance of existing steel moment-frame buildings in future earthquakes and to retrofit these buildings for improved performance.
- *FEMA-352 – Recommended Postearthquake Evaluation and Repair Criteria for Welded Steel Moment-Frame Buildings.* This publication provides recommendations for performing postearthquake inspections to detect damage in steel moment-frame buildings following an earthquake, evaluating the damaged buildings to determine their safety in the postearthquake environment, and repairing damaged buildings.
- *FEMA-353 – Recommended Specifications and Quality Assurance Guidelines for Steel Moment-Frame Construction for Seismic Applications.* This publication provides recommended specifications for the fabrication and erection of steel moment frames for seismic applications. The recommended design criteria contained in the other companion documents are based on the material and workmanship standards contained in this document, which also includes discussion of the basis for the quality control and quality assurance criteria contained in the recommended specifications.

Detailed derivations and explanations of the basis for these design and evaluation recommendations may be found in a series of State of the Art Reports prepared in parallel with these design criteria. These reports include:

- *FEMA-355A – State of the Art Report on Base Metals and Fracture*. This report summarizes current knowledge of the properties of structural steels commonly employed in building construction, and the production and service factors that affect these properties.
- *FEMA-355B – State of the Art Report on Welding and Inspection*. This report summarizes current knowledge of the properties of structural welding commonly employed in building

construction, the effect of various welding parameters on these properties, and the effectiveness of various inspection methodologies in characterizing the quality of welded construction.

- *FEMA-355C – State of the Art Report on Systems Performance of Steel Moment Frames Subject to Earthquake Ground Shaking.* This report summarizes an extensive series of analytical investigations into the demands induced in steel moment-frame buildings designed to various criteria, when subjected to a range of different ground motions. The behavior of frames constructed with fully restrained, partially restrained and fracture-vulnerable connections is explored for a series of ground motions, including motion anticipated at near-fault and soft-soil sites.
- *FEMA-355D – State of the Art Report on Connection Performance.* This report summarizes the current state of knowledge of the performance of different types of moment-resisting connections under large inelastic deformation demands. It includes information on fully restrained, partially restrained, and partial strength connections, both welded and bolted, based on laboratory and analytical investigations.
- *FEMA-355E – State of the Art Report on Past Performance of Steel Moment-Frame Buildings in Earthquakes.* This report summarizes investigations of the performance of steel moment-frame buildings in past earthquakes, including the 1995 Kobe, 1994 Northridge, 1992 Landers, 1992 Big Bear, 1989 Loma Prieta and 1971 San Fernando events.
- *FEMA-355F – State of the Art Report on Performance Prediction and Evaluation of Steel Moment-Frame Buildings*. This report describes the results of investigations into the ability of various analytical techniques, commonly used in design, to predict the performance of steel moment-frame buildings subjected to earthquake ground motion. Also presented is the basis for performance-based evaluation procedures contained in the design criteria documents, *FEMA-350, FEMA-351*, and *FEMA-352.*

In addition to the recommended design criteria and the State of the Art Reports, a companion document has been prepared for building owners, local community officials and other non-technical audiences who need to understand this issue. *A Policy Guide to Steel Moment Frame Construction (FEMA-354)* addresses the social, economic, and political issues related to the earthquake performance of steel moment-frame buildings. *FEMA-354* also includes discussion of the relative costs and benefits of implementing the recommended criteria.

1.2 Background

For many years, the basic intent of the building code seismic provisions has been to provide buildings with an ability to withstand intense ground shaking without collapse, but potentially with some significant structural damage. In order to accomplish this, one of the basic principles inherent in modern code provisions is to encourage the use of building configurations, structural systems, materials and details that are capable of ductile behavior. A structure is said to behave in a ductile manner if it is capable of withstanding large inelastic deformations without significant degradation in strength, and without the development of instability and collapse. The design forces specified by building codes for particular structural systems are related to the amount of ductility the system is deemed to possess. Generally, structural systems with more

ductility are designed for lower forces than less ductile systems, as ductile systems are deemed capable of resisting demands that are significantly greater than their elastic strength limit. Starting in the 1960s, engineers began to regard welded steel moment-frame buildings as being among the most ductile systems contained in the building code. Many engineers believed that steel moment-frame buildings were essentially invulnerable to earthquake-induced structural damage and thought that should such damage occur, it would be limited to ductile yielding of members and connections. Earthquake-induced collapse was not believed possible. Partly as a result of this belief, many large industrial, commercial and institutional structures employing steel moment-frame systems were constructed, particularly in the western United States.

The Northridge earthquake of January 17, 1994 challenged this paradigm. Following that earthquake, a number of steel moment-frame buildings were found to have experienced brittle fractures of beam-to-column connections. The damaged buildings had heights ranging from one story to 26 stories, and a range of ages spanning from buildings as old as 30 years to structures being erected at the time of the earthquake. The damaged buildings were spread over a large geographical area, including sites that experienced only moderate levels of ground shaking. Although relatively few buildings were located on sites that experienced the strongest ground shaking, damage to buildings on these sites was extensive. Discovery of these unanticipated brittle fractures of framing connections, often with little associated architectural damage, was alarming to engineers and the building industry. The discovery also caused some concern that similar, but undiscovered, damage may have occurred in other buildings affected by past earthquakes. Later investigations confirmed such damage in a limited number of buildings affected by the 1992 Landers, 1992 Big Bear and 1989 Loma Prieta earthquakes.

In general, steel moment-frame buildings damaged by the Northridge earthquake met the basic intent of the building codes. That is, they experienced limited structural damage, but did not collapse. However, the structures did not behave as anticipated and significant economic losses occurred as a result of the connection damage, in some cases, in buildings that had experienced ground shaking less severe than the design level. These losses included direct costs associated with the investigation and repair of this damage as well as indirect losses relating to the temporary, and in a few cases, long-term, loss of use of space within damaged buildings.

Steel moment-frame buildings are designed to resist earthquake ground shaking based on the assumption that they are capable of extensive yielding and plastic deformation, without loss of strength. The intended plastic deformation consists of plastic rotations developing within the beams, at their connections to the columns, and is theoretically capable of resulting in benign dissipation of the earthquake energy delivered to the building. Damage is expected to consist of moderate yielding and localized buckling of the steel elements, not brittle fractures. Based on this presumed behavior, building codes permit steel moment-frame buildings to be designed with a fraction of the strength that would be required to respond to design level earthquake ground shaking in an elastic manner.

Steel moment-frame buildings are anticipated to develop their ductility through the development of yielding in beam-column assemblies at the beam-column connections. This yielding may take the form of plastic hinging in the beams (or, less desirably, in the columns), plastic shear deformation in the column panel zones, or through a combination of these

mechanisms. It was believed that the typical connection employed in steel moment-frame construction, shown in Figure 1-1, was capable of developing large plastic rotations, on the order of 0.02 radians or larger, without significant strength degradation.

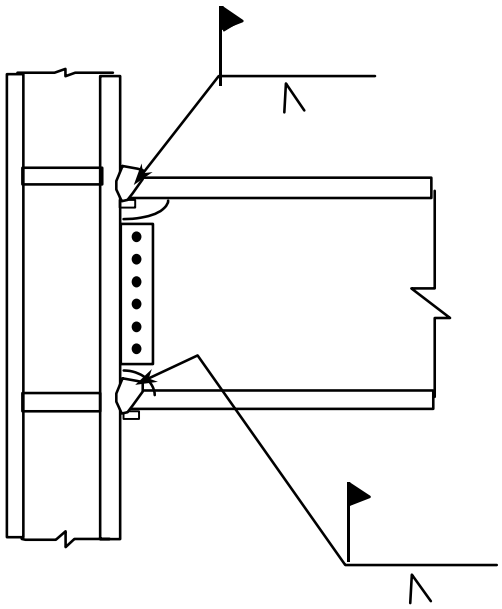

Figure 1-1 Typical Welded Moment-Resisting Connection Prior to 1994

Observation of damage sustained by buildings in the 1994 Northridge earthquake indicated that, contrary to the intended behavior, in many cases, brittle fractures initiated within the connections at very low levels of plastic demand, and in some cases, while the structures remained essentially elastic. Typically, but not always, fractures initiated at the complete joint penetration (CJP) weld between the beam bottom flange and column flange (Figure 1-2). Once initiated, these fractures progressed along a number of different paths, depending on the individual joint conditions.

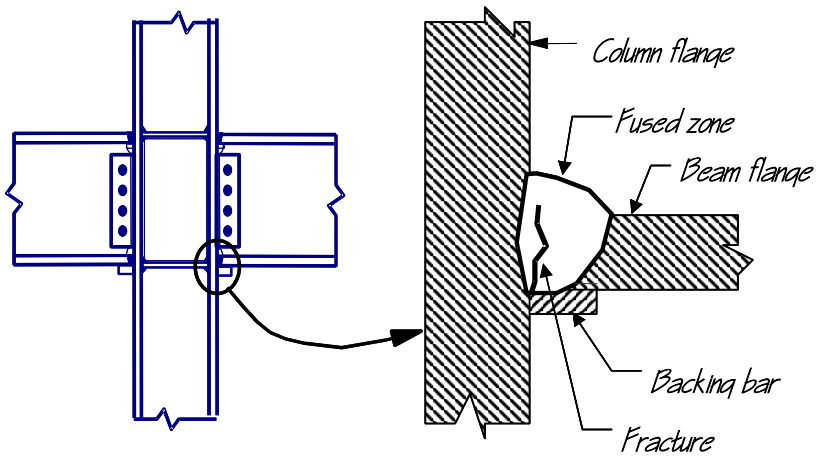

Figure 1-2 Common Zone of Fracture Initiation in Beam-Column Connection

In some cases, the fractures progressed completely through the thickness of the weld, and when fire protective finishes were removed, the fractures were evident as a crack through exposed faces of the weld, or the metal just behind the weld (Figure 1-3a). Other fracture patterns also developed. In some cases, the fracture developed into a crack of the column flange material behind the CJP weld (Figure 1-3b). In these cases, a portion of the column flange remained bonded to the beam flange, but pulled free from the remainder of the column. This fracture pattern has sometimes been termed a “divot” or “nugget” failure.

A number of fractures progressed completely through the column flange, along a near-horizontal plane that aligns approximately with the beam lower flange (Figure 1-4a). In some cases, these fractures extended into the column web and progressed across the panel zone (Figure 1-4b). Investigators have reported some instances where columns fractured entirely across the section.

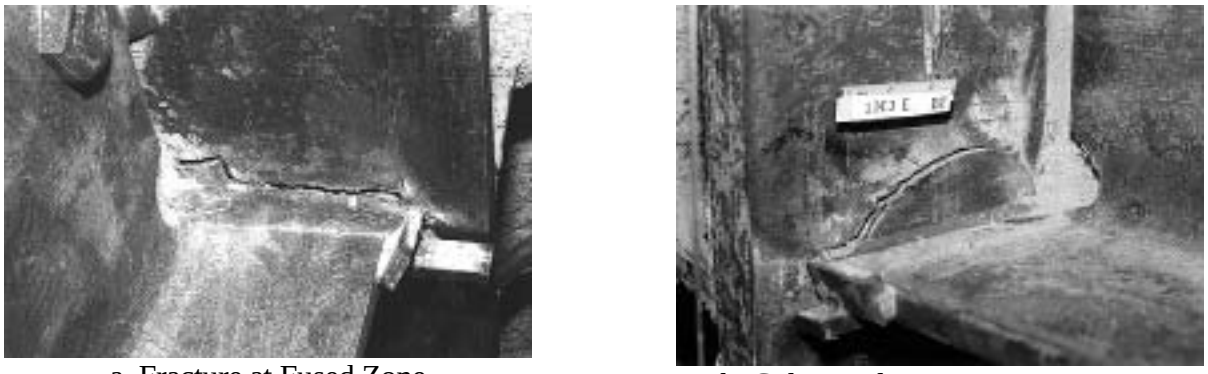

a. Fracture at Fused Zone

b. Column Flange "Divot" Fracture

Figure 1-3 Fractures of Beam-to-Column Joints

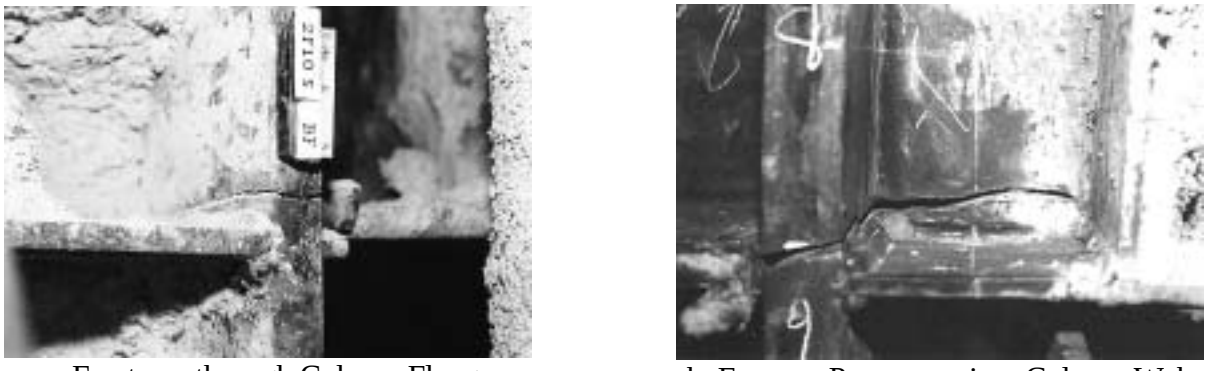

a. Fractures through Column Flange

b. Fracture Progresses into Column Web

Figure 1-4 Column Fractures

Once such fractures have occurred, the beam-column connection has experienced a significant loss of flexural rigidity and strength to resist those loads that tend to open the crack. Residual flexural strength and rigidity must be developed through a couple consisting of forces transmitted through the remaining top flange connection and the web bolts. However, in providing this residual strength and stiffness, the bolted web connections can themselves be

subject to failures. These include fracturing of the welds of the shear plate to the column, fracturing of supplemental welds to the beam web or fracturing through the weak section of shear plate aligning with the bolt holes (Figure 1-5).

Despite the obvious local strength impairment resulting from these fractures, many damaged buildings did not display overt signs of structural damage, such as permanent drifts or damage to architectural elements, making reliable postearthquake damage evaluations difficult. In order to determine if a building has sustained connection damage it is necessary to remove architectural finishes and fireproofing, and perform detailed inspections of the connections. Even if no damage is found, this is a costly process. Repair of damaged connections is even more costly. At least one steel moment-frame building sustained so much damage that it was deemed more practical to demolish the building than to repair it.

Figure 1-5 Vertical Fracture through Beam Shear Plate Connection

Initially, the steel construction industry took the lead in investigating the causes of this unanticipated damage and in developing design recommendations. The American Institute of Steel Construction (AISC) convened a special task committee in March, 1994 to collect and disseminate available information on the extent of the problem (AISC, 1994a). In addition, together with a private party engaged in the construction of a major steel building at the time of the earthquake, AISC participated in sponsoring a limited series of tests of alternative connection details at the University of Texas at Austin (AISC, 1994b). The American Welding Society (AWS) also convened a special task group to investigate the extent to which the damage was related to welding practice, and to determine if changes to the welding code were appropriate (AWS, 1995).

In September 1994, the SAC Joint Venture, AISC, the American Iron and Steel Institute and National Institute of Standards and Technology jointly convened an international workshop (SAC, 1994) in Los Angeles to coordinate the efforts of the various participants and to lay the foundation for systematic investigation and resolution of the problem. Following this workshop, FEMA entered into a cooperative agreement with the SAC Joint Venture to perform problem-focused studies of the seismic performance of steel moment-frame buildings and to develop recommendations for professional practice (Phase I of SAC Steel Project). Specifically, these recommendations were intended to address the following: The inspection of earthquake-affected

buildings to determine if they had sustained significant damage; the repair of damaged buildings; the upgrade of existing buildings to improve their probable future performance; and the design of new structures to provide reliable seismic performance.

During the first half of 1995, an intensive program of research was conducted to explore more definitively the pertinent issues. This research included literature surveys, data collection on affected structures, statistical evaluation of the collected data, analytical studies of damaged and undamaged buildings, and laboratory testing of a series of full-scale beam-column assemblies representing typical pre-Northridge design and construction practice as well as various repair, upgrade and alternative design details. The findings of these tasks formed the basis for the development of *FEMA-267 – Interim Guidelines: Evaluation, Repair, Modification, and Design of Welded Steel Moment Frame Structures*, which was published in August, 1995. *FEMA-267* provided the first definitive, albeit interim, recommendations for practice, following the discovery of connection damage in the 1994 Northridge earthquake.

In September 1995, the SAC Joint Venture entered into a contractual agreement with FEMA to conduct Phase II of the SAC Steel Project. Under Phase II, SAC continued its extensive problem-focused study of the performance of moment resisting steel frames and connections of various configurations, with the ultimate goal of developing reliable seismic design criteria for steel construction. This work has included: Extensive analyses of buildings; detailed finite element and fracture mechanics investigations of various connections to identify the effects of connection configuration, material strength, and toughness and weld joint quality on connection behavior; as well as more than 120 full-scale tests of connection assemblies. As a result of these studies, and independent research conducted by others, it is now known that the typical moment-resisting connection detail employed in steel moment-frame construction prior to the 1994 Northridge earthquake, and depicted in Figure 1-1, had a number of features that rendered it inherently susceptible to brittle fracture. These included the following:

- The most severe stresses in the connection assembly occur where the beam joins to the column. Unfortunately, this is also the weakest location in the assembly. At this location, bending moments and shear forces in the beam must be transferred to the column through the combined action of the welded joints between the beam flanges and column flanges and the shear tab. The combined section properties of these elements, for example the cross sectional area and section modulus, are typically less than those of the connected beam. As a result, stresses are locally intensified at this location.
- The joint between the bottom beam flange and the column flange is typically made as a downhand field weld, often by a welder sitting on top of the beam top flange, in a so-called "wildcat" position. To make the weld from this position each pass must be interrupted at the beam web, with either a start or stop of the weld at this location. This welding technique often results in poor quality welding at this critical location, with slag inclusions, lack of fusion and other defects. These defects can serve as crack initiators, when the connection is subjected to severe stress and strain demands.
- The basic configuration of the connection makes it difficult to detect hidden defects at the root of the welded beam-flange-to-column-flange joints. The backing bar, which was

typically left in place following weld completion, restricts visual observation of the weld root. Therefore, the primary method of detecting defects in these joints is through the use of ultrasonic testing (UT). However, the geometry of the connection also makes it very difficult for UT to detect flaws reliably at the bottom beam flange weld root, particularly at the center of the joint, at the beam web. As a result, many of these welded joints have undetected significant defects that can serve as crack initiators.

- Although typical design models for this connection assume that nearly all beam flexural stresses are transmitted by the flanges and all beam shear forces by the web, in reality, due to boundary conditions imposed by column deformations, the beam flanges at the connection carry a significant amount of the beam shear. This results in significant flexural stresses on the beam flange at the face of the column, and also induces large secondary stresses in the welded joint. Some of the earliest investigations of these stress concentration effects in the welded joint were conducted by Richard, et al. (1995). The stress concentrations resulting from this effect resulted in severe strength demands at the root of the complete joint penetration welds between the beam flanges and column flanges, a region that often includes significant discontinuities and slag inclusions, which are ready crack initiators.
- In order that the welding of the beam flanges to the column flanges be continuous across the thickness of the beam web, this detail incorporates weld access holes in the beam web, at the beam flanges. Depending on their geometry, severe strain concentrations can occur in the beam flange at the toe of these weld access holes. These strain concentrations can result in low-cycle fatigue and the initiation of ductile tearing of the beam flanges after only a few cycles of moderate plastic deformation. Under large plastic flexural demands, these ductile tears can quickly become unstable and propagate across the beam flange.
- Steel material at the center of the beam-flange-to-column-flange joint is restrained from movement, particularly in connections of heavy sections with thick column flanges. This condition of restraint inhibits the development of yielding at this location, resulting in locally high stresses on the welded joint, which exacerbates the tendency to initiate fractures at defects in the welded joints.
- Design practice in the period 1985-1994 encouraged design of these connections with relatively weak panel zones. In connections with excessively weak panel zones, inelastic behavior of the assembly is dominated by shear deformation of the panel zone. This panel zone shear deformation results in a local kinking of the column flanges adjacent to the beam-flange-to-column-flange joint, and further increases the stress and strain demands in this sensitive region.

In addition to the above, additional conditions contributed significantly to the vulnerability of connections constructed prior to 1994.

- In the mid-1960s, the construction industry moved to the use of the semi-automatic, self-shielded, flux-cored arc welding process (FCAW-S) for making the joints of these connections. The welding consumables that building erectors most commonly used inherently produced welds with very low toughness. The toughness of this material could be further compromised by excessive deposition rates, which unfortunately were commonly employed by welders. As a result, brittle fractures could initiate in welds with large defects,

at stresses approximating the yield strength of the beam steel, precluding the development of ductile behavior.

- Early steel moment frames tended to be highly redundant and nearly every beam-column joint was constructed to behave as part of the lateral-force-resisting system. As a result, member sizes in these early frames were small and much of the early acceptance testing of this typical detail was conducted with specimens constructed of small framing members. As the cost of construction labor increased, the industry found that it was more economical to construct steel moment-frame buildings by moment-connecting a relatively small percentage of the beams and columns and by using larger members for these few moment-connected elements. The amount of strain demand placed on the connection elements of a steel moment frame is related to the span-to-depth ratio of the member. Therefore, as member sizes increased, strain demands on the welded connections also increased, making the connections more susceptible to brittle behavior.
- In the 1960s and 1970s, when much of the initial research on steel moment-frame construction was performed, beams were commonly fabricated using A36 material. In the 1980s, many steel mills adopted more modern production processes, including the use of scrap-based production. Steels produced by these more modern processes tended to include micro-alloying elements that increased the strength of the materials so that despite the common specification of A36 material for beams, many beams actually had yield strengths that approximated or exceeded that required for grade 50 material. As a result of this increase in base metal yield strength, the weld metal in the beam-flange-to-column-flange joints became under-matched, potentially contributing to its vulnerability.

At this time, it is clear that in order to obtain reliable ductile behavior of steel moment-frame construction a number of changes to past practices in design, materials, fabrication, erection and quality assurance are necessary. The recommended criteria contained in this document, and the companion publications, are based on an extensive program of research into materials, welding technology, inspection methods, frame system behavior, and laboratory and analytical investigations of different connection details. The recommended criteria presented herein are believed to be capable of addressing the vulnerabilities identified above and providing for frames capable of more reliable performance in response to earthquake ground shaking.

1.3 Performance Prediction and Evaluation for Buildings under Seismic Loads

The actual performance of a building during an earthquake depends on many factors such as the structural configuration and proportions, the dynamic characteristics of the building, the strength, stiffness and ductility of the joints, the type of nonstructural components employed, the quality of the materials, fabrication and erection used in the construction of the structure, maintaining occupancy, the site conditions, and the intensity and dynamic characteristics of the earthquake ground motion at the site. Consequently, seismic performance prediction for new design or evaluation of existing buildings should consider, either explicitly or implicitly, all of these factors.

Prediction of seismic response of a new or existing structure is complex, due not only to the large number of factors that need to be considered and the complexity of seismic response, but

also due to the large inherent uncertainty associated with making these predictions. Clearly the characteristics of future earthquakes can only be approximated, leading to very large uncertainties in the loads acting on the structure. Structural properties may differ from those intended or assumed by the designer, or may change substantially during the earthquake (e.g. local fracture of connections). Analysis methods may not accurately capture the actual behavior due to simplifications in the analysis procedure (linear vs. nonlinear for instance) and modeling of the structure. Our knowledge of the behavior of structures during earthquakes is not complete, which introduces other uncertainties. Consequently, seismic performance prediction must consider these uncertainties.

Many of these issues are covered to a greater or lesser extent in current codes through the use of load and resistance factors, adjustment of various design parameters following major earthquakes, and introduction of new analytical and design procedures as they are developed and verified. In responding to the problems observed in steel moment-frame buildings observed after the Northridge and other earthquakes, the SAC steel project has attempted to develop a comprehensive understanding of the capacity of various moment-resisting connections and the demands on these connections. To achieve satisfactory building performance through design or to evaluate an existing building, one needs to reconcile expected seismic demands with acceptable performance levels while recognizing the uncertainties involved.

A reliability-based, performance-oriented approach has been adopted herein for design and evaluation. This approach was taken in order to account for uncertainties and randomness in seismic demand and capacities in a consistent manner and to satisfy identifiable performance objectives corresponding to various occupancies, damage states, and seismic hazard. In this report we will consider issues related to the performance prediction and evaluation of:

- new buildings,
- existing buildings prior to an earthquake, and
- damaged buildings following an earthquake.

There are subtle differences between performance prediction for new buildings and for existing buildings. Conservative assumptions about the material properties may be made, particular detailing of joints and members may be selected, and relatively simple analysis methods and acceptance criteria may be used with rather small impact on the cost of the new building. For an existing building that has experienced damage during an earthquake, or one that may be vulnerable to a future shock, any repair or modification may be quite expensive, particularly if occupancy is not allowed during the remedial construction. Details, materials, and member properties may not conform to code requirements for specific building types, which may require more advanced analysis procedures and acceptance criteria. This report will discuss and evaluate analysis procedures and acceptance criteria for performance prediction and evaluation of steel moment frame buildings.

1.4 Critical Issues for Performance Prediction and Evaluation

This section of the report identifies and discusses some of the critical issues involved in performance prediction and evaluation. These include analysis and modeling methods, various

performance goals, response parameters, level of seismicity, different occupancies, and legal and social issues. These items will be briefly discussed in this section and expanded in the next chapter on performance-based design and evaluation.

A variety of simple and complex analytical methods are available to the engineer to predict the seismic response of structures. These range from simple static elastic methods defined in most design codes to complex nonlinear dynamic methods. In developing design guidelines, it is desirable that these methods be used in situations where they can adequately characterize the response of a real structure. Thus, it may be necessary to limit the use of certain methods, or to adjust the methods or their input so that performance estimates obtained with different methods and modeling idealizations have consistent reliability.

The performance goals and the important response parameters are closely related. One performance goal might be to avoid collapse. The response parameter might be maximum transient or residual story drift. The performance goal might be limitation of structural and/or nonstructural damage, which might require that no yielding occur in structural members. Thus, one of the goals during design or evaluation would be the calculation of story drift or member stress levels using selected analysis and modeling procedures for a given earthquake characterization. The earthquake characterization may take the form of a design response spectrum or a set of accelerograms scaled to represent a certain hazard level which is expressed in terms of probability of exceeding a given intensity within a chosen return period. The occupancy of the building will also require special attention when selecting a target performance level. A building with high occupancy such as a high rise building, or a hospital needed for emergency treatment of earthquake victims, should be designed for a higher level of performance, or for a lower probability of non-compliance of the building to the design performance level. The probability of exceeding the design limits is another issue that should be considered. All of these items raised in this section will be described in more detail in the next chapter of this report.

1.5 Objectives

The SAC Phase II project involves several teams doing topical investigations in various areas important to the design and evaluation of steel moment frame buildings. Basic and applied research is undertaken on system performance, connection performance, material properties, welding and joining processes, and steel frame performance during past earthquakes. The project also involves the development of several products that take the form of Guidelines for design professionals, building officials, code writers, and other government agencies. The Performance Prediction and Evaluation (PPE) Team assimilates the work done by the other topical investigation teams with its own research results to formulate information required by the Guideline writers to complete their products. In a sense, the objective of this report is to provide an information bridge between the topical investigations and the Guidelines. The two main research objectives of the PPE Team were to evaluate linear and nonlinear analysis procedures and to develop a reliability framework for performance evaluation for the SAC project.

This report is not a state-of-the-art report in the traditional sense. It does not present an exhaustive coverage of the main topics that are covered. For instance, it does not consider some

of the new and exciting analysis procedures because they are still in the formative stages and require a broader review before they are ready for useful production. On the other hand, it does present a new reliability-based performance-based model for acceptance criteria that explicitly consider the randomness and uncertainties involved in the seismic design process. This performance-based evaluation procedure is at the state of the art.

In Chapter 2, several important issues related to performance-based engineering are discussed. Past work on this topic is reviewed, and basic definitions that have evolved over the past few years are given. In Chapter 3, the seismic hazard levels are discussed. The earthquake accelerograms used in the SAC project are discussed. Provisions for developing response spectra are required. Analysis procedures and modeling of structures for linear and nonlinear analysis are discussed in Chapter 4. Results of studies on the accuracy of seven analysis procedures are presented. Next, in Chapter 5, a statistical and reliability framework for comparing and evaluating predictive models for design and evaluation is presented. Performance levels and objectives, the performance evaluation process, and concepts on demand and capacity are given. A dual-performance level framework is developed which results in acceptance criteria that consider the randomness and uncertainties in the process. The development of the SAC ground motions and the different seismic hazard levels and their determination are discussed in Chapter 4. Predictive models for performance prediction are presented and evaluated in Chapter 5. Chapter 6 presents guidelines for design and performance evaluation of new steel moment frame buildings. In Chapter 7, performance evaluation of ordinary and partially restrained steel moment frames is presented. Evaluation and performance prediction for existing buildings are covered in Chapter 8, while Chapter 9 covers evaluation and performance prediction for damaged buildings.

1.6 Summary

The SAC Phase 2 project involves several teams doing basic and applied topical investigations on system performance, connection performance, material properties, welding and joining processes and other topics important to the design, evaluation and construction of steel moment frames subjected to seismic loads. The Performance Prediction and Evaluation (PPE) team was charged with assimilating research results developed by other teams with its own research in order to develop a state-of-the-art performance-based method for performance evaluation of new, existing and damaged steel moment frames.

Certain areas in the San Francisco area experienced major damage during the 1989 M7.1 Loma Prieta earthquake that shook parts of the San Francisco Bay area. Even though the level of shaking was only ¼ to ½ of the design-level earthquake in the metropolitan area, more than $7 billion of damage occurred. The 1994 Northridge earthquake caused about $20 billion of damage. Of course, this earthquake caused fractures of connections in steel moment-frame buildings and caused alarm in the minds of the public and the design profession who worried about the safety of this class of construction. This has caused a flurry of discussion and research on performance-based engineering.

Performance-based engineering takes a holistic view of functionality of a building from conception to the end of its usefulness. Therefore, it is a much broader concept than

performance-based seismic design, where the design professional develops a building design that will satisfy one or more performance levels for selected seismic hazard levels. One goal of this approach is to limit damage to buildings under minor seismic events. Although this is the correct approach for the profession to pursue, the scope is too broad for the SAC program which is focused on limiting structural damage. Nevertheless, one valuable product of the SAC project is a performance-based design and evaluation procedure that could serve as the basis of future performance-based engineering specifications.

The specific issues related to performance-based evaluation that this report addresses are the following:

- the need to reconcile information on demand and capacity on a regional basis,
- the need to account for uncertainty in performance associated with unanticipated events,
- the need to have a basis to understand performance and to set realistic expectations,
- the variability of performance for similar buildings located near one another,
- unique issues associated with fracturing of connections such as collapse,
- the need to evaluate and calibrate different analytical methods,
- the need to consider new buildings and existing ones on a consistent basis,
- the development of a reliability framework for the process,
- the need to set realistic performance levels with appropriate seismic hazard, and
- the need to understand and quantify local and global behavior leading to collapse.

The two major features of a performance based approach to seismic evaluation are the performance levels and the seismic hazards. The expression of the seismic hazard is the response spectrum acceleration. The maps developed by the USGS for the *1997 NEHRP Provisions* were adopted by the SAC project. These are maps that plot the expected spectral accelerations at a short period, and one-second period that have a 2% in 50 year (2/50) or 50% in 50 (50/50) year probability of being exceeded. The procedure for converting these spectral accelerations to design values is different for performance evaluation using the new procedure from that used for new design in the NEHRP *Provisions*. The reasons for this are discussed. The SAC project had suites of earthquake accelerograms developed for different hazard levels and soil conditions for Los Angeles, Seattle and Boston. Their role in the SAC research projects and the performance-based evaluation procedure is also explained.

One of the key objectives of the PPE team was to evaluate and calibrate predictive methods for calculating seismic demand. It was decided to include only those methods that have reached a level of maturity that their use was familiar to a broad sector of the engineering community. As a result, several exciting new procedures are not considered. So this section of the report could be labeled as the state of practice rather than the state of the art.

Eight analysis procedures were evaluated and calibrated. These are the 1997 NEHRP equivalent lateral force and modal analysis procedures, the FEMA 273 linear static, linear dynamic and nonlinear static procedures, the capacity spectrum method and linear and nonlinear

time history analysis procedures. Bias factors for each procedure are presented that remove the systematic errors associated with each and result in equal median demand predictions for given hazard level. The tables give bias factors as a function of building height, hazard level and building irregularity. The statistics of the predictions are used to develop reliability-based demand factors for use with the new evaluation procedure. State-of-the-art modeling procedures for linear and nonlinear analysis are described that include the effects of panel-zone yielding, fracturing connections, strength degradation due to local flange buckling, and moment-rotation behavior of gravity connections.

A new reliability-based performance-based evaluation procedure is presented. Two performance levels are defined. The Collapse Prevention (CP) structural performance level is defined as the postearthquake damage state in which the building is on the verge of experiencing local or global collapse. Significant degradation has occurred in the strength and stiffness of the building, which may be a total financial loss. This is paired with the 2/50 hazard level to establish a performance objective. The Immediate Occupancy performance level is defined as the postearthquake damage state in which only limited structural damage has occurred. Damage is expected to be so slight that if not found during inspection there would be no cause for alarm.

The spectral accelerations used for evaluation are median values for the hazard level of interest. Calculated demands and capacities used for evaluation are also usually median values. As a result, it should not be surprising if half of the buildings failed to meet the stated performance objectives if subjected to the design event. This is clearly unacceptable. A key and unique feature of the new performance evaluation model is that it allows the design professional to estimate the level of confidence that the building will satisfy the performance objective. The target values for the SAC project were to have a 95% confidence that a building will meet the CP performance level for the 2/50 hazard, and a 95% confidence that a building will meet the IO performance level for the 50/50 hazard.

Another key element of the new procedure is that capacity and demand are stated in terms of observable and quantifiable behavior. As a result, the acceptance criteria are expressed in terms of story drift. This required that local and global collapse be defined in terms of story drift.

A new analytical procedure is introduced for defining the state of incipient global collapse of a building under seismic attack called the Incremental Dynamic Analysis (IDA) procedure. Twenty buildings designed in accordance with the 1997 NEHRP *Provisions* and assumed to have prequalified post-Northridge moment connections that were tested by the Connection Performance team were analyzed and evaluated. The set consisted of eight 3-story, eight 9-story and four 20-story buildings with different configurations. The global collapse drifts were found to be 10% for the 3-story and 9-story buildings and 9% for the 20-story buildings. Performance evaluations of the buildings revealed that there is a 99% confidence that the 3- and 9-story buildings will satisfy the performance objective and a 93% confidence level that the 20-story building will do so as well. Additional analysis indicated that any connection behavior that satisfies the AISC test protocol should be expected to demonstrate similar performance.

The local collapse drift for pre-Northridge and post-Northridge connections were determined from laboratory tests of full-size specimens conducted by the Connection Performance team.

The local collapse drift was defined as the point at which the beams could no longer carry gravity loads. This could result from the loss of a shear tab or the development of a low-cycle fatigue crack that has progressed most of the way through the web of the beam. The local collapse criteria were evaluated for the 20 new buildings assuming that the reduced beam section connection was used. The local collapse drift for this connection is 7%. The confidence levels that the 3-, 9- and 20-story buildings will satisfy the local collapse performance objective are 96%, 93% and 96%, respectively. Similar results were found for the IO performance level for the 50/50 hazard. Based on these results, it was decided that building designs conforming to the1997 NEHRP *Provisions,* in conjunction with the new prequalified connections, will result in steel moment-frame buildings that will exhibit good performance in future earthquakes.

The performance evaluations reported above required calculating the maximum story drifts for the 20 post-Northridge buildings for 20 accelerograms representative of the 2/50 hazard level for a LA site. Several interesting results were observed as a result of these analyses. The median, 84^{th} and 95^{th} percentile drift demands for the 3-story building were 0.027, 0.039 and 0.046, respectively. For the 9-story buildings they were 0.029, 0.045 and 0.057, while they were 0.021, 0.033 and 0.050 for the 20-story buildings. Thus, the ratio of local capacity to median demand was approximately 2.7 on average.

The performance of Ordinary Moment Frames (OMF) and frames with partially restrained connections were also evaluated. OMF buildings are assumed to be less ductile than Special Moment Frame (SMF) buildings. As a result, they are designed for twice as large seismic forces, are restricted to regions of low to moderate seismicity, and have height limitations.

Three aspects of OMF frames were studied: weak panel zones, weak column designs and local flange buckling in beams and columns. The effects of local buckling were minor for two reasons. First, because they are designed for larger forces the members tend to be stocky so the degree of local buckling expected to occur is low. In addition, columns in perimeter moment frames tend to be vertical beams since the axial loads are very small compared to the bending moments that develop under seismic loads. The weak panel zones and weak column designs did not adversely affect the performance of the 3- and 9- story buildings. However, story mechanisms developed in the 20-story buildings with weak panel zones and weak column designs. They suffered global collapse for several of the accelerograms representing the 2/50 hazard level. As a result, it is recommended that frames with weak panel zones and weak column designs be restricted to 100 feet tall in SPC C regions.

Partially restrained (PR) beam connections are flexible compared to the stiffness of the beams. A connection is considered to be partially restrained (as opposed to fully restrained (FR)) if ten percent of the frame deflection results from the flexibility of the connections. PR connections can be full-strength, partial-stiffness or partial-strength, partial-stiffness configurations. Three types of connections were evaluated: T-stub, end-plate and clip angle connections. The CP team tested the first two types, and a significant amount of data was available for the third. The CP team developed procedures for modeling stiffness and identifying failure mechanisms. A number of 3- and 9-story buildings were designed for different geographic locations, seismic performance categories and site conditions. Demands and capacities were determined. A performance evaluation of each building was performed which

indicated that the confidence that each would satisfy both the CP and IO performance objectives is over 95%.

The general public and the design profession are concerned about the safety inherent in the existing steel moment frame buildings with brittle pre-Northridge connections. Fracture usually occurs at about the plastic moment capacity of the beam, which results in ductility capacity of one or less. SMF buildings are expected to experience ductility demands of three or more when subjected to the design earthquake. Although no steel buildings collapsed during the Northridge earthquake, many experienced fractured connections for ground motion levels considerably smaller than the design event. A new beam connection element was developed in order to study this problem. The element is able to model the pre-fracture and post-fracture behavior of the connections using the Drain 2DX analysis program.

Guidelines for performance evaluation of pre-Northridge buildings are presented. Such things as performance levels and objectives, material properties, condition assessment and analytical modeling procedures are discussed. Different features of the older buildings are identified that might be useful in the evaluation process. These include the year of construction and the stiffness of the building.

The seismic provisions in the UBC and the AISC specifications are reviewed for each edition going back to the early 1960's. Major changes in the codes and the years in which they occurred were noted. The two most important features that affect the expected performance are the design base shear and the drift limitations because they strongly affect the expected drift demand. Prior to 1976 there was no drift limit for seismic loads. It is surmised that some design offices used the wind drift limitations for seismic design, but is likely that many did not. In addition, there were no panel zone limitations during this period.

In order to study this problem, a 3-story, 9-story and 20-story building was designed for the UBC and AISC provisions in effect in 1973, 1985 and 1994. Actually, a prominent structural engineering firm in LA designed the 1994 buildings. The nominal member sizes and building configurations chosen for these buildings were also used for the 1973 and 1985 building designs.

IDA analyses of the 1973 designs revealed that the global collapse capacities are 10%, 8% and 7% for the 3-, 9- and 20-story buildings, respectively. The median demands for the 2/50 accelerograms were 0.062, 0.059 and 0.045. So the capacity/demand ratio averages 1.5. The local collapse drift for these connections depends on the depth of the beams and was assumed to be 0.04. None of the buildings, on average, is expected to satisfy the local collapse performance level. The confidence levels that the buildings will satisfy the global collapse performance level for the 2/50 hazard are 71, 20 and 46% for the 3-, 9- and 20-story buildings, respectively. For local collapse the confidence levels are 1, 1 and 6%.

The 1985 buildings are expected to perform somewhat better than the 1973 buildings. The 3-, 9- and 20-story buildings have global drift capacities of 10%, 9.4% and 7%, respectively, while the median demands are 5.8%, 4.8% and 3%. The confidence levels that the buildings will satisfy the global collapse performance levels for the 2/50 hazard are 76%, 69% and 71%. The 1994 buildings are expected to perform only a little better than this. They had confidence levels

of 83%, 70% and 75% that they would satisfy the collapse prevention performance objective. The ramifications of these results are discussed. It is recommended that the minimum acceptable confidence level that a building will satisfy the CP performance level should be about 90% for the 50/30 hazard level which represents a return period of about 44 years. In fact, all of the existing buildings considered in this study have a 99% confidence level that they will satisfy the CP performance level for the 50/50 hazard level which has a return period of about 72 years.

The final issue that is considered in this report is performance evaluation of damaged buildings. One of the most pressing problems facing structural engineers after a major earthquake is deciding if a building may be occupied while fractured connections are being repaired. In light of the results reported above for existing but undamaged buildings, it should be clear that the safety of damaged buildings would be difficult to ascertain. It may be required to consider the relative safety of a building before and after the damage as opposed to the absolute level of safety.

Several studies are reported which considered the pre-Northridge buildings previously described. Each building was subjected to an earthquake representing the 2/50, 10/50 and 50/50 hazard levels. The damage state was noted and then the building was subjected to the same earthquake again. The purpose was to determine the probability of a building surviving a second earthquake with the same intensity as the first. The results for the 1994 building were described in the most detail. The 3-story building suffered the worst since it experienced global collapse during the first application of the 2/50 accelerogram and local collapses after the second application of the 10/50 accelerogram. The 9-story building had most of its connections suffer bottom flange fractures during the first application of the 2/50 accelerogram and several local collapses during the second. It was able to survive both applications of the 10/50 and 50/50 accelerograms without global or local collapse. The 20-story building experienced no local or global collapse for any combination of earthquakes.

A procedure is presented for evaluating damaged buildings using static analysis procedures to analyze the building before and after the damage has occurred. Modeling procedures for handling bottom flange fractures are described and examples of “before and after” analyses are presented. One helpful feature for the damaged building is that its first-mode period of vibration is larger than for the undamaged state, which usually will reduce the demand during a second event.

Finally, the performance-based evaluation procedure is used to determine the level of safety of a damaged building. It can be a helpful tool when trying to determine if a building may remain occupied after suffering damage. The hazard level to consider in this situation is not clearly defined since the repair or rehabilitation process should only require months instead of years. A confidence level of 90% of satisfying the CP performance level for the 50/30 hazard level should be adequate. All of the buildings considered in this study had a high confidence of satisfying this performance goal if only bottom flange fractures occurred during the first event.

2. PERFORMANCE-BASED DESIGN AND EVALUATION

2.1 Background and Description of Performance-Based Design

Recent earthquakes in Northridge, California and Kobe, Japan have resulted in billions of dollars of damage to buildings, bridges, and other structures and the loss of thousands of lives. The suffering people displaced from their homes and businesses wonder why. Lessons learned from the Michoacan earthquake in Mexico City in 1985, and from the San Fernando and Loma Prieta earthquakes that rocked parts of California, have been verified in these recent earthquakes.

Major damage occurred during the 1989 M7.1 Loma Prieta Earthquake, which shook parts of the San Francisco Bay Area. Even though the level of shaking was only 1/4 to 1/2 of the design level earthquake for a metropolitan area, more than $7 billion dollars of damage occurred (SEAOC, 1995). The 1994 M6.7 Northridge earthquake caused about $20 billion of damage. These observations have stimulated much interest and activity in performance-based design philosophies. As observed in the Vision 2000 report developed by the Structural Engineers Association of California (SEAOC, 1995), "Although no loss of life occurred in modern buildings designed to recent building codes, the economic loss which occurred was judged both by the structural engineering profession and public policy makers as too large for this moderate event. A need was identified for new building design and construction procedures which could better meet society's requirement that property and business interruption losses in moderate earthquakes be controlled to acceptable levels."

The underlying philosophy for current seismic design codes and practice in the United States is expressed in the Commentary to the 1990 *Blue Book* (SEAOC, 1990):

1. No damage to either structural or nonstructural components during minor shaking.
2. Limited nonstructural damage, but no damage to structural components during moderate shaking.
3. Structural and nonstructural damage during severe shaking; total building collapse is prevented.

The goal contained in the code is one of life safety. Although this could be an excellent framework for a performance-based design code, there are at least two major flaws in its application. Minor, moderate, and major earthquakes are not specified in terms of size or probability of exceedance. Also, there is no clear calculable building response that can be associated with observable levels of damage or collapse. In fact, there is no clear connection between the code provisions and the expected performance of the building. The implicit performance level is protection against loss of life. The other two objectives given above are assumed to be met.

Performance-based design or engineering requires more than just a set of new provisions, it requires a new attitude toward seismic design. A recent report, "Performance-Based Seismic Engineering of Buildings" (SEAOC, 1995) provides an excellent discussion on philosophy and

development of performance-based seismic design codes. This report contains an insightful description of performance-based engineering. Performance-based engineering is a process that begins with the first concepts of a project and lasts throughout the life of the building. It includes selection of the performance objectives, determination of the site suitability, conceptual design, preliminary design, final design, acceptability checks during design, design review, quality assurance during construction, and maintenance during the life of the building. Each step is critical to the design and must be addressed to a level suitable to the performance objective selected. Performance-Based Engineering, not Performance-Based Design, is the most suitable title for this process since it encompasses all aspects of the effort and not just those related to design (SEAOC, 1995)." In the light of recent damaging earthquakes, there is a feeling in the engineering profession that we can do better. This has stimulated a flurry of activity and thinking about performance-based engineering and design.

Performance-based engineering is a much broader concept than performance-based design. It takes a more holistic consideration of functionality of the building from its conception to the end of its usefulness. The SAC project made a conscious decision to consider a much narrower view of the process. It was decided to consider those issues related to performance-based evaluation. To further narrow the scope, it was decided that objectives of the SAC project would not include consideration of nonstructural damage. So, only structural damage and protection of lives are considered herein. A complete performance-based design procedure must consider the operational level of performance where the structure behaves in the elastic range. Prevention of damage to architectural features and mechanical and electrical systems is the chief concern.

In a recent position paper written by R. O. Hamburger (1998), Director of Product Development for the SAC Project, an excellent description of performance-based design is given. A paraphrase follows that accurately describes the basis for the philosophy driving the SAC Steel Project.

Performance-based design of structures for seismic resistance is a new concept that is rapidly developing. As stated by SEAOC (1995), the purpose of performance-based engineering is to permit the design and construction of structures such that they will provide specific intended levels of performance within defined levels of reliability. SEAOC and several recently published design methodology documents, FEMA-273 (ATC, 1997) and ATC-40 (ATC, 1996) pioneer the practice of performance-based seismic design. Performance specifications consist of the designation of one or more limiting damage states, which should not be exceeded, given that ground shaking hazards of specific severity are experienced.

As mentioned above, typical damage states, termed performance levels, referenced by SEAOC, FEMA-273 and ATC-40, include an incipient collapse state, often termed "Collapse Prevention;" a "Life Safety" state, which is somewhat arbitrarily defined as the damage that occurs when demands are a specified fraction of those that produce the "Collapse Prevention" state; and an Immediate Occupancy state, representing a state of very limited damage with negligible compromise of original structural strength, stiffness, or deformation capacity. Ground shaking hazards are typically specified in a discrete manner, based on the probability of their not being exceeded. Typical hazard levels include hazards with 2%, 5%, 10%, and 50%

probabilities of not being exceeded in 50 years. By coupling one of these hazard levels with a corresponding performance level, or damage state, which should not be exceeded at that hazard level, a design performance objective is obtained. Although the FEMA-273 and ATC-40 methodologies prescribe engineering procedures to design for such performance objectives, no attempt has been made in these documents to characterize the reliability of the methodology. This is simply stated: Using the FEMA-273 and ATC-40 methodologies it is possible to design for a given damage state at a given hazard level. However, the probability that a structure designed using these methodologies will actually not exceed that damage is undefined. These approaches are based on mean or median values, so it should not be a surprise if 50% of the buildings designed in accordance with their provisions fail to meet the performance objective in response to the appropriate earthquake. The design procedures to be employed by the SAC project are intended to advance the state of the art by providing quantification of this reliability.

Performance-based design includes selection of appropriate building sites, systems, and configurations as well as analytical procedures used in the design process to confirm that the structure has adequate strength, stiffness, and energy dissipation capacity to respond to design ground motions without exceeding permissible damage states. The methods described in this report are applicable to evaluation used as part of the design process or for assessment of a damaged, or undamaged, existing building to determine its expected future performance capabilities.

The SAC project provides a unique opportunity for the development of performance-based design and evaluation procedures. Fundamental research is being done on a broad range of topics including system performance, connection performance, material properties and behavior, welding and joining processes, performance prediction, and evaluation and reliability and reliability-based design. In addition to the researchers, imminent engineers and social scientists from across the country are providing their expert opinion tempered by years of experience. The framework laid in the SAC project could be the basis of a future performance-based design code.

The specific issues related to performance-based evaluation that the SAC project will address include the following:

- the need to reconcile information on demand and capacity on a regional basis as developed by other SAC working groups,
- the need to account for uncertainty in performance associated with unanticipated performance and fracture,
- the need to have a basis to understand performance and to set realistic expectations,
- the variability of performance for similar buildings located near one another,
- unique issues associated with fracturing of connections such as safety against collapse,
- the need to evaluate and calibrate different analytical methods becoming available,

- the need to consider new buildings and existing ones on a consistent basis,
- the development of a reliability framework for the process,
- the need to set realistic performance levels with the appropriate seismic hazard,
- the need to have a consistent probability-based method that is transparent to the engineer and owner voluntarily electing to have a higher performance level, and
- the need to understand and quantify local and global behavior leading to collapse.

These issues are discussed below.

2.2 Basic Definitions

It will be helpful to the reader if basic definitions of important parameters and concepts are given at this point.

Acceptance Criterion	The value of a design parameter to which a specific performance can be said to be achieved with suitable confidence.
Bias Factor (C_B)	A factor used to adjust predictions of demand or capacity for systematic inaccuracies (either under-prediction or over-prediction) known to be inherent in the predictive methodology.
Capacity Factor (ϕ)	A factor applied to a capacity for a structure or structural component in order to account either for the inherent variability (randomness) or for information limitations (uncertainties) in the estimation of the structure's capacity.
Confidence Factor (λ_{con})	The ratio of the factored capacity and factored demand. Used with probability tables to determine the confidence level that a building will satisfy its performance objective.
Demand Factor (γ)	A factor applied to the demand (value of a design parameter) predicted by analysis in order to account for the inherent variability (randomness) or for information limitations (uncertainties) in the estimation of this demand.
Design Parameter	A structural response parameter that can be used as a measure of performance. Examples include component forces, plastic rotations, and story drifts.
Hazard Curve	A graphic representation of the variation in ground motion as defined by a suitable parameter, such as spectral acceleration, velocity, or displacement, with annual probability of exceedance.

	As used in SAC documents, hazard curves are assumed to be plotted on log-log paper.
Performance Level	A state of defined and observable damage of a building.
Performance Objective	The selection of a hazard level to be matched with a performance level.
Randomness	A measure of scatter of predictions of a parameter (either demand or capacity) that cannot be attributed to specific factors that can be predicted. The degree of randomness is irreducible regardless of the number of samples that we take. The yield strength of a steel member that will be purchased in the future is a random property.
Uncertainty	A measure of the scatter of predictions of a parameter (either capacity or demand) that can be attributed to specific factors, which, by themselves, have uncertain values. The degree of uncertainty is reducible with more or better knowledge. If we need to determine the yield strength of a specific steel in a column of an existing building, we can reduce the uncertainty by collecting more samples from it for testing.

2.3 Performance Levels

As defined above, a performance level is a state of defined and observable damage in a structure or structural component. This might range from collapse of a structure to cracking of windows or a facade. One of the most basic issues that needs to be addressed is the establishment and definition of appropriate performance levels and performance objectives. In a recent SAC report by Wen and Foutch (1997), the following guidelines for establishing performance levels and objectives were recommended:

1. Performance levels need to be stated in terms of probability given the large uncertainty in both loads and resistance. The performance levels need to be described directly in probabilistic terms for multiple performance goals. The performance objectives can be achieved by specifying multi-level probability based design earthquake response spectra associated ground motions and structural performance criteria that the building has to satisfy at each level.
2. The performance levels should cover the full range of performance from operational to incipient collapse and should be specified in terms of specific observable behavior that can be associated with calculable building response. A consensus needs to be established as to which calculated response and what seismic hazard level we should use as the proper limit for the performance objective, such as an interstory drift of 2% for incipient damage and 9% drift for incipient collapse.

3. The target reliability levels can be decided by comparing risk and expected loss and damage corresponding to each performance goal due to seismic hazard or other societal risks. The target reliability levels obtained for different performance goals can be used as the basis for setting acceptance criteria for evaluation and design.

In short, the performance goals should be based on reliability and uncertainty principles, they should be based on calculated response associated with observed behavior, and the acceptable risks should be determined.

The first performance-based seismic design procedure developed in the U.S. that has gone through a broad review process was developed by the Applied Technology Council (ATC) for the Building Seismic Safety Council (BSSC) and funded by the Federal Emergency Management Agency. It is entitled *NEHRP Guidelines for the Rehabilitation of Buildings* and is published as FEMA 273 (ATC, 1997a) with the *Commentary* as FEMA 274 (ATC, 1997b). This report identified four performance levels: Operational, Immediate Occupancy, Life Safety, and Collapse Prevention. The definition of a performance level is the "intended postearthquake condition of a building; a well-defined point on a scale measuring how much loss is caused by earthquake damage; in addition to casualties, loss may be in terms of property and operational loss (ATC, 1997a)." The *Vision 2000* (SEAOC, 1995) report also identified four performance levels: Fully Operational, Operational, Life-Safe, and Near Collapse. These are similar to those presented in FEMA-273.

The following descriptions of these four performance levels as described in FEMA-273 are as follows:

Operational Level - Buildings meeting this performance level are expected to sustain minimal or no damage to their structural or nonstructural components. The building is suitable for its intended use, although possibly in a slightly impaired mode, with power, water and other utilities provided from emergency sources, and possibly with some nonessential systems not functioning.

Immediate Occupancy Level - Buildings meeting this performance level are expected to sustain minimal or no damage to their structural elements and only minor damage to their nonstructural elements. While it would be safe to reoccupy a building meeting this performance level immediately following a major earthquake, nonstructural systems may not function due to either a loss of electrical power or internal damage to equipment. Therefore it may be necessary to perform some cleanup and repair, and await the restoration of utility service before the building could perform in its normal mode. For steel moment frame buildings, some connection or member damage may be discovered during post-earthquake inspection, but this would be minimal and repairable while the building remains occupied. There will be no fractures and only minor local buckling or member distortion. No permanent drift will be observed.

Life Safety Level - Buildings meeting this level may experience extensive damage to structural and nonstructural components. Repairs may be required before re-occupancy of

the building occurs, and repair may be deemed economically impractical. The risk to life in this building would be low. Hinges will form in steel moment frames. Severe joint distortion and isolated moment connection fractures will be observed. But shear connections needed to support gravity loads will remain intact. Large permanent drifts exceeding 2.5% should be expected.

Collapse Prevention Level - Buildings meeting this performance level may pose significant hazard to life safety resulting from failure of nonstructural components or major structural damage. However, because the building does not collapse, gross loss of life should not occur. Perhaps all buildings meeting this performance level will be complete economic losses. For steel moment frames, there will be extensive deformation in beams, columns, and panel zones. Many fractured moment connections will be observed, but shear connections will remain intact. Transient drifts of 5% or greater will occur.

No drift limits were established in FEMA 273. Vision 2000 stated transient and permanent drift limitations as follows: Operational: < 0.5% transient and no permanent; Life Safety: 1.5% and 0.5%; Near Collapse: 2.5% for both. There was also a difference between FEMA 273 and Vision 2000 in the suggested hazard level to combine with the performance levels to establish a performance objective.

2.4 Reliability and Performance-Based Evaluation

A method for performance evaluation based on reliability analysis and performance objectives is presented in the next chapter. Two performance levels are defined. Performance objectives are established such that the performance objectives may be satisfied within a given level of confidence. The randomness and uncertainty associated with predicting the capacity and demand are explicitly accounted for.

3. SEISMIC HAZARD AND CODE PROVISIONS

3.1 Background and Special SAC Ground Motions

3.1.1 Maximum Considered Earthquake Ground Motions

The seismic hazard is represented by an elastic response spectrum acceleration as a function of period. These spectral acceleration values used in the SAC *Recommended Criteria* (FEMA-350 to 353) were determined and mapped by the USGS for the NEHRP *Recommended Provisions for Seismic Regulations for New Buildings and Other Structures* (BSSC, 1997a) (FEMA-302). This short description paraphrases material presented in the *Commentary* to this document (BSSC, 1997b) (FEMA-303).

The intent of the NEHRP *Provisions* is to provide a uniform level of performance of structures for all regions of the U.S. The intent is to provide a uniform level of safety against collapse for the Maximum Considered Earthquake (MCE). For most regions of the U.S., the MCE is defined as the earthquake ground motion with a uniform likelihood of exceedance of 2 percent in 50 years (2/50). This represents an earthquake with a return period of 2,475 years.

"In regions of high seismicity, such as coastal California, the seismic hazard is typically controlled by large-magnitude events occurring on a limited number of defined fault systems. Ground shaking calculated at a 2% in 50 years likelihood would be much larger than that which would be expected based on the characteristic magnitudes of earthquakes on these known active faults. This is because these major active faults can produce characteristic earthquakes every few hundred years. For these regions, it is considered more appropriate to directly determine maximum considered earthquake ground motions based on the characteristic earthquakes of these defined faults. In order to provide for an appropriate level of conservatism in the design process, when this approach to calculation of the MCE ground motion is used, the median estimate of ground motion resulting from the characteristic event is multiplied by 1.5." (FEMA-303).

Unfortunately, this contaminates the reliability-based design and evaluation procedures described below. Specific references describing how the maps were generated are given in the *Commentary* to the NEHRP *Provisions* (BSSC, 1997b) (FEMA-303).

One other simplification was also introduced. The design of new buildings using the NEHRP *Provisions*, or those given in the 1997 *Uniform Building Code*, is based on elastic analysis procedures. As a result, all buildings will have significant strength above that assumed for design. This is recognized, for instance, by noting that the C_d value is less than the R value. To account for this in the design procedure, it is assumed that the lower bound on this strength ratio is 1.5 for all building systems. As a result, the spectral accelerations from the maps are multiplied by 2/3 for use in design. This further contaminates the reliability-based calculations introduced herein. A better approach would be to omit the 2/3 factor and increase the R value. Performance evaluation of buildings designed by the 97 NEHRP *Provisions* satisfy the performance objectives established by the SAC project and described in Chapter 6. As a result,

the SAC *Recommended Criteria* for design of new buildings adopt this same convention, to avoid confusion. The global and local capacities are also multiplied by 2/3 to compensate for this. For performance evaluation of new buildings, existing, or damaged buildings, however, this convention is not followed. Consequently, design of new steel frame buildings will not be considered explicitly in this report.

3.1.2 Special Ground Motion Time Histories Developed for the SAC Studies

The studies on system performance conducted by the System Performance team and the reliability based approach to performance evaluation developed by the Performance Prediction and Evaluation (PPE) team required sets of ground motion accelerograms consistent with the different hazard levels that were considered.

Several sets of accelerograms for different locations, hazard levels, and site conditions were developed for the SAC *Recommended Criteria* by Sommerville, et al. (1997). The different families of accelerograms were developed in such a way that they were representative of the natural randomness that is present in the earthquake environment.

"Ground motion estimates were developed by Sommerville and his colleagues for three locations in the United States (Boston, Seattle and Los Angeles) corresponding to seismic zones 2, 3 and 4, respectively. Suites of 20 time histories for each were provided for two probabilities of occurrence (2% in 50 years and 10% in 50 years) in each of the three locations for firm soil conditions. Time histories were also provided for 50% in 50 years for Los Angeles. Time histories for soft soil profiles were provided for 10% in 50 years in all three locations. Near fault time histories were also provided for seismic zone 4 conditions" (Sommerville, et al., 1997).

The target response spectra for the different hazard levels and locations are given in Table 3-1.

Before the PPE studies began, the average spectrum for the 20 time histories for the 2/50 hazard for the LA site was calculated and plotted with the least-squares-fit NEHRP spectrum determined for the spectral points given in Table 3-1. These plots are shown in Figure 3-1. For some reason, the average spectrum for the accelerograms did not fit the NEHRP spectrum well. In order for the reliability calculations to be meaningful, it was important that these two plots coincide. After discussing this with Sommerville, it was decided to multiply all accelerograms in the set by a scale factor of 0.83. The corrected average spectrum is also shown in Figure 3-1. This approach was taken so that the natural randomness represented in the 20 accelerograms would not be affected. Similar adjustments were also made for other sets of accelerograms. The scale factors used for each are given in Table 3-2. Plots of selected average spectra are shown in Figure 3-1 to Figure 3-3.

Table 3-1 Target Response Spectra for Site Category S_D

Return Period	Location	Period (5% damping)			
		0.3	1.0	2.0	4.0
2% 50 years					
	Boston	0.34	0.16	0.077	0.030
	Seattle	1.455	1.00	0.41	0.164
	Los Angeles	1.61	1.19	0.54	0.190
10% 50 years					
	Boston	0.12	0.052	0.028	0.0108
	Seattle	0.71	0.39	0.18	0.072
	Los Angeles	1.07	0.68	0.33	0.123
50% 50 years					
	Boston	0.0239	0.00908	0.00516	0.001
	Seattle	0.319	0.129	0.0582	0.0229
	Los Angeles	0.514	0.288	0.149	0.069
50% 30 years					
	Boston	0.0135	0.00481	0.0027	0.0005
	Seattle	0.229	0.0878	0.0397	0.0162
	Los Angeles	0.434	0.219	0.110	0.0536

These are meant to represent a NEHRP Site Category D.

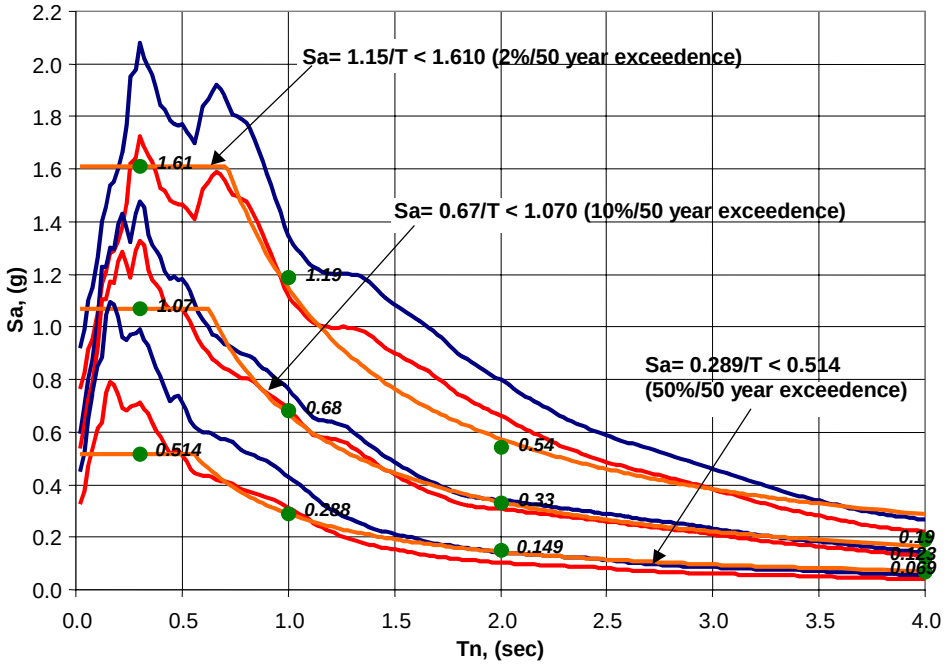

Figure 3-1 Representative 5% Damped Los Angeles Response Spectra

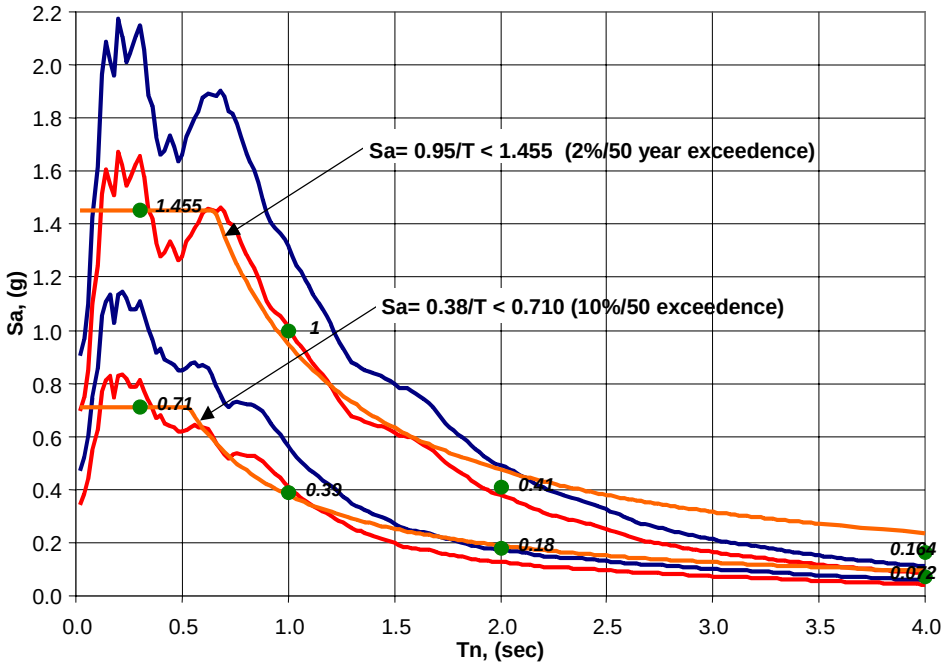

Figure 3-2 Representative 5% Damped Seattle Response Spectra

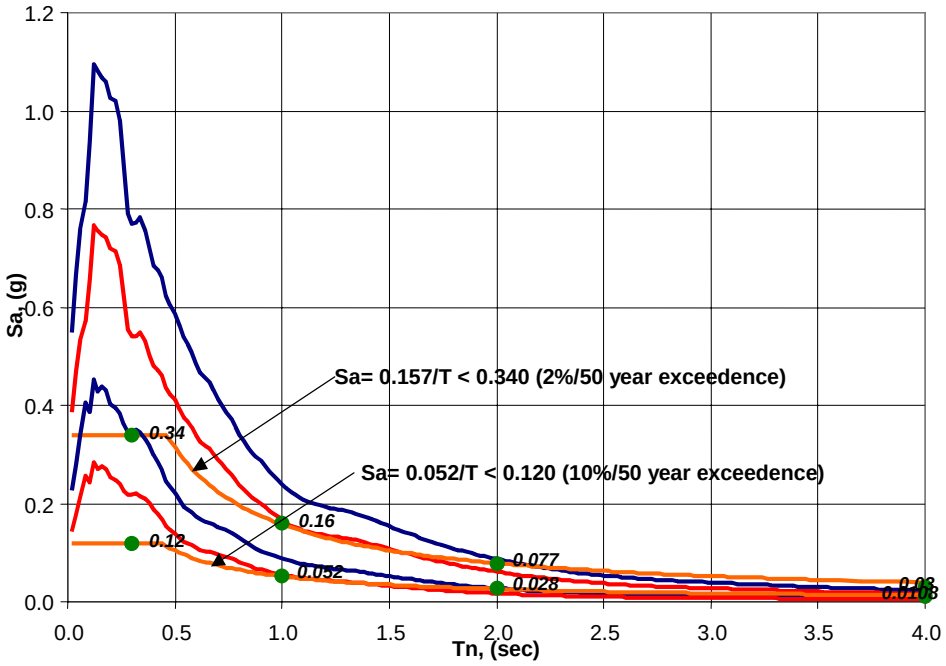

Figure 3-3 Representative 5% Damped Boston Response Spectra

Table 3-2 Scale Factors for Los Angeles, Seattle, and Boston Sites for Different Hazard Levels

	2/50 hazard	10/50 hazard	50/50 hazard
Los Angeles	0.83	0.90	0.72
Seattle	0.77	0.73	N/A
Boston	0.70	0.63	N/A

3.2 1997 NEHRP Requirements (BSSC, 1997a) (FEMA-302)

The SAC *Recommended Criteria*, FEMA-350 to 353, have adopted the maps and methods for determining design ground motions and response spectra given in the 1997 NEHRP *Provisions* (FEMA-302). Selected portions of these *Provisions* are given in this document for reference purposes. In the NEHRP *Provisions*, the design spectral acceleration is obtained by multiplying the spectral acceleration for the Maximum Considered Earthquake by 2/3 to account for the fact that the building will be "at least" 1.5 times stronger than assumed for design. This overstrength should be modeled on the capacity side and not the demand side of the design equation as discussed in Section 3.1.1. For performance evaluation, this 2/3 factor is not used. This report does not consider design of new buildings.

3.2.1 Procedures for Determining Maximum Considered Earthquake and Design Earthquake Ground Motion Accelerations and Response Spectra

"Ground motion accelerations, represented by response spectra and coefficients derived from these spectra, shall be determined in accordance with the general procedure of Section 4.1.2 of FEMA-302, (see Sec. 3.2.1.2, or the site-specific procedure of Sec. 4.1.3 of FEMA-302). The general procedure in which spectral response acceleration parameters for the maximum considered earthquake ground motions are derived using Maps 1 through 24, modified by site coefficients to include local site effects and scaled to design values, are permitted to be used for any structure except as specifically indicated in these *Provisions*. The site-specific procedure also is permitted to be used for any structure and shall be used where specifically required by these provisions." (From FEMA-302.)

3.2.1.1 Maximum Considered Earthquake Ground Motions

"The maximum considered earthquake ground motions shall be as represented by the mapped spectral response acceleration S_S at short period, and S_1 at 1 second obtained from Maps 1 through 24 of these *Provisions*" (and adjusted for Site Class effects using the site coefficients of Sec. 3.2.1.2D, herein). "When a site-specific procedure is used, maximum considered earthquake ground motion shall be determined in accordance with Sec. 4.1.3 of FEMA-302." (From FEMA-302.)

3.2.1.2 General Procedure for Determining Maximum Considered Earthquake and Design Spectral Response Accelerations

"The mapped maximum considered earthquake spectral response acceleration S_S at short periods, and S_1 at 1 second, shall be determined from Maps 1 through 24.

For structures located within those regions of the maps having values of the short period spectral response acceleration, S_S, less than or equal to 0.15g and values of the 1-second period spectral response acceleration, S_1, less than or equal to 0.04g, accelerations need not be determined. Such structures are permitted to be directly categorized as Seismic Design Category A in accordance with Sec. 3.2.2.1, (herein).

For other buildings and structures, the Site Class shall be determined in accordance with Sec. 3.2.1.2A, (herein.) The maximum considered earthquake spectral response accelerations adjusted for Site Class effects, S_{MS} and S_{M1}, shall be determined in accordance with Sec. 3.2.1.2D, (herein), and the design spectral response accelerations, S_{DS} and S_{D1}, shall be determined in accordance with Sec. 3.2.1.2E, (herein.) The general response spectrum, when required by these *Provisions*, shall be determined in accordance with Sec. 3.2.1.2F, (herein.)" (From FEMA-302.)

"**A. Site Class Definitions**: For all structures located within those regions of the maps having values of the short period spectral response acceleration, S_S, greater than 0.15g or values of the 1 second period spectral response acceleration, S_1, greater than 0.04g, the site shall be classified as one of the following classes:

A. Hard rock with measured shear wave velocity, $\bar{v}_s$ > 5,000 ft/sec (1500 m/s)

B. Rock with 2,500 ft/sec < $\bar{v}_s$ ≤ 5,000 ft/sec (760 m/s < $\bar{v}_s$ ≤ 1500 m/s)

C. Very dense soil and soft rock with 1,200 ft/sec < $\bar{v}_s$ ≤ 2,500 ft/sec (360 m/s < $\bar{v}_s$ ≤ 760 m/s) or with either $\bar{N}$ > 50 or $\bar{S}_u$ > 2,000 psf (100 k

D. Stiff soil with 600 ft/sec ≤ $\bar{v}_s$ ≤ 1,200 ft/sec (180 m/s ≤ 360 m/s) or with either 15 ≤ $\bar{N}$ ≤ 50 or 1,000 psf ≤ $\bar{S}_u$ ≤ 2,000 psf (50 kPa ≤ $\bar{S}_u$ ≤ 100 kPa)

E. A soil profile with $\bar{v}_s$ < 600 ft/sec (180 m/s) or with either

$$\bar{N}<15,\ \bar{S}_u < 1{,}000 \text{ psf},$$

or any profile with more than 10 ft (3m) of soft clay defined as soil with PI > 20, w ≥ 40%, and S_u < 500 psf (25 kPa).

F. Soils requiring site-specific evaluations:

1. Soils vulnerable to potential failure or collapse under seismic loading such as liquefiable soils, quick and highly sensitive clays, collapsible weakly cemented soils.

2. Peats or highly organic clays (H > 10 ft [3m] of peat or highly organic clay where H = thickness of soil)

3. Very high plasticity clays (H > 25 ft [8m] with PI > 75)

4. Very thick soft/medium stiff clays (H > 120 ft [36m])

Exception: When the soil properties are not known in sufficient detail to determine the Site Class, Class D shall be used. Site Classes E or F need not be assumed unless the authority having jurisdiction determines that Site Classes E or F could be present at the site or in the event that Site Classes E or F are established by geotechnical data." (From FEMA-302.)

"**B. Steps for Classifying a Site** (also see Table 3-3 below):

Step 1: Check for the four categories of Site Class F requiring site-specific evaluation. If the site corresponds to any of these categories, classify the site as Site Class F and conduct a site-specific evaluation.

Step 2: Check for the existence of a total thickness of soft clay > 10 ft (3m) where a soft clay layer is defined by: S_u < 500 psf (25 kPa), w ≥ 40 percent, and PI > 20. If these criteria are satisfied, classify the site as Site Class E.

Step 3: Categorize the site using one of the following three methods with $\bar{v}_s$, $\bar{N}$, and $\bar{S}_u$ computed in all cases as specified by the definitions in Sec. 4.1.2.2 of FEMA-302:

a. $\bar{v}_s$ for the top 100 ft (30m) ($\bar{v}_s$ method)

b. $\overline{N}$ for the top 100 ft (30m) ($\overline{N}$ method)

c. $\overline{N}_{ch}$ for cohesionless soil layers (PI < 20) in the top 100 ft (30m) and average $\overline{S}_u$ for cohesive soil layers (PI > 20) in the top 100 ft (30m) ($\overline{S}_u$ method).

Table 3-3 Site Classification

Site Class	$\overline{v}_s$	$\overline{N}$ or $\overline{N}_{ch}$	$\overline{s}_u$
E	< 600 fps (< 180 m/s)	< 15	< 1,000 psf (< 50 kPa)
D	600 to 1,200 fps (180 to 360 m/s)	15 to 50	1,000 to 2,000 psf (50 to 100 kPa)
C	> 1,200 to 2,500 fps (360 to 760 m/s)	> 50	> 2,000 (> 100 kPa)

NOTE: If the $\overline{S}_u$ method is used and the $\overline{N}_{ck}$ and $\overline{S}_u$ criteria differ, select the category with the softer soils (for example, use Site Class E instead of D).

The shear wave velocity for rock, Site Class B, shall be either measured on site or estimated for competent rock with moderate fracturing and weathering. Softer and more highly fractured and weathered rock shall either be measured on site for shear wave velocity or classified as Site Class C.

The hard rock category, Site Class A, shall be supported by shear wave velocity measurements either on site or on profiles of the same rock type in the same formation with an equal or greater degree of weathering and fracturing. Where hard rock conditions are known to be continuous to a depth of 100 ft (30m), surfacial shear wave velocity measurements may be extrapolated to assess $\overline{v}_s$.

The rock categories, Site Classes A and B, shall not be used if there is more than 10 ft (3m) of soil between the rock surface and the bottom of the spread footing or mat foundation." (From FEMA-302.)

"**C. Definitions of Site Class Parameters**: The definitions presented below apply to the upper 100 ft (30m) of the site profile. Profiles containing distinctly different soil layers shall be subdivided into those layers designated by a number that ranges from 1 to *n* at the bottom where there are a total of *n* distinct layers in the upper 100 ft (30m). The symbol i then refers to any one of the layers between 1 and *n*.

v_{si} = shear wave velocity in ft/sec (m/s).

d_i = thickness of any layer between 0 and 100 ft (30m).

$\overline{v}_s$ is:

$$\overline{v}_s = \frac{\sum_{i=1}^{n} d_i}{\sum_{i=1}^{n} \frac{d_i}{v_{si}}} \tag{3-1}$$

where $\sum_{i=1}^{n} d_i$ is equal to 100 ft (30m):

N_i is the Standard Penetration Resistance (ASTM D1586-84) not to exceed 100 blows/ft as directly measured in the field without corrections.

$\overline{N}$ is:

$$\overline{N} = \frac{\sum_{i=1}^{n} d_i}{\sum_{i=1}^{n} \frac{d_i}{N_i}} \tag{3-2}$$

$\overline{N}_{ch}$ is:

$$\overline{N}_{ch} = \frac{d_s}{\sum_{i=1}^{m} \frac{d_i}{N_i}} \tag{3-3}$$

where $\sum_{i=1}^{m} d_i = d_s$:

(Use only d_i and N_i for cohesionless soils.)

d_s = total thickness of cohesionless soil layers in the top 100 ft (30m).

s_{ui} = undrained shear strength in psf (kPa), not to exceed 5,000 psf (250 kPa), ASTM D2166-91 or D2850-87.

$\overline{S_u}$ is

$$\overline{s_u} = \frac{d_c}{\sum_{i=1}^{k} \frac{d_i}{s_{ui}}} \tag{3-4}$$

where $\sum_{i=1}^{k} d_i = d_c$:

d_c = total thickness (100 - d_s) of cohesive soil layers in the top 100 ft (30m).

PI = plasticity index, ASTM D4318-93.

w = moisture content in percent, ASTM D2216-92."
(From FEMA-302.)

"**D. Site Coefficients and Adjusted Maximum Considered Earthquake Spectral Response Acceleration Parameters**: The maximum considered earthquake spectral response acceleration S_{MS} for short periods and S_{M1} at 1 second, adjusted for site class effects, shall be determined by Equations 3-5 and 3-6, respectively:

$$S_{MS} = F_a S_S \tag{3-5}$$

and

$$S_{M1} = F_v S_1 \tag{3-6}$$

where site coefficients F_a and F_v are defined in Tables 3-4 and 3-5, respectively."
(From FEMA-302.)

Table 3-4 Values of F_a as a Function of Site Class and Mapped Short-Period Maximum Considered Earthquake Spectral Acceleration

Site Class	Mapped Maximum Considered Earthquake Spectral Response Acceleration at Short Periods				
	$S_S \leq 0.25$	$S_S = 0.50$	$S_S = 0.75$	$S_S = 1.00$	$S_S \geq 1.25$
A	0.8	0.8	0.8	0.8	0.8
B	1.0	1.0	1.0	1.0	1.0
C	1.2	1.2	1.1	1.0	1.0
D	1.6	1.4	1.2	1.1	1.0
E	2.5	1.7	1.2	0.9	a
F	a	a	a	a	a

NOTE: Use straight line interpolation for intermediate values of S_S.

[a] Site-specific geotechnical investigation and dynamic site response analyses shall be performed.

Table 3-5 Values of F_a as a Function of Site Class and Mapped 1-Second Period Maximum Considered Earthquake Spectral Acceleration

Site Class	Mapped Maximum Considered Earthquake Spectral Response Acceleration at 1-Second Period				
	$S_1 \leq 0.1$	$S_1 = 0.2$	$S_1 = 0.3$	$S_1 = 0.4$	$S_1 \geq 0.5$
A	0.8	0.8	0.8	0.8	0.8
B	1.0	1.0	1.0	1.0	1.0
C	1.7	1.6	1.5	1.4	1.3
D	2.4	2.0	1.8	1.6	1.5
E	3.5	3.2	2.8	2.4	a
F	a	a	a	a	a

NOTE: Use straight line interpolation for intermediate values of S_1.

[a] Site-specific geotechnical investigation and dynamic site response analyses shall be performed.

"**E. Design Spectral Response Acceleration Parameters**: Design earthquake spectral response acceleration at short periods, S_{DS}, and at 1 second period, S_{D1}, shall be determined from Equations 3-7 and 3-8, respectively:

$$S_{DS} = (2/3)S_{MS} \tag{3-7}$$

$$S_{D1} = (2/3)S_{M1} \tag{3-8}$$

3.2.2 Seismic Design Category

Each structure shall be assigned a Seismic Design Category in accordance with Sec. 3.2.2.1, herein. Seismic Design Categories are used in these *Provisions* to determine permissible structural systems, limitations on height and irregularity, those components of the structure that must be designed for seismic resistance, and the type of lateral force analysis that must be performed." (FEMA-302.)

3.2.2.1 Determination of Seismic Design Category

"All structures shall be assigned to a Seismic Design Category based on their Seismic Use Group and the design spectral response acceleration coefficients, S_{DS} and S_{D1}, determined in accordance with Sec. 3.2.1.2E, herein. Each building and structure shall be assigned to the most severe Seismic Design Category in accordance with Table 3-6 or 3-7, irrespective of the fundamental period of vibration T, of the structure." (From FEMA-302.)

Table 3-6 Seismic Design Category Based on Short Period Response Accelerations

Value of S_{DS}	Seismic Use Group		
	I	II	III
$S_{DS} < 0.167g$	A	A	A
$0.167g \leq S_{DS} < 0.33g$	B	B	C
$0.33g \leq S_{DS} < 0.50g$	C	C	D
$0.50g \leq S_{DS}$	D[a]	D[a]	D[a]

[a] Seismic Use Group I and II structures located on sites with mapped maximum considered earthquake spectral response acceleration at 1 second period, S_1, equal to or greater than 0.75g shall be assigned to Seismic Design Category E and Seismic Use Group III structures located on such sites shall be assigned to Seismic Design Category F.

Table 3-7 Seismic Design Category Based on 1-Second Period Response Accelerations

Value of S_{D1}	Seismic Use Group		
	I	II	III
$S_{D1} < 0.067g$	A	A	A
$0.067g \leq S_{D1} < 0.133g$	B	B	C
$0.133g \leq S_{D1} < 0.20g$	C	C	D
$0.20g \leq S_{D1}$	D[a]	D[a]	D[a]

[a] Seismic Use Group I and II structures located on sites with mapped maximum considered earthquake spectral response acceleration at 1 second period, S_1, equal to or greater than 0.75g shall be assigned to Seismic Design Category E, and Seismic Use Group III structures located on such sites shall be assigned to Seismic Design Category F.

3.2.2.2 Site Limitation for Seismic Design Categories E and F

"A structure assigned to Seismic Design Category E or F shall not be sited where there is the potential for an active fault to cause rupture of the ground surface at the structure.

Exception: Detached one- and two-family dwellings of light-frame construction." (From FEMA-302.)

3.2.3 Occupancy Importance Factor

An occupancy importance factor, I, shall be assigned to each structure in accordance with Table 3-8.

Table 3-8 Occupancy Importance Factors, I

Seismic Use Group	I
I	1.0
II	1.25
III	1.5

3.3 Comparison of Seismic Demand for Design from Various Specifications

Welded steel moment frames began to be built in the 1950s. The seismic design requirements, as well as the specifications for designing steel structures, have changed a great deal between then and the present. The design spectra from selected past UBC provisions for a Los Angeles site are shown in Figure 3-4. Also shown is the design spectrum for the LA site from the current 1997 NEHRP *Provisions*. A direct comparison of these spectra from the older

codes with those from the current code can be misleading, since the older designs used allowable stress design while the new *Provisions* are based on strength (LRFD) design.

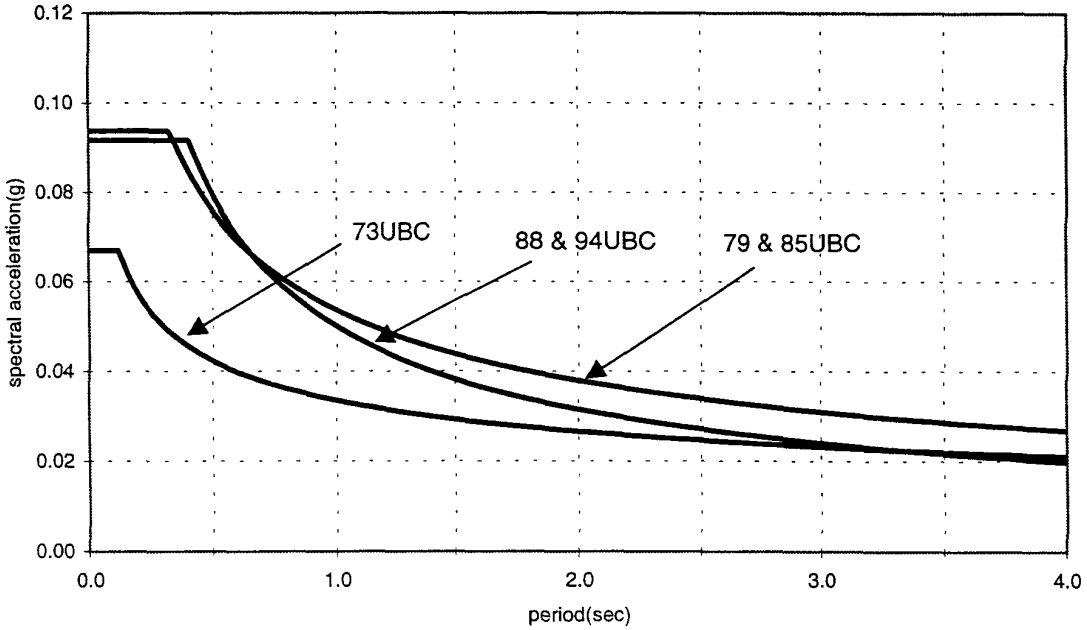

Figure 3-4 Design Response Spectrum for Special Steel Moment Frames 1973 UBC and Later Years, Los Angeles

4. ANALYSIS METHODS FOR EVALUATION OF BUILDINGS

4.1 Introduction

4.1.1 Background

Seismic design codes have been used in parts of the U.S. for over 60 years. An excellent historical review of past codes and critical review of current codes was recently published by the Applied Technology Council (ATC) under the title *A Critical Review of Current Approaches to Earthquake Resistant Design* (ATC, 1995). This document was heavily used in the development of this report.

Currently there are three model building codes that are used in the United States: the *Uniform Building Code* (UBC), (ICBO, 1997); the *National Building Code* (NBC) (BOCA, 1999); and the *Standard Building Code* (SBC) (SBCCI, 1999). Most local jurisdictions adopt all or most of the seismic provisions given in one of these model codes. Only Wisconsin has not adopted at least one of the model codes.

The *UBC* seismic provisions are based on the SEAOC "Blue Book" (SEAOC, 1997) recommendations. The *NBC* and *SBC* seismic provisions are based on FEMA-302 recommendations. In the year 2000, all three model building codes will be combined to form the *International Building Code* (IBC). The *IBC* seismic provisions will be based on an updated version of FEMA-302, the 1997 NEHRP *Provisions*.

4.1.2 Brief Summary of Past Code Provisions

The performance of steel frame buildings during an earthquake is influenced by four factors that are defined and specified in various codes: (1) the characterization of the intensity of the ground motion; (2) the design base shear and distribution of specified design forces; (3) the acceptance criteria based on the capacity of the structural members and the allowable story drift; and (4) the detail requirements such as $b_f/2t_f$ values for Special Moment Frames. Of course, there are also many factors that are not covered in the code, as discussed in Chapters 1 and 2. Changing the requirements in any one of these parameters will affect the structure's design and, therefore, its performance during an earthquake. As a result, it is neither useful nor adequate to consider any one of these factors without acknowledging and quantifying the effects of the others. A historical perspective of how these factors have been specified in the *UBC* is included in Chapter 7 on evaluation of existing buildings.

4.2 Description of Analysis Methods

Eight analysis and design procedures were evaluated for this project. The four elastic procedures that were considered are the FEMA-302 equivalent lateral force and modal analysis procedures, the FEMA-273 linear static and linear dynamic procedures, and the linear time history analysis procedure. The three inelastic procedures that were considered are the FEMA-273 nonlinear static procedure, the capacity spectrum procedure (Skokan and Hart, 1999), and the nonlinear time history analysis procedure.

It is not feasible or necessary to review all of the design requirements for each procedure. This section of the report will focus on the following features of each code: (1) the seismic hazard and the depiction of the seismic demand; (2) description of the design forces and their vertical distribution; and (3) the acceptance criteria. Most of the descriptive material is taken verbatim from the appropriate code or report. The material on seismic hazard and depiction of seismic demand is given in Chapter 3 for each design procedure. The reason for including this material is for completeness and to facilitate comparisons. Most design professionals are familiar with the elastic procedures found in one or two of the model codes. This document includes linear dynamic, nonlinear static, and nonlinear dynamic procedures.

Acceptance criteria for each procedure will not be discussed since the SAC project has acceptance criteria based on story drift. Only those provisions related to calculating story drift will be given. In some cases there is a modification of the original procedures in order to be consistent within the SAC methodology. It should be remembered that this document considers only performance evaluation and not design of new buildings. It is pointed out in the text where this distinction is important.

4.2.1 1997 NEHRP Equivalent Lateral Force Procedure – N97-LSP (FEMA-302)

4.2.1.1 Background

The first NEHRP *Provisions* were published in 1985 (BSSC, 1985). They were modeled in part on the ATC-3-06 recommendations (ATC, 1978). They were prepared for FEMA by the Building Seismic Safety Commission. "The Building Seismic Safety Commission was established under the auspices of the National Institute of Building Sciences as an entirely new type of instrument for dealing with complex regulatory, technical, social and economic issues involved in developing and promulgating building earthquake hazard mitigation regulatory provisions that are national in scope. By bringing together in the BSSC all of the needed expertise and all relevant public and private interests, it was believed that issues related to seismic safety of the built environment could be resolved and jurisdictional problems overcome through authoritative guidance and assistance backed by a broad consensus" (FEMA-302). So, the NEHRP *Provisions* were developed as a national standard. The *UBC* provisions, on the other hand, were primarily developed by the Structural Engineers Association of California.

4.2.1.2 Design Forces

A. Seismic Base Shear: The seismic base shear, V, in a given direction shall be determined in accordance with the following equation:

$$V = C_s W \tag{4-1}$$

where:

C_s = the seismic response coefficient determined by Equation 4-2

W = the total dead load and applicable portions of other loads

The seismic response coefficient, C_s, shall be determined in accordance with the following equation:

$$C_s = \frac{S_{DS}}{R} \tag{4-2}$$

where:

S_{DS} = the design spectral acceleration in the short period range as determined below,

R = the response modification factor given in Table 4-1.

The value of the seismic response coefficient computed in accordance with Equation 4-2 need not exceed the following:

$$C_s = \frac{S_{D1}}{TR} \tag{4-3}$$

but shall not be taken less than:

$$C_s = 0.044 S_{DS} \tag{4-4}$$

nor for buildings and structures in Seismic Design Categories E and F:

$$C_s = \frac{0.55\, S_{D1}}{R} \tag{4-5}$$

where R is defined above and

S_{D1} = the design spectral acceleration at a period of 1.0 seconds as determined below,

T = the fundamental period of the structure as determined below,

S_1 = the mapped maximum considered earthquake spectral acceleration determined in accordance with provisions given below.

For performance evaluation, the limits given by Equations 4-4 and 4-5 do not apply. These are included for design to provide a cushion of safety for tall buildings for potential problems such as P-Δ effects. This is not appropriate for performance evaluation. Only Equations 4-2 and 4-3 apply.

B. Period Determination: The fundamental period of the building, T, in the direction under consideration shall be established using the structural and deformational characteristics of the resisting elements in a properly substantiated analysis. Alternatively, the period may be calculated as

$$T = 2\pi\sqrt{\frac{\sum w_i \delta_i^2}{g\sum f_i \delta_i}} \tag{4-6}$$

where:

w_i = weight at each floor
g = gravity acceleration
f_i = applied force at floor level i
δ_i = displacement at floor level i

Research conducted by the PPE team demonstrated that the natural periods of steel frame buildings measured during earthquakes are very well approximated by these procedures (Lee and Foutch, 2000). The simple formulas given in the code for calculating T are conservative.

Table 4-1 Coefficients and Factors for Performance Evaluation of Steel Moment-Resisting Frame Systems

Basic-Seismic-Force-Resisting System	Response Modification Coefficient, R	System Over-Strength Factor Ω_o	Deflection Amplification Factor, C_d
Special steel moment frames	8	3	5-1/2
Intermediate steel moment frames	6	3	4-1/2[1]
Ordinary steel moment frames	4	3	3-1/2

[1] This has been changed from the NEHRP Provisions

4.2.1.3 Drift Determination

The lateral load F_x applied at any floor level x shall be determined from the following equations:

$$F_x = C_{vx} V \tag{4-7}$$

$$C_{vx} = \frac{w_x h_x^k}{\sum_{i=1}^{n} w_i h_i^k} \tag{4-8}$$

where:

k	=	1.0 for $T \leq 0.5$ second
	=	2.0 for $T \geq 2.5$ seconds
		Linear interpolation shall be used to estimate values of k for intermediate values of T.
C_{vx}	=	Vertical distribution factor
V	=	Seismic base shear from Equation 4-1
w_i	=	Portion of the total building weight W located on or assigned to floor level i
w_x	=	Portion of the total building weight W located on or assigned to floor level x
h_i	=	Height (in ft) from the base to floor level i
h_x	=	Height (in ft) from the base to floor level x

Determination of story drifts shall be based on the application of the design seismic forces determined by Equation 4-7 to a mathematical model of the structure. The model shall include the panel zone deformations. The design story drift, Δ, shall be computed as the difference between the deflections at the center of mass at the top and the bottom of the story under consideration.

The calculated story drift, δ_x, in story x shall be determined in accordance with the following:

$$\delta_x = C_d \, \delta_{xe} \tag{4-9}$$

where:

C_d	=	deflection amplification factor in Table 4-1,
δ_{xe}	=	deflections determined by an elastic analysis.

The drift angle Δ_x is then calculated by

$$\Delta_x = \frac{(\delta_x - \delta_{x-1})}{h_x} \tag{4-10}$$

h_x is the height of the story directly under floor x. The demand drift, $\hat{D}$, is then calculated as

$$\hat{D} = C_B \, \theta_m \tag{4-11}$$

where:

$\hat{D}$	=	seismic demand
C_B	=	bias factor (see Section 4.4)
θ_m	=	the maximum story drift angle, Δ_x, for all stories.

4.2.2 1997 UBC Static Force Procedure: UBC97-LSP (ICBO, 1997)

4.2.2.1 Background

The future UBC *Provisions* will be the same as given in the 2000 NEHRP *Provisions*. As a result, the analysis methods given in the 1997 *UBC* were not evaluated and will not be described in detail here.

4.2.3 FEMA-273 Linear Static Procedure: F273-LSP (ATC, 1997a)

4.2.3.1 Background

The NEHRP *Guidelines for the Seismic Rehabilitation of Buildings*, FEMA-273, (ATC, 1997a) and the NEHRP *Commentary on the Guidelines for the Seismic Rehabilitation of Buildings*, FEMA-274 (ATC, 1997b) were the culmination of over 13 years and thousands of man-hours of effort. They contain systematic guidance enabling design professionals to formulate effective and reliable rehabilitation approaches that will limit the expected earthquake damage to a specified range for a specified level of ground motion. They also represent the first attempt to develop a standardized performance-based engineering procedure. The reader is encouraged to read the *Guideline* and *Commentary*. In the FEMA-273 *Guidelines*, acceptance criteria were calculated from member forces. As a result, there are no drift limitations given. For the SAC *Recommended Criteria*, FEMA-350 to 353, all acceptance criteria are based on story drifts.

4.2.3.2 Design Forces

A. Seismic Base Shear: Under F273-LSP design, seismic forces are determined and distributed over the height of the building. A linear static analysis of the building is used to calculate the deflections in each story and the internal member forces.

The building is modeled using linear elastic stiffness properties and equivalent viscous damping appropriate for the building as it approaches the elastic limit. The design earthquake demands are expressed as a set of forces whose sum is equal to the 'pseudo lateral load' as given in Equation 4-12. On the surface, this appears to be identical to the NEHRP and UBC Linear Static Procedures. However, there is a subtle difference. For the F273-LSP, the pseudo lateral load is chosen such that when the design forces are applied to the linear elastic model of the building, the calculated displacements and member deformations will be approximately the same as those calculated for a nonlinear time history analysis. The calculated member forces, on the other hand, will be much higher than the actual member forces, which will be limited by inelastic action.

The pseudo lateral load for a given horizontal direction of a building is determined using Equation 4-12. This load shall be increased as necessary to account for torsion.

$$V = C_1 C_2 C_3 C_4 S_a W \tag{4-12}$$

where:

V = pseudo lateral load

C_1 = modification factor to relate expected maximum inelastic displacements to displacements calculated for linear elastic response

$C_1 = 1.5$ for $T<0.10$ second

$C_1 = 1.0$ for $T>T_0$. Linear interpolation shall be used to calculate C_1 for intermediate values of T.

T = fundamental period of the building

T_0 = characteristic period of the design response spectrum, defined as the period associated with transition from the constant acceleration segment of the spectrum to the constant velocity segment

C_2 = modification factor to represent the effect of stiffness degradation and strength deterioration on maximum displacement response. For steel moment frames $C_2=1.0$

C_3 = modification factor to account for P-delta effects

$C_3 = 1.0$: for $\theta < 0.1$

$C_3 = 1 + 5\,(\theta-0.1) / T$: for $\theta > 0.1$

θ is the maximum value of θ_i for all $_i$ stories

$\theta_i = \dfrac{P_i\,\delta_i}{V_i\,h_i}$. (See Equation 2-14 in FEMA-273.)

C_4 = modification factor to account for effects of overstrength

C_4 = 1.0 for all frame types for IO performance level

C_4 = 0.7 for Special Moment Frames for CP level

C_4 = 0.8 for Intermediate Moment Frames for CP level

C_4 = 0.9 for Ordinary Moment Frames for CP level

S_a = response spectrum acceleration at the fundamental period and damping ratio of the building in the direction under consideration as given in Equation 4.2.1.2-2 for the hazard level as discussed in Chapter 4

W = total dead load and anticipated live load, see Section 3.3.1.3A of FEMA-273.

B. Period Determination: The period determination follows the same procedures as those given in Section 4.2.1.2 for the 1997 NEHRP *Provisions*.

C. Vertical Distribution of Seismic Forces: The vertical distribution of the seismic forces follows the same procedures as those given in the 1997 NEHRP *Provisions*.

4.2.3.3 Acceptance Criteria

For the NEHRP-LSP, the elastic level forces are reduced by the Response Modification Factor, R, to determine the reduced seismic member forces. These reduced seismic forces are then included in the appropriate load factor combinations to determine the design member

actions that are compared to the strength capacities of each member given in the appropriate code. In addition, the calculated story drifts are multiplied by a deflection modifier coefficient, C_d, then compared to the specified drift limits. This overstrength is accounted for using the coefficient C_4 in Equation 4-12.

The acceptance criteria for the FEMA-273 procedure are quite different from these, and are based on member deformation capacities. The calculated non-reduced seismic member forces for the appropriate load combinations are compared to the expected strength of the member multiplied by a demand modifier (ductility factor) times the yield strength of the member. Although on the surface this appears to be a strength-based procedure, the effect is that the expected maximum seismic deformation demand is actually compared to the member deformation capacity. For this document, acceptance criteria for this procedure will be the same for all procedures as described in Chapter 5. The acceptance criteria for FEMA-273 is described here for reference only.

4.2.3.4 Story Drift Calculation

The base shear is applied to the building model using the vertical distribution procedure referred to above. The story drift angle for story x is then calculated as the difference in deflection between floor x and floor x-1

$$\Delta_x = \frac{(\delta_x - \delta_{x-1})}{h_x} \tag{4-13}$$

and the demand story drift, $\hat{D}$, is

$$\hat{D} = C_B \theta_m \tag{4-14}$$

where:

δ_x, δ_{x-1} = deflection at floors x and x-1

h_x = the height of story x measured as the distance between the girder centerlines at floors x and x-1

Δ_x = the drift angle of story x

4.2.4 1997 NEHRP Modal Analysis Procedure – N97-MAP (BSSC, 1997a)

4.2.4.1 Background

This procedure requires calculation of mode shapes and periods calculated from a computer model of the structure. Actually, two approaches may be taken when using a modal analysis procedure. One approach is a static procedure that calculates the response in each mode using a design spectrum. The modal responses are combined in an appropriate manner to determine the total response. This is the analysis approach described in this section. The other approach requires calculating the time history response of each mode using an earthquake accelerogram.

The individual modal responses are then combined at each instant of time to determine the total response. This method will be described in the next section of this report.

A. Modeling: A mathematical model of the structure shall be constructed that represents the spatial distribution of mass and stiffness throughout the structure. For regular structures with independent orthogonal seismic-force-resisting systems, independent two-dimensional models may be constructed to represent each system. For irregular structures or structures without independent orthogonal systems, a three-dimensional model incorporating a minimum of three dynamic degrees of freedom consisting of translation in two orthogonal plan directions and torsional rotation about the vertical axis shall be included at each level of the structure. Where the diaphragms are not rigid compared to the vertical elements of the lateral-force-resisting system, the model should include representation of the diaphragm's flexibility and such additional dynamic degrees of freedom as are required to account for the participation of the diaphragm in the structure's dynamic response. More specific modeling information is given in Section 4.3.

B. Modes: An analysis shall be conducted to determine the natural modes of vibration for the structure including the period of each mode, the modal shape vector φ, the modal participation factor, and modal mass. The analysis shall include a sufficient number of modes to obtain a combined modal mass participation of at least 90 percent of the actual mass in each of two orthogonal directions.

C. Modal Properties: The required periods, mode shapes, and participation factors of the structure shall be calculated by established methods of structural analysis for the fixed-base condition using the masses and elastic stiffnesses of the seismic-force-resisting system.

4.2.4.2 Design Forces

A. Modal Base Shear: The portion of the base shear contributed by the m^{th} mode, V_m, shall be determined from the following equations:

$$V_m = C_{sm} \overline{W_m} \tag{4-15}$$

$$\overline{W_m} = \frac{\left(\sum_{i=1}^{n} w_i \varphi_{im} \right)^2}{\sum_{i=1}^{n} w_i \varphi_{im}^2} \tag{4-16}$$

where:

C_{sm} = the modal seismic response coefficient determined below,

$\overline{W_m}$ = the effective modal gravity load including portions of the live load as defined in Sec. 5.3.2 of FEMA-302,

w_i = the portion of the total gravity load of the structure at Level *i*, and

ϕ_{im} = the displacement amplitude at the i^{th} level of the structure when vibrating in its m^{th} mode.

The modal seismic response coefficient, C_{sm}, shall be determined in accordance with the following equation:

$$C_{sm} = \frac{S_{am}}{R/I} \tag{4-17}$$

where:

S_{am} = the design spectral response acceleration at period T_m determined from either the general design response spectrum of Sec. 3.2.1.2 or a site specific response spectrum of Sec. 4.1.3 of FEMA-302,

R = the response modification factor determined from Table 4-1,

I = the occupancy importance factor determined in accordance with Sec.3.2.3,

T_m = the modal period of vibration (in seconds) of the m^{th} mode of the structure.

B. Modal Forces, Deflections, and Drifts: The modal force, F_{xm}, at each level shall be determined by the following equations:

$$F_{xm} = C_{vxm} V_m \tag{4-18}$$

and

$$C_{vxm} = \frac{w_x \phi_{xm}}{\sum_{i=1}^{n} w_i \phi_{im}} \tag{4-19}$$

where:

C_{vsm} = the vertical distribution factor in the m^{th} mode,

V_m = the total design lateral force or shear at the base in the m^{th} mode,

w_i, w_x = the portion of the total gravity load, W, located or assigned to level i or x,

ϕ_{xm} = the displacement amplitude at the x^{th} level of the structure when vibrating in its m^{th} mode, and

ϕ_{im} = the displacement amplitude at the i^{th} level of the structure when vibrating in its m^{th} mode.

The modal deflection at each level shall be determined by the following equations:

$$\delta_{xm} = C_d \delta_{xem} / I \tag{4-20}$$

$$\delta_{xem} = \left(\frac{g}{4\pi^2} \right) \left(\frac{T_m^2 F_{xm}}{w_x} \right) \tag{4-21}$$

$$\Delta_{xm} = \frac{(\delta_{xm} - \delta_{x-1m})}{h_x} \tag{4-22}$$

and

$$\hat{D} = C_B \theta_m \tag{4-23}$$

where:

δ_{xem} = the deflection of level x in the m^{th} mode at the center of the mass at level x determined by an elastic analysis,

g = the acceleration due to gravity (ft/s^2 or m/s^2),

I = the occupancy importance factor determined in accordance with Sec.3.2.3,

T_m = the modal period of vibration, in seconds, of the m^{th} mode of the structure,

F_{xm} = the portion of the seismic base shear in the m^{th} mode, induced at level x,

w_x = the portion of the total gravity load of the structure, W, located or assigned to level x.

Δ_{xm} = drift angle for level x for mode m

θ_m = the maximum drift angle for all stories = $\max\left[\left(\sum_{m=1}^{n} \Delta_{xm}^2\right)\right]^{1/2}$

C_B = the bias factor given in Table 4-8

$\hat{D}$ = the demand drift for the building

δ_{xm}, δ_{x-1m} = Deflection of floor x and floor x-1 in mode m

h_x = story height from centerline of beam at level x to centerline of beam at level x-1

C. Modal Story Shears and Moments: The story shears, story overturning moments, and the shear forces and overturning moments in vertical elements of the structural system at each level due to the seismic forces determined from the appropriate equation in Sec. 4.2.4.2 shall be computed for each mode by linear static methods.

D. Design Values: The design value for the modal base shear, V_t, each of the story shear, moment and drift quantities, and the deflection at each level shall be determined by combining their modal values as obtained from Sec. 4.2.4.2. The combination shall be carried out by taking the square root of the sum of the squares of each of the modal values or by the complete quadratic combination technique.

The base shear, V, using the equivalent lateral force procedure in Section 4.2.1 shall be calculated using a fundamental period of the structure, T, in seconds, as given by Equation 4-6. Where the design value for the modal base shear, V_t, is less than the calculated base shear, V,

using the equivalent lateral force procedure, the design story shears, moments, drifts, and floor deflections shall be multiplied by the following modification factor:

$$\frac{V}{V_t} \tag{4-24}$$

4.2.5 1997 NEHRP Dynamic Linear Time History Procedure – N97-LTH

4.2.5.1 Background

This chapter provides required standards for the linear time history analysis procedure of seismic analysis of structural demands. Two different methods are available within this class of analysis procedures. One method, the mode superposition method, uses mode shapes and modal periods calculated using a computer model of the building as described for the N97-MAP procedure described in Section 4.2.4. The symbols used in this method of analysis have the same meaning as those for similar terms used in Sec. 4.2.4, with the subscript m denoting quantities in the m^{th} mode. The information on number of modes and other restrictions required in the N97-MAP procedure apply here (where appropriate) as well. The other procedure utilizes a direct integration of the equations of motion for a computer model of the building using any widely accepted integration method such as the Newmark β-method and the Wilson θ-method. Many requirements for using linear time history methods apply to both of these methods.

4.2.5.2 Modeling

A mathematical model of the structures shall be constructed that represents the spatial distribution of mass and stiffness throughout the structure. For regular structures with independent orthogonal seismic-force-resisting systems, independent two-dimensional models may be constructed to represent each system. For irregular structures or structures without independent orthogonal systems, a three-dimensional model incorporating a minimum of three dynamic degrees of freedom consisting of translation in two orthogonal plan directions and torsional rotation about the vertical axis shall be included at each level of the structure. Where the diaphragms are not rigid compared to the vertical elements of the lateral-force-resisting system, the model should include representation of the diaphragm flexibility and such additional dynamic degrees of freedom as are required to account for the participation of the diaphragm in the structure's dynamic response. Modeling guidelines are given below in Section 4.3.

4.2.5.3 Modes

For the modal superposition method, an analysis shall be conducted to determine the natural modes of vibration for the structure including the period of each mode, the modal shape vector φ, the modal participation factor, and modal mass. The analysis shall include a sufficient number of modes to obtain a combined modal mass participation of at least 90 percent of the actual mass in each of two orthogonal directions.

4.2.5.4 Modal Properties

For the modal superposition method, the required periods, mode shapes, and participation factors of the structure shall be calculated by established methods of structural analysis for the fixed-base condition using the masses and elastic stiffnesses of the seismic-force-resisting system.

4.2.5.5 Damping

A survey of damping in buildings excited by dynamic forces revealed that the average damping values are as follows: 3-stories 4.3%; 9-stories 3.6%; and 20-stories 2.3%. These values should be used for the analyses. Interpolation may be used for building heights between these. For building heights below 3-stories, use 5%, and for buildings taller than 20-stories use 2%.

4.2.5.6 Earthquake Accelerograms

A total of 7 or more earthquake accelerograms should be used. Where possible, the accelerograms should be representative of the seismic environment and soil conditions at the site. The accelerograms must be scaled to the design spectrum for the site according to the provisions given in Chapter 3. This may be done by scaling the accelerogram such that its response spectrum ordinate at the fundamental period of the building is equal to the design response spectrum ordinate at the same period (Luco and Cornell, 1998). Care must be taken so that the spectral accelerations at the fundamental period of the buildings are not all at extreme peaks for all accelerograms. This possibility can be avoided by using a least square fit to the design spectrum in the vicinity of the first period of the building. If the spectrum is calculated at 0.02 second intervals, using the spectral values of the accelerogram at the fundamental period and those other values on each side of this one would be one way to do this. This approach is demonstrated in Figure 4-1 using a 3-story building with a fundamental period of 0.88 second. An example for both approaches is shown for one accelerogram in Figure 4-2. The scale factor of 0.74 is observed for the method using only the fundamental period. A significantly different scale factor of 1.01 was observed using a period range from 0.58 seconds to 1.18 seconds. When averaged over several accelerograms, these differences are irrelevant. (Shome and Cornell, 1999)

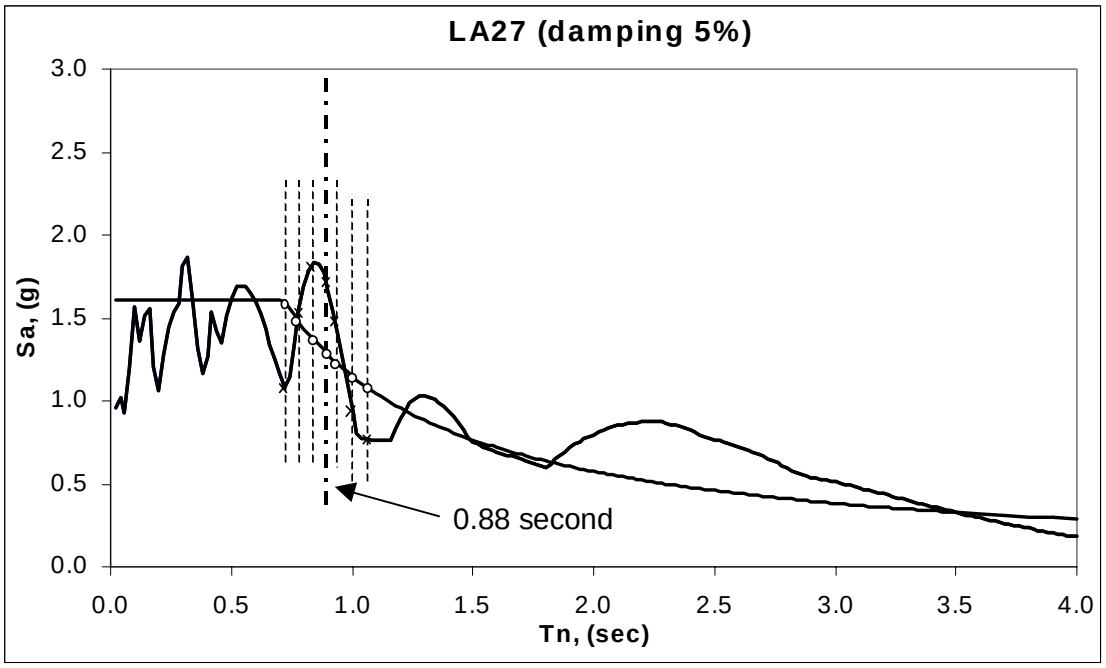

Figure 4-1 Scaling Method Using a Least Square Fit to the Design Spectrum in the Vicinity of the First Period of the Building

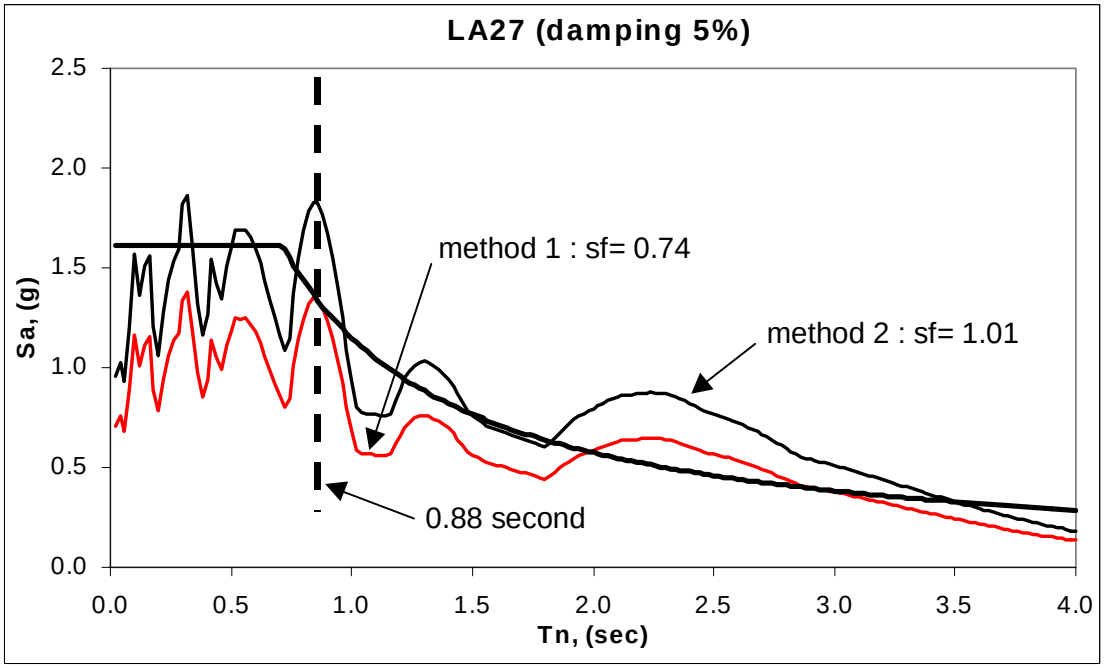

Figure 4-2 Comparison of the Two Different Scaling Methods for the 3-Story SMF with T_1 = 0.88 (sec)

4.2.5.7 Calculation of Story Drift Demands

The maximum drift angle, θ_m, calculated for any story should be determined for each accelerogram. The median value (θ_{med}) for this set of maximum drift angles should be determined. The demand drift angle, $\hat{D}$, is

$$\hat{D} = C_B \sqrt{\sum_{m=1}^{n} \theta_m^2} = C_B \theta_m \qquad (4\text{-}25)$$

where C_B is the bias factor from Table 4-8.

4.2.6 FEMA-273 Nonlinear Static Procedure – F273-NSP

4.2.6.1 Background

Under the F273-NSP, a model that accounts for inelastic material behavior P-delta effects is used for the analysis of the frame. The model is loaded monotonically until a target displacement is reached or the structure collapses or becomes unstable. This is sometimes referred to as a static force-controlled pushover analysis. The analysis may also be done by applying increments of displacements to each floor until the target displacement is reached. This is referred to as a static displacement-controlled pushover analysis. The target displacement is intended to represent the maximum displacements likely to occur during the earthquake. The target displacement may be calculated by any procedure that accounts for the effects of nonlinear response on displacement response. One such method is presented in Section 4.2.6.2. Because the mathematical model directly accounts for material inelastic behavior, the calculated internal member forces and deformations will be reasonable approximations of those expected during the design earthquake.

4.2.6.2 Design Forces

A. Lateral Load Pattern: The F273-NSP requires that a pattern of loads be specified. These loads are then increased monotonically until the target displacement is reached or the building becomes unstable. Lateral loads shall be applied to the building in profiles that approximately bound the likely distribution of inertial forces in the earthquake. At least two vertical distributions of horizontal load shall be considered. The first pattern shall be based on lateral forces that are proportional to the weight at each floor. The second pattern shall be taken from one of the following two options.

- A lateral load pattern represented by values of C_{vx} given in Equation 4-8 may be used if more than 75% of the total mass participates in the fundamental mode in the direction under consideration.

- A lateral load pattern proportional to story inertial forces consistent with story shear distribution calculated by a combination of modal forces using (1) response spectrum

analysis of the building including a sufficient number of modes to capture 90% of total mass, and (2) the appropriate ground motion spectrum.

B. Period Determination: The effective fundamental period T_e in the direction under consideration shall be calculated using the force-displacement relationship of the NSP. The nonlinear relationship between base shear and displacement of the target node shall be replaced with a bilinear relation to estimate the effective lateral stiffness, K_e, and the yield strength, V_y, of the building. The effective lateral stiffness shall be taken as the secant stiffness calculated at a base shear force equal to 60% of the yield strength. See Figure 4-3 for further details.

$$T_e = T_i \sqrt{\frac{K_i}{K_e}}$$

where:

T_i = elastic fundamental period in the direction under consideration calculated by elastic dynamic analysis

K_i = elastic lateral stiffness of the building in the direction under consideration

K_e = effective lateral stiffness of the building in the direction under consideration

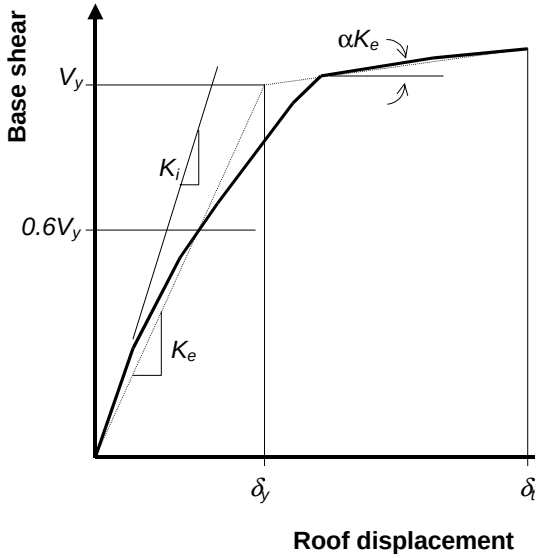

Figure 4-3 Calculation of Effective Stiffness, K_e

C. Target Displacement: The target displacement, δ_t, for a building shall be estimated using an established procedure that accounts for the likely nonlinear response of the building. Actions and deformations corresponding to the control node displacement equaling or exceeding the target displacement shall be used for component checking.

One procedure for evaluating the target displacement is given by the following equation:

$$\delta_t = C_0 C_1 C_2 C_3 S_a \frac{T_e^2}{4\pi^2} g \quad (4\text{-}26)$$

where:

T_e = effective fundamental period (sec.) of the building in the direction under consideration

C_0 = modification factor to relate spectral displacement to roof displacement

Estimates for C_0 can be calculated using one of the following:

- the first modal participation factor at the level of the control node
- the modal participation factor at the level of the control node calculated using a shape vector corresponding to the deflected shape of the building at the target displacement
- the approximate value given in Table 4-2

Table 4-2 Values for Modification Factor, C_0

Number of stories	modification factor[1], C_0
1	1.0
2	1.2
3	1.3
5	1.4
10+	1.5
[1] Linear interpolation should be used to calculate intermediate values	

C_1 = modification factor to relate expected maximum inelastic displacements to displacements calculated for linear elastic response,

= 1.0 for $T_e \geq T_0$

= $[1.0 + (R\text{-}1)\, T_0/T_e]/R$ for $T_e < T_0$

Values for C_1 shall not be taken as less than 1.0 nor greater than those values given in Section 4.2.3.2.

T_0 = a characteristic period of the response spectrum defined as the period associated with the transition from the constant acceleration segment of the spectrum to the constant velocity segment as given by Equation 4-12.

R = ratio of elastic strength demand to calculated yield strength coefficient as given below in Equation 4-27.

C_2 = modification factor to represent the effect of hysteresis shape on the maximum displacement response. Values for C_2 may be taken as 1.0 for steel moment frames.

C_3 = modification factor to represent increased displacements due to dynamic P-delta effects. For buildings with positive post yield stiffness, C_3 may be set equal to 1.0. For buildings with negative post yield stiffness values, C_3 shall be calculated using Equation 4-28. Values for C_3 need not exceed the values set forth in Section 4.2.3.2.

S_a = response spectrum acceleration (in g) at the effective fundamental period and damping ratio of the building in the direction under consideration.

The strength ratio R shall be calculated as:

$$R = \frac{S_a}{V_y C_0 / W} \tag{4-27}$$

where S_a and C_0 are defined above and:

V_y = yield strength calculated using the F273-NLP, where the nonlinear force-displacement (i.e., base shear force vs. roof displacement) is characterized as a bilinear relation as shown in Figure 4-3.

W = total dead load and anticipated live load.

The coefficient C_3 shall be calculated as follows if the relation between base shear force and control node displacement exhibits negative post-yield stiffness.

$$C_3 = 1.0 + \frac{|\alpha|(R-1)^{3/2}}{T_e} \tag{4-28}$$

where R and T_e are defined above and

α = ratio of post yield stiffness to effective elastic stiffness where the nonlinear force-deflection relation is characterized by a bilinear relation as shown in Figure 4-3.

4.2.6.3 Acceptance Criteria

When the tangent displacement is reached, the drift of each story *x* is

$$\Delta_x = \frac{(\delta_x - \delta_{x-1})}{h_x} \tag{4-29}$$

where:

δ_x, δ_{x-1} = deflection of story *x* and *x-1*
h_x = height of story x
Δ_x = drift angle of story

The demand drift angle, $\hat{D}$, is calculated as

$$\hat{D} = C_B \theta_m \tag{4-30}$$

where θ_m is the maximum story drift calculated by Equation 4-29.

4.2.7 Capacity Spectrum Procedure – CSP-NSP (ATC-40)

4.2.7.1 Background

The Capacity Spectrum Method was originally developed for the evaluation of existing buildings. This method is recommended for the evaluation of existing reinforced concrete buildings in ATC-40 (ATC, 1996).

4.2.7.2 Calculation of Floor Displacements

Using this method, the capacity curve obtained from the pushover analysis is first transformed to equivalent spectral coordinates. For each point on the capacity curve, the base shear and roof displacement quantities are transformed into equivalent spectral acceleration and spectral displacement quantities, respectively. The transformations come from the basic principles of structural dynamics and are based on first mode relationships between building response quantities and spectral quantities. The base shear from the capacity curve is transformed to an equivalent spectral acceleration by the following,

$$S_a = \frac{V/g}{\Gamma_1 L_1} \tag{4-31}$$

where V is a value of base shear from the capacity curve, Γ_1 is the first mode participation factor defined as

$$\Gamma_1 = \frac{\{\varphi_1\}^T [M]\{1\}}{\{\varphi_1\}^T [M]\{\varphi_1\}} \tag{4-32}$$

and L_1 is defined as,

$$L_1 = \{\phi_1\}^T [M]\{1\} \tag{4-33}$$

The roof displacement from the capacity curve is transformed to an equivalent spectral displacement by the following:

$$S_d = \frac{\Delta_r}{\phi_{1,r}\,\Gamma_1} \tag{4-34}$$

where Δ_r is a value of roof displacement from the capacity curve, and $\phi_{1,r}$ is the value of the fundamental mode shape at the roof level.

After transforming the capacity curve to spectral coordinates, the resulting values of spectral acceleration and spectral displacement comprise what is known as the capacity spectrum. An example of a capacity spectrum plot is shown in Figure 4-4. The target displacement is calculated by finding the intersection between the capacity spectrum and the demand spectrum. The demand spectrum, sometimes called the composite spectrum, is a plot of spectral acceleration versus spectral displacement. The demand spectrum is calculated from the response of a SDOF oscillator, at a given level of damping, to an earthquake ground motion. The demand spectrum corresponding to a level of damping equal to the inherent structural damping, β_i in a building is shown in Figure 4-4. This spectrum represents the demand spectrum for purely elastic response of the building. Note that each pair of points on the demand spectrum curve corresponds to a different period of vibration of the SDOF system. For purely elastic response of the building, the elastic capacity spectrum is a straight line corresponding to the initial elastic period of the building and is shown in Figure 4-4. The intersection of this line with the demand spectrum corresponding to β_i results in a spectral target displacement equal to the elastic spectral displacement, $(S_d)_{elastic}$, at the initial building period.

For nonlinear response of a building to an earthquake ground motion, the demand spectrum must be modified to account for the energy dissipated by hysteresis during the building's response to the earthquake ground motion. Chopra (1995) showed that an equivalent viscous damping can be defined such that, for an elastic SDOF system, the energy dissipated by this equivalent viscous damping is equal to the energy dissipated by hysteresis during the response of the building to the earthquake ground motion. The equivalent viscous damping, β_o, is defined as,

$$\beta_o = \frac{E_D}{4\pi E_{so}} \tag{4-35}$$

where E_D is the energy dissipated by hysteresis in the actual structure, and E_{so} is the strain energy calculated at the maximum displacement. Estimates of these quantities can be obtained by assuming that the force-deformation response of the building during an earthquake ground motion can be adequately modeled by the bilinear representation of the capacity curve, as shown in Figure 4-5. E_D is calculated from the area enclosed by one hysteresis loop of the bilinear capacity curve with a maximum displacement equal to the target displacement, and Eso is the strain energy calculated at the target displacement. Substituting the definitions of the energy quantities given in Figure 4-5 into Equation 4-35 results in

$$\beta_o = 0.637\left[\frac{(S_a)_y (S_d)_t - (S_a)_t (S_d)_y}{(S_a)_t (S_d)_t}\right] \tag{4-36}$$

The demand spectrum is calculated using an effective viscous damping, defined as follows

$$\beta_{eff} = \kappa \beta o + \beta_i \tag{4-37}$$

where β_i is a damping constant representing the inherent viscous damping of the building, β_o is the equivalent viscous damping that accounts for the energy dissipated by hysteresis given in Equation 4-36, and κ is a hysteresis modification factor. The coefficient κ in Equation 4-37 modifies the effective damping to account for the fact that the cyclic nonlinear behavior of the building may not be adequately represented by a bilinear relationship. The values of κ account for the effects of strength and stiffness deterioration on the equivalent viscous damping calculated from the bilinear representation of the capacity curve. For new buildings, the value of κ recommended in ATC-40 is given by

$$\kappa = 1.0 \quad \text{for} \quad \beta_o \leq 16.25\%$$

$$\kappa = 1.13 - 0.80\beta_o \quad \text{for} \quad \beta_o > 16.25\% \tag{4-38}$$

The method used to calculate the demand spectrum corresponding to the effective damping depends on whether the demand spectrum is the composite spectrum calculated from the response of a SDOF system to a particular earthquake ground motion record, or a smooth representation of the composite spectrum. If the composite spectrum is used, then the demand spectrum is simply calculated from the earthquake response of a SDOF system having a damping equal to the effective damping, β_{eff}. If a smooth demand spectrum is used, then the demand spectrum is reduced using spectral reduction factors that are a function of the effective damping. The spectral reduction factors given in ATC-40 were developed based on the work of Newmark and Hall (1982). The spectral reduction factor of the constant acceleration range, SR_A, is calculated from the following:

$$SR_A = \frac{3.21 - 0.68\ln\beta_{eff}}{3.21 - 0.68\ln\beta_i} \tag{4-39}$$

The spectral reduction factor for the constant velocity range, SR_V, is calculated from the following:

$$SR_v = \frac{2.31 - 0.41\ln\beta_{eff}}{2.31 - 0.41\ln\beta_i} \tag{4-40}$$

The spectral reduction factor for the constant displacement range, SR_D, is calculated from the following:

$$SR_D = \frac{1.82 - 0.27 \ln \beta_{eff}}{1.82 - 0.27 \ln \beta_i} \quad (4\text{-}41)$$

Note that the damping values β_i and β_{eff}, in Equation 4-39, 4-40 and 4-41 should be expressed as percentages.

Once the demand spectrum and capacity spectrum curves have been calculated, the target spectral displacement is calculated from the intersection of the demand spectrum and the capacity spectrum. This value of spectral displacement can be used to calculate a value of target roof displacement by reversing the operation in Equation 4-34.

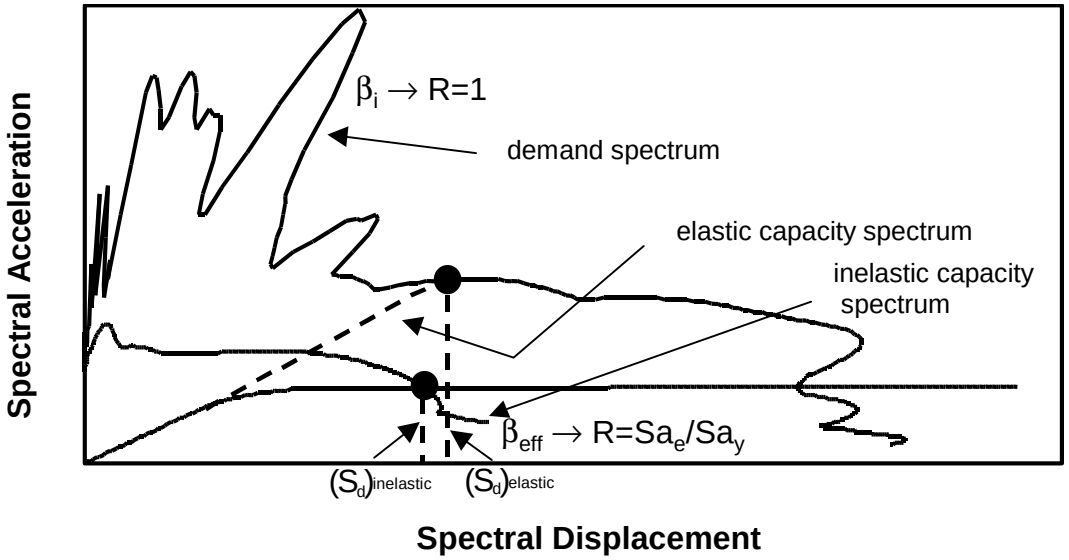

Figure 4-4 Demand and Capacity Spectrum Curves

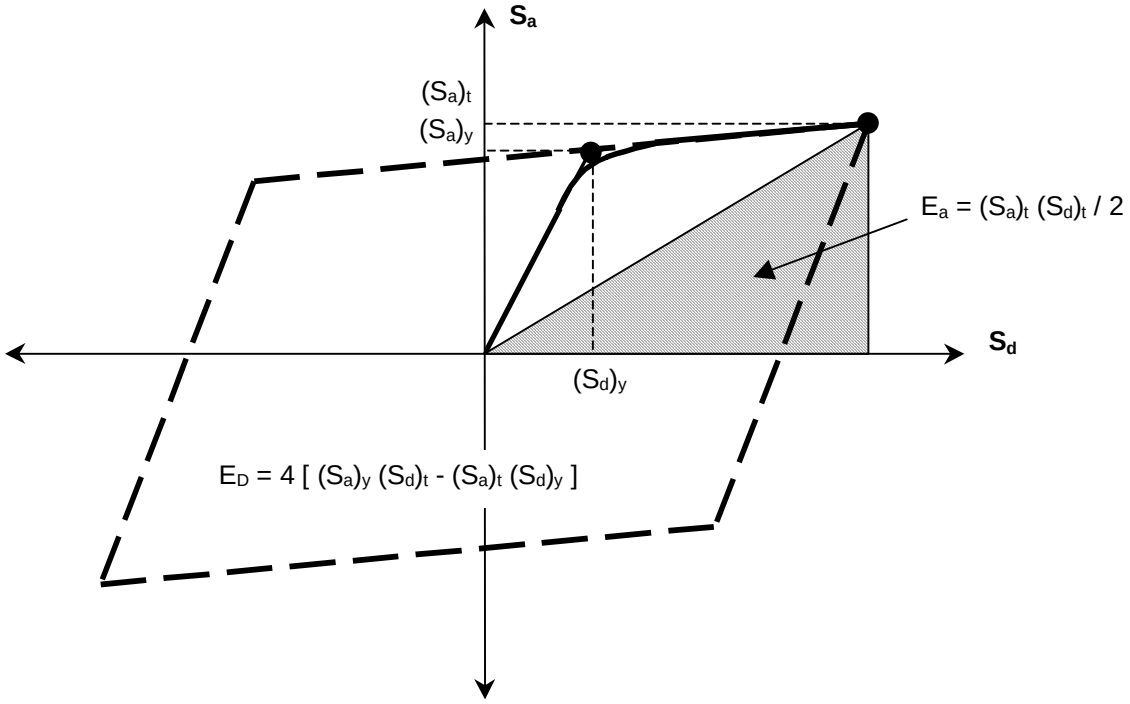

Figure 4-5 Effective Damping Calculation

4.2.7.3 Acceptance Criteria

When the target displacement is reached, the drift is calculated as

$$\Delta_x = \frac{(\delta_x - \delta_{x-1})}{h_x} \tag{4-42}$$

where:

δ_x, δ_{x-1} = deflection of story *x* and *x-1*

h_x = height of story x

Δ_x = drift angle of story x

The demand drift angle, $\hat{D}$, is calculated as

$$\hat{D} = C_B \theta_m \tag{4-43}$$

where θ_m is the maximum story drift at any level from Equation 4-42.

4.3 Modeling of New Steel Moment Frames for Performance Prediction

4.3.1 Background

The engineer's ability to model buildings has increased quickly over the past several years with the development of advanced analysis programs and the competition among software developers. In fact, our ability to model structural behavior probably exceeds our ability to understand fully the observed behavior.

The first structural analysis programs that were developed in the early 1960s could handle only linear prismatic beam and column members with fully restrained or pinned joints and centerline dimensions. Programs in use today have a number of elements that model material and geometric nonlinearities, rigid or partially restrained connections, and flexible foundations and diaphragms. This section will cover commonly used modeling procedures for steel moment frames. Additional information may be found in *the State of the Art Report on System Performance* (FEMA-355C) and the two SAC reports, SAC/BD-00/26, and Lee and Foutch (2000).

A word of caution is required. Although the modeling procedures described herein are detailed and match measured behavior well, it must be remembered that this is still greatly simplified from the case of a real building which has cladding, partitions, mechanical equipment, stairways, and many other discounted attributes. A real building might have irregularities that are important but not included here. It is important to remember that these calculations are only estimates of actual behavior, and caution is advised.

4.3.2 Linear Elastic Models

4.3.2.1 Linear Centerline Models

When designing new buildings or evaluating existing or damaged buildings, two acceptance criteria must be checked: member strength and building stiffness (drift). For new steel moment frame buildings, the drift limitation always governs in high seismic regions.

For performance evaluation using the SAC Guidelines, the acceptance criterion is stated in terms of the maximum demand drift angle where:

$$\hat{D} = C_B \, \theta_m \tag{4-44}$$

θ_m is the maximum story drift angle demand calculated by one of the analysis procedures, and C_B is the bias factor given in Table 4-8. As a result, any model that will conservatively predict the drift angle is acceptable.

Research done by Krawinkler (2000) has shown that a linear elastic model using centerline dimensions is acceptable for Special Moment-Resisting Frames. The beam moments may be checked at the location in the beam where it intersects the column flange. Even though this model gives adequate results for story drift, it will not always give good estimates of the

distribution of shears, moments, and axial forces throughout the building. Centerline dimensions are not acceptable for Ordinary Moment-Resisting Frames with weak panel zones.

4.3.2.2 Elastic Models with Panel Zones Included

The next increase in reality is to include the panel zone behavior in the model. The panel zone is the region in the column web defined by the extension of the beam flange lines into the column as shown in Figure 4-6. The simplest way to model the panel zone for linear analysis is referred to as the scissors model also shown in Figure 4-7. The beams and column are modeled with a rigid link through the panel zone region, and a hinge in the beam is placed at the intersection of the beam and column centerlines. A rotational spring with stiffness k_θ is then used to tie the beam and column together. The rigid links stiffen the structure, but the panel zone spring adds flexibility. The net result is that this building model is usually stiffer than the centerline model. Since it is stiffer, it will help in satisfying the drift design criteria. It will also give better estimates of shears, moments, and axial forces in the members. Most finite element programs currently used by engineers for seismic analysis have this feature. The method for determining the stiffness to be used for the flexibility of the panel zone is first to find the yielding properties of the panel and then to use them to calculate the stiffness of the panel zone. The yielding properties of the panel zone are:

$$\gamma_y = \frac{F_y}{\sqrt{3}G} = \theta_y \tag{4-45}$$

$$M_y = V_y d_b = 0.55 F_y d_c t d_b \tag{4-46}$$

where:

F_y = the yielding strength of the panel zone

G = the shear modulus = $\dfrac{E}{2(1+\nu)}$

d_c = depth of column

t = thickness of panel zone which is the thickness of the web of the column plus the thickness of the doubler plates if they are utilized.

d_b = depth of beam

ν = Poisson's ratio = 0.30

So, the stiffness of the panel becomes

$$K_\theta = \frac{M_y}{\theta_y} \tag{4-47}$$

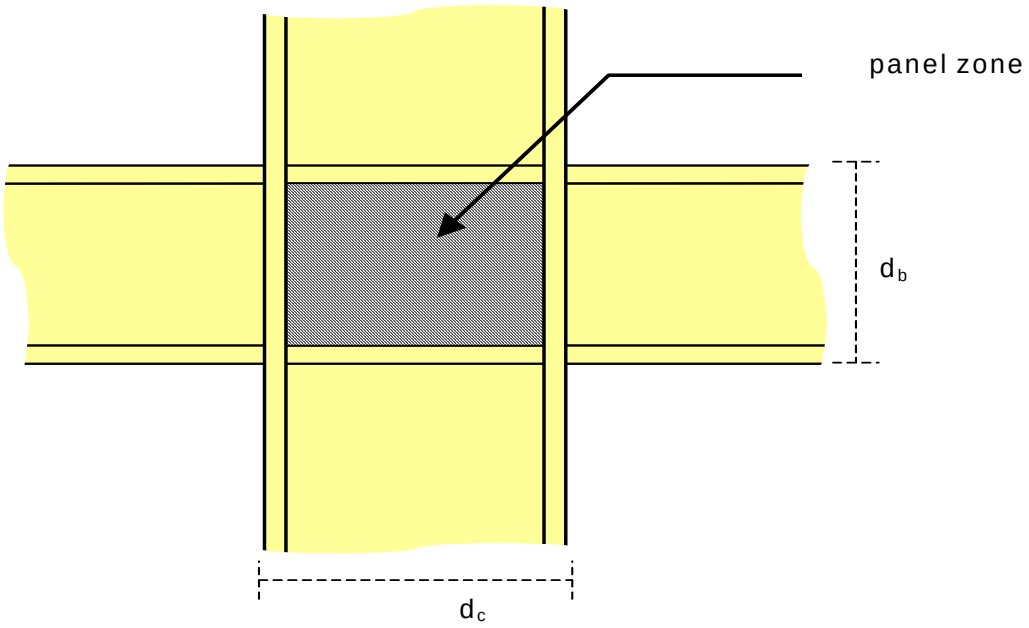

Figure 4-6 Definition of Panel Zone

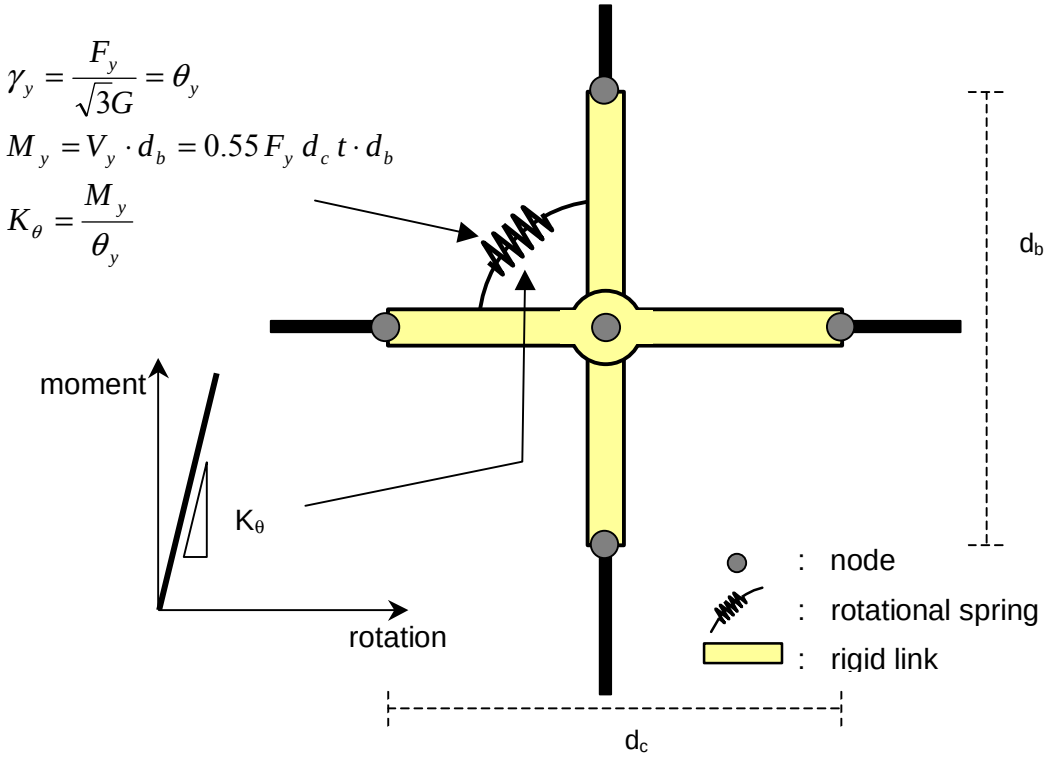

Figure 4-7 Scissors Model for Panel Zone Modeling

4.3.2.3 Nonlinear Centerline Models

Models that allow yielding in the beams and columns are much more realistic than linear models. Most of the programs commonly used today model this behavior by including a nonlinear flexural spring at the ends of elastic beam and column members. The springs should be assigned very high stiffness compared to that of the beam or column. However, the spring yields at the plastic moment capacity of the member. The correct structure elastic stiffness is maintained because it comes from the actual members rather than from the spring. This model is shown schematically in Figure 4-8.

The spring is rigid until the plastic moment of the member is reached. After yielding, a post-yield stiffness is assigned to the spring which represents the strain hardening behavior of the member. A strain hardening coefficient, α, is assigned to the spring after yielding. A value of α equal to 0.03 is a reasonable choice. The spring behavior and member plus spring behavior are shown in Figure 4-8. The value of α equal to 0.03 is a good choice for calculating story drift angles out to about 3% - 4%. After this, local flange buckling will begin to occur that causes α to gradually decrease to zero and then it can become negative with larger drifts. Most programs will not allow a negative value of α. For calculating building behavior beyond 4%, it is best to choose a strain hardening factor of zero.

For performance evaluation, the expected values of the yield strengths of the steels should be used. Expected yield strengths of commonly used steels are given in Table 4-3 (Roeder, 2000).

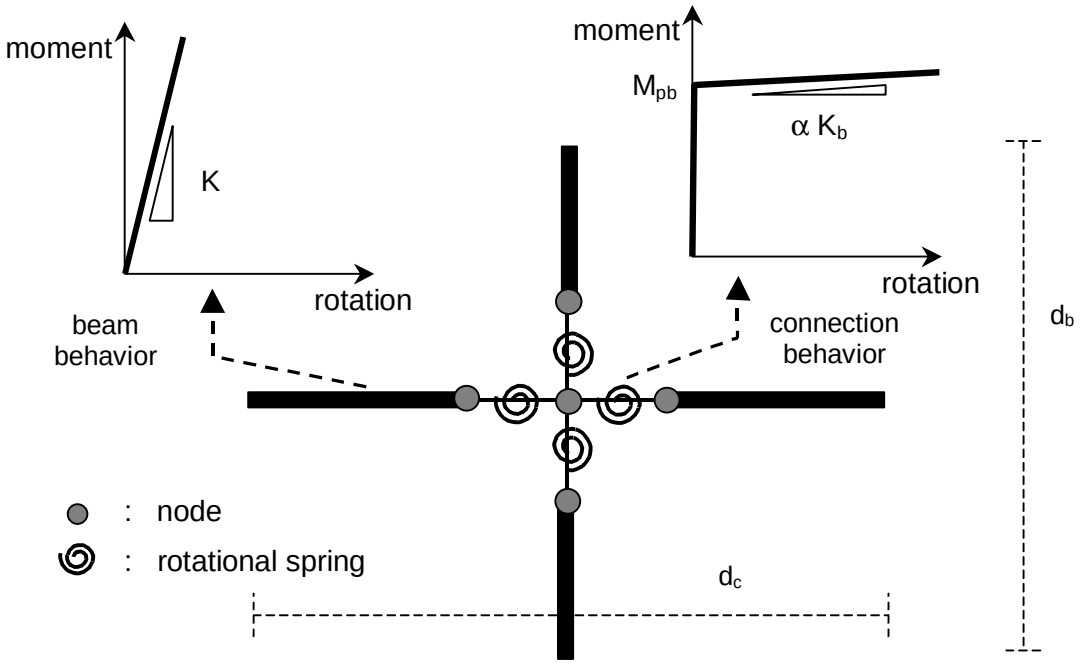

Figure 4-8 Centerline Model with Nonlinear Elements

Table 4-3 Expected and Lower Bound Material Properties for Structural Steel of Various Grades[1, 2] (Frank, 2000 and Roeder, 2000)

		Yield Strength		Tensile Strength	
Material Specification	**Year of Construction**	**Lower Bound**	**Expected**	**Lower Bound**	**Expected**
ASTM, A36	**1961 – 1990**				
Group 1		41	51	60	70
Group 2		39	47	58	67
Group 3		36	46	58	68
Group 4		34	44	60	71
Group 5		39	47	68	80
ASTM, A572	**1961 -**				
Group 1		47	58	62	75
Group 2		48	58	64	75
Group 3		50	57	67	77
Group 4		49	57	70	81
Group 5		50	55	79	84
A36 and Dual Grade 50	**1990 – 1999**				
Group 1		48	55	66	73
Group 2		48	58	67	75
Group 3		52	57	72	76
Group 4		50	54	71	76

Notes:
[1] Lower bound values for material are mean – 2 standard deviation values from statistical data. Expected values for material are mean values from statistical data.
[2] For wide flange shapes, indicated values are representative of material extracted from the web of the section. For flange, reduce indicated values by 5%.

4.3.2.4 Nonlinear Models with Panel Zones

Most of the pioneering work on nonlinear panel zone modeling has been done by Krawinkler. His state-of-the-art report (Krawinkler, 2000) provides a good discussion of this topic and includes references to his earlier work (Krawinkler et al., 1971, 1987). Two methods of modeling the nonlinear behavior of frames with yielding beams, columns, and panel zones are available. One procedure is based on the scissors model shown in Figure 4-7. The panels zone springs as well as the springs at the ends of the members are nonlinear. The behavior of the member spring is exactly the same as described in the previous section. The panel zone spring is assigned a stiffness of

$$K_\theta = \frac{M_y}{\theta_y} \tag{4-48}$$

where:

$$M_y = V_y \cdot d_b = 0.55 F_y d_c t \cdot d_b \tag{4-49}$$

$$\theta_y = \gamma_y = \frac{F_y}{\sqrt{3}G} \tag{4-50}$$

In most cases, panel zones have a much steeper stiffness and post yield stiffness. Therefore, a value of α equal to 0.06 is a reasonable value to use.

A better model is shown in Figure 4-9. This model holds the full dimension of the panel zone with rigid links and controls the deformation of the panel zone using two bilinear springs that work as a tri-linear behavior. With this, the large strength difference between the real behavior and the model is reduced.

The first slope past yield is steep and represents the behavior between the time that yielding is initiated and the full plastic capacity is reached. After the plastic capacity is reached, a small slope (2 %) or zero slope may be used. This is shown in Figure 4-10.

Since yielding in the beams, columns, and panel zones is represented well by this model, the actual distribution of yielding throughout the structure will be represented well. For design of new Special Moment Frames, the panel zones often yield first. But, because of the steep strain-hardening slope for the panel zones, the beams will yield shortly thereafter.

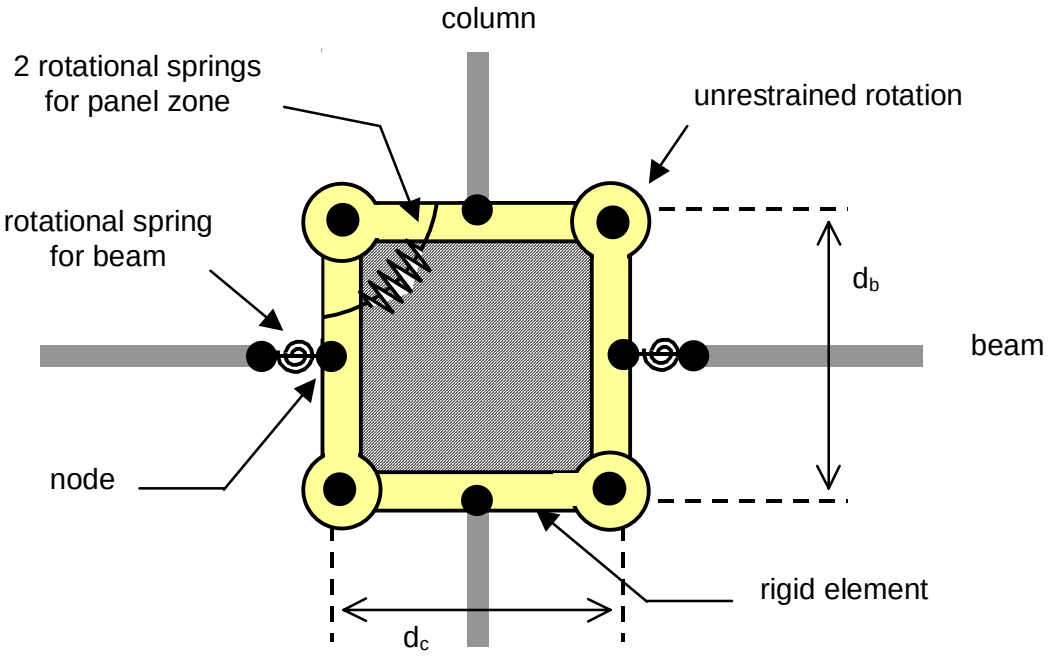

Figure 4-9 Panel Zone Modeling

In Figure 4-10, the following equations hold.

$$\gamma_y = \frac{F_y}{\sqrt{3}G} \qquad \gamma_p = 4\gamma_y$$

$$V_y = 0.55F_y \cdot d_c \cdot t \qquad V_p = V_y\left(1 + \frac{3b_c\, t_{cf}^2}{d_b\, d_c\, t}\right) \qquad V = \left(\frac{\Delta M}{d_c} - V_{col}\right)$$

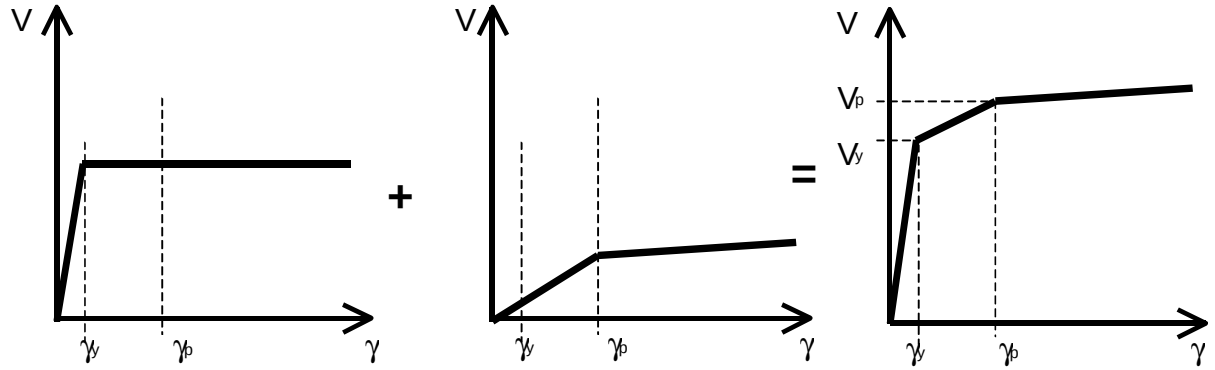

(a) Elastic – perfectly plastic (b) Bilinear (c) Trilinear

Figure 4-10 Panel Zone Modeling

Figure 4-11 shows a 9-story building that was designed according to the 1994 UBC. This building will be used for comparing the different models described here. The pushover analysis of the buildings is shown in Figure 4-12. 'M1' in the figure is the modeling case with the centerline dimensions, whereas, 'M2' is for the clear length plus panel zone modeling case. M2 also includes the modeling of the panel zones. The panel zone is modeled with tri-linear model spring and the full dimension of the member for the analysis. As can be seen, the M2 model case is a little stiffer in the elastic region than the M1 model case. The M1 model with P-Δ gives the lowest strength. Care should be taken when plotting the roof drift ratio versus the total base shear. The roof drift ratio can be misleading because it is incapable of capturing local drift concentration. A good example of this case can be seen for the 20-story building for the weak-column strong-beam design which collapsed due to large P-Δ effects. The concentration of plastic deformations around the 10th level was the controlling region. Figure 4-13 shows the plot of global roof drift ratio, top story drift ratio, and the 10th level story drift ratio versus total base shear. Global roof drift ratio is defined as the roof displacement divided by the total height of the building. Top story drift ratio is the story drift divided by the height of the story level. While the global drift ratio shows the averaged drift ratio over the whole height, when each story drift ratio is plotted, the 10th level concentration of plastic deformation is clearly noticeable. A plot of displaced shapes of the building with increasing roof displacement is also shown in Figure 4-14. The story level where the tangential slope is small indicates the large change in drift ratio. The concentration of plastic deformation can clearly be seen in Figure 4-15 where the story drift ratio for each story level with increasing lateral load is plotted. These results indicate that any nonlinear static procedure that relies on roof drift is highly questionable.

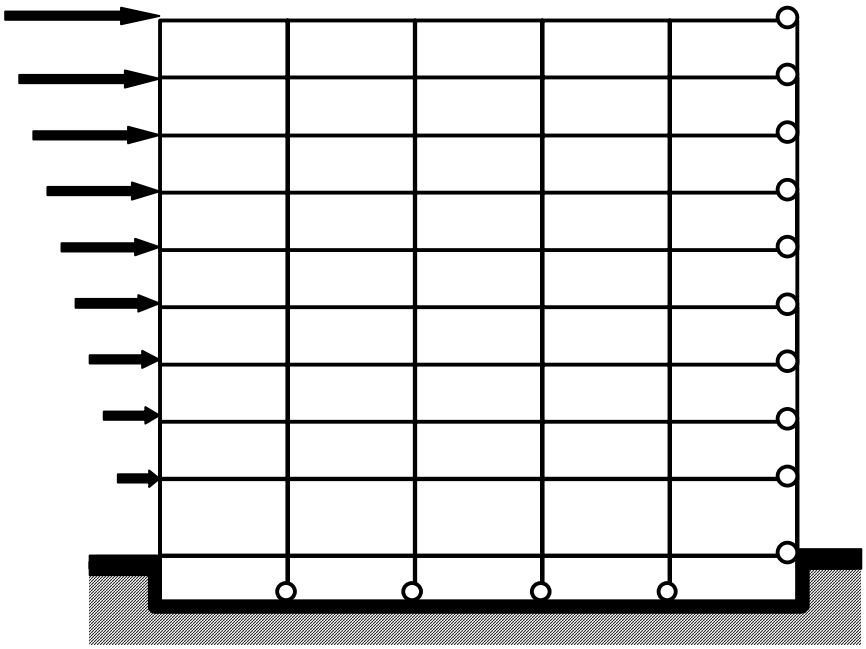

Figure 4-11 1994 UBC 9-Story Building

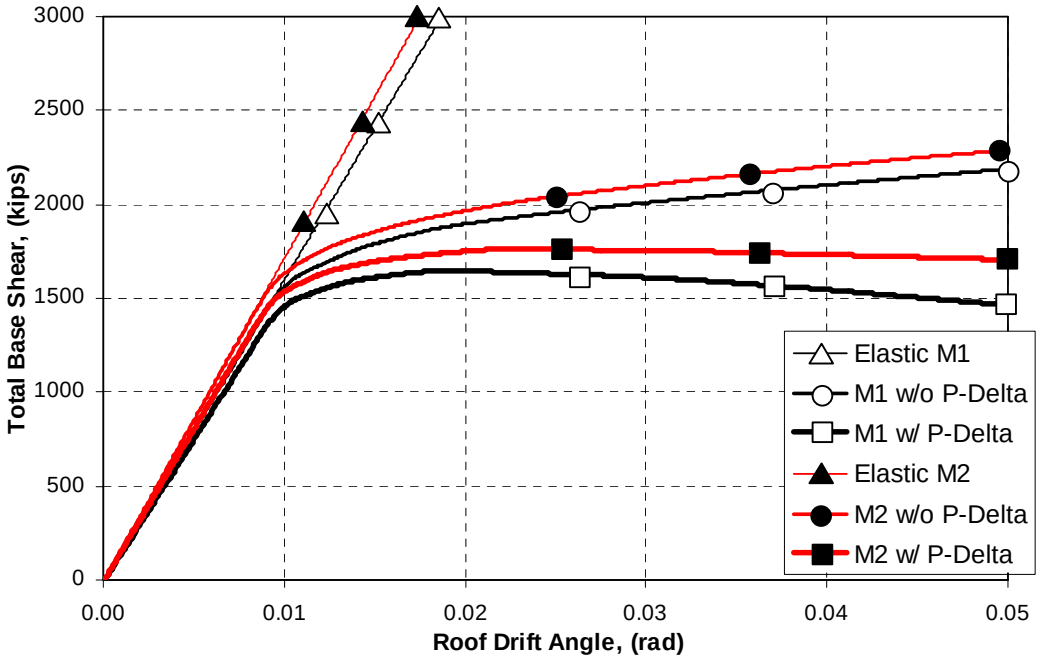

Figure 4-12 Comparison of Modeling for 1994 UBC 9-Story Building

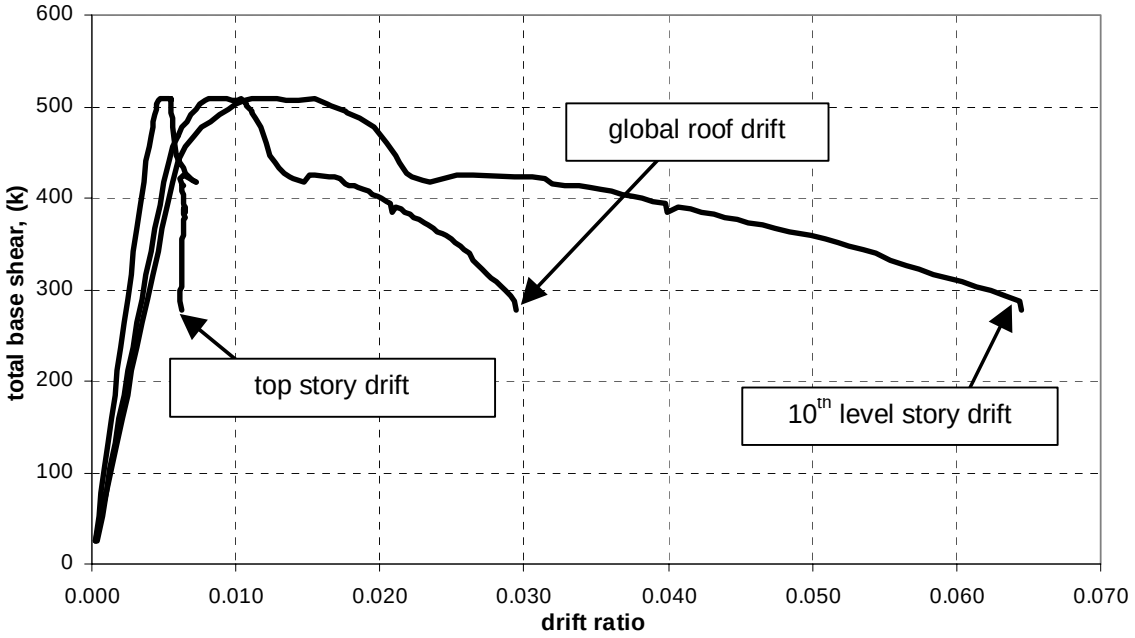

Figure 4-13 Comparison Between Global Drift Ratio vs. Story Drift Ratios for 20-Story OMF WCSB Building

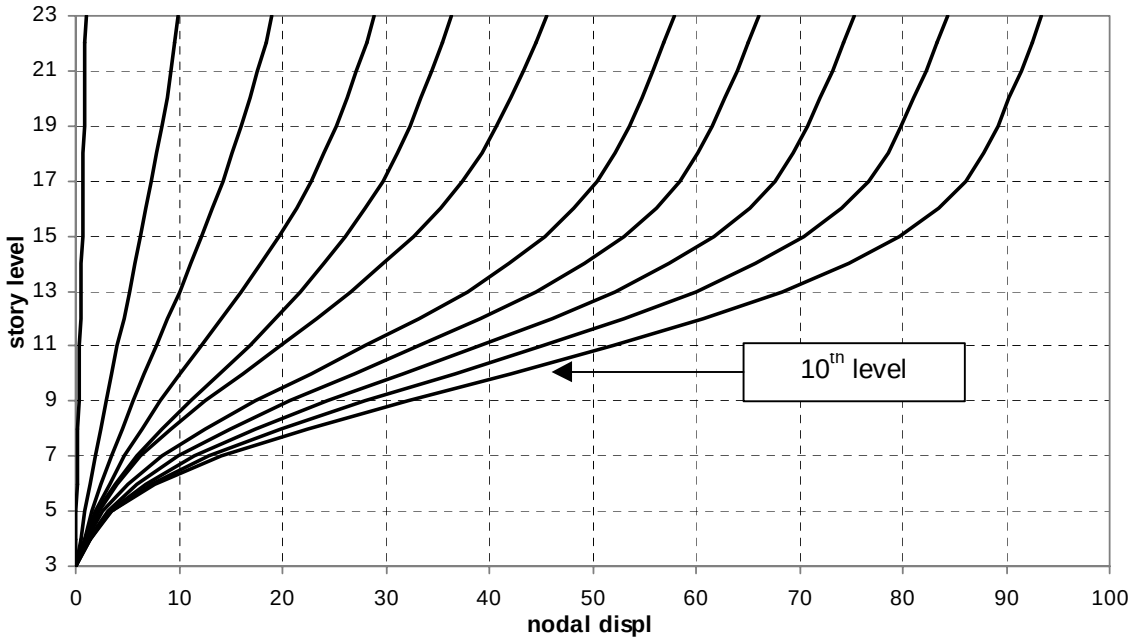

Figure 4-14 Displaced Shape from Static Pushover Analysis for 20-Story OMF WCSB Building

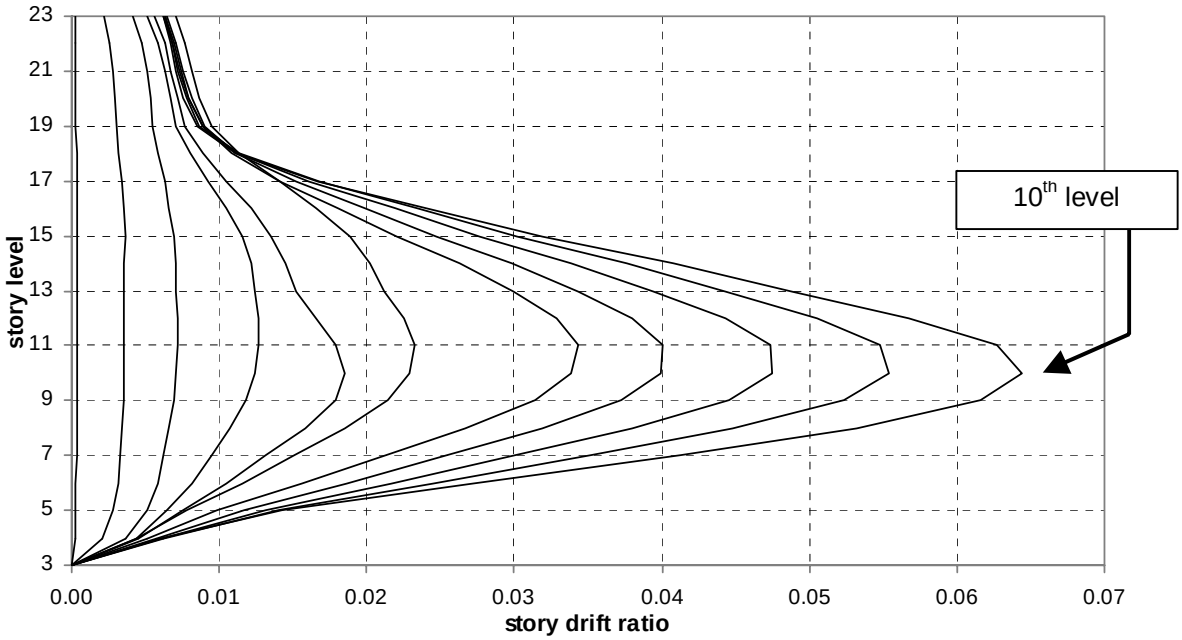

Figure 4-15 Story Drift Ratio from Static Pushover Analysis for 20-Story OMF WCSB Building

4.3.3 Nonlinear Springs for Beams, Columns, and Panel Zones

4.3.3.1 Reduced Beam Section Connection

For new buildings, reduced beam sections, which are also referred to as dog-bone members, were used for the analysis. They exhibit very good hysteretic behavior with stable loops and good energy dissipation. Tests were performed by Venti and Engelhardt (1999). A typical case of the hysteretic behavior is shown in Figure 4-16. This test used a w14x398 column member and w36x150 beam section. Both members have nominal strength of 50 ksi. A model for the analysis using the DRAIN-2DX program is shown in Figure 4-17. The behavior of the member was modeled using a tri-linear model. The model simulated the specimen well. The ratio between the beam plastic moments to the first yielding point as well as the second moment value were calculated and used for determining the yielding properties of the other member sizes. 74% of the plastic moment of the beam was used as the first yielding moment for both positive and negative moments. For the second yielding moment value, a factor of 132% of the first yielding moment for the positive side and 120% of that for the negative side of the connection were used. The rotational value for the second yielding moment of 0.03 radians for the positive side and 0.017 radians for the negative side were used for the protocol model. The rotational values that are proportional to the plastic section modulus were assigned for the other beam sections. The strength degradation ratio, that is, the drop of the strength at each plastic excursion, was assigned a value of 0.83. This value was fixed for all member sizes although in reality, there would be variations from member to member. The drift demand is not significantly affected by the choice of this ratio. Differences in drift demand calculations would not vary by more than two or three percent because of this difference. An illustration of the yielding values for the protocol member

(w36x150) and the first floor beam in the 3-story WCSB building (w30x90) are shown in Figure 4-18. The plastic moments for the members are 33,750 (k-in) for w36x150 and 16,423 (k-in) for the w30x90 member.

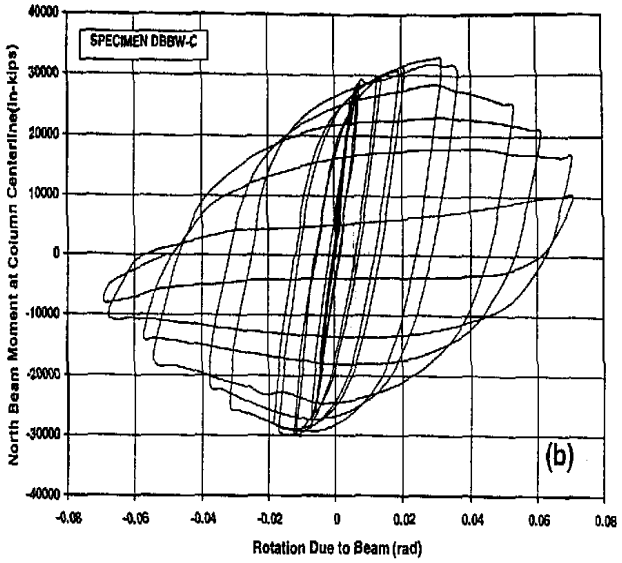

Figure 4-16 Measured Moment-Rotation Behavior of RBS Connection (Venti and Engelhardt, 1999)

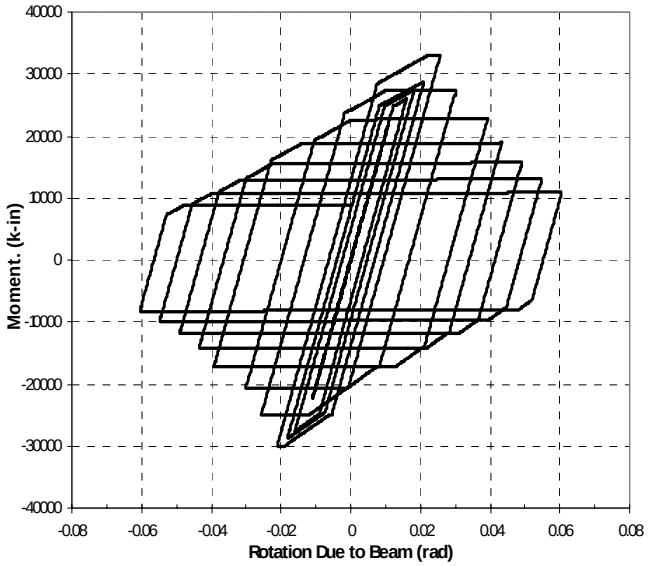

Figure 4-17 Model of Moment-Rotation Behavior of RBS Connection (Lee and Foutch, 2000)

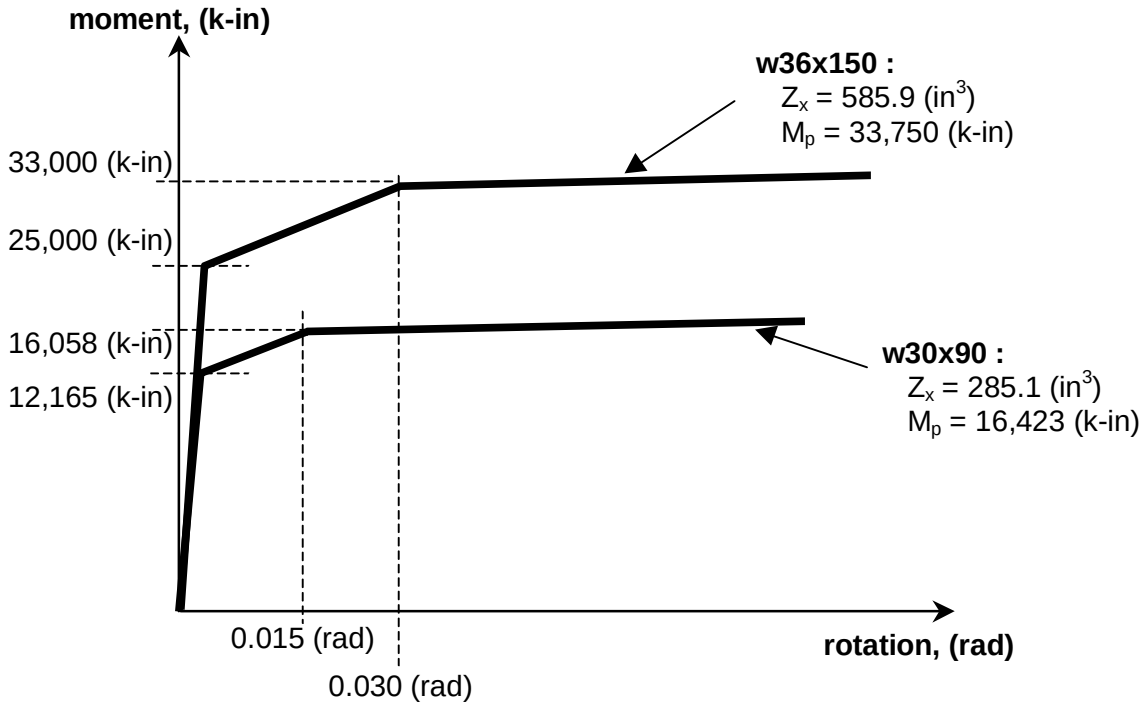

Figure 4-18 Illustration of Yielding Values for w36x150 (Protocol) and w30x90 (SDC C, 3-Story WCSB Building)

4.3.3.2 Bolted T-Stub, Partially Restrained, Connection

Experimental data provided by Leon (2000) served as the basis for estimating the stiffness and the strength of the T-stub connection. A typical T-stub connection is shown in Figure 4-19. Connection experiments with the w21x44 beam connected to the w14x311 column were selected and simulated using a spring element from the DRAIN-2DX program. The stiffness equation specified in the FEMA-273 for PR connections together with 50% of the strength of the beam was used. The stiffness equation in FEMA-273 is as follows:

$$K_\theta = \frac{M_{CE}}{0.005} \tag{4-51}$$

With the strain-hardening ratio of 20%, the hysteresis from the spring element matched the response of the experiment very well. The ratio of stiffness of the connection divided by that of beam, which is written as

$$\frac{K_\theta}{EI_b / l_b} \tag{4-52}$$

was calculated to be 8.15. This is less than the stiffness ratio of 20 specified for a rigid connection, as will be described in the Chapter 7.

Since none of the tests were cycled to failure, 4% of the connection rotation value was used as a limiting rotation before the strength dropped down drastically. This was the recommended value provided by personal communication with Roeder (1999). Due to the lack of modeling parameters provided in the modified version of the analysis program, DRAIN-2DX (Foutch and Shi, 1996), two individual springs were used to model the connection behavior. The illustration of two springs used for the model is shown in Figure 4-20. The first spring is perfectly elasto-plastic with strength dropping to 15% of the strength of the spring at 4% rotation. The second spring is elastic until the rotation reaches the value of 4%. The strength of the connection again drops down to 15% of the spring strength. The measured moment-rotation behavior of the connection and the model of it are shown in Figure 4-21 and Figure 4-25, respectively. The behavior of the two springs for the cyclic loading are also shown in Figure 4-22 and Figure 4-23. Figure 4-24 shows the total rotation behavior of the joint.

The connection stiffness values of the rest of the connections were determined using the stiffness ratio of 8.15 and 50% of the beam strength. Again, two springs for each end of the beam were used to model the strain hardening with fracturing behavior of the joint. Therefore, the rotation at which the strain hardening starts varies according to the beam size. The stiffer the member is, the smaller the rotation at which the strain hardening starts. The range of the rotation for the 9-story building with PR connections is 0.0041 radian for the lower stories to 0.0051 radian for the top story.

A similar procedure was taken for modeling the clip angle connection behavior. A more detailed description of the modeling and the behavior of the connection, as well as the behavior as a whole, are addressed in Chapter 7.

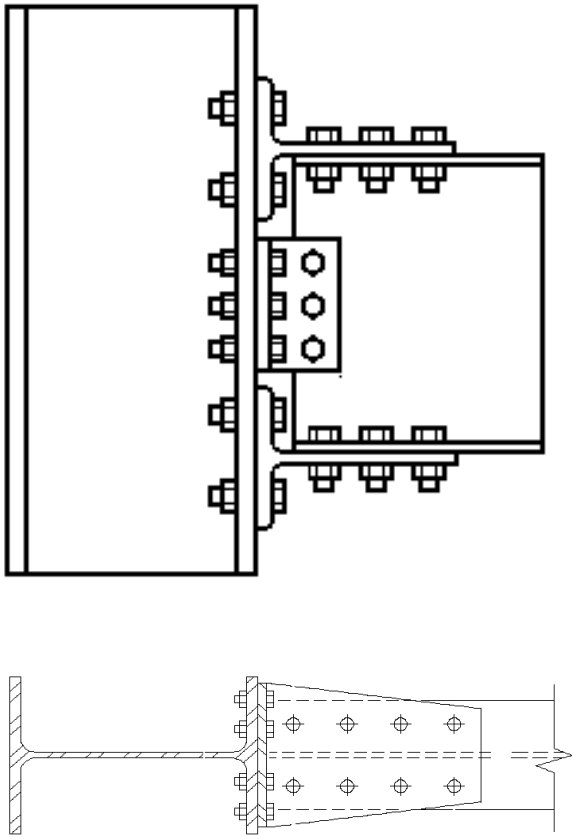

Figure 4-19 Typical T-Stub Connection (Leon, et al., 2000, Roeder, 2000)

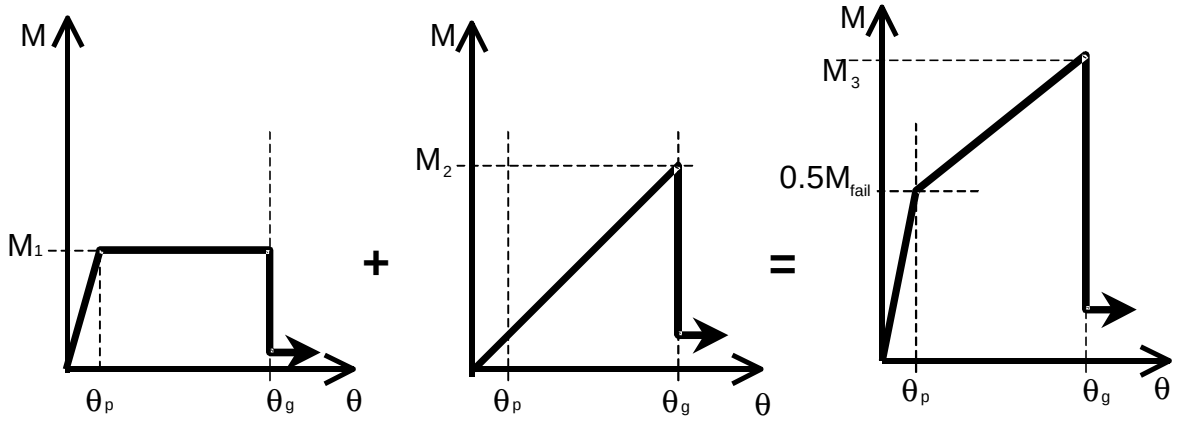

Figure 4-20 T-Stub Connection Modeling Used for Study

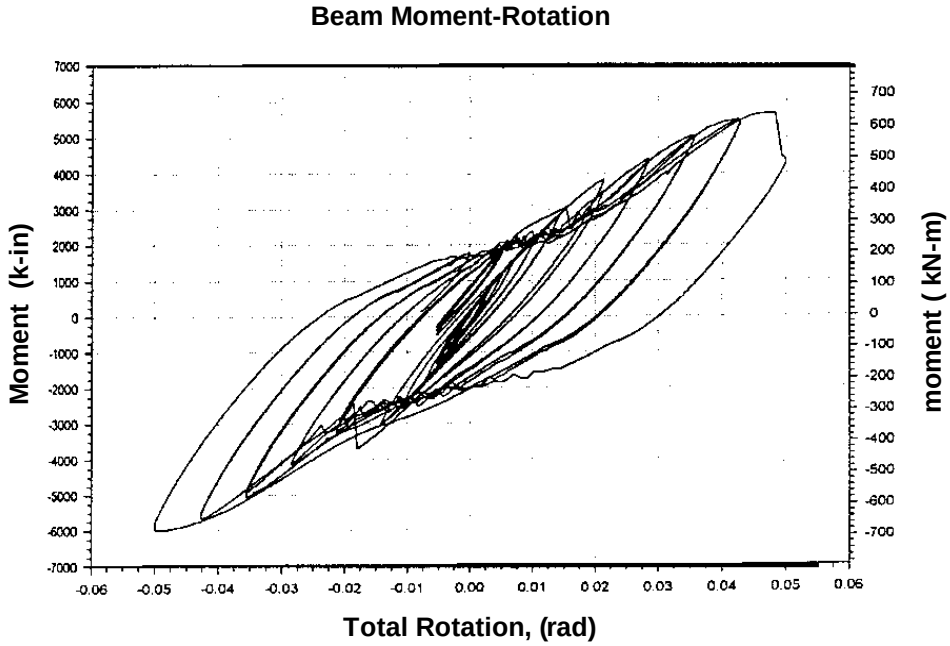

Figure 4-21 Measured Moment-Rotation Behavior of T-Stub Partially Restrained Connection (Leon, et al., 1999)

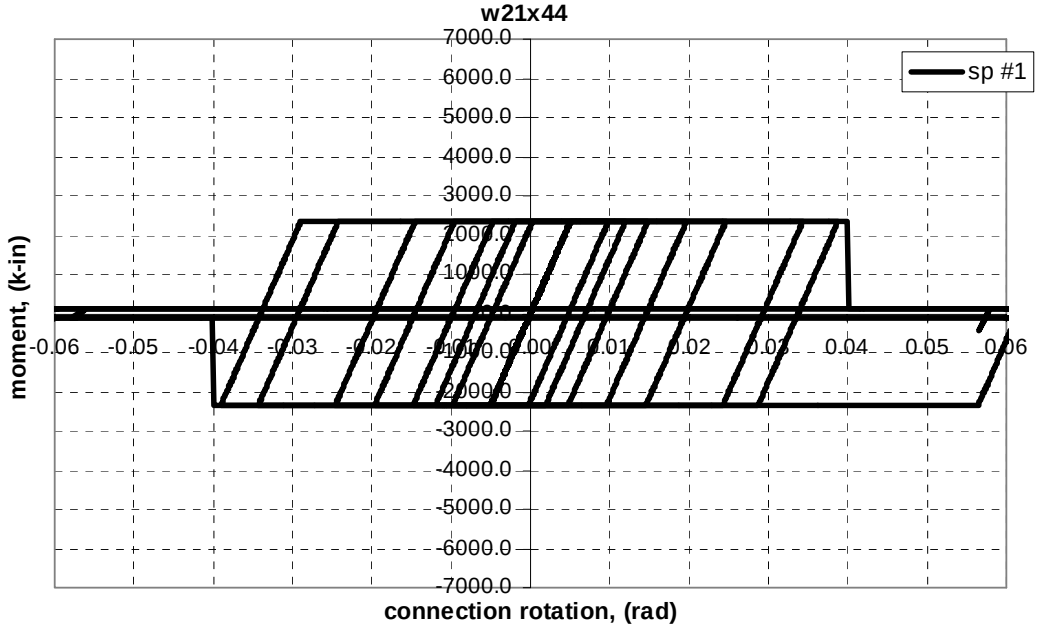

Figure 4-22 Model of Moment-Rotation Behavior of T-Stub Partially Restrained Connection Spring #1

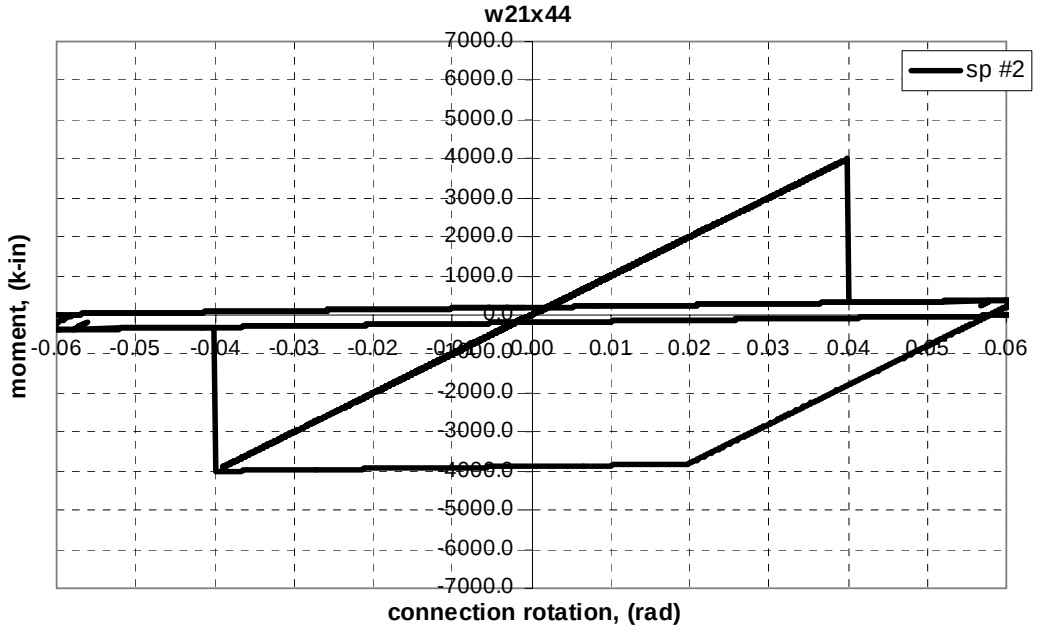

Figure 4-23 Model of Moment-Rotation Behavior of T-Stub Partially Restrained Connection Spring #2

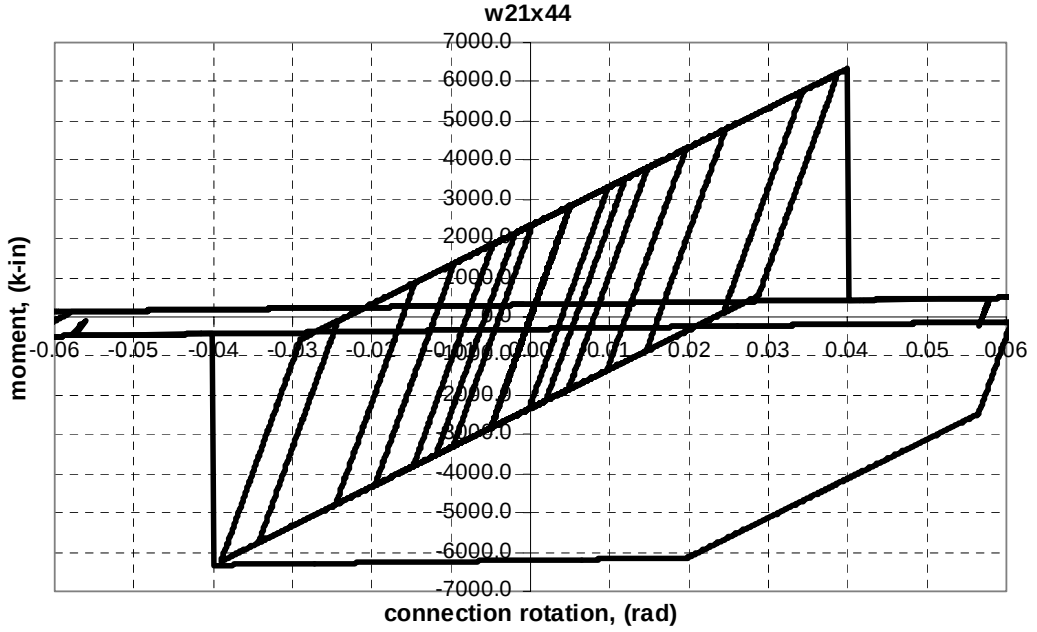

Figure 4-24 Model of Moment-Rotation Behavior of T-Stub Partially Restrained Connection Spring #1 and Connection Spring #2

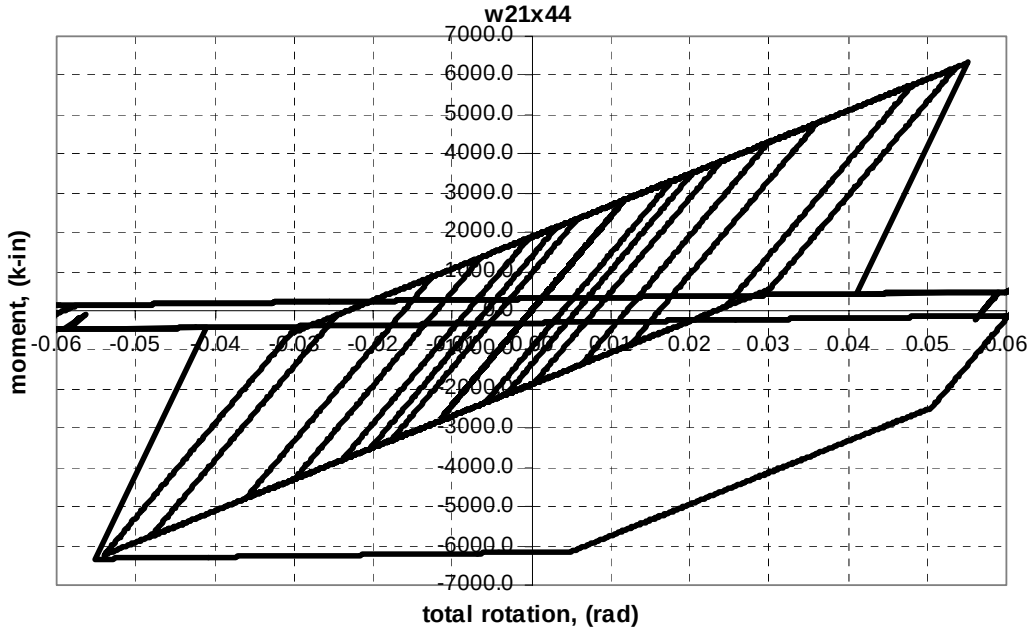

Figure 4-25 Model of Moment-Rotation Behavior of T-Stub Partially Restrained Connection

4.3.3.3 Local Buckling Behavior in Columns

The reduced beam section experiment case with w36x150 beams that was addressed in Section 4.3.3.1 was selected for the study. The amount of strength degradation for the next loading cycle was altered to represent the actual case correctly. The degradation ratio of 0.83 matched the response very well for the member size. In reality, the amount of degradation is dependent on the amount of the plastic deformation occurring in a cycle. The more plastic deformation occurs, the more strength degradation is observed. Therefore, for the incrementally increasing load cyclic experiments, the amount of strength drop is small in the low amplitude cycles, whereas the drop is large for the high amplitude cycles. However, in the DRAIN-2DX model, it is somewhat the opposite. The strength drop is represented using a factor multiplied by the strength at the cycle. Therefore, the drop is larger for the smaller amplitudes since the strength is larger. The drop is smaller for the larger amplitude cycles since the remaining strengths for the cycles are small. This can be observed from Figure 4-26. Again, modest differences between hysteresis relationships have only a small effect on calculated drifts (Shi and Foutch, 1997).

The strength degradation ratios of the member sizes were assigned proportional to the slenderness of the corresponding column sizes. The slenderness ratio is defined as $b_f/2t_f$. The value for the w36x150 is 6.37. The ratios used for the study are listed in Table 4-4.

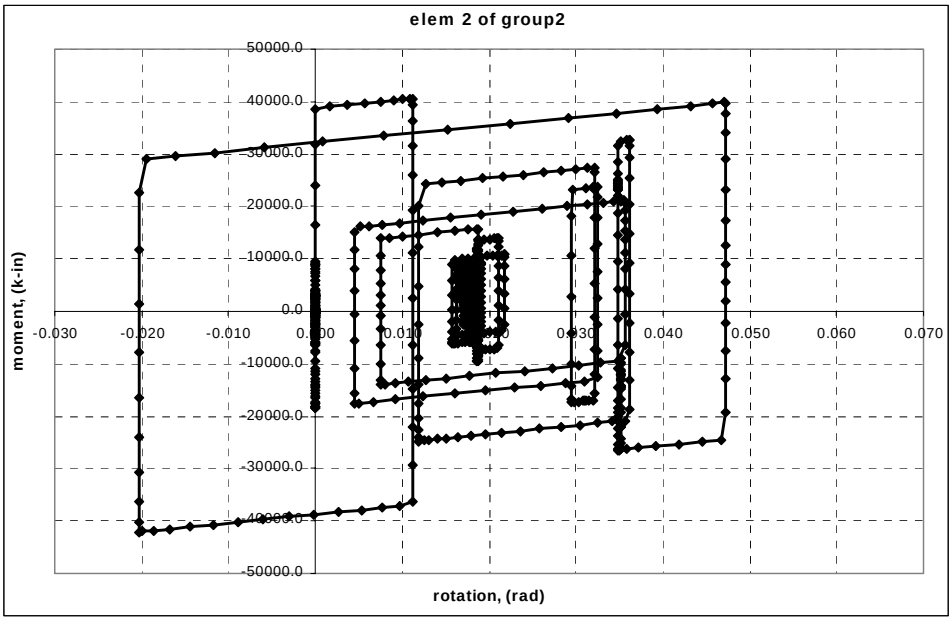

Figure 4-26 Hysteresis with Degradation Ratio of 0.83

Table 4-4 Strength Degradation Ratios Assigned for Each Column Member

SDC = D			SDC = C								
3-story	bf/2tf	ratio	3-story	bf/2tf	ratio	9-story	bf/2tf	ratio	20-story	bf/2tf	ratio
w14x342	3.31	0.91	w14x159	6.54	0.83	w14x233	4.62	0.88	w24x192	4.43	0.88
w14x311	3.59	0.90	w14x99	9.34	0.75	w14x159	6.54	0.83	w24x176	4.81	0.97
						w14x132	7.15	0.81	w24x146	5.92	0.84
						w14x99	9.34	0.75	w24x131	6.70	0.82
						w14x90	10.23	0.73	w24x117	7.53	0.80
						w14x74	6.41	0.83	w24x104	8.50	0.77
						w14x43	7.54	0.80	w24x103	4.59	0.88
									w24x84	5.86	0.84
									w24x68	7.66	0.80
									w21x50	6.10	0.84
									w21x44	7.22	0.81
									w18x35	7.06	0.81

4.3.4 Simple Connection in Gravity Frames

The gravity frames are usually thought of as frames with no resistance to the lateral load since the beam flanges are not connected to the column flanges. The frame is sometimes modeled with pinned connections to capture the P-delta effect due to additional gravity load from the interior frames. However, according to the experimental results from Liu and Astaneh-Asl (1999) the resistance not only exists but sometimes is significant due to the additional resistance occurring when a compression force in the composite floor slab is combined with a tension force in the shear tab. Additional resistance is encountered when the flanges of the beam come in contact with the column. An illustration of the connection is shown in Figure 4-27. Figure 4-28 shows a typical case where the shear tab with concrete slab on top resists lateral load for many cycles of motion. This is a case with a w18x35 beam connected to the w14x90 column with a shear tab and with a concrete slab. Minimum reinforcement was used for the slabs. The moment-rotation behavior of the connection was modeled with a nonlinear spring that drops in strength at specified rotations. The model of the connection is shown in Figure 4-29. A portion of the beam stiffness was used for the stiffness of the connection since it will not be like the rigid cases. The proportion was determined to be 25% of the stiffness of the beam. Also, the connections cannot be expected to develop the full plastic moment capacity. The maximum moment for the positive moment was taken as 38% of M_p and that for the negative side as 11% because these values resulted in a good match between experiment and analysis. The fact that the positive side develops higher moment is attributed to the compressive resistance of the concrete slab on top of the girder. The tensile strength of the slab cannot be expected to help, since minimum reinforcement is used. The rotation at which the strength drops is assigned a value of 0.045 radians for the positive side and 0.05 radians for the negative side of the connection. The drop in strength was assigned a value of 53% for the positive side and 89% for the negative. The rotational values for the other sections were calculated using the disproportional value to the depth of the beam. Again, gradual degradation of strength was modeled using 0.97 as the strength degradation factor. As will be seen later in Chapter 4 and Chapter 5, the resistance from the gravity frame is significant. However, most of the contribution is not from the connection but from the flexural resistance from the continuous columns. As was addressed previously, the differences in responses between the models with the simple connection are negligible as long as the continuity of the gravity frame columns is modeled. This is due to the fact that the connections lose strength at very early stages of the ground motion leaving only the columns to resist the lateral load. Figure 4-30 shows an illustration of the yielding properties of a protocol connection and the connection from the first floor of SDC C WCSB 3-story building.

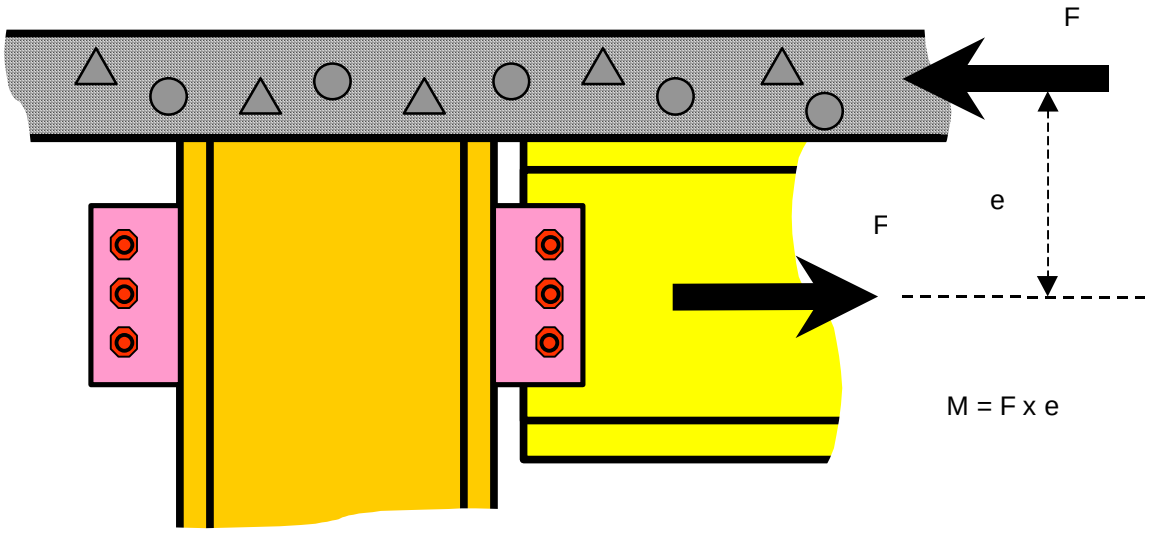

Figure 4-27 Illustration of Simple Connection in Gravity Frames

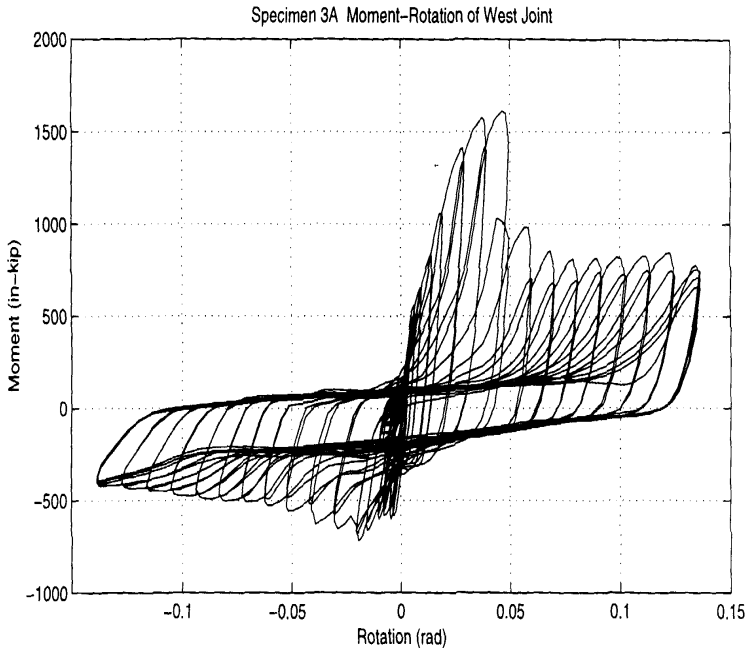

Figure 4-28 Measured Moment-Rotation Behavior of Simple Beam in Gravity Frame (Liu and Astaneh-Asl, 1999)

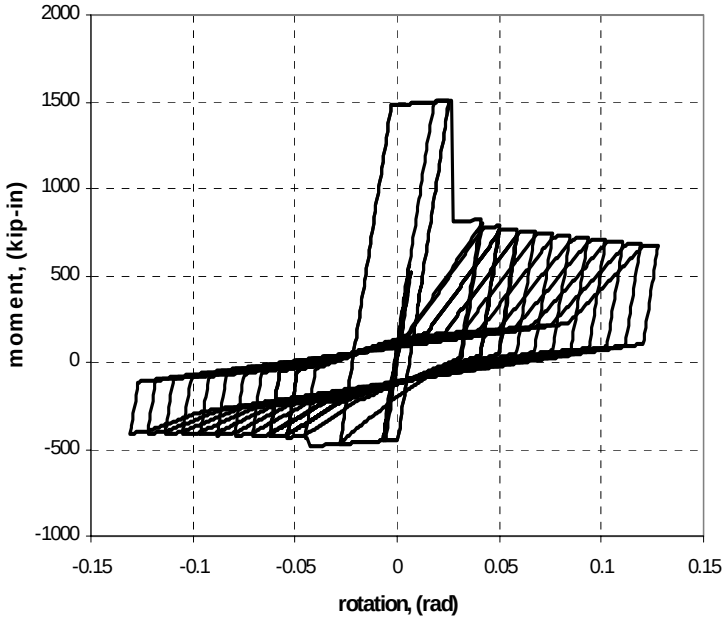

Figure 4-29 Model of Moment-Rotation Behavior of Simple Beam in Gravity Frame (Lee and Foutch, 2000)

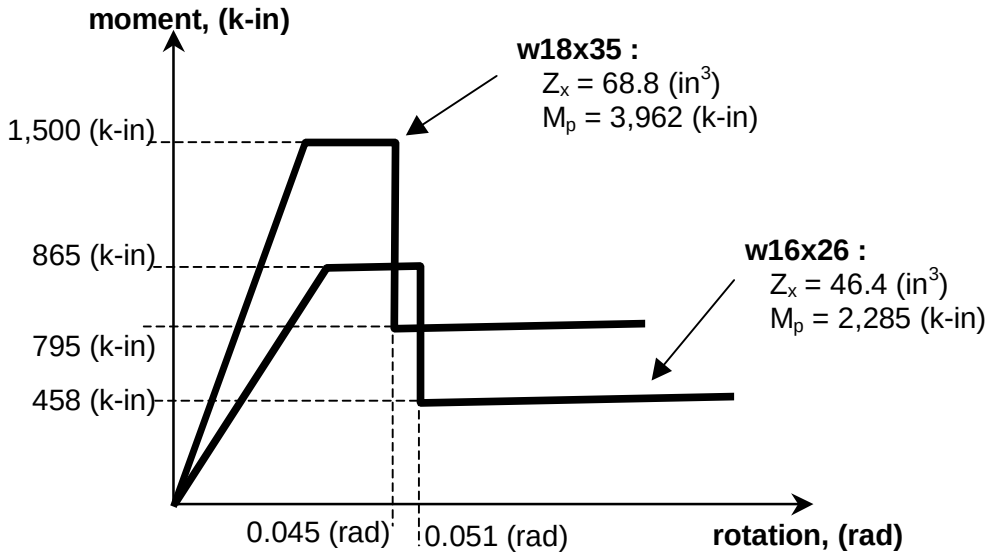

Figure 4-30 Illustration of Yielding Properties for w18x35 (Protocol) and w16x26 Beams in Gravity Frames (SDC C WCSB 3-Story Building)

4.3.5 Other Modeling Attributes

Another feature that should be included for the analysis of tall buildings, or shorter buildings taken out to large drifts, is the P-Δ effect. When the structure is displaced laterally, the gravity forces acting throughout the increasing displacement cause additional overturning moments to develop in the structure. For a perimeter frame building, this can be a significant effect since the

perimeter frames must carry the overturning moments of the entire building including the gravity frames.

One way to do this is to provide a dummy column in the model that carries the gravity loads in the building not directly carried by the moment frame. The column is connected to the moment frame using rigid links with hinges at each end as shown in Figure 4-31. The columns are hinged at both top and bottom. By doing this, only additional overturning moment from the lateral displacement will be induced. The columns will not help carry any of the lateral load since they are pinned. However in reality, the interior columns do help the moment frames since the columns are not connected with a hinge and some resistance exists for the shear tab connection in the beams due to the slab on top. An additional bay that has the equivalent properties for the whole interior frames can be used. The columns and beams will have the equivalent stiffness and strength for the corresponding stories of the interior frames. The beam springs used for the gravity frame have the hysteresis behavior described in Figure 4-28. The contribution of the equivalent gravity bay comes from both the flexural resistance of the columns and well as those from the beam springs used. However, since the strengths of the beam springs are very small compared to the moment frame springs, most of them will yield at a very early stage of the excitation.

A study using strength and stiffness calculated based on different recommendations for the simple connection with slab was performed. A total of three different connection models were used for the 3-story and the 9-story buildings which were designed according to the 1994 UBC. The first two models are based on the AISC Design Guideline document *Partially Restrained Composite Connections* (Leon, 1996). The guideline only describes the cases with reinforcements in the concrete slab. Since our case only has minimum reinforcement for shrinkage, some assumptions were made to use the equations given in the document for calculating the stiffness and the strength of the connection. The first case, noted as PR-CC_1, is to assume that there are two shear tabs with distance to the neutral axis of the concrete slab taken as zero since the concrete is assumed to have no tensile resistance. The second model, noted as PR-CC_3, is to have only one shear tab but with half the thickness of the concrete slab as the additional lever arm for development of moment. The third model, noted as Krawinkler, is to fix the rotation where the yielding starts to the value of 0.02 radians and evaluate the connection for a minimum failure mechanism. This model usually developed more flexible connections but with higher strengths compared to the other models. The differences in the connection models are shown in Figure 4-33. The 'PR-CC' represents the partially restrained composite connection cases and 'Krawinkler' represents his recommendation described in SAC report (1995).

LA38, which is one of the strongest ground motions from the 2% in 50 year hazard level for LA, was selected for the study. The static pushover curves and the demands of the analysis are plotted in Figures 4-34, and 4-35 for a 3-story and 9-story building, respectively. These buildings were designed using the strong-column weak-beam concept. As can be seen from the plots, the differences between the different models of the connections are very small. However, the difference between the behavior of the cases without the gravity bay is significant. It also shows that the contribution from the gravity frame is more prominent for the 9-story building compared to the 3-story building. The WCSB designed buildings are more affected than the

SCWB designed buildings since the bay helps to distribute the deformations over the height instead of being concentrated in a few stories. This is shown in Figure 4-36 for the 3-story building designed using the WCSB concept. Although the effects of the gravity frames seems small in these examples, they have a more significant effect on the results of the IDA analysis where global stability is studied in Chapter 7 and Chapter 8.

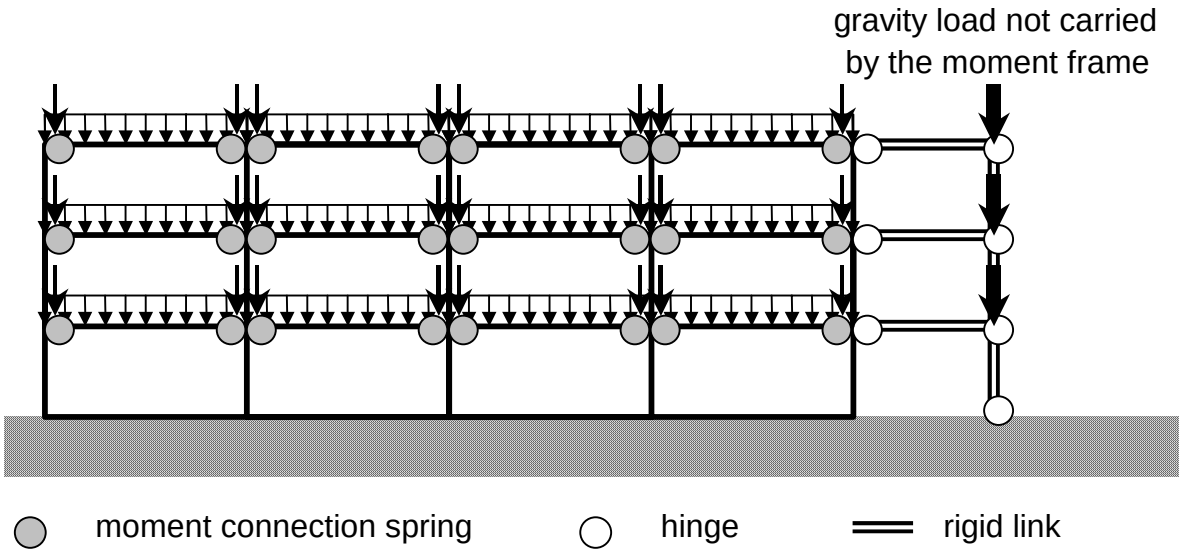

Figure 4-31 Modeling Interior Columns for P-Δ Effect Only

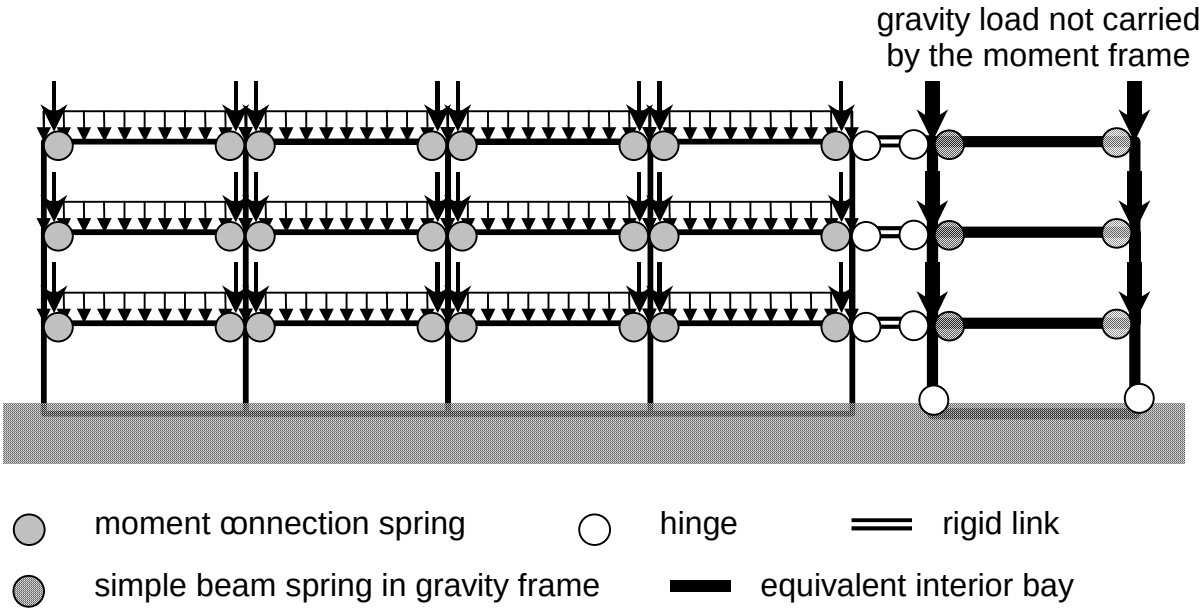

Figure 4-32 Modeling Interior Columns for P-Δ Effect and Resistance from the Equivalent Interior Bay

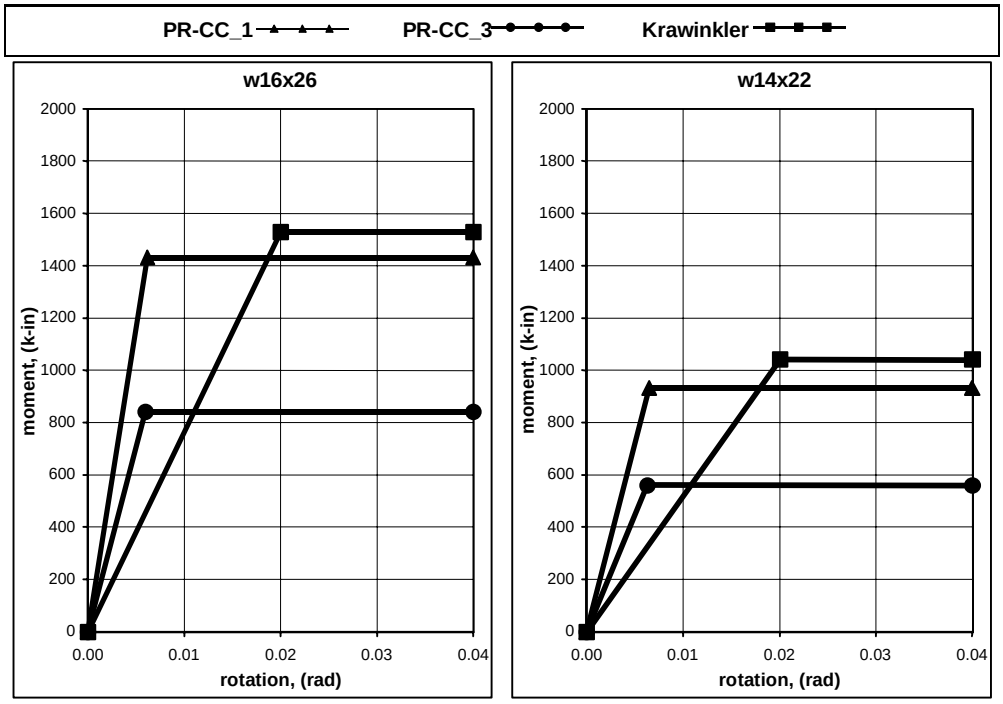

Figure 4-33 Connection Models for Simple Connection with Slab on Top for the 3-Story Building

4.4 Determination of Bias Factors

4.4.1 Background

Each analysis procedure described above has a systematic error, or bias, and random error associated with it. All of the procedures utilize an average elastic response spectrum to characterize the design ground motion. The result of the design calculation is an estimate of the maximum story drift for the building if it is shaken by the design earthquake. As discussed in Chapter 3, the "design earthquake" is a random event in intensity, time, and space. For instance, each suite of 20 accelerograms represents a collection of ground motions each of which may be said to represent the design earthquake. The generation of these suites of accelerograms was discussed in Chapter 3.

If the nonlinear time history response of a building is calculated for each accelerogram, the maximum drift that occurs for each earthquake will be different. The median value of this set of 20 maximum drifts is an estimate of the expected value of the maximum drift for the seismic hazard represented by the sample ground motions. The maximum drift calculated by any of the above analysis procedures is an estimate of the expected value of the maximum drift. The difference between the calculated design drift and the median value calculated from the nonlinear time history analyses is the bias for the method. The bias factor is the ratio of the expected maximum drift and the calculated design drift. Once the bias factor is known, the best estimate of the maximum expected drift is the product of the calculated design drift and the bias factor. The level of uncertainty in the design drift is greatly reduced when this approach is taken. Two of the research projects of the PPE team focused on determining the bias factors for

the linear (Duan and Anderson, 2000) and nonlinear (Skokan and Hart, 2000) analysis procedures described in this Chapter. This section reviews selected results of these projects and describes how these results are used to calculate the bias factors.

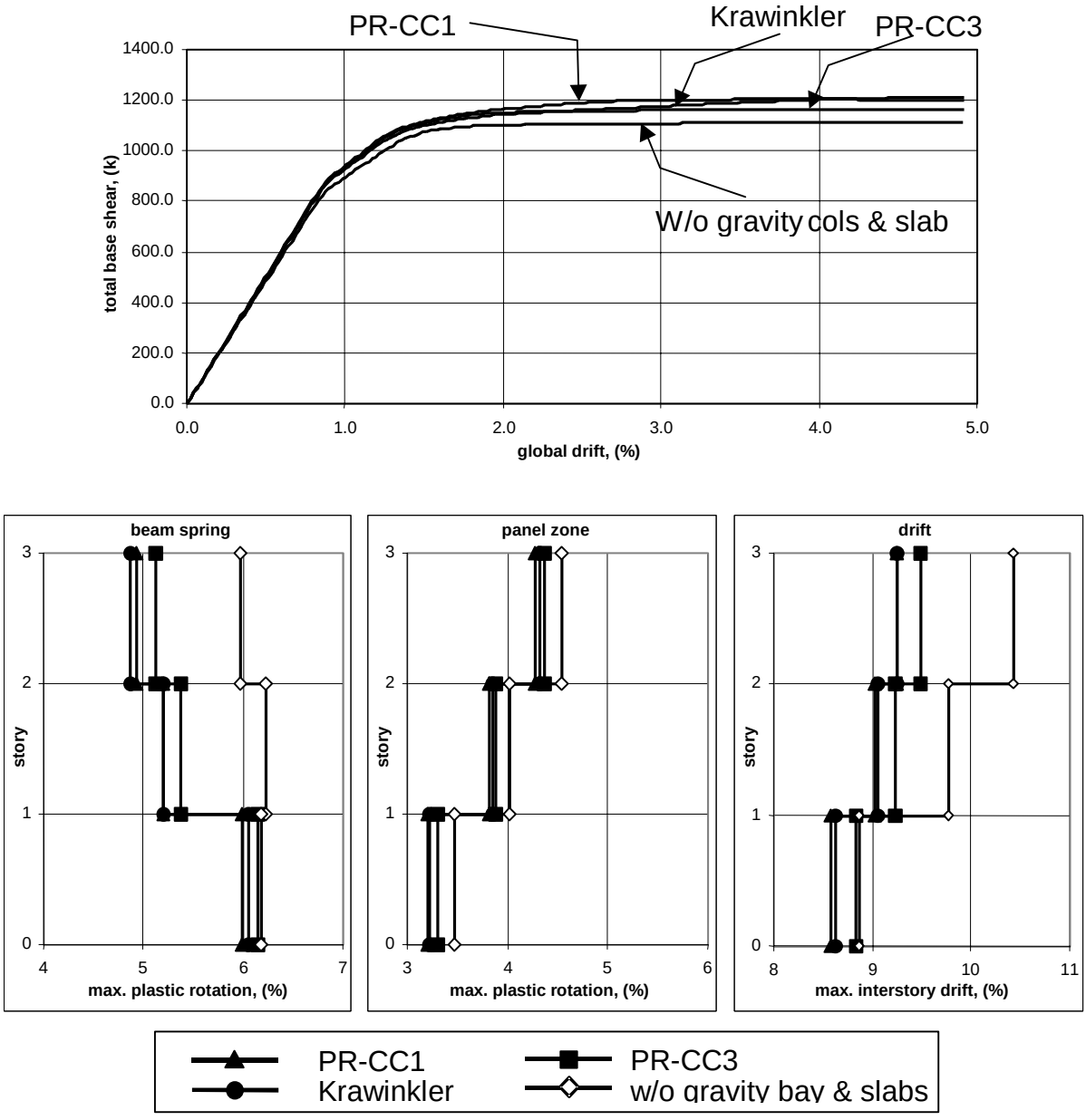

Figure 4-34 Response of SCWB 3-Story Building Using Different Models for the Simple Beam Connection with Slab on Top

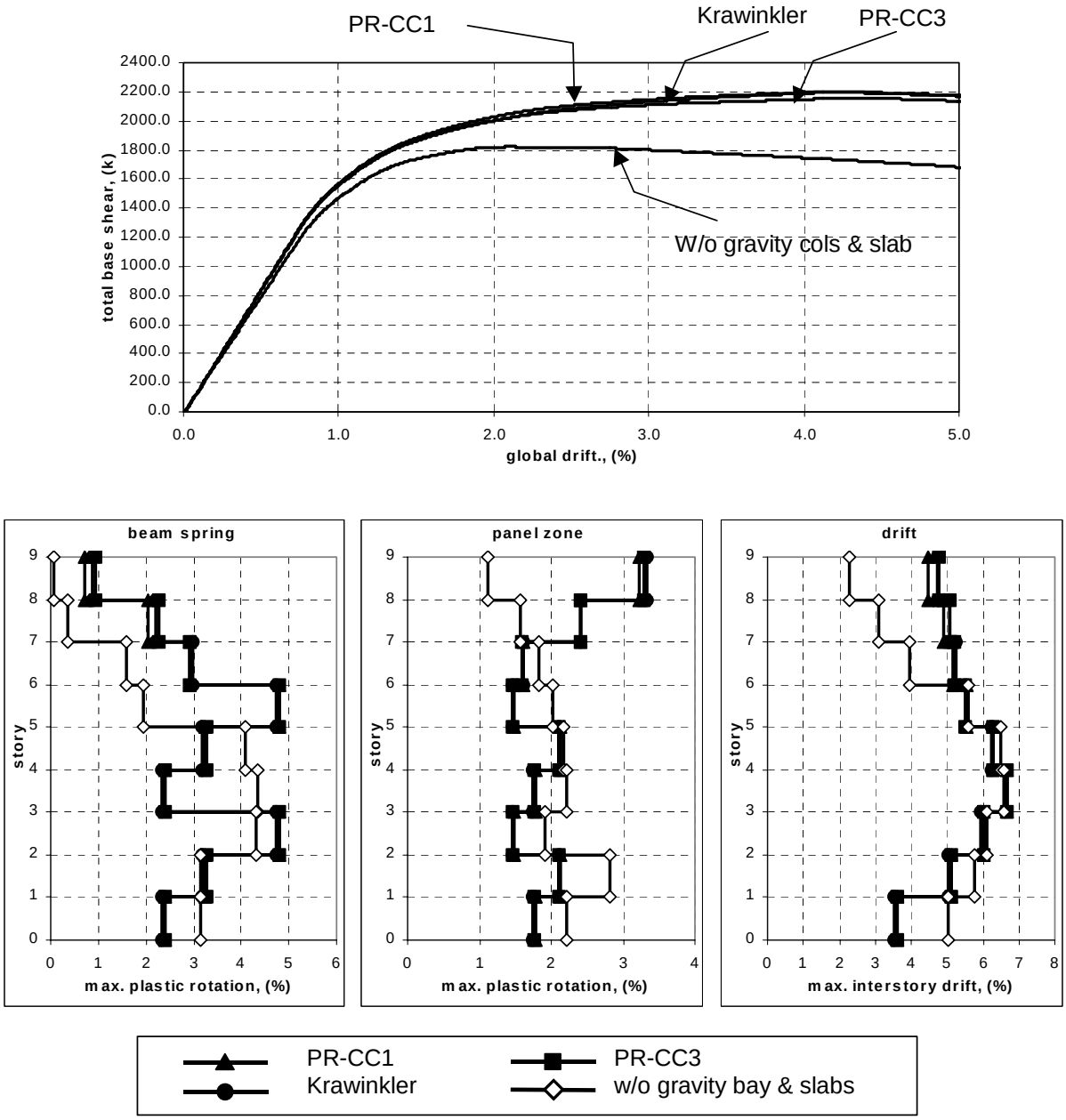

Figure 4-35 Response of SCWB 9-Story Building Using Different Models for the Simple Beam Connection with Slab on Top

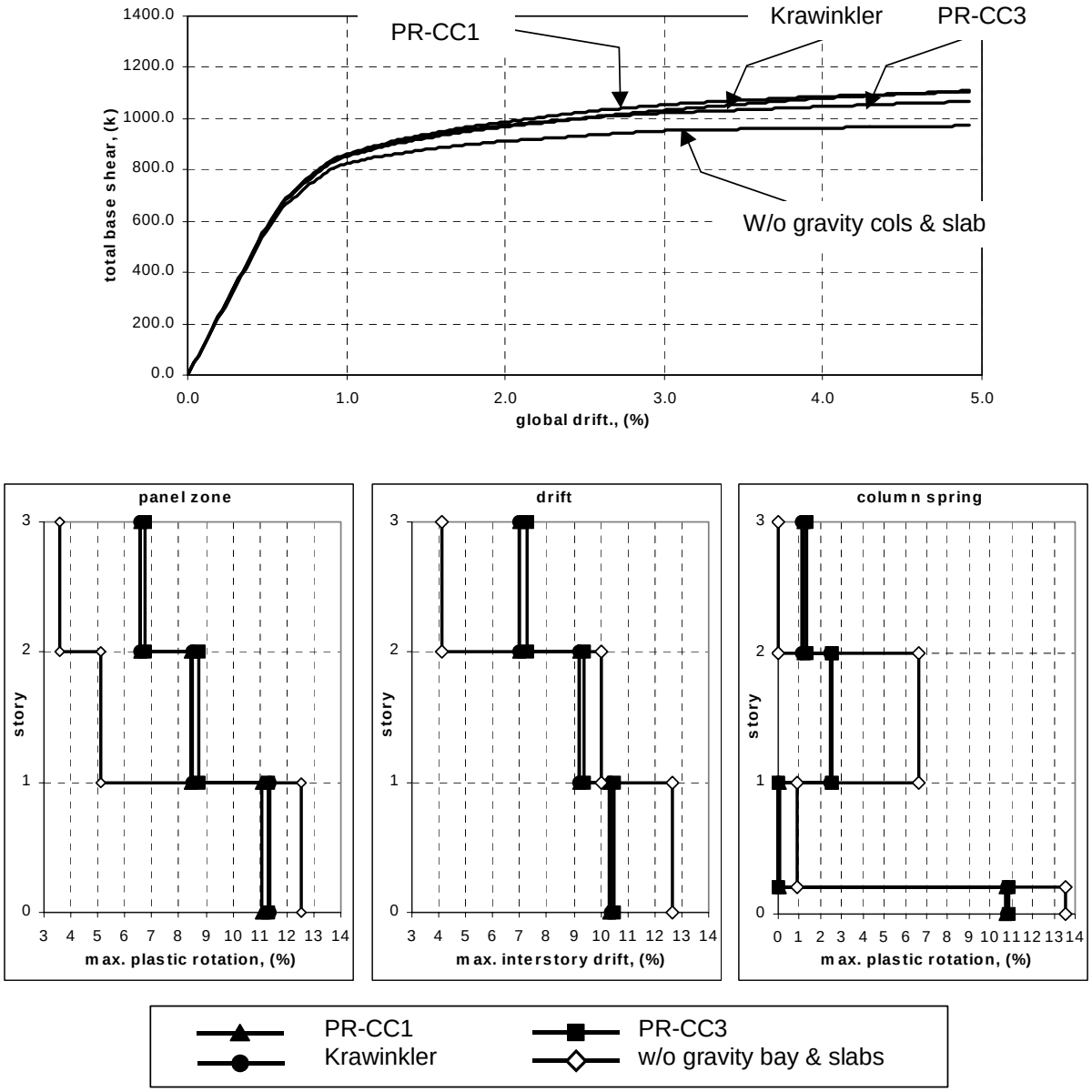

Figure 4-36 Response of WCSB 3-Story Building Using Different Models for the Simple Beam Connection with Slab on Top

4.4.2 Calculation of Bias Factors

Twenty buildings were designed using the 1997 NEHRP *Provisions* for the SAC Los Angeles site. There were eight 3-story buildings, eight 9-story buildings and four 20-story buildings. For each group, four column sizes, (W14, W24, W30 and W36) were used. For the 3-story and 9-story buildings, four upper bound and four lower bound buildings were designed. The upper bound buildings were designed using the period calculated from the empirical equation given in the code. The lower bound buildings were designed using a period calculated

using a structural analysis program. The equivalent lateral force (in the 1997 NEHRP *Provisions*) was used for each design. The period of the 20-story building was in the region of the design spectrum that is defined by a lower bound constant that is not a function of period given in Equation 4-4 and 4-5. As a result, only four 20-story buildings could be designed. The resulting designs are given in Figure 4-37 with member sizes given in Table 4-10.

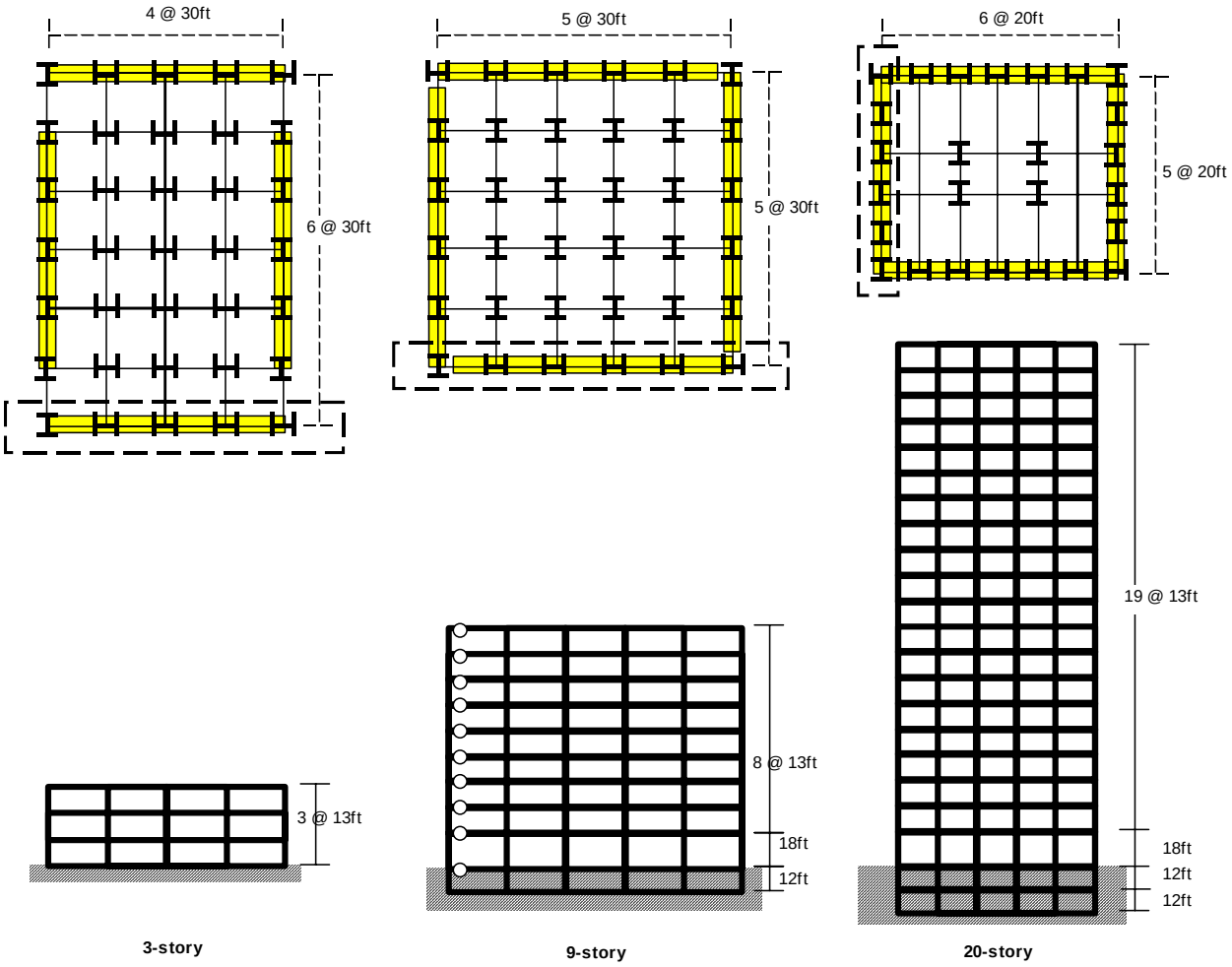

Figure 4-37 Plan and Elevation View of the 3, 9, and 20-Story Buildings Designed According to the 1997 NEHRP *Provisions*

Each building was analyzed for each of the 20 accelerograms in a suite using a nonlinear time history analysis. The reduced beam section was assumed to be the connection system used. The behavior of the panel zones was included in the model. The gravity frames were also included in the model, and P-Δ effects were calculated. The hysteresis behavior of the RBS connection and the gravity beam-column connection are shown in Figures 4-17 and 4-29, respectively. The median maximum drift was then calculated for each building. This was done for the 2/50 and 50/50 hazard levels and the LA site. These were then used to calculate the bias factors.

The bias factor is defined as follows:

$$B.F. = \frac{drift\ due\ to\ NTH}{drift\ due\ to\ corresponding\ analysis\ method} \tag{4-53}$$

The variability of each method with the corresponding bias factor is also calculated. The variations of the corrected drift values due to the analysis method were calculated by taking the coefficient of variation of the maximum drifts. The values of the variations are expected to be very small since the bias factor will shift the drift values very close to the correct drift value.

The USC team headed by Anderson has studied the Linear Static Procedures (Duan and Anderson, 2000). The UCLA team headed by Hart has performed the Nonlinear Static Procedures and the Capacity Spectrum Procedure (Skokan and Hart, 1999). The fundamental periods of each of the structures that were used for the study are shown in Table 4-5. The calculated drift values for each of the buildings for each of the methods are given in Table 4-6 for the 2% in 50 year hazard level and in Table 4-7 for the 50% in 50 year hazard level. This table includes the average values for each of the story heights as well as the weighted average for all of the story heights.

Since different teams performed the work, two changes in the data values were necessary to correctly calculate the bias factor and the variance of the drifts. The first change was for the difference in the strength reduction factor, R, and the displacement amplification factor, C_d, used in the 1997 NEHRP *Provisions*. The second change was to account for the same damping levels for each structure.

The first change that was made to calculate drift values was to account for the difference in the strength reduction factor, R, and the displacement amplification factor, C_d, used in the 1997 NEHRP *Provisions*. Since the 1997 NEHRP *Provisions* gave the best estimation for the drifts, all of the calculated drift values from the FEMA Linear Static procedures (F273L and F273M) were multiplied by the factor of 5.5/8.0, which is 0.70.

The second change involved the damping value used in the analysis. The LTH and NTH calculations used the correct average damping values for the 3-story (4.3%), 9-story (3.6%), and 20-story (2.3%) buildings. The LSP calculations were done using the NEHRP design spectrum. So the bias factor calculations are direct. The engineer uses LSP using the 5% damping spectrum and multiplies this by the bias factor to get the drift value for the correct damping level. The NSP and CSP were done using the elastic spectrum for the correct damping levels. So if the designer uses a 5% damped spectrum, the values have to be scaled upward to match those for the correct damping level. These scale factors were 1.04, 1.06, and 1.11 for the 3-, 9-, and 20-story buildings, respectively (Yun, et al., 2000). The final value in Table 4-8 incorporates these factors with some rounding and engineering judgment. Table 4-9 gives the bias factors for existing buildings built prior to the 1997 NEHRP *Provisions*.

As can be seen from the results, all of the analysis methods for the 2% in 50 year hazard level somewhat fail to capture the P-delta effects as the structures get taller. Therefore, the

methods underpredict the drift for taller structures. The linear static procedure from both the 1997 NEHRP *Provisions* and FEMA-273 predicts the response the best. The FEMA-273 Modal Analysis Procedure failed to predict the response of the taller stories better even though three modes were used for the drift calculation of the 20-story building, whereas one mode for the 3-story and 2 modes for the 9-story were used. For all of the story heights, the Linear Time History method over-predicted the response of the structure. All of the methods for the 50% in 50 year hazard level predicted the response much better since the responses stay pretty much in the elastic range with small drift values. Not much effect from P-delta is expected.

Table 4-5 Fundamental Period of Each Structure

Column	design	3-story	9-story	20-story
w14	**LB**	1.00 (sec)	2.45 (sec)	3.47 (sec)
	UB	0.88 (sec)	2.16 (sec)	
w24	**LB**	1.00 (sec)	2.47 (sec)	3.43 (sec)
	UB	0.87 (sec)	2.18 (sec)	
w30	**LB**	1.00 (sec)	2.44 (sec)	3.43 (sec)
	UB	0.86 (sec)	2.18 (sec)	
w36	**LB**	0.99 (sec)	2.47 (sec)	3.46 (sec)
	UB	0.84 (sec)	2.18 (sec)	

4.5 Analytical Studies of Post-Northridge Buildings

4.5.1 Description of Building Designs

Twenty buildings were designed for a Los Angles site using the 1997 NEHRP *Provisions*. These buildings (3-, 9-, and 20-stories) were designed for a Seattle site. The soil was assumed to be stiff and defined as a soil type D in the NEHRP *Provisions*. The buildings were designed for the 2/50 hazard level response spectra discussed in Chapter 3. In addition, 3-, 9-, and 20-story buildings were designed on a soft-soil site in Seattle. Plan and elevation views of the buildings are shown in Figure 4-37. The member sizes are given in Table 4-10. The 20-story buildings designed for the LA site used four different column sections (w14, w24, w30, and w36) in order to consider different frame conditions. Upper-bound designs for each building configuration were developed by using the empirical value of T as a function of height given in the NEHRP *Provisions* to calculate the design base shear. Lower-bound designs for the 3- and 9-story buildings were developed by using the value of T calculated by the SAP 2000 structural analysis program, but subjected to the limitations in the NEHRP *Provisions*. The lower-bound value of

the base shear for buildings with long natural periods precludes the development of a lower-bound design for the 20-story building. Other details of the buildings including the one in Seattle are given in SAC/BD-00/25, by Lee and Foutch (2000).

Table 4-6 Drift and Variance Values for Different Analysis Methods Using LA 2% in 50 Year Hazard Level Before Corrections

LA 2/50	column	design	NTH	N97L		F273L		F273M		ETH		F273N		CSP	
				drift	B.F.	drift	B.F.	drift	B.F.	drift	B.F.	drift	B.F.	drift	B.F.
3-story	w14	LB	0.030	0.030	1.00	0.048	0.63	0.036	0.83	0.033	0.90	0.034	0.87	0.023	1.31
		UB	0.027	0.030	0.91	0.047	0.58	0.033	0.83	0.032	0.85	0.035	0.78	0.023	1.18
	w24	LB	0.029	0.030	0.96	0.048	0.60	0.037	0.78	0.033	0.86	0.034	0.84	0.022	1.28
		UB	0.025	0.030	0.83	0.047	0.53	0.032	0.78	0.032	0.78	0.034	0.74	0.022	1.13
	w30	LB	0.028	0.030	0.94	0.045	0.63	0.037	0.76	0.034	0.84	0.040	0.70	0.022	1.31
		UB	0.024	0.030	0.81	0.039	0.63	0.032	0.76	0.031	0.78	0.029	0.84	0.018	1.34
	w36	LB	0.028	0.030	0.94	0.046	0.62	0.037	0.77	0.034	0.83	0.033	0.85	0.021	1.32
		UB	0.024	0.030	0.81	0.039	0.62	0.031	0.78	0.032	0.76	0.029	0.83	0.019	1.31
	μ		0.027	0.030	0.90	0.045	0.60	0.034	0.79	0.033	0.82	0.034	0.81	0.021	1.27
	σ		0.0022	0.0000	0.0742	0.0038	0.0344	0.0026	0.0283	0.0011	0.0479	0.0035	0.0610	0.0019	0.0754
	COV		0.08		0.08		0.06		0.04		0.06		0.08		0.06

LA 2/50	column	design	NTH	N97L		F273L		F273M		ETH		F273N		CSP	
				drift	B.F.	drift	B.F.	drift	B.F.	drift	B.F.	drift	B.F.	drift	B.F.
9-story	w14	LB	0.036	0.030	1.20	0.048	0.75	0.034	1.06	0.042	0.85	0.042	0.85	0.027	1.32
		UB	0.036	0.030	1.19	0.041	0.87	0.028	1.28	0.040	0.90	0.037	0.97	0.023	1.54
	w24	LB	0.034	0.030	1.14	0.048	0.71	0.032	1.07	0.042	0.82	0.041	0.83	0.025	1.39
		UB	0.033	0.030	1.10	0.042	0.78	0.029	1.13	0.039	0.85	0.035	0.93	0.023	1.44
	w30	LB	0.035	0.030	1.16	0.047	0.74	0.031	1.12	0.042	0.83	0.043	0.81	0.027	1.30
		UB	0.032	0.030	1.07	0.042	0.76	0.028	1.15	0.038	0.84	0.031	1.03	0.023	1.40
	w36	LB	0.034	0.030	1.13	0.050	0.68	0.032	1.06	0.042	0.81	0.044	0.77	0.027	1.25
		UB	0.034	0.030	1.12	0.043	0.78	0.028	1.20	0.039	0.86	0.038	0.88	0.024	1.39
	μ		0.034	0.030	1.14	0.045	0.76	0.030	1.13	0.040	0.84	0.039	0.88	0.025	1.38
	σ		0.0013	0.0000	0.0447	0.0035	0.0580	0.0023	0.0774	0.0018	0.0300	0.0044	0.0867	0.0019	0.0891
	COV		0.04		0.04		0.08		0.07		0.04		0.10		0.06

LA 2/50	column	design	NTH	N97L		F273L		F273M		ETH		F273N		CSP	
				drift	B.F.	drift	B.F.	drift	B.F.	drift	B.F.	drift	B.F.	drift	B.F.
20-story	w14	L&UB	0.024	0.018	1.34	0.027	0.89	0.024	1.01	0.029	0.83	0.033	0.74	0.020	1.19
	w24	L&UB	0.024	0.018	1.34	0.028	0.86	0.024	1.01	0.030	0.81	0.031	0.77	0.020	1.21
	w30	L&UB	0.024	0.018	1.36	0.028	0.87	0.024	1.02	0.030	0.81	0.031	0.78	0.020	1.23
	w36	L&UB	0.024	0.018	1.34	0.028	0.86	0.024	1.00	0.030	0.80	0.033	0.73	0.020	1.20
	μ		0.024	0.018	1.35	0.028	0.87	0.024	1.01	0.030	0.81	0.032	0.75	0.020	1.20
	σ		0.0002	0.0000	0.0087	0.0005	0.0156	0.0000	0.0065	0.0004	0.0090	0.0008	0.0219	0.0002	0.0162
	COV		0.01		0.01		0.02		0.01		0.01		0.03		0.01

LA 2/50	column	design	NTH	N97L		F273L		F273M		ETH		F273N		CSP	
				drift	B.F.	drift	B.F.	drift	B.F.	drift	B.F.	drift	B.F.	drift	B.F.
3, 9, and 20-story	μ				1.13		0.75		0.98		0.83		0.82		1.29
	σ				0.192		0.119		0.154		0.034		0.081		0.097
	COV				0.17		0.16		0.16		0.04		0.10		0.08

Table 4-7 Drift and Variance Values for Different Analysis Methods Using LA 50% in 50 Year Hazard Level Before Corrections

LA 2/50	column	design	NTH	N97L		F273L		F273M		ETH		F273N		CSP	
				drift	B.F.	drift	B.F.	drift	B.F.	drift	B.F.	drift	B.F.	drift	B.F.
3-story	w14	LB	0.009	0.009	0.99	0.009	0.99	0.008	1.10	0.009	0.96	0.007	1.30	0.006	1.48
		UB	0.007	0.009	0.81	0.009	0.81	0.008	0.90	0.009	0.85	0.007	1.04	0.006	1.20
	w24	LB	0.007	0.009	0.80	0.009	0.80	0.008	0.89	0.009	0.80	0.007	1.06	0.006	1.20
		UB	0.006	0.009	0.69	0.009	0.69	0.008	0.77	0.009	0.72	0.007	0.90	0.006	1.04
	w30	LB	0.007	0.009	0.80	0.009	0.80	0.008	0.89	0.009	0.79	0.007	1.04	0.006	1.23
		UB	0.006	0.007	0.88	0.007	0.88	0.006	0.98	0.008	0.81	0.006	1.04	0.005	1.22
	w36	LB	0.007	0.009	0.83	0.009	0.83	0.008	0.92	0.009	0.79	0.007	1.09	0.006	1.26
		UB	0.006	0.007	0.90	0.007	0.90	0.006	1.00	0.008	0.80	0.006	1.05	0.005	1.23
	μ		0.007	0.009	0.84	0.009	0.84	0.008	0.93	0.009	0.82	0.007	1.06	0.006	1.23
	σ		0.0009	0.0009	0.0894	0.0009	0.0894	0.0008	0.0993	0.0007	0.0684	0.0004	0.1085	0.0004	0.1209
	COV		0.13		0.11		0.11		0.11		0.08		0.10		0.10

LA 2/50	column	design	NTH	N97L		F273L		F273M		ETH		F273N		CSP	
				drift	B.F.	drift	B.F.	drift	B.F.	drift	B.F.	drift	B.F.	drift	B.F.
9-story	w14	LB	0.009	0.008	1.06	0.008	1.06	0.007	1.22	0.009	0.98	0.006	1.37	0.006	1.53
		UB	0.008	0.008	1.03	0.008	1.03	0.006	1.31	0.008	0.97	0.006	1.29	0.005	1.45
	w24	LB	0.008	0.008	1.03	0.008	1.03	0.007	1.17	0.009	0.92	0.006	1.32	0.006	1.49
		UB	0.007	0.008	0.93	0.008	0.93	0.006	1.21	0.008	0.87	0.006	1.16	0.006	1.31
	w30	LB	0.008	0.008	1.02	0.008	1.02	0.007	1.18	0.009	0.93	0.006	1.32	0.006	1.48
		UB	0.007	0.008	0.92	0.008	0.92	0.006	1.20	0.008	0.87	0.006	1.16	0.006	1.30
	w36	LB	0.008	0.008	0.96	0.008	0.96	0.007	1.15	0.009	0.92	0.006	1.26	0.006	1.42
		UB	0.007	0.008	0.92	0.008	0.92	0.006	1.21	0.008	0.88	0.006	1.15	0.006	1.30
	μ		0.008	0.008	0.98	0.008	0.98	0.007	1.21	0.009	0.92	0.006	1.25	0.006	1.41
	σ		0.0005	0.0002	0.0555	0.0002	0.0555	0.0005	0.0480	0.0003	0.0428	0.0001	0.0842	0.0001	0.0944
	COV		0.07		0.06		0.06		0.04		0.05		0.07		0.07

LA 2/50	column	design	NTH	N97L		F273L		F273M		ETH		F273N		CSP	
				drift	B.F.	drift	B.F.	drift	B.F.	drift	B.F.	drift	B.F.	drift	B.F.
20-story	w14	L&UB	0.006	0.004	1.46	0.004	1.46	0.006	1.08	0.007	0.98	0.004	1.81	0.004	1.85
	w24	L&UB	0.007	0.005	1.46	0.005	1.46	0.006	1.09	0.007	0.98	0.004	1.79	0.004	1.83
	w30	L&UB	0.007	0.005	1.48	0.005	1.48	0.006	1.13	0.007	0.99	0.004	1.84	0.004	1.87
	w36	L&UB	0.007	0.005	1.44	0.005	1.44	0.006	1.10	0.007	0.99	0.004	1.78	0.004	1.81
	μ		0.007	0.005	1.46	0.005	1.46	0.006	1.10	0.007	0.98	0.004	1.81	0.004	1.84
	σ		0.0001	0.0001	0.0174	0.0001	0.0174	0.0000	0.0226	0.0001	0.0033	0.0001	0.0250	0.0001	0.0246
	COV		0.02		0.01		0.01		0.02		0.00		0.01		0.01

LA 2/50	column	design	NTH	N97L		F273L		F273M		ETH		F273N		CSP	
				drift	B.F.	drift	B.F.	drift	B.F.	drift	B.F.	drift	B.F.	drift	B.F.
3, 9, and 20-story	μ				1.09		1.09		1.08		0.91		1.37		1.49
	σ				0.277		0.277		0.131		0.083		0.331		0.274
	COV				0.25		0.25		0.12		0.09		0.24		0.18

Table 4-8 Default Values for the C_B for the Collapse Prevention and Immediate Occupancy Performance Levels for New Buildings[5,6]

No higher modes, regular						
	3-story		9-story		20-story	
	2/50	50/50	2/50	50/50	2/50	50/50
N97-LSP	0.90	0.90	1.15	1.10	1.35	1.05
F273-LSP	0.65	0.90	0.85	1.10	1.00	1.05
N97-MAP	0.80	0.80	1.05	0.90	1.10	1.10
F273-LDP	0.80	1.00	1.15	1.10	1.00	1.15
LTHP	0.85	0.85	0.90	1.00	0.90	1.00
F273-NSP	0.85	NA[1]	0.95	NA[1]	0.85	NA[1]
CSM-NSP	1.30	NA[1]	1.50	NA[1]	1.35	NA[1]

Higher modes[3]						
	3-story		9-story		20-story	
	2/50	50/50	2/50	50/50	2/50	50/50
N97-LSP	NP[2]	NP[2]	NP[2]	NP[2]	NP[2]	NP[2]
F273-LSP	NP[2]	NP[2]	NP[2]	NP[2]	NP[2]	NP[2]
N97-MAP	0.80	0.80	1.05	0.90	1.10	1.10
F273-LDP	0.80	1.00	1.15	1.10	1.00	1.15
LTHP	0.85	0.85	0.90	1.00	0.90	1.00
F273-NSP	NP[2]	NP[2]	NP[2]	NP[2]	NP[2]	NP[2]
CSM-NSP	NP[2]	NP[2]	NP[2]	NP[2]	NP[2]	NP[2]

Irregular[4]						
	3-story		9-story		20-story	
	2/50	50/50	2/50	50/50	2/50	50/50
N97-LSP	NP[2]	1.00	NP[2]	1.20	NP[2]	1.15
F273-LSP	NP[2]	1.00	NP[2]	1.20	NP[2]	1.15
N97-MAP	0.85	0.85	1.10	0.95	1.15	1.15
F273-LDP	0.85	1.05	1.20	1.15	1.05	1.20
LTHP	0.90	0.90	0.95	1.05	0.95	1.05
F273-NSP	0.90	NA[1]	1.00	NA[1]	0.90	NA[1]
CSM-NSP	1.35	NA[1]	1.55	NA[1]	1.40	NA[1]

1. NA: Not appropriate. Assume linear behavior.
2. NP: Not permitted.
3. Use this if $T_1/T_0 \geq 2.5$.
4. Use this for NEHRP plan irregularity 1a or 1b or vertical irregularity 1a, 1b, 2 or 3.
5. $C_B = 1.0$ for nonlinear time history analysis.
6. Use T determined by analysis with these bias factors. See Appendix B for others.

Table 4-9 Default Values for the C_B for the Collapse Prevention and Immediate Occupancy Performance Levels for Existing Buildings[5,6]

No higher modes, regular						
	3-story		9-story		20-story	
	2/50	50/50	2/50	50/50	2/50	50/50
N97-LSP	1.25	0.75	1.40	0.80	1.00	0.75
F273-LSP	0.90	0.75	1.00	0.80	0.70	0.75
N97-MAP	0.90	0.70	1.00	0.60	1.10	0.80
F273-LDP	1.20	1.00	1.30	1.05	1.20	1.30
LTHP	1.35	0.95	1.20	1.05	1.00	1.15
F273-NSP	1.25	NA[1]	1.35	NA[1]	1.30	NA[1]
CSM-NSP		NA[1]		NA[1]		NA[1]

Higher modes[3]						
	3-story		9-story		20-story	
	2/50	50/50	2/50	50/50	2/50	50/50
N97-LSP	NP[2]	NP[2]	NP[2]	NP[2]	NP[2]	NP[2]
F273-LSP	NP[2]	NP[2]	NP[2]	NP[2]	NP[2]	NP[2]
N97-MAP	0.90	0.70	1.00	0.60	1.10	0.80
F273-LDP	1.20	1.00	1.30	1.05	1.20	1.30
LTHP	1.35	0.95	1.20	1.05	1.00	1.15
F273-NSP	NP[2]	NP[2]	NP[2]	NP[2]	NP[2]	NP[2]
CSM-NSP	NP[2]	NP[2]	NP[2]	NP[2]	NP[2]	NP[2]

Irregular[4]						
	3-story		9-story		20-story	
	2/50	50/50	2/50	50/50	2/50	50/50
N97-LSP	NP[2]	0.85	NP[2]	0.90	NP[2]	0.85
F273-LSP	NP[2]	0.85	NP[2]	0.90	NP[2]	0.85
N97-MAP	0.95	0.75	1.05	0.65	1.15	0.85
F273-LDP	1.25	1.05	1.35	1.10	1.25	1.35
LTHP	1.40	1.00	1.25	1.10	1.05	1.20
F273-NSP	1.30	NA[1]	1.40	NA[1]	1.35	NA[1]
CSM-NSP		NA[1]		NA[1]		NA[1]

1. NA: Not appropriate. Assume linear behavior.
2. NP: Not permitted.
3. Use this if $T_1/T_0 \geq 2.5$.
4. Use this for NEHRP plan irregularity 1a or 1b or vertical irregularity 1a, 1b, 2 or 3.
5. $C_B = 1.0$ for nonlinear time history analysis.
6. Use T determined by analysis with these bias factors. See Appendix B for others.

Table 4-10 Member Sizes for the 3, 9, and 20-Story Buildings Designed According to the 1997 *NEHRP Provisions*

-story SMF, 1997 NEHRP (Upper Bound)

w14					w24					w30					w36				
Columns		Doubler plate		Beam	Columns		Doubler plate		Beam	Columns		Doubler plate		Beam	Columns		Panle-zone		Beam
Exterior	interior	Ext.	Int.		Exterior	interior	Ext.	Int.		Exterior	interior	Ext.	Int.		Exterior	interior	Ext.	Int.	
w14x342	w14x398	0	0	w24x76	w24x192	w24x207	0	0	w24x76	w30x173	w30x173	0	0	w24x62	w36x135	w36x135	0	0	w24x76
w14x342	w14x398	0	0	w33x130	w24x192	w24x207	0	0.625	w33x118	w30x173	w30x173	0.125	0.625	w33x118	w36x135	w36x135	0.125	0.625	w33x130
w14x342	w14x398	0	0	w30x108	w24x192	w24x207	0	0.5	w30x108	w30x173	w30x173	0	0.375	w30x108	w36x135	w36x135	0	0.5	w30x108

-story SMF, 1997 NEHRP (Lower Bound)

w14					w24					w30					w36				
Columns		Doubler plate		Beam	Columns		Doubler plate		Beam	Columns		Doubler plate		Beam	Columns		Panle-zone		Beam
Exterior	interior	Ext.	Int.		Exterior	interior	Ext.	Int.		Exterior	interior	Ext.	Int.		Exterior	interior	Ext.	Int.	
w14x257	w14x283	0	0	w21x68	w24x162	w24x192	0	0	w21x68	w30x132	w30x148	0	0	w21x68	w36x135	w36x135	0	0	w18x65
w14x257	w14x283	0	1	w33x118	w24x162	w24x192	0.25	0.75	w30x99	w30x132	w30x148	0.125	0.625	w30x90	w36x135	w36x135	0.125	0.375	w30x90
w14x257	w14x283	0	0.875	w30x99	w24x162	w24x192	0	0.5	w27x84	w30x132	w30x148	0	0.5	w27x84	w36x135	w36x135	0	0.5	w24x84

-story SMF, 1997 NEHRP (Upper Bound)

w14					w24					w30					w36				
Columns		Doubler plate		Beam	Columns		Doubler plate		Beam	Columns		Doubler plate		Beam	Columns		Panle-zone		Beam
Exterior	interior	Ext.	Int.		Exterior	interior	Ext.	Int.		Exterior	interior	Ext.	Int.		Exterior	interior	Ext.	Int.	
w14x342	w14x398	0	0	w21x62	w24x207	w24x250	0	0	w21x62	w30x173	w30x191	0	0	w21x62	w36x135	w36x150	0	0	w21x62
w14x342	w14x398	0	0	w27x94	w24x207	w24x250	0	0	w27x94	w30x173	w30x191	0	0.125	w27x94	w36x135	w36x150	0	0.125	w27x94
w14x398	w14x455	0	0	w33x118	w24x250	w24x279	0	0	w33x118	w30x191	w30x211	0	0.625	w33x118	w36x150	w36x182	0	0.5	w33x118
w14x398	w14x455	0	0	w33x118	w24x250	w24x279	0	0.125	w33x118	w30x191	w30x211	0	0.625	w33x118	w36x150	w36x182	0	0.5	w33x118
w14x455	w14x550	0	0	w36x150	w24x279	w24x335	0	0.125	w36x150	w30x211	w30x261	0	0.5	w36x150	w36x182	w36x210	0	0.5	w36x150
w14x455	w14x550	0	0	w36x150	w24x279	w24x335	0	0.25	w36x150	w30x211	w30x261	0	0.625	w36x150	w36x182	w36x210	0	0.5	w36x150
w14x550	w14x550	0	0	w36x150	w24x335	w24x335	0	0.375	w36x150	w30x261	w30x261	0	0.625	w36x150	w36x210	w36x256	0	0.5	w36x150
w14x550	w14x550	0	0	w40x183	w24x335	w24x335	0	0.625	w36x182	w30x261	w30x261	0	0.875	w36x182	w36x210	w36x256	0	0.5	w36x150
w14x550	w14x605	0	0	w40x183	w24x335	w24x408	0	0.25	w36x182	w30x261	w30x326	0	0.75	w36x182	w36x210	w36x280	0	0.875	w36x182
w14x550	w14x605	0	0	w40x183	w24x335	w24x408	0	0	w36x182	w30x261	w30x326	0	0	w36x182	w36x210	w36x280	0	0	w36x182

-story SMF, 1997 NEHRP (Lower Bound)

w14					w24					w30					w36				
Columns		Doubler plate		Beam	Columns		Doubler plate		Beam	Columns		Doubler plate		Beam	Columns		Panle-zone		Beam
Exterior	interior	Ext.	Int.		Exterior	interior	Ext.	Int.		Exterior	interior	Ext.	Int.		Exterior	interior	Ext.	Int.	
w14x257	w14x283	0	0	w21x62	w24x176	w24x192	0	0	w21x62	w30x148	w30x148	0	0	w18x50	w36x135	w36x135	0	0	w18x50
w14x257	w14x283	0	0	w27x94	w24x176	w24x192	0	0.25	w27x94	w30x148	w30x148	0	0.375	w27x94	w36x135	w36x135	0	0.375	w27x94
w14x283	w14x398	0	0	w30x116	w24x192	w24x229	0	0.5	w30x116	w30x148	w30x173	0	0.5	w27x94	w36x135	w36x160	0	0.375	w27x94
w14x283	w14x398	0	0	w30x116	w24x192	w24x229	0	0.75	w30x116	w30x148	w30x173	0	0.75	w30x116	w36x135	w36x160	0	0.625	w30x116
w14x398	w14x455	0	0	w33x141	w24x229	w24x279	0	0.625	w33x118	w30x173	w30x211	0	0.875	w33x141	w36x160	w36x194	0	0.625	w33x130
w14x398	w14x455	0	0	w33x141	w24x229	w24x279	0	0.625	w33x118	w30x173	w30x211	0	0.875	w33x141	w36x160	w36x194	0	0.625	w33x130
w14x455	w14x500	0	0	w33x141	w24x279	w24x279	0	1	w33x141	w30x211	w30x235	0	0.875	w33x141	w36x194	w36x210	0	0.5	w33x130
w14x455	w14x500	0	0	w36x150	w24x279	w24x279	0	1	w33x141	w30x211	w30x235	0	0.875	w33x141	w36x194	w36x210	0	0.5	w33x130
w14x500	w14x550	0	0	w36x150	w24x279	w24x335	0	0.75	w36x150	w30x235	w30x261	0	0.75	w36x150	w36x210	w36x232	0	0.5	w36x135
w14x500	w14x550	0	0	w36x150	w24x279	w24x335	0	0	w36x150	w30x235	w30x261	0	0.125	w36x150	w36x210	w36x232	0	0	w36x135

0-story SMF, 1997 NEHRP (Upper & Lower Bound)

w14					w24					w30					w36				
Columns		Doubler plate		Beam	Columns		Doubler plate		Beam	Columns		Doubler plate		Beam	Columns		Panle-zone		Beam
Exterior	interior	Ext.	Int.		Exterior	interior	Ext.	Int.		Exterior	interior	Ext.	Int.		Exterior	interior	Ext.	Int.	
15x15x0.5	w14x370	0	0	w18x46	15x15x0.5	w24x207	0	0	w18x46	15x15x0.5	w30x148	0	0	w18x46	15x15x0.5	w36x135	0	0	w18x46
15x15x0.5	w14x370	0	0	w24x55	15x15x0.5	w24x207	0	0	w24x55	15x15x0.5	w30x148	0	0	w24x55	15x15x0.5	w36x135	0	0	w24x55
15x15x0.75	w14x426	0	0	w27x84	15x15x0.75	w24x250	0	0	w27x84	15x15x0.75	w30x191	0	0.125	w27x84	15x15x0.75	w36x135	0	0.125	w27x84
15x15x0.75	w14x426	0	0	w30x108	15x15x0.75	w24x250	0	0.125	w30x108	15x15x0.75	w30x191	0	0.375	w30x108	15x15x0.75	w36x135	0	0.375	w30x108
15x15x1.0	w14x500	0	0	w30x108	15x15x1.0	w24x279	0	0	w30x108	15x15x1.0	w30x211	0	0.375	w30x108	15x15x1.0	w36x194	0	0.25	w30x108
15x15x1.0	w14x500	0	0	w30x108	15x15x1.0	w24x279	0	0.25	w33x118	15x15x1.0	w30x211	0	0.5	w33x118	15x15x1.0	w36x194	0	0.375	w30x108
15x15x1.0	w14x500	0	0	w33x118	15x15x1.0	w24x279	0	0.375	w33x118	15x15x1.0	w30x211	0	0.625	w33x118	15x15x1.0	w36x194	0	0.5	w33x118
15x15x1.0	w14x605	0	0	w33x118	15x15x1.0	w24x335	0	0.125	w33x118	15x15x1.0	w30x261	0	0.375	w36x135	15x15x1.0	w36x245	0	0.375	w33x118
15x15x1.0	w14x605	0	0	w36x135	15x15x1.0	w24x335	0	0.25	w36x135	15x15x1.0	w30x261	0	0.625	w36x135	15x15x1.0	w36x245	0	0.5	w36x135
15x15x1.0	w14x605	0	0	w36x135	15x15x1.0	w24x335	0	0.25	w36x135	15x15x1.0	w30x261	0	0.625	w36x135	15x15x1.0	w36x245	0	0.5	w36x135
15x15x1.25	w14x605	0	0	w36x135	15x15x1.25	w24x408	0	0	w36x135	15x15x1.25	w30x326	0	0.375	w36x135	15x15x1.25	w36x260	0	0.5	w36x135
15x15x1.25	w14x605	0	0	w36x135	15x15x1.25	w24x408	0	0	w36x135	15x15x1.25	w30x326	0	0.5	w36x135	15x15x1.25	w36x260	0	0.625	w36x135
15x15x1.25	w14x605	0	0	w36x135	15x15x1.25	w24x408	0	0	w36x135	15x15x1.25	w30x326	0	0.5	w36x135	15x15x1.25	w36x260	0	0.625	w36x135
15x15x1.25	w14x665	0	0	w36x135	15x15x1.25	w24x408	0	0	w36x135	15x15x1.25	w30x326	0	0.5	w36x135	15x15x1.25	w36x260	0	0.75	w36x135
15x15x1.25	w14x665	0	0	w36x135	15x15x1.25	w24x408	0	0.125	w36x135	15x15x1.25	w30x326	0	0.5	w36x135	15x15x1.25	w36x260	0	0.75	w36x135
15x15x1.25	w14x665	0	0	w36x135	15x15x1.25	w24x408	0	0.125	w36x135	15x15x1.25	w30x326	0	0.5	w36x135	15x15x1.25	w36x260	0	0.75	w36x135
15x15x2.0	w14x730	0	0	w36x135	15x15x2.0	w24x492	0	0	w36x135	15x15x2.0	w30x391	0	0.25	w36x135	15x15x2.0	w36x300	0	0.625	w36x135
15x15x2.0	w14x730	0	0	w33x118	15x15x2.0	w24x492	0	0	w33x118	15x15x2.0	w30x391	0	0	w33x118	15x15x2.0	w36x300	0	0.375	w33x118
15x15x2.0	w14x730	0	0	w33x118	15x15x2.0	w24x492	0	0	w33x118	15x15x2.0	w30x391	0	0	w33x118	15x15x2.0	w36x300	0	0.375	w33x118
15x15x2.0	w14x808	0	0	w33x130	15x15x2.0	w24x492	0	0	w33x118	15x15x2.0	w30x391	0	0	w33x118	15x15x2.0	w36x300	0	0.375	w33x118
15x15x2.0	w14x808	0	0	w33x130	15x15x2.0	w24x492	0	0	w33x118	15x15x2.0	w30x391	0	0	w33x118	15x15x2.0	w36x300	0	0	w33x118
15x15x2.0	w14x808	0	0	w14x22	15x15x2.0	w24x492	0	0	w14x22	15x15x2.0	w30x391	0	0	w14x22	15x15x2.0	w36x300	0	0	w14x22

4.5.2 Static Pushover Analysis

A static pushover analysis was performed on each building to evaluate its lateral strength and post-yield behavior. Force and displacement relationships obtained from the static pushover analysis are very useful to evaluate the capacity of a structure experiencing substantial inelastic deformation. The force and displacement relationship was plotted in terms of the seismic base shear coefficient and roof drift angle. The seismic base shear coefficient was calculated from the ratio of lateral force to structural seismic weight. The roof drift angle was obtained from the roof displacement divided by the total height of the structure. All lateral forces were distributed along the height of the structure based on the 1997 NEHRP *Provisions*. In this analysis model, a bi-linear connection model representing ductile behavior was used along with the P-delta effect. Displacement control was used for the pushover analyses.

Figure 4-38 shows the seismic coefficient to top-story drift angle relationships for the 3-story buildings designed for the upper-bound limit. The frames designed by the upper-bound limitation have a higher strength and stiffness than those from the lower-bound designs. This indicates that increasing seismic design force or the drift requirement leads to an increase in the stiffness and strength when the drift limit controls the frame design. It is interesting to note that usually the frame designed with W14 column members results in less stiffness and more strength than those using other section types such as W24, W30, and W36 column members. This is because the W14 column member must have a much higher plastic section modulus in order to provide the same stiffness as the deeper sections. In addition, the relatively thick web plate in the W14 member does not require putting a doubler plate in the column web to satisfy the panel zone requirement. The doubler plates attached to the frames using W24, W30, and W36 column members add significant strength and stiffness in the beam-to-column connections and result in increasing the initial stiffness of the structures.

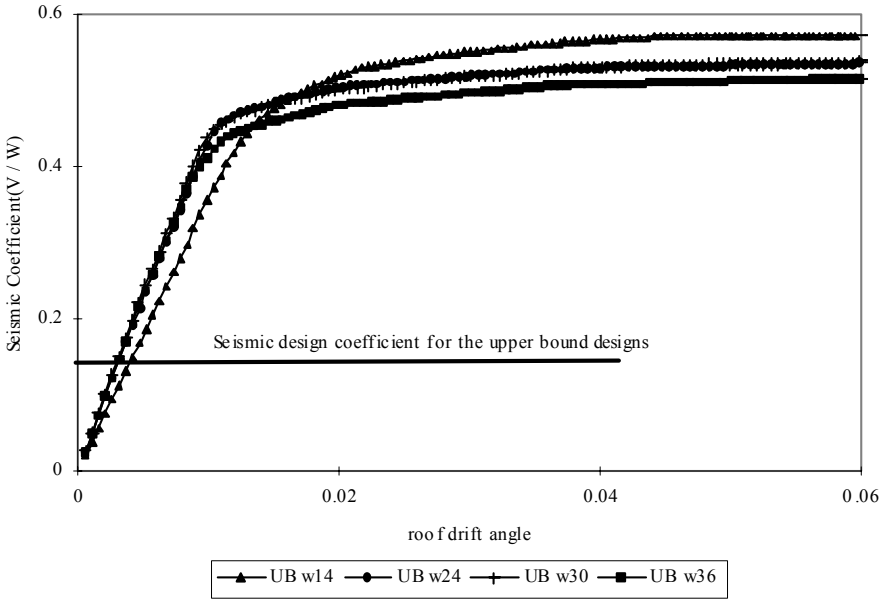

Figure 4-38 Static Pushover Analysis for LA 3-Story Upper Bound Designs

An over-strength ratio was calculated to examine the strength of a structural system for seismic evaluation. The over-strength ratio was defined here as the ratio of ultimate strength of the frame to the design strength used as the minimum design force in the 1997 NEHRP *Provisions*. A peak point from the static pushover analysis was selected as the ultimate strength of the frame. Since the post-yield strengths increased continuously as the drift increased, a point corresponding to the roof drift angle of 0.03 was chosen and calculated as the ultimate strength. The over-strength ratios ranged from 3.3 to 3.7 for 3-story upper-bound designs and from 3.9 to 4.5 for the lower bound designs. For the 9-story upper-bound designs, the over-strength ratios varied between 3.3 and 3.8. For the lower-bound designs, the range was 3.7 to 4.1.

For the 20-story building design, the frame with W14 column members has an over-strength factor of 3.6, while others have values of 3.6, 3.4, and 3.4 for the frames with W24, W30, and W36 column members, respectively. The displacement-controlled pushover analysis allows one to observe the load-deflection behavior after the slope becomes negative. Figure 4-39 indicates that the slope of the load-drift curve becomes negative at a drift of about 0.03. The negative slope gradually increases as the building is pushed to larger deflections. This is discussed further in relation to the pushover results for the 20-story building.

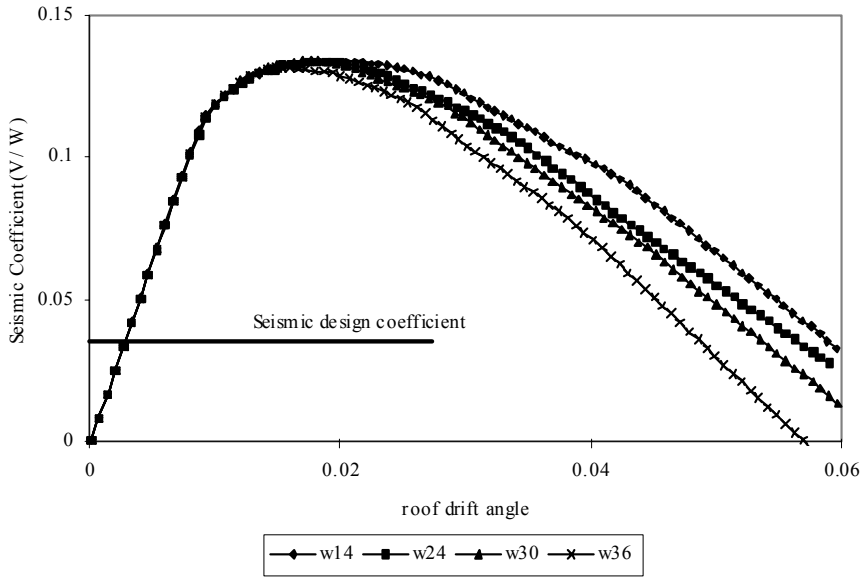

Figure 4-39 Static Pushover Analysis for LA 20-Story Designs

Figure 4-39 illustrates the lateral strength capacity of the 20-story SMRF buildings. As described previously, the minimum constant design force defined in the 1997 NEHRP *Provisions* controlled both the upper and lower-bound design. As a result, the UB and LB design for the 20-story buildings are the same design. The pushover analyses show that the P-delta effects cause negative stiffness in the 20-story building after a roof drift angle of 0.01 is reached. Using the different column depths does not result in a significant difference in the initial elastic stiffness of each building. However, the post-yield behavior of the frames is different as the frames

experience substantial inelastic drift. The general trends of the post-yield strength observed in the 3- and 9-story buildings are very similar for the 20-story buildings. The frame using W14 columns shows the highest post-yield strength, while the frame using the W36 column has the lowest one. Krawinkler (2000) observed similar post-yield behavior for the 20-story pre-Northridge building and was quite concerned by it.

The P-delta effect was further investigated for the 9-story and 20-story buildings where the building frames are more vulnerable to the geometric instability. Figure 4-40 shows the deflected shape of the 20-story buildings during the static pushover analyses. The building experiences substantial displacements in the lower stories when the top floor drift angle exceeds 1%. After the frame enters the negative stiffness region, the drifts at the lower stories are increased at a much higher rate due to the detrimental P-delta effect. Figure 4-41 shows the drift angle at the 5th floor and roof for comparison. Each story displacement was divided by height corresponding to the location of each floor. As the drift angle exceeds about 1%, the drift angle at the 5th floor becomes larger than the one for the roof, indicating that large drift demands are concentrated in the lower stories.

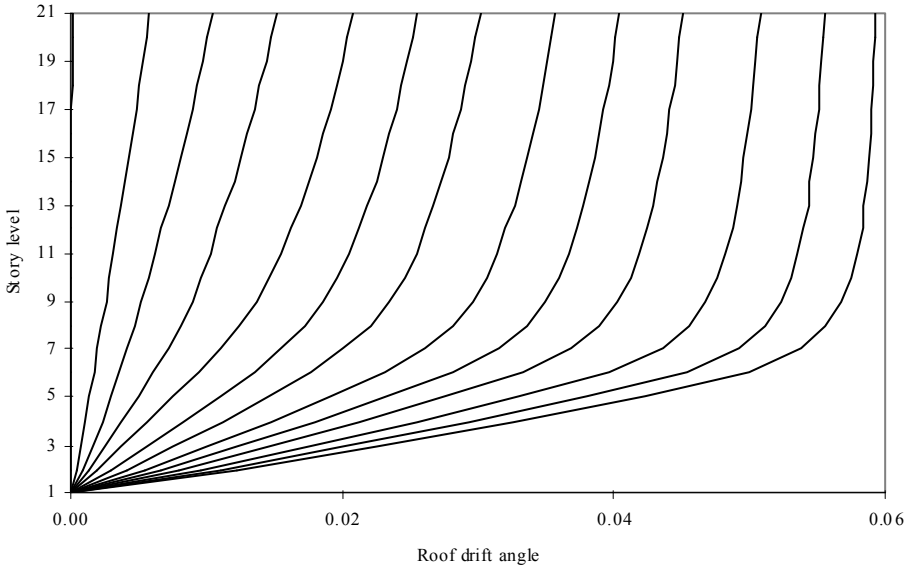

Figure 4-40 Deflected Shape During Pushover Analysis – LA 20-Story Designs

The pushover results for the 20-story building demonstrate that this analysis procedure may be misleading. They suggest that the building will collapse if the roof drift exceeds 2% to 3%. However, the dynamic analyses described in the next chapter demonstrate that the median drift at global collapse is about 9%. Inspection of the equations used to calculate the time history response indicate that the equivalent positive stiffness represented by changing the velocity of the mass over a time step overshadows the negative structural stiffness. The pushover analyses were conducted using the displacement control in order to be able to observe the negative stiffness without collapse. This is an artificial representation, however, because it is required to apply forces in the opposite direction to hold the structure up. If force control is used for the

pushover analysis, the structure will collapse as soon as a negative stiffness is encountered. This casts a considerable amount of doubt on analysis procedures that utilize nonlinear pushover analysis, especially those that use roof drift versus base shear.

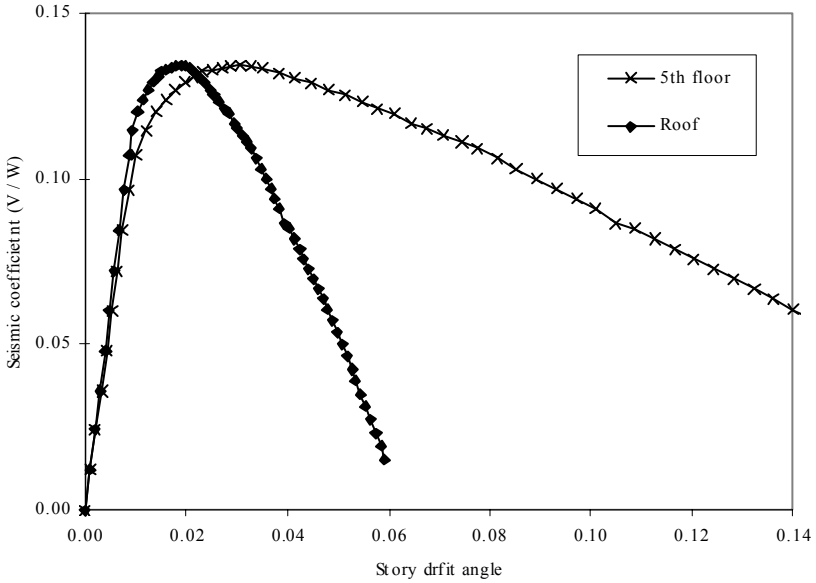

Figure 4-41 Static Pushover Analysis – LA 20-Story Designs

4.5.3 Drift Demands for Typical Post-Northridge SMRF Buildings

The results discussed here were obtained from the three typical building types: 3-story UB with W14 columns, 9-story UB with W14 columns, and 20-story building with W24 columns. These buildings were selected as typical building frames since previous SAC studies have been done based on these structural configurations. Each of the 20 ground motions with 2/50, 10/50 and 50/50 hazard levels were used to evaluate the statistical performance of the post-Northridge SMRF buildings.

Figure 4-42 shows the median, 84th, and 95th percentile values of maximum story drifts from the 20 ground motions representing the 2/50 and 50/50 hazard levels. For the 3-story building with 2/50 ground motions, the difference of drift demand between the second and roof floor level becomes smaller as the percentile values are increased. The maximum drift demands of 0.027, 0.039, and 0.046 were calculated for the median, 84th, and 95th percentile response levels, respectively. All maximum drift demands occurred in the second story. The smaller drift demand at the first story for the 2/50 motions is the result of the fixed columns at the base.

For the 9-story building, the median distribution along the height is relatively uniform, while the 84th and 95th percentile values have a distinct concentration of large drifts in the middle stories. This trend was not observed from the static pushover analyses. The maximum values for the median, 84th, and 95th percentile levels are 0.029, 0.045, and 0.057, respectively.

For the 20-story buildings, large concentrations of drift demands in the lower stories were observed from the inelastic analysis for the 85th and 95th percentiles of response. The maximum drift demands occurred in the fourth story, and the drift values of 0.021, 0.033, and 0.050 were observed for the median, 84th, and 95th percentile calculations, respectively. The drift values from the 95th percentile clearly show that the significant P-delta effect produced the large drift concentration in the lower stories. It is interesting to note that the response at the 84th and 95th percentile levels predict the lower stories mechanism that was predicted using the static pushover analysis procedure. This is because of the P-delta effects, which are greater in the lower stories. P-delta effects do not explain all features of the results, however, since the maximum drifts in the 9-story building were larger than those for the 20-story buildings.

Figure 4-42 illustrates the performance of the post-Northridge buildings subjected to 20 ground motions in LA representing the 50/50 hazard level. The median, 84th, and 95th percentile values for drift demand were calculated and plotted along the height. All median values observed in these results are much less than the drift of 0.01, which is considered to be the average elastic drift limit of typical moment frames (97AISC/LRFD Commentary). This result indicates that most structural members remain in the elastic range, which is necessary to satisfy the Immediate Occupancy performance level. The median maximum drift demands were observed to be 0.070, 0.070, and 0.065 for the 3-, 9-, and 20-story buildings, respectively.

4.5.4 Axial Force Demand in Column

Axial forces generated for the 2/50 LA ground motions are plotted in Figure 4-43. Exterior columns that produce high axial forces resulting from overturning moments were used to calculate the axial force demand. The compression forces are shown in the left side using the ratio of the axial force demand to the column critical load (P_{cr}). The tension forces are plotted in the right side using the ratio of axial force demand to the column yield load (P_y). While the axial force demands for the 3- and 9-story buildings are relatively small, those for the 20-story building have a relatively large demand/capacity ratio. It shows that the large overturning moments induced by severe ground motions cause high axial force demand. For compression, the ratio of P/P_{cr} was 0.52 for the median value and 0.67 for the 95th percentile. The maximum recommended ratio is 0.75. On the tension side, for the 20-story building, P/P_y reached 0.35 for the median response and 0.57 for the 95th percentile.

In addition to the axial force demands from the nonlinear time history (NLTH) analyses, a simplified method was investigated for estimating maximum column axial load demands. By assuming formation of plastic hinges at the beam ends in all stories, the simplified method could provide engineers with a reasonable estimation of maximum forces in the columns.

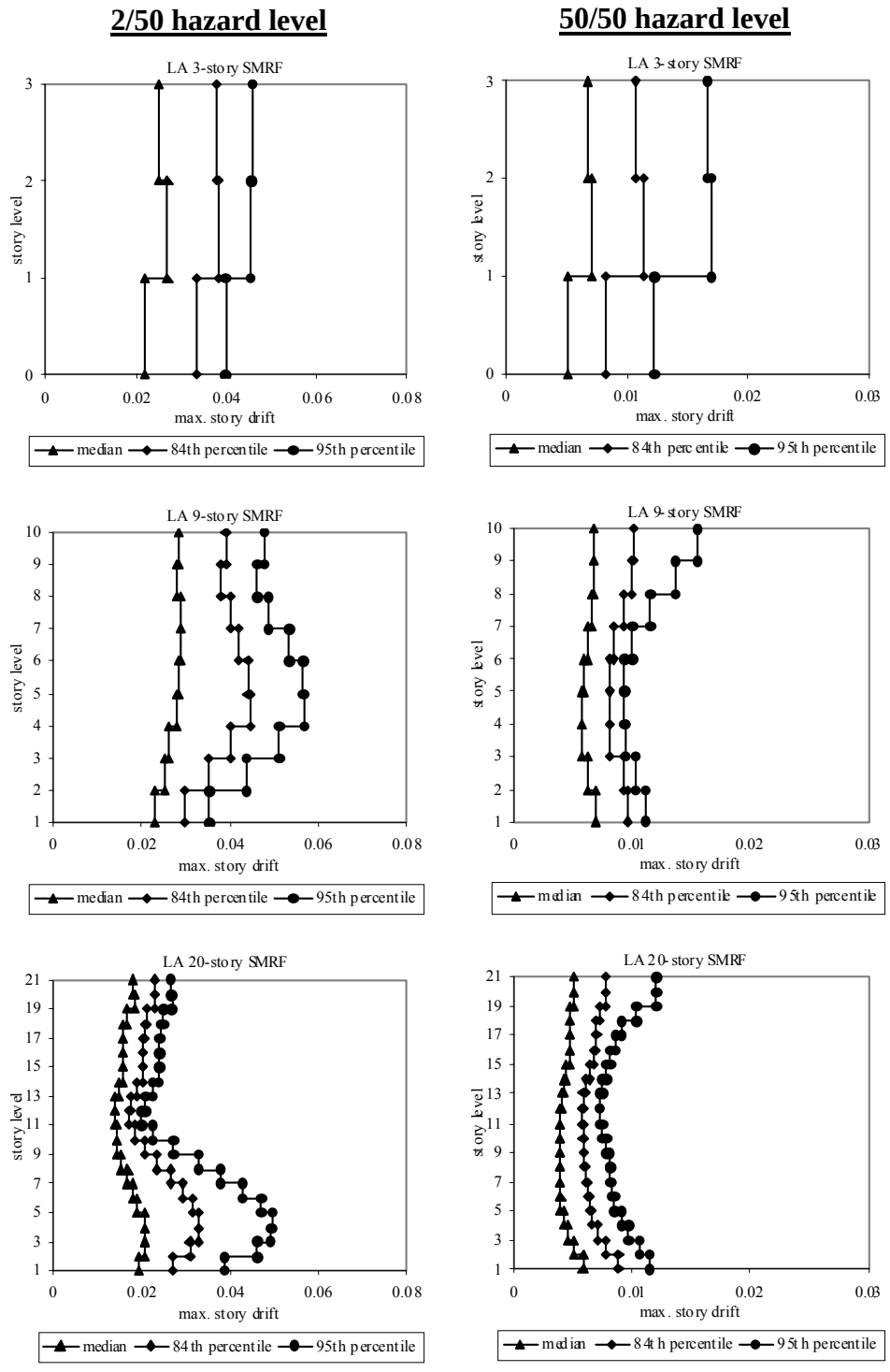

Figure 4-42 Drift Demands for Post-Northridge Typical Buildings

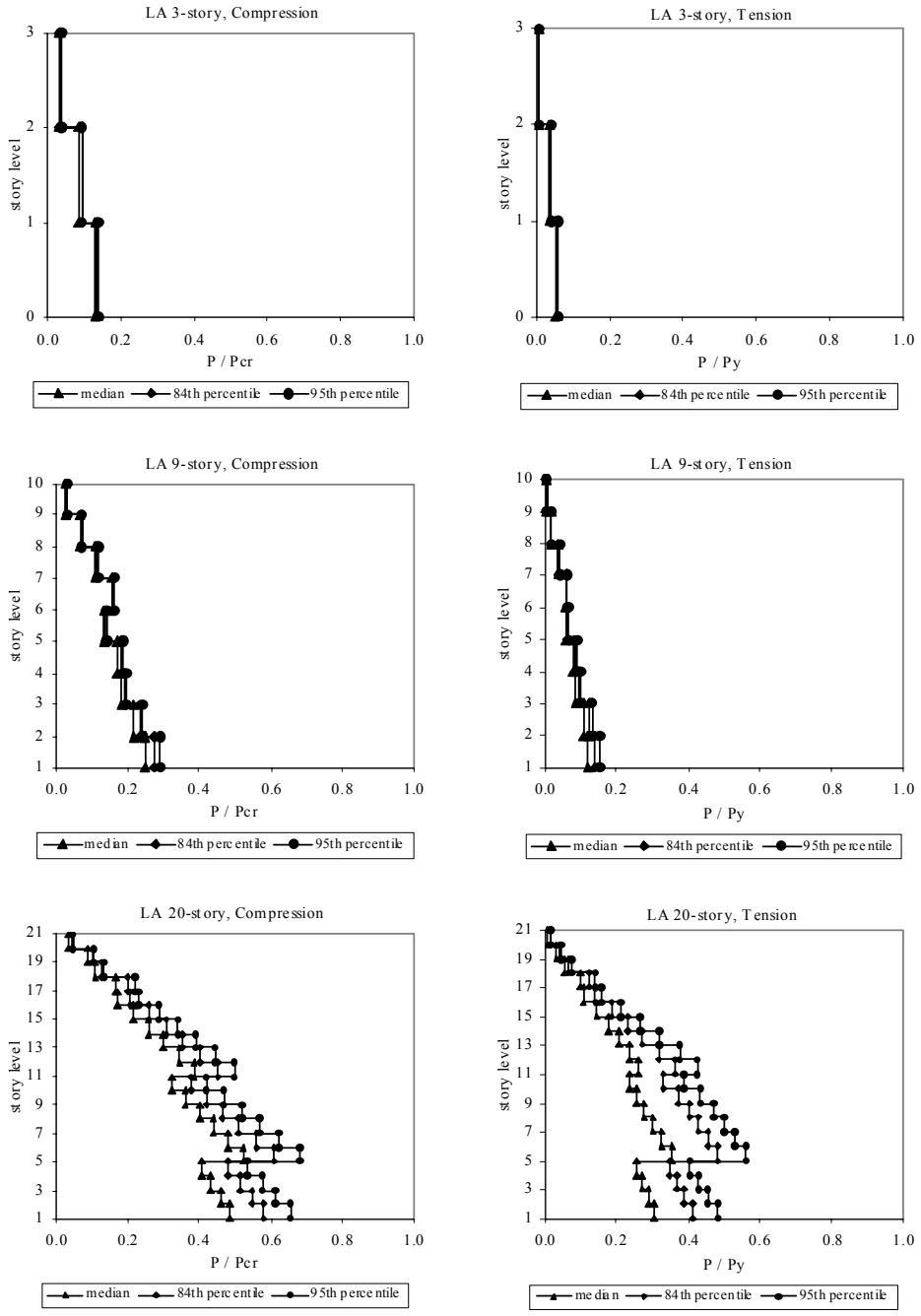

Figure 4-43 Column Axial Force Demand for Post-Northridge Typical Buildings

Figure 4-44 shows the formations of plastic hinges at the beam ends. The column compression and tension forces obtained from the beam shear forces ($\Sigma 2M_p/L$) are shown. These axial forces are then summed from top to bottom of the column and added to the gravity loads. Assuming that all beam elements experience inelastic deformation at the same time in all stories, the results from the simplified method are usually conservative. Figure 4-45 shows the comparison of the axial force demands of the exterior columns calculated from the two different approaches: one is the NLTH analyses and the other is the simplified method. Note that the column axial force demands from the NLTH analyses were added or subtracted from the gravity axial forces based on the compression or tension consideration. From the NLTH results based on the 20 LA ground motions for the 2/50 hazard level, four results were selected, which provide the 6th, 8th, 10th, and 12th largest drift demands for the three different buildings. The axial force demands for the exterior columns were averaged and compared with those from the simplified method.

As expected, all the ratios shown here are more than 1.0, implying that the simplified method provides conservative estimations compared to those for the NLTH analyses. For instance, the errors in estimating the axial force demands for the 3-story buildings are only about 10% and 20% for the compression and tension forces, respectively. For the 9-story building, the differences between the simplified method and NLTH analyses remain in the same range providing about a 20% difference in estimates from the simple model compared to the NLTH results. The difference becomes greater for the 20-story building where estimations are larger by about 40%. The estimation for the 20-story building provides a rather high over-estimation compared to those for the lower buildings. Nevertheless, the estimation of the seismic column axial forces, which are a critical aspect to ensure structural safety, using the $\Sigma 2M_p/L$ mechanism provides reasonable and conservative results without excessive effort. The estimated forces from the simple model will still be smaller than those calculated using Ω_0. It is very important to note that expected yield strength as opposed to nominal yield strengths must be used to calculate M_p.

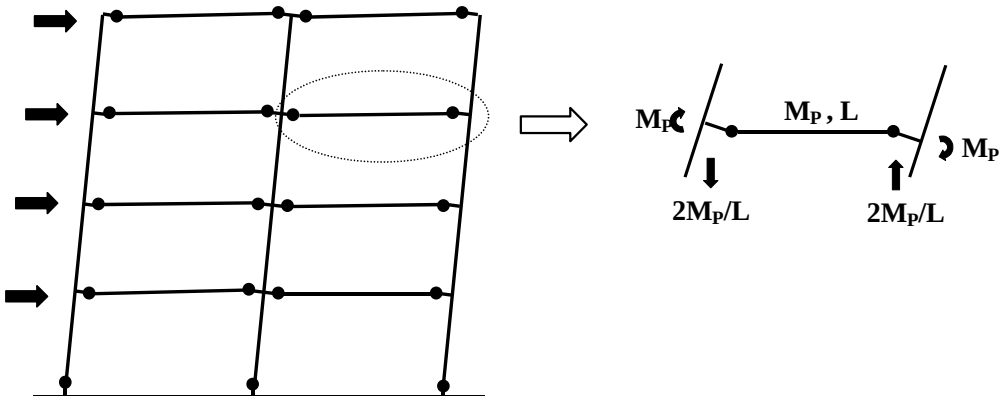

Figure 4-44 Estimation of Column Axial Force Using $\Sigma 2M_p/L$

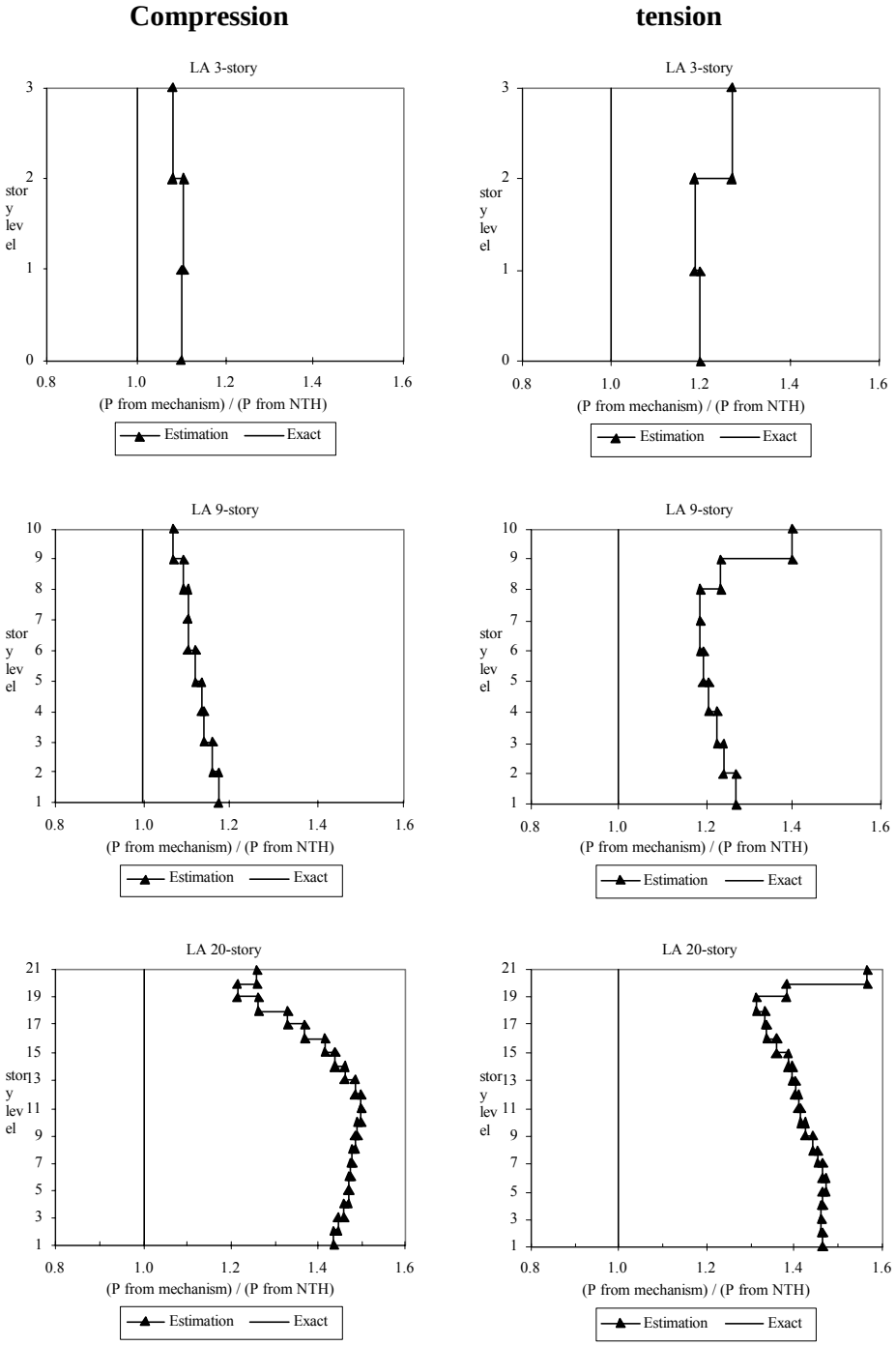

Figure 4-45 Comparison of Axial Force Estimation (NLTH Analysis vs. Simplified Method)

4.5.5 Other Analysis Results

The results presented herein are included to provide an overview of the results reported in SAC/BD-00/25 by Lee and Foutch. They are also provided to substantiate drift demands that are

used in the performance evaluation procedures described in the next chapter. The reader is referred to this report for more details and results.

4.6 Effects of Modeling, Structural Configuration, and Other Attributes on System Performance

It is highly recommended that the engineer read FEMA-355C, the State of the Art Report on *Systems Performance of Steel Moment Frames Subject to Earthquake Ground Shaking* (Krawinkler, 2000). This report summarizes the results of investigations by the SP Team. Space limitations do not allow for an adequate summary of this report. The topics covered include inelastic cyclic characteristics of structural elements, methods for predicting seismic demands, selected issues affecting the seismic performance of SMRF structures, seismic demands for frames with rigid connections, behavior of frames with pre-Northridge connections, and behavior of frames with partially restrained connections.

4.7 Recent Advances in the Development of Predictive Methods

It was mentioned earlier in this report that a policy decision was made to restrict efforts to evaluate predictive methods to those that are accepted by the engineering community and have reached a relatively high level of maturity. The R-method, included as the equivalent lateral force procedure in the NEHRP *Provisions*, is the simplest method currently available for use in design. The vast majority of new buildings designed today are designed using this procedure. Even though it is well known that it is based on several faulty assumptions, it is still preferred because of its simplicity and the fact that it usually produces a building that will perform well in an earthquake. If we think of it as a design tool rather than an analysis method, it is a little easier to accept. For some buildings, particularly those with short periods, it is not a good choice. But for steel frame buildings, which are usually flexible (a three story building with a period of one second!), the method is conservative.

The accuracy of the analysis procedure used for design of steel frame buildings is not an important issue as long as an acceptable level of conservatism is used. One reason for this is that the incremental cost incurred from the over-conservatism is minimal. For evaluation, however, this is not the case. If a decision has to be made to evacuate a building for repair or rehabilitate every connection in a steel moment frame, the cost can be substantial. This is one of the reasons that the SAC Steel Project has focused on evaluation rather than design.

One of the major flaws of the R-method is that it does not result in buildings that have a uniform level of ductility demand over the complete range of periods. For instance, if we design a building with a 0.2 second period using an R of 6, the ductility demand might be 10 or 12 for a building with little over-strength when subjected to the design earthquake. A building with a period of 2 seconds on the other hand might have a ductility demand of 3. So one great improvement that could be made would be to have R a function of period. Bertero (Bertero et al., 1986, 1988; Miranda and Bertero, 1994) has long been a proponent of replacing the current R-method.

The next level of advancement would be to have a series of coefficients that are multiplied together to account for differences in behavior among different structures. These could be referred to as coefficient methods. The FEMA-273 LSP described in this report is one such model. There is a period-dependent coefficient and coefficients to account for P-delta effects and deterioration of stiffness and strength. A recent development in this approach was reported by Han and co-workers (1999) that has coefficients to account for period, target ductility, strain hardening rate, strength degradation, and degree of pinching.

The methods discussed so far are linear elastic procedures. There have been a number of relatively new methods that include nonlinear analysis. One family of these could be labeled as equivalent single-degree-of-freedom methods. The basic concept of these methods is that a static nonlinear pushover analysis of a building can be made, and the results related to nonlinear dynamic analysis results for a single-degree-of-freedom model. The FEMA-273 NSP and Capacity Spectrum Method are two such procedures. Another similar method was developed (Collins, 1995; Collins, et al., 1996) that introduced the concept of the bias factor that was incorporated into the SAC methodology. Chen and Collins (1999) recently improved this procedure. Black and Aschheim (2000) recently reported a new approach called the Capacity Spectrum Method which holds great promise for use in performance-based design.

Another class of procedures is based on energy principles. Bertero and Uang (1992) discussed issues related to energy methods. Leelataviwat, Goel, and Stojadinovic (1998) have proposed the most well developed procedure to date based on energy principles.

Although this is not an exhaustive coverage of the broad range of research on new predictive methods, it does show that there is activity in this area. It takes continued exposure before a research method is incorporated into engineering practice. Great strides have been made in the practice of earthquake engineering practice over the past ten years. Although the R-method is used for new design, many firms now routinely use nonlinear pushover analysis for evaluation and rehabilitation. This will increase in the future as more documents like FEMA-273 adopt new procedures and legitimize them.

5. STATISTICAL AND RELIABILITY FRAMEWORK FOR ESTABLISHING PERFORMANCE OBJECTIVES

5.1 Background

Structural failures observed in the Northridge and Kobe earthquakes have exposed the weakness of current design and construction procedures and shown the need for new concepts and methodologies for evaluation of building performance and design. A central issue is proper treatment and incorporation of the large uncertainty in both seismic loading and building resistance in the evaluation and design process. The state of the art of statistical and reliability methods that can be used for this purpose has been reviewed, and several critical issues directly related to the mission of the SAC Project have been discussed in the report "Critical Issues in Developing Statistical Framework for Evaluation and Design" (Wen and Foutch, 1997). Based on the review, a statistical and reliability framework for the purpose of comparing and evaluating predictive models for structural performance evaluation and design was developed. This was further advanced by Hamburger (1998) and Jalayer and Cornell (1999). From this basis, the load and resistance factor approach described below has been adopted by the SAC Phase 2 Project. Technical details and justifications of the proposed framework can be found in papers by Luco and Cornell (1998) and Hamburger, Foutch, and Cornell (2000).

5.2 Performance Levels

Two performance levels are defined herein. These are termed Collapse Prevention and Immediate Occupancy**.**

The Collapse Prevention (CP) structural performance level is defined as the postearthquake damage state in which a structure is on the verge of experiencing either local or total collapse. Substantial damage to the building has occurred, including significant degradation in strength and stiffness of the lateral-force-resisting system, large permanent deformation of the structure, and possibly some degradation of the gravity-load-carrying system. However, all significant components of the gravity-load-carrying system must continue to be functional.

The Collapse Prevention (CP) level is not achieved if any of the following occurs:

1. The structure experiences excessive drift resulting in initiation of a P-Δ instability and global collapse.
2. Beam-column connections in the structure, including those in gravity frames, experience sufficient inelastic rotation demand to cause excessive damage to the shear-resisting elements, which may lead to local loss of gravity-carrying capacity and collapse.
3. A column in a frame experiences sufficient axial load demand to induce buckling. It is recommended that P/P_{cr} be less than 0.75.
4. A column splice in a frame experiences sufficient axial tension plus bending demand to induce splice fracture. Fracture of a bottom column connection to the base plate should be avoided.

For this performance level, it is expected that the building may be a total financial loss and that occupancy of the building before extensive repairs are made will not be permitted.

The Immediate Occupancy (IO) structural performance level is defined as the post-earthquake damage state in which only slight structural damage has occurred. Damage is anticipated to be so slight that, if not found during inspection, there would be no cause for concern. The basic vertical-and-lateral-load-carrying systems still have most, if not all, of their strength and stiffness. Buildings meeting this performance level should be safe for occupancy immediately after the earthquake, presuming that damage to nonstructural components is light and utility service is available.

The Immediate Occupancy (IO) performance level is not achieved if any of the following occurs:

1. Damage detected after the design earthquake is significant enough that repair would be required. This would allow some yielding in the members, minor local buckling in some beams but not in any columns.
2. More than 15% of the connections fracture on any floor.
3. Observable damage occurs at any base plate.
4. Yielding of any column splice plate occurs.
5. Permanent residual drift exceeds 0.5% in any story.

Maximum interstory drift angle, θ_x, at any story will be the primary design parameter used to determine if the damage states related to connection fractures, loss of the gravity-load-carrying ability of connections, buckling of beam and column flanges, permanent lateral drift, and global instability are exceeded. Column axial force and moment will be the design parameters used to determine if the column buckling or column splice fracture damage states have been exceeded.

Interstory drift capacity may be limited by global response of the structure, or by local behavior of the beam-column connection. This is discussed more thoroughly in the next section, and median drift capacities for the various connections are given.

The probable behavior of beam-column connections at various demand levels can best be determined by full-scale laboratory testing. Such testing can provide indications of the probable physical behavior of such assemblies in buildings. Depending on the characteristics of the connection assembly being tested, meaningful behavior may include the onset of local buckling, initiation of fractures in welds, base metal, or bolts, a drop in the moment below some designated threshold, and the loss of gravity-carrying capacity. If enough experimental data are gathered, it should be possible to obtain statistics on the demand levels at which this meaningful behavior will occur.

In the past, most laboratories used plastic rotation as the demand parameter by which a beam-column connection assembly was judged. However, since plastic deformations may occur at a number of places within a connection assembly, including within the panel zone, the laboratories

have reported plastic rotation angles from testing in an inconsistent manner. Therefore, in the *Guidelines*, connection assembly drift angle, consisting of the deflection of the point of contraflexure of the beam under load, relative to its unloaded position, divided by the linear distance between the point of contraflexure and the center line of the column, is recommended as the demand parameter for reporting laboratory data. This parameter is less subject to interpretation by various testing laboratories and also has the advantage that it is approximately equal to the interstory drift angle predicted by structural analyses.

5.3 Load and Resistance Factor Format for Evaluation and Design of Building Systems at Multiple Performance Levels

This approach to performance-based evaluation was developed over a period of time by several people involved in the SAC project working closely together. The issues considered and the theoretical background for this approach are given in several publications (Wen and Foutch, 1997; Hamburger, 1998; Luco and Cornell, 1998; Jalayer and Cornell, 1999; Hamburger, Foutch and Cornell, 2000). Its development is described in the next several sections of this report. The description here is for the design of SMF buildings (Foutch, 2000). The application to OMF buildings will be described following SMF buildings.

5.4 Performance Objectives

A building's desired performance level is characterized by performance objectives. A performance objective is a specification of the performance level that is to be achieved together with a seismic hazard level. The 1997 NEHRP *Provisions* (FEMA, 1997) specify that the primary design performance objective for Seismic Use Group 1 buildings is the Collapse Prevention Level of performance not to be exceeded for a Maximum Considered Earthquake ground motion assumed to be taken as that having a 2% probability of being exceeded in 50 years (abbreviated, 2/50). The approximate return period for this event is 2,475 years. The NEHRP *Provisions* also imply that a performance objective consisting of Immediate Occupancy (IO) performance level, which is similar to the SAC IO level, for a ground motion having a 50% probability of exceedance in 50 years, can also be achieved for conforming buildings. FEMA-273, however, suggests that Immediate Occupancy be paired with a ground motion with a 50% probability of exceedance in 30 years (BSSC, 1997c), but the definitions of acceptable damage within the IO performance level are not identical in the two documents.

It is recommended, herein, that the only performance objective that should be specified in the *Guidelines* is the Collapse Prevention performance level, paired with the 2%-in-50-year (2/50) seismic hazard level, rephrased as a performance objective that there be less than a 2% probability of collapse in 50 years. It is recommended that a 95% confidence in achieving this performance objective be adopted. A description of how this is attained through the design, evaluation and rehabilitation, or repair is given below. The other performance levels deal with damage control. The structural design requirements necessary to achieve IO performance, for example, are given later in this document. The design professional working with the owner or developer should decide which hazard level to use and the associated confidence level. Combining the IO performance with the 50/50 hazard level is a reasonable performance objective.

For evaluation of an existing building, or one that has been damaged by an earthquake, this level of confidence will probably not be attainable without upgrading the building. The design professional and owner should decide on the level of confidence that is appropriate for the building and its current occupancy. In Chapters 8 and 9, which deal with existing and damaged buildings, respectively, this issue is discussed further. It is recommended that a minimum confidence level of 90% of achieving the CP Performance level for the 50/30 hazard level be required for the building to remain occupied. If not, upgrade or repair should be required.

5.5 Performance Evaluation Process for New Buildings

The specific criteria for performance evaluation will be determined by the design professional in consultation with the owner and building authorities. This requires the selection of a performance objective and a degree of confidence that the performance will not be worse, or the damage greater. For new design, the performance objective is Collapse Prevention (CP) for the seismic hazard which has only a 2% probability of being exceeded in 50 years (2/50 hazard). The CP performance level is defined by a maximum design drift capacity, $\hat{C}$, times a resistance factor, ϕ. The design capacity and resistance factor are given in Table 5-1 for each connection type that has been tested for the SAC project (Roeder, 2000). The procedure required for determining capacity for other connection types is given in Section 4.7.

Table 5-1 Default Drift Capacities and Resistance Factors as Limited by Local Connection Response - Ductile Welded Connections (Roeder, 2000)

Connection Type	Strength Degradation Limit Drift Angle (radians) θ_{SD}	Immediate Occupancy		Collapse Prevention	
		Limit Drift Angle (radians) θ_{IO}	Capacity Reduction Factor ϕ	Limit Drift Angle[1] (radians) θ_{CP}	Capacity Reduction Factor[2] ϕ
WUF-B[3]	0.031-0.0003d_b	0.015	0.9	0.060-0.0006 d_b	0.9
WUF-W[4]	0.051	0.020	0.9	0.064	0.9
FF[5]	0.077-0.0012 d_b	0.020	0.9	0.10-0.0016 d_b	0.9
RBS[6]	0..060-0.0003 d_b	0.020	0.9	0.08-0.0003 d_b	0.9
WFP[7]	0.12-0.023 d_b	0.020	0.9	0.10-0.0011 d_b except that θ_{SD} should be used if w14 or less	0.9
End-plate	Not pre-qualified for the *Guidelines*				

1. These capacities are for local collapse. For global collapse use $\hat{C} = 0.085$.
2. These ϕ factors are for local collapse. For global collapse use $\phi = 0.85$.
3. WUF-B: Welded Unreinforced Flange – Bolted connection.
4. WUF-W: Welded Unreinforced Flange – Welded Web connection.
5. FF: Free Flange connection.
6. RBS: Reduced Beam Section connection.
7. WFP: Welded Flange Plate connection.

For the Collapse Prevention performance level, the desired performance is to prevent global or local collapse. Global collapse is assumed to have occurred when the numerical calculation of dynamic response becomes unstable or a drift of 10% in any story has been reached. Local collapse is assumed to have occurred when the rotation at each end of a girder is so large that the gravity-load-carrying capacity is lost. Methods for determining these capacities for connections not tested for the SAC Project are given in Section 5.6.1.2.

For local collapse, the resistance factor, ϕ, is a function of the randomness in the ground motion and the uncertainty in the connection performance. The development of ϕ for connections not tested for the SAC project is described in Section 5.6.1.2. Additional information is given in the State of the Art Report on Connection Behavior (FEMA-355D).

The seismic demand is determined by multiplying the median estimate of the seismic demand, $\hat{D}$, by demand factor, γ, and an analysis demand factor, γ_a. The demand, $\hat{D}$, is calculated as the product of the estimated median story drift, θ_m, and the bias factor, C_B:

$\hat{D} = \theta_m C_B$. The bias factor is dependent on the analysis procedure used to calculate θ_m. Values of C_B are given in Table 4-7. Default values for γ, γ_a and the confidence level are given in this section. Methods for calculating these factors are given in Section 5.6.

The provisions for new design given in the *Guidelines* are established such that, given the mean estimate of the hazard at the site, there is a 95% confidence of less than 2% probability of global or local collapse in 50 years. The calculation of this confidence level is described in the next section.

Although design for the Immediate Occupancy (IO) performance level is not required for new buildings, it is highly recommended. It should also be a part of any performance evaluation. The IO performance level is assumed to have been exceeded (there is more damage, or poorer performance) if there is enough observable damage to connections that repair is necessary, or if there is a permanent drift exceeding 0.5% in any story. Default median capacities and demands, resistance factors, and demand factors are given below. Methods for determining the load and resistance factors are similar to those used for the CP performance level and are also given in the corresponding sections below.

The acceptance criteria described above may be written in equation form as

$$\lambda_{con} = \frac{\phi \hat{C}}{\gamma \gamma_a \hat{D}} \tag{5-1}$$

where:

$\hat{D}$	=	estimate of median drift demand
$\hat{C}$	=	estimate of median drift capacity – Section 5.6.1 or Tables 5-1 to 5-3
ϕ	=	resistance factor – Section 5.6.1 or Tables 5-1 to 5-3

γ	=	demand factor – Section 5.6.2.1 or Table 5-4
γ_a	=	analysis demand factor – Section 5.6.2.2 or Table 5-4
λ_{con}	=	confidence factor – used to determine the confidence level from Table 5-6

A brief description of the steps to take will be addressed in this section. Procedures for doing more detailed, or customized, application of the basic performance evaluation are given in the following sections. A method for calculating λ_{con} is given in Section 5.6.3.

$\hat{D}$ is the median estimate of the demand drift calculated using the appropriate hazard level response spectrum and any of the analysis procedures calibrated as part of the SAC Project. Any commonly used structural analysis program may be used to calculate $\hat{D}$. Default values for $\hat{C}$, ϕ, γ_a and λ_{con} are given in this section. The default values for the demand factor, γ, are listed in Table 5-4.

The global and local median collapse drifts are derived for the reduced beam section (RBS) connection. The default values for ϕ, γ and λ_{con} and for parameters given in Table 5-1 and Table 5-6 are based on studies of 20 buildings designed for a Los Angeles site. The buildings had different configurations and included eight 3-story, eight 9-story, and four 20-story buildings (Lee and Foutch, 2000). Another variable used in calculating these factors is k, which is the slope of the hazard curve for a 1.0-second period. A value of k equal to 3.0 was used for the default value which represents an average of 25 sites in California. Definitions and calculations for these parameters are given below. Although Equation 5-1 appears to be complicated, its application is straightforward, as will be demonstrated in Chapter 6.

Procedures for doing more detailed, or customized, application of the basic performance evaluation are given in the following sections. Generation and use of each uncertainty and randomness term will be described. Summary of the uncertainty and randomness are given in Table 5-25 at the end of the chapter. A method for calculating λ_{con} is given in Section 5.6.3.

The *Guidelines* writers made two changes in format to the performance evaluation procedures. The first was to combine the two coefficients, C_B and γ_a, into a single coefficient γ_a. Therefore, γ_a is now a function of the analysis procedure in the *Guidelines* and there is no C_B.

The second change affected the symbol and definition of the confidence factor. The symbol used is λ instead of λ_{con}. The relationship between λ and λ_{con} is that λ is the inverse of λ_{con} : $\lambda=1/\lambda_{con}$. So λ is the ratio of factored demand divided by factored capacity. This also required changing the values in Table 5-6 which will be introduced below.

5.6 Reliability Format Evaluation Procedures

5.6.1 Determination of Median Drift Capacity and Resistance Factors

The median drift capacities and resistance factors for connection types tested under the SAC Project are given in Tables 5-1 to 5-3. These values, corresponding to local collapse, were determined from cyclic tests of full-size connection specimens, and those for global collapse

were determined from dynamic nonlinear analysis of multi-story building models. The cyclic tests are used to determine load-deformation hysteresis behavior of the system and the maximum drift for which gravity loads may still be carried by the girders. This gravity-induced drift limit is reached when the shear tab is significantly damaged, a low-cycle fatigue crack develops in the beam web, or the load-deformation behavior of the moment connection has completely deteriorated. This local drift limit is based on the judgment of the design professional after observing the test results.

5.6.1.1 Connection Test Protocol and Determination of the Median Local Drift Capacity, $\hat{C}$

The test protocol developed for the SAC Project has been adopted by the AISC *Seismic Provisions* (SAC, 1997). Instructions on loading sequence and required response measurements are given therein. The moment vs. plastic rotation of the beam for the RBS System is shown in Figure 4-16. This is characterized by a gradual strength degradation with increasing plastic rotation. It appeared that the shear-carrying capacity was reached at a plastic rotation of about 0.06. That was also the rotation where the moment strength approached zero. One modification of the AISC test protocol that should be made is that the tests should be continued until the total drift has reached 0.06 to 0.07, so that the local collapse limit state can be determined.

Local collapse is assumed to have occurred when the rotation at each end of a girder is so large that the gravity-load-carrying capacity is lost. The default drift capacity and resistance factors as limited by local connection response for ductile welded connections are listed in Table 5-1. Those for the brittle connection representing the pre-Northridge case and partially restrained connections are listed in Table 5-2 and Table 5-3, respectively. Detailed information can be obtained from the State of the Art Report of Connection Performance (Roeder, 2000).

Table 5-2 Default Drift Capacities and Resistance Factors as Limited by Local Connection Response - Brittle (Pre-Northridge) Welded Connections (Roeder, 2000)

Connection Type	Strength Degradation Limit Drift Angle (radians) θ_{SD}	Immediate Occupancy		Collapse Prevention	
		Limit Drift Angle (radians) θ_{IO}	Capacity Reduction Factor ϕ	Limit Drift Angle[1] (radians) θ_{CP}	Capacity Reduction Factor[2] ϕ
WUF[3] (<1980)	$0.061-0.00013d_b$	0.010	0.8	Larger of $0.053-0.0006\ d_b$ or $0.061-0.00013\ d_b$	0.8
WUF[3] (>1980)	0.021	0.010	0.8	$0.053-0.0006\ d_b$	0.8

1. These capacities are for local collapse. For global collapse use $\hat{C} = 0.07$.
2. These ϕ factors are for local collapse. For global collapse use $\phi = 0.85$.
3. WUF: Welded Unreinforced Flange connection.

Table 5-3 Default Drift Capacities and Resistance Factors as Limited by Local Connection Response – Partially Restrained Connections (Roeder, 2000)

Connection Type	Strength Degradation Limit Drift Angle (radians) θ_{SD}	Immediate Occupancy		Collapse Prevention	
		Limit Drift Angle (radians) θ_{IO}	Capacity Reduction Factor ϕ	Limit Drift Angle[1] (radians) θ_{CP}	Capacity Reduction Factor[2] ϕ
DST	Full strength connections: 0.12-0.0032 d_b. Partial strength connections: $\theta_p = \frac{0.9 - 1.4 \cdot \left\{ \frac{\lvert M_{fail-TFlngFlex} - M_{fail-TStem} \rvert}{M_{fail-TFlngFlex} + M_{fail-TStem}} \right\}}{d_b}$ but no less than $\theta_p = \frac{0.6 - 1.4 \cdot \left\{ \frac{\lvert M_{fail-TFlngFlex} - M_{fail-TStem} \rvert}{M_{fail-TFlngFlex} + M_{fail-TStem}} \right\}}{d_b}$	0.030	0.90	Full strength connections: 0.14-0.0032 d_b. Partial strength connections: $\theta_p = \frac{0.9 - 1.4 \cdot \left\{ \frac{\lvert M_{fail-TFlngFlex} - M_{fail-TStem} \rvert}{M_{fail-TFlngFlex} + M_{fail-TStem}} \right\}}{d_b}$ +0.01 but no less than $\theta_p = \frac{0.6 - 1.4 \cdot \left\{ \frac{\lvert M_{fail-TFlngFlex} - M_{fail-TStem} \rvert}{M_{fail-TFlngFlex} + M_{fail-TStem}} \right\}}{d_b}$ +0.01	0.90
Clip angle	$0.5/d_b + 0.01$		0.90	$0.5/d_b + 0.03$	0.90

1. These capacities are for local collapse. For global collapse use $\hat{C} = 0.087$.
2. These ϕ factors are for local collapse. For global collapse use $\phi = 0.86$.
3. DST: Double Split Tee connection.

5.6.1.2 Calculation of Global Stability

It is important that the analytical model used for determining the global drift demand reproduce the major features of the measured response, such as sudden loss of strength or pinching. This means that the measured hysteresis behavior must be modeled as closely as possible. Figure 5-2 shows the modeled behavior of the RBS system which can be compared to the measured response given in Figure 5-1 (Veti and Engelhardt, 1999). Modeling requirements are given by Foutch (2000) and Lee and Foutch (2000). It should be noted that the connection that reaches a plastic rotation of 0.03 without significant loss of strength and 0.05 without complete loss of strength will have a median global drift capacity of 0.09 or greater, for L.A.-type ground motions. This can be thought of as the lower bound behavior of a connection that satisfies the AISC test protocol. Including the gravity columns in the model helps to stabilize the building at large drifts. If the computer program is capable of handling complex moment-rotation behavior, the moment developed in gravity beams through composite action can be included. Figure 5-3 shows a typical moment-rotation behavior for a typical interior beam-column connection (Liu and Astaneh-Asl, 1999). Figure 5-4 shows the modeled behavior. In

lieu of calculating a median drift capacity, the value $\hat{C} = 0.09$ for global stability may be used for any connection satisfying the AISC test protocol.

The global stability limit is determined using the Incremental Dynamic Analysis (IDA) technique developed by Cornell and his associates (Luco and Cornell, 1999). The procedure that was followed in doing this analysis follows:

1. Choose a suite of ten to twenty accelerograms representative of the site and hazard level. The SAC project developed typical accelerograms for Los Angeles, Seattle, and Boston sites (Somerville, 1997). These might be appropriate for similar sites.
2. Perform an elastic time-history analysis of the building for one of the accelerograms. Plot the point on a graph whose vertical axis is the spectral ordinate for the accelerogram at the first period of the building and the horizontal axis is the maximum calculated drift at any story. Draw a straight line from the origin of the axes to this point. The slope of this line is referred to as the elastic slope for the accelerogram. Calculate the slope for the rest of the accelerograms using the same procedure and calculate the median slope. The median slope is referred to as the elastic slope, S_e.
3. Perform a nonlinear time-history analysis of the building subjected to one of the accelerograms. Plot this point, as in Step 2, on the graph. Call this point Δ_1.
4. Increase the amplitude of the accelerogram and repeat step 3. This may be done by multiplying the accelerogram by a constant that increases the spectral ordinates of the accelerogram by 0.1g. Plot this point as Δ_2. Draw a straight line between points Δ_1 and Δ_2. If the slope of this line is less than 0.2 S_e, then Δ_1 is the global drift limit. This can be thought of as the point at which the inelastic drifts are increasing at five times the rate of elastic drifts.
5. Repeat step 4 until the straight line slope between consecutive points Δ_i and Δ_{i+1} is less than 0.2 S_e. When this condition is reached, Δ_i is the global drift capacity for this accelerogram. If $\Delta_{i+1} \geq 0.10$, then the drift capacity is taken as 0.10.
6. Choose another accelerogram and repeat steps 3 through 5. Do this for each accelerogram. The median capacity for global collapse is the median value of the calculated set of drift limits. An example for two accelerograms for an L.A. site for a 20-story weak-column OMF building is shown in Figure 5-5. The open triangles represent the IDA for an accelerogram where the 0.2 S_e slope determined the capacity. The open circles represent a case where the default capacity = 0.10.

The factors that affect the curve of the Incremental Dynamic Analysis (IDA) are as follows:

- P-Δ effects
- increment used for the analysis
- ground motion used
- strain-hardening ratio
- shifting of fundamental period due to nonlinearity

- higher-mode effects
- shifting of maximum-story-drift location

A strain hardening ratio of 0.03 was used for all of the analyses in this study. A ground motion intensity increment of 0.2g for the 3-story and 9-story buildings was used, whereas 0.1g was used for the 20-story buildings since sudden increases in drift were observed due to larger P-delta effects. The ground motion increment must be small enough that the drift increment is relatively small for each step. The values given above should be considered as upper bounds. The use of larger increments would usually result in a smaller drift capacity and larger variation of the capacity. Therefore, it would give conservative results.

5.6.1.3 Determination of the Resistance Factor, ϕ

The resistance factor, ϕ, accounts for the fact that the estimate of $\hat{C}$ is affected by randomness and uncertainty in the estimation process. The capacity of the building against global collapse is a function of the earthquake accelerograms used in the IDA analyses. These accelerograms are part of a random process. The capacity is also affected by the uncertainty in the load-deformation behavior of the system determined from tests. The local collapse value is also affected by uncertainties in the response of the components due to variable material properties and fabrication.

The equation for calculating ϕ is given by Jalayer and Cornell (1999)

$$\phi = \phi_{RC} \cdot \phi_{UC} \tag{5-2}$$

$$\phi_R = e^{\frac{-k\,\beta_{RC}^2}{2b}} \tag{5-3}$$

$$\phi_U = e^{\frac{-k\,\beta_{UC}^2}{2b}} \tag{5-4}$$

where:

ϕ	=	Resistance factor
ϕ_{RC}	=	Contribution to ϕ from randomness of the earthquake accelerograms
ϕ_{UC}	=	Contribution to ϕ from uncertainties in measured connection capacity
β_{RC}	=	(i) global: Standard deviation of the natural logs of the drift capacities from IDA analysis. Independent from the demand uncertainty. (ii) local: Test variability in rotation. Set to 0.20, according to Cornell (personal communication).
β_{UC}	=	Standard deviation of the natural logs of the drift capacities derived from testing. (i) global: Dependent part of the demand capacity. Negatively correlated to demand uncertainty. More description will follow in Section 5.7.10.

Therefore,

$$\beta_U = \sqrt{\beta_{Ui}^{\ 2} + \beta_{Ud}^{\ 2}} = \sqrt{\beta_{Ui}^{\ 2} + 2 \cdot \rho \cdot \beta_{dd} \cdot \beta_{cd}}$$

$$= \sqrt{3 \cdot \beta_{NTH}^{\ 2}} = \sqrt{3} \cdot \beta_{NTH}$$

where:

β_{Ui} = independent part of uncertainty

β_{Ud} = dependent part of uncertainty

	3-story	9-story	20-story
β_{NTH}	0.15	0.20	0.25
β_U	0.26	0.35	0.43

(ii) local: Calculate the coefficient of variation described in the connection Performance report (Roeder, 2000) depending on the connection type used. Set to 0.25, according to Cornell (personal communication).

k = slope of the hazard curve as discussed in Section 5.7.3

b = 1.0 for this application as discussed in Section 5.7.4

For local collapse, β_{UC} accounts for the uncertainty in the median drift capacity. This includes uncertainties in material properties, weld properties, and weld quality. The β_{RC} term would account for randomness in the natural log of the drift capacity resulting from the test setup, and testing procedure. If 10 specimens could be manufactured exactly the same way with no uncertainties and sent to ten different laboratories, the difference in test results could be associated with randomness in the testing.

The capacities determined by testing are subject to uncertainties. For new connections not considered by the SAC Project, it is likely that there will not be enough specimens tested to determine a reliable estimate of β_{UC}. In this case, it is recommended that test data from similar connections be used along with the new test results for determining β_{UC}. For SAC studies, β_{UC}= 0.25 is a representative value.

As a result,

$$\phi_{RC} = e^{\frac{-3.0x0.20^2}{2x1}} = 0.94$$

$$\phi_{UC} = e^{\frac{-3.0x0.25^2}{2x1}} = 0.91$$

$$\phi = 0.94 \times 0.91 = 0.86$$

It should be remembered that the β values are for the natural logs of the drifts and not the drifts themselves. Summaries of the uncertainty and randomness are given in Table 5-25 at the end of the chapter.

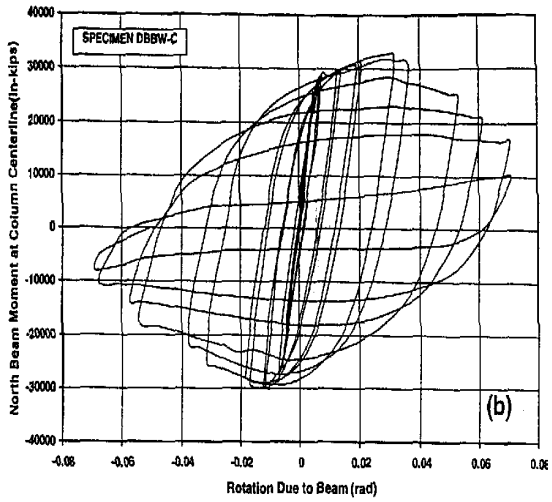

Figure 5-1 Measured Moment-Rotation Behavior of RBS Connection (Venti and Engelhardt, 1999)

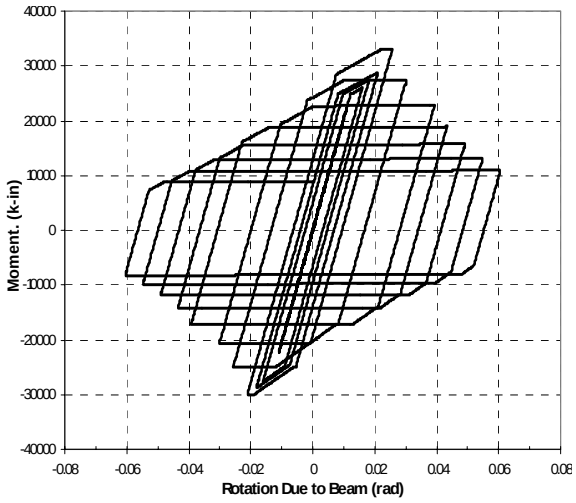

Figure 5-2 Model of Moment-Rotation Behavior of RBS Connection (Lee and Foutch, 2000)

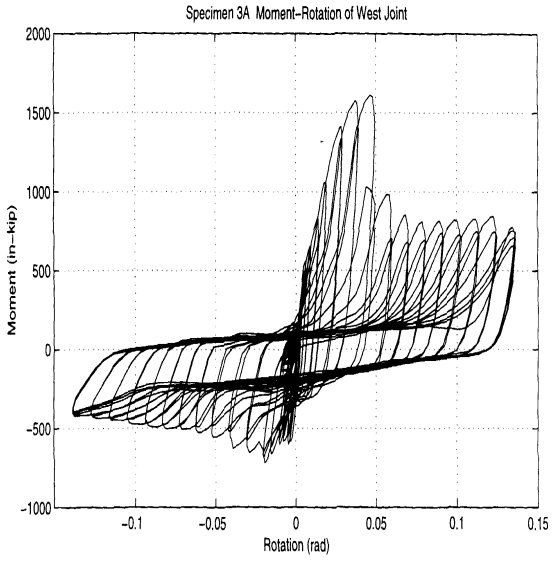

Figure 5-3 Measured Moment-Rotation Behavior of Simple Beam in Gravity Frame (Liu and Astaneh-Asl, 1999)

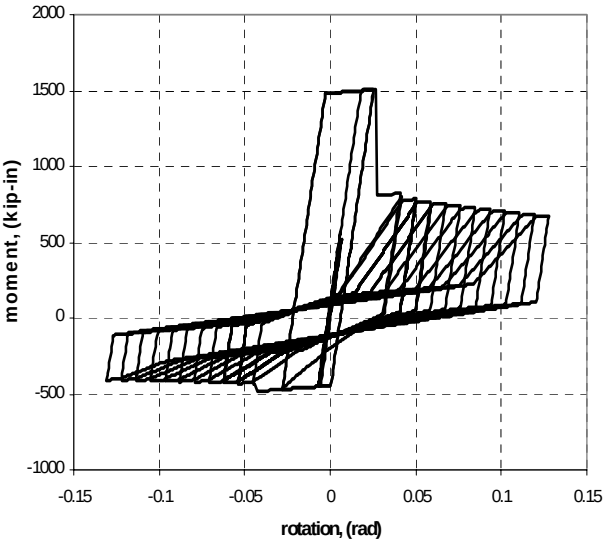

Figure 5-4 Model of Moment-Rotation Behavior of Simple Beam in Gravity Frame (Lee and Foutch, 2000)

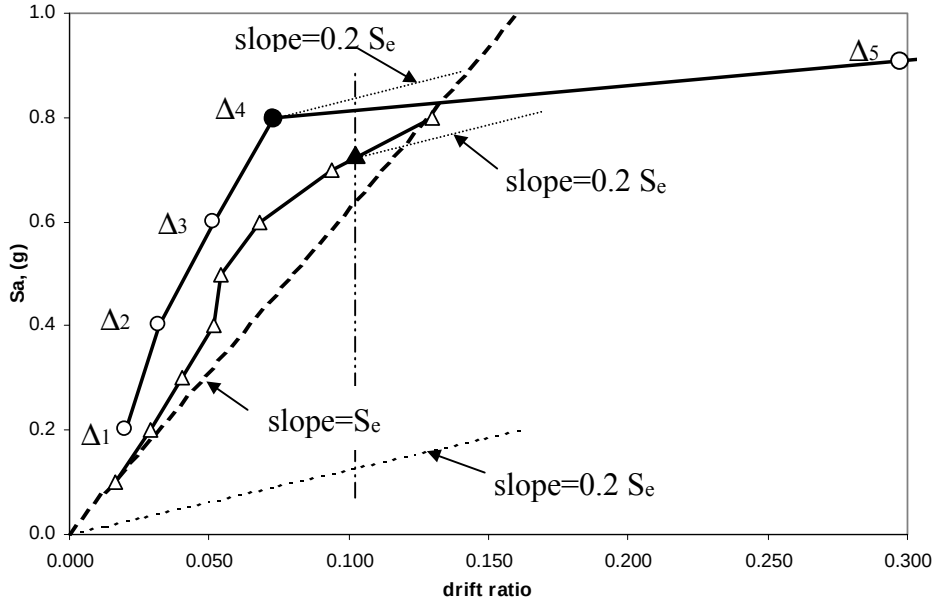

Figure 5-5 Two IDA Analyses for 9-Story WCSB OMF

5.6.2 Determination of Demand Factors, γ and γ_a

Like the resistance factor, the demand factors are subject to both random effects and uncertainty. The randomness arises from the earthquake accelerograms and orientation of the building with respect to the fault. The uncertainty comes from the nonlinear time-history analysis procedure (assumed to be 0.15, 0.20, and 0.25 for 3-story, 9-story, and 20-story, respectively) and one associated with the bias factors, which is small.

5.6.2.1 Determination of γ

The demand factor, γ, is associated with the randomness arising from the earthquake accelerograms and orientation of the building with respect to the fault. The orientation is only a factor for near-fault sites such as the LA site. For these sites the fault-parallel and fault-normal directions experience quite different shaking. For sites farther away from the fault, there is no statistical difference in the accelerograms recorded in different directions. The uncertainty from the earthquake accelerograms comes from calculating the variance of the natural log of the drift associated with the different accelerograms.

The demand factor, γ, is calculated as

$$\gamma = e^{\frac{k\beta_{RD}^2}{2b}} \tag{5-5}$$

where:

γ = the demand factor

β_{RD} = $\sqrt{\sum \beta_i^2}$ where β_i^2 is the variance of the natural log of the drifts for each element of randomness

The β values for each source of uncertainty and randomness as determined for the SAC Project are given in Section 4.7 for the 2/50 and 50/50 hazard levels, respectively. These are based on studies for three 1994 UBC-designed buildings and 20 1997-NEHRP-designed buildings for the LA site. The notation used is as follows: β_{acc}, accelerograms (demand drifts); β_{or}, orientation. The orientation factor applies only for California sites where known faults are mapped. It is recommended that the values for β given below be used for most cases. Only the β_{acc} should be determined for different sites and hazard levels. For this case, β_{acc} is the standard deviation of the log of the maximum story drifts calculated for each of 10 to 20 representative accelerograms. The default values created based on the SMF buildings designed according to the 1997 NEHRP are shown in Table 5-4. As can be seen from the table, the γ value decreases going from 3-story to 9-story but increases going to 20-story. This is due to the fact that the difference between the effect of P-Δ from the time-history analysis is larger for the 20-story than the 9-story building.

5.6.2.2 Determination of γ_a

The demand factor, γ_a, given in Table 5-4 is based on uncertainties related to the determination of demand, $\hat{D}$. The β values for each source of uncertainty as determined for the SAC Project are given in Section 5.7 for the 2/50 and 50/50 hazard levels. These are based on studies for three 1994-UBC-designed buildings and 20 1997-NEHRP-designed buildings for the LA site. The notation used is β_a for analysis procedure. The β_a is composed of five parts, and they are as follows:

- β_{NTH} associated with uncertainties in the nonlinear time-history analysis procedure.
- β_{BF} associated with uncertainty in the bias factor, which is small.
- $\beta_{damping}$ associated with uncertainty in estimating the damping value of the structure, which is small and described in Section 5.7.5.
- $\beta_{live\ load}$ associated with uncertainty in live load applied, which is small.
- $\beta_{material\ property}$ associated with uncertainty in material property, which is small.

The β_{NTH} for the results of the nonlinear time-history analysis is assumed to be 0.15, 0.20, and 0.25 for 3-story, 9-story, and 20-story, respectively. The effect of stiffnesses of structures is also combined into the nonlinear time-history analysis procedure as described in previous sections. Values of β for damping, live load, and material capacity were set to zero since the values were negligible.

The bias factor for each analysis procedure is calculated as the ratio of the median drift demand resulting from the nonlinear time-history analysis of a building for 10 to 20

accelerograms divided by the estimate of the drift demand using a particular analysis procedure. The β_{BF} for the bias factor is the coefficient of variation of the bias factors for a given building height. The values of bias factors (C_B) are given in Table 4-8.

Table 5-4 Values for γ_a and γ for CP and IO

Post-Northridge Buildings				
	γ_a		γ	
	CP	**IO**	**CP**	**IO**
3-story	1.05	1.05	1.33	1.48
9-story	1.07	1.07	1.21	1.35
20-story	1.10	1.10	1.50	1.39
Pre-Northridge Buildings				
	γ_a		γ	
	CP	**IO**	**CP**	**IO**
3-story	1.10	1.10	1.39	1.41
9-story	1.15	1.15	1.52	1.27
20-story	1.20	1.20	1.78	1.55

5.6.3 Determination of β_{UT}

The β_{UT} term is a function of the total uncertainty. Therefore, it is comprised of uncertainties associated with the demand as well as the capacity but not randomness. The β's associated with the uncertainty only are the β_U from the capacity side and the β_a from the demand side. As described earlier in this section, β_a is the combined uncertainty due to the nonlinear time-history analysis procedure, as well as the effects of P-delta. Therefore, the equation for calculating the total uncertainty is

$$\beta_{UT} = \sqrt{\left(\beta_U^{\,2} + \beta_a^{\,2}\right)} \tag{5-6}$$

The default values created based on the SMF building designs according to the 1997 NEHRP are shown in Table 5-5.

Table 5-5 Values for β_{UT} for CP and IO

Post-Northridge Buildings					
	CP against global collapse for 2/50	**CP against local collapse for 2/50**	**IO for 50/50**	**CP against global collapse for 50/50**	**CP against local collapse for 50/50**
3-story	0.32	0.30	0.30	0.32	0.30
9-story	0.40	0.32	0.32	0.40	0.32
20-story	0.50	0.35	0.35	0.50	0.35
Pre-Northridge Buildings					
	CP against global collapse for 2/50	**CP against local collapse for 2/50**	**IO for 50/50**	**CP against global collapse for 50/50**	**CP against local collapse for 50/50**
3-story	0.36	0.35	0.35	0.36	0.35
9-story	0.46	0.39	0.39	0.46	0.39
20-story	0.55	0.43	0.43	0.55	0.43

5.6.4 Calculation of the Confidence Factor, λ_{con}

The confidence factor, λ_{con}, depends on the slope of the hazard curve, k, and the uncertainty, but not randomness, associated with the natural log of the drifts. The equation for λ_{con} is (Jalayer and Cornell, 1999)

$$\lambda_{con} = e^{\left[K_x \beta_{UT} - \frac{1}{2} k \beta_{UT}^2\right]} \tag{5-7}$$

where:

λ_{con} = confidence factor

β_{UT}^2 = $\Sigma\sigma_i^2$ where σ_i is for uncertainties in the demand and capacity but not randomness

k = slope of the hazard curve

K_x = standard Gaussian variate associated with probability x of not being exceeded (found in standard probability tables)

From the preceding sections, the following β's need to be included: β_U, capacity; β_a, analysis procedures. If the relationship given in Equation 5-7 is written in terms of K_x,

$$K_x = \left[\ln(\lambda_{con}) + \frac{1}{2} \cdot k \cdot \beta_{UT}^2 \right] \cdot \frac{1}{\beta_{UT}} \tag{5-8}$$

The acceptance criteria described in Section 5.5 is written in equation form as

$$\lambda_{con} = \frac{\phi \hat{C}}{\gamma \gamma_a \hat{D}} \tag{5-9}$$

Therefore, for the evaluation purposes, one can calculate λ_{con} using Equation 5-9, and K_x using Equation 5-8. Then, the confidence level may be found in any appropriate probability reference. Since the parameters that relate the confidence level with λ_{con} are k and β_{UT}, Table 5-6 can be used to obtain the confidence level from the calculated λ_{con} value. The reverse of the procedure will work appropriately for the design process by first determining the level of confidence for the structure and then calculating the demand drift required to achieve this level of confidence.

Table 5-6 λ_{con}, as a Function of Confidence Level, Hazard Level Parameter k, and Uncertainty β_{UT}

Confidence	2%	5%	10%	20%	30%	40%	50%	60%	70%	80%	90%	95%	98%
β_{UT} = 0.3													
k=1	0.52	0.58	0.65	0.74	0.82	0.89	0.96	1.03	1.12	1.23	1.40	1.57	1.77
k=2	0.49	0.56	0.62	0.71	0.78	0.85	0.91	0.99	1.07	1.18	1.34	1.50	1.69
k=3	0.47	0.53	0.59	0.68	0.75	0.81	0.87	0.94	1.02	1.12	1.28	1.43	1.62
k=4	0.45	0.51	0.57	0.65	0.71	0.77	0.84	0.90	0.98	1.08	1.23	1.37	1.55
β_{UT} = 0.4													
k=1	0.41	0.48	0.55	0.66	0.75	0.83	0.92	1.02	1.14	1.29	1.54	1.78	2.10
k=2	0.37	0.44	0.51	0.61	0.69	0.77	0.85	0.94	1.05	1.19	1.42	1.65	1.94
k=3	0.35	0.41	0.47	0.56	0.64	0.71	0.79	0.87	0.97	1.10	1.31	1.52	1.79
k=4	0.32	0.38	0.43	0.52	0.59	0.66	0.73	0.80	0.90	1.02	1.21	1.40	1.65
β_{UT} = 0.5													
k=1	0.32	0.39	0.46	0.58	0.68	0.78	0.88	1.00	1.15	1.34	1.67	2.01	2.46
k=2	0.28	0.34	0.41	0.51	0.60	0.69	0.78	0.88	1.01	1.19	1.48	1.77	2.17
k=3	0.25	0.30	0.36	0.45	0.53	0.61	0.69	0.78	0.89	1.05	1.30	1.56	1.92
k=4	0.22	0.27	0.32	0.40	0.47	0.53	0.61	0.69	0.79	0.92	1.15	1.38	1.69
β_{UT} = 0.6													
k=1	0.24	0.31	0.39	0.50	0.61	0.72	0.84	0.97	1.14	1.38	1.80	2.24	2.86
k=2	0.20	0.26	0.32	0.42	0.51	0.60	0.70	0.81	0.96	1.16	1.51	1.87	2.39
k=3	0.17	0.22	0.27	0.35	0.43	0.50	0.58	0.68	0.80	0.97	1.26	1.56	2.00
k=4	0.14	0.18	0.23	0.29	0.36	0.42	0.49	0.57	0.67	0.81	1.05	1.31	1.67
β_{UT} = 0.7													
k=1	0.19	0.25	0.32	0.43	0.54	0.66	0.78	0.93	1.13	1.41	1.92	2.48	3.30
k=2	0.15	0.19	0.25	0.34	0.42	0.51	0.61	0.73	0.88	1.10	1.50	1.94	2.58
k=3	0.11	0.15	0.20	0.27	0.33	0.40	0.48	0.57	0.69	0.86	1.18	1.52	2.02
k=4	0.09	0.12	0.15	0.21	0.26	0.31	0.38	0.45	0.54	0.68	0.92	1.19	1.58

5.7 Modeling of Uncertainty and Randomness in Evaluation Process

5.7.1 Background

As discussed previously, a procedure for seismic performance evaluation based on nonlinear dynamics and reliability theory was developed to predict and evaluate the performance of moment-frame systems. It features full integration over the three key stochastic models: ground motion hazard curve, nonlinear dynamic displacement demand, and displacement capacity. Further, uncertainties in our knowledge and of specific events are evaluated and carried through the analysis. A number of uncertainty sources were input to the procedure such as period, live load, material properties, damping, analysis procedure, and orientation of the structure. Several limit states are defined instead of the traditional single state. The confidence percentage was obtained through the procedure and not simply a mean estimate of the annual probability.

Many parameters affect the response of the structure. Not all engineers, for example, will have the same location, same design methods, same member sizes, and same configuration. To account for all variabilities in response due to these parameters, sensitivity studies have been performed. The work from Duan and Anderson (2000), Hart and Skokan (2000), Foutch (2000), and Lee and Foutch (2000) are combined to accomplish this study. In this section, all of the variables studied will be laid out first with a description of how they were handled and how the variance of each variable was obtained.

5.7.2 Buildings Used for the Study

There are two groups of buildings used for the study. For the investigation of the variation in the parameters such as damping, period of the structure, and orientation of the ground motions analyses have been performed using the original SAC buildings that are designed according to the 1994 UBC. However, for the investigation of the analysis methods, new buildings designed according to the 1997 NEHRP *Provisions* were used.

The three buildings designed according to the 1994 UBC used the approximate periods in the code that usually give smaller values of period for conservatism. Therefore, the structure is stronger and stiffer than might actually be needed. Figure 5-6 shows the plan and elevation view for the 3-story, the 9-story, and the 20-story buildings. The member sizes for the buildings are given in Table 5-7.

Twenty buildings were designed to study the effect of building configuration on the mean and variance of the capacity and demand variables. All of the buildings were designed in accordance with the 1997 NEHRP *Provisions*. For each building height, two periods were used to calculate the design base shear. One period was the empirical one given in the *Provisions* that is a function of building height (referred to as an upper bound). The other period was calculated using the Improved Rayleigh Quotient. This equation is

$$T = 2\pi \sqrt{\frac{\sum w_i \delta_i^2}{g \sum f_i \delta_i}} \tag{5-10}$$

where:

w_i	=	weight at each floor
g	=	gravity acceleration
f_i	=	applied force at floor level i
δ_i	=	displacement at floor level i

This was referred to as a lower-bound design. For each building height, four column sizes were used: w14, w24, w30, and w36.

Since the calculated period for the 20-story building was limited by the upper bound of the period specified in the NEHRP *Provisions*, the distinction between the upper and lower bound was not possible. Therefore, a total of 20 buildings were designed according to the 1997 *Provisions* for the study. The elevation view and the plan view of the buildings are shown in Figure 4-37. The member sizes for the buildings are shown in Table 4-9. Due to the new restriction on the redundancy of the structure, an additional bay was designed to be a part of the lateral-load-resisting system for the 3-story buildings.

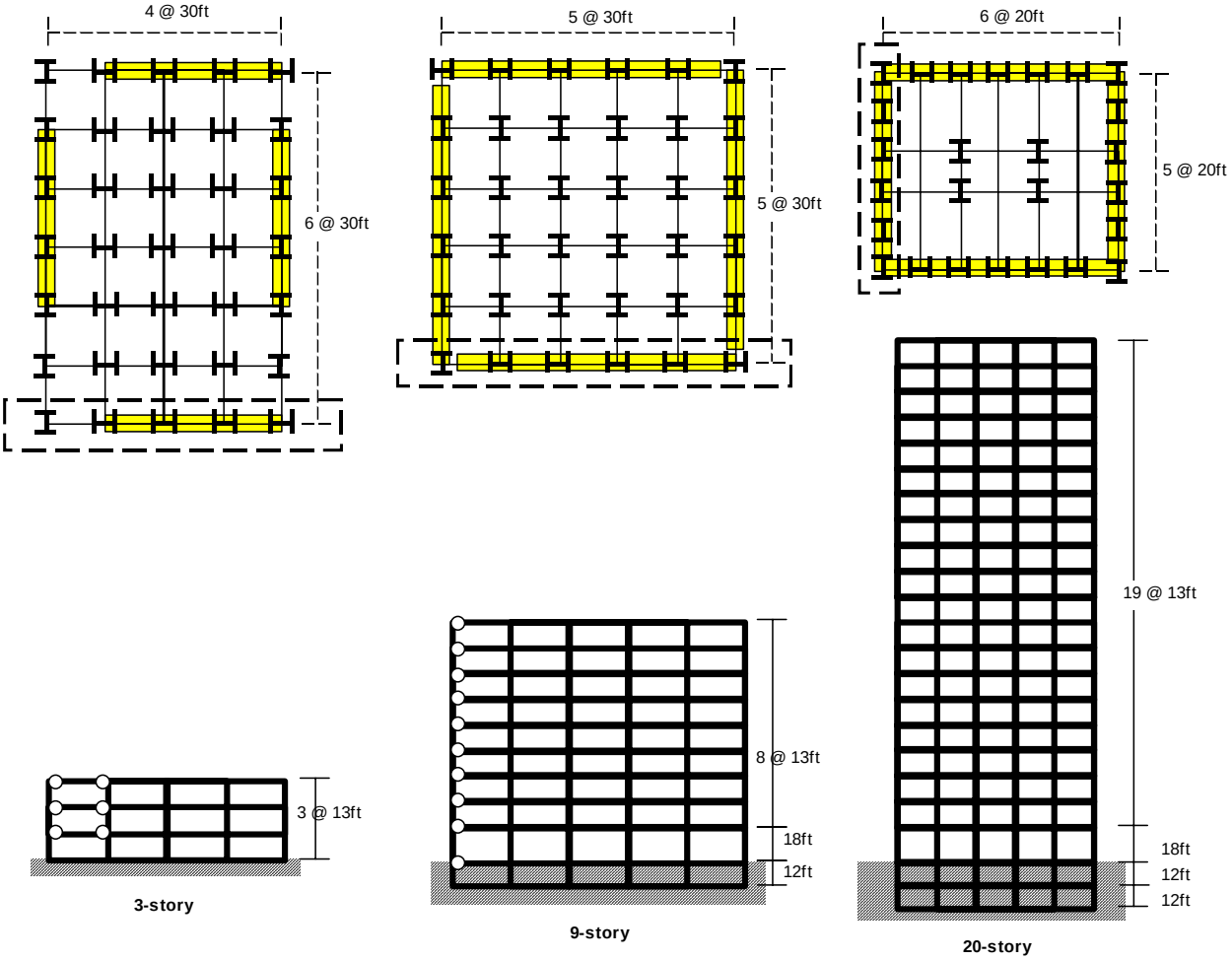

Figure 5-6 Plan and Elevation View of the 3, 9, and 20-Story Buildings Designed According to the 1994 UBC

Table 5-7 Member Sizes for the 3, 9, and 20-Story Designed According to the 1994 UBC Buildings

1994 UBC 3-story			1994 UBC 9-story			1994 UBC 20-story		
Ext. Col.	Int. Col.	Beam	Ext. Col.	Int. Col.	Beam	Ext. Col.	Int. Col.	Beam
W14x257	w14x311	w24x68	w14x233	w14x257	w24x68	15x15x0.50	w24x84	w21x50
W14x257	w14x311	w30x116	w14x257	w14x283	w27x84	15x15x075	w24x117	w24x62
W14x257	w14x311	w33x118	w14x257	w14x283	w30x99	15x15x0.75	w24x117	w27x84
			w14x283	w14x370	w36x135	15x15x0.75	w24x131	w27x84
			w14x283	w14x370	w36x135	15x15x0.75	w24x131	w30x99
			w14x370	w14x455	w36x135	15x15x0.75	w24x131	w30x99
			w14x370	w14x455	w36x135	15x15x1.00	w24x192	w30x99
			w14x370	w14x500	w36x160	15x15x1.00	w24x192	w30x99
			w14x370	w14x500	w36x160	15x15x1.00	w24x192	w30x99
			w14x370	w14x500	w36x160	15x15x1.00	w24x229	w30x99
						15x15x1.00	w24x229	w30x108
						15x15x1.00	w24x229	w30x108
						15x15x1.00	w24x229	w30x108
						15x15x1.00	w24x229	w30x108
						15x15x1.00	w24x229	w30x108
						15x15x1.25	w24x335	w30x108
						15x15x1.25	w24x335	w30x99
						15x15x1.25	w24x335	w30x99
						15x15x2.00	w24x335	w30x99
						15x15x2.00	w24x335	w30x99
						15x15x2.00	w24x335	w30x99
						15x15x2.00	w24x335	w14x22

5.7.3 Local Variation of the Slope of the Hazard Curve, k

The first parameter that was investigated was the k value, that is, the slope of the hazard curve. This parameter is a function of the hazard level, location, and period. USGS maps give S_s and S_1 for the 2/50 and 10/50 hazard levels for all locations in the U.S. This information is also available on their web site. The S_1 values are the most appropriate for steel moment frames. The hazard curve is a plot of probability of exceedance of a spectral ordinate versus spectral amplitude for a given period and is usually plotted on a log-log scale. In functional form, it is expressed as

$$H_{Si}(S_i) = k_0 S_i^{-k} \tag{5-11}$$

The value of k can be obtained by re-arranging the above equation with the two spectral values for any two hazard levels. In this study, 2% in 50 years and 10% in 50 years hazard levels were used to calculate the slope of the curve, k. The equation is in the form

$$k = \frac{\ln\left[\dfrac{H_{Sa}(Sa_{10\%})}{H_{Sa}(Sa_{2\%})}\right]}{\ln\left[\dfrac{Sa_{2\%}}{Sa_{10\%}}\right]} \tag{5-12}$$

where:

$Sa_{10\%}$	=	spectral amplitude for 10/50 hazard level
$Sa_{2\%}$	=	spectral amplitude for 2/50 hazard level
$H_{Sa}(Sa_{10\%})$	=	probability of exceedance for 10% in 50 years = 1/474 = 0.0021
$H_{Sa}(Sa_{2\%})$	=	probability of exceedance for 2% in 50 years = 1/2475 = 0.00040
i	=	period of interest (0.3 seconds for S_s and 1.0 seconds for S_1)

An example of a hazard curve for a 9-story building designed according to the 1994 UBC is shown in Figure 5-7. The two darkened points in the plot represent the 10% in 50 year and the 2% in 50 year hazard levels.

The USGS web site for a given postal zip code is used for the study. A few cities on the west coast, the central U.S., and the east coast were selected as shown in Figures 5-8 to 5-10. Twenty-five cities were selected for the state of California since it is the most seismically active state in the U.S. Table 5-8 lists the cities, corresponding spectral accelerations, and k values. The table is prepared with the β's from the 9-story building designed according to the 1997 NEHRP *Provisions*. The β's are defined as the standard deviation of the natural log of the drift due to the variation of a variable. As prescribed in the previous sections, β_R stands for the randomness in capacity from the ground motions and β_U stands for the uncertainty. β_{acc} stands for the randomness in demand from the ground motions, β_{or} is for the randomness in the orientation of the ground motions and β_a is to account for the variation from the analysis method used. Since the value of k is only dependent on the site, the values of k will not change for different buildings used in the calculations. Some typical average values of k for various locations in the U.S. are listed in Table 5-9. As a result, this table will be conservative for other parts of the country since ϕ, γ, γ_a and λ_{con} all are functions of k. As a result, the ratio

$$\frac{\phi}{\gamma \gamma_a \lambda_{con}} \tag{5-13}$$

is the most meaningful measure of variation across the country. This ratio is also listed in Table 5-8 for confidence levels of 84%, 90%, and 95%. In California, this ratio varies between 0.30 (Sacramento) and 0.36 for 25 coastal and inland locations for the 95% confidence level. For other parts of the U.S., the range was 0.30 (Sacramento, CA) to 0.41 (Dyersburg,TN). So, the confidence level will be slightly unconservative for LA and some other California sites and conservative for other parts of the country. Table 5.8 gives values of k, λ_{con} and Equation 5-13 for different parts of the U.S. for confidence levels of 84%, 90%, and 95%. However, if Equation 5-1 is rewritten as

$$\hat{D} \le \frac{\phi \cdot \hat{C}}{\gamma \cdot \gamma_a \cdot \lambda_{con}} \tag{5-14}$$

then a change in Equation 5-13 represents a difference in the required stiffness needed to satisfy the 95% confidence level. Therefore, for California, the difference between the largest value and the smallest value of this ratio is 0.36/0.30 = 1.20. This represents a difference in frame stiffness of 20%, which is fairly large. This is why Sections 5.7 is included here. All of the values of the various β's given here can probably be used anywhere in the U.S. As a result, the design professional need only recalculate ϕ, γ, γ_a and λ_{con} using the appropriate value of k for the location of a building site. Section 5.6.4 gives instructions for calculating λ_{con}.

Figure 5-11 shows how to find the $S_{1\text{-}10\%}$ and $S_{1\text{-}2\%}$ from the USGS web site for a given zip code. The zip code used for the example is for the Los Angeles site. The S_1 for the 10% in 50 year hazard level and 2% in 50 year hazard level are 0.45g and 0.77g, respectively. A database keyed to latitude and longitude of a site is also available at the same web site.

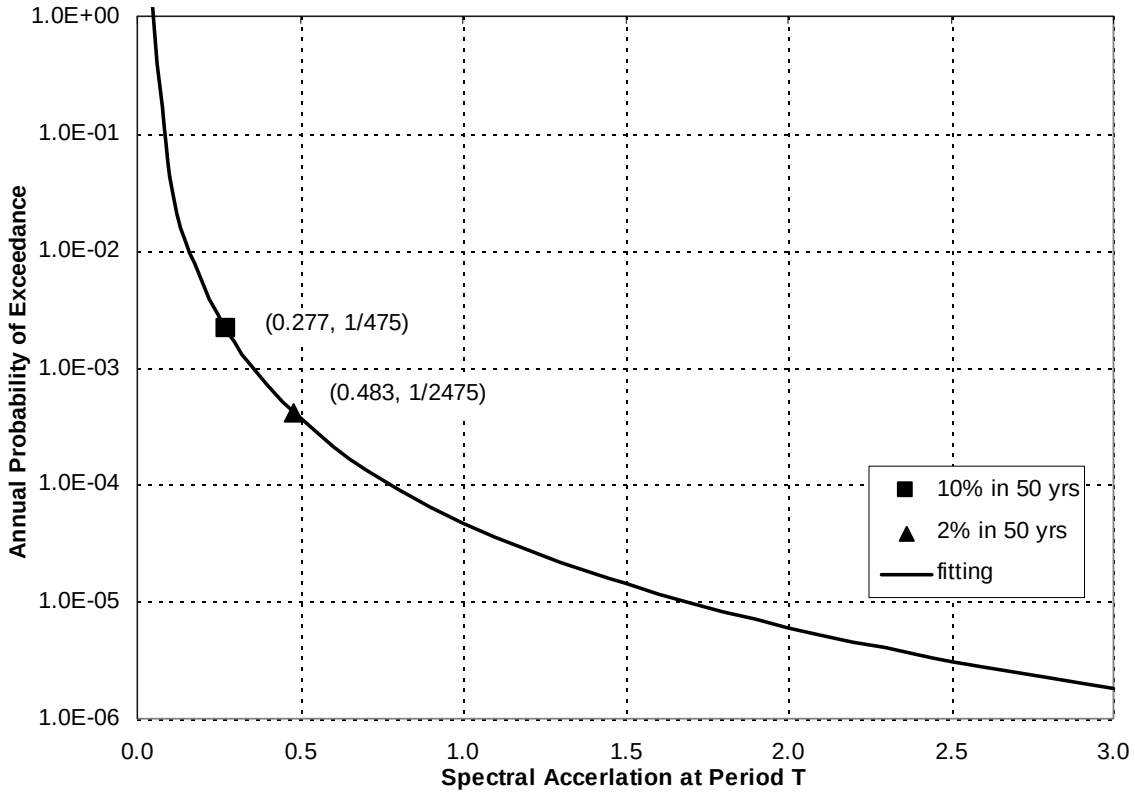

Figure 5-7 Hazard Curve for 1994 UBC 9-Story Building

Figure 5-8 Cities Selected for Study in the West Coast

Figure 5-9 Cities Selected for Study in the East Coast

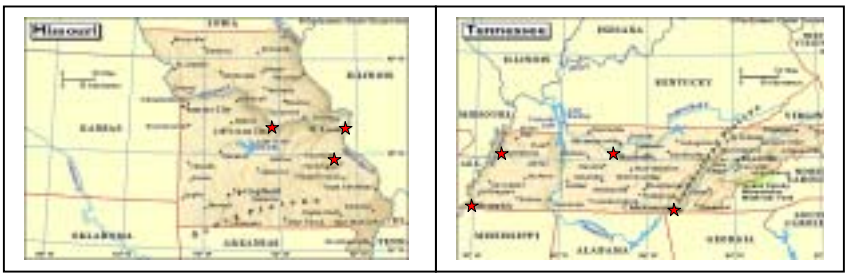

Figure 5-10 Cities Selected for Study in the Central U. S.

Table 5-8 Values of k, λ_{con} and Equation 5-13 at 1.0-Second Period for the 2/50 Hazard Level (β_R= 0.00, β_U= 0.35, β_{acc}= 0.30, β_{or}= 0.19, β_a= 0.20)

	location	10%Sa	2%Sa	k	λ_{con84}	λ_{con90}	λ_{con95}	ϕ	γ	γ_a	$\phi/\gamma\gamma_a\lambda_{con84}$	$\phi/\gamma\gamma_a\lambda_{con90}$	$\phi/\gamma\gamma_a\lambda_{con95}$
WASHINGTON	Seattle	*0.221*	*0.560*	1.7730	1.29	1.46	1.65	0.90	1.12	1.04	0.60	0.53	0.47
	Tacoma	*0.206*	*0.403*	2.4524	1.23	1.38	1.56	0.86	1.17	1.05	0.57	0.51	0.45
	Olympia	*0.204*	*0.411*	2.3578	1.24	1.39	1.57	0.87	1.16	1.05	0.58	0.51	0.45
	Port Angeles	*0.224*	*0.505*	2.0354	1.27	1.43	1.61	0.88	1.14	1.04	0.59	0.52	0.46
	Forks	*0.218*	*0.789*	1.2824	1.35	1.52	1.71	0.92	1.08	1.03	0.62	0.55	0.49
	Shelton	*0.221*	*0.452*	2.3058	1.24	1.40	1.58	0.87	1.16	1.05	0.58	0.51	0.45
OREGON	Portland	*0.174*	*0.352*	2.3419	1.24	1.39	1.57	0.87	1.16	1.05	0.58	0.51	0.45
	Salem	*0.178*	*0.389*	2.1167	1.26	1.42	1.60	0.88	1.14	1.04	0.59	0.52	0.46
	Springfield	*0.158*	*0.363*	1.9934	1.27	1.43	1.62	0.89	1.13	1.04	0.59	0.52	0.46
	Tillamook	*0.277*	*0.724*	1.7192	1.30	1.47	1.65	0.90	1.11	1.03	0.60	0.53	0.47
	Newport	*0.305*	*0.811*	1.6861	1.30	1.47	1.66	0.90	1.11	1.03	0.60	0.53	0.47
	Coos Bay	*0.305*	*0.838*	1.6341	1.31	1.48	1.66	0.90	1.11	1.03	0.60	0.54	0.47
CALIFORNIA	Santa Rosa	*0.545*	*0.966*	2.8871	1.18	1.34	1.51	0.84	1.20	1.06	0.56	0.49	0.44
	San Francisco	*0.577*	*1.001*	2.9938	1.17	1.32	1.49	0.83	1.21	1.06	0.55	0.49	0.43
	Berkeley	*0.696*	*1.309*	2.6123	1.21	1.36	1.54	0.85	1.18	1.05	0.57	0.50	0.45
	San Jose	*0.582*	*0.996*	3.0668	1.17	1.32	1.48	0.83	1.21	1.06	0.55	0.49	0.43
	Santa Cruz	*0.483*	*0.873*	2.7858	1.19	1.35	1.52	0.84	1.19	1.06	0.56	0.50	0.44
	Salinas	*0.430*	*0.750*	2.9678	1.18	1.33	1.50	0.83	1.21	1.06	0.55	0.49	0.44
	Carmel	*0.374*	*0.690*	2.6922	1.20	1.36	1.53	0.85	1.18	1.06	0.56	0.50	0.44
	Santa Maria	*0.233*	*0.452*	2.4920	1.22	1.38	1.55	0.86	1.17	1.05	0.57	0.51	0.45
	Santa Barbara	*0.435*	*0.830*	2.5483	1.22	1.37	1.55	0.86	1.17	1.05	0.57	0.50	0.45
	Burbank	*0.521*	*0.982*	2.6055	1.21	1.37	1.54	0.85	1.18	1.05	0.57	0.50	0.45
	Los Angeles	*0.381*	*0.667*	2.9422	1.18	1.33	1.50	0.84	1.20	1.06	0.55	0.49	0.44
	Anaheim	*0.322*	*0.640*	2.4087	1.23	1.39	1.56	0.86	1.16	1.05	0.57	0.51	0.45
	Oceanside	*0.252*	*0.427*	3.1350	1.16	1.31	1.48	0.83	1.22	1.06	0.55	0.49	0.43
	San Diego	*0.249*	*0.558*	2.0468	1.27	1.43	1.61	0.88	1.14	1.04	0.59	0.52	0.46
	Yreka	*0.135*	*0.277*	2.2893	1.24	1.40	1.58	0.87	1.16	1.05	0.58	0.51	0.46
	Red Bluff	*0.139*	*0.269*	2.5040	1.22	1.38	1.55	0.86	1.17	1.05	0.57	0.51	0.45
	Chico	*0.123*	*0.211*	3.0431	1.17	1.32	1.49	0.83	1.21	1.06	0.55	0.49	0.43
	Yuba City	*0.125*	*0.203*	3.4258	1.13	1.28	1.44	0.81	1.24	1.07	0.54	0.48	0.42
	Sacramento	*0.135*	*0.211*	3.7247	1.11	1.25	1.41	0.80	1.26	1.08	0.53	0.47	0.41
	Modesto	*0.164*	*0.282*	3.0656	1.17	1.32	1.48	0.83	1.21	1.06	0.55	0.49	0.43
	Fresno	*0.124*	*0.202*	3.3801	1.14	1.28	1.45	0.81	1.24	1.07	0.54	0.48	0.42
	Visalia	*0.117*	*0.198*	3.1548	1.16	1.31	1.47	0.82	1.22	1.07	0.55	0.49	0.43
	Barstow	*0.221*	*0.480*	2.1307	1.26	1.42	1.60	0.88	1.14	1.04	0.58	0.52	0.46
	San Bernardino	*0.786*	*1.283*	3.3739	1.14	1.28	1.45	0.81	1.24	1.07	0.54	0.48	0.42
	Palm Springs	*0.448*	*0.748*	3.2154	1.15	1.30	1.47	0.82	1.22	1.07	0.55	0.48	0.43
MASSACHUSETTS	Boston	*0.029*	*0.090*	1.4570	1.33	1.50	1.69	0.91	1.10	1.03	0.61	0.54	0.48
	Lynn	*0.030*	*0.091*	1.4714	1.33	1.50	1.69	0.91	1.10	1.03	0.61	0.54	0.48
	Weymouth	*0.028*	*0.086*	1.4558	1.33	1.50	1.69	0.91	1.10	1.03	0.61	0.54	0.48
NEW YORK	New York	*0.029*	*0.095*	1.3902	1.33	1.50	1.70	0.92	1.09	1.03	0.61	0.54	0.48
	Mt. Vernon	*0.029*	*0.094*	1.3929	1.33	1.50	1.70	0.92	1.09	1.03	0.61	0.54	0.48
	Middletown	*0.028*	*0.087*	1.4716	1.33	1.50	1.69	0.91	1.10	1.03	0.61	0.54	0.48
SOUTH CAROLINA	Charleston	*0.070*	*0.403*	0.9426	1.38	1.56	1.76	0.94	1.06	1.02	0.63	0.56	0.50
	Georgetown	*0.058*	*0.394*	0.8610	1.39	1.57	1.77	0.95	1.06	1.02	0.63	0.56	0.50
	Columbia	*0.061*	*0.196*	1.4030	1.33	1.50	1.70	0.92	1.09	1.03	0.61	0.54	0.48
MISSOURI	St. Louis	*0.056*	*0.188*	1.3634	1.34	1.51	1.70	0.92	1.09	1.03	0.61	0.54	0.48
	Jefferson City	*0.033*	*0.106*	1.4026	1.33	1.50	1.70	0.92	1.09	1.03	0.61	0.54	0.48
	Park Hills	*0.060*	*0.210*	1.3210	1.34	1.51	1.71	0.92	1.09	1.03	0.62	0.55	0.48
TENNESSEE	Dyersburg	*0.089*	*0.881*	0.7192	1.41	1.59	1.79	0.96	1.05	1.01	0.64	0.57	0.50
	Memphis	*0.069*	*0.423*	0.9125	1.39	1.56	1.76	0.95	1.06	1.02	0.63	0.56	0.50
	Nashville	*0.049*	*0.147*	1.5078	1.32	1.49	1.68	0.91	1.10	1.03	0.61	0.54	0.48
	Chattanooga	*0.053*	*0.142*	1.6899	1.30	1.47	1.66	0.90	1.11	1.03	0.60	0.53	0.47

Table 5-9 Typical Average Values for k for Various Locations

Location	California	Oregon	Washington	Memphis	Boston
k:	2.86	1.91	2.03	0.91	1.46

Seismic Hazards for a location by Zip Code

1. Logon to http://www.usps.gov/ncsc/ to find the zip code of your location.
2. Logon to http://geohazards.cr.usgs.gov/eq/ for Hazard values.
3. Select 'Hazard by Zip Code' in 'SEISMIC HAZARD' category on the left of the screen.
4. Type in the Zip Code of the location(s) you wish to find hazard for.
5. Click on the 'Submit Query' icon.
6. Note that the output data are in '***%' value of (g).***

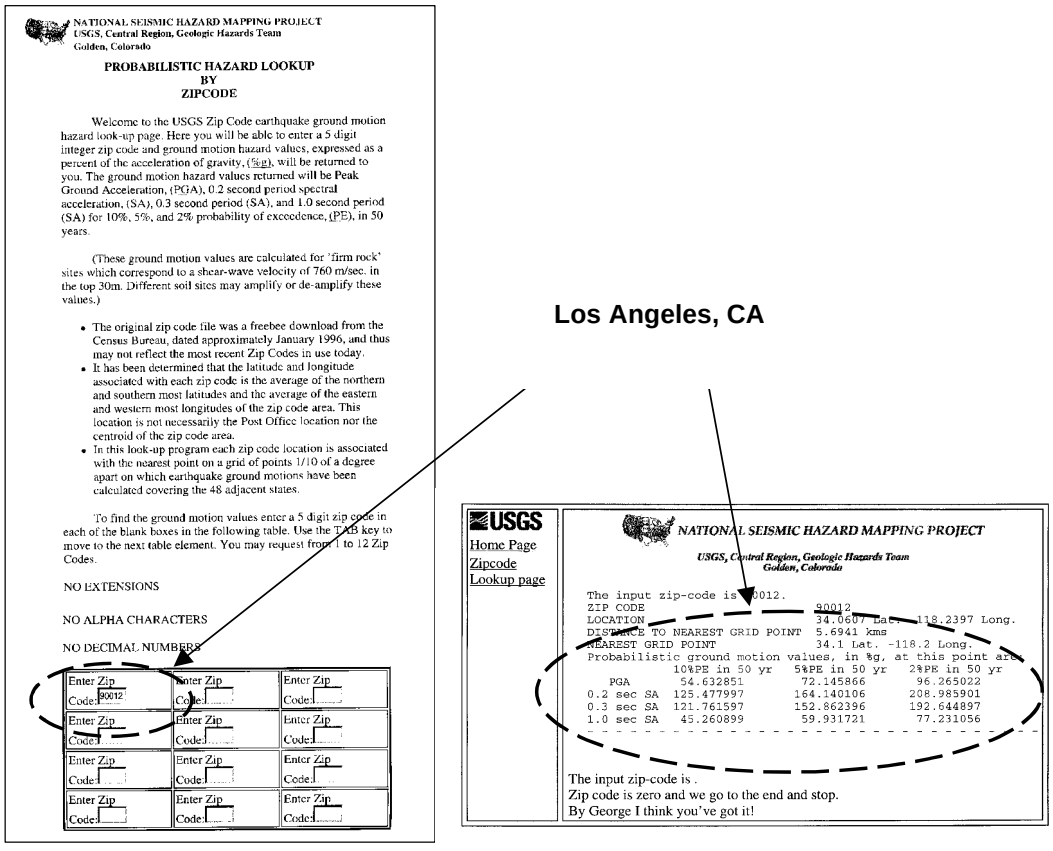

Figure 5-11 Determination of $S_{1\text{-}2\%}$ and $S_{1\text{-}10\%}$ from USGS Web Site for a Given Postal Zip Code

Example for calculating *k* at City Hall in LA:

Get S_i values from Figure 5-11 : $S_{1\text{-}10\%} = 0.45$, $S_{1\text{-}2\%} = 0.77$

$$k = \frac{\ln\left[\frac{0.0021}{0.0004}\right]}{\ln\left[\frac{0.77}{0.45}\right]} = 3.08$$

The value of S_1 for the 50/50 hazard level is needed for checking the MD performance level, but this is not listed at the USGS web site. However, it can be calculated from the data that are given.

When S_s for the 2/50 hazard level is less than 1.5g

$$\ln(S_{1-50\%}) = \ln(S_{1-10\%}) + [\ln(S_{1-2\%}) - \ln(S_{1-10\%})] \cdot [0.606\ln(P_R) - 3.73] \qquad (5\text{-}15)$$

where:

$S_{1\text{-}50\%}$ = spectral amplitude for 50/50 hazard at 1.0 second period
$S_{1\text{-}10\%}$ = spectral amplitude for 10/50 hazard at 1.0 second period
$S_{1\text{-}2\%}$ = spectral amplitude for 2/50 hazard at 1.0 second period

When S_s for 2/50 hazard is greater than or equal to 1.5g

$$S_{1-50\%} = S_{1-10\%}\left(\frac{P_R}{475}\right)^n \qquad (5\text{-}16)$$

values for the exponent n are given in Table 3.3.6-1 and

$$P_R = \frac{1}{1 - e^{0.02\ln(1-P_{E50})}} \qquad (5\text{-}17)$$

where:

P_R = return period
P_{E50} = probability of exceedance in 50 years
So P_{E50} for 50% probability of exceedance in 50 years is 0.50

$$P_R = \frac{1}{1 - e^{0.02\ln(1-0.50)}} = 72 \text{ years}$$

Values for exponent n for determination of spectral amplitude S_s and S_1

Region	S_s	S_1
California	0.29	0.29
Pacific Northwest	0.56	0.67
Intermountain	0.50	0.60
Central US	0.98	1.09
Eastern US	0.93	1.05

Example for LA City Hall for determination of $S_{1\text{-}50\%}$:

$S_s = 1.93g > 1.50g$ so use Equation 5-16

$$S_{1-50\%} = 0.45\left(\frac{72}{465}\right)^{0.29} = 0.26g$$

5.7.4 Determination of b Value

In the reliability format, the site-specific hazard curve is developed, and the value of k is determined. The relationship between the spectral acceleration and the story drift of the structure is obtained from the analysis. The relationship is assumed to be in the form of

$$\theta = S_a{}^b \tag{5-18}$$

where:

θ = story drift angle of the structure
S_a = spectral acceleration at the period of the structure
b = slope of the curve

Taking the natural log of each side of this equation results in

$$\ln(\theta) = b \cdot \ln(S_a) \tag{5-19}$$

When Equation 5-19 is re-arranged to a more familiar form for plotting

$$\ln(S_a) = \frac{1}{b} \cdot \ln(\theta) \tag{5-20}$$

So, the term b represents the slope of the curve. Therefore, the larger the value of b, the smaller the slope of the curve becomes as shown in Figure 5-6. According to Cornell (1999), for the

demand calculations, taking the value of b equal to 1.0 is reasonable since the drifts do not get unstable even at most of the 2%-in-50-year ground motion levels. However, when the capacity of the structure is calculated using the Dynamic Incremental Analysis (IDA), the slope of the curve will be small for some of the ground motions since the change in interstory drift due to a constant increase in the ground motion will be large. There are others for which the limiting drift value of 0.10 is reached before the structure becomes unstable. In those cases, the slope of the curve would be too small. Therefore, it is difficult to keep track of each slope of the dynamic analysis performed, and each of the ground motions would have a different value of b. This would be challenging to implement into the procedure and is really not necessary. Therefore taking the b value of 1.0 for both demand and capacity would simplify the procedure and be slightly conservative. The illustration of the levels at which the demands and capacities are calculated is shown in Figure 5-13.

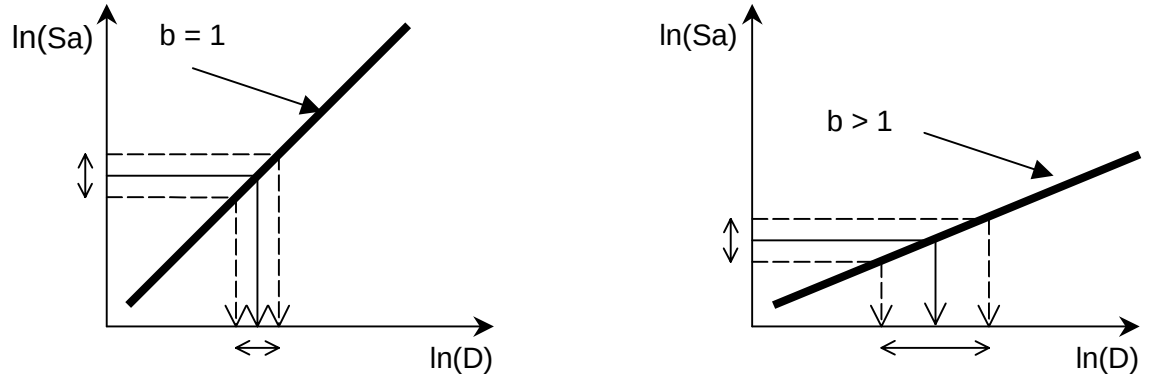

Figure 5-12 Log-log Plot of the Demand vs. Spectral Acceleration

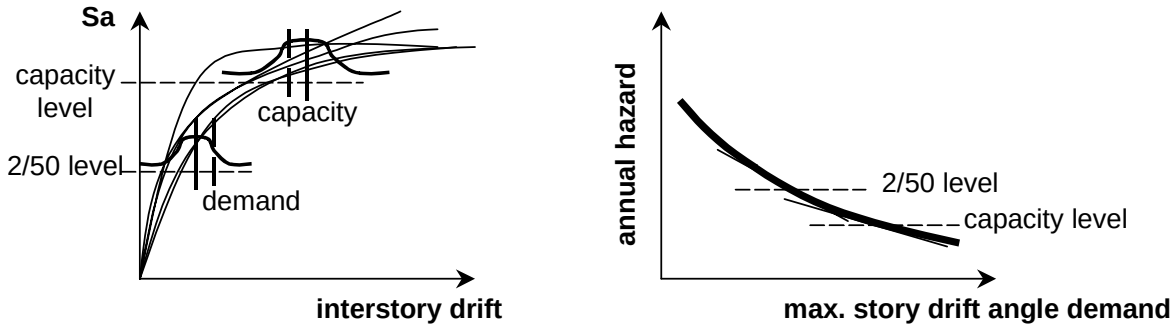

Figure 5-13 Illustration of Levels of Demand and Capacity Calculations

5.7.5 Variabilities in Damping of Structures

The standard deviation of the natural log of the variable β, for each source of uncertainty and randomness as determined for the SAC project will be given below for the 2/50 hazard level. The analyses are based on studies for three buildings designed for the LA site according to the 1994 UBC.

The uncertainty in estimating the period and damping of the structure was calculated using a collection of measured data. The major part of the data is from the report by Goel and Chopra (1997). The collected data were plotted by height verses the variable, in this case damping. Some of the data, far removed from the median values, were omitted from the study. The best-fit line from the regression analysis of the data was calculated for damping and is shown in Figure 5-14. A constant standard deviation was assumed. The changes in drift values due to the variation in the variables were then calculated. The damping values corresponding to the fundamental period of the 1994 UBC buildings are 4.31%, 3.57%, and 2.30% for 3-story (0.99 seconds), 9-story (2.17 seconds), and 20-story (3.59 seconds) buildings, respectively.

The procedure for calculating the variance of the natural log of the maximum drift associated with different sources of uncertainty is as follows:

1. Run 10 or 20 time histories using the mean of the variable and call this value μ_1.
2. Find the mean of the natural log of the corresponding maximum drifts, λ_{m1}.
3. Run 10 or 20 time histories using the mean+stdev of the variable and call this value μ_2.
4. Find the mean of the natural log of the corresponding maximum drifts, λ_{m2}.
5. Calculate the sensitivity,

$$\frac{(\lambda_{m2} - \lambda_{m1})}{(\mu_2 - \mu_1)} \tag{5-21}$$

6. The variance of the natural log of the drift with respect to the variable is the square of the sensitivity times the variance of the variable.

$$VAR = \left[\frac{(\lambda_{m2} - \lambda_{m1})}{(\mu_{\text{var}} + \sigma_{\text{var}}) - \mu_{\text{var}}}\right]^2 \times \sigma_{\text{var}}^2 = (\lambda_{m2} - \lambda_{m1})^2 \tag{5-22}$$

Therefore,

$$\beta_{\ln Drift} = \sqrt{\left[\frac{(\lambda_{m2} - \lambda_{m1})}{(\mu_{\text{var}} + \sigma_{\text{var}}) - \mu_{\text{var}}}\right]^2 \times \sigma_{\text{var}}^2} = |\lambda_{m2} - \lambda_{m1}| \tag{5-23}$$

The calculated results from the dynamic analysis using 2%-in-50-year ground motions for the LA site are listed in Table 5-10. The natural logs of the drifts as well as the variances of the variable for each story height are shown in Table 5-11. For damping, the $\beta_{lnDrift}$ values are 0.024 for 3-story, 0.030 for 9-story, and 0.034 for 20-story buildings.

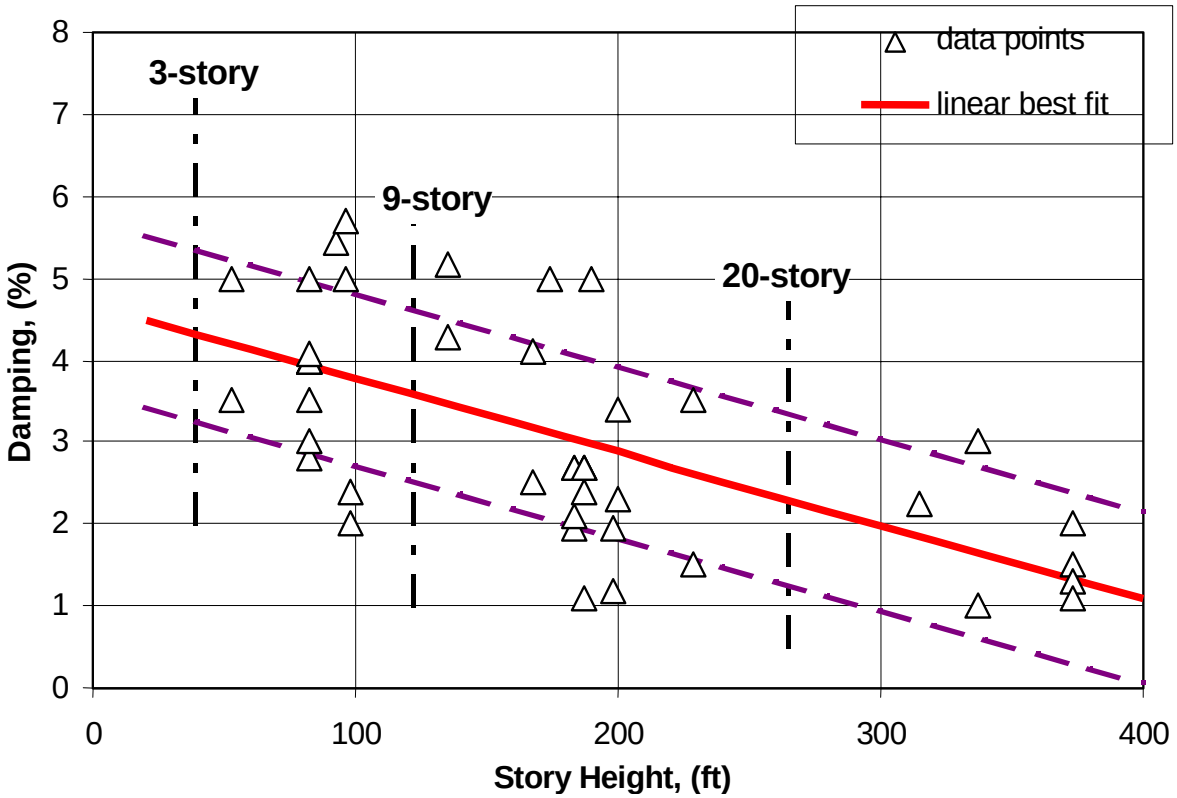

Figure 5-14 Damping Value vs. Story Height

Table 5-10 Calculated Maximum Drifts Due to Different Damping Values for 3-Story, 9-Story, and 20-Story Buildings

		3-story			9-story			20-story	
		T1=	0.9934		T1=	2.1746		T1=	3.5861
		T2=	0.2000		T2=	0.2000		T2=	0.3842
		μ	μ+σ		μ	μ+σ		μ	μ+σ
ξ		4.31	5.35		3.57	4.62		2.30	3.34
α		0.453838	0.563349		0.188924	0.244490		0.072797	0.105714
β		0.002284	0.002835		0.002081	0.002693		0.002541	0.003689
		Δμ	Δμ+σ		Δμ	Δμ+σ		Δμ	Δμ+σ
Ia21		0.0384	0.0374		0.0345	0.0337		0.0215	0.0210
Ia22		0.0411	0.0399		0.0409	0.0393		0.0235	0.0225
Ia23		0.0158	0.0156		0.0176	0.0170		0.0154	0.0146
Ia24		0.0232	0.0230		0.0528	0.0497		0.0389	0.0379
Ia25		0.0413	0.0401		0.0307	0.0303		0.0179	0.0177
Ia26		0.0472	0.0458		0.0345	0.0340		0.0221	0.0214
Ia27		0.0355	0.0344		0.0345	0.0332		0.0184	0.0185
Ia28		0.0329	0.0320		0.0260	0.0256		0.0277	0.0270
Ia29		0.0179	0.0179		0.0236	0.0226		0.0142	0.0136
Ia30		0.0197	0.0191		0.0283	0.0278		0.0504	0.0464
mean		0.0313	0.0305		0.0323	0.0313		0.0250	0.0240

Table 5-11 Natural Log of the Maximum Drifts and Variances

	3-story		9-story		20-story	
	LN(Δμ)	LN(Δμ+σ)	LN(Δμ)	LN(Δμ+σ)	LN(Δμ)	LN(Δμ+σ)
la21	-3.2593	-3.2862	-3.3668	-3.3903	-3.8414	-3.8639
la22	-3.1908	-3.2226	-3.1966	-3.2365	-3.7507	-3.7943
la23	-4.1480	-4.1634	-4.0399	-4.0745	-4.1751	-4.2256
la24	-3.7622	-3.7727	-2.9412	-3.0018	-3.2479	-3.2738
la25	-3.1873	-3.2170	-3.4835	-3.4966	-4.0222	-4.0365
la26	-3.0541	-3.0828	-3.3668	-3.3814	-3.8107	-3.8436
la27	-3.3388	-3.3695	-3.3668	-3.4052	-3.9981	-3.9912
la28	-3.4156	-3.4411	-3.6497	-3.6652	-3.5879	-3.6127
la29	-4.0225	-4.0253	-3.7465	-3.7898	-4.2535	-4.3007
la30	-3.9269	-3.9600	-3.5649	-3.5827	-2.9876	-3.0712
λ	-3.5306	-3.5540	-3.4723	-3.5024	-3.7675	-3.8014
sensitivity	-0.0226		-0.0287		-0.0325	
β	0.0235		0.0301		0.0338	
β^2	0.0006		0.0009		0.0011	

5.7.6 Variabilities in Orientation of the Ground Motions

Variation of maximum drifts due to the randomness in the orientation of the structures to the ground motion was investigated. For this study, the LA 2%-in-50-years ground motions that were not rotated 45 degrees were used. The structures were excited by ten fault-parallel components and ten fault-normal components of ground motion. The procedure for the orientation is similar to the procedure previously described for damping and period except that the orientation is a uniformly distributed function instead of a log-normally distributed function. The orientation of fault parallel (0^0) and fault normal (90^0) were selected for the study. The equation is

$$\beta_{\ln Drift} = \sqrt{\left[\frac{\left(\lambda_{90^o} - \lambda_{0^o}\right)}{\left(90^o - 0^o\right)}\right]^2 \times \sigma_{ori}^2} \tag{5-24}$$

where:

λ_{0^o} = median drift for the 0^0 rotated (fault parallel) ground motions

λ_{90^o} = median drift for the 90^0 rotated (fault normal) ground motions

σ_{ori} = standard deviation of uniform distribution from 0^o to $90^o = 26^0$

Ten pairs of ground motion were used. The acceleration time history and the response spectra for the ground motions are presented in Appendix A.2 for reference. The drift values from the dynamic analysis are listed in Table 5-12, and the natural log of the values for variance calculations are shown in Table 5-13. The $\beta_{lnDrift}$ for the orientation of the building was 0.21 for 3-story, 0.19 for 9-story, and 0.26 for 20-story buildings. The $\beta_{lnDrift}$ for 9-story building came out to be smaller than that for 20-story building. This is due to the fact that the P-Δ effect from the time-history analysis is larger for the 20-story than for the 9-story building.

One thing that is worth noting is that since the ground motions in reality are applied in pairs, the worst case would not be the case when one component is 90^0. That is because the other component, which is orthogonal to it, will be 0^0. Therefore, the worst case would be the case when the first component is located between 45^0 to 90^0 and the orthogonal component is located at larger than 90^0. An illustration of this is shown in Figure 5-15.

Table 5-12 Calculated Maximum Drifts Due to Different Orientations for 3-Story, 9-Story, and 20-Story Building Sensitivity of Period

	3-story		9-story		20-story	
	T1= 0.9934		T1= 2.1746		T1= 3.5861	
	T2= 0.2000		T2= 0.2000		T2= 0.3842	
	normal	parallel	normal	parallel	normal	parallel
	90.0	0.0	90.0	0.0	90.0	0.0
ξ	4.31	4.31	3.57	3.57	2.30	2.30
α	0.453838	0.453838	0.188924	0.188924	0.072797	0.072797
β	0.002284	0.002284	0.002081	0.002081	0.002541	0.002541
	90.0	0.0	90.0	0.0	90.0	0.0
LF21, 22	0.0528	0.0237	0.0510	0.0230	0.0270	0.0190
LF23, 24	0.0207	0.0179	0.0389	0.0215	0.0410	0.0197
LF25, 26	0.0518	0.0165	0.0336	0.0219	0.0287	0.0138
LF27, 28	0.0421	0.0263	0.0358	0.0298	0.0446	0.0199
LF29, 30	0.0177	0.0165	0.0270	0.0167	0.0273	0.0264
LF31, 32	0.0392	0.0309	0.0353	0.0225	0.0320	0.0244
LF33, 34	0.0279	0.0225	0.0415	0.0264	0.0589	0.0161
LF35, 36	0.0757	0.0212	0.0984	0.0208	0.1510	0.0147
LF37, 38	0.1078	0.0153	0.0726	0.0150	0.0655	0.0129
LF39, 40	0.0533	0.0191	0.0350	0.0317	0.0369	0.0175
mean	0.0489	0.0210	0.0469	0.0229	0.0513	0.0184

Table 5-13 Natural Log of the Drifts and Variances

	3-story		9-story		20-story	
	LN(90)	LN(0)	LN(90)	LN(0)	LN(90)	LN(0)
LF21, 22	-2.9422	-3.7427	-2.9759	-3.7723	-3.6119	-3.9633
LF23, 24	-3.8757	-4.0238	-3.2468	-3.8397	-3.1942	-3.9271
LF25, 26	-2.9607	-4.1043	-3.3932	-3.8213	-3.5509	-4.2831
LF27, 28	-3.1681	-3.6401	-3.3298	-3.5132	-3.1100	-3.9170
LF29, 30	-4.0353	-4.1052	-3.6119	-4.0923	-3.6009	-3.6344
LF31, 32	-3.2379	-3.4786	-3.3439	-3.7942	-3.4420	-3.7132
LF33, 34	-3.5784	-3.7946	-3.1821	-3.6344	-2.8319	-4.1289
LF35, 36	-2.5811	-3.8530	-2.3187	-3.8728	-1.8905	-4.2199
LF37, 38	-2.2278	-4.1819	-2.6228	-4.1997	-2.7257	-4.3505
LF39, 40	-2.9323	-3.9576	-3.3524	-3.4514	-3.2995	-4.0456
λ	-3.1539	-3.8882	-3.1377	-3.7991	-3.1258	-4.0183
sensitivity	0.0082		0.0073		0.0099	
β	0.2121		0.1911		0.2578	
β^2	0.0450		0.0365		0.0665	

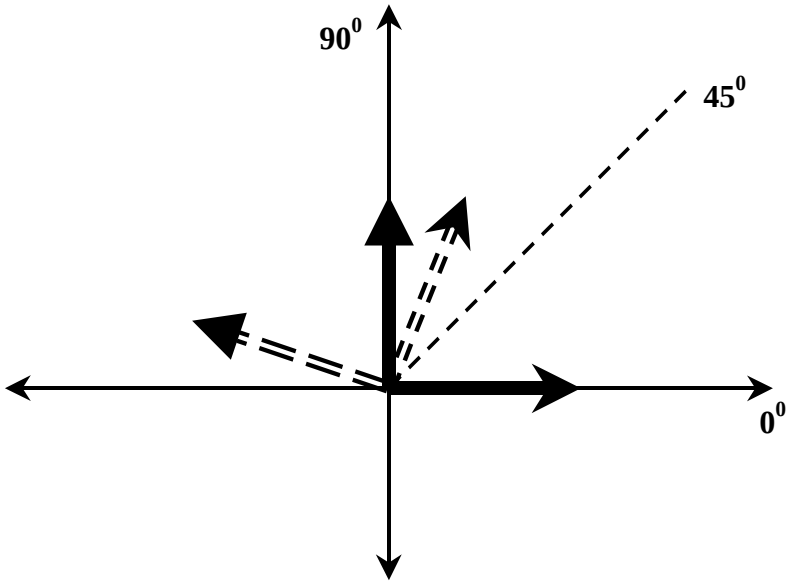

Figure 5-15 Illustration of the Worst Ground Motion Pair

5.7.7 Uncertainties in Analysis Methods

The β values for each source of uncertainty and randomness as determined for the SAC project are given below for the 2/50 and 50/50 hazard levels. These are based on studies for 20 buildings designed for the LA site. The values are averaged from eight 3- and 9-story buildings and four 20-story buildings.

The analysis procedures that are investigated are as follows:

- 1997 NEHRP Linear Static Procedure - 97NEHRP-LSP
- FEMA-273 Linear Static Procedure - F273-LSP
- FEMA-273 Modal Analysis Procedure - F273-MAP
- Linear Time-History Procedure - LTHP
- FEMA-273 Nonlinear Static Procedure - F273-NSP
- Capacity Spectrum Procedure - CSM-NSP
- Nonlinear Time-History Procedure - NTHP

Detailed procedures for each of the analysis methods will not be discussed in this report. They can be found from the reports by Hart and Skokan (2000) and Duan and Anderson (2000).

The main purpose of this part of the study is to get the bias factor that would correct the drift of the corresponding analysis method to the nonlinear time-history analysis method. This is based on the assumption that the nonlinear time-history analysis method is exact. The β_{NTH} for the nonlinear time-history procedure is included independently. The bias factor is defined as follows:

$$B.F. = \frac{drift\ due\ to\ NTH}{drift\ due\ to\ corresponding\ analysis\ method} \tag{5-25}$$

The variability of each method with the corresponding bias factor is also calculated. The variations of the corrected drift values due to the analysis method were calculated by taking the coefficient of variation of the maximum drifts. The values of the variations are expected to be very small since the bias factor will shift the drift values very close to the correct drift value.

The USC team headed by Anderson has studied the Linear Procedures (Duan and Anderson, 2000). The UCLA team headed by Hart studied the Nonlinear Static Procedures as well as the Capacity Spectrum Method (Hart and Skokan, 2000). The fundamental periods of each of the structures that were used for the study are shown in Table 5-14. The calculated drift values for each of the buildings for each of the methods are given in Table 5-15 for the 2%-in-50-year hazard level and in Table 5-16 for the 50%-in-50-year hazard level. This table includes the average values for each of the story heights as well as the weighted average for all of the story heights.

Since different teams performed the work, one change in the data values was necessary to calculate the bias factor and the variance of the drifts correctly. The change to the calculate drift values was to account for the different damping levels used for the different analysis procedures of the structure. The 5%-damped spectra were used for the 1997 NEHRP *Provisions* and FEMA-273 Modal Analysis Procedure, whereas the other FEMA-273 procedures and the Capacity Spectrum methods used the spectra corresponding to the damping levels calculated for different story heights in Section 4.2.7. Therefore, damping levels for the 3-story (4.31%), the 9-story (3.57%), and the 20-story (2.30%) needed to be converted to the 5% damping level. This was tried using three different methods. The first two methods gave somewhat unreasonable values, so the third method was selected for the study.

The first method of converting different damping levels to 5% was to use the damping conversion table given in FEMA-273. The response spectra values for different damping values are given. The table in FEMA-273 and B_S and B_1 values calculated using the linear interpolation are shown in Table 5-17 and Table 5-18. B_s and B_1 are damping coefficients. The response spectra for the corresponding damping levels as well as for the 5% damping level are plotted in Figure 5-16. The spectral acceleration values at each fundamental period of the structures were found and divided by those values for the 5% damped spectra. Then the average of those values for each story height was calculated. They are 0.94, 0.91, and 0.84 for 3-story, 9-story, and 20-story buildings, respectively. Although the values decreased with the height of the structure as expected, the coarseness of the damping points for linear interpolation in addition to the somewhat smaller ratio than expected made this method not appropriate.

The second method that was investigated required calculating the elastic response spectrum corresponding to each damping level. Therefore, 5%, 4.3%, 3.6%, and 2.3% damped spectra were generated for the 2%-in-50-year hazard level. The plot of those spectra with the smooth response spectra, which is usually generated for the 5% damping level is shown in Figure 5-17. The method of getting the conversion factor for different damping levels was to take the difference between the smooth response spectra and the different damped response spectra at the

fundamental periods of the structures. Again, the average value of those factors for each story height was calculated. They are 1.03, 0.94, and 1.14 for the 3-story, 9-story, and 20-story buildings, respectively. This method seemed inappropriate since the factors decrease and increase with the increase in height.

The third method that is selected for the study used the same plot shown in Figure 5-17. However, instead of using the smooth response spectra, the real response spectra for the 5% damping level was used to calculate the conversion factor. This was done by taking the average of the ratio of the median spectral acceleration values at the fundamental period of the structures for 5% and those for the corresponding damping levels. Again, 0.83 scaled ground motions were used for the LA 2%-in-50-year hazard level. Table 5-19 to Table 5-21 show the calculated spectral values as well as the average scale factor to be used for each story height. The average of the ratios came out to be 0.96, 0.93, and 0.90 for the 3-story, the 9-story, and the 20-story buildings, respectively. These values were used to scale the drift values down to the 5% damping level. The same factors were used to correct the drift values for the 50%-in-50-year hazard level. The final corrected drift values for all the described analysis methods are shown in Table 5-22 and Table 5-23. By rounding off the values in these tables and using engineering judgment, Table 4-8 was developed.

As can be seen from the results, all of the analysis methods for the 2%-in-50-year hazard level somewhat fail to capture the P-delta effects as the structures get taller. Therefore, the methods under-predict the drift for taller structures. The linear static procedure from both the 1997 NEHRP *Provisions* and FEMA-273 predicts the response the best. The NEHRP and FEMA-273 Modal Analysis Procedures failed to predict accurately the response of the taller stories even though three modes were used for the drift calculation of the 20-story building. One mode for the 3-story and two modes for the 9-story were used. For all of the story heights, the Linear Time History method over-predicted the response of the structure. All of the methods for the 50%-in-50-year hazard level predicted the response better since the responses stay mostly in the elastic range with small drift values. Not much effect from P-delta is expected.

Table 5-14 Fundamental Period of Each Structure

Column	design	3-story	9-story	20-story
w14	**LB**	1.00 (sec)	2.45 (sec)	3.47 (sec)
	UB	0.88 (sec)	2.16 (sec)	
w24	**LB**	1.00 (sec)	2.47 (sec)	3.43 (sec)
	UB	0.87 (sec)	2.18 (sec)	
w30	**LB**	1.00 (sec)	2.44 (sec)	3.43 (sec)
	UB	0.86 (sec)	2.18 (sec)	
w36	**LB**	0.99 (sec)	2.47 (sec)	3.46 (sec)
	UB	0.84 (sec)	2.18 (sec)	

Table 5-15 Drift and Variance Values for Different Analysis Methods Using LA 2% in 50 Year Hazard Level Before Corrections (Hart and Skokan, 2000 and Duan and Anderson, 2000)

LA 2/50	column	design	NTH	N97L		F273L		F273M		ETH		F273N		CSP	
				drift	B.F.	drift	B.F.	drift	B.F.	drift	B.F.	drift	B.F.	drift	B.F.
3-story	w14	LB	0.030	0.030	1.00	0.048	0.63	0.036	0.83	0.033	0.90	0.034	0.87	0.023	1.31
		UB	0.027	0.030	0.91	0.047	0.58	0.033	0.83	0.032	0.85	0.035	0.78	0.023	1.18
	w24	LB	0.029	0.030	0.96	0.048	0.60	0.037	0.78	0.033	0.86	0.034	0.84	0.022	1.28
		UB	0.025	0.030	0.83	0.047	0.53	0.032	0.78	0.032	0.78	0.034	0.74	0.022	1.13
	w30	LB	0.028	0.030	0.94	0.045	0.63	0.037	0.76	0.034	0.84	0.040	0.70	0.022	1.31
		UB	0.024	0.030	0.81	0.039	0.63	0.032	0.76	0.031	0.78	0.029	0.84	0.018	1.34
	w36	LB	0.028	0.030	0.94	0.046	0.62	0.037	0.77	0.034	0.83	0.033	0.85	0.021	1.32
		UB	0.024	0.030	0.81	0.039	0.62	0.031	0.78	0.032	0.76	0.029	0.83	0.019	1.31
	μ		0.027	0.030	0.90	0.045	0.60	0.034	0.79	0.033	0.82	0.034	0.81	0.021	1.27
	σ		0.0022	0.0000	0.0742	0.0038	0.0344	0.0026	0.0283	0.0011	0.0479	0.0035	0.0610	0.0019	0.0754
	COV		0.08		0.08		0.06		0.04		0.06		0.08		0.06

LA 2/50	column	design	NTH	N97L		F273L		F273M		ETH		F273N		CSP	
				drift	B.F.	drift	B.F.	drift	B.F.	drift	B.F.	drift	B.F.	drift	B.F.
9-story	w14	LB	0.036	0.030	1.20	0.048	0.75	0.034	1.06	0.042	0.85	0.042	0.85	0.027	1.32
		UB	0.036	0.030	1.19	0.041	0.87	0.028	1.28	0.040	0.90	0.037	0.97	0.023	1.54
	w24	LB	0.034	0.030	1.14	0.048	0.71	0.032	1.07	0.042	0.82	0.041	0.83	0.025	1.39
		UB	0.033	0.030	1.10	0.042	0.78	0.029	1.13	0.039	0.85	0.035	0.93	0.023	1.44
	w30	LB	0.035	0.030	1.16	0.047	0.74	0.031	1.12	0.042	0.83	0.043	0.81	0.027	1.30
		UB	0.032	0.030	1.07	0.042	0.76	0.028	1.15	0.038	0.84	0.031	1.03	0.023	1.40
	w36	LB	0.034	0.030	1.13	0.050	0.68	0.032	1.06	0.042	0.81	0.044	0.77	0.027	1.25
		UB	0.034	0.030	1.12	0.043	0.78	0.028	1.20	0.039	0.86	0.038	0.88	0.024	1.39
	μ		0.034	0.030	1.14	0.045	0.76	0.030	1.13	0.040	0.84	0.039	0.88	0.025	1.38
	σ		0.0013	0.0000	0.0447	0.0035	0.0580	0.0023	0.0774	0.0018	0.0300	0.0044	0.0867	0.0019	0.0891
	COV		0.04		0.04		0.08		0.07		0.04		0.10		0.06

LA 2/50	column	design	NTH	N97L		F273L		F273M		ETH		F273N		CSP	
				drift	B.F.	drift	B.F.	drift	B.F.	drift	B.F.	drift	B.F.	drift	B.F.
20-story	w14	L&UB	0.024	0.018	1.34	0.027	0.89	0.024	1.01	0.029	0.83	0.033	0.74	0.020	1.19
	w24	L&UB	0.024	0.018	1.34	0.028	0.86	0.024	1.01	0.030	0.81	0.031	0.77	0.020	1.21
	w30	L&UB	0.024	0.018	1.36	0.028	0.87	0.024	1.02	0.030	0.81	0.031	0.78	0.020	1.23
	w36	L&UB	0.024	0.018	1.34	0.028	0.86	0.024	1.00	0.030	0.80	0.033	0.73	0.020	1.20
	μ		0.024	0.018	1.35	0.028	0.87	0.024	1.01	0.030	0.81	0.032	0.75	0.020	1.20
	σ		0.0002	0.0000	0.0087	0.0005	0.0156	0.0000	0.0065	0.0004	0.0090	0.0008	0.0219	0.0002	0.0162
	COV		0.01		0.01		0.02		0.01		0.01		0.03		0.01

LA 2/50	column	design	NTH	N97L		F273L		F273M		ETH		F273N		CSP	
				drift	B.F.	drift	B.F.	drift	B.F.	drift	B.F.	drift	B.F.	drift	B.F.
3, 9, and 20-story	μ				1.13		0.75		0.98		0.83		0.82		1.29
	σ				0.192		0.119		0.154		0.034		0.081		0.097
	COV				0.17		0.16		0.16		0.04		0.10		0.08

Table 5-16 Drift and Variance Values for Different Analysis Methods Using LA 50% in 50 Year Hazard Level Before Corrections (Hart and Skokan, 2000 and Duan and Anderson, 2000)

LA 2/50	column	design	NTH	N97L		F273L		F273M		ETH		F273N		CSP	
				drift	B.F.	drift	B.F.	drift	B.F.	drift	B.F.	drift	B.F.	drift	B.F.
3-story	w14	LB	0.009	0.009	0.99	0.009	0.99	0.008	1.10	0.009	0.96	0.007	1.30	0.006	1.48
		UB	0.007	0.009	0.81	0.009	0.81	0.008	0.90	0.009	0.85	0.007	1.04	0.006	1.20
	w24	LB	0.007	0.009	0.80	0.009	0.80	0.008	0.89	0.009	0.80	0.007	1.06	0.006	1.20
		UB	0.006	0.009	0.69	0.009	0.69	0.008	0.77	0.009	0.72	0.007	0.90	0.006	1.04
	w30	LB	0.007	0.009	0.80	0.009	0.80	0.008	0.89	0.009	0.79	0.007	1.04	0.006	1.23
		UB	0.006	0.007	0.88	0.007	0.88	0.006	0.98	0.008	0.81	0.006	1.04	0.005	1.22
	w36	LB	0.007	0.009	0.83	0.009	0.83	0.008	0.92	0.009	0.79	0.007	1.09	0.006	1.26
		UB	0.006	0.007	0.90	0.007	0.90	0.006	1.00	0.008	0.80	0.006	1.05	0.005	1.23
	μ		0.007	0.009	0.84	0.009	0.84	0.008	0.93	0.009	0.82	0.007	1.06	0.006	1.23
	σ		0.0009	0.0009	0.0894	0.0009	0.0894	0.0008	0.0993	0.0007	0.0684	0.0004	0.1085	0.0004	0.1209
	COV		0.13		0.11		0.11		0.11		0.08		0.10		0.10

LA 2/50	column	design	NTH	N97L		F273L		F273M		ETH		F273N		CSP	
				drift	B.F.	drift	B.F.	drift	B.F.	drift	B.F.	drift	B.F.	drift	B.F.
9-story	w14	LB	0.009	0.008	1.06	0.008	1.06	0.007	1.22	0.009	0.98	0.006	1.37	0.006	1.53
		UB	0.008	0.008	1.03	0.008	1.03	0.006	1.31	0.008	0.97	0.006	1.29	0.005	1.45
	w24	LB	0.008	0.008	1.03	0.008	1.03	0.007	1.17	0.009	0.92	0.006	1.32	0.006	1.49
		UB	0.007	0.008	0.93	0.008	0.93	0.006	1.21	0.008	0.87	0.006	1.16	0.006	1.31
	w30	LB	0.008	0.008	1.02	0.008	1.02	0.007	1.18	0.009	0.93	0.006	1.32	0.006	1.48
		UB	0.007	0.008	0.92	0.008	0.92	0.006	1.20	0.008	0.87	0.006	1.16	0.006	1.30
	w36	LB	0.008	0.008	0.96	0.008	0.96	0.007	1.15	0.009	0.92	0.006	1.26	0.006	1.42
		UB	0.007	0.008	0.92	0.008	0.92	0.006	1.21	0.008	0.88	0.006	1.15	0.006	1.30
	μ		0.008	0.008	0.98	0.008	0.98	0.007	1.21	0.009	0.92	0.006	1.25	0.006	1.41
	σ		0.0005	0.0002	0.0555	0.0002	0.0555	0.0005	0.0480	0.0003	0.0428	0.0001	0.0842	0.0001	0.0944
	COV		0.07		0.06		0.06		0.04		0.05		0.07		0.07

LA 2/50	column	design	NTH	N97L		F273L		F273M		ETH		F273N		CSP	
				drift	B.F.	drift	B.F.	drift	B.F.	drift	B.F.	drift	B.F.	drift	B.F.
20-story	w14	L&UB	0.006	0.004	1.46	0.004	1.46	0.006	1.08	0.007	0.98	0.004	1.81	0.004	1.85
	w24	L&UB	0.007	0.005	1.46	0.005	1.46	0.006	1.09	0.007	0.98	0.004	1.79	0.004	1.83
	w30	L&UB	0.007	0.005	1.48	0.005	1.48	0.006	1.13	0.007	0.99	0.004	1.84	0.004	1.87
	w36	L&UB	0.007	0.005	1.44	0.005	1.44	0.006	1.10	0.007	0.99	0.004	1.78	0.004	1.81
	μ		0.007	0.005	1.46	0.005	1.46	0.006	1.10	0.007	0.98	0.004	1.81	0.004	1.84
	σ		0.0001	0.0001	0.0174	0.0001	0.0174	0.0000	0.0226	0.0001	0.0033	0.0001	0.0250	0.0001	0.0246
	COV		0.02		0.01		0.01		0.02		0.00		0.01		0.01

LA 2/50	column	design	NTH	N97L		F273L		F273M		ETH		F273N		CSP	
				drift	B.F.	drift	B.F.	drift	B.F.	drift	B.F.	drift	B.F.	drift	B.F.
3, 9, and 20-story	μ				1.09		1.09		1.08		0.91		1.37		1.49
	σ				0.277		0.277		0.131		0.083		0.331		0.274
	COV				0.25		0.25		0.12		0.09		0.24		0.18

Table 5-17 Response Spectra Values for Different Damping Levels Specified in FEMA-273

damping, (%)	B_S	B_1
2.0	0.8	0.8
5.0	1.0	1.0
10.0	1.3	1.2

Table 5-18 Calculated Response Spectra Values for Different Damping Levels Using Values in FEMA-273

damping, (%)	B_S	B_1
4.3	0.95	0.95
3.6	0.91	0.91
2.3	0.82	0.82

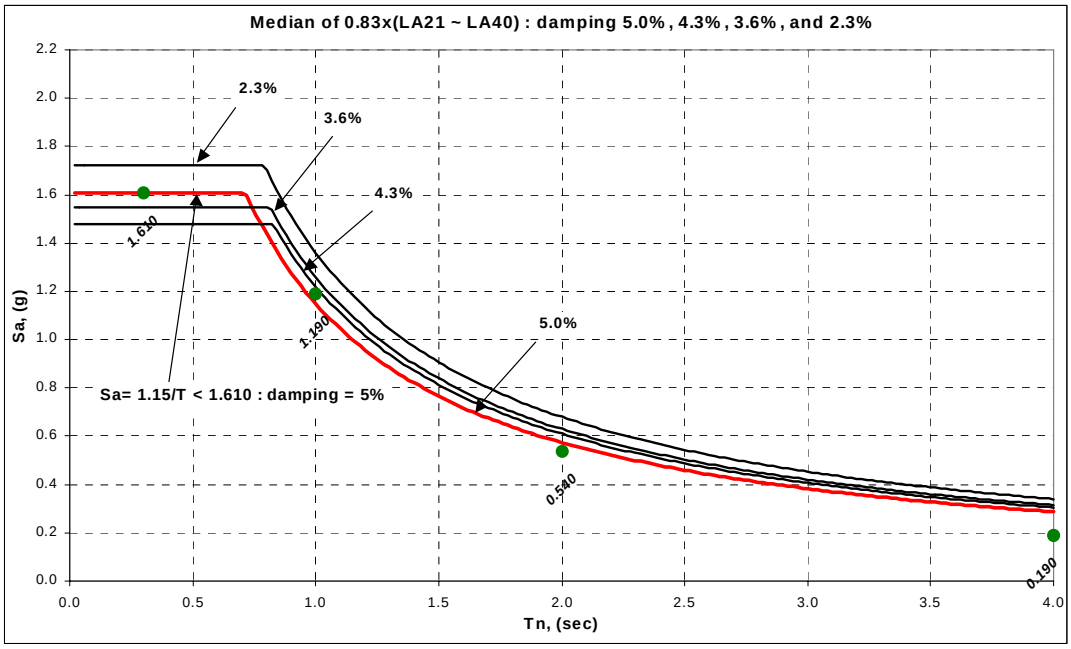

Figure 5-16 Response Spectra of 5.0%, 4.3%, 3.6%, and 2.3% Damping for FEMA-273

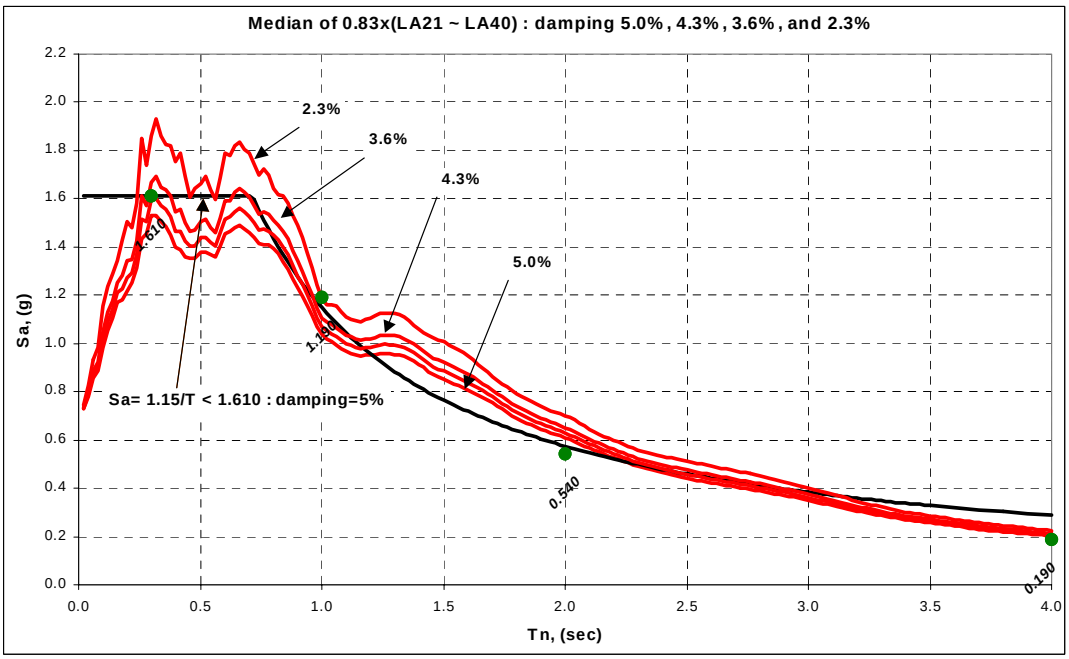

Figure 5-17 Median Response Spectra of 5.0%, 4.3%, 3.6%, and 2.3% Damping for 2%-in-50-Years Hazard Level

Table 5-19 Spectral Acceleration Values for 3-Story Buildings with 5.0% and 4.3% Damping for 2% in 50 Years Hazard Level

LA 2/50	column	design	Period, T_1	Sa at 5.0% damping	Sa at 4.3% damping	ratio, $Sa_{5\%}$ / $Sa_{4.3\%}$	average
3-story	w14	LB	1.00 (sec)	1.04	1.07	0.97	0.96
		UB	0.88 (sec)	1.27	1.32	0.96	
	w24	LB	1.00 (sec)	1.04	1.07	0.97	
		UB	0.87 (sec)	1.27	1.32	0.96	
	w30	LB	1.00 (sec)	1.04	1.07	0.97	
		UB	0.86 (sec)	1.31	1.37	0.96	
	w36	LB	0.99 (sec)	1.04	1.07	0.97	
		UB	0.84 (sec)	1.34	1.40	0.96	

Table 5-20 Spectral Acceleration Values for 9-Story Buildings with 5.0% and 3.6% Damping for 2% in 50 Years Hazard Level

LA 2/50	column	design	Period, T_1	Sa at 5.0% damping	Sa at 3.6% damping	ratio, $Sa_{5\%}$ / $Sa_{3.6\%}$	average
9-story	w14	LB	2.45 (sec)	0.45	1.07	0.93	0.93
		UB	2.16 (sec)	0.54	1.32	0.94	
	w24	LB	2.47 (sec)	0.45	1.07	0.93	
		UB	2.18 (sec)	0.53	1.32	0.94	
	w30	LB	2.44 (sec)	0.46	1.07	0.93	
		UB	2.18 (sec)	0.53	1.37	0.94	
	w36	LB	2.47 (sec)	0.45	1.07	0.93	
		UB	2.18 (sec)	0.53	1.40	0.94	

Table 5-21 Spectral Acceleration Values for 20-Story Buildings with 5.0% and 2.3% Damping for 2% in 50 Years Hazard Level

LA 2/50	column	design	Period, T_1	Sa at 5.0% damping	Sa at 2.3% damping	ratio, $Sa_{5\%}$ / $Sa_{2.3\%}$	average
20-story	w14	L&UB	3.47 (sec)	0.26	0.29	0.90	0.90
	w24	L&UB	3.43 (sec)	0.27	0.29	0.90	
	w30	L&UB	3.43 (sec)	0.27	0.29	0.90	
	w36	L&UB	3.46 (sec)	0.26	0.29	0.90	

Table 5-22 Drift and Variance Values for Different Analysis Methods Using LA 2% in 50 Year Hazard Level After Corrections

LA 2/50	column	design	NTH	N97-LSP		F273-LSP		N97-MAP		F273-LDP		LTHP		F273-NSP		CSP-NSP	
				drift	B.F.	drift	B.F.	drift	B.F.	drift	B.F.	drift	B.F.	drift	B.F.	drift	B.F.
3-story	w14	LB	0.030	0.030	1.00	0.046	0.65	0.039	0.77	0.036	0.83	0.032	0.94	0.033	0.91	0.022	1.36
		UB	0.027	0.030	0.91	0.045	0.60	0.031	0.88	0.033	0.83	0.031	0.89	0.034	0.81	0.022	1.23
	w24	LB	0.029	0.030	0.96	0.046	0.62	0.041	0.70	0.037	0.78	0.032	0.90	0.033	0.88	0.021	1.34
		UB	0.025	0.030	0.83	0.045	0.55	0.031	0.80	0.032	0.78	0.031	0.81	0.032	0.77	0.021	1.18
	w30	LB	0.028	0.030	0.94	0.043	0.65	0.041	0.69	0.037	0.76	0.032	0.87	0.039	0.73	0.021	1.36
		UB	0.024	0.030	0.81	0.037	0.65	0.030	0.81	0.032	0.76	0.030	0.81	0.028	0.88	0.017	1.40
	w36	LB	0.028	0.030	0.94	0.044	0.64	0.040	0.71	0.037	0.77	0.033	0.86	0.032	0.88	0.021	1.38
		UB	0.024	0.030	0.81	0.037	0.65	0.028	0.87	0.031	0.78	0.031	0.79	0.028	0.87	0.018	1.36
	μ		0.027	0.030	0.90	0.043	0.63	0.035	0.78	0.034	0.79	0.031	0.86	0.032	0.84	0.020	1.33
	σ		0.0022	0.0000	0.0742	0.0036	0.0358	0.0056	0.0741	0.0026	0.0283	0.0011	0.0499	0.0034	0.0636	0.0018	0.0785
	COV		0.08		0.08		0.06		0.10		0.04		0.06		0.08		0.06

LA 2/50	column	design	NTH	N97-LSP		F273-LSP		N97-MAP		F273-LDP		LTHP		F273-NSP		CSP-NSP	
				drift	B.F.	drift	B.F.	drift	B.F.	drift	B.F.	drift	B.F.	drift	B.F.	drift	B.F.
9-story	w14	LB	0.036	0.030	1.20	0.045	0.80	0.038	0.95	0.034	1.06	0.040	0.91	0.039	0.92	0.025	1.42
		UB	0.036	0.030	1.19	0.038	0.94	0.029	1.23	0.028	1.28	0.037	0.97	0.034	1.04	0.022	1.65
	w24	LB	0.034	0.030	1.14	0.045	0.77	0.036	0.95	0.032	1.07	0.039	0.88	0.038	0.89	0.023	1.49
		UB	0.033	0.030	1.10	0.039	0.84	0.029	1.13	0.029	1.13	0.036	0.92	0.033	1.00	0.021	1.54
	w30	LB	0.035	0.030	1.16	0.044	0.80	0.036	0.97	0.031	1.12	0.039	0.89	0.040	0.87	0.025	1.40
		UB	0.032	0.030	1.07	0.039	0.82	0.029	1.11	0.028	1.15	0.036	0.90	0.029	1.10	0.021	1.51
	w36	LB	0.034	0.030	1.13	0.047	0.73	0.036	0.94	0.032	1.06	0.039	0.87	0.041	0.83	0.025	1.35
		UB	0.034	0.030	1.12	0.040	0.84	0.029	1.16	0.028	1.20	0.036	0.93	0.035	0.95	0.022	1.50
	μ		0.034	0.030	1.14	0.042	0.82	0.033	1.05	0.030	1.13	0.038	0.91	0.036	0.95	0.023	1.48
	σ		0.0013	0.0000	0.0447	0.0032	0.0623	0.0041	0.1172	0.0023	0.0774	0.0016	0.0323	0.0041	0.0933	0.0018	0.0959
	COV		0.04		0.04		0.08		0.11		0.07		0.04		0.10		0.06

LA 2/50	column	design	NTH	N97-LSP		F273-LSP		N97-MAP		F273-LDP		LTHP		F273-NSP		CSP-NSP	
				drift	B.F.	drift	B.F.	drift	B.F.	drift	B.F.	drift	B.F.	drift	B.F.	drift	B.F.
20-story	w14	L&UB	0.024	0.018	1.34	0.024	0.99	0.022	1.10	0.024	1.01	0.026	0.92	0.029	0.82	0.018	1.32
	w24	L&UB	0.024	0.018	1.34	0.025	0.96	0.022	1.10	0.024	1.01	0.027	0.90	0.028	0.85	0.018	1.34
	w30	L&UB	0.024	0.018	1.36	0.025	0.97	0.022	1.11	0.024	1.02	0.027	0.90	0.028	0.86	0.018	1.36
	w36	L&UB	0.024	0.018	1.34	0.025	0.96	0.022	1.10	0.024	1.00	0.027	0.89	0.030	0.81	0.018	1.33
	μ		0.024	0.018	1.35	0.025	0.97	0.022	1.10	0.024	1.01	0.027	0.90	0.029	0.84	0.018	1.34
	σ		0.0002	0.0000	0.0087	0.0004	0.0173	0.0000	0.0071	0.0000	0.0065	0.0003	0.0100	0.0007	0.0243	0.0002	0.0180
	COV		0.01		0.01		0.02		0.01		0.01		0.01		0.03		0.01

LA 2/50	column	design	NTH	N97-LSP		F273-LSP		N97-MAP		F273-LDP		LTHP		F273-NSP		CSP-NSP	
				drift	B.F.	drift	B.F.	drift	B.F.	drift	B.F.	drift	B.F.	drift	B.F.	drift	B.F.
3, 9, and 20-story	μ				1.13		0.81		0.98		0.98		0.89		0.88		1.38
	σ				0.192		0.148		0.164		0.154		0.040		0.083		0.100
	COV				0.17		0.18		0.17		0.16		0.05		0.10		0.07

Table 5-23 Drift and Variance Values for Different Analysis Methods Using LA 50% in 50 Year Hazard Level After Corrections

LA 2/50	column	design	NTH	N97-LSP		F273-LSP		N97-MAP		N97-LTH		F273-NSP		CSP-NSP	
				drift	B.F.	drift	B.F.	drift	B.F.	drift	B.F.	drift	B.F.	drift	B.F.
3-story	w14	LB	0.009	0.009	1.03	0.009	1.03	0.008	1.10	0.009	1.00	0.007	1.35	0.006	1.55
		UB	0.007	0.009	0.84	0.009	0.84	0.008	0.90	0.008	0.88	0.007	1.08	0.006	1.25
	w24	LB	0.007	0.009	0.84	0.009	0.84	0.008	0.89	0.009	0.83	0.007	1.10	0.006	1.25
		UB	0.006	0.009	0.72	0.009	0.72	0.008	0.77	0.008	0.75	0.007	0.94	0.006	1.09
	w30	LB	0.007	0.009	0.83	0.009	0.83	0.008	0.89	0.009	0.82	0.007	1.08	0.006	1.28
		UB	0.006	0.007	0.92	0.007	0.92	0.006	0.98	0.007	0.84	0.006	1.08	0.005	1.28
	w36	LB	0.007	0.009	0.86	0.009	0.86	0.008	0.92	0.009	0.83	0.007	1.13	0.006	1.31
		UB	0.006	0.007	0.94	0.007	0.94	0.006	1.00	0.008	0.83	0.006	1.09	0.005	1.28
	μ		0.007	0.008	0.87	0.008	0.87	0.008	0.93	0.008	0.85	0.006	1.11	0.006	1.29
	σ		0.0009	0.0009	0.0931	0.0009	0.0931	0.0008	0.0993	0.0006	0.0713	0.0004	0.1130	0.0004	0.1259
	COV		0.13		0.11		0.11		0.11		0.08		0.10		0.10

LA 2/50	column	design	NTH	N97-LSP		F273-LSP		N97-MAP		N97-LTH		F273-NSP		CSP-NSP	
				drift	B.F.	drift	B.F.	drift	B.F.	drift	B.F.	drift	B.F.	drift	B.F.
9-story	w14	LB	0.009	0.008	1.13	0.008	1.13	0.010	0.85	0.008	1.06	0.006	1.47	0.005	1.65
		UB	0.008	0.007	1.11	0.007	1.11	0.008	0.98	0.008	1.05	0.006	1.39	0.005	1.56
	w24	LB	0.008	0.007	1.10	0.007	1.10	0.010	0.82	0.008	0.99	0.006	1.42	0.005	1.60
		UB	0.007	0.007	1.00	0.007	1.00	0.008	0.90	0.008	0.93	0.006	1.25	0.005	1.40
	w30	LB	0.008	0.007	1.10	0.007	1.10	0.010	0.82	0.008	1.00	0.006	1.42	0.005	1.59
		UB	0.007	0.007	0.99	0.007	0.99	0.008	0.90	0.008	0.94	0.006	1.25	0.005	1.40
	w36	LB	0.008	0.008	1.04	0.008	1.04	0.010	0.81	0.008	0.98	0.006	1.35	0.005	1.53
		UB	0.007	0.007	0.99	0.007	0.99	0.008	0.91	0.008	0.95	0.006	1.24	0.005	1.39
	μ		0.008	0.007	1.06	0.007	1.06	0.009	0.87	0.008	0.99	0.006	1.35	0.005	1.52
	σ		0.0005	0.0002	0.0597	0.0002	0.0597	0.0011	0.0597	0.0003	0.0460	0.0001	0.0906	0.0001	0.1015
	COV		0.07		0.06		0.06		0.07		0.05		0.07		0.07

LA 2/50	column	design	NTH	N97-LSP		F273-LSP		N97-MAP		N97-LTH		F273-NSP		CSP-NSP	
				drift	B.F.	drift	B.F.	drift	B.F.	drift	B.F.	drift	B.F.	drift	B.F.
20-story	w14	L&UB	0.006	0.007	1.00	0.007	1.00	0.006	1.08	0.006	1.09	0.003	2.02	0.003	2.05
	w24	L&UB	0.007	0.007	1.01	0.007	1.01	0.006	1.09	0.006	1.09	0.003	1.99	0.003	2.03
	w30	L&UB	0.007	0.006	1.06	0.006	1.06	0.006	1.13	0.006	1.09	0.003	2.04	0.003	2.08
	w36	L&UB	0.007	0.007	1.02	0.007	1.02	0.006	1.10	0.006	1.10	0.003	1.98	0.003	2.02
	μ		0.007	0.006	1.02	0.006	1.02	0.006	1.10	0.006	1.09	0.003	2.01	0.003	2.05
	σ		0.0001	0.0000	0.0287	0.0000	0.0287	0.0000	0.0226	0.0001	0.0036	0.0001	0.0278	0.0001	0.0273
	COV		0.02		0.03		0.03		0.02		0.00		0.01		0.01

LA 2/50	column	design	NTH	N97-LSP		F273-LSP		N97-MAP		N97-LTH		F273-NSP		CSP-NSP	
				drift	B.F.	drift	B.F.	drift	B.F.	drift	B.F.	drift	B.F.	drift	B.F.
3, 9, and 20-story	μ				0.98		0.98		0.97		0.98		1.49		1.62
	σ				0.103		0.103		0.118		0.112		0.397		0.337
	COV				0.10		0.10		0.12		0.11		0.27		0.21

5.7.8 Other Uncertainties

Uncertainties in live load and material properties were also investigated. However, they were neglected since the variances are small.

Initially, an uncertainty value of 0.25 was assigned with engineering judgment to account for the fact that the time history method is not perfect. However, this value is changed due to the reasons described in the following section.

5.7.9 Coupling and Double Counting of Uncertainties in Capacity and Demand

Careful consideration should be given to the coupling or double counting of uncertainties in capacity and demand. Particularly, the relationship among the period, bias factors and the nonlinear time history results should be looked at more closely. A summary of all of the variables that were covered follows:

Variables	3-story	9-story	20-story	Comments
k	Height dependency was relieved by taking 1.0 second value for each hazard level. Still dependent on site. Can be calculated using Equation 4.7.3-2 or use typical average value listed in Table 4.7.3-2.			
b	1.0	1.0	1.0	Decided for both demand and capacity calculations.
$\beta_{damping}$	0.024	0.030	0.034	Calculated using LA 2/50 ground motions.
$\beta_{orientation}$	0.21	0.19	0.26	Calculated using unrotated LA 2/50 ground motions
$\beta_{analysis\ method}$	0.08	0.10	0.03	Maximum value among the LA 2/50 ground motions.
β_{NTH}	0.25	0.25	0.25	To account for imperfectness of nonlinear time history analysis. Decided by engineering judgment.

For the uncertainties on the demand side, the period depends on the stiffness of the structure which is related to the analysis method as well as the model in the nonlinear time history method. Therefore, period, analysis method, and nonlinear time history values are inter-related. Moreover, the uncertainty due to nonlinear time history should also be height-dependent due to the uncertainty in stiffness estimation and P-delta effects. Therefore, β_a, which combines the analysis method with the stiffness of the structure as well as the consideration for the height dependency is introduced. The values of 0.15, 0.20, and 0.25 are assigned for the β_{NTH} for the 3-story, 9-story, and 20-story buildings, respectively. The variance from the analysis method, variance due to nonlinear time history model, which includes the stiffness (period) as well as P-delta effects is listed with the final value of β_a. The $\beta_{B.F.}$ values listed are corresponding values from Table 5-22 and Table 5-23. The resulting table is shown in Table 5-24.

On underestimating the P-delta effect, lower demand and higher capacity results are expected. Therefore, demand and capacity are not independent but have a negative correlation. After a few long meetings and discussions, a procedure for treating the demand uncertainty marginally, and adding the $2\ \rho\ \beta_{dd}\ \beta_{cd}$ to the capacity variance (β_{Ui}^2), was adopted (Cornell, 1999). For simplicity and conservatism, this negative correlation was assumed to be perfect. It was decided that, because of the uncertainty in capacity is zero due to stiffness, the dependents for both demand (β_{dd}) and capacity (β_{cd}) are those for the nonlinear time history only. Therefore, $\sqrt{2\rho} \cdot \beta_{NTH}$ should be added to the uncertainty in global capacity. Since ρ for perfectly negative correlation is -1, the additional uncertainty becomes $\sqrt{2} \cdot \beta_{NTH}$. The period of global stiffness was set to zero since the stiffness should affect absolute drift demand but not drift capacity, because this is dominated by P-delta, which depends on the drift level, not the stiffness.

Therefore, the variance in the global capacity is in the form

$$\beta_U = \sqrt{\beta_{Ui}^2 + \beta_{Ud}^2} = \sqrt{\beta_{Ui}^2 + 2 \cdot \rho \cdot \beta_{dd} \cdot \beta_{cd}} = \sqrt{3 \cdot \beta_{NTH}^2} = \sqrt{3} \cdot \beta_{NTH} \qquad (5\text{-}26)$$

where:

β_{Ui} = independent part of uncertainty

β_{Ud} = dependent part of uncertainty

β_{dd} = dependent part of demand

β_{cd} = dependent part of capacity

and the variances are as follow:

	3-story	9-story	20-story
β_{NTH}	0.15	0.20	0.25
β_U	0.26	0.35	0.43

Therefore, β values for uncertainties and randomness that will be used for the evaluation process are given in Table 5-25.

A summary of all performance evaluation coefficients and bias factors for new and existing buildings is given in Appendix B. There are some other minor differences between the *Guidelines* and this State of the Art Report. A complete documentation of this information is given in Yun and Foutch (2000).

5.8 Implication for Evaluation of Existing Buildings

Using this same approach, it is possible to perform an evaluation of the expected performance of existing damaged or undamaged buildings. An analytical model can be constructed of the building in the damaged or undamaged state, and an analysis performed for the ground motion corresponding to various hazard levels. By interpolation, it should be possible to find the hazard level ground motion likely to result in exceedance of the Collapse Prevention performance level at various levels of confidence, and which can be reported as the performance capability of the structure. If there is insufficient confidence that a damaged structure will provide Collapse Prevention performance at a suitable ground motion exceedance probability, then a decision could be made to "red-tag" the building. This is discussed in detail in Chapters 8 and 9. Examples are presented in Appendix A.

5.9 Evaluating the Relative Effect of Reducing the Uncertainty in Various Design Parameters from a Safety and Reliability Point of View

The reliability of the building systems in general can be improved by increasing the mean capacity against the limit state and/or reducing the uncertainty in the capacity. The increase in mean capacity can be achieved by more stable configuration, more redundancy of the systems,

and stronger and stiffer components, including connections, against overload and low-cycle fatigue failures. This increase would result in lower response at each level and hence lower limit state probability.

In view of the practical difficulty in enforcing reduction in resistance and modeling uncertainty, and in view of the relatively small impact on structural reliability, emphasis should be on increasing the capacity or decreasing the demand. The latter is accomplished by making the building stiffer. The relative effect of various improvement measures on the safety and reliability of the building can be evaluated by comparing the change in the long-term reliability to the different improvement measures. A sensitivity analysis may be carried out for this purpose to rank the improvement measures at each level.

Table 5-24 β_a Values for Different Analysis Procedures

3-story						
Analysis Procedure	$\beta_{B.F.}$		β_{NTH}		β_a	
	2/50	**50/50**	**2/50**	**50/50**	**2/50**	**50/50**
97 NEHRP-LSP	0.08	0.11	0.15	0.15	0.17	0.18
F273-LSP	0.06	0.11	0.15	0.15	0.16	0.18
F273-MAP	0.04	0.11	0.15	0.15	0.15	0.18
Linear-THP	0.06	0.08	0.15	0.15	0.16	0.17
F273-NSP	0.08	0.10	0.15	0.15	0.17	0.18
CSM-NSP	0.06	0.10	0.15	0.15	0.16	0.18
9-story						
Analysis Procedure	$\beta_{B.F.}$		β_{NTH}		β_a	
	2/50	**50/50**	**2/50**	**50/50**	**2/50**	**50/50**
97 NEHRP-LSP	0.04	0.06	0.20	0.20	0.20	0.21
F273-LSP	0.08	0.06	0.20	0.20	0.21	0.21
F273-MAP	0.07	0.04	0.20	0.20	0.21	0.20
Linear-THP	0.04	0.05	0.20	0.20	0.20	0.21
F273-NSP	0.10	0.07	0.20	0.20	0.21	0.21
CSM-NSP	0.06	0.07	0.20	0.20	0.21	0.21
20-story						
Analysis Procedure	$\beta_{B.F.}$		β_{NTH}		β_a	
	2/50	**50/50**	**2/50**	**50/50**	**2/50**	**50/50**
97 NEHRP-LSP	0.01	0.03	0.25	0.25	0.25	0.25
F273-LSP	0.02	0.03	0.25	0.25	0.25	0.25
F273-MAP	0.01	0.03	0.25	0.25	0.25	0.25
Linear-THP	0.01	0.00	0.25	0.25	0.25	0.25
F273-NSP	0.03	0.01	0.25	0.25	0.25	0.25
CSM-NSP	0.01	0.01	0.25	0.25	0.25	0.25

Table 5-25 Summary of Uncertainties and Randomness to be used for the Evaluation Process

	Randomness	**Uncertainty**
Capacity: Local	β_{RC} = 0.20	β_{UC} = 0.25
Capacity: Global	β_{RC} = standard deviation of log of the calculated drifts from Incremental Dynamic Analysis (IDA)	$\beta_{UC} = \sqrt{3} \cdot \beta_{NTH}$
Demand	β_{RD} = standard deviation of log of the calculated drifts from time history analysis for a hazard level β_{ori} = associated with orientation of the structure to the ground motion	β_{NTH} = associated with uncertainties in the nonlinear time history analysis procedure (0.15, 0.20 and 0.25 for 3-story, 9-story and 20-story, respectively) $\beta_{C.B.}$ = associated with uncertainty in the bias factor which is quite small $\beta_{damping}$ = associated with uncertainty in the estimating the damping value of the structure which is quite small. Therefore, $\beta_{damping}$ = 0.0 $\beta_{live\ load}$ = associated with uncertainty in live load applied which is quite small. Therefore, $\beta_{live\ load}$ = 0.0 $\beta_{material\ property}$ = associated with uncertainty in material property which is quite small. Therefore, $\beta_{material\ property}$ = 0.0

6. PERFORMANCE EVALUATION FOR NEW BUILDINGS

6.1 Introduction

This chapter provides criteria for evaluating the expected performance of a new moment-resisting frame building. Two performance levels are considered: Collapse Prevention (CP), and Immediate Occupancy (IO). The damage associated with these performance levels is given in Chapter 5. A load and resistance format is used for the acceptance criteria. The level of confidence that a building will satisfy the performance objective is also estimated.

Performance evaluation should be a part of the design process for all new buildings. This is discussed to some extent in Chapter 2. This should cover all levels of performance from fully operational, where no structural or nonstructural damage is expected to occur, to collapse prevention, where no local or global collapse occurs, but the building will be a financial ruin. As discussed in Chapter 2, the leadership on the SAC project decided that the scope of the project included a range of performance between immediate occupancy with limited structural damage (IO) to incipient collapse (CP).

6.2 Performance Levels

Two performance levels are defined Collapse Prevention and Immediate Occupancy.

The Collapse Prevention (CP) structural performance level is defined as the post-earthquake damage state in which a structure is on the verge of experiencing either local or total collapse. Substantial damage to the building has occurred, including significant degradation in strength and stiffness of the lateral-force-resisting system, large permanent deformation of the structure, and possibly some degradation of the gravity-load-carrying system. However, all significant components of the gravity-load-carrying system must continue to be functional. For this performance level it is expected that the building may be a total financial loss and that occupancy of the building before extensive repairs are made will not be permitted. Specific criteria are given in Chapter 5.

The Immediate Occupancy (IO) structural performance level is defined as the post-earthquake damage state in which only slight structural damage has occurred. Damage is anticipated to be so slight, that if not found during inspection, there would be no cause for concern. The basic vertical and lateral-load-carrying systems still have most, if not all, of their strength and stiffness. Buildings meeting this performance level should be safe for occupancy immediately after the earthquake, presuming that damage to nonstructural components is light and utility service is available. Specific criteria are given in Chapter 5.

Maximum interstory drift angle at any story will be the primary design parameter used to determine if the damage states related to connection fractures, loss of the gravity-load-carrying ability of connections, buckling of beam and column flanges, permanent lateral drift, and global instability states are exceeded. Column axial force and moment will be the design parameters

used to determine if the column buckling or column splice fracture damage states have been exceeded. Additional information on performance is given in Chapter 5.

As mentioned in the previous section and discussed more thoroughly in Chapter 2, protection of nonstructural systems is not in the scope of the SAC project. However, it should be a part of any performance evaluation. The performance level might be labeled as operational. This is discussed in great length, and recommendations are given in Vision 2000 (1995) and FEMA-273 (FEMA, 1997). The expectation for this performance level is that there will be no structural damage since elastic response is required. Only minimal nonstructural damage would occur. Full operation of the building would be expected after checking on the operation of the mechanical and electrical systems. A reasonable interstory drift demand limitation in the range of 0.003 to 0.005 might be appropriate. The hazard level of 50/30 and a 90% confidence level of achieving this performance level should be specified.

6.3 Seismic Hazard and Design Spectra

6.3.1 Design Spectral Accelerations for Linear Static Procedures

The recommended design elastic response spectrum accelerations and other seismic demand characterizations are those given in Chapter 3. They are similar to those given in the 1997 NEHRP *Provisions* with some important exceptions.

The 1997 NEHRP *Provisions* specify that the short-period and one-second period spectral accelerations, S_{DS} and S_{D1}, are determined by multiplying the S_{MS} and S_{M1} spectral accelerations by 2/3 to account for the expected overstrength of about 1.5. The 2/3 factor is changed to 1.0 for performance evaluation. The overstrength is accounted for on the capacity side of the equation as discussed in Chapters 3 and 5. Additional information is given in Chapter 5.

6.3.2 Earthquake Accelerograms for Time-History Analysis

It is recommended that seven to ten accelerograms be used for performance evaluation. Where possible, accelerograms from actual earthquakes recorded in the same geographic location and with magnitudes consistent with the hazard level under consideration be used. The USGS has a very large database of recorded earthquake accelerograms available on CD ROM that can be obtained at a modest fee (Seekins, et al., 1998).

Once the accelerograms are selected, they must be scaled to be consistent with the hazard level under consideration. The first step is to construct the NEHRP design spectrum for the hazard level and site conditions. There are several methods for scaling accelerograms. Two methods are described in Chapter 4.

6.3.3 Concurrence of Seismic Ground Motions

In codes prior to 1994, the building's response to shaking in the direction under consideration was required to be combined with 30% of the response to shaking in the orthogonal direction. This is done in the following manner. Assume that the building has two orthogonal axes of orientation in the N-S and E-W directions. Usually the structural systems

carrying lateral loads in each direction are considered independently. So, the base shear in the N-S direction is distributed to the N-S frames according to their stiffness. However, these N-S forces cause torsion of the building even if only accidental torsion is present. The twisting of the building due to this torsion cause forces to develop in the E-W frames. The maximum responses in the N-S and E-W directions do not occur simultaneously. As a result, only 30% of the forces in the E-W frames caused by torsion induced by the N-S seismic forces are considered This is very important for buildings that have a torsional irregularity as defined in the NEHRP *Guidelines*. For some unknown and/or unstated reason, this was dropped from all current codes. Results from SAC studies (Krawinkler, 2000) indicate that predictions of torsional motions may be grossly under-predicted without this term for buildings with torsional asymmetries. This 30%-rule should be required for buildings with plan irregularities as defined in the 1997 NEHRP *Provisions* and recommended for regular buildings.

6.4 Performance Evaluation

6.4.1 Performance Evaluation Process for New Buildings

The specific criteria for performance evaluation will be determined by the design professional in consultation with the owner and building authorities. This requires the selection of a performance objective and a degree of confidence in achieving the performance objective. For new design, the recommended performance objective is Collapse Prevention (CP) for the seismic hazard which has only a 2% probability of being exceeded in 50 years (2/50 hazard). The CP performance level is defined by a maximum design drift capacity, $\hat{C}$, times a resistance factor, ϕ. The design capacity and resistance factor are given in Table 6-1 for each connection type that has been tested for the SAC project (Roeder, 2000). The procedure required for determining capacity for other connection types is given in Section 5.6.1.

For the Collapse Prevention performance level, the desired performance is to prevent global or local collapse. Global collapse is assumed to have occurred when the numerical calculation of dynamic response becomes unstable or a drift of 10% in any story has been reached (Yun and Foutch, 1999). Local collapse is assumed to have occurred when the rotation at each end of a girder is so large that the gravity-load-carrying capacity is lost. Methods for determining these capacities for connections not tested for the SAC project are given in Section 5.6.1.2. Additional requirements are given in Chapter 5.

The resistance factor, ϕ, is a function of the randomness in the ground motions and the uncertainty in the connection performance. The development of ϕ for connections not tested for the SAC project is described in Section 5.6.1. Additional information is given in the *State of the Art Report on Connection Performance* (Roeder, 2000).

The seismic demand is determined by multiplying the median estimate of the seismic demand, $\hat{D}$, by a general demand factor, γ, and an analysis demand factor, γ_a. The demand, $\hat{D}$, is calculated as the product of the maximum story drift, θ_m, and the bias factor, C_B: $\hat{D} = \theta_m C_B$. The bias factor is dependent on the analysis procedure used to calculate θ_m. Values of C_B and γ_a

are given in Table 4-8 and Table 5-4. Methods for calculating these factors are given in Chapter 5.

If median values of $\hat{C}$ and $\hat{D}$ are used in these equations in conjunction with the 2/50 hazard, there is a 50% probability of not achieving the performance level. The provisions for new design given in the *Guidelines* are established such that for the hazard level given by the USGS maps there is a 95% confidence of less than 2% in 50 year probably of not achieving the performance level. The calculation of this confidence level is described in the next section.

Although design for the Immediate Occupancy (IO) performance level is not required for new buildings, it is highly recommended. It should also be a part of any performance evaluation. The IO performance level is assumed to be exceeded, i.e., damage is greater, if there is enough observable damage to connections that repair is necessary, or if there is a permanent drift exceeding 0.5% in any story. A more complete description of IO is given in Section 5.2. Default median capacities and demands, resistance factors and demand factors are also given in Chapter 5. Methods for determining the load and resistance factors are similar to those used for the CP performance level and are also given in the corresponding sections below.

The acceptance criteria described in Chapter 5 may be written in equation form as

$$\lambda_{con} = \frac{\phi \hat{C}}{\gamma \gamma_a \hat{D}} \tag{6-1}$$

where:

$\hat{D}$ = estimate of median drift demand
$\hat{C}$ = estimate of median drift capacity – Table 5-1
ϕ = resistance factor – Table 5-1
γ = demand factor – Table 5-4
γ_a = analysis demand factor – Table 5-4
λ_{con} = confidence factor – used to determine the confidence level from Table 5-6

$\hat{D}$ is the median estimate of the demand drift calculated using the appropriate hazard level response spectrum and any of the analysis procedures calibrated as part of the SAC project. Any commonly used structural analysis program may be used to calculate $\hat{D}$. Default values for $\hat{C}$, ϕ, γ_a and λ_{con} are given in Chapter 5. The default values for the demand factor, γ, are listed in Table 5-4.

The global and local median collapse drifts are derived for the reduced beam section (RBS) connection. The default values for ϕ, γ and λ_{con} and for parameters given in Table 5-4 and Table 5-6 are based on studies of 20 buildings designed for a Los Angeles site. The buildings had different configurations and included eight 3-story, eight 9-story, and four 20-story buildings (Lee and Foutch, 2000). Another variable used in calculating these factors is k, the slope of the

hazard curve for a 1-second period. A value of k = 3.0 was used, which represents an average of 25 sites in California. Definitions and calculations for these parameters are given below.

The evaluation of a building designed and built using any of the connections given in Table 6-1 would proceed as follows:

1. Determine S_s and S_1 for the site from maps or the USGS web site. Determine the design response spectrum following the 1997 NEHRP *Provisions*, but replace the 2/3 factor by 1.0 for determining S_{DS} and S_{D1}.
2. Calculate the maximum drift demand, θ_m, using any of the analysis procedures given in Table 4-8. The demand drift, $\hat{D}$, is then calculated as

$$\hat{D} = C_B \theta_m \tag{6-2}$$

where:

θ_m = the maximum story drift angle, Δ_x, for all stories

C_B = bias factor from Table 4-8

3. Get values for $\hat{C}$ and ϕ from Table 6-1 for the connection type used and the Performance Level of interest.
4. Get value of γ_a for the height and performance level from Table 5-4. Also, select γ for the CP performance level or for the IO performance level from the table.
5. Calculate λ_{con} using Equation 6-1.
6. Get the β_{UT} value from Table 5-5. Check the confidence level in achieving the performance objective from Table 5-6. Decide if the confidence is acceptable. If not, redesign the frame to make it stiffer and, therefore, reduce $\hat{D}$.

Procedures for doing more detailed, or customized, application of the basic performance evaluation are given in Chapter 5. Examples are also given below. A method for calculating λ_{con} is given in Section 3.3.6.

6.4.2 Modeling and Analysis

Analysis procedures recognized by the SAC project are described in Chapter 4. Recommendations on modeling are also given in Chapter 4.

6.4.3 Example for Performance Evaluation of 3-Story Post-Northridge Building

An example is given in Appendix A.

Table 6-1 Default Drift Capacities and Resistance Factors as Limited by Local Connection Response – Ductile Welded Connections

Connection Type	Strength Degradation Limit Drift Angle (radians) θ_{SD}	Immediate Occupancy		Collapse Prevention	
		Limit Drift Angle (radians) θ_{IO}	Capacity Reduction Factor ϕ	Limit Drift Angle[1] (radians) θ_{CP}	Capacity Reduction Factor[2] ϕ
WUF-B[3]	0.031-0.0003d_b	0.015	0.9	0.060-0.0006 d_b	0.9
WUF-W[4]	0.051	0.020	0.9	0.064	0.9
FF[5]	0.077-0.0012 d_b	0.020	0.9	0.10-0.0016 d_b	0.9
RBS[6]	0..060-0.0003 d_b	0.020	0.9	0.08-0.0003 d_b	0.9
WFP[7]	0.12-0.023 d_b	0.020	0.9	0.10-0.0011 d_b except that should used θ_{SD} if w14 or less	0.9
End-plate	Not pre-qualified for the Guidelines				

1. These capacities are for local collapse. For global collapse use $\hat{C}$ = 0.085.
2. These ϕ factors are for local collapse. For global collapse use ϕ = 0.85.
3. WUF-B: Welded Unreinforced Flange – Bolted connection.
4. WUF-W: Welded Unreinforced Flange – Welded Web connection.
5. FF: Free Flange connection.
6. RBS: Reduced Beam Section connection.
7. WFP: Welded Flange Plate connection.

7. PERFORMANCE OF ORDINARY AND PARTIALLY RESTRAINED STEEL MOMENT FRAMES

7.1 Background

The 1997 NEHRP (FEMA, 1997a) and 1997 UBC (ICBO, 1997) seismic provisions recognize three classes of steel moment-resisting frame systems. Two of these, Intermediate Moment Frames (IMF) and Ordinary Moment Frames (OMF), have limited ductility capacity. The proportioning and configuration of these frames are less restricted than for Special Moment Frames (SMF). As a result, their performance is expected to deteriorate at lower drift levels than that of an SMF. This is accounted for in design by prescribing a smaller response modification factor, R, with a corresponding smaller deflection amplification factor, C_d. In addition, there are restrictions on when and where they can be used.

There are several frame attributes and design considerations that distinguish the SMF from the IMF and OMF. These include member flange slenderness ratio ($b_f/2t_f$)**,** panel zone requirements, strong-column-weak-beam configurations, and connection type. These issues were studied by Yun and Foutch (1999). The results of this study and other studies performed by the SP team are used to develop design guidelines for IMF and OMF buildings.

7.2 Effects of Panel-Zone Strength and Stiffness on Member and Frame Deformation Demands

The 3-story and 9-story buildings designed according to the 1994 UBC were used for the study. To investigate the contribution of panel-zone strength to the global and local behavior of the frame system, different strengths of the panel zone were assigned to panel-zone properties of the model. The strength requirement of the panel zone presented in the *Seismic Provisions for Structural Steel Buildings* (AISC, 1994) is as follows:

$$R_v = 0.6 \cdot F_y \cdot d_c \cdot t_p \cdot \left[1 + \frac{3 \cdot b_{cf} \cdot t_{cf}^2}{d_b \cdot d_c \cdot t_p} \right] \geq R_u \qquad (7\text{-}1)$$

where:

R_v = required shear strength of the panel zone, however, it need not exceed the shear force determined from $0.8 \sum R_y M_p$

Panel zone strengths of $0.70M_p$, $0.80M_p$, $0.90M_p$, and $1.00M_p$ were chosen for the analysis. Figure 7-1 and Figure 7-2 show the results for the 3-story and the 9-story buildings. The 2%-in-50-year earthquakes were used as the ground motion input. The average responses for twenty earthquakes are plotted for comparison.

As expected, it was observed that a gradual transition of the plastic rotations from panel zones to beams occurs as the strength ratio goes up. Although the global maximum story drifts

became smaller, the difference was not significant. Since most of the panel-zone strengths of the original building were higher than 1.00, most of the plastic deformations occurred in the beams.

These results indicate that there is a predictable relationship between story drifts, beam rotations, and panel-zone rotations depending on the strength ratio of the panel-zone rotation and the beam plastic-moment capacity. The lack of a restriction on panel-zone strength for ordinary steel moment frames is insignificant. For some connections, distortion of the panel zone might lead to weld fracture. This is certainly the case for pre-Northridge connections. Test results indicate that the total drift is the most important parameter (Roeder, 2000). For new design, the drift demands for ordinary frames are small enough that all of the pre-qualified connections will result in acceptable designs regardless of the ratio of the panel-zone strength to the beam plastic moment. However, it will be shown in the next section that a height restriction must be placed on buildings with weak panel zones.

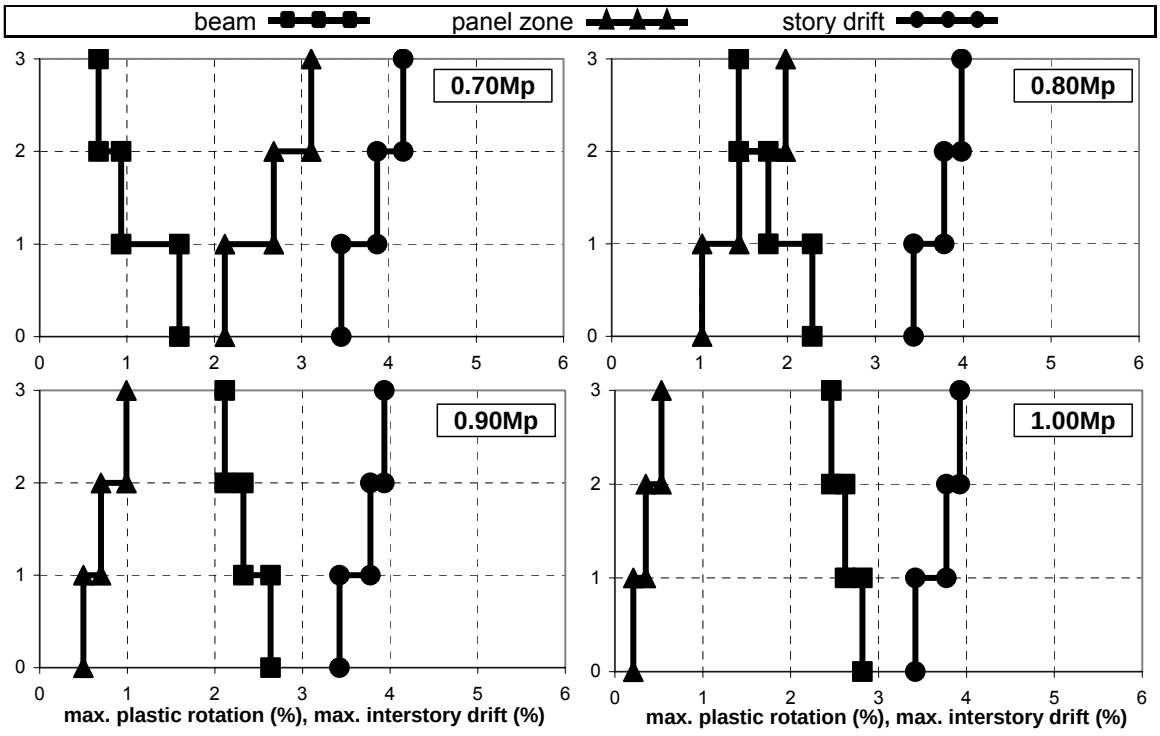

Figure 7-1 1994 UBC 3-Story Building

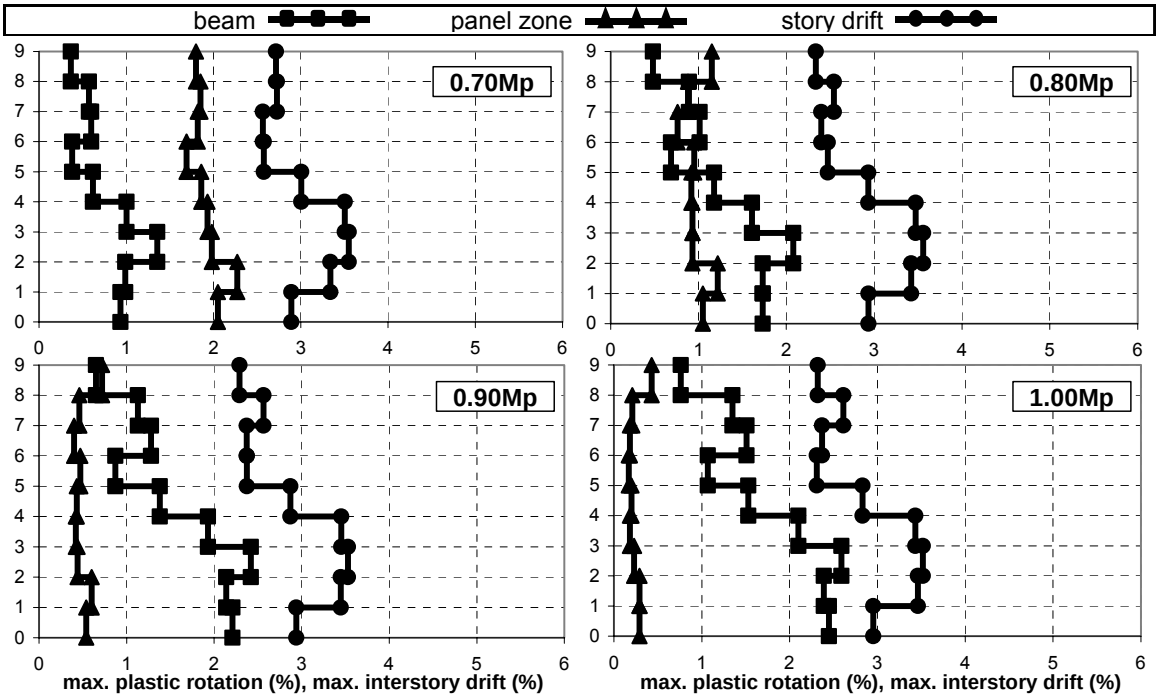

Figure 7-2 1994 UBC 9-Story Building

7.3 Effects of Weak-Column Designs

7.3.1 Background

One of the biggest concerns about OMF is the possibility of using a weak-column-strong-beam (WCSB) design. The fear is that a weak story will result in very large drift demands because all of the deformation and energy dissipation will occur in a single story or a few stories. A report by Yun and Foutch (2000) describes results of their investigation of this feature. Several weak-column buildings were designed for the LA and Seattle sites. Effects of local buckling of column flanges were also considered. Details and results are reported by Yun and Foutch (2000). These results and conclusions are summarized in this section.

7.3.2 Features of Weak-Column Designs Used for the Study

The weak-column-strong-beam (WCSB) design procedure was taken for the study of the ordinary moment frame system as a lower bound design. The column-beam moment capacity ratio specified in the LRFD seismic provision for SMFs is as follows:

$$\frac{\sum M^{*}_{pc}}{\sum M^{*}_{pb}} > 1.0 \qquad (7\text{-}2)$$

where:

$\sum M^*_{pc}$ = the sum of the moments in the column above and below the joint at the intersection of the beam and column centerlines. It is permitted to take $\sum M^*_{pc} = \sum Z_c \left(F_{yc} - P_{uc} / A_g\right)$

$\sum M^*_{pb}$ = the sum of the moment(s) in the beam(s) at the intersection of the beam and column centerline. It is permitted to take $\sum M^*_{pb} = \sum \left(1.1 R_y M_p + M_y\right)$, where M_y is the additional moment due to shear amplification.

P_{uc} = column axial compression force, kips

There is no such restriction for OMFs.

A three-story building for Seismic Design Category (SDC) D and 3-story, 9-story, and 20-story buildings were designed in accordance with the 1997 NEHRP *Provisions*. They were designed with a strength ratio of 0.9 for Equation 7-2. Plan and elevation views are the same as the original SAC buildings except for the 20-story building. For the 20-story building, wide flange sections replaced the outer columns. This was done so that all the joints were weak column designs. Plan and elevation views are shown in Figure 7-3. Both of the 3-story buildings were governed by drift, but the 9- and 20- story buildings were partially governed by strength and partially by drift.

For SDC D, the twenty LA ground motions for the 2/50 hazard were used. For SCD C the LA 10/50 were used but they were scaled to fit a 97 NEHRP spectrum for the 2/50 hazard level with S_s = 0.75 g and S_1 = 0.30 g. These are the maximum values for a SDC C region. The average response spectrum for the 20 records and the NEHRP design spectrum are shown in Figure 7-4. Strictly speaking, this 3-story weak-column design would not be allowed at this LA site because it is slightly too tall. This is included here to represent an upper bound on the system.

7.3.3 Evaluation of Response of WCSB Buildings

Even though these were nominally designed as WCSBs, yielding occurred in other elements. Since there is no requirement on panel zones, no doubler plates were used. As a result, the main plastic deformations formed in the panel zones. Some yielding occurred in the columns of the SDC D 3-story building, but hinges did not form in the columns. The 20-story building collapsed for most of the 2/50 ground motions. The 3- and 9-story buildings performed adequately. The story drift at each level for the 20-story building during a static pushover analysis shown in Figure 7-5 reveals the problem with this design. The drift demands for the middle stories are much higher than those for the rest of the building. Although this is not technically a story mechanism, the result is the same. The mechanism is forming over a few stories.

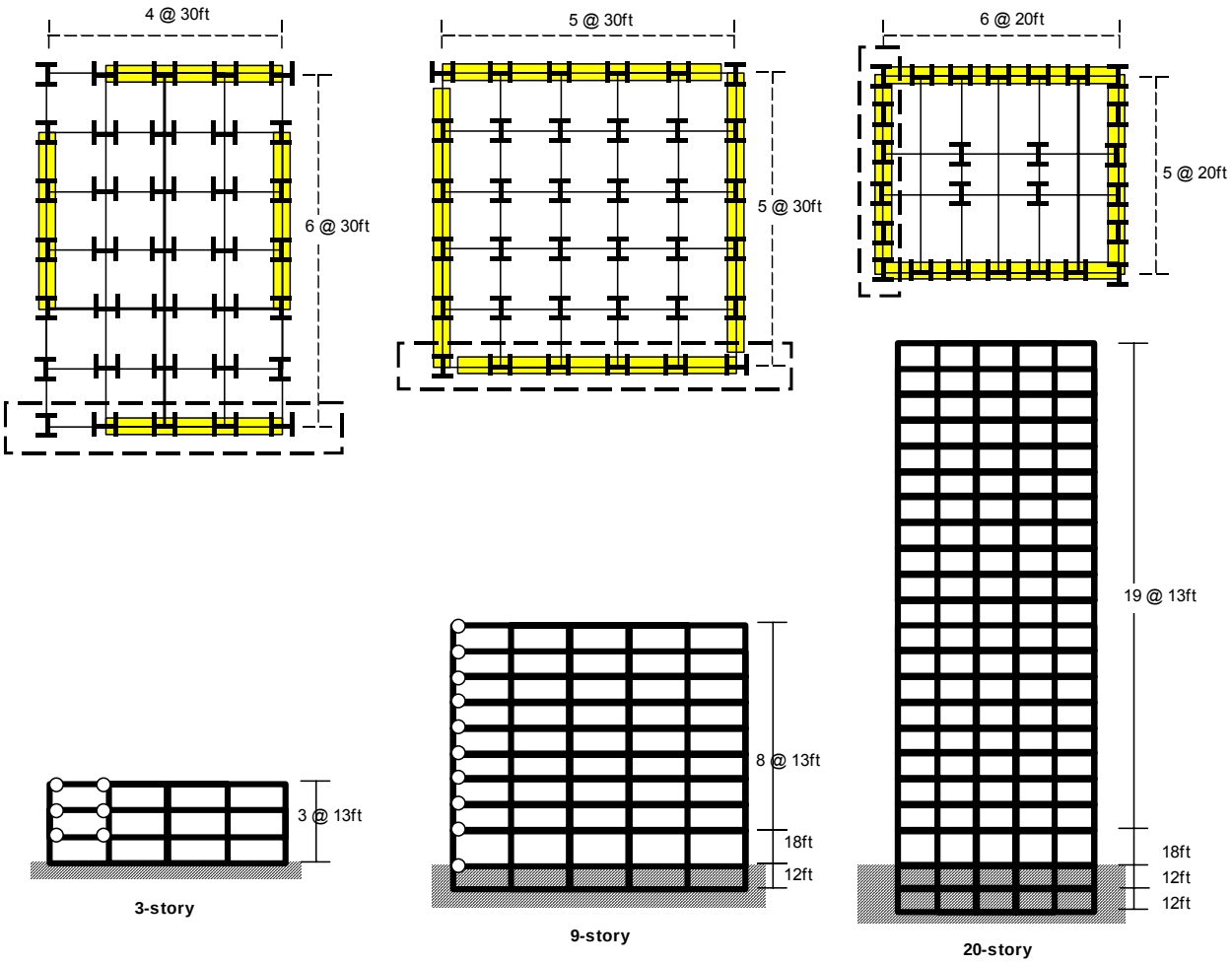

Figure 7-3 Plan and Elevation View of the 3, 9, and 20-Story WCSB Buildings

After this, doubler plates were added so that no hinging in the panel zones would occur. In this case, yielding occurred in the columns. However, in some cases yielding in some beams in the outside bays also occurred. The reason for this was the fluctuation of the column axial forces for the outside columns. Figure 7-6 demonstrates this phenomenon. As the frame moves to the right, the shear in the left-most girder acts upward and opposes the gravity compression force in the column. This changes the ratio in Equation 7-2 which results in yielding in the girder.

The results for the column above and below a joint of the 9-story building are shown in Figure 7-7. The axial force vs. time for the two columns is shown in the upper figure. The moment capacity of the two columns at the joint and the strength ratio at the joint as given by Equation 7-2 are shown in the plot. The results show that the hinging alternates between the columns and the adjacent beams. This prevented story mechanisms from forming.

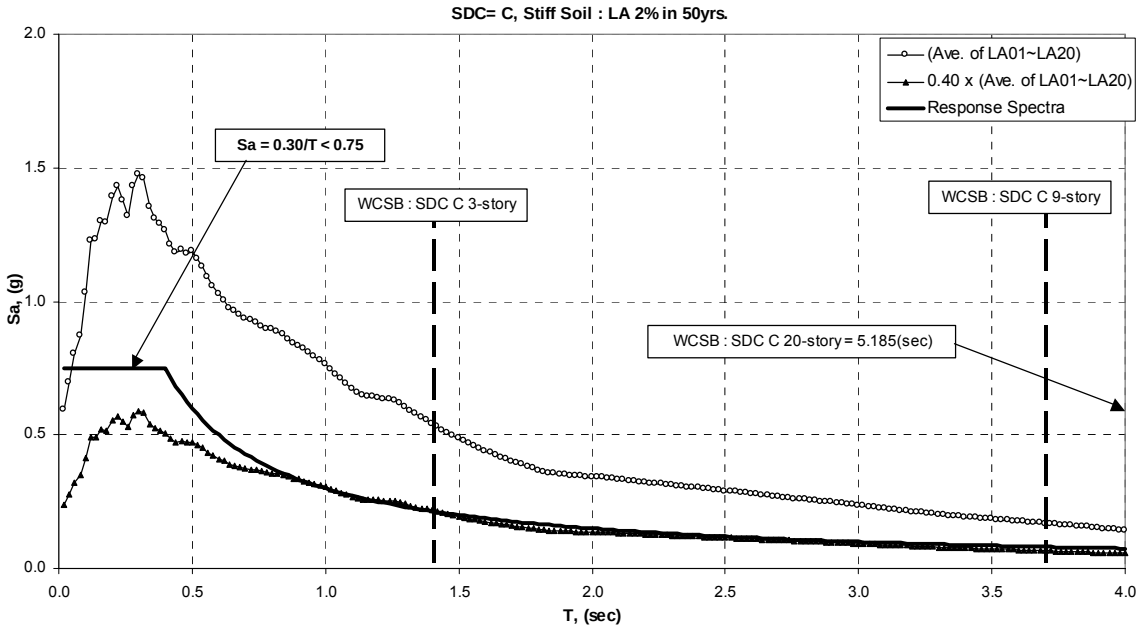

Figure 7-4 Average Response Spectrum for 20 Records and the NEHRP Design Spectrum

Next, the plastic moment capacities of the beams were assumed to be strengthened to prevent them from yielding. At this point, all of the plastic hinges occurred in the columns. The overall strength of the building was much greater than required for this site. Thus, even though hinges formed in the columns, the demands were so small that the buildings performed well.

The 9-story building was redesigned with stiff and strong beams and doubler plates. Although drift governed for most stories, the strength of the columns governed in some cases.

Static pushover results for the two 3-story buildings are shown in Figure 7-8. Pushover results for the 3-, 9-, and 20-story buildings are shown in Figure 7-9. The vertical distribution of forces for the pushover analysis was the same as that used for the NEHRP equivalent lateral force method. The results for the 3-story buildings clearly show the increase in strength of the buildings when the panel zones are strengthened. Similar results were also seen for the 9- and 20-story buildings. The pushover result for the 20-story building has a negative slope at the very low drift of about 0.007 radians, which explains its poor performance.

After being redesigned with stiff and strong beams and panel zones, the frame is stronger and stiffer than the original design with weak panel zones. As a result, the 9-story building had low enough demands that there were no collapses, even though story mechanisms occurred.

The effects of moment capacity degradation in the columns due to local buckling were studied next. The 9-story building with stiff and strong beams and panel zones was used for this study. Figure 7-10 shows a typical moment vs. plastic-rotation hysteresis behavior for one column during the earthquake.

Results are shown in Figure 7-11. The left-most figure shows the ratio of P/P_{cr} for compression and P/P_y for tension. The solid points are median values and the open symbols are the maximum values. The axial forces are relatively small, so no problems will occur. The plastic rotations and drifts are shown in the middle figure. The median drifts are all below 1.5%. The maximum drift exceeds 3% at the top of the building, but no collapse occurred. The median, 84th and 95th percentiles of the drift demands are shown in the rightmost figure. These are well within acceptable limits. A 3-story and 9-story building in SDC C were designed for the Seattle location. Similar results were found.

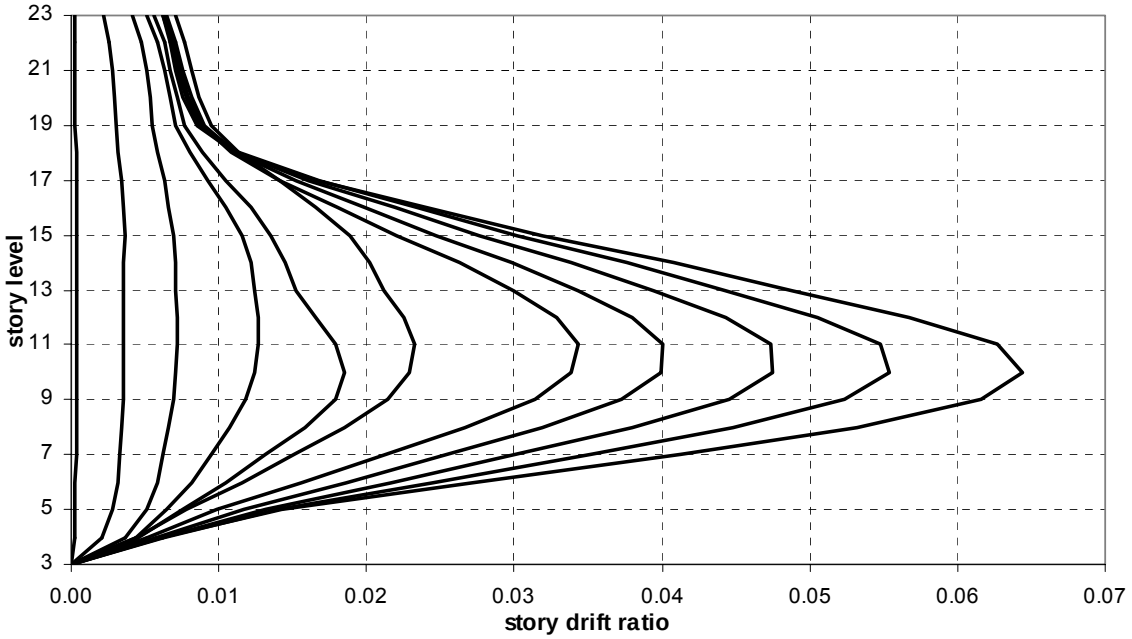

Figure 7-5 Story Drift Distribution, Static Pushover for 20-Story WCSB Buildings

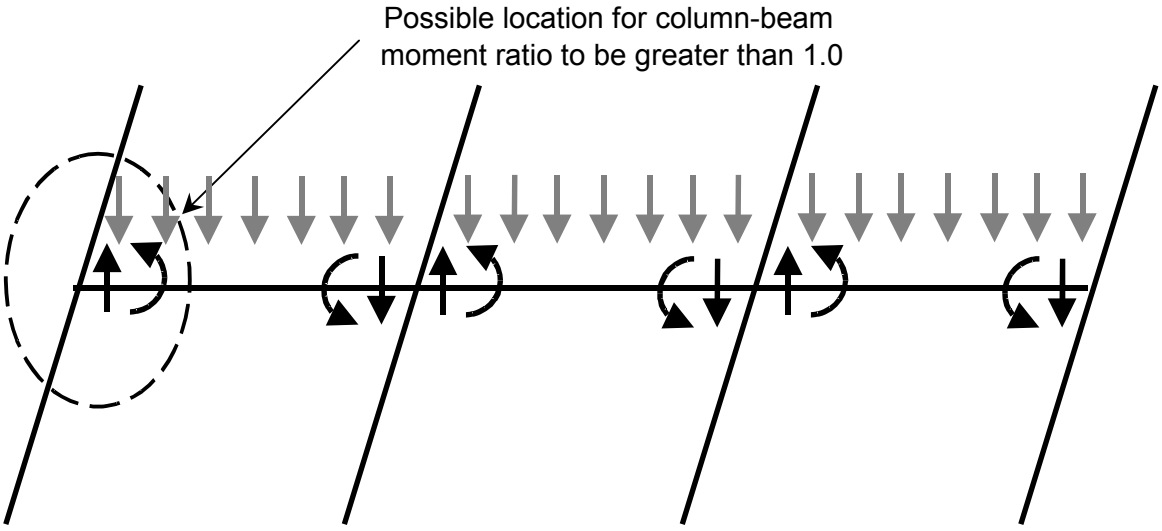

Figure 7-6 Forces in a Typical Portion of a Frame

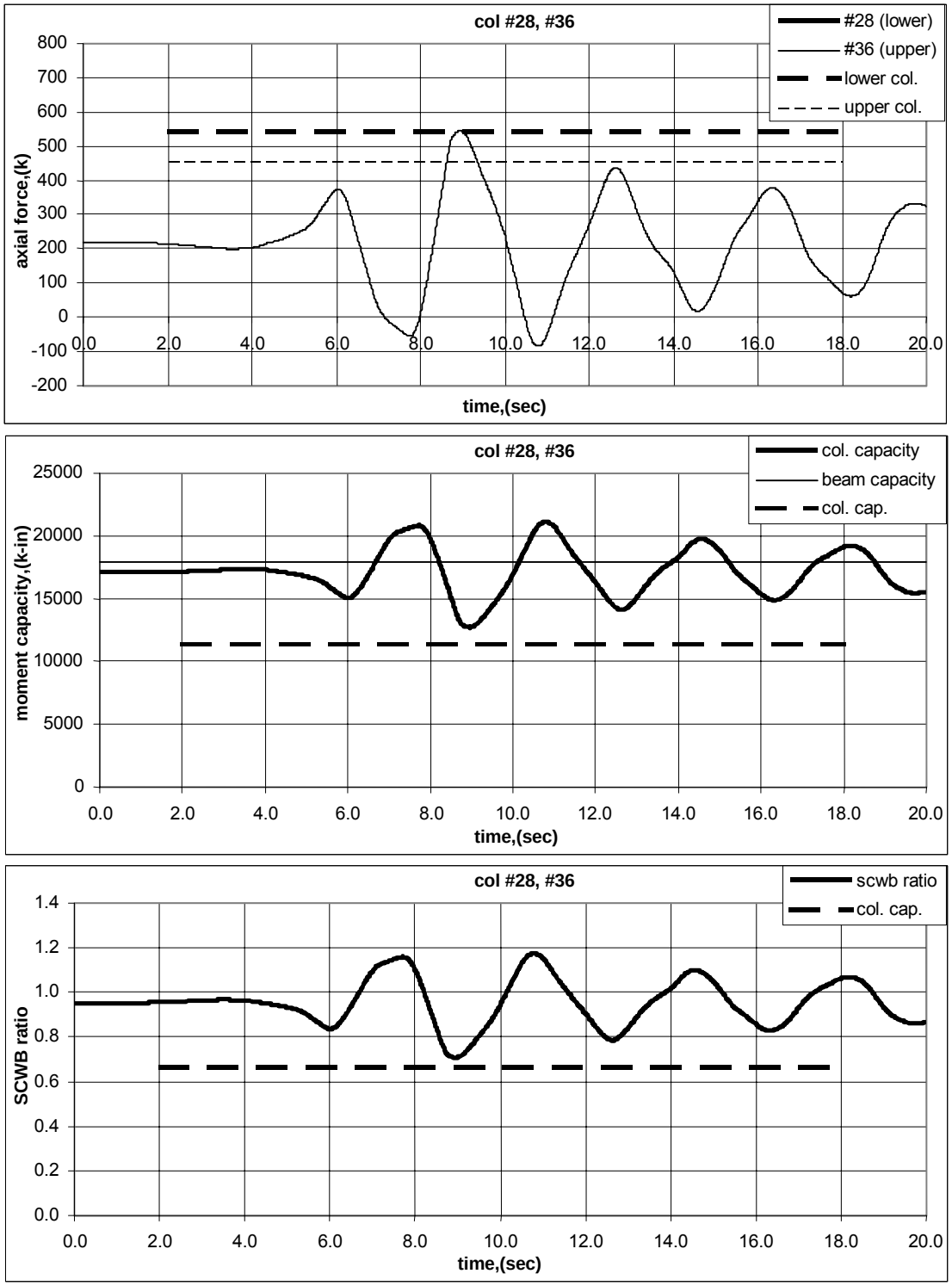

Figure 7-7 Time-History of Capacity, and Capacity Ratio, for 9-Story WCSB Building

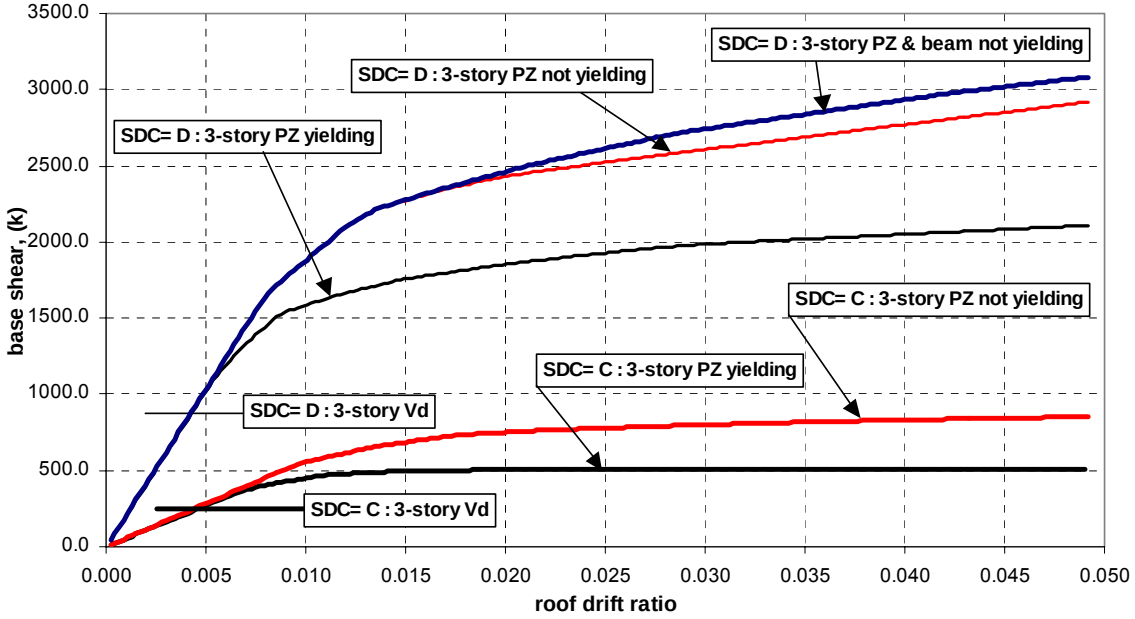

Figure 7-8 Static Pushover of 3-Story Buildings for Both SDC=D and SDC=C

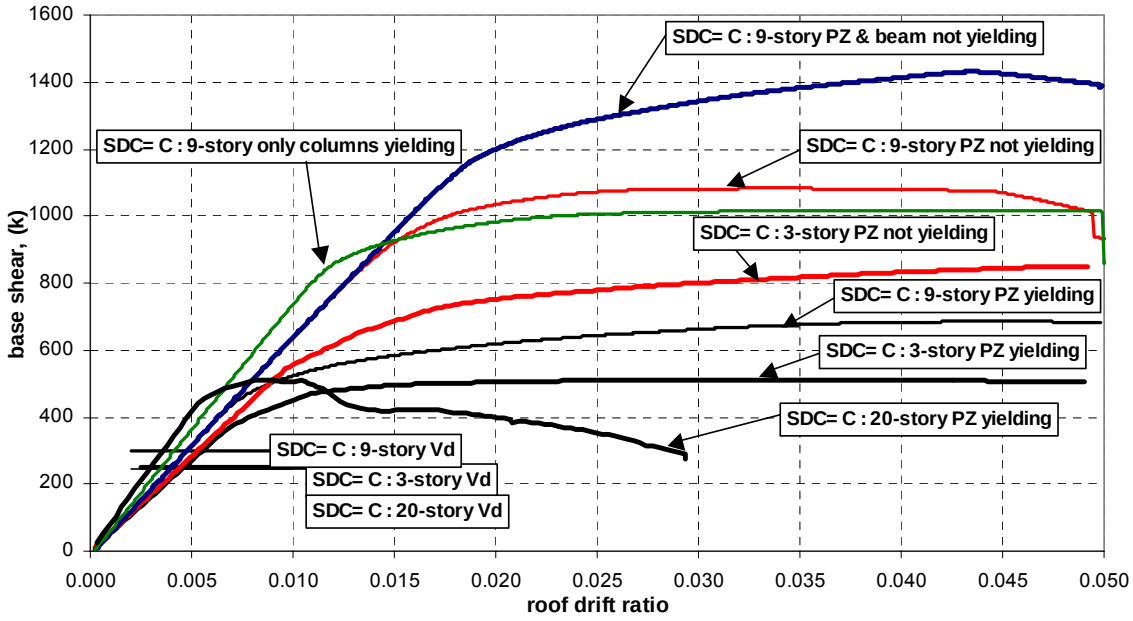

Figure 7-9 Static Pushover of 3, 9, and 20-Story Buildings for SDC=C

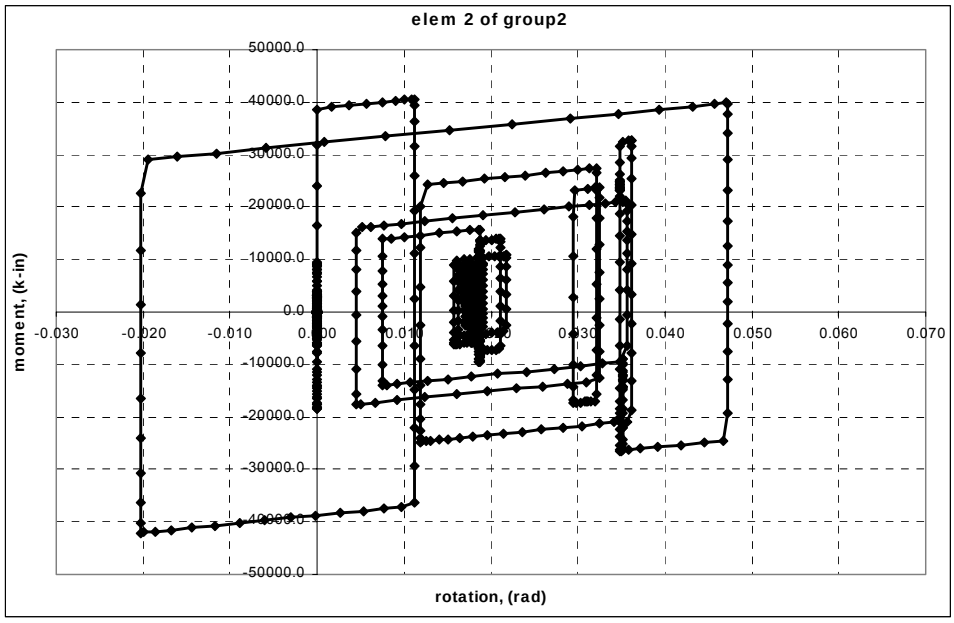

Figure 7-10 Typical Hysteresis Model of Strength-Degrading Column Spring

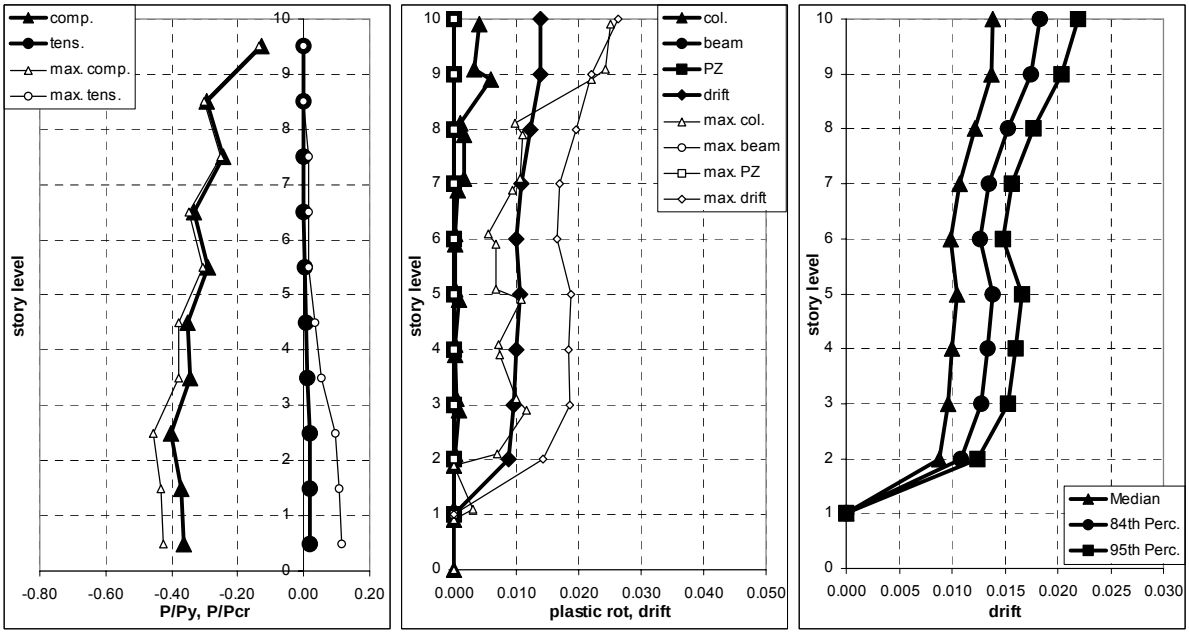

Figure 7-11 9-Story WCSB in SDC C with Stiff and Strong Beam and Panel Zone with Column Spring for LA

7.3.4 Performance Evaluation of WCSB Buildings

Performance evaluations were done for all of the WCSB buildings except for the 20-story building that collapsed. Values for C, β_R, β_U, ϕ, D, β_{acc}, γ,β_a, γ_a, λ_{con} β_{UT}^2, K_x in LA are given in

Table 7-1 to Table 7-3. Those in Seattle are given in Table 7-4 to Table 7-6. The local drift capacities for the buildings with WCSB configuration are not defined since the beams do not yield and lose gravity-carrying capacity. These were calculated using the provisions set out in Chapter 5. The confidence level for CP for the 2/50 hazard and IO for the 50/50 hazard for all buildings is 99%. This is true only if WCSB buildings are limited to 100 feet in height.

Table 7-1 CP Confidence Level Against Global Collapse for LA 2/50 Hazard

	$\hat{C}$	β_r	β_u	ϕ	$\hat{D}$	β_{acc}	β_{or}	γ	β_a	γ_a	λ_{con}	β_{UT}^2	K_x	C.L.
1997 NEHRP WCSB, SDC= D														
3-story	0.100	0.00	0.26	0.90	0.026	0.37	0.21	1.31	0.17	1.04	2.54	0.10	3.46	99%
1997 NEHRP WCSB, SDC= C														
3-story	0.100	0.01	0.26	0.90	0.011	0.39	0.00	1.26	0.17	1.04	6.26	0.10	6.37	99%
9-story	0.091	0.12	0.35	0.82	0.016	0.22	0.00	1.08	0.20	1.06	4.07	0.16	4.11	99%
20-story	Collapse													
1997 NEHRP WCSB, SDC= C : with very stiff beams														
9-story	0.097	0.08	0.35	0.83	0.015	0.24	0.00	1.09	0.20	1.06	4.62	0.16	4.43	99%

Table 7-2 IO Confidence Level for LA 50/50 Hazard

	$\hat{C}$	β_r	β_u	ϕ	$\hat{D}$	β_{acc}	β_{or}	γ	β_a	γ_a	λ_{con}	β_{UT}^2	K_x	C.L.
1997 NEHRP WCSB, SDC= D														
3-story	0.045	0.20	0.25	0.86	0.005	0.67	0.00	1.95	0.18	1.05	3.76	0.09	4.76	99%
1997 NEHRP WCSB, SDC= C														
3-story	0.014	0.20	0.25	0.86	0.003	0.41	0.00	1.29	0.18	1.05	2.96	0.09	3.98	99%
9-story	0.014	0.20	0.25	0.86	0.004	0.44	0.00	1.34	0.21	1.07	1.90	0.11	2.46	99%
20-story	0.033	0.20	0.25	0.86	0.002	0.39	0.00	1.25	0.25	1.10	8.59	0.13	6.61	99%
1997 NEHRP WCSB, SDC= C : with very stiff beams														
9-story	0.014	0.20	0.25	0.86	0.004	0.44	0.00	1.33	0.21	1.07	2.16	0.11	2.85	99%

Table 7-3 CP Confidence Level Against Global Collapse for LA 50/50 Hazard

	$\hat{C}$	β_r	β_u	ϕ	$\hat{D}$	β_{acc}	β_{or}	γ	β_a	γ_a	λ_{con}	β_{UT}^2	K_x	C.L.
1997 NEHRP WCSB, SDC= D														
3-story	0.100	0.00	0.26	0.90	0.005	0.67	0.00	1.95	0.18	1.05	8.81	0.10	7.36	99%
1997 NEHRP WCSB, SDC= C														
3-story	0.100	0.01	0.26	0.90	0.003	0.41	0.00	1.29	0.18	1.05	22.3	0.10	10.3	99%
9-story	0.091	0.12	0.35	0.81	0.004	0.44	0.00	1.34	0.21	1.07	11.7	0.17	6.65	99%
20-story	Collapse													
1997 NEHRP WCSB, SDC= C : with very stiff beams														
9-story	0.097	0.08	0.35	0.82	0.004	0.44	0.00	1.33	0.21	1.07	14.4	0.17	7.15	99%

Table 7-4 CP Confidence Level Against Global Collapse for SE 2/50 Hazard

	$\hat{C}$	β_r	β_u	ϕ	$\hat{D}$	β_{acc}	β_{or}	γ	β_a	γ_a	λ_{con}	β_{UT}^2	K_x	C.L.
1997 NEHRP WCSB, SDC= C														
3-story	0.099	0.03	0.26	0.93	0.011	0.28	0.00	1.08	0.17	1.03	7.55	0.10	6.81	99%
9-story	0.092	0.11	0.35	0.88	0.014	0.32	0.00	1.11	0.20	1.04	4.99	0.16	4.40	99%
20-story	Collapse													
1997 NEHRP WCSB, SDC= C : with very stiff beams														
9-story	0.077	0.24	0.35	0.84	0.014	0.44	0.00	1.21	0.20	1.04	3.64	0.16	3.62	99%

Table 7-5 IO Confidence Level for SE 50/50 Hazard

	$\hat{C}$	β_r	β_u	ϕ	$\hat{D}$	β_{acc}	β_{or}	γ	β_a	γ_a	λ_{con}	β_{UT}^2	K_x	C.L.
1997 NEHRP WCSB, SDC= C														
3-story	0.014	0.20	0.25	0.90	0.003	0.39	0.00	1.16	0.18	1.03	3.62	0.09	4.49	99%
9-story	0.014	0.20	0.25	0.90	0.005	0.28	0.00	1.08	0.21	1.05	2.49	0.11	3.12	99%
20-story	0.033	0.20	0.25	0.90	0.002	0.25	0.00	1.07	0.25	1.06	12.5	0.13	7.50	99%
1997 NEHRP WCSB, SDC= C : with very stiff beams														
9-story	0.014	0.20	0.25	0.90	0.004	0.32	0.00	1.11	0.21	1.05	2.66	0.11	3.33	99%

Table 7-6 CP Confidence Level Against Global Collapse for SE 50/50 Hazard

	$\hat{C}$	β_r	β_u	ϕ	$\hat{D}$	β_{acc}	β_{or}	γ	β_a	γ_a	λ_{con}	β_{UT}^2	K_x	C.L.
1997 NEHRP WCSB, SDC= C														
3-story	0.099	0.03	0.26	0.93	0.003	0.39	0.00	1.16	0.18	1.03	25.6	0.10	10.7	99%
9-story	0.092	0.11	0.35	0.87	0.005	0.28	0.00	1.08	0.21	1.05	15.82	0.17	7.17	99%
20-story	Collapse													
1997 NEHRP WCSB, SDC= C : with very stiff beams														
9-story	0.077	0.24	0.35	0.84	0.004	0.32	0.00	1.11	0.21	1.05	13.6	0.17	6.79	99%

7.3.5 Summary of Results for WCSB Buildings

Except for the 20-story building, all of the WCSB buildings designed in accordance with the 1997 NEHRP *Provisions* satisfied the SAC performance objectives for CP and IO. As a result, no further restrictions are required for these buildings.

The 20-story WCSB building designed in accordance with the 1997 NEHRP *Provisions* collapsed when subjected to LA and Seattle 2/50 ground motions. As a result, it is recommended that WCSB designs be restricted to 100 feet in height. This restriction also applies to weak-panel-zone designs which behave like frames with weak columns. Since the 9-story frames demonstrate adequate behavior, this restriction could be raised.

7.4 Ordinary Moment Frame Buildings with Partially Restrained Connections

7.4.1 Background

Partially Restrained (PR) connections occur in those steel moment frames in which the strength and stiffness of the frame is strongly influenced by the strength and the stiffness of the connection. PR connections are permitted in both Intermediate and Ordinary Moment Frames. PR connections may be partial stiffness, partial strength, or both. Partial stiffness PR connections are somewhat flexible. That is, significant rotation may occur in the connection before the connection develops its ultimate resistance. Connection flexibility of PR connections varies greatly as illustrated in Figure 7-12. PR connections can be categorized into stiff PR connections, PR connections with intermediate stiffness, and flexible PR connections. Details on each of the connection types in each category and the behavior of them can be found in the State of the Art Report on Connection Performance (Roeder, 2000). T-stub connections, which are in the intermediate category, have been investigated for this study, and a summary of the results are given in this section.

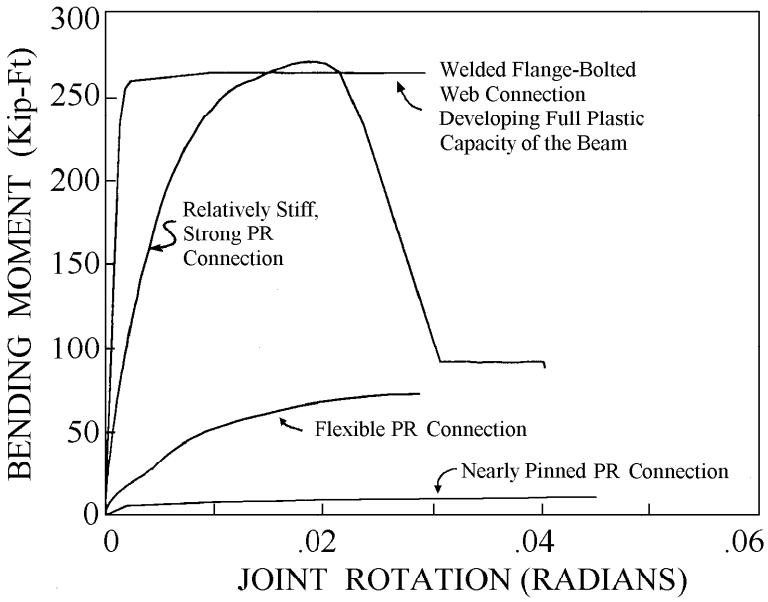

Figure 7-12 Relative Strength and Stiffness of PR Connections (Roeder, 2000)

7.4.2 Stiffness for PR Connection

The connection stiffness can have a large impact on the behavior of the building. If the connections are rigid, that is the centerlines of the columns and beams remain orthogonal, or if the connection is just pinned, the modeling can be easily done by any of the commercial programs. Since the PR connections have stiffnesses less than the rigid case and greater than the pinned case, a special element accounting for the flexibility of the connection is needed.

Accounting for the flexibility of the connection can be achieved by putting in, at each end of the beam, rotational spring elements that have the proper stiffness. This is shown in Figure 7-13. One end of the spring is connected to the beam and the other to the column. However, not all structural analysis programs have a rotation spring element.

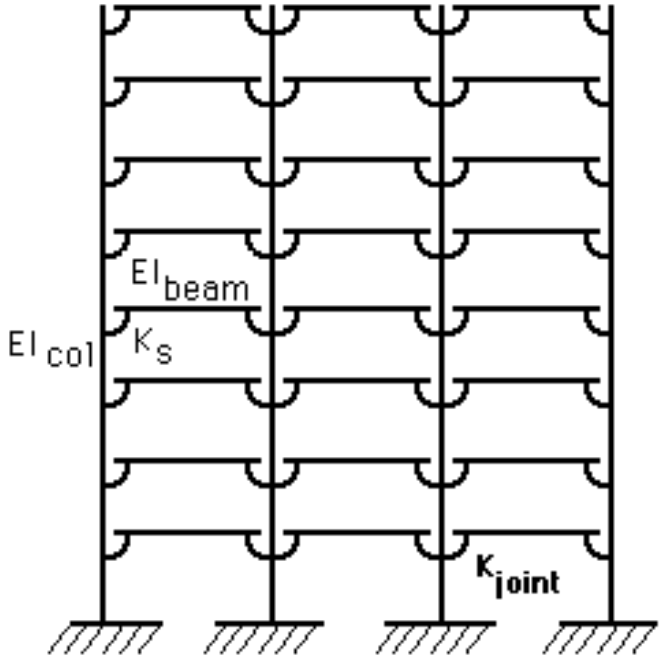

Figure 7-13 Modeling of Connection Flexibility with Rotational Spring Elements (Roeder, 2000)

An alternative method that is described in FEMA-273 (FEMA, 1997c) can be used for designing a building with PR connections. This method allows an analysis with rigid connections, but the beam stiffness, EI_b, is reduced to $EI_{b\ adj}$ to account for the rotational spring stiffness of the joint. This is based on a single-story moment-frame subassemblage as shown in Figure 7-14. This frame has rigid connections with bending stiffness of EI for the beams and columns. The elastic story drift-deflection, *u*, can be estimated by the equation

$$u = \frac{P \cdot h^3}{12 E I_c} + \frac{P h l_b^2}{12 E I_b} \tag{7-3}$$

where:

h = story height, in
l_b = beam length, in
I_b = moment of inertia of beam, in^4
I_c = moment of inertia of column, in^4

The deflection, u, is made up of two parts: bending of columns and bending of beams. If the loads and the beam and column stiffness are unchanged, the story drift deflection for a frame with flexible connections becomes

$$u = \frac{P \cdot h^3}{12 E I_c} + \frac{P h l_b^2}{12 E I_b} + \frac{P h^2}{2 K_s} \tag{7-4}$$

To achieve the same deflection, Equation 7-3 and Equation 7-4 can be used to obtain the following equation. Only the bending stiffness of the beam is adjusted.

$$u = \frac{P \cdot h^3}{12 E I_c} + \frac{P h l_b^2}{12 E I_{b\,adj}} \tag{7-5}$$

where:

$$EI_{b\,adj} = \frac{1}{\frac{6h}{l_b^2 K_\theta} + \frac{1}{E I_b}} \tag{7-6}$$

$$K_\theta = \frac{M_{PE}}{0.003} \tag{7-7}$$

for the case where the connection is encased and develops composite action and

$$K_\theta = \frac{M_{PE}}{0.005} \tag{7-8}$$

for others,

where:

K_θ = the rotational stiffness of the connection
M_{PE} = the moment capacity of the connection

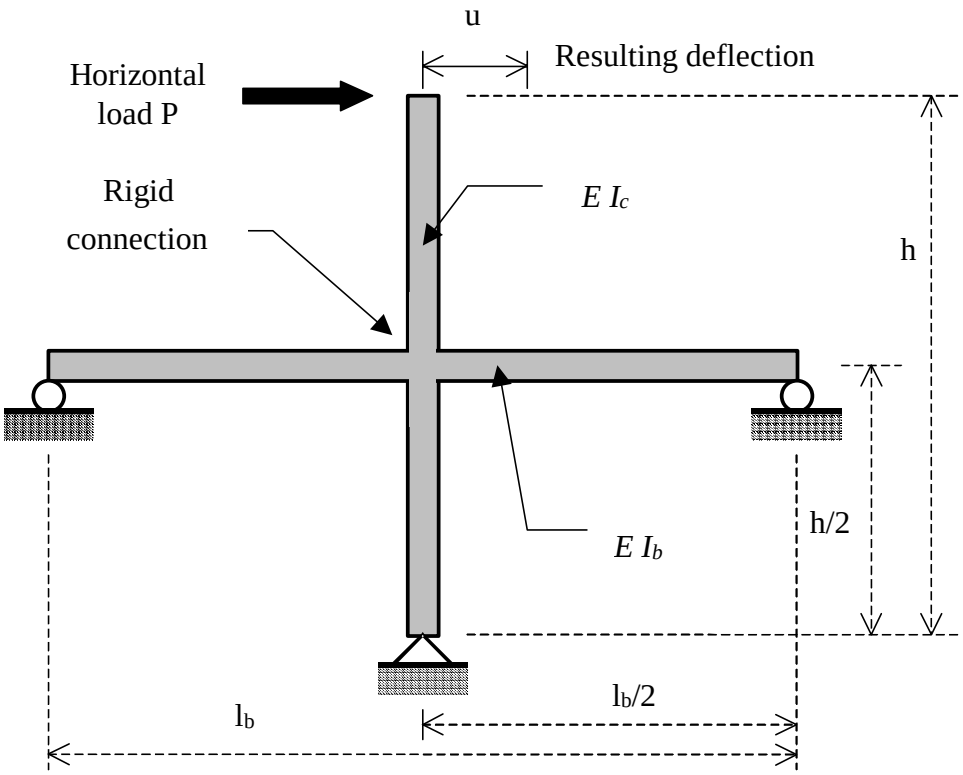

Figure 7-14 A Single-Story Moment Frame Subassemblage

Verification of Equation 7-6 has been performed using the SAP2000 program for modeling the rigid connection case and also the case with $I_{b\,adj}$. The DRAIN-2DX program was used to model the building with flexible connection springs. The 9-story building designed with T-stub connections for the LA site was used for the study. Figure 7-15 shows the comparison between the three cases. The open symbols represent the partially restrained cases, the circle representing the case with adjusted moment of inertia for the beam, and the square representing the case with flexible springs. As expected, the fully restrained case gave the smallest drifts over the height. Both procedures for modeling of the partially restrained connections gave similar responses. Therefore, modeling with adjusted beam moment of inertia with Equation 7-6 is adequate for design. However, when nonlinear behavior of the connection is to be investigated, the alternative method described in FEMA-273 will not be appropriate. Modeling of nonlinearity for the flexible connection will be covered in Section 7.4.3.3.

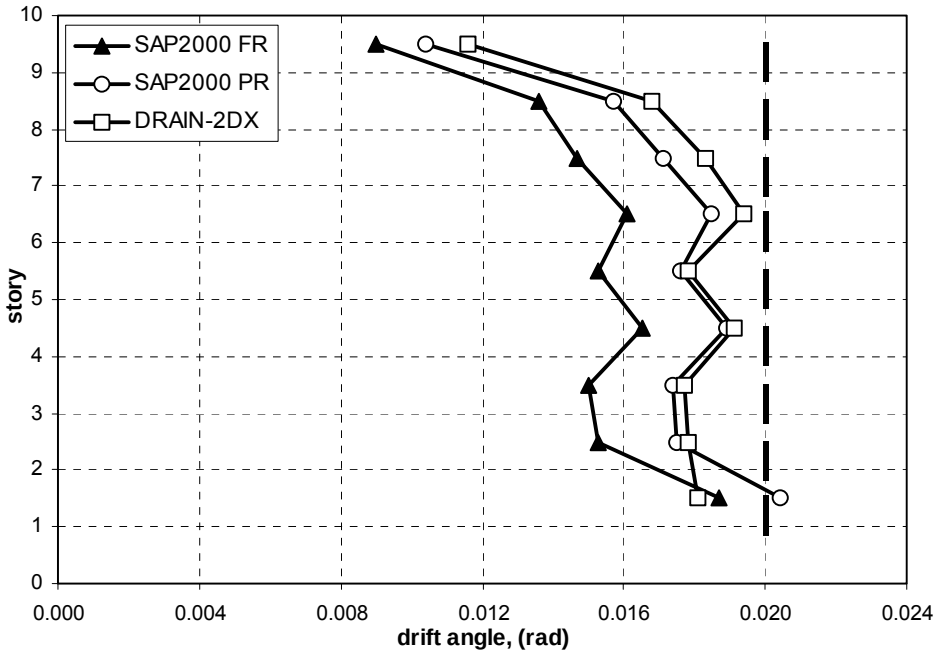

Figure 7-15 Comparison of Drift for PR and FR Cases for 9-Story Building

As described previously, the stiffness of the connection varies over a large range for PR connections. The ratio of the connection stiffness to the beam stiffness referred to as stiffness ratio is commonly used for indicating the relative stiffness. A 9-story building designed with T-stub PR connections was used for the investigation of the relative stiffnesses. According to Roeder (2000), a range of a minimum of 2 or 3 to 15 or 20 is expected to be the stiffness ratio for this kind of connection.

$$2 \sim 3 \le \frac{K_\theta}{E\, I_b / l_b} \le 15 \sim 20 \ = \text{stiffness ratio}$$

where K_θ is the stiffness of the connection spring.

The structure was pushed to the designed load for different values of stiffness ratios varying from 0.5 to 99. The result is shown in Figure 7-16. The ratio of 0.5 represents an almost pinned case, whereas the ratio of 99 represents the fully fixed case. The ratio between the roof drift for the fixed case (where ratio is 99) to that for each stiffness case is listed in the Table 7-7. It shows that the ratio of 20 is about 90% of the stiffness of the fully restrained case.

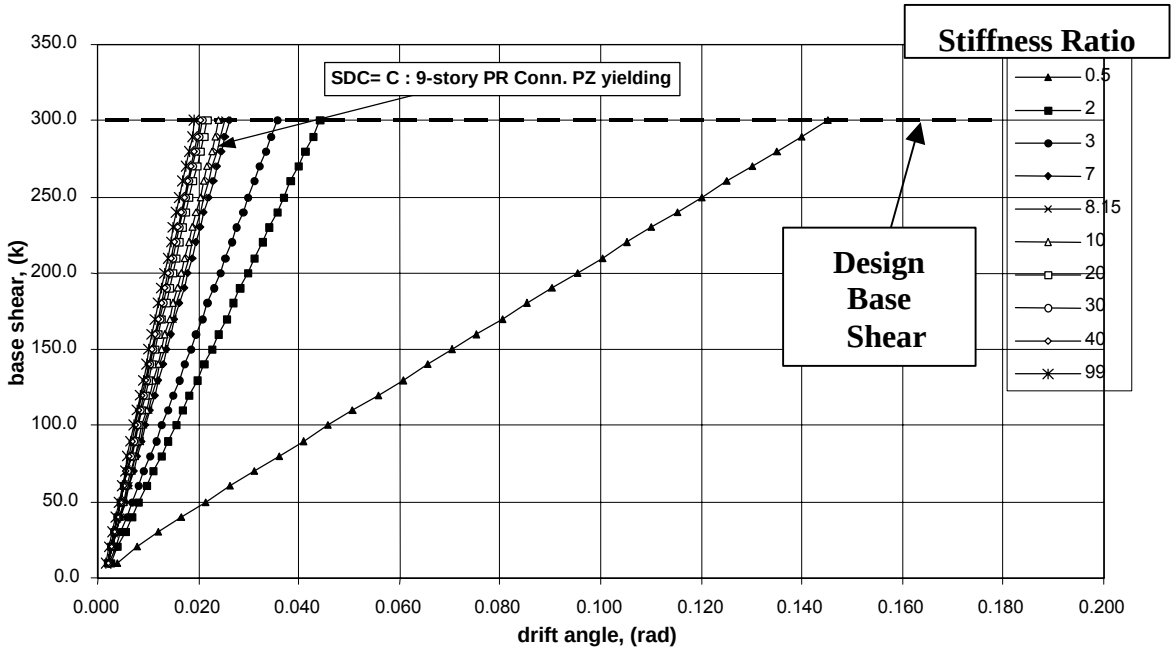

Figure 7-16 Comparison of Global (Roof) Drift Angle Due to Static Loading for Different Stiffness Ratios of the Connection Springs

Table 7-7 Comparison of Global (Roof) Drift Angle Due to Static Loading for Different Stiffness Ratios of the Connection Springs

Stiffness Ratio	99	40	30	20	10	8.15	7	3	2	0.5
Roof Drift Angle	0.0193	0.0205	0.0209	0.0217	0.0242	0.0252	0.0262	0.0357	0.0442	0.1450
ratio to the fixed case	1.00	0.94	0.92	0.89	0.80	0.76	0.74	0.54	0.44	0.13

7.4.3 Evaluation of Buildings with T-stub PR Connections

7.4.3.1 Background

PR connections can be categorized as stiff PR connections, PR connections with intermediate stiffness and flexible PR connections. The bolted T-stub connection is the only type categorized as an intermediate stiffness connection. A typical configuration of the T-stub partially restrained connection is shown in Figure 7-17. The moment capacity of the connection may be as large as the full plastic moment capacity of the beam, or it can be as small as 60% to 70% of the full plastic moment capacity. While T-stub connections are clearly PR connections, they are stiffer and stronger than some of the other PR connection alternatives. The bolted T-stub connection can also be divided into partial stiffness with full strength, and partial stiffness with partial strength. Full-strength bolted T-stub connections are designed so that the full plastic capacity of

the beam can be reached, but yielding of beams and panel-zone shear deformation are also the sources of the plastic deformation. Partial strength connections will invariably develop their plastic deformations within the T-section. T-stub connections with partial strength have been studied for this project.

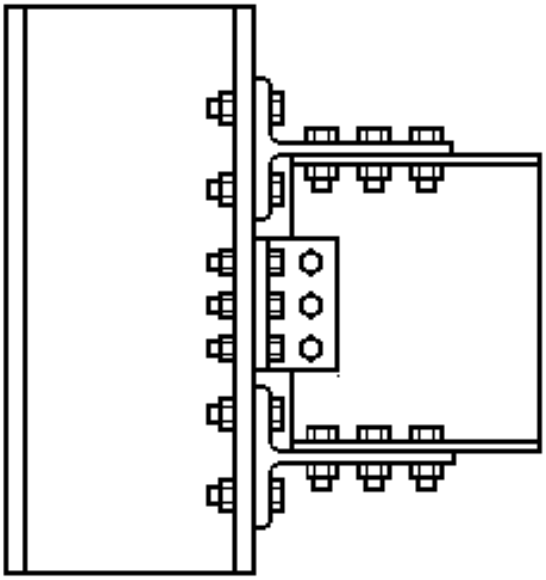

Figure 7-17 Typical T-Stub Connection

7.4.3.2 Description of Buildings Investigated

Similar to the study of the fully restrained ordinary WCSB moment frame, a 3-story building for seismic design category D and a 9-story building for seismic design category C were selected for investigation, since they showed large demands. Since T-stub connections are flexible, interior frames are also designed to act as part of the lateral-load-resisting system. The new plan views for the 3-story and the 9-story buildings are shown in Figure 7-18. The number of PR connections in the building was made to be the same for the N-S and E-W directions. The elevation views with the member sizes for those buildings are shown in Figures 7-19 and 7-20. The 3-story building now has eight moment-resisting bays with 14 T-stub PR connections per floor. The lateral-load resistance from the gravity-load only-columns and beams were also considered in the model with an additional bay. Modeling of the gravity-load-only bay is described in Section 5.4.6. The 9-story building has eight moment-resisting bays. The ground motions used for the study are 20 ground motions at the LA site for 2/50 hazard level and 20 ground motions at the Seattle site for the 2/50 hazard level. Both suites of ground motions were scaled to match the target spectra values. Since plastic deformations in panel zones were observed, cases with the addition of doubler plates were also investigated.

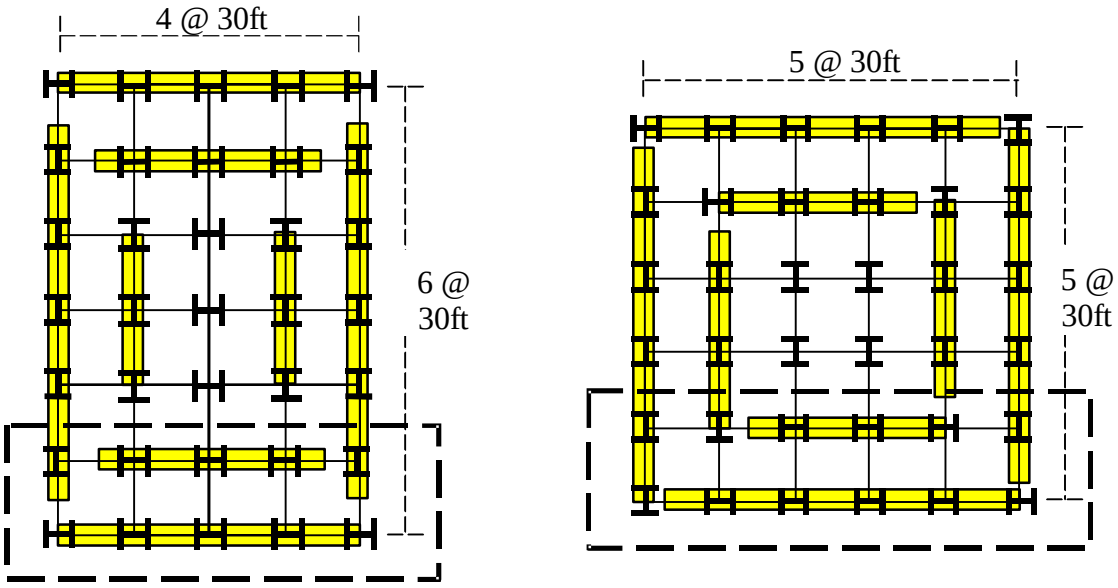

1997 NEHRP 3-story OMF T-stub PR Conn.
E-W : 28 connections
N-S : 28 connections

1997 NEHRP 9-story OMF T-stub PR Conn.
E-W : 28 connections
N-S : 28 connections

Figure 7-18 Plan View of 3-Story Building in SDC D and 9-Story Building in SDC C

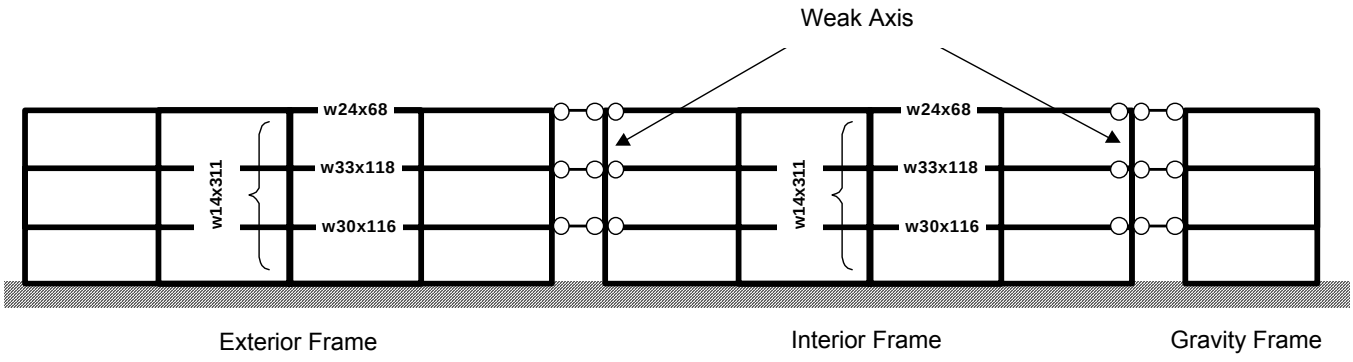

Figure 7-19 1997 NEHRP 3-Story OMF with T-Stub PR Connections

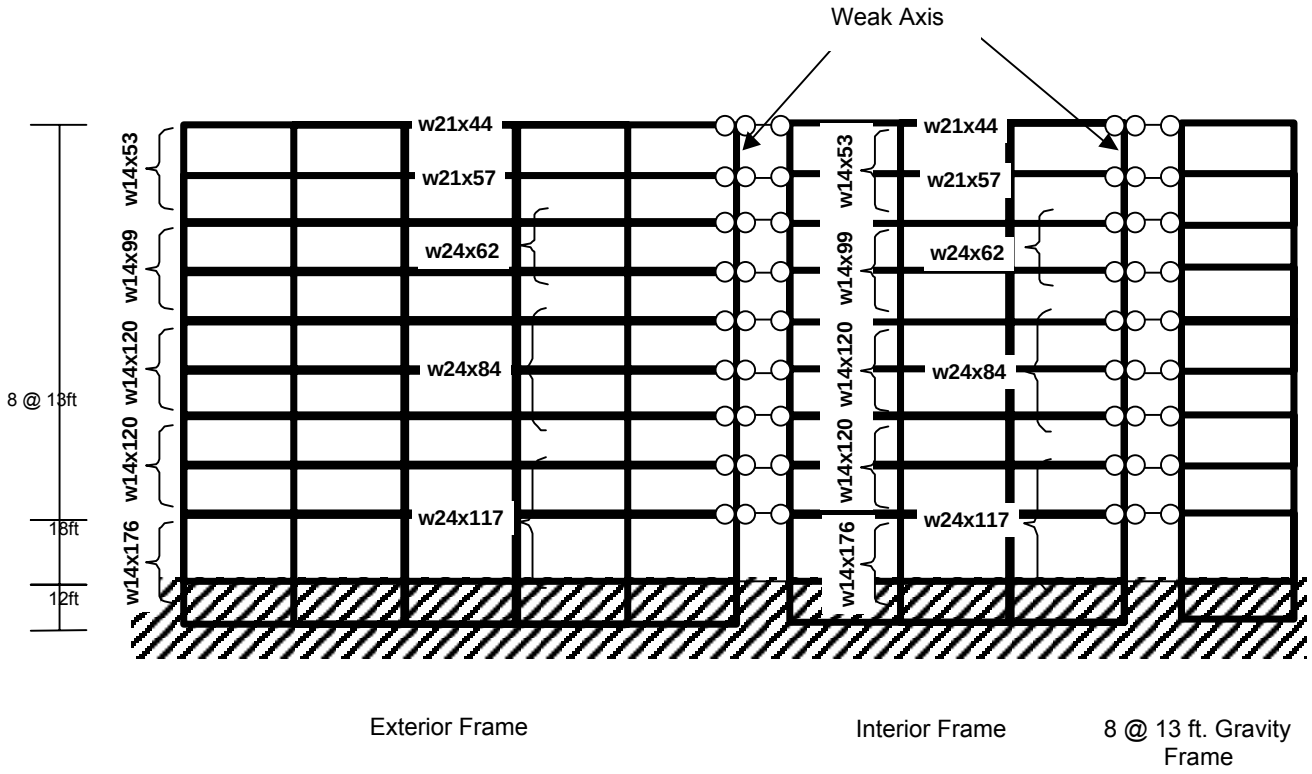

Figure 7-20 1997 NEHRP 9-Story OMF with T-Stub PR Connections

7.4.3.3 Modeling T-Stub Connections

The experimental data were provided by the Connection Performance team (Roeder, 2000). Determining the stiffness and strength of those connections is the critical issue for modeling the correct behavior. According to the report by Roeder (2000), the best performance is likely to be achieved with plastic flexural deformations of the flanges of the T-section coupled with tensile elongation of the stem of the T-section. The typical measured moment-rotation behavior of the partial stiffness and partial strength T-stub connection is shown in Figure 7-21. The model of moment-rotation behavior is shown in Figure 7-22. Due to the lack of modeling parameters provided in the modified version of the analysis program, DRAIN-2DX (Foutch and Shi, 1996), two individual springs were used to model the connection behavior. The illustration of two springs used for the model is shown in Figure 7-23. Two spring stiffnesses were combined to provide the stiffness specified in the report by Roeder (2000). The equation is as follows:

$$K_\theta = \frac{d_b \cdot M_{fail}}{0.375} \tag{7-9}$$

where:

d_b = depth of beam, in

M_{fail} = minimum of the failure mechanisms specified in Table 7-8.

The ductilities of each connection type are expressed in terms of two rotations. The first plastic rotation, θ_p, is the plastic rotation which can be achieved with a given yield mechanism and connection type without a sudden loss in resistance or deterioration in the behavior of the connection. The second plastic rotation, θ_g, is the plastic rotation at which the connection is expected to lose its capacity to support the gravity load. The plastic rotation that can be achieved with the partial strength connection depends on the relationship between the resistance, M_{fail}, of the local plastic flexure of the T-section flanges and net section fracture of the stem of the T-section. Therefore,

$$\theta_p = \frac{0.9 - 1.4\left\{\dfrac{M_{\text{fail-TFlngFlex}} - M_{\text{fail-TStem}}}{M_{\text{fail-TFlngFlex}} + M_{\text{fail-TStem}}}\right\}}{d_b} \tag{7-10}$$

where:

$M_{fail\text{-}TFlngFlex}$ = failure moment of T-section in local plastic flexure of the T-section flanges

$M_{fail\text{-}TStem}$ = failure moment of T-section flanges and net section fracture of the stem of the T-section

$$\theta_g = \theta_p + 0.01 \tag{7-11}$$

A comparable model which is simpler is shown in Figure 7-24.

The primary yield mechanisms and common failure modes for bolted T-stub connections are shown in Figure 7-25. Table 7-8 shows the yield mechanisms for the connection. The definition of symbols in the table can be referred to Figure 7-26 and 7-27. For a full strength T-stub connection, balance of yield mechanisms and failure modes is needed for ductile performance. The last row in the table should be satisfied for the partial strength connections. Failure modes for bolted T-stub connections are listed in Table 7-9. Again, the definition of symbols in the table can be referred to Figures 7-26 and 7-27. Details of each parameter are reported in the SOA report by Roeder (2000) and also shown in Figures 7-26 and 7-27.

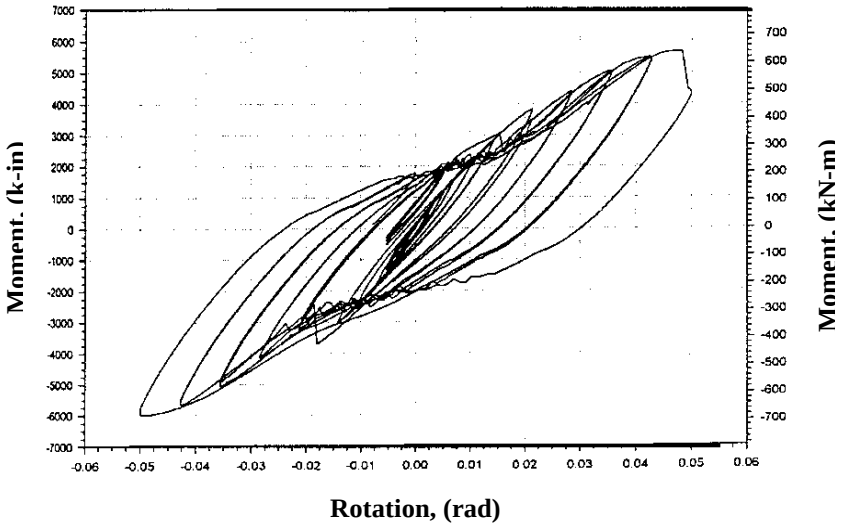

Figure 7-21 Measured Moment-Rotation Behavior of T-Stub Partially Restrained Connection (Leon et al., 1999)

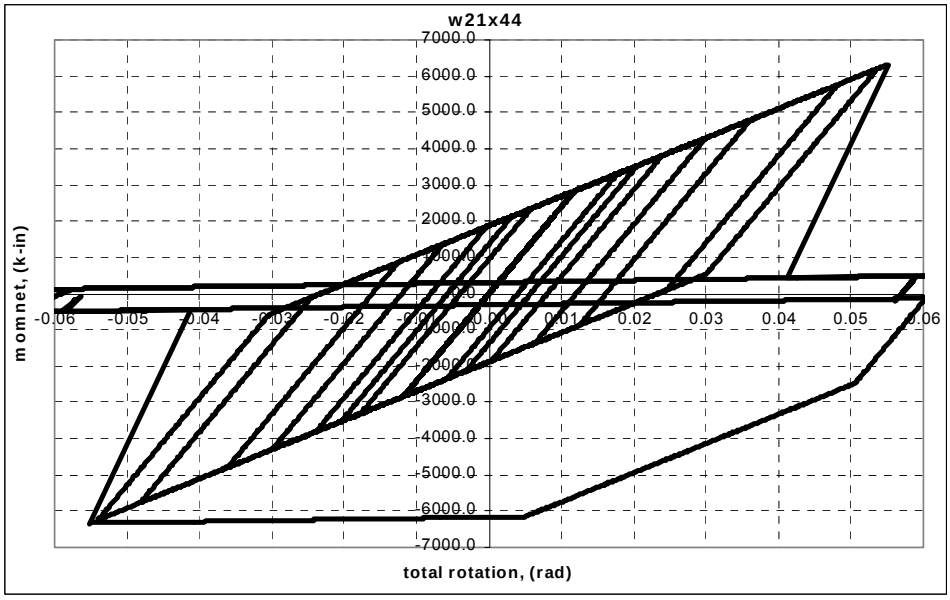

Figure 7-22 Model of Moment-Rotation Behavior of T-Stub Partially Restrained Connection (Foutch and Yun, 1999)

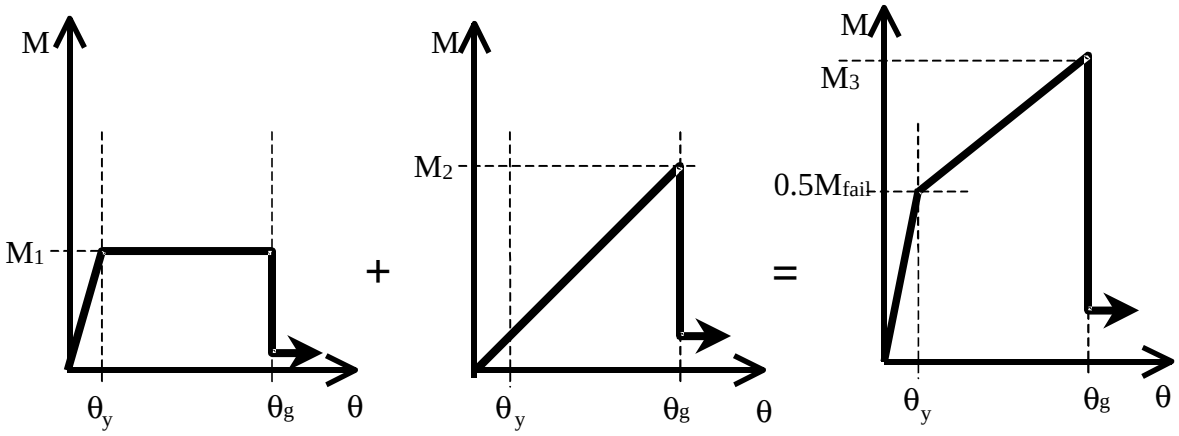

Figure 7-23 T-Stub Connection Modeling Used for Study

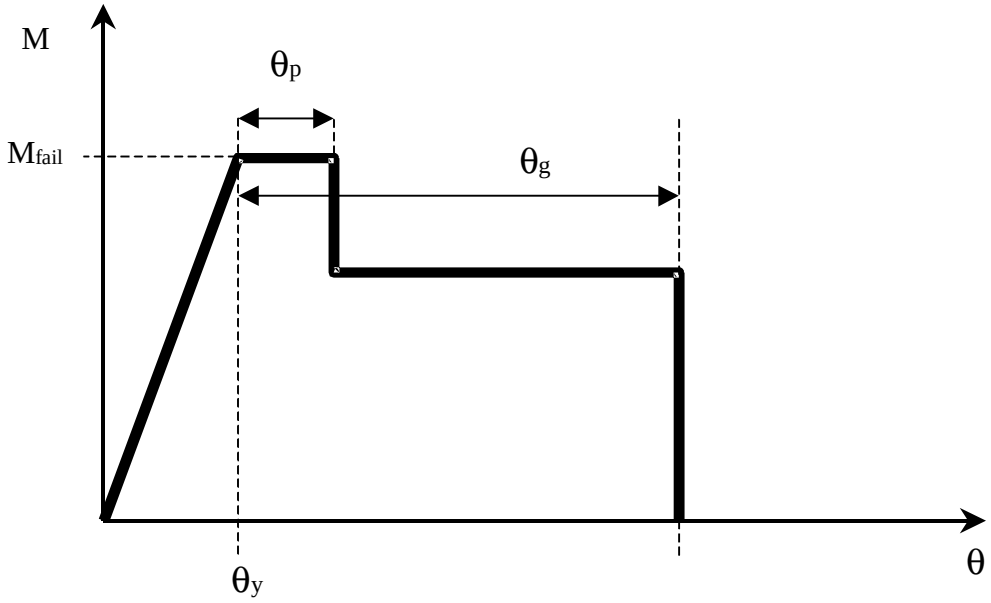

Figure 7-24 Moment-Rotation Behavior of T-Stub Connection

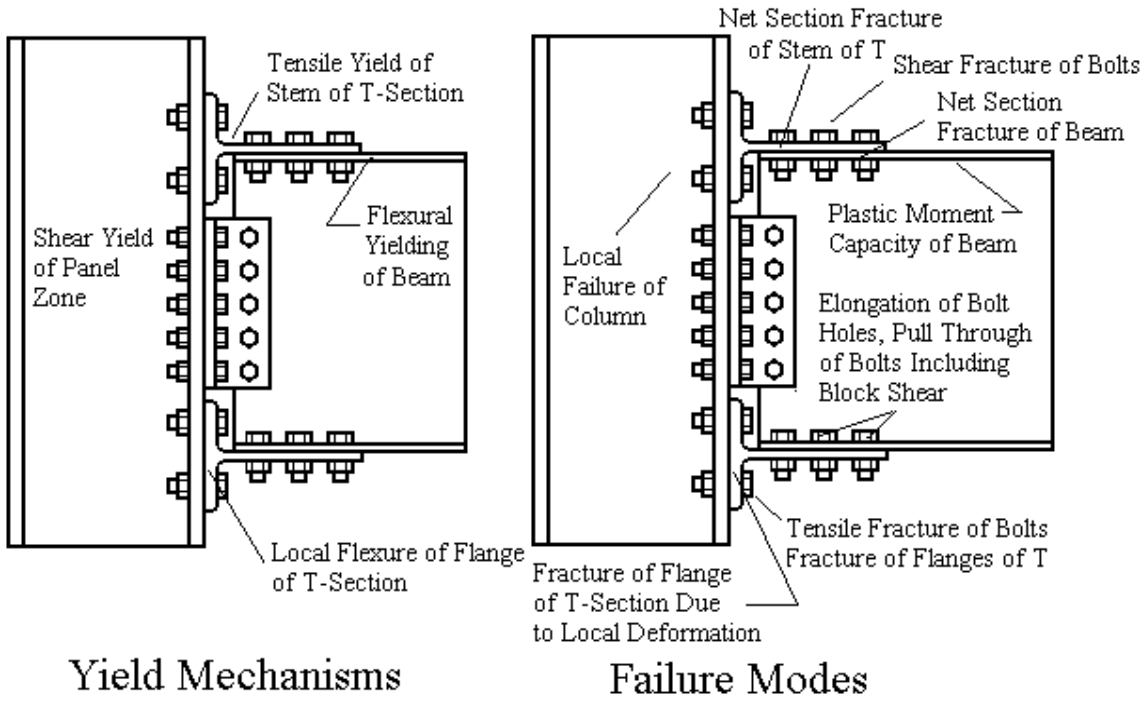

Figure 7-25 Primary Yield Mechanisms and Common Failure Modes for Bolted T-Stub Connections (Leon et al., 2000 and Roeder, 2000)

7.4.3.4 Response of the Buildings with PR Connections

The results of the static pushover analyses of the buildings with PR connections are shown in Figure 7-28 and Figure 7-29. The vertical distribution of forces was the same as used for the NEHRP equivalent lateral force procedure. Since plastic deformations in panel zones were observed, cases with doubler plates were also investigated and plotted. The results for both of the PR connection buildings clearly show lower stiffness for the PR connections than for those for the FR WCSB cases. However, the strength of the 3-story building was comparable to the WCSB 3-story building with doubler plates. The 9-story building shows some reduction in strength compared to the WCSB 9-story case. The increase in strength due to the doubler plates for the 3-story PR building is small compared to the case for the 9-story PR building.

Demands for the 3-story PR-connection building, with and without the doubler plates, excited by 2/50 ground motions, are shown in Figure 7-30. Those for 9-story PR connection buildings are shown in Figure 7-31. The plots on the left are for the case without doubler plates and those on the right are for the case with the doubler plates. The change in response due to providing doubler plates for the 3-story building case is insignificant, just like the results from the static analysis. The drift demands increased for the 9-story building when doubler plates were added. The increase in the axial compression force as well as the increase in demand for the beam connections were noticeable. The median drift for the 3-story building was approximately 0.032, whereas it was about 0.02 for the 9-story building. Both buildings performed well.

Table 7-8 Yield Mechanisms for Bolted T-Stub Connection (Leon, et al., 2000 and Roeder, 2000)

Yield Mechanism	Equation to Define Yield Mechanism Moment Resistance at the Face of the Column
Flexure of Beam	$M_{yield} = S \cdot F_{ybm} \cdot \dfrac{L - d_c}{L - d_c - 2 \cdot (S_1 + S_3)}$
Panel Zone Yielding	$M_{yield} = 0.55 \cdot d_b \cdot F_{y-col} \cdot d_c \cdot t_{w-c} \cdot \left(\dfrac{L - d_c}{L}\right) \cdot \left(\dfrac{h}{h - d_b}\right)$
Balance of Flexural and Panel Zone Yielding	$S \cdot F_{ybm} \cdot \dfrac{L - d_c}{L - d_c - 2 \cdot (S_1 + S_3)}$ $\approx 0.6 \cdot d_b \cdot F_{y-col} \cdot d_c \cdot t_{w-c} \cdot \left(\dfrac{L}{L - d_c}\right) \cdot \left(\dfrac{h - d_b}{h}\right)$
Balance of Yield Mechanisms and Failure Modes Needed for Ductile Performance	Experiments have shown that ductile behavior of the connection with full strength connection behavior can be achieved if $1.1 \cdot M_{yield} < \phi \cdot M_{fail}$ for all T-section, bolt tension, and beam net section failure modes
Balance of T-section Flange Flexural Capacity for Control of Prying Forces	The prying forces in partial strength connections must be limited to no more than 30% of bolt force associated with the failure moment acting alone.
Balance Requirement For Partial Strength Connections Using The Rotational Capacity Given In Eq. 5-12a	$M_{fail-stem\ of\ T}$ must be within 15% of $M_{fail-flange\ of\ T\ in\ flexure}$

Note: The definition of symbols are referred to Figure 7-26 and Figure 7-27.

Table 7-9 Failure Modes for Bolted T-Stub Connections (Leon, et al., 2000 and Roeder, 2000)

Failure Mode	Equation for Failure Moment at the Face of the Column	Related Issues
Fracture of Shear Bolts	$M_{fail} = 2\,N\,A_b\,(0.6\,F_{u\text{-}bolt})\,(d_b + t_{stem\text{-}t})\,\frac{L}{L - (S_1 + S_3)}$	A_b is the cross sectional area of bolt
Net Section Fracture of Stem of T-Section	$M_{fail} = F_{u\text{-}t\text{-}stub}\,(W - 2\,(\Phi_{bolt} + .125))\,t_{stem\text{-}t}\,(d_b + t_{stem\text{-}t})\,\frac{L}{L - 2\,S_1}$ where W is lesser of $W \le W_1$ and $W \le g_{shear} + S_3 \tan\theta_{eff}$.	Φ_{bolt} is the bolt diameter and $\theta_{eff} = 60\,t_{stem\text{-}t}$ except $15^o < \theta_{eff} < 30^o$
Plastic Capacity of Flanges of T-Section	$M_{fail} = \frac{(2a' - \frac{d_b}{4})\,W\,F_{y\text{-}t\text{-}section}\,t_f^2\,(d_b + t_{stem\text{-}t})}{4a'\,b' - d_b\,(b' + a')}$	Geometry is defined in Figure 6.3.3-6 and $a' = a + \frac{\Phi_{bolt}}{2}$
Tension Capacity of Bolts Including Prying Force	$M_{fail} = N_{tb}\,(d_b + t_{stem\text{-}t})\{R_n + \frac{p\,F_{y\text{-}t}\,t_{f\text{-}t}^2}{4\,a'}\}\frac{a' + b'}{a'}$	R_n is nominal tensile resistance of bolts and $p = \frac{2\,W}{N_{tb}}$
Net Section Fracture of Beam	$M_{fail} = \{F_{u\text{-}bm}\,(b_f - 2\,(\Phi_{bolt} + .125))\,t_{bf}\,(d_b - t_f) + 0.25\,F_{y\text{-}bm}\,(A_{bm} - 2\,b_f\,t_f)\,(d_b - 2\,t_f)\}\,\frac{L - d_c}{L - d_c - 2\,(S_1 + S_3)}$	A_{bm} is cross sectional area of beam
Block Shear	AISC LRFD Block Shear criteria must be applied to the block shear and bolt pull-through patterns illustrated in Fig. 7-26.	See Figure 7-26 for geometry
Flange Buckling	for flange, $\frac{b_f}{2\,t_f} \le \frac{52}{\sqrt{F_y}}$	
Web Buckling	for web, $\frac{d_b}{t_w} \le \frac{375}{\sqrt{F_y}}$	
Lateral Torsional Buckling	$L_b < \frac{2500\,r_y}{F_y}$ L_b is the unsupported length.	Equation from AISC LRFD Seismic Provisions

Table 7-9 Failure Modes for Bolted T-Stub Connections (Leon, et al., 2000 and Roeder, 2000) (continued)

Failure Mode	Equation for Failure Moment at the Face of the Column	Related Issues
Column Flange Thickness **Requirements for No Stiffener to the Beam Tension Flange**	For column flanges without stiffeners or continuity plates, the minimum thickness of column, t_{cf}, must be greater than $t_{cf} > \sqrt{\frac{1.1\, R_y F_{yb} Z_b}{d_b - t_{bf}} \frac{(\frac{g}{2} - k_1)}{2.02\, F_{yc}\, c}}$ Stiffeners required to carry the unbalanced portion of the force, $\frac{1.1\, R_y F_{yb} Z_b}{d_b - t_{bf}}$, if the column flange thickness does not satisfy this requirement.	The dimensions are defined in the figure except that k_1 is distance from centerline of column web to flange toe of fillet. - This equation is the same as 4 bolt unstiffened end plate.
Plastic Bending Capacity of Stiffened Column Flanges	The column flange thickness, t_{fc}, must be larger than $t_{fc} > \sqrt{\frac{1.1\, R_y F_{yb} Z_b}{2(d_b - t_{bf})} \frac{}{0.81\, F_{yc}\, Y_c}}$ where: $Y_c = (\frac{c}{2} + s)(\frac{1}{\frac{b_{fc} - g}{2}} + \frac{2}{\frac{g}{2} - k_1}) + (\frac{b_{fc} - g}{2} + \frac{g}{2} - k_1)(\frac{4}{c} + \frac{2}{s})$ and $s = \sqrt{\frac{(\frac{g}{2} - k_1)\frac{b_{fc} - g}{2}}{\frac{b_{fc} - g}{2} + g - 2\, k_1} (2b_{fc} - 4\, k_1)}$	Yield line theory of bending of column flanges. - This equation is the same as 4 bolt unstiffened end plate.
Column Stiffener **Requirements for Beam Compression Flange**	No Stiffener required if $\frac{1.1\, R_y F_{yb} Z_b}{d_b - t_{bf}} < (6\, k + c)\, F_{yc}\, t_{wc}$ Stiffeners required to carry the unbalanced portion of the force, $\frac{1.1\, R_y F_{yb} Z_b}{d_b - t_{bf}}$, if the column flange thickness does not satisfy this requirement. This equation recognizes the greater spreading of beam flange force to the column web provided by the end plate.	k is the beam fillet distance from the extreme fiber of beam flange to the web toe of fillet. - This equation is the same as 4 bolt unstiffened end plate.
Strong Column Weak Beam	$1.1 < \frac{\Sigma\, Z_c (F_{yc} - \frac{P_{uc}}{A_g})}{\Sigma\, Z_b\, F_{yb} \frac{L - d_c}{L - d_c - 2(S_1 + S_3)}}$	Based on plastic moment capacity of beam at the last bolt of T-section.

Note: The definition of symbols are referred to Figure 7-26 and Figure 7-27.

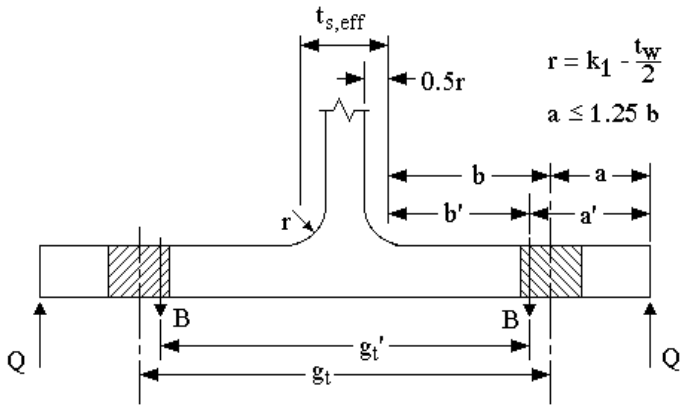

Figure 7-26 Geometry for Prying Forces and Bending of T-Section Flanges (Leon et al., 2000 and Roeder, 2000)

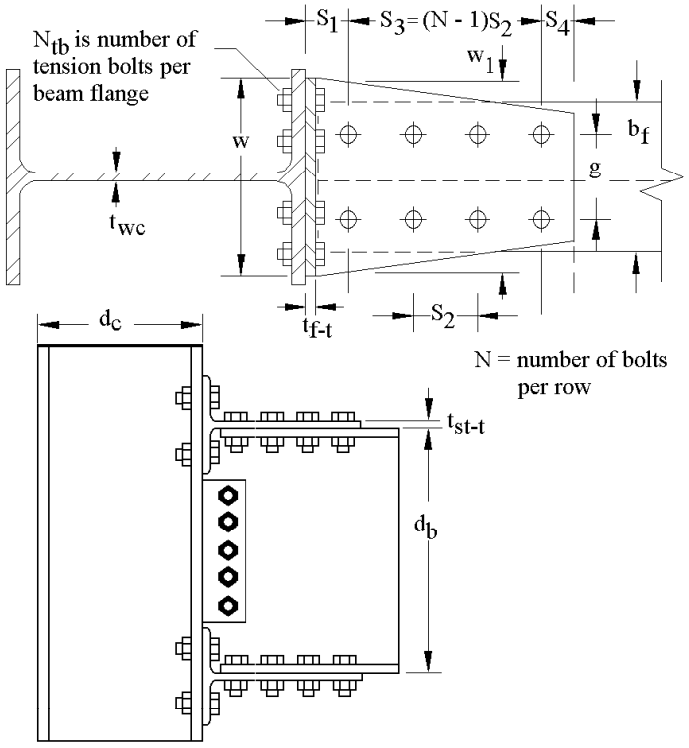

Figure 7-27 Geometry for Other T-Stub Failure Modes (Leon et al., 2000; Roeder, 2000)

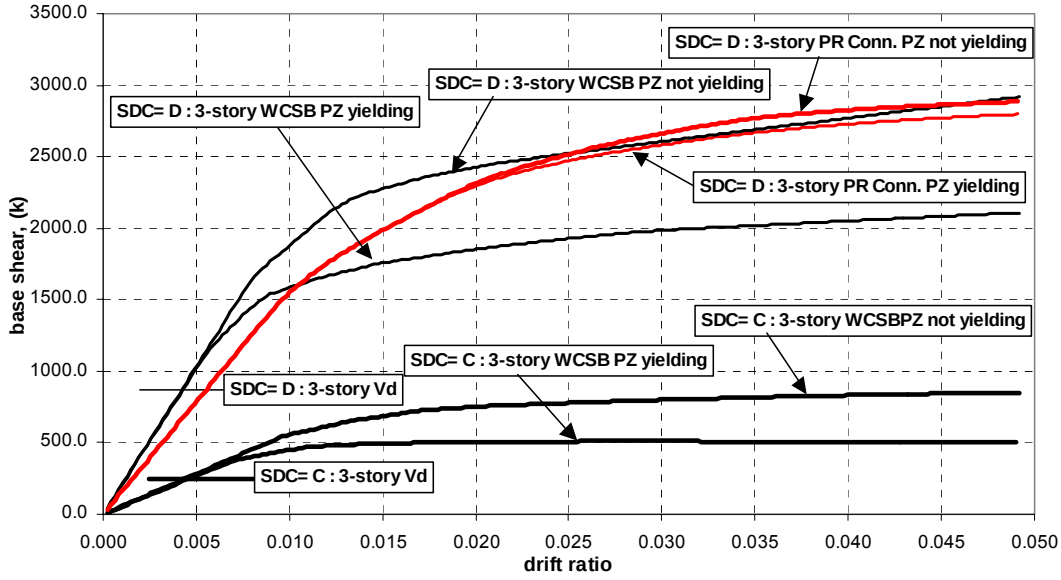

Figure 7-28 Comparison of Static Pushovers for 3-Story Buildings with PR Connections

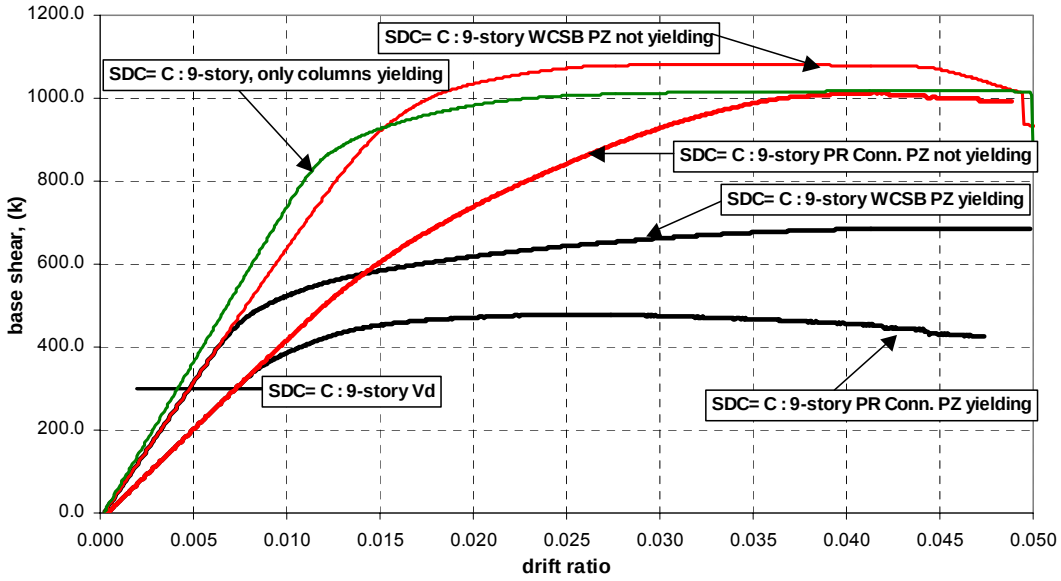

Figure 7-29 Comparison of Static Pushovers for 9-Story Buildings with PR Connections

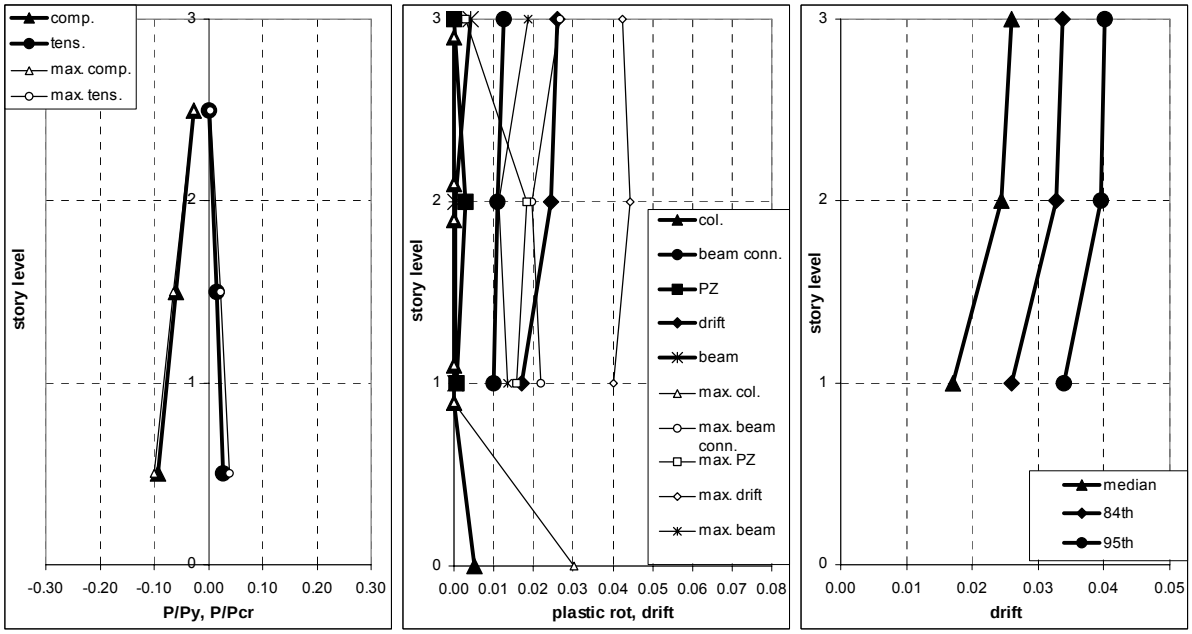

Figure 7-30 Median and Maximum Demands for the LA 3-Story Building with Yielding Panel Zones

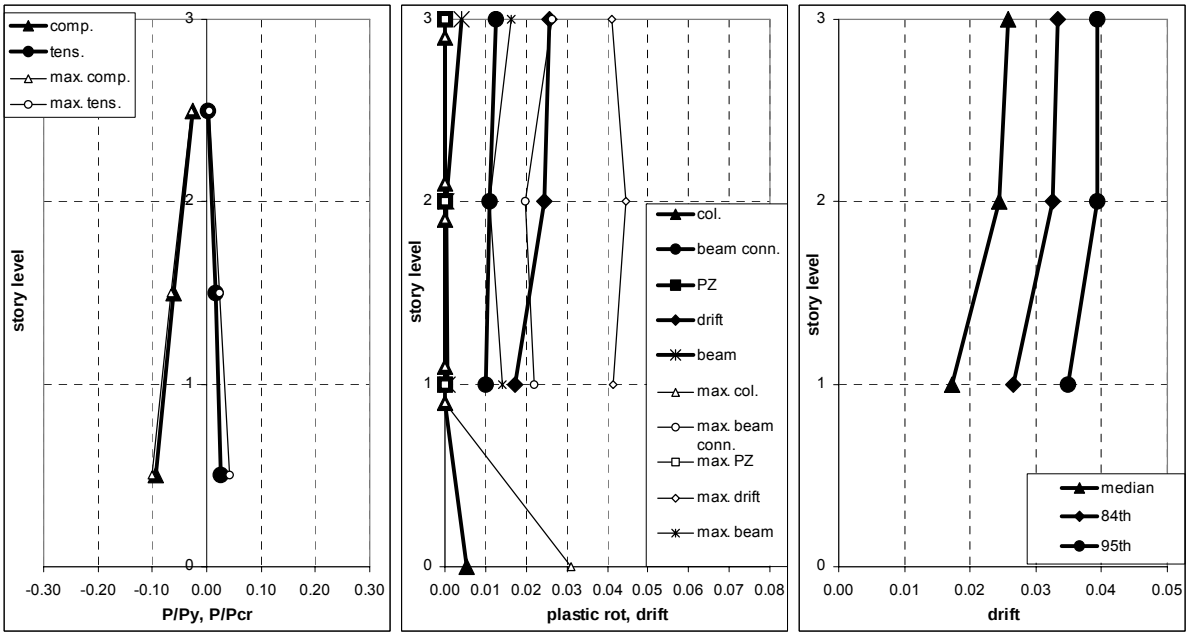

Figure 7-31 Median and Maximum Demands for the LA 3-Story Building with Panel Zones Prevented from Yielding

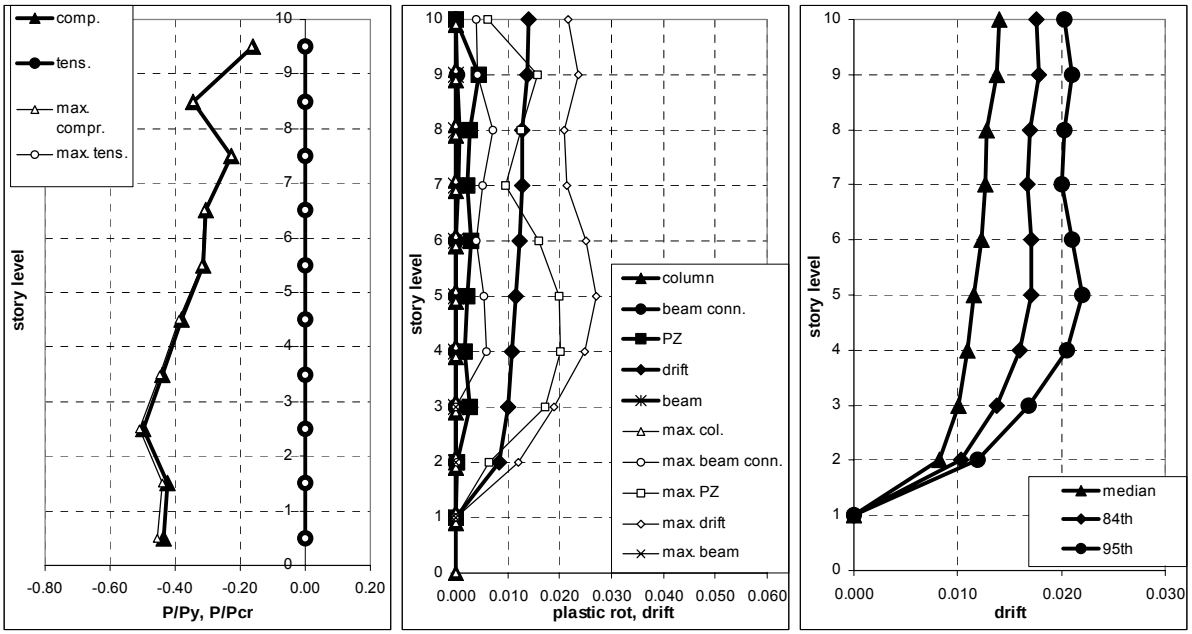

Figure 7-32 Median and Maximum Demands for the LA 9-Story Building with Yielding Panel Zones

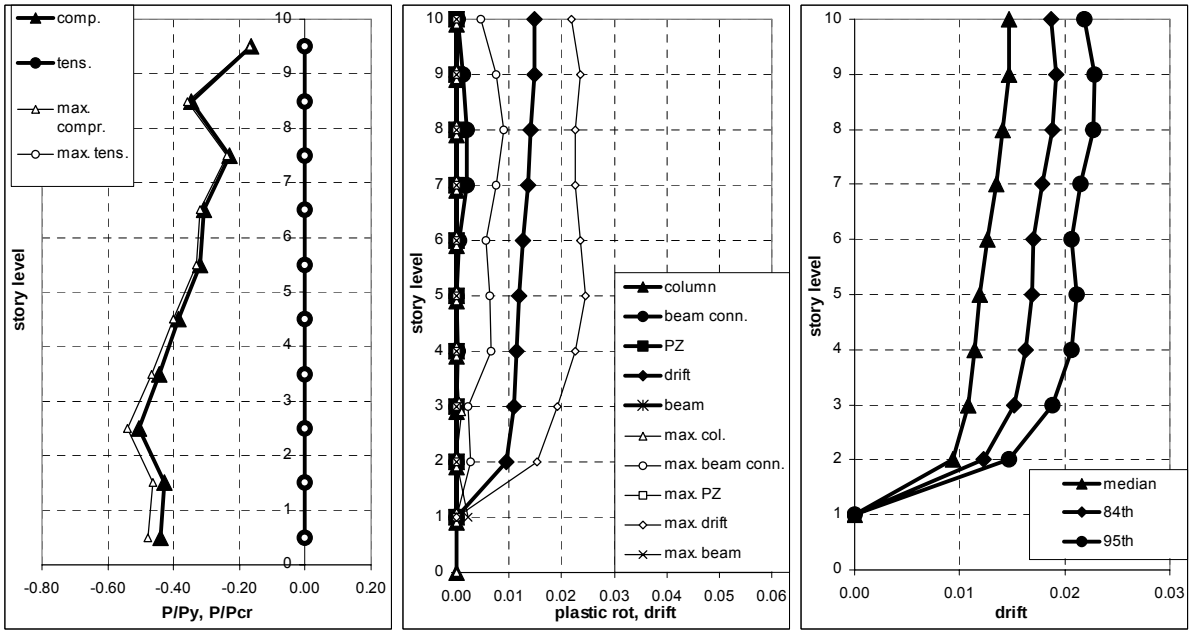

Figure 7-33 Median and Maximum Demands for the LA 9-Story Building with Panel Zones Prevented from Yielding

7.4.4 Performance Evaluation of Buildings with PR Connections

Performance evaluations were completed for all of the buildings with T-stub PR connections. Values for $\hat{C}$, β_R, β_U, ϕ, $\hat{D}$, β_{acc}, γ, β_a, γ_a, λ_{con}, β_{UT}^2, K_x for the LA site are given in Table 7-10 to Table 7-14. The results for the Seattle site are shown in Table 7-15 to Table 7-19. These were calculated using the provisions set out in Chapter 5.

The global capacities for each of the buildings were calculated using the IDA analysis. The 3-story building showed a median drift value of 10%. The median drift capacity for the original 9-story building showed 8.7%. The median demand drifts for both 2%-in-50-year hazard level and 50%-in-50-year hazard level have been presented and discussed in the previous section. Since the local drift capacity for buildings with T-stub PR connections was not defined in Table 5-3, it has been calculated individually. Since the strength of the connection was dropped down to 15% of the beam moment capacity at 4% rotation, a drift value of 4% plus the elastic drift observed from the static pushover analysis in Figure 7-28 and Figure 7-29 was used as the local drift capacity. Therefore, local drift capacity for the 3-story building was calculated to be 5% and that for the 9-story building calculated to be 4.8%. The drift criterion for the immediate occupancy level is listed in the table and its value was 3%.

A confidence level of 99% for the CP level and IO level for both of the buildings was observed, except for the 3-story building. The confidence level is 92%, which is lower than the acceptable value of 95%, but probably acceptable. A better estimation of the local drift capacity of the T-stub connection may make this building acceptable. A local drift capacity of 5.4% would result in 95% confidence.

Table 7-10 CP Confidence Level Calculations Against Global Collapse for Scaled LA 2/50 Hazard

	$\hat{C}$	β_r	β_u	ϕ	$\hat{D}$	β_{acc}	β_{or}	γ	β_a	γ_a	λ_{con}	β_{UT}^2	K_x	C.L. %
1997 NEHRP PR Connection, SDC= D														
3-story	0.100	0.00	0.26	0.90	0.026	0.27	0.21	1.19	0.17	1.04	2.79	0.10	3.77	99
1997 NEHRP PR Connection, SDC= C														
9-story	0.087	0.16	0.35	0.80	0.016	0.25	0.00	1.10	0.20	1.06	3.65	0.16	3.84	99

Table 7-11 CP Confidence Level Calculations Against Local Collapse for Scaled LA 2/50 Hazard

	$\hat{C}$	β_r	β_u	ϕ	$\hat{D}$	β_{acc}	β_{or}	γ	β_a	γ_a	λ_{con}	β_{UT}^2	K_x	C.L. %
1997 NEHRP PR Connection, SDC= D														
3-story	0.050	0.20	0.25	0.86	0.026	0.27	0.21	1.19	0.17	1.04	1.32	0.09	1.38	92
1997 NEHRP PR Connection, SDC= C														
9-story	0.048	0.20	0.25	0.86	0.016	0.25	0.00	1.10	0.20	1.06	2.15	0.10	2.87	99

Table 7-12 IO Confidence Level Calculations for Scaled LA 50/50 Hazard

	$\hat{C}$	β_r	β_u	ϕ	$\hat{D}$	β_{acc}	β_{or}	γ	β_a	γ_a	λ_{con}	β_{UT}^2	K_x	C.L. %
1997 NEHRP PR Connection, SDC= D														
3-story	0.030	0.20	0.25	0.86	0.002	0.72	0.00	2.16	0.18	1.05	5.96	0.09	6.26	99
1997 NEHRP PR Connection, SDC= C														
9-story	0.030	0.20	0.25	0.86	0.005	0.39	0.00	1.25	0.21	1.07	4.19	0.11	4.88	99

Table 7-13 CP Confidence Level Calculations Against Global Collapse for Scaled LA 50/50 Hazard

	$\hat{C}$	β_r	β_u	ϕ	$\hat{D}$	β_{acc}	β_{or}	γ	β_a	γ_a	λ_{con}	β_{UT}^2	K_x	C.L. %
1997 NEHRP PR Connection, SDC= D														
3-story	0.010	0.00	0.26	0.90	0.002	0.72	0.00	2.16	0.18	1.05	21.0	0.10	10.1	99
1997 NEHRP PR Connection, SDC= C														
9-story	0.087	0.16	0.35	0.80	0.005	0.39	0.00	1.25	0.21	1.07	11.4	0.17	6.56	99

Table 7-14 CP Confidence Level Calculations Against Local Collapse for Scaled LA 50/50 Hazard

	$\hat{C}$	β_r	β_u	ϕ	$\hat{D}$	β_{acc}	β_{or}	γ	β_a	γ_a	λ_{con}	β_{UT}^2	K_x	C.L. %
1997 NEHRP PR Connection, SDC= D														
3-story	0.005	0.20	0.25	0.86	0.002	0.72	0.00	2.16	0.18	1.05	9.94	0.09	7.92	99
1997 NEHRP PR Connection, SDC= C														
9-story	0.048	0.20	0.25	0.86	0.005	0.39	0.00	1.25	0.21	1.07	6.71	0.11	6.32	99

Table 7-15 CP Confidence Level Calculations Against Global Collapse for Scaled Seattle 2/50 Hazard

	$\hat{C}$	β_r	β_u	ϕ	$\hat{D}$	β_{acc}	β_{or}	γ	β_a	γ_a	λ_{con}	β_{UT}^2	K_x	C.L. %
1997 NEHRP PR Connection, SDC= C														
9-story	0.082	0.19	0.35	0.86	0.015	0.30	0.00	1.09	0.20	1.04	4.08	0.16	3.90	99

Table 7-16 CP Confidence Level Calculations Against Local Collapse for Scaled Seattle 2/50 Hazard

	$\hat{C}$	β_r	β_u	ϕ	$\hat{D}$	β_{acc}	β_{or}	γ	β_a	γ_a	λ_{con}	β_{UT}^2	K_x	C.L. %
1997 NEHRP PR Connection, SDC= C														
9-story	0.048	0.20	0.25	0.90	0.015	0.30	0.00	1.09	0.20	1.04	2.52	0.10	3.91	99

Table 7-17 IO Confidence Level Calculations for Scaled Seattle 50/50 Hazard

	$\hat{C}$	β_r	β_u	ϕ	$\hat{D}$	β_{acc}	β_{or}	γ	β_a	γ_a	λ_{con}	β_{UT}^2	K_x	C.L. %
1997 NEHRP PR Connection, SDC= C														
9-story	0.030	0.20	0.25	0.90	0.005	0.29	0.00	1.08	0.21	1.05	5.31	0.11	5.44	99

Table 7-18 CP Confidence Level Calculations Against Global Collapse for Scaled Seattle 50/50 Hazard

	$\hat{C}$	β_r	β_u	ϕ	$\hat{D}$	β_{acc}	β_{or}	γ	β_a	γ_a	λ_{con}	β_{UT}^2	K_x	C.L. %
1997 NEHRP PR Connection, SDC= C														
9-story	0.082	0.19	0.35	0.85	0.005	0.29	0.00	1.08	0.21	1.05	13.7	0.17	6.82	99

Table 7-19 CP Confidence Level Calculations Against Local Collapse for Scaled Seattle 50/50 Hazard

	$\hat{C}$	β_r	β_u	ϕ	$\hat{D}$	β_{acc}	β_{or}	γ	β_a	γ_a	λ_{con}	β_{UT}^2	K_x	C.L. %
1997 NEHRP PR Connection, SDC= C														
9-story	0.048	0.20	0.25	0.90	0.005	0.29	0.00	1.08	0.21	1.05	8.49	0.11	6.88	99

7.4.5 Summary of Results for the Buildings with T-Stub PR Connections

The 9-story building designed with T-stub PR connections for SDC C in accordance with the 1997 NEHRP *Provisions* satisfied the SAC performance objectives for the CP and the IO performance levels. However, the 3-story building designed with T-stub PR connections for SDC D in accordance with the 1997 NEHRP *Provisions* did not satisfy the SAC performance objectives for the CP performance at a confidence level of 95%. However, the confidence level was 92%, which is probably acceptable.

For the 3-story building, a maximum plastic rotation of 2.5% was observed in the beam connections, but only about 1% median plastic rotation was observed. Similarly, a large drift value of 4% was observed for the 95th percentile, but a median drift value of 2.5% was observed

which is acceptable. For the 9-story building, the maximum plastic rotation was observed in the panel zones. Maximum plastic rotation of 2% was observed for the panel zones when only 0.8% was observed for the beam connections. The building with doubler plates resulted in a maximum connection plastic rotation of 1%. Drifts of 2.2% and 1.4% were observed for the 95th percentile and median, respectively. Therefore, the 9-story buildings performed well.

A 9-story building for the Seattle site was analyzed for the 2%-in-50-year ground motions. The median drifts and 95th percentile drifts were 1.5% and 2.5%, respectively. These were slightly larger than for the 9-story building in LA. Overall, the structure performed well.

The adequacy of rotational capacity for the T-stub PR connection due to gravity load and lateral load was also investigated. For the 9-story building with T-stub PR connections in SDC C, the 8th level had the largest plastic rotational demand among all the levels, which was about 0.009 radians. Total rotational demand for the corresponding level is 0.013 radians. Another 9-story building in SDC B was designed and analyzed. This building was mostly governed by strength requirements. A maximum plastic rotation of 0.003 radians was observed at the 3rd level. Although the capacities of the connections were smaller than those for the SDC C structure, the calculated rotational demands were small enough that the connection performed well. Therefore, the rotational capacity for the T-stub PR connection due to gravity load and lateral load was adequate for both SDC C and SDC B.

The column axial force ratios were calculated and checked for acceptability. The maximum P/P_{cr} ratio observed was 0.5, which is well below the limiting ratio of 0.75. Only a small amount of tension was observed in the 3-story building. Therefore, the axial forces are all acceptable.

The permanent residual drifts due to 50/50 hazard ground motions were investigated. The maximum residual drift of 0.1% was observed from the 9-story building. The 3-story building had small residual drift values. Therefore, the building is again acceptable.

Finally, the confidence level calculations according to the procedure presented in Chapter 5 were performed. The confidence levels for CP for the 2/50 hazard and IO for the 50/50 hazard for all buildings were 99%, except for the 3-story building in SDC D with T-stub PR connections, which resulted in a 92% confidence level, which is lower than the acceptable value of 95% but probably acceptable. A better estimation of the local drift capacity of the T-stub connection may make this building acceptable. A local drift capacity of 5.4% would result in 95% confidence.

7.5 Evaluation of Buildings with End-Plate Connections

7.5.1 Background

The bases for determining the behavior of the end-plate connection is found in the experimental research by Murray (2000). This type of connection is considered to be in the category of stiff, partially restrained connections. As will be seen from the measured moment-rotation behavior of the connection, the connection has large stiffness as well as strength for most of the failure mechanisms. Hence, it will behave similarly to the fully restrained

connections. Therefore, this type of connection was moved to the fully restrained connection category from the partially restrained category. Therefore, just a brief description of the findings for the connection from the SOA report by Roeder will be addressed here.

7.5.2 Summary of Findings for End-Plate Connection from Connection Performance Team

More than 150 experiments were performed for the study of the connection behavior. Mixed results were obtained, due to the fact that most of the experiments in the past were monotonic loading cases, or they utilized very slender members which cannot develop significant inelastic deformations. A typical end-plate connection is shown in Figure 7-34.

The primary yield mechanisms and common failure modes for bolted extended-end-plate connections is shown in Figure 7-35. The measured moment-rotation behavior of connections for different failure mechanisms are shown in Figure 7-36 to Figure 7-38. The connections exhibited stable behavior with full hysteresis loops except for the connection with bolt fracture. A summary of the tests performed for the SAC project is shown in Table 7-20. Equations for calculating the failure mode of the 4-bolt unstiffened extended-end-plate connection and the 8-bolt stiffened extended-end-plate connection are listed in Table 7-21 and Table 7-22. The descriptions of the geometry parameters needed for the calculations are shown in Figure 7-39.

Based on the experiments performed for the SAC project, the plastic rotations achieved with the extended end-plate are large and they are strongly dependent upon the beam depth. A regression analysis of the results produced the following results.

$$\theta_p = 0.0607 - 0.0013\, d_b \text{ (radians with } d_b \text{ in inches)} \tag{7-12}$$

The standard deviation of the rotation is

$$\sigma_p = 0.006 - 0.0003\, d_b \text{ (radians with } d_b \text{ in inches)} \tag{7-13}$$

θ_g is estimated as

$$\theta_g = \theta_p + 0.01 = 0.0707 - 0.0013\, d_b \text{ (radians with } d_b \text{ in inches)}, \tag{7-14}$$

and the standard deviation of the rotation is

$$\sigma_g = \sigma_p \tag{7-15}$$

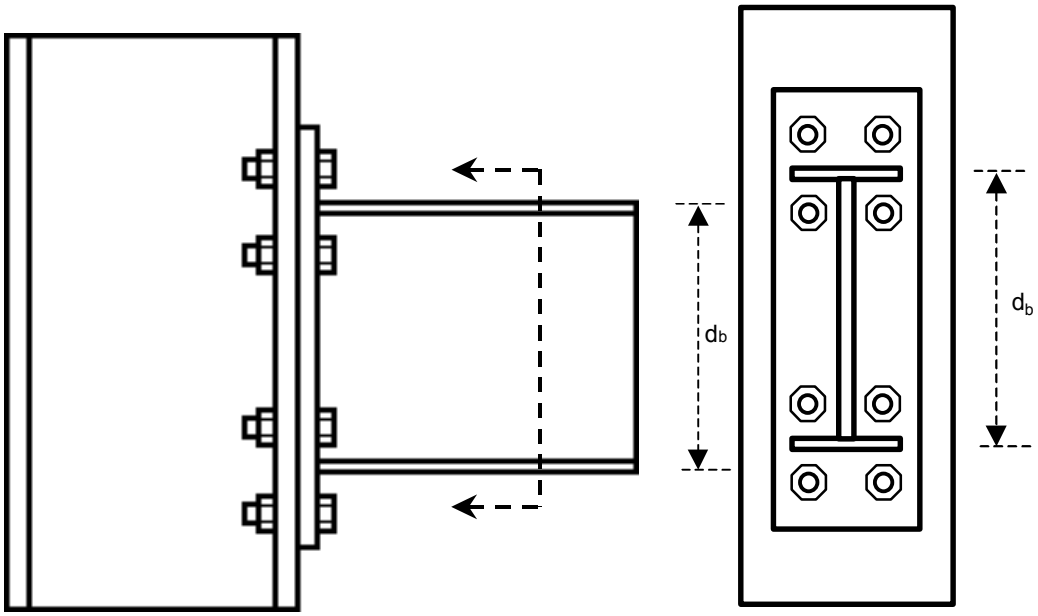

Figure 7-34 Typical Extended End-Plate Connection

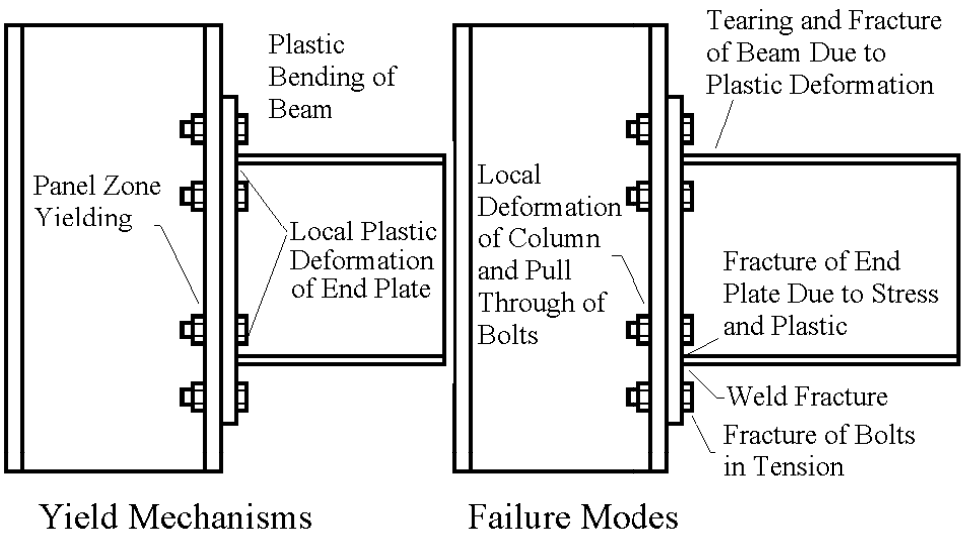

Figure 7-35 Primary Yield Mechanisms and Common Failure Modes for Bolted Extended-End-Plate Connections (Roeder, 2000)

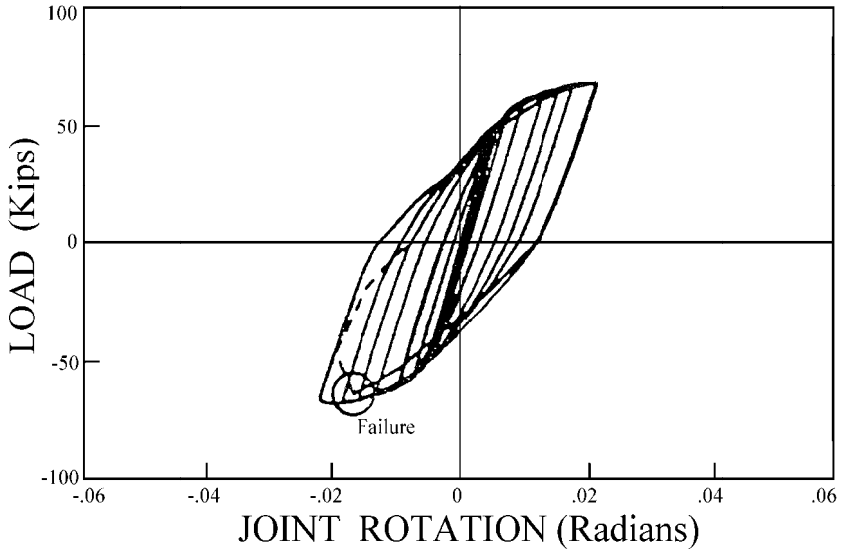

Figure 7-36 Moment-Rotation Behavior for Extended-End-Plate Connection with Bolt Fracture (Roeder, 2000)

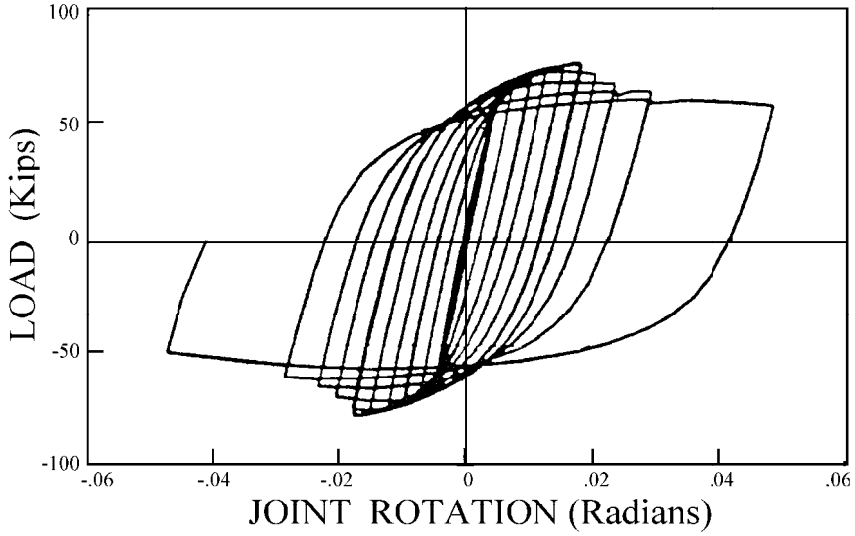

Figure 7-37 Moment-Rotation Behavior for Extended-End-Plate Connection with Plastic Deformation of the End Plate (Roeder, 2000)

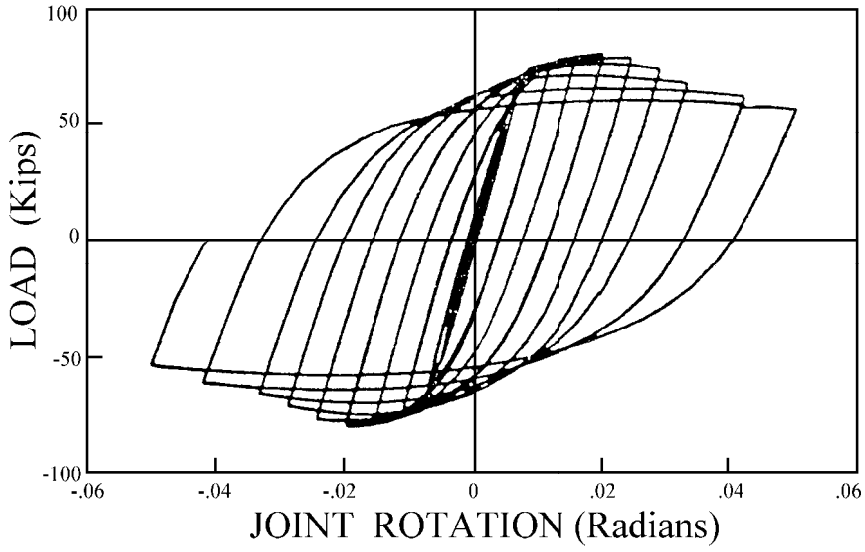

Figure 7-38 Moment-Rotation Behavior for Stiffened Extended-End-Plate Connection which Develops the Full Plastic Capacity of the Beam (Roeder, 2000)

Table 7-20 Yield Mechanisms for Both 4-Bolt Unstiffened and 8-Bolt Stiffened Extended-End-Plate Connections (Roeder, 2000)

Yield Mechanism	Equation to Define Yield Mechanism Moment Resistance at the Face of the Column
Plastic Flexure of Beam	for unstiffened end plate, $M_{yield} = S F_{ybm}$ for stiffened end plate, $M_{yield} = S F_{ybm} \frac{L - dc}{L - dc - Lstiffener}$
Panel Zone Yielding	$M_{yield} = 0.6 d_b F_{y\text{-}col} d_{eff} t_{w\text{-}c} (\frac{L-dc}{L})(\frac{h}{h - deff})$
Balance of Panel Zone Yielding and Flexural Yielding	$M_{yield\ Panel\ Zone} \approx M_{yield\ Flexural\ Yield}$
Requirements for Balance of Failure Modes to Assure Ductility	$1.1 R_y M_{fail\text{-}Beam\ Flexure} < M_{fail\text{-}Bolt\ Tension}$ and $1.22 R_y M_{fail\text{-}Beam\ Flexure} < M_{fail\text{-}Plate\ Bending}$

Table 7-21 Failure Modes for 4-Bolt Unstiffened Extended-End-Plate Connections (Roeder, 2000)

Failure Mode	Equation for Failure Moment at the Face of the Column	Related Issues
Plastic Deformation of Beam	For 4 bolt Unstiffened Connection $$M_{fail} = Z_b \frac{F_y + F_{ub}}{2}$$	
Tensile Fracture of Bolts	$$M_{fail} = N\, T_b \frac{d_o + d_i}{2}$$ where N is 4 for 4 bolt unstiffened connection; d_o and d_i are the distances defined in Figure 6.4.2-6; and $T_b = 90\, A_{bolt}$ for A325 bolts or $113\, A_{bolt}$ for A490 bolts	This model requires thick plate design so that prying forces can be neglected.
Plastic Bending of End Plate	$$M_{fail} = t_p^2\, F_{yp}\{(h - pt)[\frac{b_p}{2}(\frac{1}{p_f} + \frac{1}{s}) + (p_f + s)\frac{2}{g}] + \frac{b_p}{2}(\frac{h}{p_f} + \frac{1}{2})\}$$ where $s = \sqrt{b_p\, g}$ and ϕ_b is the bolt diameter.	Based on yield line analysis with dimensions given in Figure 6.4.2-6.
Shear Yielding of End Plate	Plate thickness, t_p, must satisfy $$\frac{1.1\, R_y\, F_{yb}\, Z_b}{2(d_b - t_{bf})} < \phi\, 0.6\, F_{yp}\, b_p\, t_p$$	Checks to ensure that the plate is not too thin to develop yield line mechanism.
Shear Capacity	Shear force, V, at the face of the column is based upon plastic bending at each end of beam and must be designed so that it does not control the capacity of the connection. For unstiffened 4 bolt connection $$\frac{2.2\, R_y\, F_{yb}\, Z}{L - d_c} < \phi\, 4\, F_v\, A_b$$ F_v and A_b are the nominal shear strength by AISC LRFD and the bolt area,	Equations assume shear is carried by bolts in compression.
Column Flange Thickness **Requirements for No Stiffener to the Beam Tension Flange**	For column flanges without stiffeners or continuity plates the minimum thickness of column, t_{cf}, must be greater than $$t_{cf}, > \sqrt{\frac{\frac{1.1\, R_y\, F_{yb}\, Z_b}{d_b - t_{bf}}(\frac{g}{2} - k_1)}{2.02\, F_{yc}\, c}}$$ Stiffeners required to carry the unbalanced portion of the force, $\frac{1.1\, R_y\, F_{yb}\, Z_b}{d_b - t_{bf}}$, if the column flange thickness does not satisfy this requirement.	The dimensions are defined in the figure except that k_1 is distance from centerline of column web to flange toe of fillet.

Table 7-21 Failure Modes for 4-Bolt Unstiffened Extended-End-Plate Connections (Roeder, 2000) (continued)

Failure Mode	Equation for Failure Moment at the Face of the Column	Related Issues
Plastic Bending Capacity of Stiffened Column Flanges	The column flange thickness, t_{fc}, must be larger than $t_{fc} > \sqrt{\frac{1.1\, R_y\, F_{yb}\, Z_b}{2(d_b - t_{bf})} \Big/ 0.81\, F_{yc}\, Y_c}$ where $Y_c = (\frac{c}{2} + s)(\frac{1}{\frac{b_{fc} - g}{2}} + \frac{2}{\frac{g}{2} - k_1}) + (\frac{b_{fc} - g}{2} + \frac{g}{2} - k_1)(\frac{4}{c} + \frac{2}{s})$ and $s = \sqrt{\frac{(\frac{g}{2} - k_1)\frac{b_{fc} - g}{2}}{\frac{b_{fc} - g}{2} + g - 2k_1}(2b_{fc} - 4k_1)}$	Yield line theory of bending of column flanges.
Column Stiffener Requirements for Beam Compression Flange	No Stiffener required if $\frac{1.1\, R_y\, F_{yb}\, Z_b}{d_b - t_{bf}} < (6k + c)\, F_{yc}\, t_{wc}$ Stiffeners required to carry the unbalanced portion of the force, $\frac{1.1\, R_y\, F_{yb}\, Z_b}{d_b - t_{bf}}$, if the column flange thickness does not satisfy this requirement. This equation recognizes the greater spreading of beam flange force to the column web provided by the end plate.	k is the beam fillet distance from the extreme fiber of beam flange to the web toe of fillet.
Weld Fracture	Experiments have shown that E71T-1 Gas Shielded FCAW welds. Flange welds are full penetration with no weld cope but under side of beam flange sealed with $^3/_8$" fillet weld and complete penetration weld welded against fillet weld seal after initial backgouging. Webs may be full penetration or fillet welds.	
Flange Buckling	for flange - $\frac{b_f}{2\, t_f} \le \frac{52}{\sqrt{F_y}}$	
Web Buckling	for web - $\frac{d_b}{t_w} \le \frac{375}{\sqrt{F_y}}$	
Lateral Torsional Buckling	$L_b < \frac{2500\, r_y}{F_y}$ L_b is the unsupported length.	Equation from AISC LRFD Seismic Provisions

Table 7-21 Failure Modes for 4-Bolt Unstiffened Extended-End-Plate Connections (Roeder, 2000) (continued)

Strong Column Weak Beam	$1.1 < \dfrac{\Sigma Zc\left(F_{yc} - P_{uc}/A_g\right)}{\Sigma Z_b\left(F_{yb} + F_{ub}\right)\left(L - d_c\right)/\left(2\left(L - d_c - 2L_{st}\right)\right)}$	Based on plastic moment capacity of beam

Table 7-22 Failure Modes for 8-Bolt Stiffened Extended-End-Plate Connections (Roeder, 2000)

Failure Mode	Equation for Failure Moment at the Face of the Column	Related Issues
Plastic Deformation of Beam	$M_{fail} = Z_b \dfrac{F_y + F_{ub}}{2} \dfrac{L - d_c}{L - 2L_{st} - d_c}$	
Tensile Fracture of Bolts	$M_{fail} = N T_b \dfrac{d_o + d_i}{2}$ where N is 6.8 for the 8 bolt stiffened connection; d_o and d_i are the distances defined in Figure 6.4.2-6; and $T_b = 90\ A_{bolt}$ for A325 bolts or $113\ A_{bolt}$ for A490 bolts	This model requires thick plate design so that prying forces can be neglected.
Plastic Bending of End Plate	For 8 bolt stiffened connection must be designed to have a minimum thickness of the end plate t_p must satisfy $t_p > \dfrac{0.00609\ p_f^{0.873}\ g^{0.577}\ F_{fu}^{0.917}}{\phi_b^{0.924}\ t_s^{0.112}\ b_p^{0.882}}$ and $t_p > \dfrac{0.00413\ p_f^{0.257}\ g^{0.148}\ F_{fu}^{1.017}}{\phi_b^{0.719}\ t_s^{0.162}\ b_p^{0.319}}$ where $F_{fu} = \dfrac{1.1\ R_y\ F_{yb}\ Z}{d_b - t_{bf}}$	Equations are empirical but are based upon yield line theory. The dimension ϕ_b is the bolt diameter. All other dimensions given in Figure 7-39.
Shear Capacity	Shear force, V, at the face of the column is based upon plastic bending at each end of beam and must be designed so that it does not control the capacity of the connection. For 8 bolt stiffened connection $\dfrac{2.2\ R_y\ F_{yb}\ Z}{L - d_c} < \phi\ 8\ F_v\ A_b$ F_v and A_b are the nominal shear strength by AISC LRFD and the bolt area, respectively. Note that bearing capacity of bolts on bolt holes must also be checked for both end plate and column flange.	Equation assumes shear is carried by bolts in compression.

Table 7-22 Failure Modes for 8-Bolt Stiffened Extended-End-Plate Connections (Roeder, 2000) (continued)

Failure Mode	Equation for Failure Moment at the Face of the Column	Related Issues
Column Flange Thickness and Stiffener Requirements at Beam Tension Flange	For column flanges without stiffeners or continuity plates the minimum thickness of column, t_{cf}, is $t_{cf} > \sqrt{\frac{\alpha_m F_{fu} (\frac{g}{2} - \frac{\phi b}{4} - k_1)}{0.9 F_{yc} (3.5 p_b + c)}}$ where $\alpha_m = C_a C_b (\frac{A_f}{A_w})^{1/3} (\frac{\frac{g}{2} - \frac{\phi b}{4} - k_1}{\phi b})^{1/4}$ If the column flange thickness does not satisfy the above requirement,, tension stiffeners are required. The stiffeners must have enough capacity to reduce the flange force, F_{fu}, to a level were the required flange thickness is less than that provided.	Dimensions defined in the figure. F_{fu} is defined with the end plate thickness equations above. C_a depends upon the materials used in the analysis and C_b is normally taken as 1.0.
Column Stiffener Requirements for Beam Compression Flange	No Stiffener required if $\frac{1.1 R_y F_{yb} Z_b}{d_b - t_{bf}} < (6 k + c) F_{yc} t_{wc}$ Stiffeners required to carry the unbalanced portion of the force, $\frac{1.1 R_y F_{yb} Z_b}{d_b - t_{bf}}$, if the column flange thickness does not satisfy this requirement. This equation recognizes the greater spreading of beam flange force to the column web provided by the end plate.	k is the beam fillet distance from the extreme fiber of beam flange to the web toe of fillet.
Bending of Stiffened Column Flange	Not yet available.	Checks the column flange to ensure "thick plate" assumption applies
Weld Fracture	Experiments have shown that E71T-1 Gas Shielded FCAW welds. Flange welds are full penetration with no weld cope but under side of beam flange sealed with $^3/_8$" fillet weld and complete penetration weld welded against fillet weld seal after initial backgouging. Web welds may be full penetration or fillet welds.	
Flange Buckling	for flange, $\frac{b_f}{2 t_f} \leq \frac{52}{\sqrt{F_y}}$	
Web Buckling	for web, $\frac{d_b}{t_w} \leq \frac{375}{\sqrt{F_y}}$	

Table 7-22 Failure Modes for 8-Bolt Stiffened Extended-End-Plate Connections (Roeder, 2000) (continued)

Failure Mode	Equation for Failure Moment at the Face of the Column	Related Issues
Lateral Torsional Buckling	$L_b < \frac{2500\, r_y}{F_y}$ L_b is the unsupported length.	Equation from AISC LRFD Seismic Provisions
Strong Column Weak Beam	for stiffened end plate, $1.1 < \frac{\Sigma Z_c (F_{yc} - \frac{P_{uc}}{A_g})}{\Sigma Z_b F_{yb} \frac{L - d_c}{L - d_c - 2L_{st}}}$	Based on plastic moment capacity of beam at end of stiffener

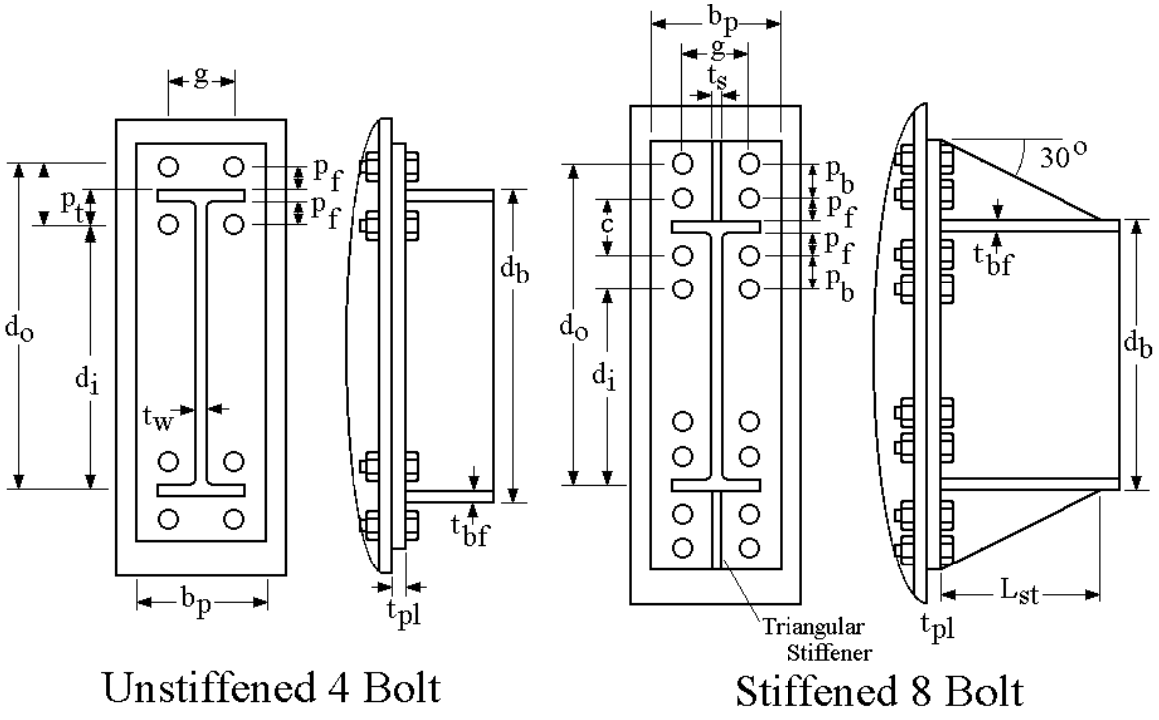

Figure 7-39 Geometry Needed to Define Panel-Zone Models (Roeder, 2000)

7.5.3 Summary for the Response of the Buildings with End-Plate Connections

New buildings with the end-plate connections are expected to perform well based on the SMF studies by Lee and Foutch (2000). The 1997 NEHRP *Provisions* were adequate for achieving excellent performance.

7.6 Evaluation of Buildings with Clip-Angle PR Connections

7.6.1 Background

Determining the behavior of the clip-angle connection is based on the experimental research by Leon and Schrauben (2000). This type of connection is considered to be in the flexible connection category. A typical configuration of the clip-angle partially restrained connection is shown in Figure 7-40. According to Roeder (2000), this type of connection was typically used in shorter buildings or in the top stories of tall buildings. The clip-angle-connections are flexible and weaker than T-stub connections. Therefore, they usually develop only 20% to 50% of the plastic moment capacity of the beam. Since they are flexible and weak, more connections from the interior bays should act in the lateral-load-resisting system. They are usually used in lowest seismicity regions.

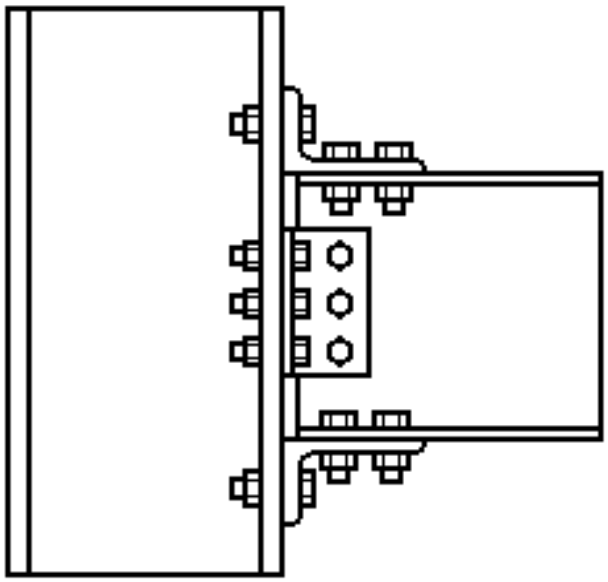

Figure 7-40 Typical Flange Clip Angle Connection

7.6.2 Summary of Findings for Clip-Angle Connections from Connection Performance Team

The experimental data were provided by the Connection Performance team (Leon and Schrauben, 2000 and Roeder, 2000). The full-scale tests performed by the CP team are listed in Table 7-23. Component tests were also performed to identify the behavior of the clip angles themselves. A brief description of the behavior of the clip-angle connection based on those reports will be addressed here.

Different types of yield mechanisms and observed failure modes are shown in Figure 7-41. The rotational spring stiffness of the bolted clip angle connection is proposed as

$$k_s < \frac{M_{fail}}{0.01} \tag{7-16}$$

where M_{fail} is the critical failure mode for the connection from Table 7-23. The definitions of the symbols in the table can be referred to Figure 7-42. Therefore, the stiffness of the connection should be modeled for analysis.

The plastic rotational capacity proposed is

$$\theta_p < \frac{0.50}{d_b} \tag{7-17}$$

and the plastic rotation at which the connection is expected to lose its gravity-carrying capacity can be conservatively estimated as

$$\theta_g < \frac{0.50}{d_b} + 0.02 \tag{7-18}$$

According to Roeder (2000), this rotational limit is strongly dependent on the beam depth. However, it is independent of span length, since all of the deformation occurs in the connection element.

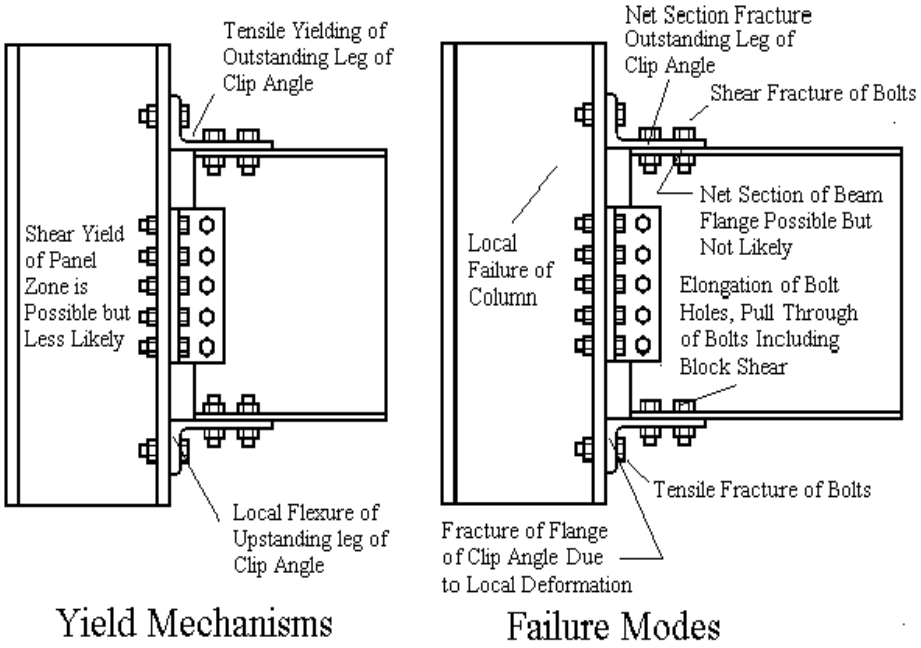

Figure 7-41 Primary Yield Mechanisms and Common Failure Modes for the Bolted Clip-Angle Connection (Roeder, 2000)

Table 7-23 Failure Modes for Bolted Clip Angle Connections (Roeder, 2000)

Failure Mode	Equation for Failure Moment at the Face of the Column	Related Issues
Plastic Bending Capacity of Upstanding Leg of the Angle	$M_{fail} = \frac{.5\, w\, t_a^2\, Fy}{d' - \frac{t_a}{2}} (d_b + d')$	See geometry of Figure 7-42
Shear Fracture of Bolts Between Outstanding Leg of Angle and Beam Flange	$M_{fail} = 2\, N\, A_b\, (0.6\, F_{u\text{-}bolt})\, (d_b + t_a) \frac{L - d_c}{L - d_c - (S_1 + S_3)}$	A_b is the cross sectional area of bolt
Fracture of Tension Bolts	$M_{fail} = P_{bolt}\, (d + d') - \frac{0.25\, w\, t_a^2\, F_{ya}}{a}$ where $a = l_a - d'$ and P_{bolt} = proof load capacity of the high strength bolt	Prying force is needed to plastically deform angle. Bolt force limited to proof load.
Net Section Fracture of Outstanding Leg of Angle	$M_{fail} = F_{u\text{-}angl}\, (W - 2\, (\Phi_{bolt} + .125))\, t_a\, (d_b + t_a) \frac{L - d_c}{L - d_c - 2\, S_1}$ where W is lesser of $W \le W_1$ and $W \le g + S_3 \tan \theta_{eff}$. Because both legs of the angle have the same thickness, this is less likely to control the capacity than the other modes.	Φ_{bolt} is the bolt diameter and $\theta_{eff} = 60\, t_{stem\text{-}t}$ except $15^o < \theta_{eff} < 30^o$
Bolt Elongation, Bolt Pull-Through, and Block Shear	Block shear, bolt hole elongation and bolt pull through must be checked by normal AISC criteria, but they are less likely to control the design of these connections than the bolted T-Stub or other connections.	
Other Issues	Balance of panel zone stress state, continuity plates, and flange and web slenderness requirements would apply to these connections, but they are unlikely to affect the design since the connection develops a sufficiently small moment capacity that the members are unlikely to be stressed high enough to develop problems in these areas. Weak beam-strong column requirements may be a problem even with the relatively small moments in the beams and connections, because of the large axial loads in the columns due to gravity load.	
Recommended Balance Condition	$M_{fail\text{-}Flexure\ of\ angle\ leg} < 1.1\, M_{fail\text{-}\ All\ Other\ modes}$ Other modes include tension fracture of bolts, shear fracture of bolts, and net section fracture of outstanding leg.	

Note: Geometric symbols are defined in Figure 7-42.

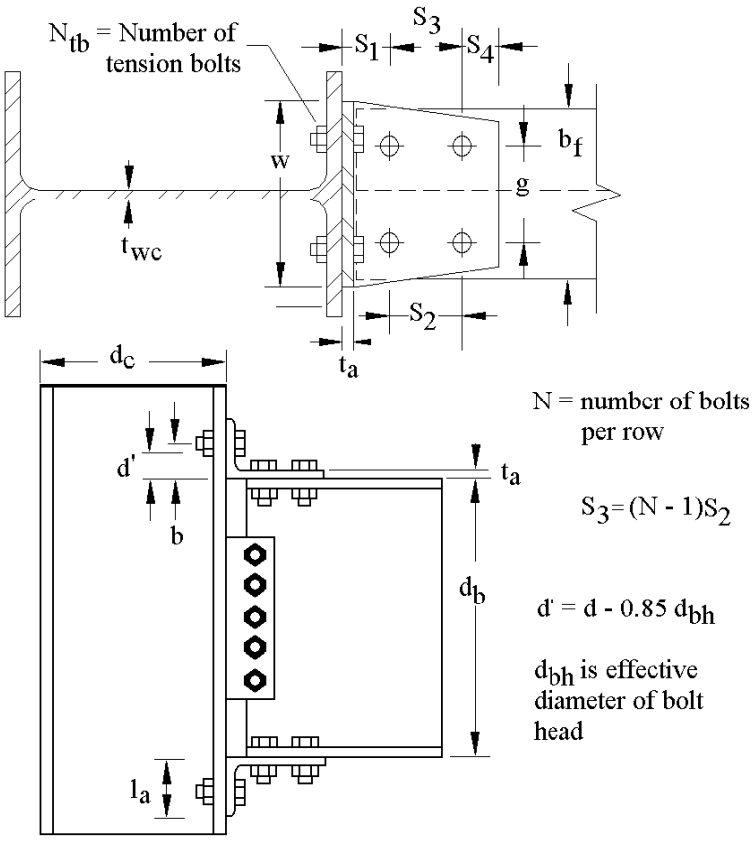

Figure 7-42 Geometry for Failure Mode Evaluation of Clip-Angle Connections (Roeder, 2000)

7.6.3 Properties of Clip-Angle Connections for this Study

Experimental data provided by Leon and Schrauben (2000) and Roeder (2000) permitted the estimation of the stiffness and the strength of the clip-angle PR connections, but none of the equations for the connection were available at the time of this study. Connection experiments with a w18x40 beam connected to a w14x145 column were selected, and simulated using a spring element from the DRAIN-2DX program. The stiffness equation specified in FEMA-273 for PR connections together with 35% of the strength of the beam were used. This value was less than the minimum of 50% of the moment capacity of the beam specified in the seismic section of the LRFD for Ordinary Moment Frames. However, according to the experimental research, Leon concluded that the connection usually develops only 20% to 50% of the plastic moment capacity of the beam.

With a procedure similar to that taken for the T-stub PR connections, the spring parameters that best represent the behavior of the measured moment-rotation relationship were obtained. The stiffness equation in FEMA-273, which is

$$K_\theta = \frac{M_{CE}}{0.005} \tag{7-19}$$

again adequately represented the stiffness of the connection. A less stiff slope than for the T-stub connection case is observed since M_{ce} is 35% of the moment capacity of the beam instead of 50%. With the strain-hardening ratio of 20%, the hysteresis from the spring element matched the response of the experiment very well. The ratio of stiffness of the connection divided by that of beam was calculated to be 6.46. This is well below the stiffness ratio for the rigid connection case, which is 20 as described in the previous section.

Since failure due to tension bolt failure at the total rotation of 4%, the 4% value was used as a limiting rotation before the strength drops down drastically. Therefore, in modeling the connection behavior, a rotation value of 3% was used. Due to the lack of modeling parameters provided in the modified version of the analysis program, DRAIN-2DX (Shi and Foutch, 1996), two individual springs were used to model the connection behavior. The illustration of two springs used for the model is again shown in Figure 7-43. The first spring is perfectly elasto-plastic, with strength dropping to 15% of the strength of the spring at the 3% rotation. The second spring is elastic until the rotation reaches the value of 3%. The strength of the connection again drops down to 15% of the spring strength. The measured moment-rotation behavior of the connection and the model of it are shown in Figure 7-44 and Figure 7-45, respectively. Figure 7-45 shows the total rotation behavior of the joint.

The connection stiffness values for the rest of the connections were determined using the stiffness calculated using Equation 7-19 and 35% of the beam strength. Again, two springs for each end of the beam were used to model the strain hardening with fracturing behavior of the joint.

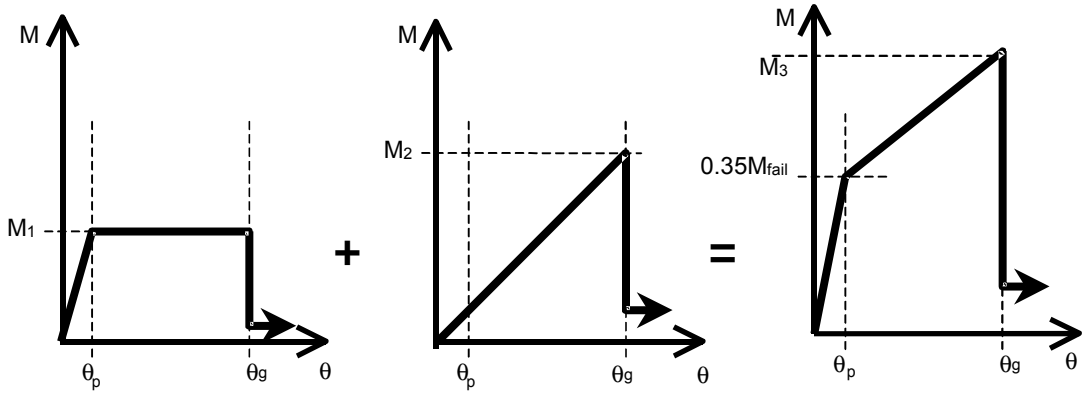

Figure 7-43 Clip-Angle Connection Modeling Used for Study

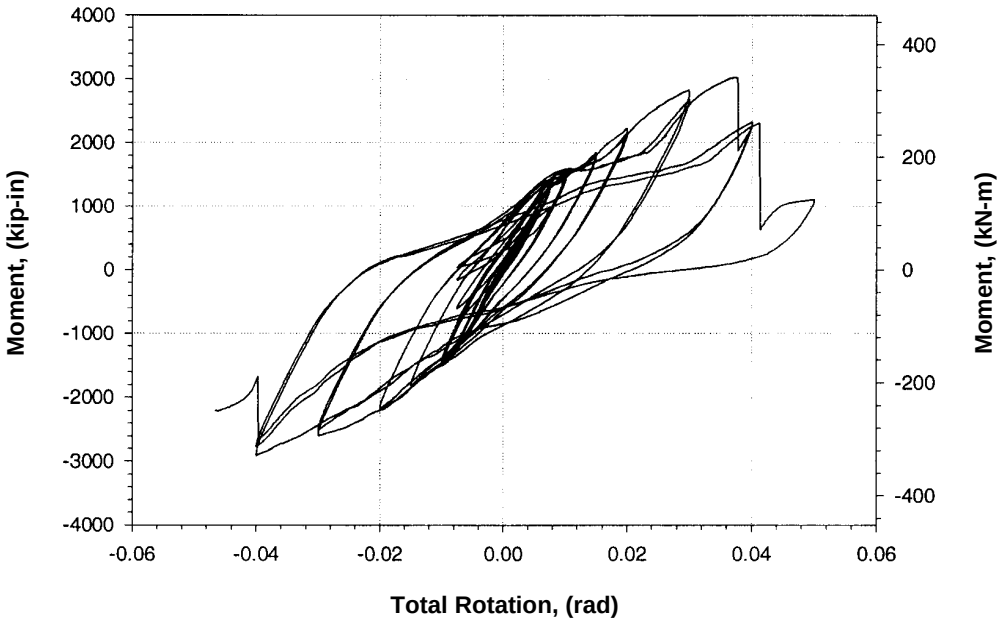

Figure 7-44 Measured Moment-Rotation Behavior of Clip-Angle Partially Restrained Connection (Leon and Schrauben, 2000)

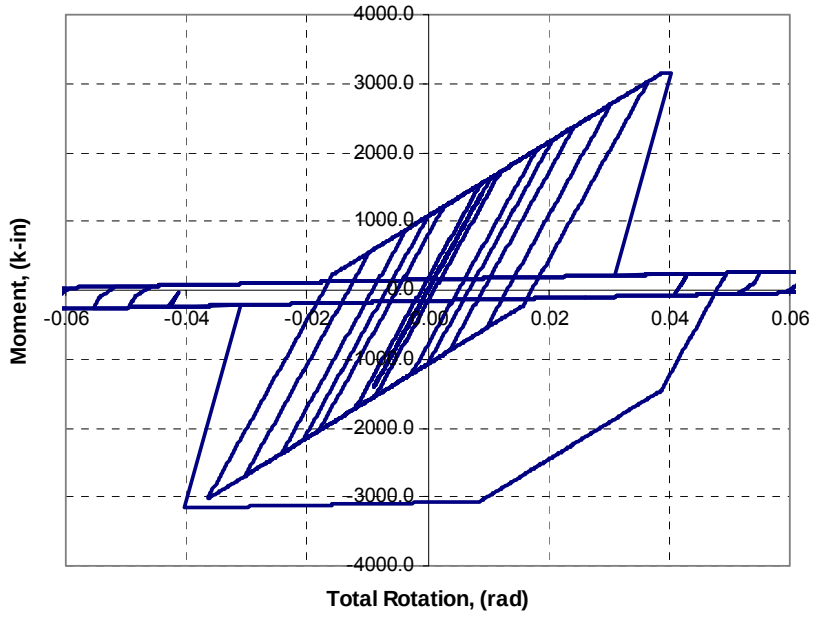

Figure 7-45 Model of Moment-Rotation Behavior of Clip-Angle Partially Restrained Connection

7.6.4 Description of Building Investigated

A 9-story building for seismic design category C was selected for investigation since it showed large demands for the WCSB configuration case. Since clip-angle connections are flexible compared with the T-stub connections, all of the interior frames were also designed to act as the lateral-load-resisting system. The new plan views for the 9-story building are shown in Figure 7-46. The number of PR connections in the building is the same for the N-S and E-W directions. The elevation view with the member sizes for the building is shown in Figure 7-47. The 9-story building now has fifteen moment-resisting bays with thirty clip-angle PR connections per floor. Therefore, an additional bay to represent the gravity frame was not needed. Since the partially restrained connections are permitted in OMFs, a strength reduction factor of four was used for the design. Initially, the members of the structure were changed so that the drifts were satisfied according to the 1997 NEHRP *Provisions*. Increases in beam sizes were necessary to meet the drift requirements. Strengths of the members and the connections were checked. Detailed design of the connections was not performed. Instead, 35% of the strength of the beam was used as described in Section 7.5.3. This is below the limiting strength ratio of 50% for OMF partially restrained connections specified in the LRFD *Seismic Provisions*. However, according to the experimental research, Leon concluded that the connections usually develop only 20% to 50% of the plastic moment capacity of the beam. A connection strength of 35% of the beam strength was adequate for all of the connections in the 9-story building. More description on how the connection model was introduced is given in Section 7.5.3. Doubler plates were not used since the panel-zone check requirements are not enforced for the OMF systems. Since the strengths of the connections are small, only a small amount of plastic deformation was observed for the panel zone. Therefore, a case with doubler plates was not investigated. The design force and the fundamental period for the structure were 300 kips and 3.88 seconds, respectively.

The ground motions used for the study are the 20 ground motions for the LA site for the 2/50 hazard level and the 20 ground motions for the Seattle site for the 2/50 hazard level, as described in Chapter 3. Both suites of ground motions were scaled to match the target spectra values.

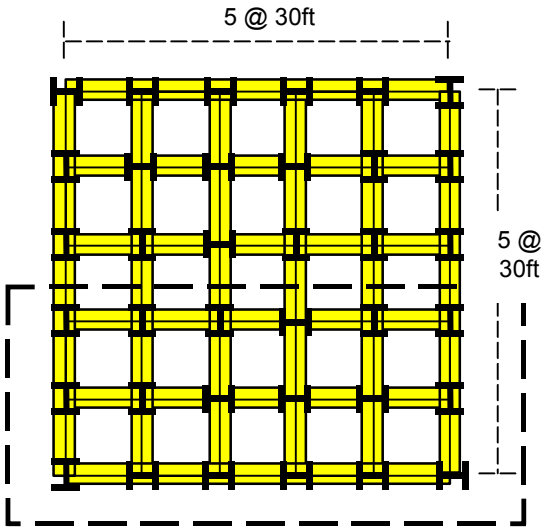

1997 NEHRP 9-story OMF T-stub PR Conn.
E-W : 60 connections
N-S : 30 connections

Figure 7-46 Plan View 9-Story Building in SDC C

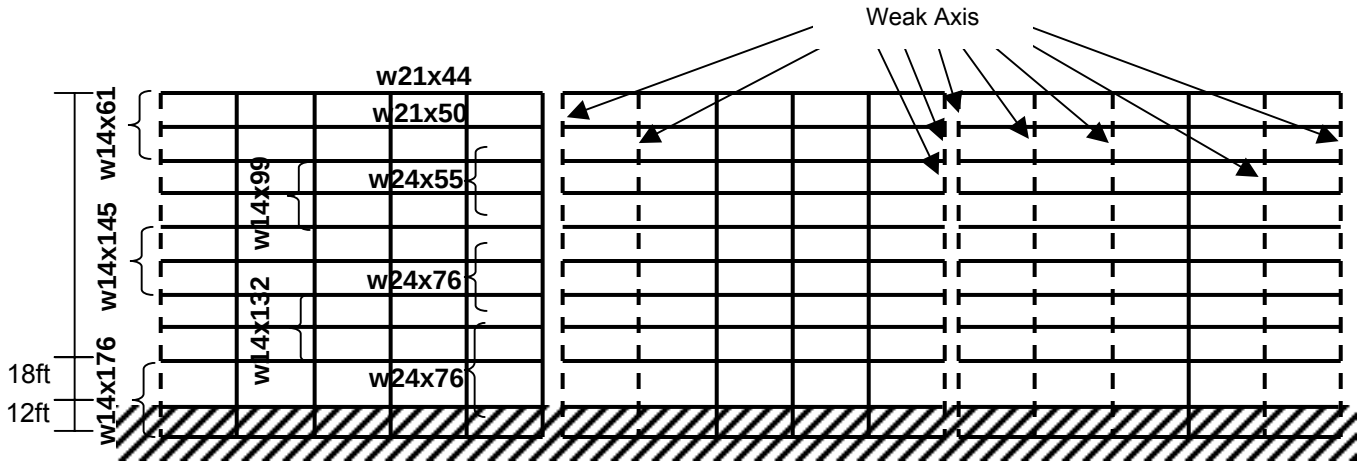

Figure 7-47 1997 NEHRP 9-Story OMF with Clip-Angle PR Connections

7.6.5 Response of Buildings with Clip Angle PR Connections

7.6.5.1 Demand Responses

A comparison of the static pushover response of the buildings with PR connections and buildings with WCSB configurations is shown in Figure 7-48. Since only small plastic deformations in panel zones were observed, a case with doubler plates was not investigated. The 9-story building with clip angle PR connections shows strength comparable to the WCSB cases with doubler plates and T-stub connections. This is because only small demands were observed for the panel zone and more connections are resisting the lateral force. However, the building drastically lost its strength after reaching 3% of the global drift. This is due to the limited capacity of the clip-angle connections.

Demands for the 9-story building with clip-angle PR connections excited by LA 2/50 ground motions are shown in Figure 7-49. Those for the Seattle site are shown in Figure 7-50. The solid symbols represent the median response values whereas the open symbols represent the maximum response. The plot on the left represents the axial force ratios of columns. The P/P_{cr} and P/P_y are compressive axial force ratio and tensile axial force ratio, respectively. The negative values represent compressive values. The middle plot shows the plastic rotation demands for each of the components as well as the drifts. The right plot shows the median, 84^{th} percentile, and 95^{th} percentile drifts observed from the analysis.

The responses from both sites give similar results. For the LA site, a maximum plastic rotation of 1.2% was observed in the beam connection but only about 0.5% median plastic rotation was observed. A drift value of 2% was observed for the 95^{th} percentile but a median drift value of 1.2% was observed, which is acceptable. Maximum plastic rotation observed in the building was only 0.5%, which is smaller than that in WCSB and T-stub PR connection cases. Similar but somewhat larger demands were observed for the building in Seattle. Again maximum drifts were observed in the top story. The axial compression force ratio stayed at about 0.4 while no tension force was observed. Very little fluctuation of the axial forces was observed from the results both for LA and Seattle. This is due to the small rotational capacity and thus reduction of stiffness after yielding of the connection model. Therefore, the 9-story building performed well.

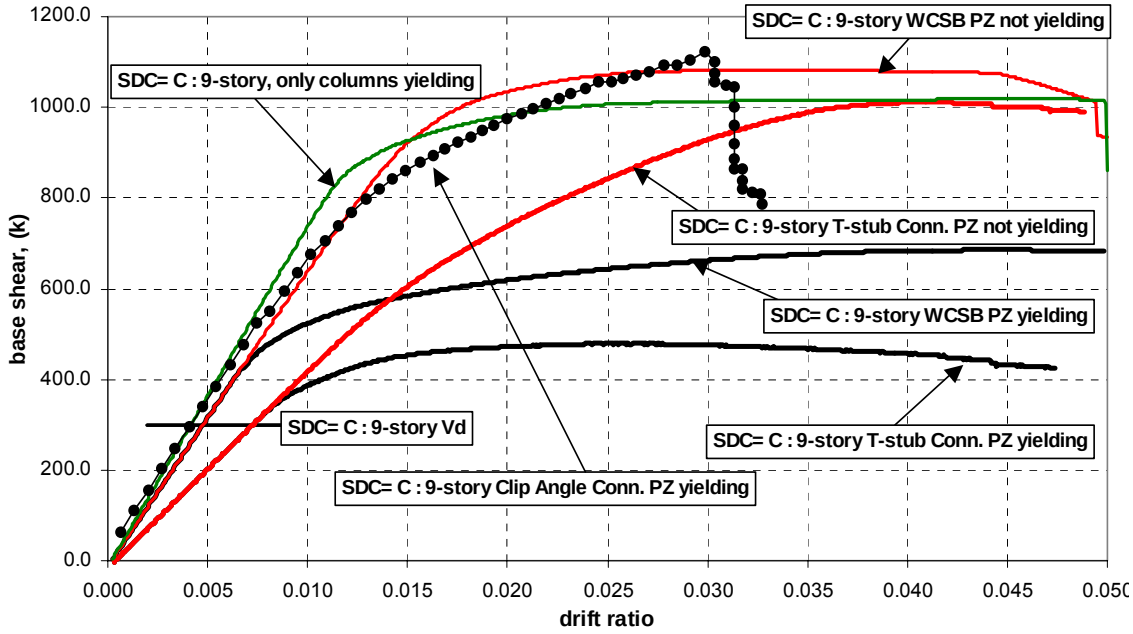

Figure 7-48 Comparison of Static Pushovers for 9-Story Building with WCSB Configuration, T-Stub Connections, and Clip-Angle Connections

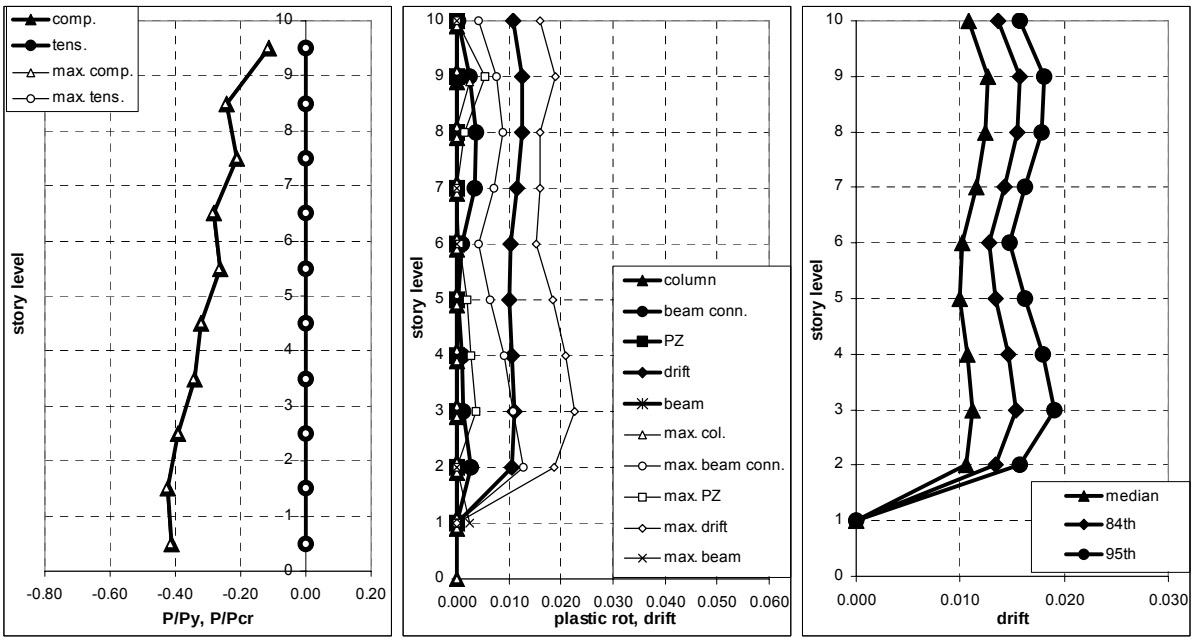

Figure 7-49 Median and Maximum Demands for the Case with Panel Zones Yielding for LA 9-Story Building with Clip-Angle PR Connections

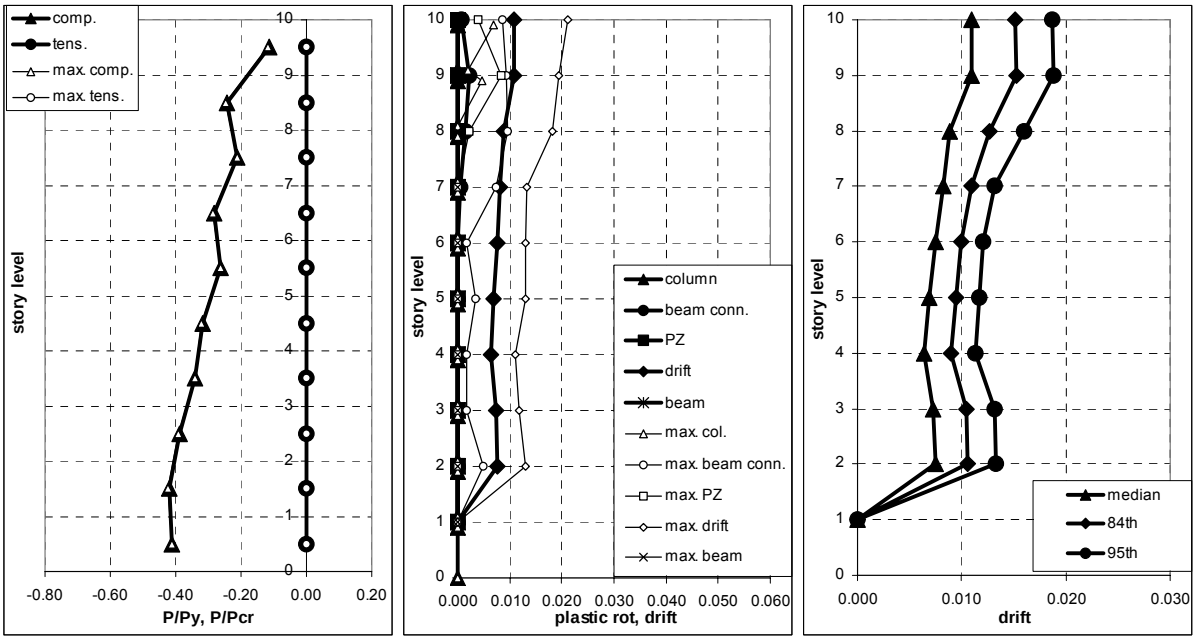

Figure 7-50 Median and Maximum Demands for the Case with Panel Zones Yielding for Seattle 9-Story Building with Clip-Angle PR Connections

7.6.6 Performance Evaluation of Buildings with Clip Angle Connections

Performance evaluations were done for all of the building with clip-angle PR connections. Values for $\hat{C}$, β_R, β_U, ϕ, $\hat{D}$, β_{acc}, γ, β_a, γ_a, λ_{con}, β_{UT}^2, K_x for the LA site are given in Table 7-24 to Table 7-28. The results for the Seattle site are shown in Table 7-29 to Table 7-33. These were calculated using the provisions set out in Chapter 5.

The global capacities for each of the buildings were calculated using the IDA analysis. The median drift capacity for the original 9-story building in LA was 4.9% and in Seattle it was 5.8%, which is low when compared with other buildings studied. The median demand drifts for both 2%-in-50-years hazard level and 50%-in-50-years hazard level have been presented and discussed in the previous section. Since the local drift capacity for the buildings with clip-angle PR connections has not yet been defined in Table 5-2, in Section 5.6.1.1 it has been calculated individually. Since the strength of the connection dropped to 15% of beam moment capacity at 3% rotation, a drift value of 3% plus the elastic drift observed from the static pushover analysis in Figure 7-48 was used as the local drift capacity. Therefore, local drift capacity for the 9-story building was calculated to be 4%. The drift criterion for the immediate occupancy level was also not provided. Therefore, the 3% drift capacity, which is the same value as used for the T-stub PR connections listed in the table for the IO levels, was used.

Although the drift capacities calculated were small for the buildings with clip angles compared to the other buildings, the drift demands calculated were also the smallest. This is due to the large resistance coming from the larger number of the moment bays. Therefore, a

confidence level of 99% for the CP level and IO level for both of the buildings was observed for the 9-story building.

Table 7-24 CP Confidence Level Calculations Against Global Collapse for Scaled LA 2/50 Hazard

	$\hat{C}$	β_r	β_u	ϕ	$\hat{D}$	β_{acc}	β_{or}	γ	β_a	γ_a	λ_{con}	β_{UT}^2	K_x	C.L. %
1997 NEHRP PR Connection, SDC= C														
9-story	0.049	0.28	0.35	0.74	0.014	0.21	0.00	1.07	0.20	1.06	2.23	0.16	2.60	99

Table 7-25 CP Confidence Level Calculations Against Local Collapse for Scaled LA 2/50 Hazard

	$\hat{C}$	β_r	β_u	ϕ	$\hat{D}$	β_{acc}	β_{or}	γ	β_a	γ_a	λ_{con}	β_{UT}^2	K_x	C.L. %
1997 NEHRP PR Connection, SDC= C														
9-story	0.040	0.20	0.25	0.86	0.014	0.21	0.00	1.07	0.20	1.06	2.11	0.10	2.81	99

Table 7-26 IO Confidence Level Calculations for Scaled LA 50/50 Hazard

	$\hat{C}$	β_r	β_u	ϕ	$\hat{D}$	β_{acc}	β_{or}	γ	β_a	γ_a	λ_{con}	β_{UT}^2	K_x	C.L. %
1997 NEHRP PR Connection, SDC= C														
9-story	0.030	0.20	0.25	0.86	0.003	0.41	0.00	1.29	0.21	1.07	5.48	0.11	5.70	99

Table 7-27 CP Confidence Level Calculations Against Global Collapse for Scaled LA 50/50 Hazard

	$\hat{C}$	β_r	β_u	ϕ	$\hat{D}$	β_{acc}	β_{or}	γ	β_a	γ_a	λ_{con}	β_{UT}^2	K_x	C.L. %
1997 NEHRP PR Connection, SDC= C														
9-story	0.049	0.28	0.35	0.74	0.003	0.41	0.00	1.29	0.21	1.07	7.75	0.17	5.63	99

Table 7-28 CP Confidence Level Calculations Against Local Collapse for Scaled LA 50/50 Hazard

	$\hat{C}$	β_r	β_u	ϕ	$\hat{D}$	β_{acc}	β_{or}	γ	β_a	γ_a	λ_{con}	β_{UT}^2	K_x	C.L. %
1997 NEHRP PR Connection, SDC= C														
9-story	0.040	0.20	0.25	0.86	0.003	0.41	0.00	1.29	0.21	1.07	7.31	0.11	6.58	99

Table 7-29 CP Confidence Level Calculations Against Global Collapse for Scaled Seattle 2/50 Hazard

	$\hat{C}$	β_r	β_u	ϕ	$\hat{D}$	β_{acc}	β_{or}	γ	β_a	γ_a	λ_{con}	β_{UT}^2	K_x	C.L. %
1997 NEHRP PR Connection, SDC= C														
9-story	0.058	0.32	0.35	0.80	0.012	0.32	0.00	1.11	0.21	1.04	3.44	0.16	3.47	99

Table 7-30 CP Confidence Level Calculations Against Local Collapse for Scaled Seattle 2/50 Hazard

	$\hat{C}$	β_r	β_u	ϕ	$\hat{D}$	β_{acc}	β_{or}	γ	β_a	γ_a	λ_{con}	β_{UT}^2	K_x	C.L. %
1997 NEHRP PR Connection, SDC= C														
9-story	0.040	0.20	0.25	0.90	0.012	0.32	0.00	1.11	0.20	1.04	2.68	0.10	3.40	99

Table 7-31 IO Confidence Level Calculations for Scaled Seattle 50/50 Hazard

	$\hat{C}$	β_r	β_u	ϕ	$\hat{D}$	β_{acc}	β_{or}	γ	β_a	γ_a	λ_{con}	β_{UT}^2	K_x	C.L. %
1997 NEHRP PR Connection, SDC= C														
9-story	0.030	0.20	0.25	0.90	0.004	0.30	0.00	1.09	0.21	1.05	6.59	0.11	6.10	99

Table 7-32 CP Confidence Level Calculations Against Global Collapse for Scaled Seattle 50/50 Hazard

	$\hat{C}$	β_r	β_u	ϕ	$\hat{D}$	β_{acc}	β_{or}	γ	β_a	γ_a	λ_{con}	β_{UT}^2	K_x	C.L. %
1997 NEHRP PR Connection, SDC= C														
9-story	0.058	0.32	0.35	0.80	0.004	0.30	0.00	1.08	0.21	1.05	11.3	0.17	6.34	99

Table 7-33 CP Confidence Level Calculations Against Local Collapse for Scaled Seattle 50/50 Hazard

	$\hat{C}$	β_r	β_u	ϕ	$\hat{D}$	β_{acc}	β_{or}	γ	β_a	γ_a	λ_{con}	β_{UT}^2	K_x	C.L. %
1997 NEHRP PR Connection, SDC= C														
9-story	0.040	0.20	0.25	0.90	0.004	0.30	0.00	1.09	0.21	1.05	8.79	0.11	6.98	99

7.6.7 Summary of Results for Buildings with Clip Angle Connections

The 9-story building designed with clip-angle connections for SDC C in accordance with the 1997 NEHRP *Provisions* satisfied the SAC performance objectives for the CP and the IO performance levels.

For the 9-story building, a maximum plastic rotation of 2.2% was observed for the connections. The maximum panel zone rotation observed was only 0.9%. Drift ratios of 1.9% and 1.2% were observed for the 95^{th} percentile and median, respectively. Therefore, the 9-story building with clip angle connections performed well.

A 9-story building for the Seattle site was also analyzed for the 2%-in-50-year ground motions. The median drifts and 95^{th} percentile drifts were 1.1% and 1.9%, respectively, which is similar to those for the LA site. Overall, the structure performed well.

The column axial force ratios were calculated and checked for acceptability. The maximum P/P_{cr} ratio observed was a little over 0.4, which is well below the limiting ratio of 0.75. No tension was observed in the 9-story building. Therefore, the axial forces are all acceptable.

The permanent residual drift due to 50/50 ground motion hazard was investigated. The 9-story building in LA had below 0.1% of permanent residual drift ratio, which is significantly below the failure criterion. However, the 9-story building in Seattle resulted in 0.64% permanent residual drift ratio. This is attributable to the characteristics of the SE19 ground motions and higher mode effects. Therefore, the building is considered to have failed the CP performance objective.

Finally, the confidence level calculations were performed according to the procedure presented in Chapter 5. Although the calculated drift capacities were small for the buildings with clip angles compared with those for other buildings, the calculated drift demands were also the smallest. This is due to the large resistance from the larger number of moment bays. Therefore, the confidence level of 99% was observed for the 9-story building for the CP and IO levels.

7.7 Summary of Results and Conclusions for Seismic Behavior of Frames with PR Connections

A 3-story building in SDC D, a 9-story building in SDC C with T-stub PR connections, and a 9-story building in SDC C with clip-angle PR connections were designed and analyzed for this study. As seen from the measured moment-rotation behavior of the end-plate connection, the connection has large stiffness and strength for most of the failure mechanisms. Hence, it will behave similarly to the fully restrained connections. Therefore, the performance of the buildings with the end-plate connections is expected to be good based on the SMRF studies performed by Lee and Foutch (2000).

For the buildings with T-stub PR connections, maximum plastic rotation was observed in the panel zone. Therefore, buildings with doubler plates inserted were also investigated. Maximum

plastic rotation was observed in beam connections for the building with clip-angle PR connections.

For the 3-story building with T-stub PR connections, a maximum plastic rotation of 2.5% was observed in the beam connections, but only about 1% median plastic rotation was observed. Similarly, a large drift value of 4% was observed for the 95th percentile, but an acceptable median drift value of 2.5% was observed. For the 9-story building with T-stub connections, the maximum plastic rotation was observed in the panel zones. A maximum plastic rotation of 2% was observed for the panel zones when only 0.8% was observed for the beam connections. The building with doubler plates resulted in a maximum connection plastic rotation of 1%. Drift ratios of 2.2% and 1.4% were observed for the 95th percentile and median, respectively. Therefore, the 9-story buildings performed well. A 9-story building for the Seattle site was analyzed for the 2%-in-50-year ground motions. The median drifts and 95th percentile drifts were 1.5% and 2.5%, respectively, which is slightly larger than for the LA site. Overall, the structure performed well.

For the 9-story building with clip-angle PR connections, the maximum plastic rotation was observed in the connections. A maximum plastic rotation of 2.2% was observed for the connections, but the maximum panel zone rotation observed was only 0.9%. Drift ratios of 1.9% and 1.2% were observed for the 95th percentile and median, respectively. Therefore, the 9-story building with clip-angle connections performed well. A 9-story building for the Seattle site was also analyzed for the 2%-in-50-year ground motions. The median drifts and 95th percentile drifts were 1.1% and 1.9%, respectively, which are similar to those for the LA site.

The adequacy of rotational capacity for the T-stub PR connection due to gravity load and lateral load was investigated. For the 9-story building with T-stub PR connections in SDC C, the 8th level had the largest plastic rotational demand of about 0.009 radians. Total rotational demand for the corresponding level was 0.013 radians. Another 9-story building in SDC B was designed and analyzed. This building was mostly governed by strength requirements. The maximum plastic rotation of 0.003 radians was observed at the 3rd level. Although the capacities of the connections were smaller than for those for the SDC C structure, the calculated rotational demands were small enough that the connection performed well. Therefore, the rotational capacity for the T-stub PR connection due to gravity load and lateral load is adequate for both SDC C and SDC B.

The column axial force ratios were calculated and checked for acceptability. The maximum P/P_{cr} ratios observed for the building with T-stub PR connections and clip-angle PR connection were 0.5 and 0.4 respectively, which is well below the limiting ratio of 0.75. No tension was observed for all of the 9-story buildings and only a small amount was observed in the 3-story building with T-stub PR connections. Therefore, the axial forces are all acceptable.

The permanent residual drift due to 50/50 hazard ground motions was investigated. The maximum residual drift observed for a building with T-stub connections was from the 9-story building, where it was 0.001. However, a large permanent residual drift value of 0.0064 was observed for the 9-story building with clip-angle connections. This is attributable to the

characteristics of the SE19 ground motion and effects from the higher modes. The value observed exceeds the target value of 0.005. The 3-story building had small residual drift values. Therefore, the building is again acceptable.

Finally, the confidence level calculations according to the procedure presented in Chapter 5 were performed. The confidence levels for CP for the 2/50 hazard and IO for the 50/50 hazard for all buildings were 99% except for the 3-story building in SDC D with T-stub PR connections, which resulted in 92% confidence level, which is probably acceptable. A local drift capacity of 5.4% would result in 95% confidence.

8. PERFORMANCE EVALUATION OF EXISTING BUILDINGS

8.1 Introduction

Seismic evaluation and upgrade of buildings is being performed in almost all parts of the country. Recently, a major national project funded by FEMA resulted in the development of *Guidelines* and *Commentary for the Seismic Rehabilitation of Buildings*. These were published as FEMA Reports 273 and 274 (FEMA, 1997c, d) and are described in Chapter 4.

8.2 Evaluation and Rehabilitation Objectives and Process

8.2.1 Evaluation and Rehabilitation Objectives

Performance evaluation for existing buildings is covered in this chapter. Rehabilitation procedures and objectives are covered in FEMA-273 and in the *Guidelines*.

8.2.2 Evaluation Process

The evaluation process for existing buildings follows the same general steps as those given in Chapters 5 and 6. However, it is necessary to determine the material properties and condition of the existing buildings.

8.3 General Requirements

8.3.1 Scope

This chapter gives recommendations for systematic evaluation and rehabilitation of existing steel moment frame buildings. The recommendations follow closely those given in FEMA-273 and 274 (FEMA, 1997c, d). These documents are highly recommended for design professionals. Some significant changes to FEMA-273 are recommended. These changes result from the Northridge earthquake experience and the large volume of research results that have been produced since then, including the two SAC projects.

8.3.2 Performance Levels and Objectives

Two performance levels are recognized in this document: Collapse Prevention (CP) and Immediate Occupancy (IO). These are defined and described in Chapters 2 and 5. For design of new buildings, the stated performance object is 95% confidence in achieving Collapse Prevention for the 2/50 hazard. Although this is an excellent goal for evaluation and rehabilitation, it may not always be attainable due to the cost and other factors. To satisfy this performance objective for new buildings, it only requires using a better connection that results in only a small increment in cost. To take this approach for an existing building might require rehabilitating every moment connection in the building. This would be very costly.

This chapter presents a performance-based procedure for evaluating the confidence in satisfying a given performance level for a steel moment-frame building for a given hazard level.

The procedure is based on the groundwork presented in Chapter 5 and follows closely the developments for performance evaluation of new buildings given in Chapter 6.

The two broad issues that face the design professional and building owner are these: (1) What is the minimum acceptable level of protection against collapse and loss of life for a given hazard level? (2) What level of damage is acceptable for a given hazard level? This document will not attempt to answer these questions in general terms because every building, occupancy and situation are different. The objective of this report is to provide tools that will allow the design professional to evaluate the risk.

8.3.3 Seismic Hazard and Design Spectrum

The seismic hazard and design acceleration response spectra are the ones given in Chapter 3. They are identical to those given in the 1997 NEHRP *Provisions* with one important exception. In the NEHRP *Provisions*, the design spectrum ordinates, S_{DS} and $S_{D1,}$ are calculated by multiplying S_{MS} and S_{M1} by 2/3. For these SAC *Guidelines*, the 2/3 factor is replaced by 1.0. Justification for this is given in Chapter 3.

8.4 Material Properties and Condition Assessment

8.4.1 General

Quantification of in-place material properties and verification of the existing system configuration and condition are necessary to analyze or evaluate a building. This section identifies properties requiring consideration and provides guidelines for their acquisition. Condition assessment is an important aspect of planning and executing the seismic rehabilitation of an existing building. One of the most important steps in condition assessment is a visit to the building for visual inspection.

The extent of in-place materials testing and condition assessment that must be accomplished is related to availability and accuracy of construction and as-built records, the quality of materials used and construction performed, and the physical condition of the structure. Data such as the properties and grades of material used in component and connection fabrication may be effectively used to reduce the amount of in-place testing required. The design professional is encouraged to research and acquire all available records from the original construction.

8.4.2 Properties of In-Place Materials and Components

8.4.2.1 Material Properties

Mechanical properties of component and connection material dictate the structural behavior of the component under load. Mechanical properties of greatest interest include the expected yield (F_{ye}) and tensile (F_{ue}) strengths of base and connection material, ductility, toughness, elongational characteristics, and weldability. The term “expected strength” is used throughout this document in place of “nominal strength” since expected yield and tensile strengths are used in place of nominal values specified in AISC (1994a and b).

The effort required to determine these properties is related to the availability of original and updated construction documents, original quality of construction, accessibility, and condition of materials.

The determination of material properties is best accomplished through removal of samples and laboratory testing. Sampling may take place in regions of reduced stress, such as flange tips at beam ends and external plate edges, to minimize the effects of reduced area. Types and sizes of specimens should be in accordance with ASTM standards. Mechanical and metallurgical properties usually can be established from laboratory testing on the same sample. Default values for material properties recognized by the SAC project are given in Table 8-1. There are two factors that require mill test data to be adjusted. The first is that coupons are taken from the web, which has a strength of about 5% higher than the flange. The second is the mill load rate.

Table 8-1 Expected and Lower-Bound Material Properties for Structural Steel of Various Grades

	Yield Strength (ksi)		Tensile Strength (ksi)	
Material Specification	**Lower Bound**	**Expected**	**Lower Bound**	**Expected**
ASTM, A36	1961 – 1990			
Group 1	41	47	60	70
Group 2	39	47	58	67
Group 3	36	46	58	68
Group 4	34	44	60	71
Group 5	39	47	68	80
ASTM, A572	1961 -			
Group 1	47	54	62	75
Group 2	48	58	64	75
Group 3	50	57	67	77
Group 4	49	57	70	81
Group 5	50	55	79	84
A36 and Dual Grade 50	1990 – 1999			
Group 1	48	55	66	73
Group 2	48	58	67	75
Group 3	52	57	72	76
Group 4	50	54	71	76

Notes:
1. Lower-bound values for material are mean – 2 standard deviation values from statistical data. Expected values for material are mean values from statistical data.
2. For wide-flange shapes, indicated values are representative of material extracted from the web of the section. For flange, reduce indicated values by 5%.

8.4.2.2 Component Properties

Behavior of beams and columns is dictated by such properties as area, width-to-thickness and slenderness ratios, lateral torsional buckling resistance, and connection details. Component properties of interest are:

- original cross-sectional shape and physical dimensions,
- size and thickness of additional connected materials, including cover plates, bracing, and stiffeners,
- existing cross-sectional area, section moduli, moments of inertia, and torsional properties at critical sections,
- as-built configuration of intermediate, splice, and end connections, and
- current physical condition of base metal and connector materials, including the presence of deformation.

Each of these properties is needed to characterize building performance in the seismic analysis. The starting point for establishing component properties should be construction documents. Preliminary review of these documents shall be performed to identify primary vertical- and lateral-load-carrying elements and systems, and their critical components and connections. In the absence of a complete set of building drawings, the design professional must direct a testing agency to perform a thorough inspection of the building to identify these elements and components. In the absence of degradation, statistical analysis has shown that mean component cross-sectional dimensions are comparable to the nominal published values by AISC, AISI, and other organizations. Variance in these dimensions is also small.

8.4.3 Condition Assessment

8.4.3.1 General

A condition assessment of the existing building and site conditions shall be performed as part of the seismic evaluation process. The goals of this assessment are:

- to examine the physical condition of primary and secondary components and the presence of any degradation
- to verify or determine the presence and configuration of components and their connections, and the continuity of load paths between components, elements, and systems
- to review other conditions such as neighboring party walls and buildings, the presence of nonstructural components, and limitations for rehabilitation that may influence building performance.

The physical condition of existing components and elements, and their connections, must be examined for the presence of degradation. Degradation may include environmental effects (e.g., corrosion, fire damage, chemical attack) or past or current loading effects (e.g., overload, damage from past earthquakes, fatigue, fracture). The condition assessment shall also examine for configuration problems observed in recent earthquake, including effects of discontinuous

components, improper welding, and poor fit-up. If design or construction drawings are available, then the lateral-load-resisting system does not need to be verified by inspection. The condition of the components and the requirement for inspection shall be determined by the design professional based on the past history of the building.

Component orientation, plumbness, and physical dimensions should be confirmed during an assessment. The wide-flange section can usually be determined by measuring the appropriate dimensions of the beams and columns. Connections in steel components, elements, and systems require special consideration and evaluation. The load path for the system must be determined, and each connection in the load path(s) must be evaluated. This includes diaphragm-to-component and component-to-component connections. FEMA-267 (SAC, 1995) provides recommendations for inspection of welded steel moment frames.

The condition assessment also affords an opportunity to review other conditions that may influence steel elements and systems and overall building performance. Of particular importance is the identification of other elements and components that may contribute to, or impair, the performance of the steel system in question, including infills, neighboring buildings, and equipment attachments. Limitations posed by existing coverings, wall and ceiling space, infills, and other conditions shall also be defined so that prudent rehabilitation measures may be planned.

8.4.3.2 Scope and Procedures

The scope of a condition assessment shall include all primary structural elements and components involved in gravity and lateral-load resistance. If coverings or other obstructions exist, then local removal of covering materials will be necessary.

- If detailed design or construction drawings exist and the structure has not experienced an earthquake peak ground acceleration of 0.20 g or higher, no exposure of joints or members is required.
- If detailed design and construction drawings exist and the structure has experienced an earthquake peak ground acceleration of 0.20 g or more, the inspection procedures described in the SAC *Guidelines* should be followed.
- In the absence of construction drawings, the design professional shall establish inspection protocol that will provide adequate knowledge of the building needed for reliable evaluation. For steel elements encased in concrete, it may be more cost-effective to provide an entirely new lateral-load-resisting system than to remove concrete for inspection.

8.4.3.3 Quantifying Results

The results of the condition assessment shall be used in the preparation of building system models in the evaluation of seismic performance. To aid in this effort, the results shall be quantified and reduced, with the following specific topics addressed.

- Component section properties and dimensions
- Connection configuration and presence of any eccentricities
- Type and location of column splices
- Interaction of nonstructural components and their involvement in lateral-load resistance

The acceptance criteria for existing components depend on the design professional's knowledge of the condition of the structural system and material properties (as previously noted). All deviations noted between available construction records and as-built conditions shall be accounted for and considered in the structural analysis.

8.5 Analytical Evaluation Methods for Existing Steel Moment Frames

8.5.1 General

Moment-resisting connections with calculable resistance are required between the members in steel moment frames. The frames are categorized by the types of connections used and by the local and global stability of the members. Moment frames may act alone to resist seismic loads, or they may act in conjunction with concrete or masonry shear walls or with braced steel frames to form a dual system. Special rules for design of new dual systems are included in AISC (1997) and FEMA (1997a).

Connections between the members may be fully restrained (FR), partially restrained (PR), or nominally unrestrained (simple shear or pinned). The components may be bare steel, steel with a nonstructural coating for fire protection, or steel with either concrete or masonry encasement for fire protection.

Two types of frames are categorized in this document. Fully restrained (FR) moment frames are those frames for which no more than 10% of the lateral deflections arise from connection deformation. Partially restrained (PR) moment frames are those frames for which more than 10% of the lateral deflections result from connection deformation. In each case, the 10% value refers only to deflection due to beam-column connection deformation and not to frame deflections that result from column panel-zone deformation. Information on PR connections is given in Chapter 7. Existing welded connections are covered here.

8.5.1.1 Design Forces Using Various Analysis Procedures

Any of the analysis procedures described and calibrated in Chapter 4 may be used. Appropriate coefficients for each are given below.

8.5.2 Modeling and Analysis

8.5.2.1 General

Fully restrained (FR) moment frames are those moment frames with rigid connections. The connection shall be at least as strong as the weaker of the two members being joined. Connection deformation may contribute no more than 10% (not including panel-zone

deformation) to the total lateral deflection of the frame. If either of these conditions is not satisfied, the frame shall be characterized as partially restrained. The most common beam-to-column connection used in steel FR moment frames since the late 1950s required the beam flange to be welded to the column flange using complete joint penetration groove welds. These are commonly referred to as pre-Northridge connections. Many of these connections have fractured during recent earthquakes. The design professional is referred to FEMA-267 (SAC, 1995) and other documents prepared for the SAC Phase 1 and Phase 2 projects.

Fully restrained moment frames encompass both Special Moment-Resisting Frames and Ordinary Moment-Resisting Frames, defined in the *Seismic Provisions for Structural Steel Buildings* in Part 6 of AISC (1997). Requirements for general or seismic design of steel components given in AISC (1997) or FEMA (1997a) may be followed unless superseded by provisions in this report. In all cases, the expected strength will be used in place of the nominal design strength by replacing F_y with F_{ye}. Ordinary Moment Resting Frames are discussed in Chapter 7 of this document.

8.5.2.2 Stiffness for Analysis

A. Linear Static and Dynamic Procedures

Information on modeling buildings for analysis is given in Chapter 4 of this document.

B. Nonlinear Static Procedure

- Use elastic component properties as outlined in Chapter 4.
- Use appropriate nonlinear moment-curvature and interaction relationships for beams and beam-columns to represent plastification. These may be derived from experiment or analysis. See Chapter 4 for more information.
- Linear and nonlinear behavior of panel zones may be included as described in Chapter 4.

C. Nonlinear Dynamic Procedure

The hysteretic behavior of each component must be properly modeled. This behavior must be verified by experiment. A study by Shi and Foutch (1998) showed that the maximum drifts calculated using a nonlinear time-history analysis are not sensitive to the hysteresis model. Only major features of the hysteresis model are important such as sudden loss of strength and extreme pinching.

8.5.2.3 Modeling Nonlinear Behavior of Connections

Modeling the nonlinear behavior of new connections pre-qualified by the SAC project is described in Chapter 4. Modeling the nonlinear behavior of pre-Northridge connections is given here.

The nonlinear behavior of pre-Northridge connections is very complex. This is because of the brittle-type behavior of the weld. The hysteresis behavior of a typical pre-Northridge connection is shown in Figure 8-5. The first departure from linear behavior is usually the fracture of the bottom flange weld when the beam is under positive moment. A reasonable estimate of when this occurs is when the plastic moment capacity of the beam is reached. This is followed by a sudden loss of strength and stiffness. The strength drops to a value of about 0.2 M_p. It does not go to zero because the shear tab acting with the composite slab will generate some moment resistance. If the deformation continues, the top flange or shear tab will fracture leading to loss of gravity-carrying capability. When the deformation is reversed, there is no resistance until the crack in the fractured bottom flange closes. At this point the connection acts as if no fracture occurred, and negative moment builds. This could continue until the top flange, which is now in tension, fractures. If the load is reversed before fracturing the top flange, the moment will reduce to zero and remain at zero as the crack opens. The moment will increase until it reaches the $0.2M_p$ value. Generally, when the previous maximum positive rotation is reached, the crack will still continue to propagate with nearly constant moment until complete fracture occurs.

For the nonlinear static procedure, this behavior can be approximated in a reasonably easy manner. The behavior under positive moment can be modeled as shown in Figure 8-1. The control points are given in the *State of the Art Report on Connection Performance* (Roeder, 2000) as follows:

$$\theta_p = 0.051 - 0.0013\, d_b \tag{8-1}$$

and

$$\theta_g = 0.043 + 0.00058\, d_b \tag{8-2}$$

where:

θ_p = plastic rotation at which the bottom tension flange fractures

θ_g = plastic rotation at which top compression flange or shear tab fails

d_b = beam depth

This assumes that the engineer has an analysis program that not only does nonlinear analysis, but also allows the engineer to input custom moment-rotation models. There are currently commercial programs available with this capability.

Figure 8-1 depicts the behavior of the connection under positive moment. The behavior under negative moment is shown in Figure 8-2. When a static pushover analysis is conducted such as the F273-NSP described in Chapter 4, as the structure is loaded to the right, all connections on the right side of each column will be under positive moment and each connection on the left of each column will be under negative moment. The right-side connections should be modeled as shown in Figure 8-1 and each left-side connection should be modeled as shown in

Figure 8-2. It is recommended that a small amount of strain hardening be used for both connections in all regions of response.

For nonlinear time-history analysis, the connection model must have complex loading and unloading rules. Programs that allow this are not readily available. The SAC studies used a custom element for the Drain 2DX program developed by Shi and Foutch (1998). The behavior of the model connection is shown in Figure 8-6.

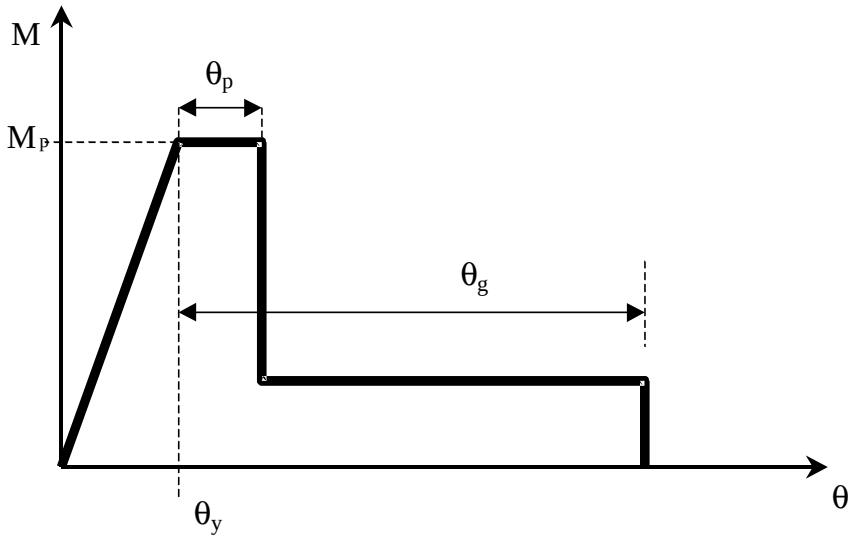

Figure 8-1 Moment-Rotation Behavior of Pre-Northridge Connection under Positive Moment

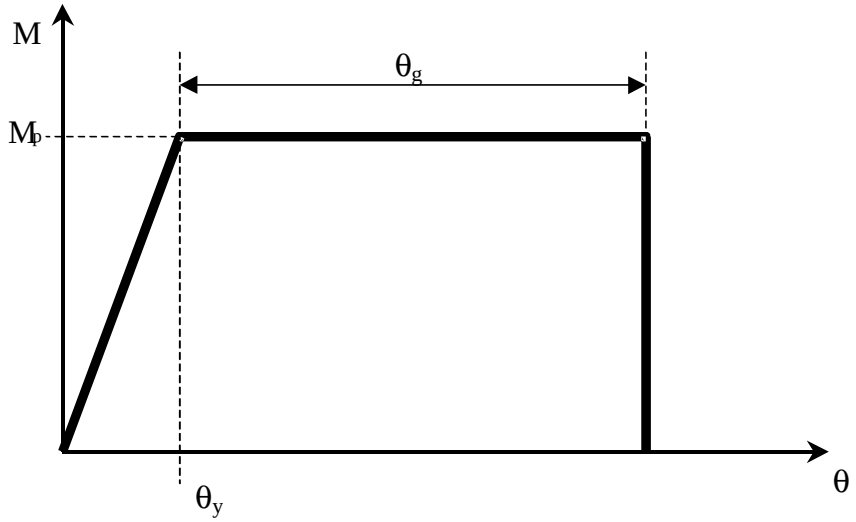

Figure 8-2 Moment-Rotation Behavior of Pre-Northridge Connection under Negative Moment

8.6 Performance Evaluation of Buildings Designed and Constructed Before the Northridge Earthquake

8.6.1 Background

There are many steps to take in the evaluation of an existing building. These include collecting design and construction drawings if available, determination of the condition of the building, and identification of the gravity and seismic-load-carrying systems and load paths. These and other important items are discussed in the body of the *Guidelines*. This section deals only with using analysis procedures for evaluation. It is assumed that the date of construction is known and the members and material properties of the gravity and seismic-load-carrying systems have been identified through the design documents or inspection and material tests as described above.

The year of construction can be an important indicator for seismic performance. Table 8-2 provides a summary of key specifications from the *UBC* for the years 1958 through 1997. The seismic and steel design requirements remained relatively unchanged from 1958 through 1970. Welded steel moment frames built during this period are characterized by four potential deficiencies. The most serious of these is the lack of a drift limit for seismic loads. Although not required for seismic design, many firms imposed a drift limit of 0.0025, which was the commonly used limit for wind loads. The second key aspect is the lack of a requirement for strength of panel zones. Frames designed in this period may have a ratio of plastic panel-zone strength to the sum of the strengths of the beams framing into the column as low as 0.40. The third important aspect is low design base shear. The fourth is the lack of restrictions on weak column designs.

Prior to 1970, there were no restrictions for steel buildings. In 1970, local buckling and connection strength requirements were added. An important addition to the code was made in 1976. A drift limit of 0.005 was imposed. The drift was equal to the calculated drift from elastic analysis divided by K. A new equation for determining the period of a building based on the improved Rayleigh quotient was also added. In 1988, four major changes took place. The current base shear format using a response modification factor, $R_{w,}$ and a requirement on panel zone strength were adopted. The drift limit was changed to the smaller of $0.04/R_w$ or 0.005. Also, a requirement on the ratio of strength of columns and girders framing into a joint was imposed. For all of these years up to, and including, 1994, only allowable stress design was recognized. In 1997, a near-source multiplier on the member strength requirements and a redundancy term were added.

Figure 8-3 shows the design response spectrum for 1973 and later years. The 1973 spectrum is considerably lower than the later ones for short periods and longer periods out to about two seconds. The response spectrum for the past years was for Zone 4, which assumed a peak ground acceleration at bedrock of 0.40g. The current codes recognize that the response spectrum for different sites in what was previously classified as Zone 4 can vary significantly. The level of the response spectrum is only half of the picture, however. The drift limitation is also very important, and there was none in 1973.

Table 8-2 A Summary of Key Specification from the UBC for the Years 1958 Through 1994

	94UBC	88UBC	85UBC	82UBC
UBC SEISMIC PART				
Allowable stress	All allowable stresses can be increased 1/3 when considering earthquake forces.	All allowable stresses can be increased 1/3 when considering earthquake forces.	All allowable stresses can be increased 1/3 when considering earthquake forces.	All allowable stresses can be increased 1/3 when considering earthquake forces.
Load combination	1.DL+LL+SnowL 2.DL+LL+WL(Seismic) 3.DL+LL+WL+Snow/2 4.DL+LL+Snow+Wind/2 5.DL+LL+Snow+Seismic	1.DL+LL+SnowL 2.DL+LL+WL(Seismic) 3.DL+LL+WL+Snow/2 4.DL+LL+Snow+Wind/2 5.DL+LL+Snow+Seismic	1.DL+LL+SnowL 2.DL+LL+WL(Seismic) 3.DL+LL+WL+Snow/2 4.DL+LL+Snow+Wind/2 5.DL+LL+Snow+Seismic	1.DL+LL+SnowL 2.DL+LL+WL(Seismic) 3.DL+LL+WL+Snow/2 4.DL+LL+Snow+Wind/2 5.DL+LL+Snow+Seismic
Live load reduction	Allowed	allowed	allowed	allowed
Seismic zone(LA)	Zone No. 4	Zone No. 4	Zone No. 4	Zone No. 4
Base shear	V=ZICW/Rw $C=1.25S/T^{2/3}$ - Rw=12 for SMRF	V=ZICW/Rw $C=1.25S/T^{2/3}$ - Rw=12 for SMRF	V=ZIKCSW $C=1/(15*T^{1/2})$ - K=0.67 for SMRF - S=coefficient for site-structure resonance	V=ZIKCSW $C=1/(15*T^{1/2})$ - K=0.67 for SMRF - S=coefficient for site-structure resonance
Period(T)	$T = 2\pi\sqrt{\left(\sum \omega_i \delta_i^2\right) \div \left(g \sum f_i \right.}$ $T=Ct(hn)^{3/4}$	$T = 2\pi\sqrt{\left(\sum \omega_i \delta_i^2\right) \div \left(g \sum f_i \delta_i\right)}$ $T=Ct(hn)^{3/4}$	$T = 2\pi\sqrt{\left(\sum \omega_i \delta_i^2\right) \div \left(g \sum f_i \delta_i\right)}$ $T=0.05hn/D^{1/2}$ T=0.1N for SMRF	$T = 2\pi\sqrt{\left(\sum \omega_i \delta_i^2\right) \div \left(g \sum f_i \delta_i\right)}$ $T=0.05hn/D^{1/2}$ T=0.1N for SMRF
Distribution of lateral forces	V=Ft+ΣFi Ft=0.07TV	V=Ft+ΣFi Ft=0.07TV	V=Ft+ΣFi Ft=0.07TV	V=Ft+ΣFi Ft=0.07TV
Story drift limit	* T ≤ 0.7sec limit=0.04/Rw or 0.005*hn * T > 0.7sec limit=0.03/Rw or 0.004*hn	* h ≤ 65' limit=0.04/Rw or 0.005*hn * h > 65' limit=0.03/Rw or 0.004*hn	Story drift≤0.005 Drift=displacement*(1/K)	Story drift≤0.005 Drift=displacement*(1/K)
ASD STEEL PART				
Bending	Fb=0.66Fy , ($65/Fy^{1/2}$)	Fb=0.66Fy , ($65/Fy^{1/2}$)	Fb=0.66Fy , ($65/Fy^{1/2}$)	Fb=0.66Fy , ($65/Fy^{1/2}$)
Axial + bending	$\frac{f_a}{F_a} + \frac{C_m f_b}{\left(1-\frac{f_a}{F'_e}\right)F_b} \le 1.0$	$\frac{f_a}{F_a} + \frac{C_m f_b}{\left(1-\frac{f_a}{F'_e}\right)F_b} \le 1.0$	$\frac{f_a}{F_a} + \frac{C_m f_b}{\left(1-\frac{f_a}{F'_e}\right)F_b} \le 1.0$	$\frac{f_a}{F_a} + \frac{C_m f_b}{\left(1-\frac{f_a}{F'_e}\right)F_b} \le 1.0$
SMRF requirements	-panel zone strength -panel zone thickness -strength ratio (strong col. weak beam)	-panel zone strength -panel zone thickness -strength ratio (strong col. weak beam)	-connections are able to develop full plastic capacity -local buckling=> satisfy plastic design	-connections are able to develop full plastic capacity -local buckling=> satisfy plastic design

Table 8-2 A Summary of Key Specification from the UBC for the Years 1958 Through 1994 (continued)

UBC SEISMIC PART	**79UBC**	**76UBC**	**73UBC**	**70UBC**
Allowable stress	All allowable stresses can be increased 1/3 when considering earthquake forces.	All allowable stresses can be increased 1/3 when considering earthquake forces.	All allowable stresses can be increased 1/3 when considering earthquake forces.	All allowable stresses can be increased 1/3 when considering earthquake forces.
Load combination	Wind load and earthquake load are not combined	Wind load and earthquake load are not combined	Wind load and earthquake load are not combined	Wind load and earthquake load are not combined
Live load reduction	allowed	allowed	Allowed	Allowed
Seismic zone(LA)	Zone No. 4	Zone No. 4	Zone No. 3	Zone No. 3
Base shear	V=ZIKCSW $C=1/(15*T^{1/2})$ - K=0.67 for SMRF - S=coefficient for site-structure resonance	V=ZIKCSW $C=1/(15*T^{1/2})$ - K=0.67 for SMRF - S=coefficient for site-structure resonance	V=ZKCW $C=0.05/T^{1/3}$ - K=0.67 for SMRF	V=ZKCW $C=0.05/T^{1/3}$ - K=0.67 for SMRF
Period(T)	$T=2\pi\sqrt{\left(\sum \omega_i \delta_i^2\right)\div\left(g\sum f_i\delta_i\right)}$ $T=0.05hn/D^{1/2}$ T=0.1N for SMRF	$T=2\pi\sqrt{\left(\sum \omega_i \delta_i^2\right)\div\left(g\sum f_i\delta_i\right)}$ $T=0.05hn/D^{1/2}$ T=0.1N for SMRF	$T=0.05hn/D^{1/2}$ T=0.1N for SMRF	$T=0.05hn/D^{1/2}$ T=0.1N for SMRF
Distribution of lateral forces	V=Ft+ΣFi Ft=0.07TV	V=Ft+ΣFi Ft=0.07TV	V=Ft+ΣFi Ft=0.004V(hn/D)^2	V=Ft+ΣFi Ft=0.004V(hn/D)^2
Story drift limit	Story drift≤0.005 Drift=displacement*(1/K)	Story drift≤0.005 Drift=displacement*(1/K)	Drift shall be considered in accordance with accepted engineering practice	Drift shall be considered in accordance with accepted engineering practice
ASD STEEL PART				
Bending	$Fb=0.66Fy$, $(65/Fy^{1/2})$	$Fb=0.66Fy$, $(65/Fy^{1/2})$	$Fb=0.66Fy$, $(52.2/Fy^{1/2})$	$Fb=0.66Fy$, $(52.2/Fy^{1/2})$
Axial + bending	$\frac{f_a}{F_a}+\frac{C_m f_b}{\left(1-f_a/F'_e\right)F_b}\le 1.0$	$\frac{f_a}{F_a}+\frac{C_m f_b}{\left(1-f_a/F'_e\right)F_b}\le 1.0$	$\frac{f_a}{F_a}+\frac{C_m f_b}{\left(1-f_a/F'_e\right)F_b}\le 1.0$	$\frac{f_a}{F_a}+\frac{C_m f_b}{\left(1-f_a/F'_e\right)F_b}\le 1.0$
SMRF requirements	-connections are able to develop full plastic capacity -local buckling=> satisfy plastic design	-connections are able to develop full plastic capacity -local buckling=> satisfy plastic design	-connections are able to develop full plastic capacity -local buckling=> satisfy plastic design	-connections are able to develop full plastic capacity -local buckling=> satisfy plastic design

Table 8-2 A Summary of Key Specification from the UBC for the Years 1958 Through 1994 (continued)

	67UBC	64UBC	61UBC	58UBC
UBC SEISMIC PART				
Allowable stress	All allowable stresses can be increased 1/3 when considering earthquake forces.	All allowable stresses can be increased 1/3 when considering earthquake forces.	All allowable stresses can be increased 1/3 when considering earthquake forces.	All allowable stresses can be increased 1/3 when considering earthquake forces.
Load combination	Wind load and earthquake load are not combined	Wind load and earthquake load are not combined	Wind load and earthquake load are not combined	Wind load and earthquake load are not combined
Live load reduction	Allowed	Allowed	Allowed	Allowed
Seismic zone(LA)	Zone No. 3	Zone No. 3	Zone No. 3	Zone No. 3
Base shear	V=ZKCW $C=0.05/T^{1/3}$ - K=0.67 for SMRF	V=ZKCW $C=0.05/T^{1/3}$ - K=0.67 for SMRF	V=ZKCW $C=0.05/T^{1/3}$ - K=0.67 for SMRF	F=CW C=Horizontal force factor
Period(T)	$T=0.05hn/D^{1/2}$ T=0.1N for SMRF	$T=0.05hn/D^{1/2}$ T=0.1N for SMRF	$T=0.05hn/D^{1/2}$ T=0.1N for SMRF	
Distribution of lateral forces	V=Ft+ΣFi Ft=0.004V(hn/D)^2	V=Ft+ΣFi Ft=0.004V(hn/D)^2	V=Ft+ΣFi Ft=0.1*V	
Story drift limit	Drift shall be considered in accordance with accepted engineering practice	Drift shall be considered in accordance with accepted engineering practice	Drift shall be considered in accordance with accepted engineering practice	
ASD STEEL PART				
Bending	$Fb=0.66Fy$, $(13330/Fy^{1/2}$ psi)	$Fb=0.66Fy$, $(13330/Fy^{1/2}$ psi)	20,000psi ,when (Ld/bt)<600	20,000psi ,when (Ld/bt)<600
Axial + bending	$\frac{f_a}{F_a}+\frac{C_m f_b}{\left(1-f_a/F'_e\right)F_b}\le 1.0$	$\frac{f_a}{F_a}+\frac{C_m f_b}{\left(1-f_a/F'_e\right)F_b}\le 1.0$	$17{,}000-0.485(L/r)^2$ when L/r<120	$17{,}000-0.485(L/r)^2$ when L/r<120
SMRF REQUIREMENTS	- no seismic regulation	- no seismic regulation	- no seismic regulation	- no seismic regulation

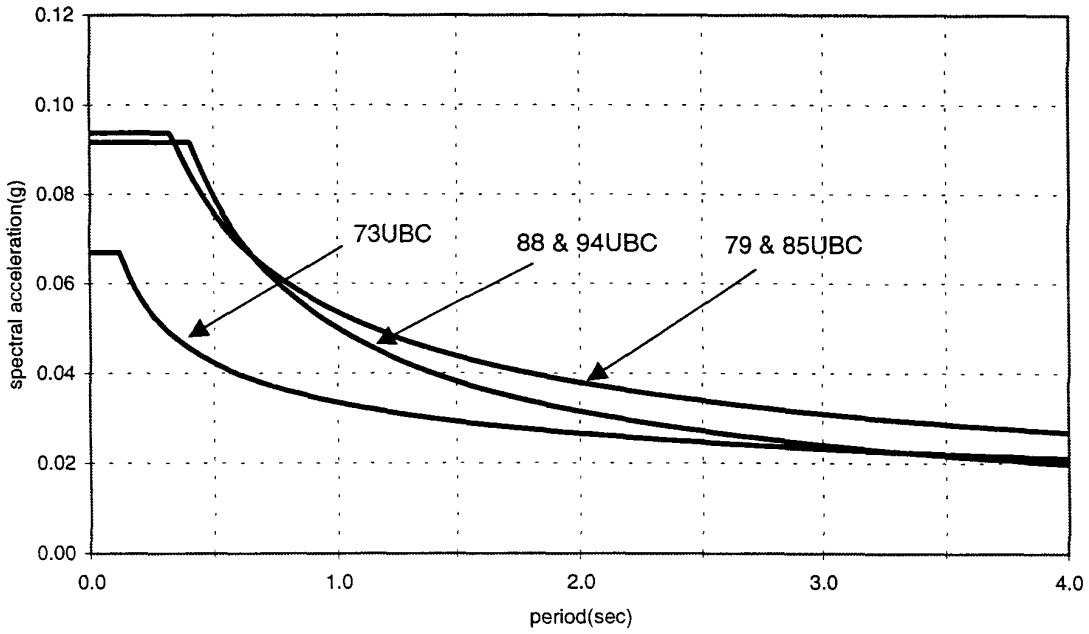

Figure 8-3 Design Response Spectrum for Special Moment Frames, 1973 UBC, and Later Years

Perhaps the greatest deficiencies in all the welded steel moment frames constructed prior to the Northridge earthquake are the welding material and joint configuration. Laboratory tests revealed that most bottom flange welds fractured at or below the plastic moment capacity of the beams, which limits the ductility capacity of the beams to about 1. Recent tests of pre-Northridge connections indicate that weak panel zones will cause fracture at about the same joint rotation as for a frame with strong panel zones. This indicates that the distortion of the panel zone can cause the beam-column flange welds to fracture even when the rotation of the beam is not sufficient to cause flexural yielding.

8.6.2 Expected Performance of Existing Welded Steel Moment Frames Based on Year of Construction

Major investigations were undertaken for the SAC Phase 2 project. The System Performance (SP), Connection Performance (CP), and Performance Prediction and Evaluation (PPE) Teams were established for this research. Summaries of this work may be found in the State of the Art Reports (SOA) for these groups (Krawinkler, 2000; Roeder, 2000). More complete reports of this activity are referenced in the SOA reports.

The PPE team designed a number of buildings for an LA site in accordance with the various codes mentioned above. Three story, 9-story, and 20-story buildings were designed for the 1973, 1985, and 1994 *UBC* requirements. An additional set of buildings was designed for the 1973 *UBC*, the first set with no drift limit and the second with a drift limit of 0.0025. The building configurations were the same as those for which outside consultants designed buildings for sites in Los Angeles, Seattle, and Boston. Twenty buildings with these and other configurations were designed in accordance with the 1997 NEHRP *Provisions*. Floor plans and elevations for these

buildings are shown in Figure 8-4. Note that one more bay of moment frame was added to the three-story building designed for the 1997 NEHRP *Provisions* in order to satisfy the redundancy requirement for an SMF. The member sizes and other information for all of these buildings are given in the report by Lee and Foutch (1999).

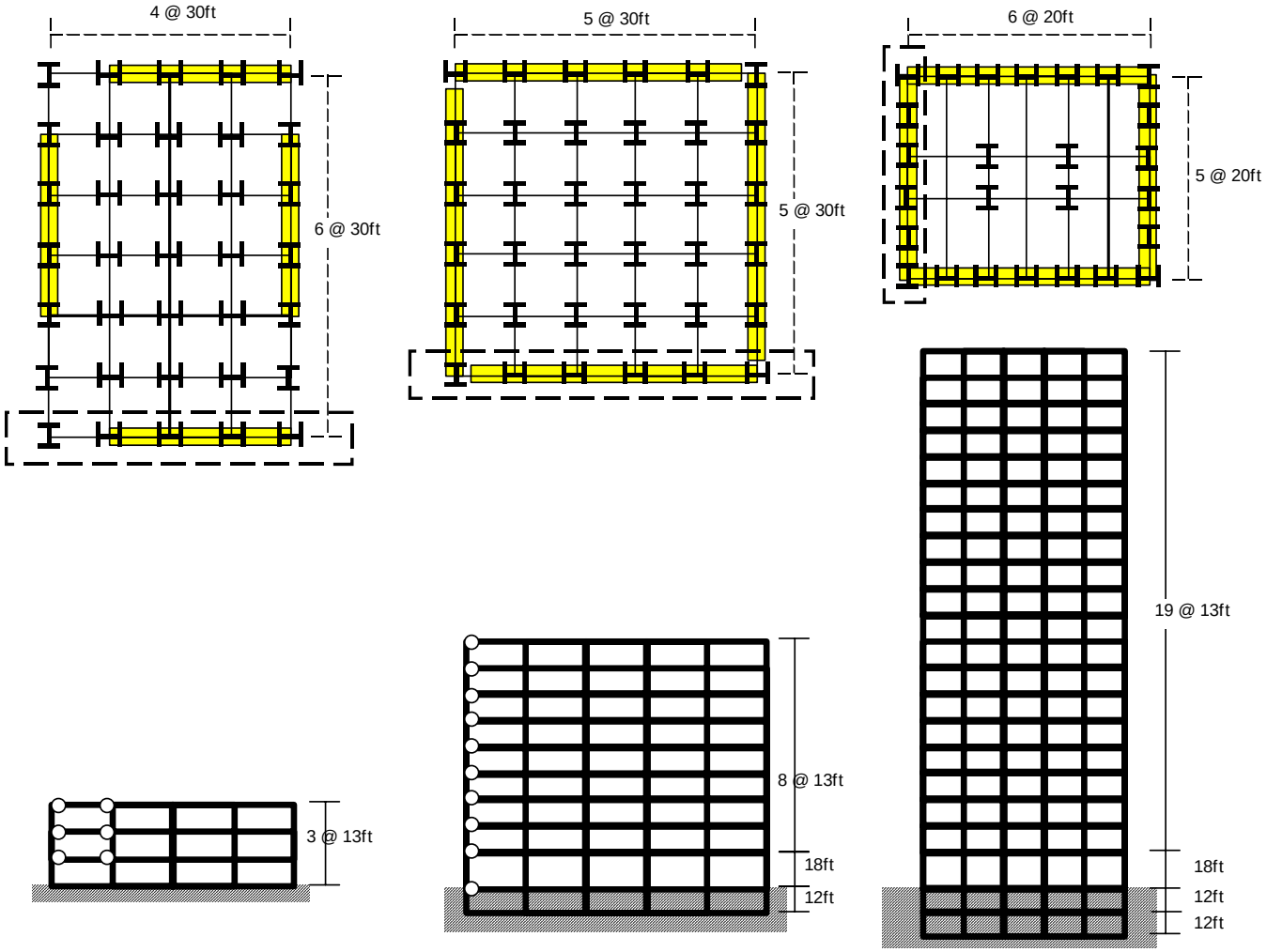

Figure 8-4 Floor Plans and Elevations for the Pre-Northridge Buildings

The modeling of the 1997 buildings is described in Chapters 4 and 5. The hysteresis behavior from tests of beam-column connections is shown in Figures 5-1 for an RBS connection and Figure 5-3 for a beam-column shear tab connection in a gravity frame. The models used in these studies for this behavior are shown in Figures 5-2 and 5-4. The measured and modeled hysteresis behavior of the pre-Northridge connections used for the moment frames are shown in Figures 8-5 and 8-6. The response in the upper quadrant represents the response for positive moment where the bottom flange fractures. This is characterized by sudden fracture of the bottom flange followed by severe pinching thereafter. The large increase in strength and stiffness after a plateau of zero strength and stiffness represents closure of the crack in the bottom flange. The element model (Shi and Foutch, 1997) used for these analyses reproduces

the measured behavior well. The lower left quadrant represents behavior for negative moment where the crack in the bottom flange is fully closed and the top flange is in tension. At a rotation of about 0.04, either the top flange or the shear tab usually fractures, resulting in nearly zero strength and stiffness. The connection model is not able to model this well. The model gradually loses strength and arrives at about zero capacity at a rotation of 0.04, so the calculated results are a little conservative. The response calculations are not particularly sensitive to this difference. It is expected that the calculated responses are perhaps 1% larger for the model used.

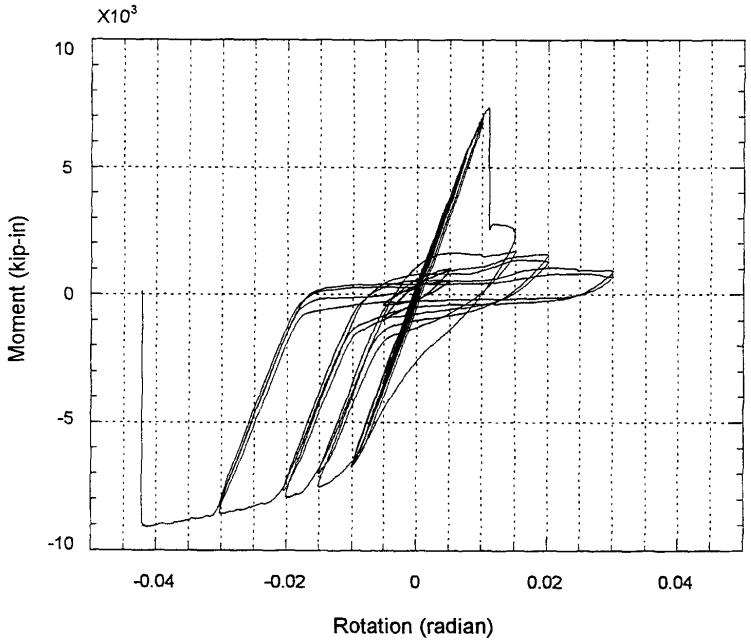

Figure 8-5 Measured Moment-Rotation Behavior of Pre-Northridge Connection

Demands placed on these buildings by the SAC LA ground motions and IDA analyses were completed for each building. Typical results for IDA analyses are shown in Figure 8-7. For the 1997 NEHRP building, it was assumed that the RBS system was used. Plots of median, 84th and 95th percentiles of maximum drift for each story for each building for both the 2/50 and 50/50 accelerograms are shown in Figure 8-8. Global collapse capacities for each building were determined using IDA analyses. Median demands for the 2/50 LA accelerograms were also calculated and are given with the capacities in Table 8-3.

The results show that the expected performance of a steel moment-frame building depends on the code for which it was designed. The buildings designed prior to 1973 with no drift limit should be expected to perform worse than buildings designed under more recent codes. These pre-1973 buildings had median drift demands of approximately 6%, 5%, and 4% for the 3, 9, and 20-story buildings, respectively. At the 84th percentile, the drift demands are about 8%. This is alarming given that the global collapse drift for the 9 and 20-story buildings are smaller than this and the local collapse drift is 4% for all the buildings. The results also indicate that the taller buildings should be expected to perform worse than shorter ones for LA type ground motions.

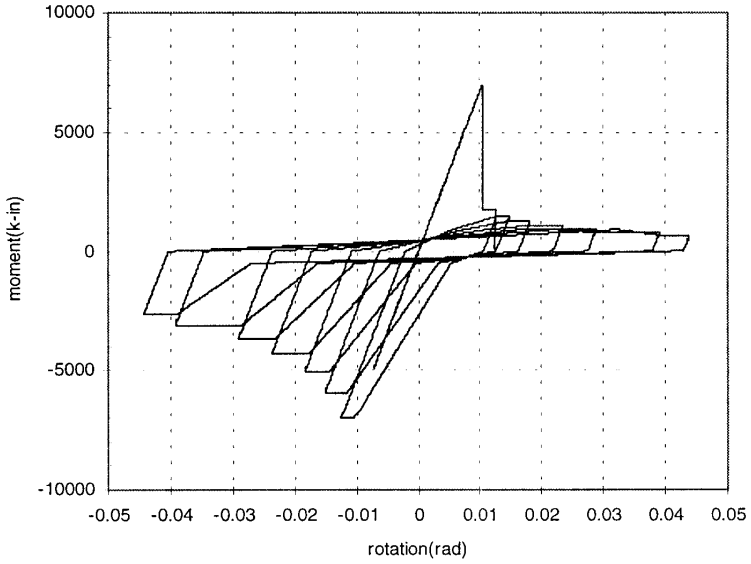

Figure 8-6 Model of Moment-Rotation Behavior of Pre-Northridge Connection

The results show that, as the year of construction becomes older, the capacity decreases and the demand increases. This effect is most pronounced for the 20-story building where the demand-to-capacity ratio is 0.34 for 1997 NEHRP design and 0.58 for the 1973 *UBC* design. The results in Table 8-3 are for a specific set of buildings designed for a specific site and subjected to 20 accelerograms (Lee and Foutch, 2000) developed for this site for the SAC project. Each building is unique. It may have more or less strength and stiffness than these case study buildings and it will obviously be designed for different site conditions. Also, these are the result of calculations for a highly idealized model using procedures that have not been tested for a real building shaken to drifts approaching collapse. Therefore, the results given in Table 8-3 and in tables and figures shown below should not be used indiscriminately. They are given here merely for reference and as a rough indicator of possible average performance based on year of construction. The judgement of the design professional is crucial for effective evaluation of existing and damaged buildings.

Table 8-3 Demand and Global Capacities for 2/50 Hazard Level for Buildings Designed for Different Building Codes

	97NEHRP		94UBC		85UBC		73UBC w/ drift limit		73UBC w/o drift limit	
	capcity	demand	capcity	demand	capcity	demand	capcity	demand	capcity	demand
3-story	0.100	0.027	0.100	0.047	0.100	0.058	0.100	0.056	0.100	0.062
9-story	0.100	0.034	0.078	0.043	0.094	0.048	0.077	0.046	0.079	0.059
20-story	0.085	0.024	0.072	0.031	0.070	0.030	0.069	0.045	0.069	0.045

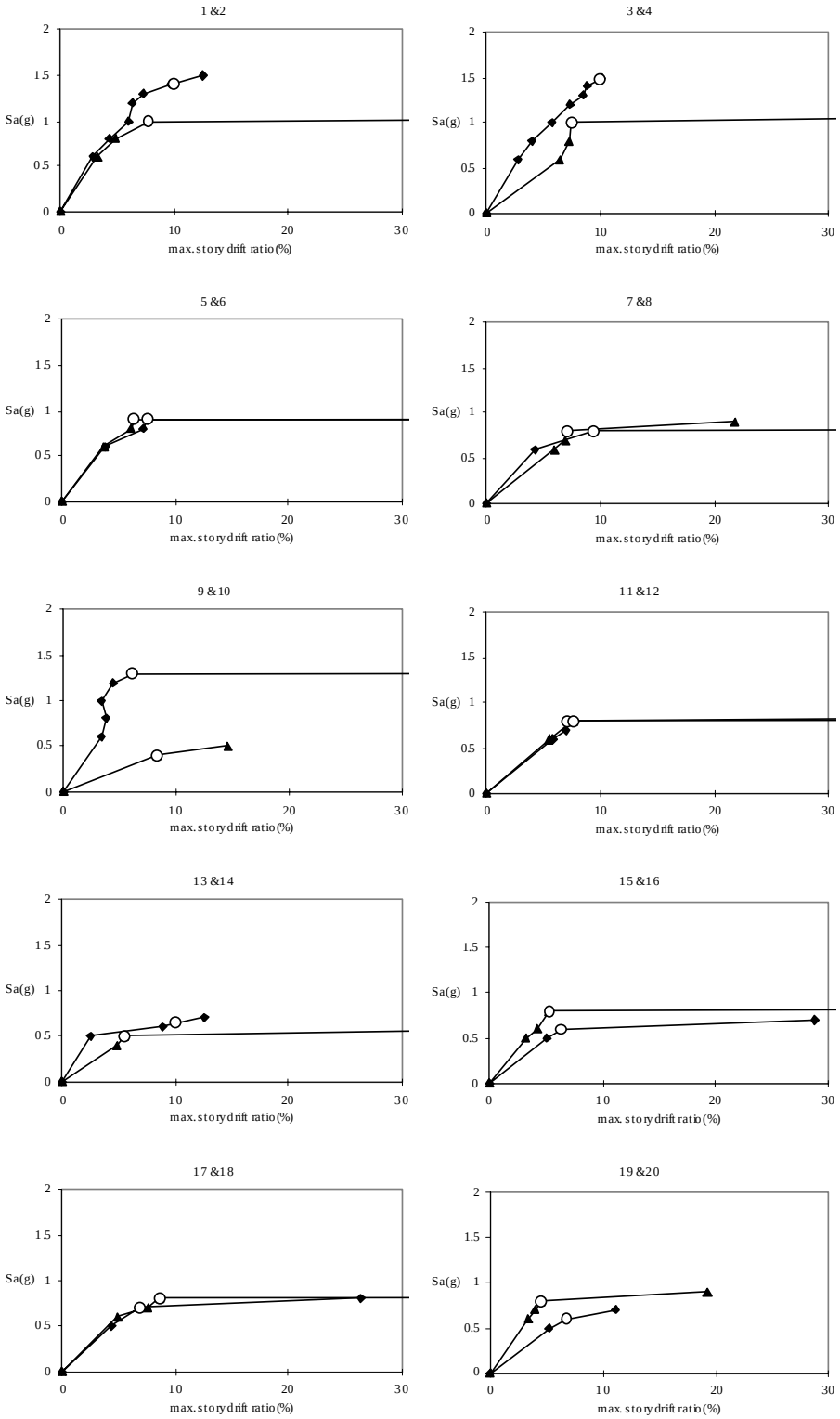

Figure 8-7 Typical IDA Analyses for Existing 20-Story Building

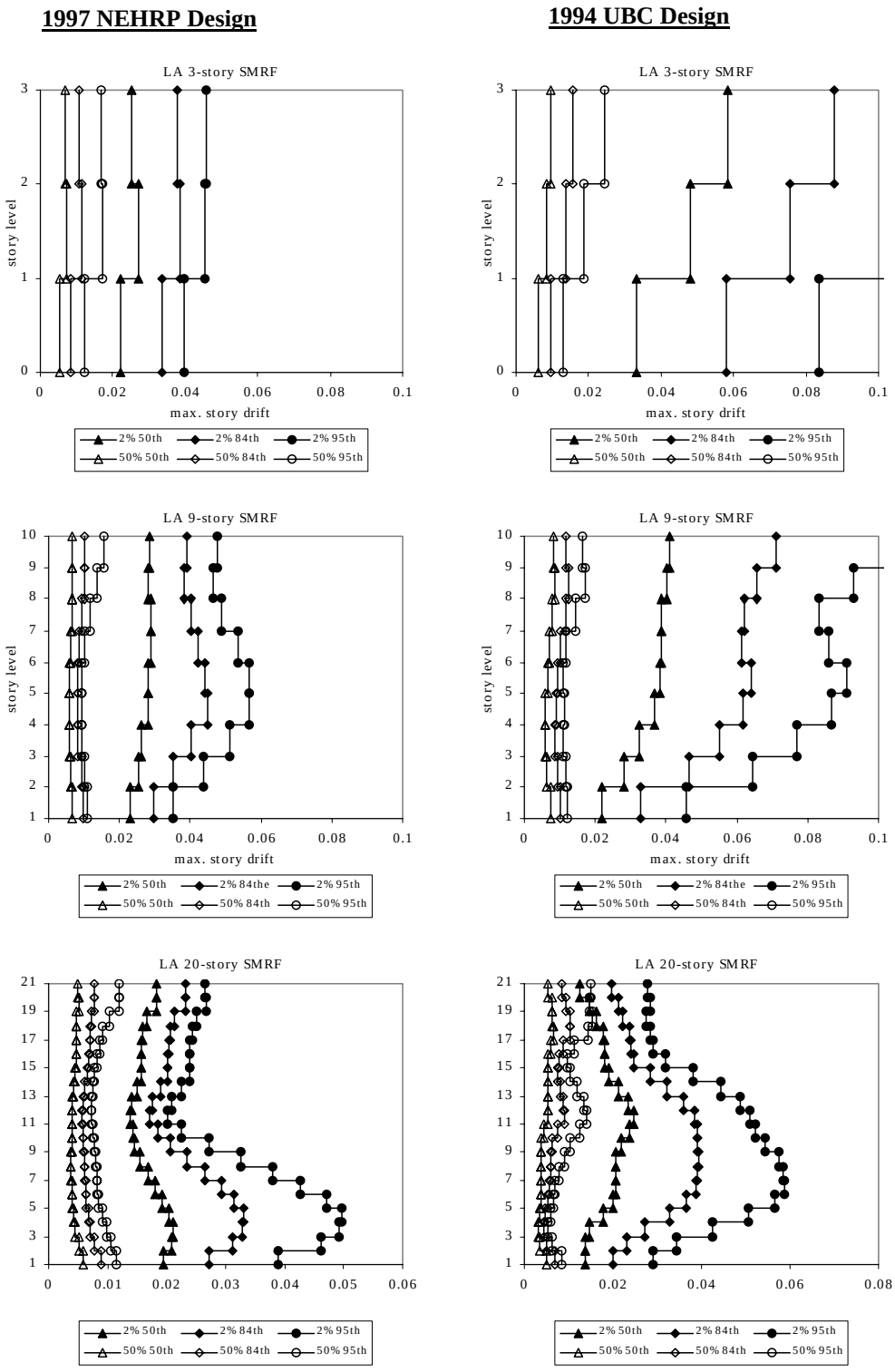

Figure 8-8 Median, 84th and 95th Percentile of Maximum Drift for Each Story

1985 UBC Design **1973 UBC Design**

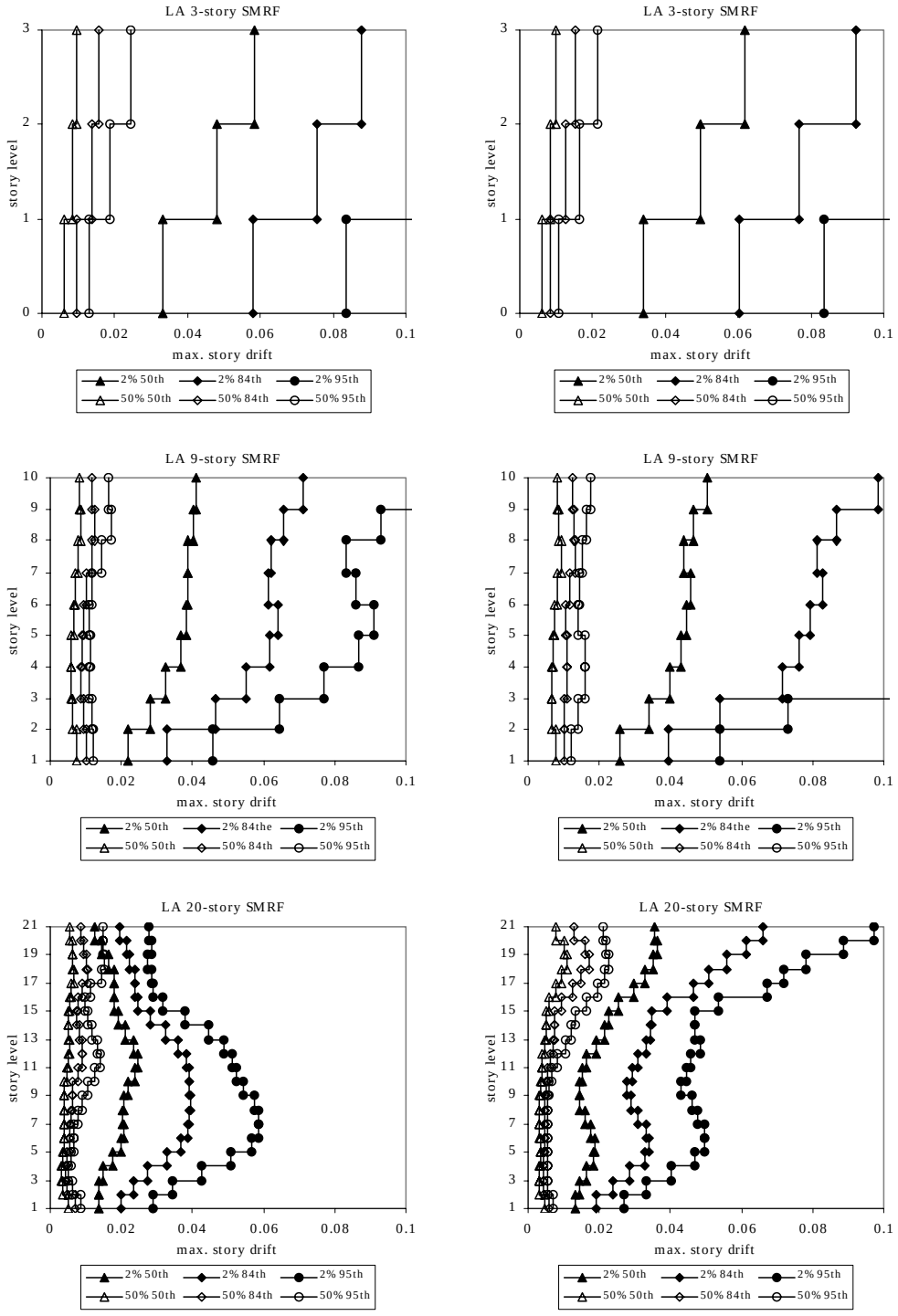

Figure 8-8 Median, 84th and 95th Percentile of Maximum Drift for Each Story (continued)

8.6.3 Expected Performance of Existing Buildings Based on Stiffness

The information presented in the previous section was based on the assumption that all existing buildings were designed to be in exact conformance with the *UBC* and AISC *Provisions* that were in effect at the time they were designed. This is certainly not true. Buildings built prior to 1973 may have been designed for any drift limit (including none) that was common practice for the design office. Buildings designed for any of the years may or may not have had doubler plates regardless of code requirements. Some buildings may have been designed for much larger or smaller live loads than are currently in place in the building. Some buildings may have been designed for a higher (or lower) level of performance than the minimum required by the design code. As a result, knowing the year of design and construction of a building is only a very crude indicator of expected performance.

A useful indicator of performance is the stiffness of a building. The fact that buildings of the same height have widely varying periods of vibration is an indication that the stiffnesses of buildings may vary substantially. Steel moment frames in Seismic Performance Categories D, E and F (and many in SPC B and C) of the NEHRP *Provisions* will be governed by drift and, therefore, stiffness.

Since the buildings considered in these studies were designed for different base shear and design drift levels, a comparison of the calculated drift for each building based on the lateral force for which it was designed would not be particularly useful. Instead, each building was analyzed for the current requirements in the 1997 NEHRP *Provisions* (but with $S_{D1} = F_v S_s$) to investigate how buildings might perform as a function of stiffness. The calculated displacements and drifts are for the elastic drift for the reduced forces, and are multiplied by $C_d = 5.5$ to estimate the maximum inelastic displacements and drifts. One other change was also made to the 1997 NEHRP *Provisions*. The lower bound on the response spectrum was eliminated for performance evaluation as discussed in Chapter 4. This lower bound is not appropriate for the evaluations of buildings using the procedures described herein (Yun and Foutch, 2000).

Results of these analyses are shown in Figure 8-9. It is clear from these results that buildings designed under different codes and office practices may have different stiffnesses. The pre-1976 buildings designed for no drift limit are clearly more flexible than those designed after 1976. The IDA-determined global stability capacities given in Table 8-3 are also much smaller for the more flexible buildings. The calculated drifts are also given in Figure 8-9. To put these drifts into context, the equivalent maximum allowable drift demand for a new building is 0.03. The local collapse drift for pre-Northridge buildings is 0.04. The global stability limits from Table 8-3 range from 0.10 for all of the 3-story buildings to 0.057 for the 1973 20-story building.

The results indicate that if the pre-1997 buildings were designed exactly according to the corresponding building code requirements, on average the 1973 buildings designed with no drift requirement, and the 1985 buildings, would not be expected to satisfy the local collapse criteria.

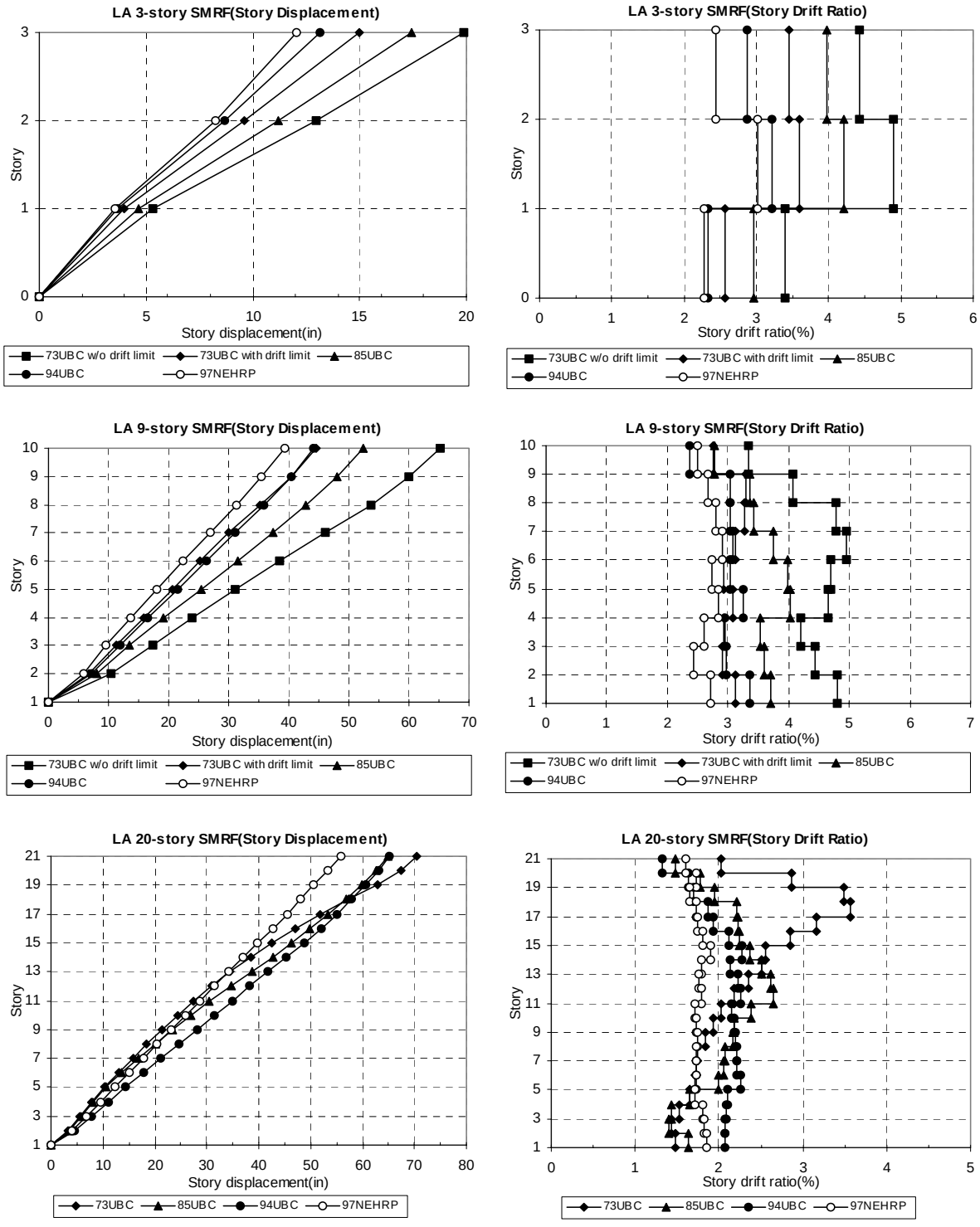

Figure 8-9 A Comparison of the Calculated Drift for Each Building Based on the 1997 NEHRP Lateral Force

8.6.4 Performance Prediction using Confidence Level Calculations

Another tool that the designer may use for predicting performance is the confidence level calculation described in Chapter 5. The level of confidence in an existing building satisfying the CP and IO performance levels described in Chapter 2 may be calculated and used in an absolute fashion or in comparison with buildings designed by the 1997 NEHRP *Provisions*. An example is given in Appendix A.

Tables 8-4 and 8-5 give the confidence level of satisfying the global and local collapse limit states for the 2/50 hazard level for each of the case-study buildings. The tables also give the β, γ and γ_a values used for these calculations. It is possible that some of the earlier buildings were constructed using an E7018 or other notch-tough electrode and the SMAW welding process. In this case, the building would be expected to perform only slightly better than those constructed with the T4 electrode. There have been few tests of these connections.

The results indicate that, in general, the newer the building the more confidence we have in its ability to survive during an earthquake. However, even for a 1994 building, the confidence level that a 9-story building will avoid global collapse is only 56% and local collapse only 14%. The situation is much worse for a 1973 building designed with no drift limit. The confidence that a 9-story building will avoid global collapse is 45% and for local collapse it is only 7%!

Table 8-6 gives the confidence levels for satisfying the IO performance level for the 50/50 hazard level for all of these buildings. The capacity for the 1997 building is a story drift of 0.018 that corresponds roughly with the onset of local buckling. For the pre-Northridge buildings, fracture of the bottom flange represents the damage state which occurs at a drift of 0.01. The results indicate that only the 1997 building provides a satisfactory level of confidence.

Tables 8-7 and 8-8 give the confidence level of satisfying the global and local CP limit state for the 50/50 hazard level that corresponds to a return period of 72 years. Fortunately, all of the buildings have a high level of confidence that they will satisfy this performance level. It is this author's opinion that the minimum acceptable state for an existing building to be acceptable without rehabilitation is a 90% confidence of satisfying the CP performance level for the 50/30 hazard level.

Examples of how these calculations are made are given in Appendix A.

Table 8-4 CP Confidence Level Calculations Against Global Collapse for 2/50 Hazard

	C	β_r	β_u	ϕ	D	β_{acc}	β_{or}	γ	β_a	γ_a	λ_{con}	β_{UT}^2	K_x	C.L.(%)
1997 NEHRP														
3-story	0.100	0.00	0.26	0.90	0.027	0.38	0.21	1.33	0.17	1.04	2.41	0.10	3.30	**99**
9-story	0.100	0.00	0.35	0.84	0.034	0.30	0.19	1.21	0.20	1.06	1.91	0.16	2.21	**99**
20-story	0.085	0.29	0.43	0.67	0.024	0.45	0.26	1.50	0.25	1.10	1.43	0.25	1.47	**93**
1994 UBC														
3-story	0.100	0.00	0.26	0.90	0.047	0.51	0.21	1.58	0.17	1.04	1.16	0.10	0.94	**83**
9-story	0.078	0.22	0.35	0.78	0.043	0.41	0.19	1.37	0.20	1.06	0.97	0.16	0.53	**70**
20-story	0.072	0.22	0.43	0.70	0.031	0.47	0.26	1.53	0.25	1.10	0.97	0.25	0.69	**75**
1985 UBC														
3-story	0.100	0.00	0.26	0.90	0.058	0.41	0.21	1.38	0.17	1.04	1.08	0.10	0.71	**76**
9-story	0.094	0.22	0.35	0.77	0.048	0.48	0.19	1.49	0.20	1.06	0.95	0.16	0.49	**69**
20-story	0.070	0.35	0.43	0.63	0.030	0.43	0.26	1.46	0.25	1.10	0.91	0.25	0.56	**71**
1973 UBC : with drift limit= 0.0025														
3-story	0.100	0.00	0.26	0.90	0.056	0.37	0.21	1.31	0.17	1.04	1.18	0.10	0.99	**84**
9-story	0.077	0.22	0.35	0.78	0.046	0.50	0.19	1.54	0.20	1.06	0.79	0.16	0.02	**51**
20-story	governed by wind. therefore same as 1973 UBC without drift limit													
1973 UBC : without drift limit														
3-story	0.100	0.00	0.26	0.90	0.062	0.40	0.21	1.36	0.17	1.04	1.02	0.10	0.54	**71**
9-story	0.079	0.27	0.35	0.75	0.059	0.56	0.19	1.68	0.20	1.06	0.56	0.16	-0.83	**20**
20-story	0.069	0.23	0.43	0.70	0.045	0.44	0.26	1.49	0.25	1.10	0.66	0.25	-0.09	**46**

Table 8-5 CP Confidence Level Calculations Against Local Collapse for 2/50 Hazard

	C	β_r	β_u	ϕ	D	β_{acc}	β_{or}	γ	β_a	γ_a	λ_{con}	β_{UT}^2	K_x	C.L.(%)
1997 NEHRP														
3-story	0.070	0.20	0.25	0.86	0.027	0.38	0.21	1.33	0.17	1.04	1.60	0.09	2.01	**98**
9-story	0.070	0.20	0.25	0.86	0.034	0.30	0.19	1.21	0.20	1.06	1.37	0.10	1.47	**93**
20-story	0.070	0.20	0.25	0.86	0.024	0.45	0.26	1.50	0.25	1.10	1.52	0.13	1.71	**96**
1994 UBC														
3-story	0.037	0.20	0.25	0.86	0.047	0.51	0.21	1.58	0.17	1.04	0.41	0.09	-2.51	**1**
9-story	0.037	0.20	0.25	0.86	0.043	0.41	0.19	1.37	0.20	1.06	0.51	0.10	-1.62	**5**
20-story	0.037	0.20	0.25	0.86	0.031	0.47	0.26	1.53	0.25	1.10	0.61	0.13	-0.88	**19**
1985 UBC														
3-story	0.037	0.20	0.25	0.86	0.058	0.41	0.21	1.38	0.17	1.04	0.38	0.09	-2.75	**0**
9-story	0.037	0.20	0.25	0.86	0.048	0.48	0.19	1.49	0.20	1.06	0.42	0.10	-2.24	**1**
20-story	0.037	0.20	0.25	0.86	0.030	0.43	0.26	1.46	0.25	1.10	0.66	0.13	-0.65	**26**
1973 UBC : with drift limit= 0.0025														
3-story	0.057	0.20	0.25	0.86	0.056	0.37	0.21	1.31	0.17	1.04	0.64	0.09	-1.04	**15**
9-story	0.057	0.20	0.25	0.86	0.046	0.50	0.19	1.54	0.20	1.06	0.65	0.10	-0.85	**20**
20-story	governed by wind. therefore same as 1973 UBC without drift limit													
1973 UBC : without drift limit														
3-story	0.057	0.20	0.25	0.86	0.062	0.40	0.21	1.36	0.17	1.04	0.55	0.09	-1.50	**7**
9-story	0.057	0.20	0.25	0.86	0.059	0.56	0.19	1.68	0.20	1.06	0.47	0.10	-1.87	**3**
20-story	0.057	0.20	0.25	0.86	0.045	0.44	0.26	1.49	0.25	1.10	0.66	0.13	-0.62	**27**

Table 8-6 IO Confidence Level Calculations for 50/50 Hazard

	C	β_r	β_u	ϕ	D	β_{acc}	β_{or}	γ	β_a	γ_a	λ_{con}	β_{UT}^2	K_x	C.L.(%)
1997 NEHRP														
3-story	0.020	0.20	0.25	0.86	0.007	0.51	0.00	1.48	0.17	1.04	1.59	0.09	1.98	**98**
9-story	0.020	0.20	0.25	0.86	0.008	0.45	0.00	1.35	0.20	1.06	1.49	0.10	1.71	**96**
20-story	0.020	0.20	0.25	0.86	0.007	0.47	0.00	1.39	0.25	1.10	1.60	0.13	1.86	**97**
1994 UBC														
3-story	0.010	0.20	0.25	0.86	0.009	0.50	0.00	1.45	0.17	1.04	0.65	0.09	-0.96	**17**
9-story	0.010	0.20	0.25	0.86	0.009	0.39	0.00	1.25	0.20	1.06	0.74	0.10	-0.46	**32**
20-story	0.010	0.20	0.25	0.86	0.007	0.58	0.00	1.67	0.25	1.10	0.63	0.13	-0.76	**22**
1985 UBC														
3-story	0.010	0.20	0.25	0.86	0.010	0.49	0.00	1.43	0.17	1.04	0.57	0.09	-1.41	**8**
9-story	0.010	0.20	0.25	0.86	0.010	0.37	0.00	1.23	0.20	1.06	0.68	0.10	-0.72	**24**
20-story	0.010	0.20	0.25	0.86	0.008	0.54	0.00	1.54	0.25	1.10	0.63	0.13	-0.77	**22**
1973 UBC : with drift limit= 0.0025														
3-story	0.010	0.20	0.25	0.86	0.010	0.49	0.00	1.43	0.17	1.04	0.59	0.09	-1.27	**10**
9-story	0.010	0.20	0.25	0.86	0.009	0.41	0.00	1.29	0.20	1.06	0.69	0.10	-0.64	**26**
20-story	governed by wind. therefore same as 1973 UBC without drift limit													
1973 UBC : without drift limit														
3-story	0.010	0.20	0.25	0.86	0.010	0.44	0.00	1.33	0.17	1.04	0.62	0.09	-1.11	**13**
9-story	0.010	0.20	0.25	0.86	0.011	0.41	0.00	1.29	0.20	1.06	0.57	0.10	-1.27	**10**
20-story	0.010	0.20	0.25	0.86	0.011	0.51	0.00	1.49	0.25	1.10	0.46	0.13	-1.64	**5**

Table 8-7 CP Confidence Level Calculations Against Global Collapse for 50/50 Hazard

	C	β_r	β_u	ϕ	D	β_{acc}	β_{or}	γ	β_a	γ_a	λ_{con}	β_{UT}^2	K_x	C.L.(%)
1997 NEHRP														
3-story	0.100	0.00	0.26	0.90	0.007	0.51	0.00	1.48	0.17	1.04	8.36	0.10	7.29	**99**
9-story	0.100	0.00	0.35	0.84	0.008	0.45	0.00	1.35	0.20	1.06	7.24	0.16	5.53	**99**
20-story	0.085	0.29	0.43	0.67	0.007	0.47	0.00	1.39	0.25	1.10	5.28	0.25	4.08	**99**
1994 UBC														
3-story	0.100	0.00	0.26	0.90	0.009	0.50	0.00	1.45	0.17	1.04	6.87	0.10	6.66	**99**
9-story	0.078	0.22	0.35	0.78	0.009	0.39	0.00	1.25	0.20	1.06	5.23	0.16	4.72	**99**
20-story	0.072	0.22	0.43	0.70	0.007	0.58	0.00	1.67	0.25	1.10	3.73	0.25	3.38	**99**
1985 UBC														
3-story	0.10	0.00	0.26	0.90	0.010	0.49	0.00	1.43	0.17	1.04	5.98	0.10	6.22	**99**
9-story	0.09	0.22	0.35	0.77	0.010	0.37	0.00	1.23	0.20	1.06	5.76	0.16	4.96	**99**
20-story	0.07	0.35	0.43	0.63	0.008	0.54	0.00	1.54	0.25	1.10	3.23	0.25	3.10	**99**
1973 UBC : with drift limit= 0.0025														
3-story	0.100	0.00	0.26	0.90	0.010	0.49	0.00	1.43	0.17	1.04	6.25	0.10	6.36	**99**
9-story	0.077	0.22	0.35	0.78	0.009	0.41	0.00	1.29	0.20	1.06	4.82	0.16	4.51	**99**
20-story	governed by wind. therefore same as 1973 UBC without drift limit													
1973 UBC : without drift limit														
3-story	0.10	0.00	0.26	0.90	0.010	0.44	0.00	1.33	0.17	1.04	6.56	0.10	6.51	**99**
9-story	0.08	0.27	0.35	0.75	0.011	0.41	0.00	1.29	0.20	1.06	3.90	0.16	3.99	**99**
20-story	0.07	0.23	0.43	0.70	0.011	0.51	0.00	1.49	0.25	1.10	2.61	0.25	2.67	**99**

Table 8-8 CP Confidence Level Calculations Against Local Collapse for 50/50 Hazard

	C	β_r	β_u	ϕ	D	β_{acc}	β_{or}	γ	β_a	γ_a	λ_{con}	β_{UT}^2	K_x	C.L.(%)
1997 NEHRP														
3-story	0.070	0.20	0.25	0.86	0.007	0.51	0.00	1.48	0.17	1.04	5.56	0.09	6.11	**99**
9-story	0.070	0.20	0.25	0.86	0.008	0.45	0.00	1.35	0.20	1.06	5.20	0.10	5.60	**99**
20-story	0.070	0.20	0.25	0.86	0.007	0.47	0.00	1.39	0.25	1.10	5.61	0.13	5.40	**99**
1994 UBC														
3-story	0.037	0.20	0.25	0.86	0.009	0.50	0.00	1.45	0.17	1.04	2.41	0.09	3.36	**99**
9-story	0.037	0.20	0.25	0.86	0.009	0.39	0.00	1.25	0.20	1.06	2.73	0.10	3.60	**99**
20-story	0.037	0.20	0.25	0.86	0.007	0.58	0.00	1.67	0.25	1.10	2.34	0.13	2.94	**99**
1985 UBC														
3-story	0.037	0.20	0.25	0.86	0.010	0.49	0.00	1.43	0.17	1.04	2.10	0.09	2.90	**99**
9-story	0.037	0.20	0.25	0.86	0.010	0.37	0.00	1.23	0.20	1.06	2.51	0.10	3.34	**99**
20-story	0.037	0.20	0.25	0.86	0.008	0.54	0.00	1.54	0.25	1.10	2.34	0.13	2.93	**99**
1973 UBC : with drift limit= 0.0025														
3-story	0.057	0.20	0.25	0.86	0.010	0.49	0.00	1.43	0.17	1.04	3.38	0.09	4.47	**99**
9-story	0.057	0.20	0.25	0.86	0.009	0.41	0.00	1.29	0.20	1.06	3.96	0.10	4.75	**99**
20-story	governed by wind. therefore same as 1973 UBC without drift limit													
1973 UBC : without drift limit														
3-story	0.057	0.20	0.25	0.86	0.010	0.44	0.00	1.33	0.17	1.04	3.55	0.09	4.63	**99**
9-story	0.057	0.20	0.25	0.86	0.011	0.41	0.00	1.29	0.20	1.06	3.24	0.10	4.13	**99**
20-story	0.057	0.20	0.25	0.86	0.011	0.51	0.00	1.49	0.25	1.10	2.65	0.13	3.29	**99**

Example: 1985 UBC, 9-story, near City Hall in LA

A 9-story building located near City Hall in LA has the same configuration as the building shown in Figure 8-4. The building was constructed according the 1985 UBC code. Check the confidence in avoiding collapse for 2/50, 10/50, and 50/50 hazard levels.

Collapse against 2/50 hazard

Determine S_{DS} and S_{D1} for the site:

$S_{DS} = 1.0 \times S_{MS} = 1.0 \times F_a \times S_{S\text{-}2\%} = 1.0 \times 1.0 \times 1.93g = 1.93g$

$S_{D1} = 1.0 \times S_{M1} = 1.0 \times F_v \times S_{1\text{-}2\%} = 1.0 \times 1.3 \times 0.77g = 1.00g$

Use the 1997 NEHRP-LSP to calculate:

For a SMF 2/50 hazard, $R = 8$, $C_d = 5.5$

Analyzing the structure for the design base shear of 478 kips yields a maximum elastic drift of

$\delta_{xe} = 0.0044$ $\qquad \Delta = \delta_{xe} \times 5.5 = 0.024$

$\theta_m = 0.024$

Get C_B value for 9-story NEHRP LSP procedure Table 4-8: $C_B = 1.15$

Therefore, $C_B \theta_m = 1.15 \times 0.024 = 0.028$

For CP global: *$\hat{C} = 0.07$, $\phi = 0.85$, (Table 5-2)*

CP: $\gamma = 1.21$

For 1997 NEHRP in Table 5-4 $\gamma_a = 1.07$

Global collapse:

Get β_{UT} from Table 5-5: $\beta_{UT} = 0.40$

From Table 5-6: confidence level = 97 %

For CP local: *$\theta_{CP} = 0.054$, $\phi = 0.80$*

CP: $\gamma = 1.21$, $\gamma_a = 1.07$

Local collapse:

Get β_{UT} from Table 5-5: $\beta_{UT} = 0.32$

From Table 5-6: confidence level = 84 %

Collapse against 10/50 hazard

Determine S_{DS} and S_{D1} for the site:

$S_{DS} = 1.0 \times S_{MS} = 1.0 \times F_a \times S_{S\text{-}10\%} = 1.0 \times 1.0 \times 1.22g = \mathbf{1.22g}$

$S_{D1} = 1.0 \times S_{M1} = 1.0 \times F_v \times S_{1\text{-}10\%} = 1.0 \times 1.35 \times 0.45g = \mathbf{0.61g}$

Use the 1997 NEHRP-LSP to calculate $\hat{D}$:

For a SMF 10/50 hazard, $R = 8$, $C_d = 5.5$

Base shear of 290 kips will give elastic drift of

$$\delta_{xe} = 0.0044 \times \frac{290}{478} = 0.0027$$

$$\Rightarrow \quad \Delta = \delta_{xe} \times 5.5 = 0.015$$

Since values of γ, γ_a, and C_B are defined for 10/50 hazard level those larger of 2/50 and 50/50 values were used for this example calculations.

$C_B = 1.15$ is used. Therefore, $\hat{D} = C_B \theta_m = 1.15 \times 0.015 = 0.017$

$\gamma = 1.35$, $\gamma_a = 1.07$, $\beta_{UT} = 0.40$ for CP global, $\beta_{UT} = 0.32$ for CP local

Global collapse:

$$\lambda_{con} = \frac{0.85 \times 0.07}{1.35 \times 1.07 \times 0.017} = 2.42$$

$\beta_{UT} = 0.40$: confidence level = 99 %

Local collapse:

$$\lambda_{con} = \frac{0.80 \times 0.054}{1.35 \times 1.07 \times 0.017} = 1.76$$

$\beta_{UT} = 0.32$: confidence level = 97 %

Collapse against 50/50 hazard

Determine S_{DS} and S_{D1} for the site:

From the example in Section 5.7.3,

$S_{1\text{-}50\%}$ = 0.26g

Similarly using Equation 5-16,

$$S_{S-50\%} = 1.22\left(\frac{72}{474}\right)^{0.29} = 0.71g$$

***S_{DS}** = 1.0 x S_{MS} = 1.0 x F_a x $S_{S\text{-}50\%}$ = 1.0 x 1.12 x 0.71g = 0.79g*

***S_{D1}** = 1.0 x S_{M1} = 1.0 x F_v x $S_{1\text{-}50\%}$ = 1.0 x 1.54 x 0.26g = 0.40g*

Use the 1997 NEHRP-LSP to calculate $\hat{D}$:

For a SMF 50/50 hazard: R = 1, C_d = 1.0

Base shear of 1,539 kips will give elastic drift of

$$\delta_{xe} = 0.0044 \times \frac{1{,}539}{478} = 0.014 \Rightarrow \Delta = 0.018 \text{ x } 1.0 = 0.014$$

Get C_B value for 9-story NEHRP LSP procedure : C_B = 1.10

Therefore, $\hat{D} = C_B \theta_m$ = 1.10 x 0.014 = 0.015

***For 1997 NEHRP in Table 5-4:** γ = 1.43, γ_a = 1.07*

Global collapse:

$$\lambda_{con} = \frac{0.86 \times 0.07}{1.43 \times 1.07 \times 0.015} = 2.62$$

Get β_{UT} from Table 5-5: β_{UT} = 0.40

From Table 5-6: confidence level = 99 %

Local collapse:

$$\lambda_{con} = \frac{0.80 \times 0.054}{1.43 \times 1.07 \times 0.015} = 1.83$$

Get β_{UT} from Table 5-5: β_{UT} = 0.32

confidence level = 99 %

9. PERFORMANCE EVALUATION OF DAMAGED BUILDINGS

9.1 Introduction

After the discovery of fractured connections in steel moment frame buildings after the Northridge Earthquake, there was a genuine concern about the level of safety of badly damaged buildings. One of the most important considerations was whether or not to allow occupancy of the damaged buildings during the inspection and repair process. There are major sociological issues related to the balance of safety vs. the cost of not allowing occupancy. The issue of when and where to inspect for damage is also addressed in other SAC Guidelines.

The issues addressed here are directed at using structural analysis to evaluate the current condition of a damaged building and to estimate how the damaged structure might perform under future events that might occur before damage is repaired. Unfortunately, there are no magic equations whereby the design professional can plug in a number of pieces of information, press "enter," and wait for the red, yellow, or green light to appear. There are, however, a number of things that can be done that will help in making the difficult decisions. One fact that makes the decision harder is that each building and site are unique since the building configuration and age, occupancy, site, hazard level, and many more factors are involved. Having said all of this, the most important goal should be to protect human life.

The same tools discussed in the previous chapter regarding approaches to evaluate existing buildings may be used to predict performance of damaged buildings. These are the year of construction, the evaluation of the stiffness of the building before and after the earthquake, and the safety of the building before and after the earthquake damage was sustained. In each case, the expected level of performance before and after the damage is an important consideration.

This section is meant to address not just the pre-Northridge era of buildings, but also buildings constructed after that event using the better connection schemes. For the RBS and other improved systems, far fewer fractures should be expected than for the pre-Northridge buildings. However, there will always be situations where undiscovered problems occurred during construction, or a very large earthquake occurs that generates ground motions comparable to those expected for the 2/50 event.

In Chapter 8 of this report, the evolution of the seismic and steel codes is discussed. Important milestones are identified in Table 8-2. This is an important tool along with the other data discussed for determining the expected fragility of the building. The information provided in Chapter 8 suggests some interesting trends for pre-Northridge buildings. The older the building is, the more flexible it will probably be. The more flexible the building is, the more vulnerable it will be to local or global collapse. The confidence that we have that a pre-Northridge building will satisfy the CP performance objective is quite low even for an undamaged building. The result of this last observation is that the design professional may not be able to make a decision on the fate of the building in absolute terms but will have to compare relative (before and after) degrees of safety. The one good observation from the previous section is that buildings designed using the 1997 NEHRP *Provisions* and constructed using a SAC pre-

qualified connection system are expected to perform exceptionally well, even if subjected to ground motions comparable to those expected from the 2/50 event.

9.2 Performance Levels and Objectives

Two performance levels are recognized in this document: Collapse Prevention (CP) and Immediate Occupancy (IO). These are defined and described in Chapter 2. For design of new buildings, the stated performance object is 95% confidence in achieving Collapse Prevention for the 2/50 hazard. Although this is an excellent goal for evaluation and rehabilitation, it may never be attainable due to the cost and other factors. To satisfy this performance objective for new buildings, it only requires using a better connection that results in only a small increment in cost. To take this approach for an existing building might require rehabilitating every moment connection in the building. This would be very costly.

This chapter presents a performance based procedure for evaluating the confidence in satisfying a given performance level for a steel moment frame building for a given hazard level. The procedure is based on the groundwork presented in Chapter 5 and follows closely the developments for performance evaluation of new buildings given in Chapter 6 and existing buildings in Chapter 8.

The two broad issues that face the design professional and building owner are these: (1) What is the minimum acceptable level of protection against collapse and loss of life for a given hazard level? (2) What level of damage is acceptable for a given hazard level? This document will not attempt to answer these questions in general terms because every building, occupancy, and situation is different. The objective of this report is to provide tools that will allow the design professional to evaluate the risk.

9.3 Seismic Hazard and Design Spectrum

The seismic hazard and design acceleration response spectrum are the ones given in the 1997 NEHRP *Provisions*, but modified as discussed in Chapter 3 of this report.

9.4 Material Properties and Condition Assessment

In order to perform an evaluation of a damaged building, it is necessary to have a good understanding of the nature and condition of the building. The configuration of the building must be known. The features of the lateral load resisting systems must be identified, along with the existence and condition of the load paths. The expected material properties must be determined or assumed. These and other important aspects of condition assessment are given in Chapter 8 on evaluation of existing buildings. The 273/274 (FEMA 1997c, d) reports cover many important steps that should be undertaken for evaluation and/or rehabilitation.

9.5 Modeling and Analysis of Damaged Buildings

9.5.1 General

Moment-resisting connections with calculable resistance are required between the members in steel moment frames. The frames are categorized by the types of connections used and by the local and global stability of the members. Moment frames may act alone to resist seismic loads, or they may act in conjunction with concrete or masonry shear walls or braced steel frames to form a dual system. Special rules for design of new dual systems are included in AISC (1997) and FEMA (1997a).

Connections between the members may be fully restrained (FR), partially restrained (PR), or nominally unrestrained (simple shear or pinned). The components may be bare steel, steel with a nonstructural coating for fire protection, or steel with either a concrete or masonry encasement for fire protection.

Two types of frames are categorized in this document. Fully restrained (FR) moment frames are those frames for which no more than 10% of the lateral deflections arise from connection deformation. Partially restrained (PR) moment frames are those frames for which more than 10% of the lateral deflections result from connection deformation. In each case, the 10% value refers only to deflection due to beam-column deformation and not to frame deflections that result from column panel zone deformation. Partially restrained connections are covered in Chapter 7.

9.5.2 Modeling and Analysis of FR and PR Steel Moment Frames

In Chapters 5 and 8, the modeling and analysis of new and existing steel moment frames with FR connections are discussed. Chapter 7 discusses modeling and analysis of buildings with PR connections.

9.6 Analytical Methods for Performance Prediction and Evaluation of Damaged Buildings

9.6.1 Background

The first step in evaluating a damaged building is to gather as much information as possible about the building. This issue was discussed in Section 8.5. The information given in Section 8.6.3 on using stiffness to predict performance is also valuable for evaluating damaged buildings and should be read before proceeding. One of the first things that should be done in evaluating a damaged building is to develop a computer model of the undamaged building. The periods of vibration of the building in each direction should be calculated. It is not recommended that the empirical equation based solely on the height and type of building be used. The studies undertaken for the SAC project indicated that a high level of uncertainty is introduced by this (Yun and Foutch, 1999). The equation that has appeared in previous codes based on the improved Rayleigh's Quotient gives excellent estimates of the fundamental periods of vibration that are usually within a percent or two of the values produced using finite element programs.

This equation is

$$T = 2\pi\sqrt{\frac{\sum w_i \delta_i^2}{g\sum f_i \delta_i}} \tag{8-1}$$

where:

w_i = weight at each floor
g = gravity acceleration
f_i = applied force at floor level i
δ_i = displacement at floor level i

The next step is to apply the 1997 NEHRP (or later) design forces to the analytical model and calculate the elastic story displacements and drifts. These will be used for comparison with those attained by analyzing a model of the damaged building. The resulting displacements and drifts can be compared to the requirements for design of new buildings and to the results given in Section 8.6.2 for the case study buildings to develop a preliminary and rough idea of the expected performance of the undamaged building. If estimates of the strength of shaking at or near the building are available, the undamaged building should be analyzed for these motions or forces to give some insight into the level of damage that should have been expected. Because of the fact that so many variables influence the actual response of a building and the deformation level that will cause joint fracture, it should not be expected that the analysis will be able to identify exactly which connections actually fractured (Lee and Foutch, 1999). However, a reasonably good estimate of the overall deformations experienced by the building will be found. The results of these exercises when compared to the results given in Section 8.6.2 can also be used to determine if the building is more or less comparable to one designed to the minimum standards of the code that was in effect at the time of construction. Before discussing the next step in the evaluation of the damaged building, the results of a series of studies will be given.

The three, nine, and twenty-story buildings designed using the UBC in effect in 1973, 1985, and 1994 were studied in undamaged and damaged states in order to understand better the performance expected from damaged buildings. The first step in the process for each building was to calculate its fundamental period of vibration. Next, the design forces using the criteria given in Chapter 4 were determined, and a static analysis of the building was completed. Next, the building model was subjected to one of the LA 50/50 accelerograms (LA41, peak acceleration = 0.42g) using a nonlinear time history analysis with the pre-Northridge connection model. After this analysis, the output was checked to see which flanges of which connections had been fractured. The connection model described above was used where the bottom flange fractured at about the plastic moment capacity of the beam and the top flange was assumed to have fractured at a plastic rotation of 0.03. Two additional steps were taken after this. The damaged building was subjected to the same earthquake ground motion, and the state of the building after two back-to-back earthquakes was observed. The other step taken after the first earthquake was to change the elastic model of the building to represent the building in the

damaged state. The period of the building was recalculated, and new static forces were calculated and applied to the damaged building. This last step was repeated for the building after the second earthquake. This sequence of analyses was done for all of the building models described above. As mentioned above, these analyses were completed for all of the pre-1997 building models. Because of the large volume of results that were generated, only representative results will be shown in detail.

Figure 9-1 shows the damage that was suffered by the 1994 3-story building for the different earthquakes. The figure at the top left shows the damage after the first application of the 50/50 motion and the one at the top right shows the damage pattern after the second application of the same motion. This same information is shown in the middle two figures for the 10/50 motions (LA14, peak acceleration = 0.59g) and the bottom ones for the 2/50 motions (LA28, peak acceleration = 1.1g). At each joint there is a circle that, with the beams and columns framing into the joint, forms four sections. A darkened segment indicates fracture of a top or bottom flange

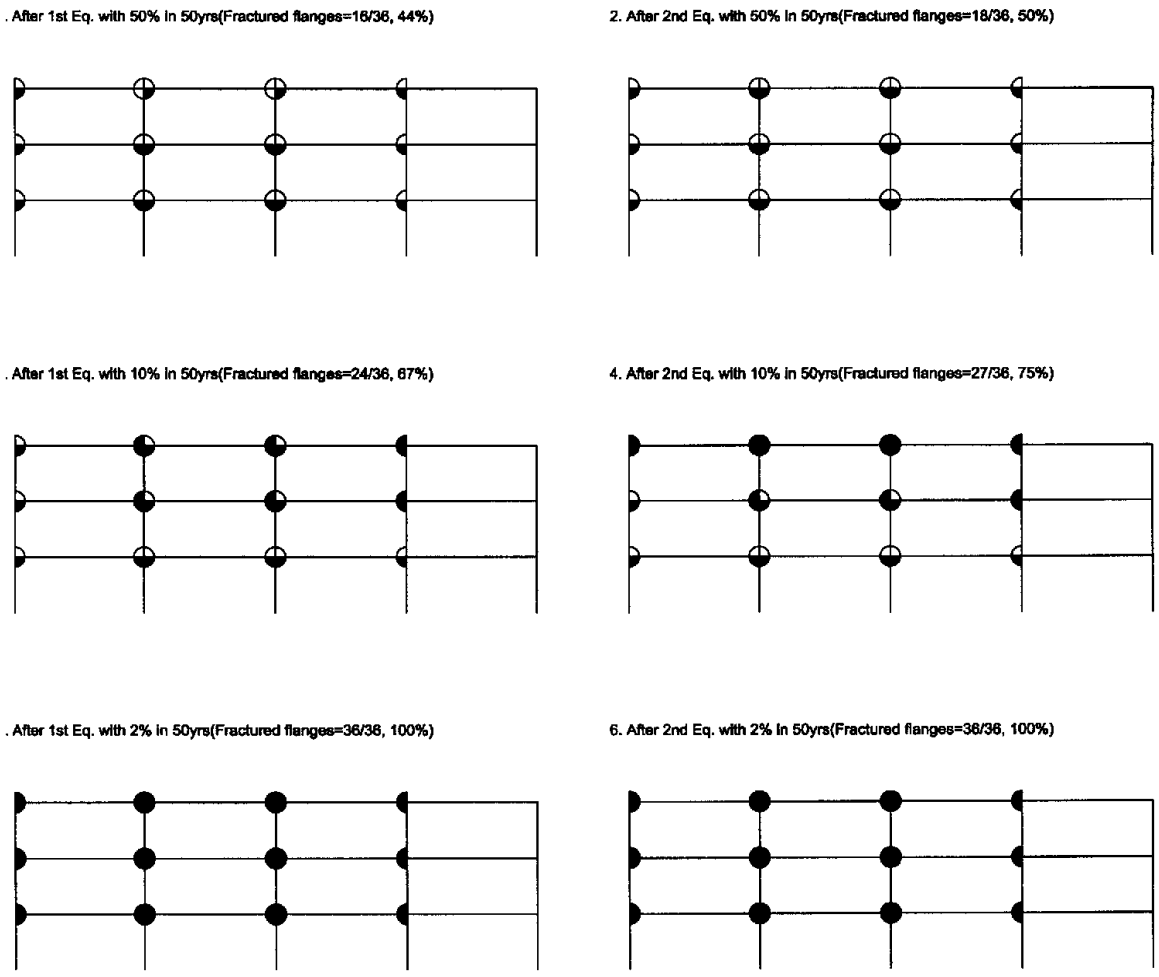

Figure 9-1 Observed Damage from First and Second Ground Motion Excitation for 1994 UBC 3-Story Building

on the left or right of the joint. The results indicate that all of the bottom flanges were fractured during this 50/50 event. (Note: The right-most beam at each floor level is actually pinned at each end. There were only three bays of moment frame provided.) This is an unfortunate, but not unanticipated, result. The small note above each figure gives the total number and percentage of flanges that fractured. A total of 16/36 (44%) flanges fractured during the first application of the 50/50 motion, and a total of 18/36 (50%) were fractured after the second earthquake. It should be noted that no global or local collapse is indicated. For this discussion, a local collapse will be assumed to have occurred if top and bottom flanges have fractured at each end of a beam.

The results for the 10/50 accelerograms are shown in the middle two figures. No global or local collapse occurred during the first earthquake, but all of the beams at the top story suffered local collapse during the second earthquake. Although the program solution for the 2/50 accelerogram ran to completion (no instability detected) the damage pattern indicates that all top and bottom flanges have fractured during the first earthquake, which creates a seemingly unstable building. The thing that kept it from "falling down" was the resistance of the columns and gravity frames. For practical purposes, this should be considered to be a global collapse.

The results for the 1994 9-story building are given in Figure 9-2. The two applications of the 50/50 record produced only a small number of flange fractures (23/180 or 13% after both earthquakes). The 10/50 records produced 73/180 (41%) fractures but no local collapse. The first application of the 2/50 accelerogram fractured all of the bottom flanges of the beams except for the first floor, but no top flanges. The second application fractured all of the top flanges in the top four floors, creating 16 local collapses and four virtual story mechanisms. A reasonable call for this building would be to not allow occupancy after the first 2/50 earthquake. However, this represents acceptable behavior since it survived the 2/50 motion and it really shouldn't be expected to be useable after the design event.

It is also highly unlikely that back to back earthquakes of this magnitude will occur within a short period of time. A more realistic test would be to subject the damaged building to a 50/50 or 50/30 accelerogram. Figure 9-3 shows the damage caused by a less severe accelerogram for the second application. Top left and right figures illustrate the damage after back-to-back earthquakes representing the 2/50 hazard level. The middle two figures show the damage from the first application of the 2/50 accelerogram followed by the second application of the 10/50 accelerogram. The first 2/50 accelerogram produced 81/180 (45%) bottom flange fractures, and the second 10/50 accelerogram caused five top flange fractures in the upper stories. The bottom two figures showed the damage from the first 2/50 and the second 50/50 or 50/30 accelerogram, which is the less severe but more likely event. The application of the second 50/50 or 50/30 ground motion fractured three more bottom flanges. The ratio of the fractured flanges is 35% and 37% for the first and second applications, respectively. Figure 9-4 shows the damage from the first 10/50 accelerogram and the second 50/50 and 50/30 earthquakes. Unlike the results obtained from the back to back earthquakes with the same magnitude, no additional damage was observed during the second 50/50 or 50/30 event.

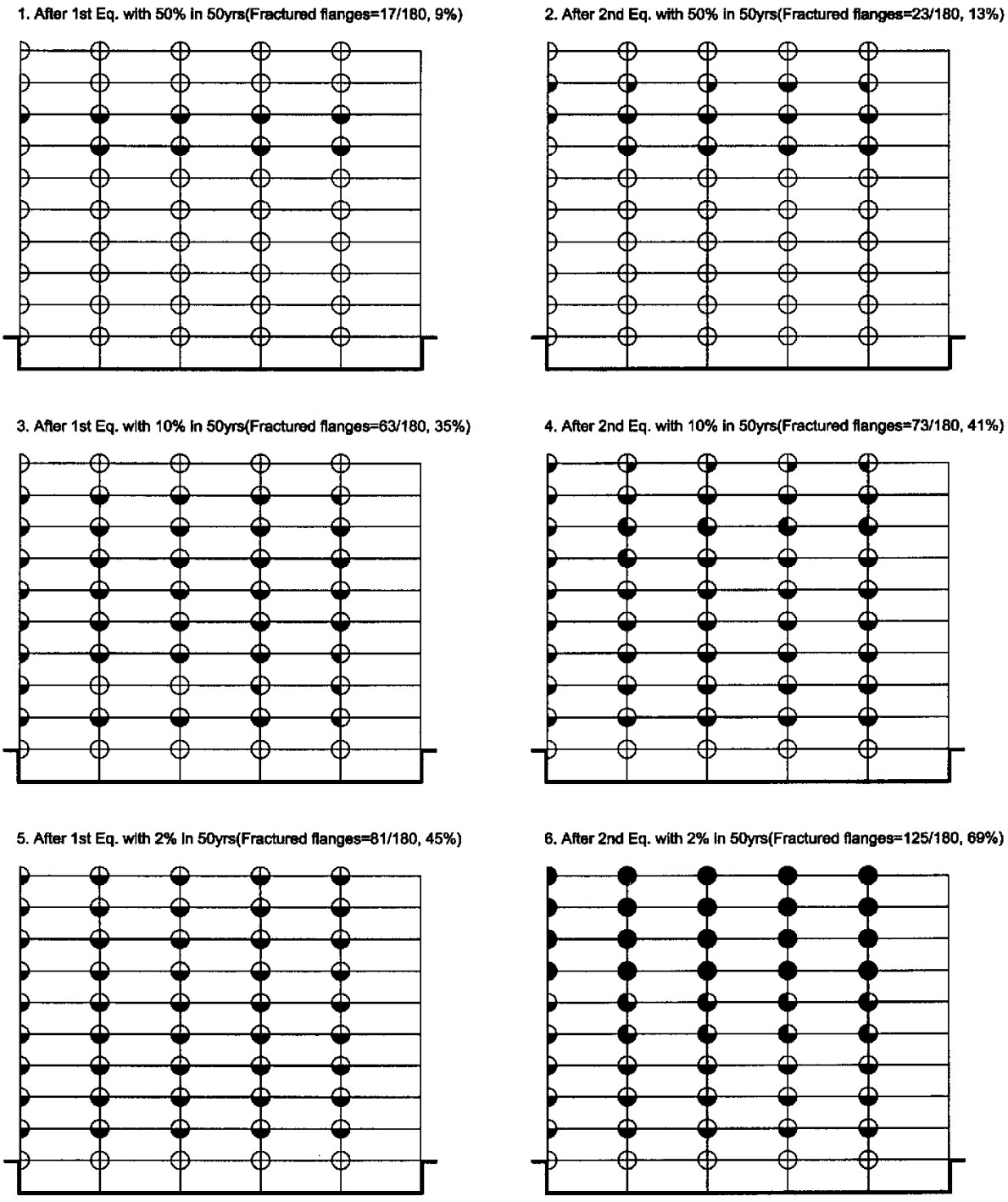

Figure 9-2 Observed Damage from First and Second Ground Motion Excitation for 1994 UBC 9-Story Building (Back-to-Back Ground Motions with Same Magnitude)

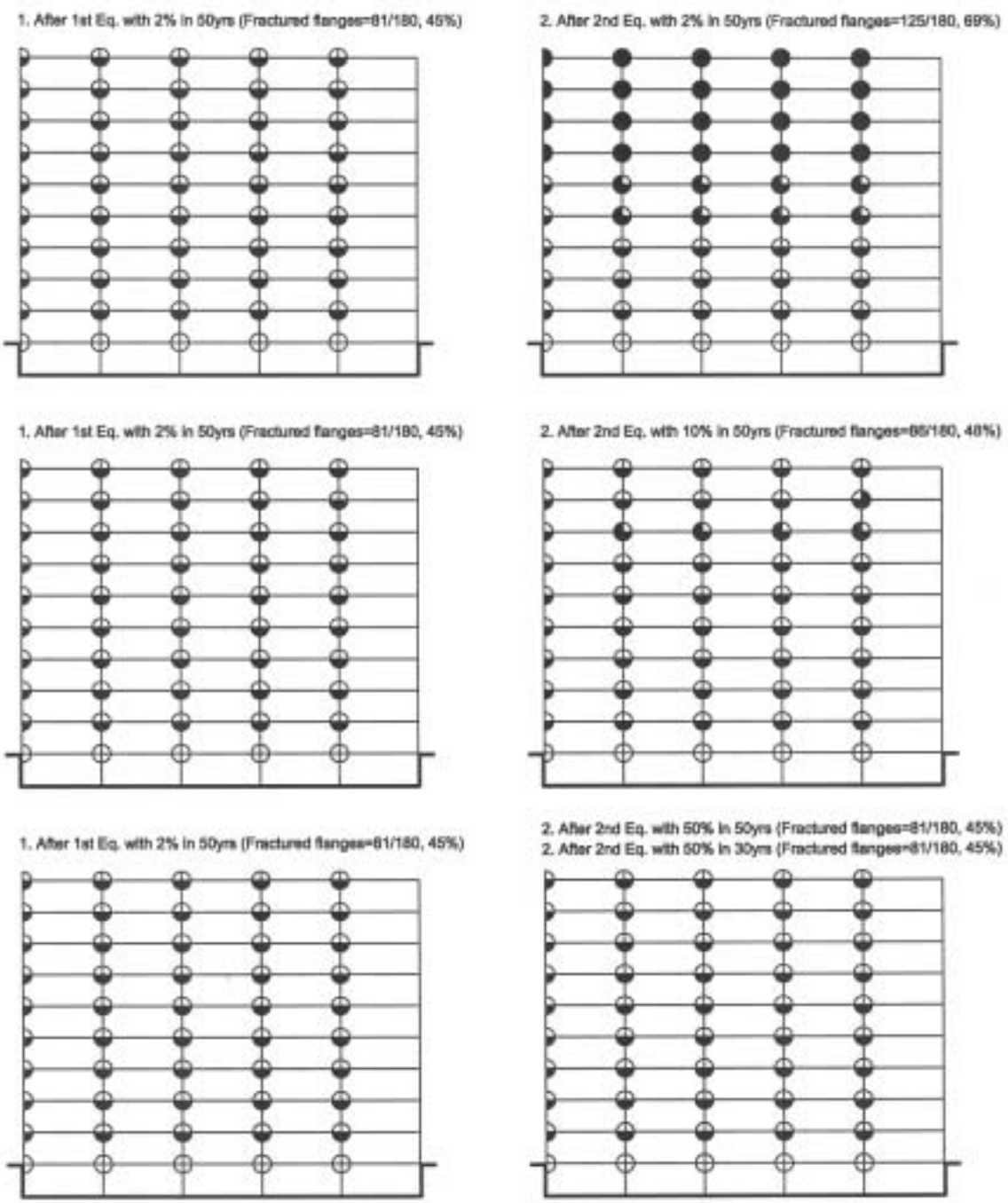

Figure 9-3 Observed Damage from First and Second Ground Motion Excitation for 1994 UBC 9-Story Building (with Less Magnitude for the Second Application)

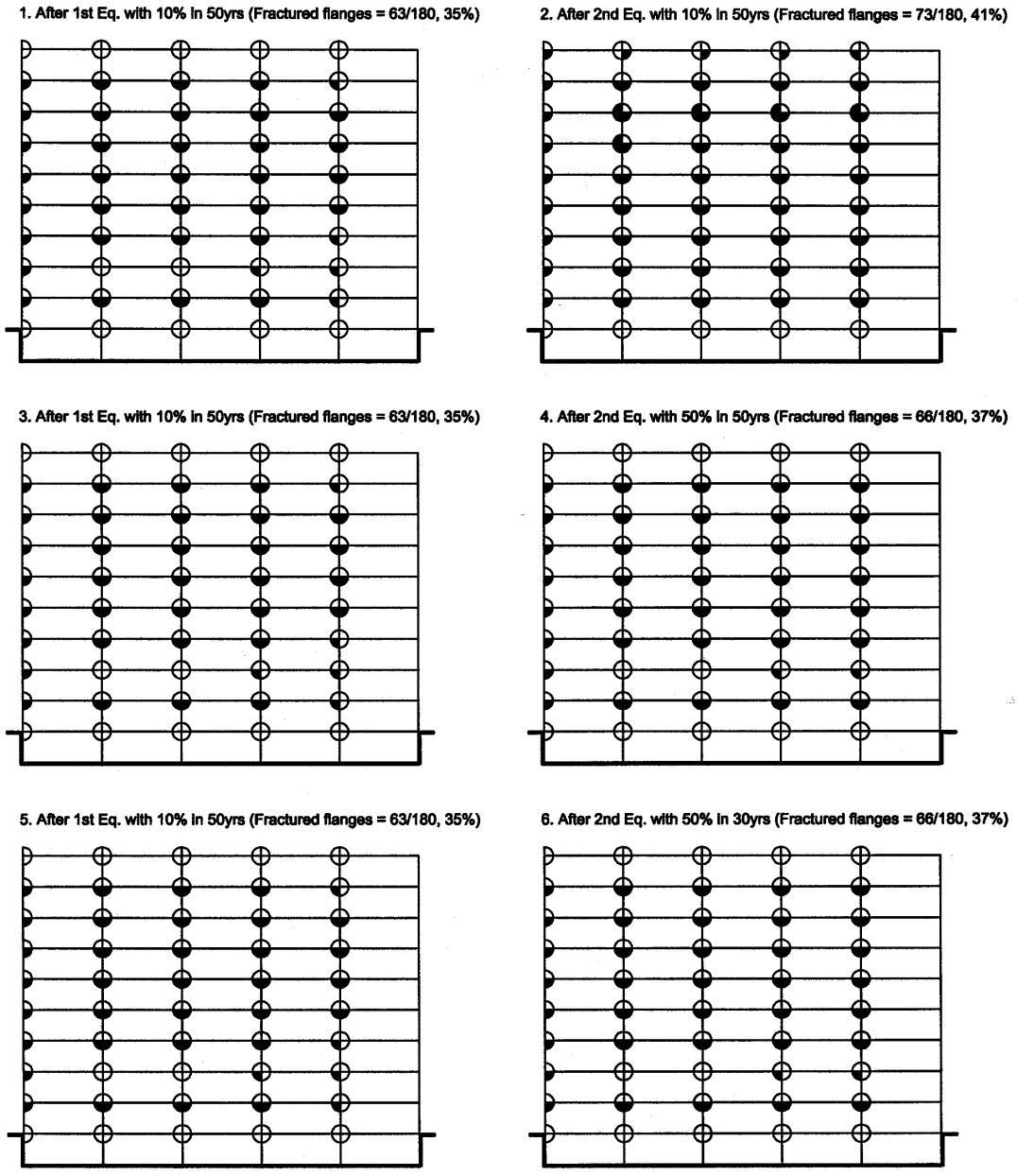

Figure 9-4 Observed Damage from First and Second Ground Motion Excitation for 1994 UBC 9-Story Building (with Less Magnitude for the Second Application)

The results for the 1994 20-story building are shown in Figure 9-5. The format of the figure is different from the previous ones. The results for each hazard level are shown one above the other. Essentially no damage occurred for either application of the 50/50 accelerogram. The first application of the 10/50 accelerogram produced 99/440 (23%) bottom flange fractures with no local collapses and the second application fractured only nine more bottom flanges. The two applications of the 2/50 earthquake fractured 152/440 (35%) bottom flanges but no top flanges. This is very good performance. A summary of all of the analytical results is given in Table 9-1.

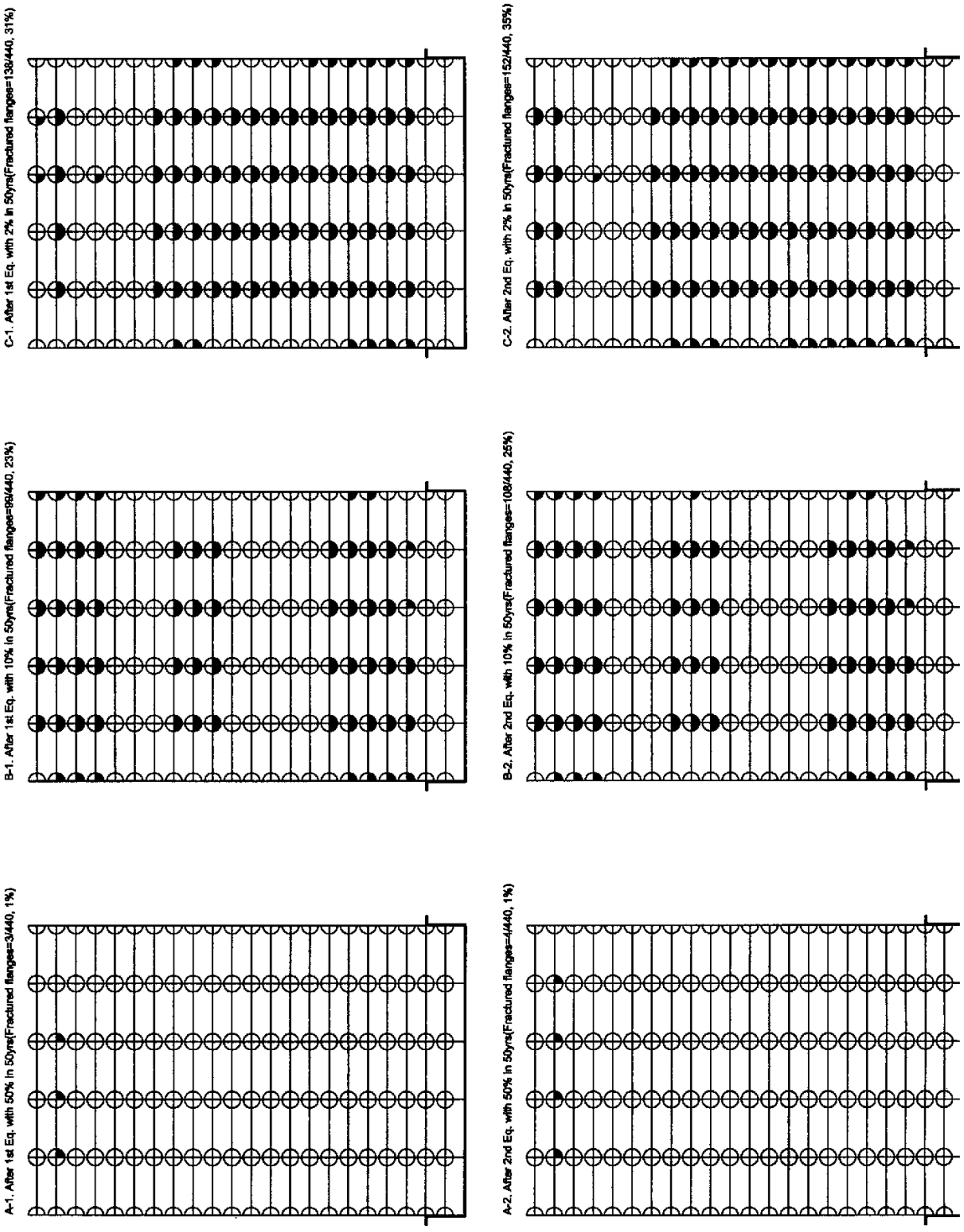

Figure 9-5 Observed Damage from First and Second Ground Motion Excitation for 1994 UBC 20-Story Building

One of the reasons for undertaking this exercise was to determine the stiffness of the building before and after each application of the ground motion to see what can be learned. Results for the 1994 3-story building are shown in Figure 9-6. The figure in the upper left portion shows the maximum story drifts calculated for the first and second applications of the 50/50 accelerogram. The figure in the upper right portion shows the results of using the 1997 NEHRP *Provisions* to determine lateral design forces for the 50/50 spectrum for the building in each damage state (including the original undamaged state). Results for the 10/50 accelerograms are shown in the middle two figures, and for the 2/50 year ones in the bottom two figures. Modeling of the building in each damage state will be discussed below.

Observing the building after the 50/50 earthquake has occurred sets the stage. Inspection of the building reveals the damage pattern shown in Figure 9-1. After an elastic analysis of the building in the undamaged state has been done, the model is changed to represent the building in its damaged state. New design forces are then calculated because the period has changed and the damaged building model is analyzed. The results indicate that the building has lost about half of its stiffness. Even if we don't know exactly what the input motion was to begin with, we know that the response exceeded about 1% drift at each story because all of the bottom flanges have been fractured. We also know that the response at all stories was less than about 4%, since no top flanges fractured. If the evaluation has progressed to this stage, then credible estimates of the ground motion are probably available. The application of the code design base shear to the damaged building model before and after the earthquake will reveal that the building has lost half of its stiffness during the earthquake. This in itself is valuable information. If no estimates of ground motion are available, then the damage pattern as discussed in this paragraph will give the engineer a rough scaling of the first earthquake. Different future seismic events can be postulated and evaluated for their potential to cause local or global collapse.

The observed damage after the 10/50 earthquake reveals a much more serious event. The fact that top flange fractures have occurred reveals that story drifts might have exceeded 4% at those levels. Also, the fact that every bottom flange has fractured along with most of the top flanges for the top two stories should be enough to not allow occupancy until repairs are made. This is the level of damage that would be expected of a new building if subjected to the 2/50 accelerogram, so it should not be surprising if the building is demolished. The results of the static analyses shown in Figure 9-6 support these conclusions.

The results for the 1994 9-story building are shown in Figure 9-7. In this case, almost no damage has occurred for the 50/50 event. Only 9% of the connections have experienced bottom flange fracture. The damage may not even be found, which is acceptable in this case. The application of the second 50/50 accelerogram results in only a small amount of additional damage.

The first application of the 10/50 accelerogram results in bottom flange fractures in about two thirds of all of the beams, but no top flange fractures. As in the previous case for the 3-story building, this indicates that the story drifts exceeded 1% in almost all of the stories, but not 4%. As a result, one might expect that the maximum story drift was substantially larger than 1%. The static analysis of the undamaged frame resulted in about 2% drift over the entire height of the

building. This is consistent with the time history results. The results of the second analysis reveals that if the earthquake occurs again, drifts of two or three stories may exceed 4% by a small amount. This indicates that local collapses may occur in a few beams. One should not expect that the analysis is able to identify exactly which floors might experience this local collapse, which could be used, for instance, to deny occupancy on a selected number of floors. The reason for this also relates to the fact that damage occurred over most of the height of the structure during the first event.

With the application of the 2/50 accelerogram 90% of the bottom flanges fractured as opposed to about 70% for the 10/50 earthquake. The more bottom flange fractures that occur during an earthquake, the greater is the likelihood that several stories will approach 4% drift. Again, this provides a basis for estimating the actual magnitude of the seismic forces in the first event. Applying these forces to the damaged building results in story drifts of 7%, indicating that global collapse is likely to occur. This is born out by the results of the second time history analysis, which resulted in story mechanisms in the top four stories.

Results for the 1994 20-story building are shown in Figure 9-8. Similar observations could be made for this case. At all levels of earthquake, no local or global collapses occurred, and none would have been predicted by the static analyses. A summary of all of the analyses is given in Table 9-1. The fundamental period of vibration of each building before and after each application of the earthquakes is given in Table 9-2. This change in period also reflects the loss of stiffness of each building after each event.

In the actual, real-life earthquake scenario, the situations will not be as nicely laid out as the ones described here. One complicating feature will be that some top flange fractures will occur at story drifts of less than 4%. Even for tests of laboratory specimens of pre-Northridge connections, there was scatter in the results. This will make estimation of the actual drift levels that the building experienced and scaling of the static forces more difficult. As a result, a range of different scenarios should be investigated. In real life, it is very unlikely that two earthquakes of the same magnitude will occur over the amount of time required to repair damaged buildings. As a result, it might be prudent to examine a number of possible occurrences of aftershocks of smaller magnitude. Of course, the possibility exists that the first occurrence is a pre-shock of a larger event to come.

Very few design offices have access to a program that has sophisticated connection elements that can model the hysteretic behavior of the pre-Northridge connection. However, meaningful analyses can still be undertaken using a linear static model. If the bottom flanges at each end of a beam have fractured, then positive moment will open the crack resulting in essentially no stiffness, or pin-like behavior. Negative moment will cause the crack to close, resulting in no loss of flexural stiffness. Since sway deformations in a building result in one end of a beam being in positive moment and the other end in negative moment, then one end will always be in negative moment and the other in positive moment. The effect of this on the elastic drift response can be modeled by putting a hinge at one end of the beam and a moment connection at the other end of the beam in the elastic model. The moments calculated in the beams will not be

correct, but the story drifts will be calculated accurately, and all of the SAC recommendations are keyed to story drift. This is demonstrated in an example in Appendix A.

9.7 Performance Prediction using Confidence Level Calculations

In Section 8.6.5, confidence level calculations were used to predict performance of undamaged pre-Northridge buildings. This might also be an effective tool for evaluating damaged buildings. The procedure would begin in exactly the same way that was described in the previous section on stiffness. The first step would be to examine the building for damage and determine the sizes of members and material properties from design documents or inspection and material tests. A computer model of the building would then be developed for the undamaged building. The confidence that the building could satisfy the CP performance level for different magnitudes of ground motion could then be evaluated. A model of the building in the damaged state could then be developed. The confidence level that the damaged building could satisfy the CP performance level for future events of similar magnitude could then be evaluated. The demands would be estimated using the static elastic analysis. All of the other information required is given in Section A.7.4. The observed damage to the building, along with the static analysis results, could provide estimates of the magnitude of the first earthquake in the same fashion as described above. Estimates of the magnitude of shaking at the building site might also be available for this purpose. This estimate of confidence could then be used along with other data to decide the fate of the building.

Example: 1985 UBC, 9-story, near City Hall in LA

A 9-story building located near City Hall in LA was considered to calculate the confidence level before and after the damage. The floor plan and elevation view are given in Figure 8-4. The building was designed based on the 1985 UBC provisions. As described in Section 8.6, one ground motion for each hazard level was selected. The damage pattern that building experienced with different hazard levels is shown in Figure 9-9. Then elastic models of damaged buildings were developed and corresponding periods were determined. The results of the elastic static analyses are shown in Figure 9-10. The summary of the confidence level calculations for global and local collapses are shown in Table 9-3 and Table 9-4, respectively.

50/50 hazard level

With the first application of the 50/50 accelerogram, the damage pattern was investigated and is shown in Figure 9-9. The bottom flanges in four of the upper stories experienced fractures resulting in 19% of total flanges being fractured. The second application of the 50/50 accelerogram produced a small amount of additional damage. The relatively small amount of damage indicates that only a few upper stories exceeded 1% drift. But it is unlikely that any of these approached 4% drift. This is supported by the nonlinear time history results shown in the upper left portion in Figure 9-10. Next, confidence levels are calculated.

Table 9-1 Results of Sequential Applications of Ground Motions to Pre-Northridge Buildings

Year/bldg.	50/50 acceleration		10/50 acceleration		2/50 acceleration	
	First Earthquake	Second Earthquake	First Earthquake	Second Earthquake	First Earthquake	Second Earthquake
1973/ 3-story, w/o drift limit	18 – 50%	18 – 50%	25 – 69% local collapse	32 – 89% story mechanism	36 – 100% story mechanism	36 – 100% story mechanism
1973/ 9-story, w/o drift limit	34 – 19%	36 – 20%	76 – 42%	91 – 51% local collapse	108 – 60% local collapse	Global collapse
1973/ 3-story, with drift limit	18 – 50%	20 – 56%	27 – 75% local collapse	32 – 89% story mechanism	36 – 100% story mechanism	36 – 100% story mechanism
1973/ 9-story, with drift limit	15 - 8%	27 – 15%	60 – 33%	78 – 43%	82 – 46%	122 – 68% story mechanism
1973/ 20-story	50 – 11%	55 – 13%	121 – 28%	180 – 41% local collapse	204 – 46% local collapse	240 – 55% story mechanism
1985/ 3-story	18 – 50%	19 – 53%	21 – 58%	32 – 89% story mechanism	36 – 100% story mechanism	36 – 100% story mechanism
1985/ 9-story	26 – 14%	31 – 17%	76 – 42%	93 – 52%	96 – 53%	124 – 69% story mechanism
1985/ 20-story	43 – 10%	57 – 13%	156 – 36%	174 – 40%	190 – 43%	202 – 46%
1994/ 3-story	16 – 44%	18 – 50%	24 – 67%	27 – 75% local collapse	36 – 100% story mechanism	36 – 100% story mechanism
1994/ 9-story	17 – 9%	23 – 13%	63 – 35%	73 – 41%	81 – 45%	125 – 69% story mechanism
1994/ 20-story	3 – 1%	4 – 1%	99 – 23%	108 – 25%	138 – 41%	152 – 35%

- Evaluation of the damaged frame from SAC Eqs with 50% in 50 years

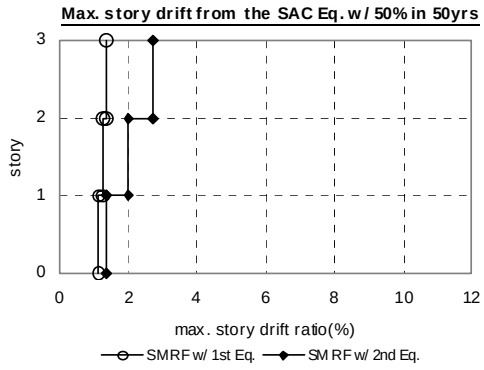

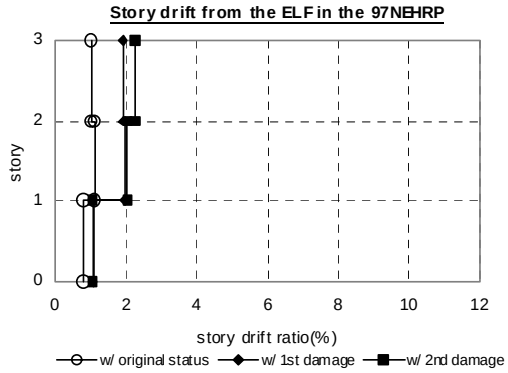

- Evaluation of the damaged frame from SAC Eqs with 10% in 50 years

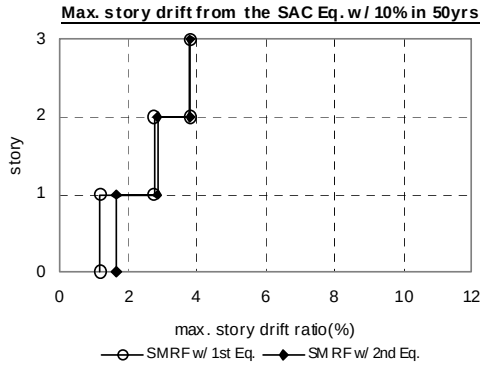

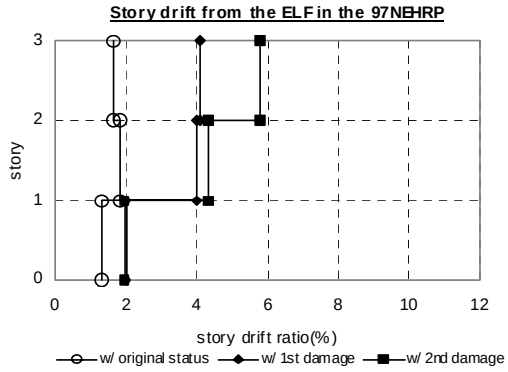

- Evaluation of the damaged frame from SAC Eqs with 2% in 50 years

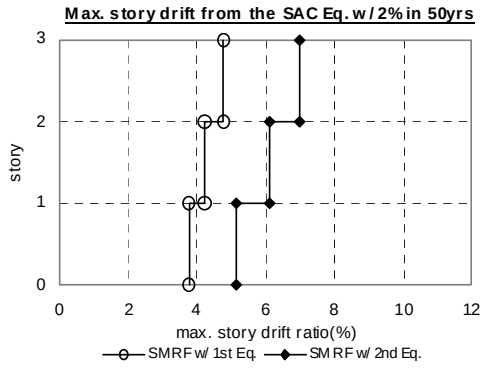

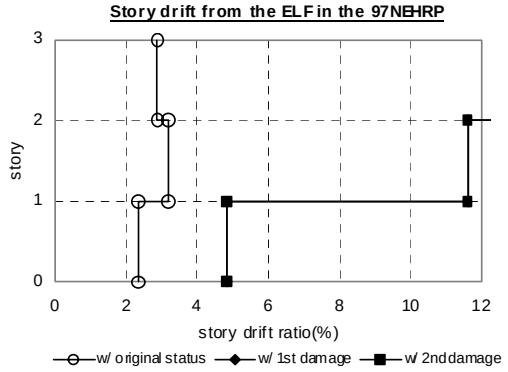

Figure 9-6 Drift Demands from Both Dynamic and Static Analysis of Damaged 1994 UBC 3-Story Building for 50/50, 10/50 and 2/50 Hazard

- Evaluation of the damaged frame from SAC Eqs with 50% in 50 years

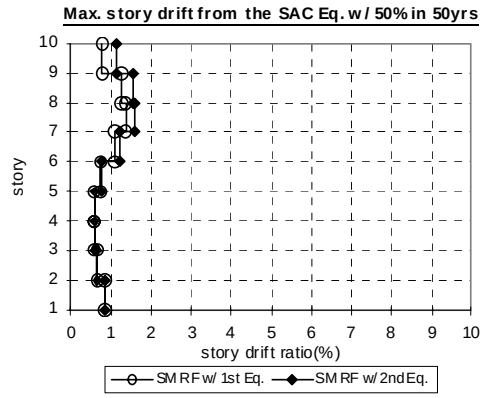

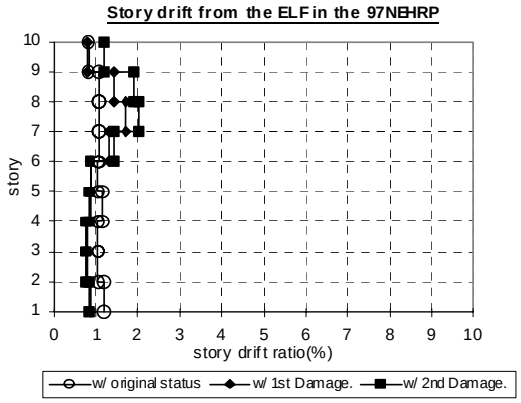

- Evaluation of the damaged frame from SAC Eqs with 10% in 50 years

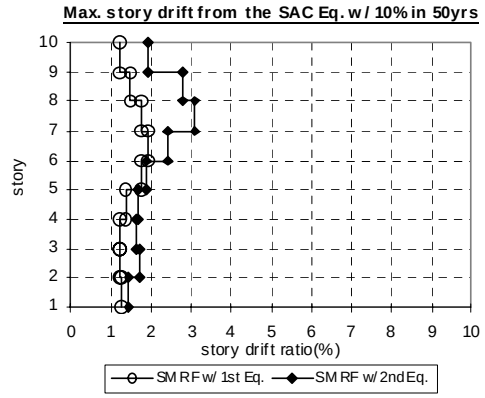

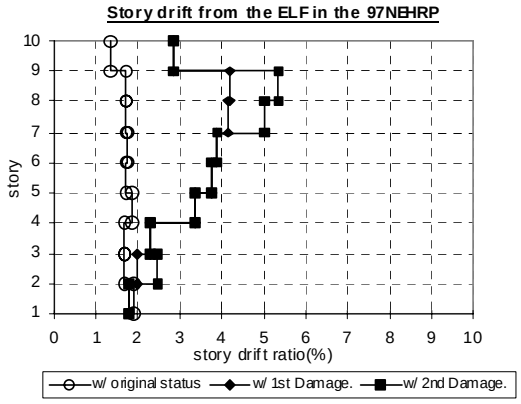

- Evaluation of the damaged frame from SAC Eqs with 2% in 50 years

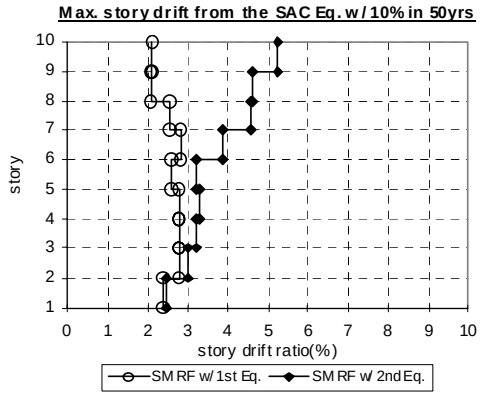

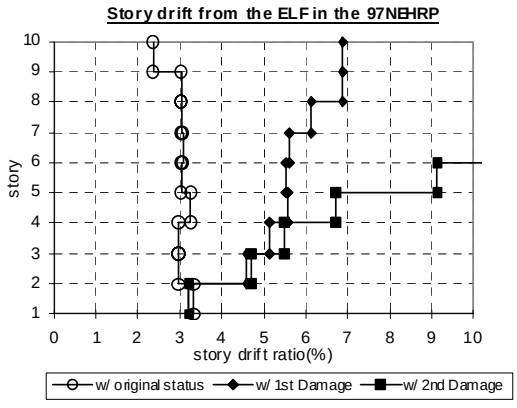

Figure 9-7 1994 UBC 9-Story Building for 50/50, 10/50 and 2/50 Hazard

- Evaluation of the damaged frame from SAC Eqs with 50% in 50 years

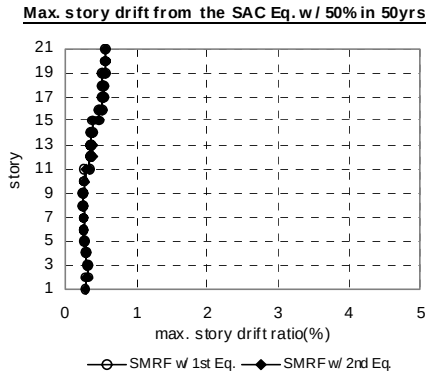

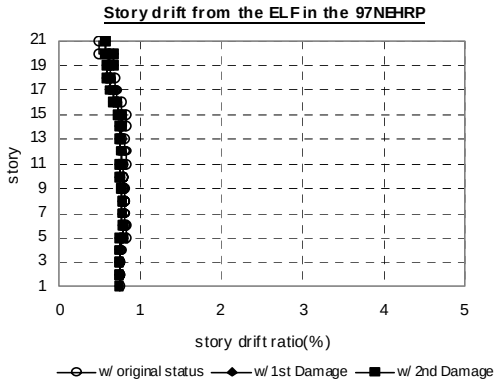

- Evaluation of the damaged frame from SAC Eqs with 10% in 50 years

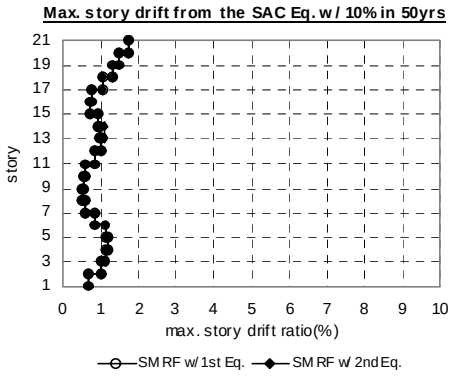

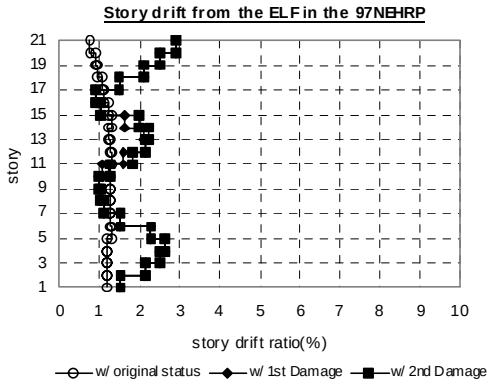

- Evaluation of the damaged frame from SAC Eqs with 2% in 50 years

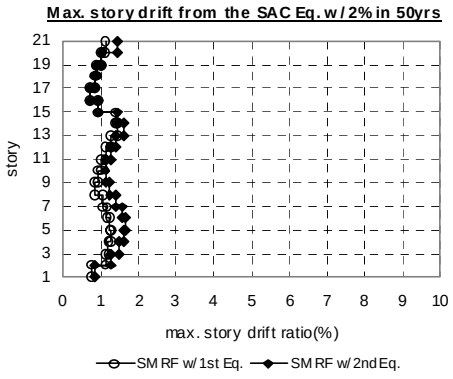

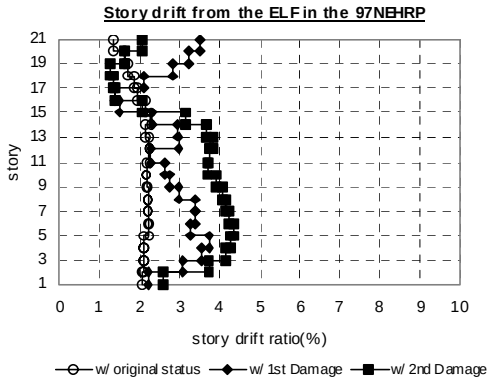

Figure 9-8 Drift Demands from Both Dynamic and Static Analysis of Damaged 1994 UBC 20-Story Building for 50/50, 10/50 and 2/50 Hazard Levels

Table 9-2 Fundamental Period of Vibration of Each Building Before and After Ground Excitation for 50/50, 10/50 and 2/50 Hazard Levels

Code Year		50/50	10/50	2/50
	$T_{undamaged}$	$T_{damaged}$	$T_{damaged}$	$T_{damaged}$
3-story				
94UBC Design	**1.09**	1.58	1.81	3.42
85UBC Design	**1.39**	2.12	2.24	4.33
73UBC Design with drift limit	**1.21**	1.84	2.18	3.75
73UBC Design without drift limit	**1.56**	2.37	2.72	4.86
9-story				
94UBC Design	**2.51**	2.68	3.58	4.01
85UBC Design	**2.94**	3.35	4.7	5.75
73UBC Design with drift limit	**2.45**	2.61	3.37	4.04
73UBC Design without drift limit	**3.65**	4.04	5.75	6.72
20-story				
94UBC Design	**4.24**	4.25	5.36	6.24
85UBC Design	**3.99**	4.24	5.5	6.28
73UBC Design (governed by wind)	**3.9**	4.28	5.54	6.31

- ***Example: Collapse Prevention for the 50/50 hazard level***
  - *Fundamental period of building (T) = 2.60 sec. (undamaged)*
  - *Seismic base shear (V) = 1539 kips*
  - *Maximum elastic drift angle (δ_{xe}) = 0.014*
  - *Maximum inelastic drift (θ_m) = δ_{xe} x C_d = 0.014 x 1.0 = 0.014*
  - *C_B = 0.81: 1997 NEHRP – LSP for pre-Northridge building: given in Table 4-9*
  - *Median drift demand ($\hat{D}$) = C_B x θ_m = 0.81 x 0.014 = 0.012*
  - *Fundamental period of building (T) = 3.07 sec. (damaged)*
  - *Seismic base shear (V) = 1303 kips*
  - *Maximum elastic drift angle (δ_{xe}) = 0.027*

- *Maximum inelastic drift (θ_m) = δ_{xe} x C_d = 0.027 x 1.0 = 0.027*
- *Median drift demand ($\hat{D}$) = C_B x θ_m = 0.81 x 0.027 = 0.022*

1. Global collapse

- *Median drift capacity ($\hat{C}$) = 0.070: given in Table 5-2 (brittle connection)*
- *Resistance factor (ϕ) = 0.85: given in Table 5-2 (brittle connection)*
- *Demand factor (γ) = 1.52: given in Table 5-4*
- *Analysis demand factor (γ_a) = 1.15: given in Table 5-4*
- ***Confidence factor,*** $\lambda_{con} = \dfrac{\phi \hat{C}}{\gamma \gamma_a \hat{D}}$ *: Equation 5-1*

$$\lambda_{con} = \frac{0.85 \times 0.070}{1.52 \times 1.15 \times 0.022} = 1.55$$

- ***Slope of hazard curve (k) = 3.0***
- ***Uncertainties (β_{UT}) = 0.46 ≅ 0.5: given in Table 5-5***
- ***Confidence level = 95%: determined using Table 5-6***

2. Local collapse

- *Median drift capacity ($\hat{C}$) = 0.037: given in Table 5-2 (brittle connection)*
- *Resistance factor (ϕ) = 0.80: given in Table 5-2 (brittle connection)*
- *Demand factor (γ) = 1.52: given in Table 5-4*
- *Analysis demand factor (γ_a) = 1.15: given in Table 5-4*
- ***Confidence factor,*** $\lambda_{con} = \dfrac{\phi \hat{C}}{\gamma \gamma_a \hat{D}}$ *: Equation 5-1*

$$\lambda_{con} = \frac{0.80 \times 0.037}{1.52 \times 1.15 \times 0.022} = 0.77$$

- ***Slope of hazard curve (k) = 3.0***
- ***Uncertainties (β_{UT}) = 0.39 ≅ 0.4: given in Table 5-5***
- ***Confidence level = 47%: determined using Table 5-6***

The confidence levels for the undamaged building were done in the previous section, and the results are given in Tables 9-3 and 9-4. The confidence levels for global collapse before and after the damage are 99% and 83%. For local collapse, they are 81% and 19%. The second occurrence of this earthquake resulted in maximum drifts of about 3% with no local collapses.

The first application of the 10/50 accelerogram resulted in almost every bottom flange being fractured. The second earthquake produced local collapse in the upper stories indicating that the maximum story drifts approached 4% drift. Elastic analyses for the building before and after the damage are shown in the middle portion in Figure 9-9. Next, the confidence levels are calculated.

- ***Example: Collapse Prevention for the 10/50 hazard level***
  - *Fundamental period of building (T) = 2.60 sec. (undamaged)*
  - *Seismic base shear (V) = 290 kips*
  - *Maximum elastic drift angle (δ_{xe}) = 0.0027*
  - *Maximum inelastic drift (θ_m) = δ_{xe} x C_d = 0.0027 x 5.5 = 0.015*
  - *C_B = 1.40: 1997 NEHRP – LSP for pre-Northridge building : given in Table 4-9*
  - *Median drift demand ($\hat{D}$) = C_B x θ_m = 1.40 x 0.015 = 0.021*
  - *Fundamental period of building (T) = 4.19 sec. (damaged)*
  - *Seismic base shear (V) = 180 kips*
  - *Maximum elastic drift angle (δ_{xe}) = 0.0047*
  - *Maximum inelastic drift (θ_m) = δ_{xe} x C_d = 0.0047 x 5.5 = 0.026*
  - *Median drift demand ($\hat{D}$) = C_B x θ_m = 1.4 x 0.026 = 0.036*

  1. Global collapse

  - *Median drift capacity ($\hat{C}$) = 0.070 : given in Table 5-2 (brittle connection)*
  - *Resistance factor (ϕ) = 0.85 : given in Table 5-2 (brittle connection)*
  - *Demand factor (γ) = 1.52 : given in Table 5-4*
  - *Analysis demand factor (γ_a) = 1.15 : given in Table 5-4*

- ***Confidence factor,*** $\lambda_{con} = \dfrac{\phi \hat{C}}{\gamma \gamma_a \hat{D}}$ *: Equation 5-1*

$$\lambda_{con} = \frac{0.85 \times 0.070}{1.52 \times 1.15 \times 0.036} = 0.95$$

- ***Slope of hazard curve (k) = 3.0***
- ***Uncertainties (β_{UT}) = 0.46 ≅ 0.5: given in Table 5-5***
- ***Confidence level = 77%: determined using Table 5-6***

2. Local collapse

- *Median drift capacity ($\hat{C}$) = 0.037: given in Table 5-2 (brittle connection)*
- *Resistance factor (ϕ) = 0.80: given in Table 5-2 (brittle connection)*
- *Demand factor (γ) = 1.52: given in Table 5-4*
- *Analysis demand factor (γ_a) = 1.15: given in Table 5-4*
- ***Confidence factor,*** $\lambda_{con} = \dfrac{\phi \hat{C}}{\gamma \gamma_a \hat{D}}$ *: Equation 5-1*

$$\lambda_{con} = \frac{0.80 \times 0.037}{1.52 \times 1.15 \times 0.036} = 0.47$$

- ***Slope of hazard curve (k) = 3.0***
- ***Uncertainties (β_{UT}) = 0.39 ≅ 0.4: given in Table 5-5***
- ***Confidence level = 10%: determined using Table 5-6***

The confidence levels before the earthquake were 99% for global collapse and 97% for local collapse. The static analysis and the confidence level calculations indicate that the building may remain occupied. This might be a difficult decision to justify given that almost every bottom flange has fractured. However, this is essentially like starting out with a building with one end of each beam hinged. This would obviously be a very flexible building, but not necessarily one that would collapse. Given this, it would still be a difficult decision to make. The low likelihood that another earthquake of this intensity would strike again before repairs could be completed might sway the argument.

The application of the first 2/50 earthquake resulted in the damage shown in the lower left plot in Figure 9-9. Not only are all of the bottom flanges fractured, but about half of the top flanges on two floors are also fractured. This indicates that two floors reached 4% drift and many other ones probably approached these levels. The first and second applications of static

forces indicate that drifts approaching 8% might occur during a second occurrence of the 2/50 ground motion. This is obviously a case where occupancy would not be allowed.

Table 9-3 CP Confidence Level Calculations Against Local Collapse for 2/50, 10/50 and 50/50 Hazard for a 1985 9-Story Building in LA

	T(sec)	V(kip)	C	ϕ	D	γ	γ_a	γ_{con}	β_{UT}^2	Kx	C. L.
LA City Hall without plateau (k=3.08) : before											
2/50	2.60	478	0.037	0.80	0.029	1.52	1.15	0.58	0.15	-0.81	**21%**
10/50	2.60	290	0.037	0.80	0.018	1.52	1.15	0.94	0.15	0.42	**66%**
50/50	2.60	1539	0.037	0.80	0.015	1.52	1.15	1.13	0.15	0.89	**81%**
LA City Hall without plateau (k=3.08) : after											
	T(sec)	**V(kip)**	**C**	ϕ	**D**	γ	γ_a	γ_{con}	β_{UT}^2	**Kx**	**C. L.**
2/50	5.18	240	0.037	0.80	0.108	1.52	1.15	0.16	0.15	-4.20	**0%**
10/50	4.19	180	0.037	0.80	0.031	1.52	1.15	0.55	0.15	-0.98	**16%**
50/50	3.07	1303	0.037	0.80	0.030	1.52	1.15	0.56	0.15	-0.90	**19%**

Table 9-4 CP Confidence Level Calculations Against Global Collapse for 2/50, 10/50 and 50/50 Hazard for a 1985 9-Story Building in LA

	T(sec)	V(kip)	C	ϕ	D	γ	γ_a	γ_{con}	β_{UT}^2	Kx	C. L.
LA City Hall without plateau (k=3.08) : before											
2/50	2.60	478	0.070	0.85	0.029	1.52	1.15	1.17	0.21	1.04	**85%**
10/50	2.60	290	0.070	0.85	0.018	1.52	1.15	1.89	0.21	2.08	**98%**
50/50	2.60	1539	0.070	0.85	0.015	1.52	1.15	2.27	0.21	2.48	**99%**
LA City Hall without plateau (k=3.08) : after											
	T(sec)	**V(kip)**	**C**	ϕ	**D**	γ	γ_a	γ_{con}	β_{UT}^2	**Kx**	**C. L.**
2/50	5.18	240	0.070	0.85	0.108	1.52	1.15	0.32	0.21	-1.83	**3%**
10/50	4.19	180	0.070	0.85	0.031	1.52	1.15	1.10	0.21	0.89	**81%**
50/50	3.07	1303	0.070	0.85	0.030	1.52	1.15	1.13	0.21	0.96	**83%**

9.8 Summary

The examples given here indicate that evaluating a damaged building is very difficult because so much is at stake. The tools discussed in this section for damaged buildings and in Chapter 8 for existing undamaged buildings should be helpful to the design professional. The possible occurrence of local collapse is the most difficult to deal with. In every case examined in Chapter 8 and Chapter 9, the level of confidence in avoiding local collapse is significantly lower than for global collapse. For global collapse, we know what will happen and we don't like it. For local collapse, we don't know what will happen. The beam is usually at the perimeter, so no one could be directly under it. The beam will have shear studs and floor beams that will help support it if a shear tab is lost. It probably is unlikely that the beam and slab would fall. Of course the operative word in this last sentence is "probably."

The level of confidence against local or global collapse for a building to remain occupied is a difficult decision that the design professional and owner must make. Perhaps a reasonable lower bound would be 90% confidence in achieving the CP performance level for the 50% probability of exceedance in 30 years hazard level. This represents a return period of 44 years. Since repairs can be completed in a period of time considerably smaller than this, the building may remain occupied during repair and/or rehabilitation.

The engineer should also check for the failure criteria on compressive forces in columns as well as tension forces in column splice locations.

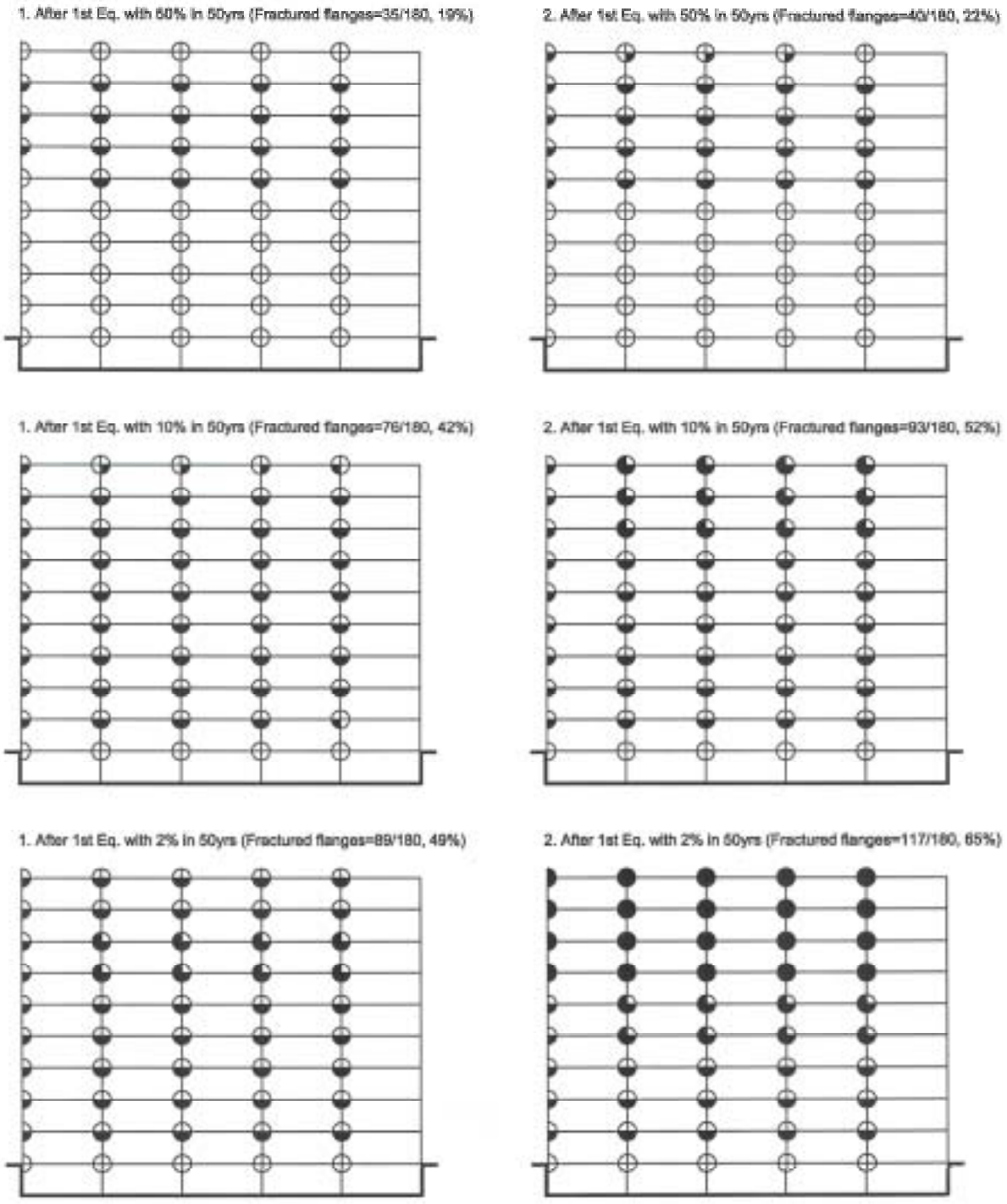

Figure 9-9 Observed Damage from First and Second Ground Motion Excitation

- Evaluation of the damaged frame from SAC Eqs with 50% in 50

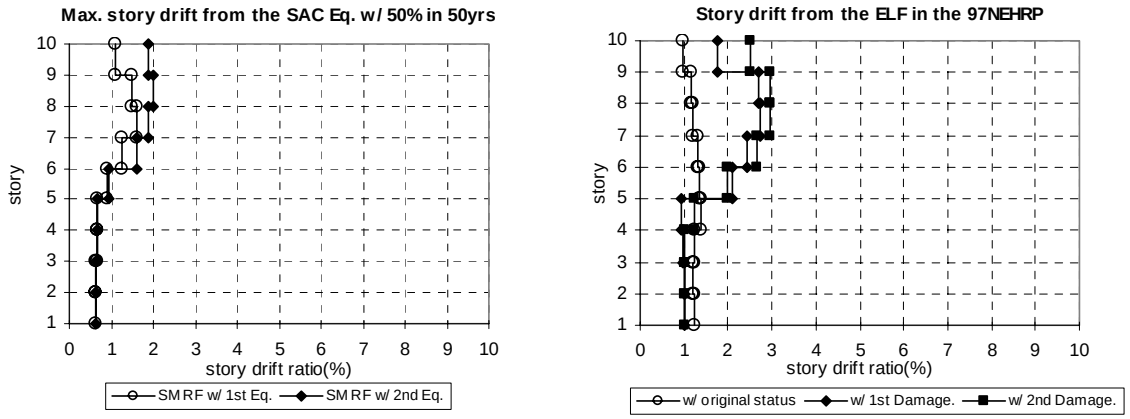

- Evaluation of the damaged frame from SAC Eqs with 10% in 50

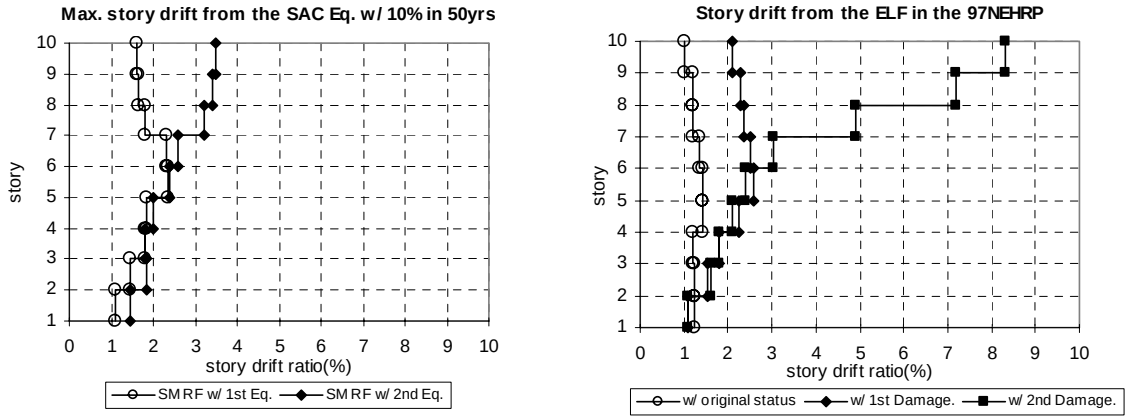

- Evaluation of the damaged frame from SAC Eqs with 2% in 50 years

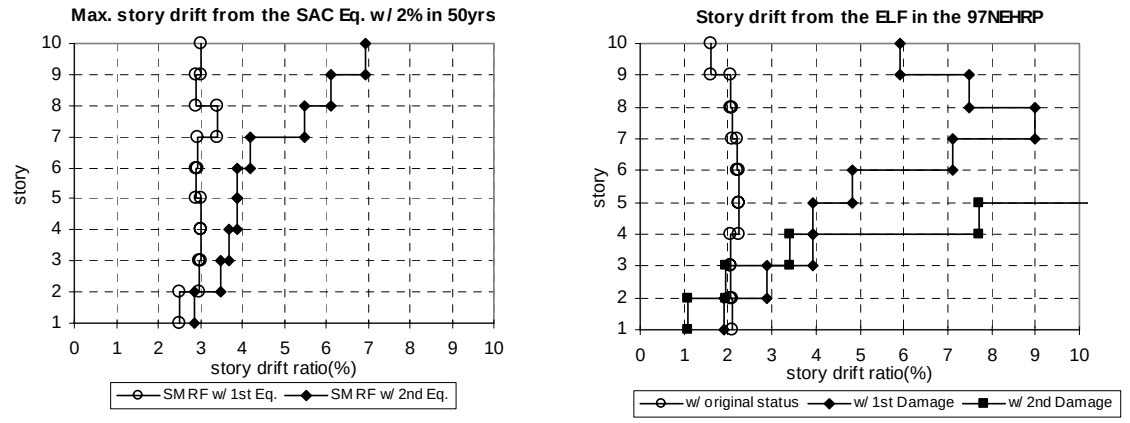

Figure 9-10 Drift Demands from Both Dynamic and Static Analyses of 9-Story Damaged Buildings for 50/50, 10/50 and 2/50 Hazard Levels

APPENDIX A. EXAMPLE FOR PERFORMANCE EVALUATION PROCEDURE

A.1 Performance Evaluation Procedure

The evaluation of a building designed and built using any of the connections given in Tables 5-1 to 5-3 would proceed as follows:

1. Determine S_s and S_1 for the site from maps or the USGS web site. Determine the design response spectrum following the 1997 NEHRP provisions, but replace the 2/3 factor by 1.0 for determining S_{DS} and S_{D1}.
2. Calculate the maximum drift demand, θ_m, using any of the analysis procedures given in Table 4-8 and Table 4-9. The demand drift, $\hat{D}$, is then calculated as:

$$\hat{D} = C_B \theta_m \quad \text{(A-1)}$$

where:

θ_m = the maximum story drift angle, Δ_x, for all stories

C_B = bias factor from Table 4-8 and Table 4-9

3. Get values for $\hat{C}$ and ϕ from Table 5-1 to Table 5-3 for the connection type used and the performance level of interest.
4. Get value of γ_a for the height and performance level from Table 5-4. Also, select γ for the CP performance level or for the IO performance level from the table.
5. Calculate λ_{con} using Equation 5-1.
6. Get β_{UT} value from Table 5-5. Check the confidence level in achieving the performance objective from Table 5-6. Decide if the confidence is acceptable. If not, redesign the frame to make it stiffer and, therefore, reduce $\hat{D}$.

A.2 Example for Performance Evaluation for 9-Story Buildings

A.2.1 LA 9-Story Post-Northridge Building Using RBS Connections

The floor plan and elevation view for a 9-story SMRF building that confirms the minimum requirement in the 1997 NEHRP provisions are shown in Figure 4-37. Type 1 (RBS) connections are assumed to be used for the post-Northridge building. Calculate confidence levels satisfying the CP for the 2/50 hazard level and IO performance levels for the 50/50 and 50/30 hazard levels.

- *Example: Collapse Prevention against global collapse for the 2/50 hazard level*
  - S_S = 1.61g, S_1 = 0.79g, F_a = 1.0, F_v = 1.5 (1997 NEHRP Provisions)
  - $S_{DS} = S_{MS} = F_a \times S_S$ = 1.61g ; $S_{D1} = S_{M1} = F_v \times S_1$ = 1.19g
  - Soil Type D (stiff soil)
  - Seismic design category (SDC) = D
  - Fundamental period of building (T) = 2.39 sec.
  - Total seismic weight (W) = 19923 kips
  - Seismic base shear (V) = 1240 kips, V_f = 620 kips (2 moment frames)
  - R = 8, C_d = 5.5 for the 2/50 hazard level
  - Maximum elastic drift angle (δ_{xe}) = 0.005

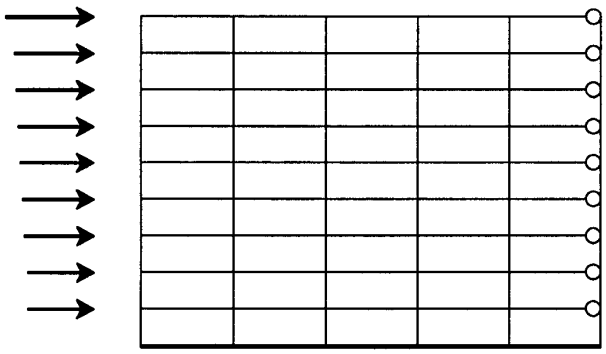

Elastic building model

Level	Fi (k)	Disp.(in)	Drift
9	164	6.29	0.004
8	125	5.67	0.004
7	100	5.04	0.005
6	78	4.29	0.005
5	58	3.54	0.004
4	42	2.92	0.005
3	28	2.21	0.004
2	17	1.53	0.004
1	8	0.86	0.004
Total	620		

Story force and story drift

1. Collapse Prevention (CP) Performance Level (LA 9-Story Post-Northridge Building)

	Global collapse for 2/50 hazard level	Local collapse for 2/50 hazard level	Symbol	PPE SOA Report
S_{DS}	1.61	1.61	$S_{DS} = S_{MS} = F_a \times S_S$	1997 NEHRP
S_{D1}	1.19	1.19	$S_{D1} = S_{M1} = F_v \times S_1$	1997 NEHRP
T (sec)	2.39	2.39	Fundamental period of building	From rational analysis
R	8	8	Response modification coefficient	1997 NEHRP Table 5.2.2
C_d	5.5	5.5	Deflection amplification factor	1997 NEHRP Table 5.2.2
C_s	0.062	0.062	$C_s = S_{D1}/(T \times R)$	1997 NEHRP
V_f (kips)	620	620	Base shear (C_s x W)	
δ_{xe}	0.005	0.005	Max. elastic drift	Elastic analysis
θ_m	0.026	0.026	Max. inelastic drift $\theta_m = \delta_{xe} \times C_d$	
C_B	1.15	1.15	Bias factor (1997 NEHRP – LSP)	Table 4-8
$\hat{D}$	0.031	0.031	Median drift demand ($C_B \times \theta_m$)	Elastic analysis
$\hat{C}$	0.090	0.070	Median drift capacity	Table 5-1
ϕ	0.86	0.90	Resistance factor	Table 5-1
γ	1.21	1.21	Demand factor	Table 5-4
γ_a	1.07	1.07	Analysis demand factor	Table 5-4
λ_{con}	**1.89**	**1.55**	**Confidence factor**	$\lambda_{con} = \frac{\phi \hat{C}}{\gamma \gamma_a \hat{D}}$
k	**2.86 ≅ 3.0**	**2.86 ≅ 3.0**	**Slope of hazard curve**	**Table 5-9**
β_{UT}	**0.4**	**0.33 ≅ 0.30**	**Uncertainties**	**Table 5-5**
C. L.	**99%**	**97%**	**Confidence Level**	**Table 5-6**

2. Immediate Occupancy (IO) Performance Level (LA 9-Story Post-Northridge Building) For IO Assume Elastic Behavior so R = 1.0 and C_d = 1.0

	IO for 50/50 hazard level	**IO for 50/30 hazard level**	**Symbol**	**PPE SOA Report**
S_{DS}	0.514	0.434	$S_{DS} = S_{MS} = F_a \times S_S$	1997 NEHRP
S_{D1}	0.288	0.219	$S_{D1} = S_{M1} = F_v \times S_1$	1997 NEHRP
T (sec)	2.39	2.39	Fundamental period of building	From rational analysis
R	1	1	Response modification coefficient	1997 NEHRP Table 5.2.2
C_d	1	1	Deflection amplification factor	1997 NEHRP Table 5.2.2
C_s	0.121	0.092	$C_s = S_{D1}/(T \times R)$	1997 NEHRP
V_f (kips)	1197	910	Base shear (C_s x W)	
δ_{xe}	0.008	0.006	Max. elastic drift	Elastic analysis
θ_m	0.008	0.006	Max. inelastic drift $\theta_m = \delta_{xe} \times C_d$	
C_B	1.1	1.1	Bias factor (1997 NEHRP – LSP)	Table 4-8
$\hat{D}$	0.009	0.007	Median drift demand ($C_B \times \theta_m$)	Elastic analysis
$\hat{C}$	0.020	0.020	Median drift capacity	Table 5-1
ϕ	0.90	0.90	Resistance factor	Table 5-1
γ	1.43	1.43	Demand factor	Table 5-4
γ_a	1.07	1.07	Analysis demand factor	Table 5-4
λ_{con}	**1.31**	**1.68**	**Confidence factor**	$\lambda_{con} = \frac{\phi \hat{C}}{\gamma \gamma_a \hat{D}}$
k	**2.86 ≅ 3.0**	**2.86 ≅ 3.0**	**Slope of hazard curve**	**Table 5-9**
β_{UT}	**0.33 ≅ 0.30**	**0.33 ≅ 0.30**	**Uncertainties**	**Table 5-5**
C. L.	**94%**	**99%**	**Confidence Level**	**Table 5-6**

A.2.2 LA 9-Story Pre-Northridge Building Using Brittle Connections

The floor plan and elevation view for a 9-story SMRF building designed based on the 1994 UBC provisions is shown in Figure 5-6. Brittle welded connections are assumed to use for the pre-Northridge building. Calculate confidence levels satisfying the CP for the 2/50, 50/50 and 50/30 hazard levels and IO performance level for the 50/50 and 50/30 hazard levels.

- Example: Collapse Prevention against global collapse for the 2/50 hazard level
  - S_S = 1.61g, S_1 = 0.79g, F_a = 1.0, F_v = 1.5 (1997 NEHRP Provisions)
  - $S_{DS} = S_{MS} = F_a \times S_S$ = 1.61g ; $S_{D1} = S_{M1} = F_v \times S_1$ = 1.19g
  - Soil Type D (stiff soil)
  - Seismic design category (SDC) = D
  - Fundamental period of building (T) = 2.51 sec.
  - Total seismic weight (W) = 19923 kips
  - Seismic base shear (V) = 1176 kips, V_f = 588 kips (2 moment frames)
  - R = 8, C_d = 5.5 for the 2/50 hazard level
  - Maximum elastic drift angle (δ_{xe}) = 0.006

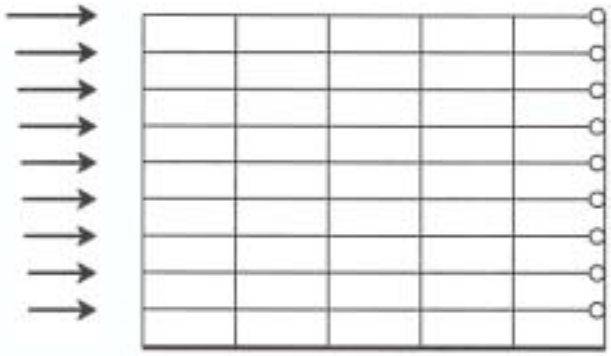

Elastic building model

Level	Fi (k)	Disp.(in)	Drift
9	190	6.78	0.005
8	80	6.02	0.005
7	71	5.30	0.006
6	63	4.54	0.005
5	54	3.80	0.005
4	45	3.10	0.005
3	37	2.38	0.004
2	28	1.71	0.004
1	20	1.04	0.005
Total	588		

Story force and story drift

1. Collapse Prevention (CP) Performance Level (LA 9-Story Pre-Northridge Building)

	Global collapse for 2/50 hazard level	**Local collapse for 2/50 hazard level**	**Symbol**	**PPE SOA Report**
S_{DS}	1.61	1.61	$S_{DS} = S_{MS} = F_a \times S_S$	1997 NEHRP
S_{D1}	1.19	1.19	$S_{D1} = S_{M1} = F_v \times S_1$	1997 NEHRP
T (sec)	2.51	2.51	Fundamental period of building	From rational analysis
R	8	8	Response modification coefficient	1997 NEHRP Table 5.2.2
C_d	5.5	5.5	Deflection amplification factor	1997 NEHRP Table 5.2.2
C_s	0.059	0.059	$C_s = S_{D1}/(T \times R)$	1997 NEHRP
V_f (kips)	588	588	Base shear ($C_s \times W$)	
δ_{xe}	0.006	0.006	Max. elastic drift	Elastic analysis
θ_m	0.033	0.033	Max. inelastic drift $\theta_m = \delta_{xe} \times C_d$	
C_B	1.15	1.15	Bias factor (1997 NEHRP – LSP)	Table 4-9
$\hat{D}$	0.040	0.040	Median drift demand ($C_B \times \theta_m$)	Elastic analysis
$\hat{C}$	0.070	0.054	Median drift capacity	Table 5-1
ϕ	0.86	0.80	Resistance factor	Table 5-1
γ	1.21	1.21	Demand factor	Table 5-4
γ_a	1.07	1.07	Analysis demand factor	Table 5-4
λ_{con}	**1.16**	**0.84**	**Confidence factor**	$\lambda_{con} = \frac{\phi \hat{C}}{\gamma \gamma_a \hat{D}}$
k	**2.86 ≅ 3.0**	**2.86 ≅ 3.0**	**Slope of hazard curve**	**Table 5-9**
β_{UT}	**0.4**	**0.33 ≅ 0.30**	**Uncertainties**	**Table 5-5**
C. L.	**81%**	**50%**	**Confidence Level**	**Table 5-6**

2. Collapse Prevention (CP) Performance Level (LA 9-story Pre-Northridge Building)

	Global collapse for 50/50 hazard level	Local collapse for 50/50 hazard level	Symbol	PPE SOA Report
S_{DS}	0.514	0.514	$S_{DS} = S_{MS} = F_a \times S_S$	1997 NEHRP
S_{D1}	0.288	0.288	$S_{D1} = S_{M1} = F_v \times S_1$	1997 NEHRP
T (sec)	2.51	2.51	Fundamental period of building	From rational analysis
R	1	1	Response modification coefficient	1997 NEHRP Table 5.2.2
C_d	1	1	Deflection amplification factor	1997 NEHRP Table 5.2.2
C_s	0.115	0.115	$C_s = S_{D1}/(T \times R)$	1997 NEHRP
V_f (kips)	1140	1140	Base shear ($C_s \times W$)	
δ_{xe}	0.010	0.010	Max. elastic drift	Elastic analysis
θ_m	0.010	0.010	Max. inelastic drift $\theta_m = \delta_{xe} \times C_d$	
C_B	1.1	1.1	Bias factor (1997 NEHRP – LSP)	Table 4-9
$\hat{D}$	0.011	0.011	Median drift demand ($C_B \times \theta_m$)	Elastic analysis
$\hat{C}$	0.070	0.054	Median drift capacity	Table 5-1
ϕ	0.86	0.80	Resistance factor	Table 5-1
γ	1.21	1.21	Demand factor	Table 5-4
γ_a	1.07	1.07	Analysis demand factor	Table 5-4
λ_{con}	**4.34**	**3.15**	**Confidence factor**	$\lambda_{con} = \frac{\phi \hat{C}}{\gamma \gamma_a \hat{D}}$
k	**2.86 ≅ 3.0**	**2.86 ≅ 3.0**	**Slope of hazard curve**	**Table 5-9**
β_{UT}	**0.4**	**0.33 ≅ 0.30**	**Uncertainties**	**Table 5-5**
C. L.	**99%**	**99%**	**Confidence Level**	**Table 5-6**

3. Immediate Occupancy (IO) Performance Level (LA 9-story Pre-Northridge Building) For IO Assume Elastic Behavior so R = 1.0 and C_d = 1.0

	IO for 50/50 hazard level	**IO for 50/30 hazard level**	**Symbol**	**PPE SOA Report**
S_{DS}	0.514	0.434	$S_{DS} = S_{MS} = F_a \times S_S$	1997 NEHRP
S_{D1}	0.288	0.219	$S_{D1} = S_{M1} = F_v \times S_1$	1997 NEHRP
T (sec)	2.51	2.51	Fundamental period of building	From rational analysis
R	1	1	Response modification coefficient	1997 NEHRP Table 5.2.2
C_d	1	1	Deflection amplification factor	1997 NEHRP Table 5.2.2
C_s	0.115	0.087	$C_s = S_{D1}/(T \times R)$	1997 NEHRP
V_f (kips)	1140	867	Base shear (C_s x W)	
δ_{xe}	0.010	0.007	Max. elastic drift	Elastic analysis
θ_m	0.010	0.007	Max. inelastic drift $\theta_m = \delta_{xe} \times C_d$	
C_B	1.1	1.1	Bias factor (1997 NEHRP – LSP)	Table 4-9
$\hat{D}$	0.011	0.008	Median drift demand ($C_B \times \theta_m$)	Elastic analysis
$\hat{C}$	0.010	0.010	Median drift capacity	Table 5-1
ϕ	0.80	0.80	Resistance factor	Table 5-1
γ	1.43	1.43	Demand factor	Table 5-4
γ_a	1.07	1.07	Analysis demand factor	Table 5-4
λ_{con}	**0.49**	**0.65**	**Confidence factor**	$\lambda_{con} = \frac{\phi \hat{C}}{\gamma \gamma_a \hat{D}}$
k	**2.86 ≅ 3.0**	**2.86 ≅ 3.0**	**Slope of hazard curve**	**Table 5-9**
β_{UT}	**0.33 ≅ 0.30**	**0.33 ≅ 0.30**	**Uncertainties**	**Table 5-5**
C. L.	**4%**	**18%**	**Confidence Level**	**Table 5-6**

A.2.3 LA 9-Story Pre-Northridge Damaged Building After 2/50 Accelerogram

The floor plan and elevation view for a 9-story SMRF building designed based on the 1994 UBC provisions is shown in Figure 5-6. Brittle welded connections are assumed to use for the pre-Northridge building. Calculate confidence levels for damaged buildings subjected to 2/50 accelerogram satisfying the CP for the 2/50 and 50/50 and IO performance levels for the 50/50 and 50/30 hazard levels.

- ***Example for calculation of maximum elastic drift after the building was hit by one of the 2/50 accelerograms.***
    - The building model was subjected to one of the LA 2/50 accelerograms and checked to see which flanges of which connections had been fractured. To represent the building in the damaged state, rigid connection in the elastic building model was changed to pin connection.
    - The period of the building was recalculated, and new static forces were calculated. These forces were applied to the damaged building to evaluate the performance level.

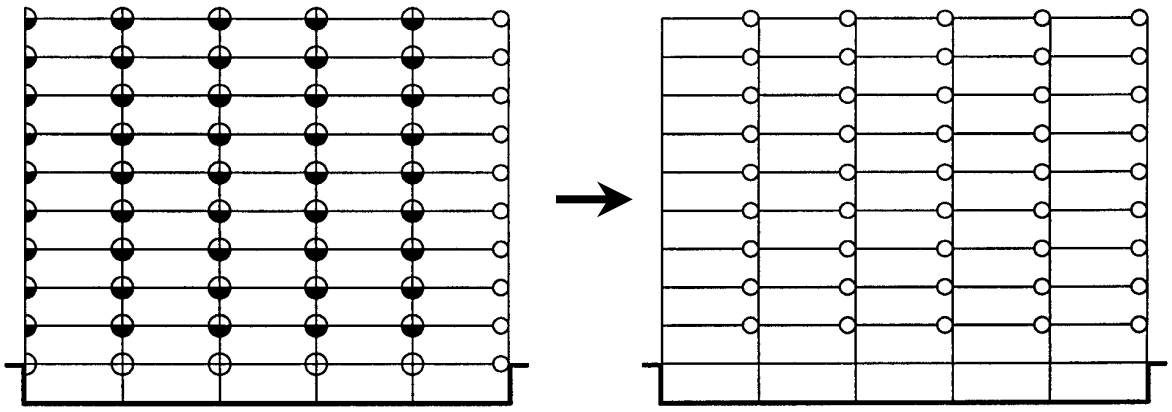

Damaged building after 2/50 Eq. **Elastic building model after damage**

    - The period of the building was recalculated and new static forces were calculated. These forces were applied to the damaged building to evaluate the performance level.

- LA 9-story pre-Northridge building subjected to 2/50 accelerogram

	Original state	Damaged state
Fundamental Period	2.51 second	4.01 second
Base Shear	588 kips	369 kips
Max. elastic drift	0.005	0.013
Max. inelastic drift	0.027	0.069

1. Collapse Prevention (CP) Performance Level (LA 9-story Pre-Northridge Damaged Building After One 2/50 Accelerogram)

	Global collapse for 2/50 hazard level	**Local collapse for 2/50 hazard level**	**Symbol**	**PPE SOA Report**
S_{DS}	1.61	1.61	$S_{DS} = S_{MS} = F_a \times S_S$	1997 NEHRP
S_{D1}	1.19	1.19	$S_{D1} = S_{M1} = F_v \times S_1$	1997 NEHRP
T (sec)	4.01	4.01	Fundamental period of building	From rational analysis
R	8	8	Response modification coefficient	1997 NEHRP Table 5.2.2
C_d	5.5	5.5	Deflection amplification factor	1997 NEHRP Table 5.2.2
C_s	0.037	0.037	$C_s = S_{D1}/(T \times R)$	1997 NEHRP
V_f (kips)	369	369	Base shear (C_s x W)	
δ_{xe}	0.013	0.013	Max. elastic drift	Elastic analysis
θ_m	0.069	0.069	Max. inelastic drift $\theta_m = \delta_{xe} \times C_d$	
C_B	1.15	1.15	Bias factor (1997 NEHRP – LSP)	Table 4-9
$\hat{D}$	0.083	0.083	Median drift demand ($C_B \times \theta_m$)	Elastic analysis
$\hat{C}$	0.070	0.054	Median drift capacity	Table 5-1
ϕ	0.86	0.80	Resistance factor	Table 5-1
γ	1.21	1.21	Demand factor	Table 5-4
γ_a	1.07	1.07	Analysis demand factor	Table 5-4
λ_{con}	**0.56**	**0.40**	**Confidence factor**	$\lambda_{con} = \frac{\phi \hat{C}}{\gamma \gamma_a \hat{D}}$
k	**2.86 ≅ 3.0**	**2.86 ≅ 3.0**	**Slope of hazard curve**	**Table 5-9**
β_{UT}	**0.4**	**0.33 ≅ 0.30**	**Uncertainties**	**Table 5-5**
C. L.	**20%**	**1%**	**Confidence Level**	**Table 5-6**

2. Collapse Prevention (CP) Performance Level (LA 9-Story Pre-Northridge Damaged Building After One 2/50 Accelerogram)

	Global collapse for 50/50 hazard level	**Local collapse for 50/50 hazard level**	**Symbol**	**PPE SOA Report**
S_{DS}	0.514	0.514	$S_{DS} = S_{MS} = F_a \times S_S$	1997 NEHRP
S_{D1}	0.288	0.288	$S_{D1} = S_{M1} = F_v \times S_1$	1997 NEHRP
T (sec)	4.01	4.01	Fundamental period of building	From rational analysis
R	1	1	Response modification coefficient	1997 NEHRP Table 5.2.2
C_d	1	1	Deflection amplification factor	1997 NEHRP Table 5.2.2
C_s	0.072	0.072	$C_s = S_{D1}/(T \times R)$	1997 NEHRP
V_f (kips)	713	713	Base shear (C_s x W)	
δ_{xe}	0.017	0.017	Max. elastic drift	Elastic analysis
θ_m	0.017	0.017	Max. inelastic drift $\theta_m = \delta_{xe} \times C_d$	
C_B	1.1	1.1	Bias factor (1997 NEHRP – LSP)	Table 4-9
$\hat{D}$	0.019	0.019	Median drift demand ($C_B \times \theta_m$)	Elastic analysis
$\hat{C}$	0.070	0.054	Median drift capacity	Table 5-1
ϕ	0.86	0.80	Resistance factor	Table 5-1
γ	1.21	1.21	Demand factor	Table 5-4
γ_a	1.07	1.07	Analysis demand factor	Table 5-4
λ_{con}	**2.40**	**1.74**	**Confidence factor**	$\lambda_{con} = \frac{\phi \hat{C}}{\gamma \gamma_a \hat{D}}$
k	**2.86 ≅ 3.0**	**2.86 ≅ 3.0**	**Slope of hazard curve**	**Table 5-9**
β_{UT}	**0.4**	**0.33 ≅ 0.30**	**Uncertainties**	**Table 5-5**
C. L.	**99%**	**99%**	**Confidence Level**	**Table 5-6**

A.2.4 LA 9-Story Pre-Northridge Damaged Building After 50/50 Accelerogram

The floor plan and elevation view for a 9-story SMRF building designed based on the 1994 UBC provisions is shown in Figure 5-6. Brittle welded connections are assumed to be used for the pre-Northridge building. Calculate confidence levels for damaged buildings subjected to 50/50 accelerogram satisfying the CP for the 2/50 and 50/50 and IO performance levels for the 50/50 and 50/30 hazard levels.

- Example for calculation of maximum elastic drift after the building was hit by one of the 50/50 accelerograms.

  - The building model was subjected to one of the LA 50/50 accelerograms and checked to see which flanges of which connections had been fractured. To represent the building in the damaged state, rigid connection in the elastic building model was changed to pin connection.

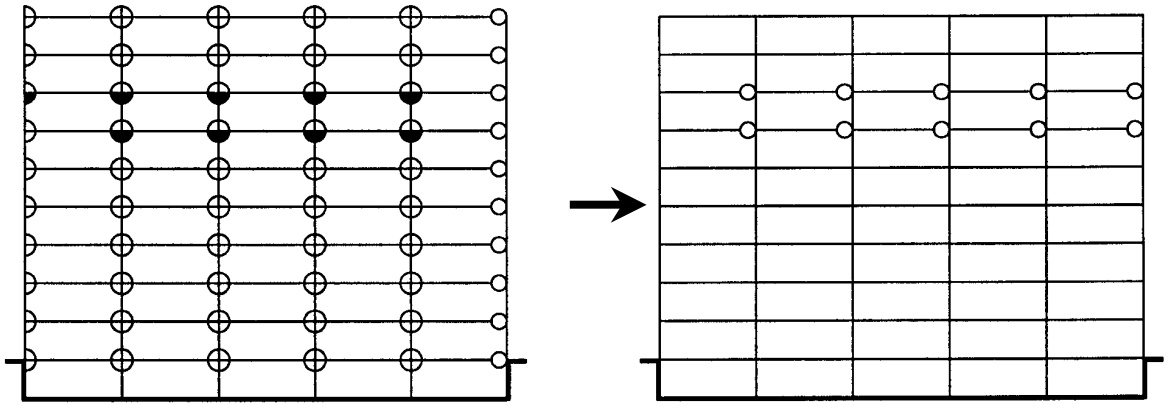

Damaged building after 50/50 Eq. **Elastic building model after damage**

  - The period of the building was recalculated and new static forces were calculated. These forces were applied to the damaged building to evaluate the performance level.

- ***LA 9-Story Pre-Northridge Building Subjected to 50/50 Accelerogram***

	Original state	Damaged state
Fundamental Period	2.51 second	2.68 second
Base Shear	588 kips	551 kips
Max. elastic drift	0.005	0.006

1. Collapse Prevention (CP) Performance Level (LA 9-Story Pre-Northridge Damaged Building After One 50/50 Accelerogram)

	Global collapse for 2/50 hazard level	**Local collapse for 2/50 hazard level**	**Symbol**	**PPE SOA Report**
S_{DS}	1.61	1.61	$S_{DS} = S_{MS} = F_a \times S_S$	1997 NEHRP
S_{D1}	1.19	1.19	$S_{D1} = S_{M1} = F_v \times S_1$	1997 NEHRP
T (sec)	2.68	2.68	Fundamental period of building	From rational analysis
R	8	8	Response modification coefficient	1997 NEHRP Table 5.2.2
C_d	5.5	5.5	Deflection amplification factor	1997 NEHRP Table 5.2.2
C_s	0.056	0.056	$C_s = S_{D1}/(T \times R)$	1997 NEHRP
V_f (kips)	551	551	Base shear (C_s x W)	
δ_{xe}	0.006	0.006	Max. elastic drift	Elastic analysis
θ_m	0.034	0.034	Max. inelastic drift $\theta_m = \delta_{xe} \times C_d$	
C_B	1.15	1.15	Bias factor (1997 NEHRP – LSP)	Table 4-9
$\hat{D}$	0.041	0.041	Median drift demand ($C_B \times \theta_m$)	Elastic analysis
$\hat{C}$	0.070	0.054	Median drift capacity	Table 5-1
ϕ	0.86	0.80	Resistance factor	Table 5-1
γ	1.21	1.21	Demand factor	Table 5-4
γ_a	1.07	1.07	Analysis demand factor	Table 5-4
λ_{con}	**1.12**	**0.82**	**Confidence factor**	$\lambda_{con} = \frac{\phi \hat{C}}{\gamma \gamma_a \hat{D}}$
k	**2.86 ≅ 3.0**	**2.86 ≅ 3.0**	**Slope of hazard curve**	**Table 5-9**
β_{UT}	**0.4**	**0.33 ≅ 0.30**	**Uncertainties**	**Table 5-5**
C. L.	**82%**	**43%**	**Confidence Level**	**Table 5-6**

2. Collapse Prevention (CP) Performance Level (LA 9-Story Pre-Northridge Damaged Building After One 50/50 Accelerogram)

	Global collapse for 50/50 hazard level	**Local collapse for 50/50 hazard level**	**Symbol**	**PPE SOA Report**
S_{DS}	0.514	0.514	$S_{DS} = S_{MS} = F_a \times S_S$	1997 NEHRP
S_{D1}	0.288	0.288	$S_{D1} = S_{M1} = F_v \times S_1$	1997 NEHRP
T (sec)	2.68	2.68	Fundamental period of building	From rational analysis
R	1	1	Response modification coefficient	1997 NEHRP Table 5.2.2
C_d	1	1	Deflection amplification factor	1997 NEHRP Table 5.2.2
C_s	0.107	0.107	$C_s = S_{D1}/(T \times R)$	1997 NEHRP
V_f (kips)	1067	1067	Base shear (C_s x W)	
δ_{xe}	0.012	0.012	Max. elastic drift	Elastic analysis
θ_m	0.012	0.012	Max. inelastic drift $\theta_m = \delta_{xe} \times C_d$	
C_B	1.1	1.1	Bias factor (1997 NEHRP – LSP)	Table 4-9
$\hat{D}$	0.013	0.013	Median drift demand ($C_B \times \theta_m$)	Elastic analysis
$\hat{C}$	0.070	0.054	Median drift capacity	Table 5-1
ϕ	0.86	0.80	Resistance factor	Table 5-1
γ	1.21	1.21	Demand factor	Table 5-4
γ_a	1.07	1.07	Analysis demand factor	Table 5-4
λ_{con}	**3.48**	**2.53**	**Confidence factor**	$\lambda_{con} = \frac{\phi \hat{C}}{\gamma \gamma_a \hat{D}}$
k	**$2.86 \cong 3.0$**	**$2.86 \cong 3.0$**	**Slope of hazard curve**	**Table 5-9**
β_{UT}	**0.4**	**$0.33 \cong 0.30$**	**Uncertainties**	**Table 5-5**
C. L.	**99%**	**99%**	**Confidence Level**	**Table 5-6**

3. Immediate Occupancy (IO) Performance Level (LA 9-Story Pre-Northridge Damaged Building After One 50/50 Accelerogram); For IO level, R=1.0 and C_d=1.0

	IO for 50/50 hazard level	IO for 50/30 hazard level	Symbol	PPE SOA Report
S_{DS}	0.514	0.434	$S_{DS} = S_{MS} = F_a \times S_S$	1997 NEHRP
S_{D1}	0.288	0.219	$S_{D1} = S_{M1} = F_v \times S_1$	1997 NEHRP
T (sec)	2.68	2.68	Fundamental period of building	From rational analysis
R	1	1	Response modification coefficient	1997 NEHRP Table 5.2.2
C_d	1	1	Deflection amplification factor	1997 NEHRP Table 5.2.2
C_s	0.107	0.082	$C_s = S_{D1}/(T \times R)$	1997 NEHRP
V_f (kips)	1067	812	Base shear (C_s x W)	
δ_{xe}	0.012	0.009	Max. elastic drift	Elastic analysis
θ_m	0.012	0.009	Max. inelastic drift $\theta_m = \delta_{xe} \times C_d$	
C_B	1.1	1.1	Bias factor (1997 NEHRP – LSP)	Table 4-9
$\hat{D}$	0.013	0.010	Median drift demand ($C_B \times \theta_m$)	Elastic analysis
$\hat{C}$	0.010	0.010	Median drift capacity	Table 5-1
ϕ	0.80	0.80	Resistance factor	Table 5-1
γ	1.43	1.43	Demand factor	Table 5-4
γ_a	1.07	1.07	Analysis demand factor	Table 5-4
λ_{con}	**0.40**	**0.52**	**Confidence factor**	$\lambda_{con} = \frac{\phi \hat{C}}{\gamma \gamma_a \hat{D}}$
k	**2.86 ≅ 3.0**	**2.86 ≅ 3.0**	**Slope of hazard curve**	**Table 5-9**
β_{UT}	**0.33 ≅ 0.30**	**0.33 ≅ 0.30**	**Uncertainties**	**Table 5-5**
C. L.	**1%**	**4%**	**Confidence Level**	**Table 5-6**

A.3 Summary

Confidence Level for the LA 9-story buildings

Building Type	Performance Level		Confidence Level
Post-Northridge Building	Collapse Prevention (CP)	Global collapse for 2/50	99%
		Local collapse for 2/50	97%
	Immediate Occupancy (IO)	IO for 50/50	94%
		IO for 50/30	99%
Pre-Northridge Building	Collapse Prevention (CP)	Global collapse for 2/50	81%
		Local collapse for 2/50	50%
		Global collapse for 50/50	99%
		Local collapse for 50/50	99%
	Immediate Occupancy (IO)	IO for 50/50	4%
		IO for 50/30	18%
Damaged building after 2/50 accelerogram	Collapse Prevention (CP)	Global collapse for 2/50	20%
		Local collapse for 2/50	1%
		Global collapse for 50/50	99%
		Local collapse for 50/50	99%
Damaged building after 50/50 accelerogram	Collapse Prevention (CP)	Global collapse for 2/50	82%
		Local collapse for 2/50	43%
		Global collapse for 50/50	99%
		Local collapse for 50/50	99%
Damaged building after 50/50 accelerogram	Immediate Occupancy (IO)	IO for 50/50	1%
		IO for 50/30	4%

These results indicate that the new post-Northridge building should be able to satisfy the IO and CP performance objectives with a high level of confidence. The IO performance objective cannot be achieved by the pre-Northridge building even for the 50/30 hazard level. There is a high level of confidence that the CP performance level can be met for the 50/50 and 50/30 hazard levels. However, the confidence level is low for satisfying the CP level for the 2/50 year event. The pre-Northridge building that was damaged even by the 2/50 event had a high level of confidence of satisfying the CP level for the 50/50 or 50/30 earthquake.

APPENDIX B. PERFORMANCE EVALUATION COEFFICIENTS AND BIAS FACTORS FOR NEW AND EXISTING BUILDINGS

B.1 Performance Evaluation Coefficients

$$\lambda_{con} = \frac{\phi \cdot \hat{C}}{\gamma \cdot \gamma_a \cdot \hat{D}}$$

$\hat{D}$ = **estimate of median drift demand**

$$\hat{D} = C_B \cdot \theta_m$$

θ_m= the calculated maximum story drift angle, Δ_x, for all stories

C_B = bias factor

***Post-Northridge*: C_B**

Analysis Procedure	3-story		9-story		20-story	
	2/50	50/50	2/50	50/50	2/50	50/50
97NEHRP-LSP	0.90	0.90	1.15	1.10	1.35	1.05
97NEHRP-LDP	0.85	0.85	1.05	0.90	1.10	1.10
Linear-THP	0.85	0.85	0.90	1.00	0.90	1.00
F273-NSP	1.20	NA	1.35	NA	1.20	NA
CSM-NSP	1.30	NA	1.50	NA	1.35	NA

NA: Not appropriate

***Pre-Northridge*: C_B**

Analysis Procedure	3-story		9-story		20-story	
	2/50	50/50	2/50	50/50	2/50	50/50
97NEHRP-LSP	1.25	0.75	1.40	0.80	1.00	0.75
97NEHRP-LDP	0.90	0.75	1.20	0.75	1.30	0.95
Linear-THP	1.25	0.90	1.35	1.10	1.30	1.30
F273-NSP	1.35	0.90	1.20	1.05	1.00	1.15
CSM-NSP	N/A	N/A	N/A	N/A	N/A	N/A

N/A: Not available

$\hat{C}$ = **estimate of median drift capacity**

(i). For global capacity:

Post-Northridge $\Rightarrow$ $\hat{C}$ = **0.085**

Pre-Northridge $\Rightarrow$ $\hat{C}$ = **0.07**

(ii). For local capacity:

***Post-Northridge*: $\hat{C}$**

Connection Type	Immediate Occupancy	Collapse Prevention
	Limit Drift Angle (radians) θ_{IO}	Limit Drift Angle[1] (radians) θ_{CP}
WUF-B[3]	0.015	0.060-0.0006 d_b
WUF-W[4]	0.020	0.064
FF[5]	0.020	0.10-0.0016 d_b
RBS[6]	0.020	0.08-0.0003 d_b
WFP[7]	0.020	0.10-0.0011 d_b except that should used θ_{SD} if w14 or less
End-plate	Not pre-qualified for the Guidelines	

***Pre-Northridge*: $\hat{C}$**

Connection Type	Immediate Occupancy	Collapse Prevention
	Limit Drift Angle (radians) θ_{IO}	Limit Drift Angle[1] (radians) θ_{CP}
WUF[3] (<1980)	0.010	Larger of 0.053-0.0006 d_b or 0.061-0.00013 d_b
WUF[3] (>1980)	0.010	0.053-0.0006 d_b

ϕ	=	**resistance factor**

$$\phi = \phi_{RC} \cdot \phi_{UC}, \qquad \phi_{RC} = e^{\frac{-k\beta_{RC}^2}{2b}}, \qquad \phi_{UC} = e^{\frac{-k\beta_{UC}^2}{2b}}$$

β_{RC} = Standard deviation of the natural logs of the drift capacities from IDA analysis.

(i). global:

Independent of the demand uncertainty.

***Post-Northridge*: β_{RC}**

	3-story	9-story	20-story
β_{RC}	0.00	0.00	0.26

***Pre- Northridge*: β_{RC}**

	3-story	9-story	20-story
β_{RC}	0.00	0.27	0.35

(ii). local: Test variability in rotation.

Post-Northridge

β_{RC} **= 0.20** : according to personal communication with Cornell (2000)

Pre-Northridge

β_{RC} **= 0.30** : according to personal communication with Hamburger (2000)

β_{UC} = Standard deviation of the natural logs of the drift capacities derived from testing.

(i). global:

Dependent part of the demand capacity. Negatively correlated to demand uncertainty.

Therefore,

$$\beta_{UC} = \sqrt{\beta_{Ui}^{\ 2} + \beta_{Ud}^{\ 2}} = \sqrt{\beta_{Ui}^{\ 2} + 2 \cdot \rho \cdot \beta_{dd} \cdot \beta_{cd}}$$

$$= \sqrt{3 \cdot \beta_{NTH}^{\ 2}} = \sqrt{3} \cdot \beta_{NTH}$$

where:

β_{Ui} = independent part of uncertainty

β_{Ud} = dependent part of uncertainty

***Post-Northridge*: β_{UC}**

	3-story	9-story	20-story
β_{NTH}	0.15	0.20	0.25
β_{UC}	0.26	0.35	0.43

***Pre-Northridge*: β_{UC}**

	3-story	**9-story**	**20-story**
β_{NTH}	0.15	0.20	0.25
β_{UC}	0.26	0.35	0.43

(ii). local: Calculate the coefficient of variation described in the Connection Performance report (Roeder, 2000) depending on the connection type used.

Post-Northridge & Pre-Northridge

β_{UC} **= 0.25** according to personal communication with Cornell (2000)

ϕ_{RC} = Contribution to ϕ from randomness of the earthquake accelerograms

(i). Global:

***Post-Northridge*: ϕ_{RC}**

	3-story	9-story	20-story
ϕ_{RC}	1.00	1.00	1.00

***Pre- Northridge*: ϕ_{RC}**

	3-story	9-story	20-story
ϕ_{RC}	1.00	0.90	0.83

(ii). Local:

***Post-Northridge*: ϕ_{RC} = 0.94**

***Pre- Northridge*: ϕ_{RC} = 0.87**

ϕ_{UC} = Contribution to ϕ from uncertainties in measured connection capacity

(i). Global:

***Post-Northridge*: ϕ_{UC}**

	3-story	9-story	20-story
ϕ_{UC}	0.90	0.83	0.76

***Pre- Northridge*: ϕ_{UC}**

	3-story	9-story	20-story
ϕ_{UC}	0.90	0.83	0.76

(ii). Local:

***Post-Northridge*: ϕ_{UC} = 0.91**

***Pre- Northridge*: ϕ_{UC} = 0.91**

Therefore, default value for ϕ is,

ϕ	Global	Local
Post-Northridge	0.85	0.90
Pre- Northridge	0.70	0.80

Demand factor

$\gamma = e^{\frac{k\,\beta_{RD}^2}{2\,b}}$ = γ_{RD} = randomness in demand

β_{RD} = $\sqrt{\sum\left(\beta_{acc}^2 + \beta_{or}^2\right)}$: near the source

= β_{acc} : not near the source

***Post-Northridge*: β_{RD}**

	near source		not near source	
	CP	**IO**	**CP**	**IO**
3-story	0.43	0.51	0.38	0.51
9-story	0.36	0.45	0.30	0.45
20-story	0.52	0.47	0.45	0.47

***Pre-Northridge*: β_{RD}**

	near source		not near source	
	CP	**IO**	**CP**	**IO**
3-story	0.47	0.48	0.42	0.48
9-story	0.53	0.40	0.49	0.40
20-story	0.62	0.54	0.56	0.54

Therefore, default value for $\gamma = \gamma_{RD}$ is

***Post-Northridge*: γ**

	near source		not near source	
	CP	**IO**	**CP**	**IO**
3-story	1.33	1.48	1.24	1.48
9-story	1.21	1.35	1.14	1.35
20-story	1.50	1.39	1.35	1.39

***Pre-Northridge*: γ**

	near source		not near source	
	CP	**IO**	**CP**	**IO**
3-story	1.39	1.41	1.30	1.41
9-story	1.52	1.27	1.43	1.27
20-story	1.78	1.55	1.60	1.55

$\gamma_a = \gamma_{UD} = e^{\frac{k\,\beta_{UD}^2}{2\,b}}$ = analysis demand factor

β_{NTH} = associated with uncertainties in the nonlinear time history analysis procedure

$\beta_{B.F.}$ = associated with uncertainty in the bias factor which is quite small

$\beta_{damping}$ = associated with uncertainty in the estimating the damping value of the structure which is quite small.

$\beta_{live\ load}$ = associated with uncertainty in live load applied which is quite small.

$\beta_{material\ property}$ = associated with uncertainty in material property which is quite small

Therefore, $\beta_a = \sqrt{\beta_{B.F.}^2 + \beta_{NTH}^2}$

***Post-Northridge*:** β_a and γ_a

Analysis Procedure	$\beta_{B.F.}$		β_{NTH}		β_a		γ_a	
3-story								
	2/50	50/50	2/50	50/50	2/50	50/50	2/50	50/50
97 NEHRP-LSP	0.08	0.11	0.15	0.15	0.17	0.18	1.04	1.05
F273-LSP	0.06	0.11	0.15	0.15	0.16	0.18	1.04	1.05
F273-MAP	0.04	0.11	0.15	0.15	0.15	0.18	1.04	1.05
Linear-THP	0.06	0.08	0.15	0.15	0.16	0.17	1.04	1.05
F273-NSP	0.08	0.10	0.15	0.15	0.17	0.18	1.04	1.05
CSM-NSP	0.06	0.10	0.15	0.15	0.16	0.18	1.04	1.05
9-story								
97 NEHRP-LSP	0.04	0.06	0.20	0.20	0.20	0.21	1.06	1.07
F273-LSP	0.08	0.06	0.20	0.20	0.21	0.21	1.07	1.07
F273-MAP	0.07	0.04	0.20	0.20	0.21	0.20	1.07	1.06
Linear-THP	0.04	0.05	0.20	0.20	0.20	0.21	1.06	1.07
F273-NSP	0.10	0.07	0.20	0.20	0.21	0.21	1.08	1.07
CSM-NSP	0.06	0.07	0.20	0.20	0.21	0.21	1.07	1.07
20-story								
97 NEHRP-LSP	0.01	0.03	0.25	0.25	0.25	0.25	1.10	1.10
F273-LSP	0.02	0.03	0.25	0.25	0.25	0.25	1.10	1.10
F273-MAP	0.01	0.03	0.25	0.25	0.25	0.25	1.10	1.10
Linear-THP	0.01	0.00	0.25	0.25	0.25	0.25	1.10	1.10
F273-NSP	0.03	0.01	0.25	0.25	0.25	0.25	1.10	1.10
CSM-NSP	0.01	0.01	0.25	0.25	0.25	0.25	1.10	1.10

***Pre-Northridge*:** β_a and γ_a

Analysis Procedure	$\beta_{B.F.}$		β_{NTH}		β_a		γ_a	
3-story								
	2/50	50/50	2/50	50/50	2/50	50/50	2/50	50/50
97 NEHRP-LSP	0.097	0.137	0.15	0.15	0.19	0.20	1.06	1.06
F273-LSP	NA	NA	NA	NA	NA	NA	NA	NA
F273-MAP	0.191	0.125	0.15	0.15	0.24	0.20	1.09	1.06
Linear-THP	0.064	0.103	0.15	0.15	0.16	0.18	1.04	1.05
F273-NSP	0.098	0.151	0.15	0.15	0.18	0.21	1.05	1.07
CSM-NSP	NA	NA	NA	NA	NA	NA	NA	NA
9-story								
97 NEHRP-LSP	0.093	0.109	0.20	0.20	0.22	0.23	1.08	1.08
F273-LSP	NA	NA	NA	NA	NA	NA	NA	NA
F273-MAP	0.235	0.100	0.20	0.20	0.31	0.22	1.16	1.08
Linear-THP	0.072	0.087	0.20	0.20	0.21	0.22	1.08	1.08
F273-NSP	0.034	0.027	0.20	0.20	0.20	0.20	1.06	1.06
CSM-NSP	NA	NA	NA	NA	NA	NA	NA	NA
20-story								
97 NEHRP-LSP	0.058	0.019	0.25	0.25	0.26	0.25	1.11	1.11
F273-LSP	NA	NA	NA	NA	NA	NA	NA	NA
F273-MAP	0.090	0.113	0.25	0.25	0.27	0.27	1.12	1.12
Linear-THP	0.223	0.170	0.25	0.25	0.34	0.30	1.19	1.15
F273-NSP	0.192	0.034	0.25	0.25	0.32	0.25	1.17	1.11
CSM-NSP	NA	NA	NA	NA	NA	NA	NA	NA

NA: not available

Therefore, default value for $\boldsymbol{\gamma_a}$ is,

	Post-Northridge	**Pre-Northridge**
	CP & IO	**CP & IO**
3-story	1.05	1.10
9-story	1.07	1.15
20-story	1.10	1.20

β_{UT} = **total uncertainty**

$$\beta_{UT} = \sqrt{\left(\beta_{UC}^{\ 2} + \beta_{UD}^{\ 2}\right)}$$

Using default values for the β_a,

***Post-Northridge*: β_{UT}**

	CP against global collapse for 2/50	CP against local collapse for 2/50	IO for 50/50	CP against global collapse for 50/50	CP against local collapse for 50/50
3-story	0.32	0.30	0.30	0.32	0.30
9-story	0.40	0.32	0.32	0.40	0.32
20-story	0.50	0.35	0.35	0.50	0.35

***Pre-Northridge*: β_{UT}**

	CP against global collapse for 2/50	CP against local collapse for 2/50	IO for 50/50	CP against global collapse for 50/50	CP against local collapse for 50/50
3-story	0.36	0.35	0.35	0.36	0.35
9-story	0.46	0.39	0.39	0.46	0.39
20-story	0.55	0.43	0.43	0.55	0.43

λ_{con} = **confidence factor – used to determine the confidence level**

$$\lambda_{con} = e^{\left[K_x \beta_{UT} - \frac{1}{2} k \beta_{UT}^2\right]}$$

where:

λ_{con} = confidence factor

β_{UT}^2 = $\Sigma\sigma_i^2$ where σ_i is for uncertainties in the demand and capacity but not randomness

k = slope of the hazard curve

K_x = standard Gaussian variate associated with probability x of not being exceeded (found in standard probability tables).

From the preceding sections, the following β's need to be included: β_U, capacity; β_a, analysis procedures. If the relationship is rewritten in terms of K_x,

$$K_x = \left[\ln(\lambda_{con}) + \frac{1}{2} \cdot k \cdot \beta_{UT}^2 \right] \cdot \frac{1}{\beta_{UT}}$$

B.2 Bias Factors

B.2.1 Post-Northridge Bias Factors

(i). Calculated Bias Factors

Bias Factors Using Empirical Equation for Fundamental Period

	3-story		9-story		20-story	
	2/50	**50/50**	**2/50**	**50/50**	**2/50**	**50/50**
N97-LSP	***0.72***	***0.62***	***0.81***	***0.76***	***1.15***	***0.87***
F273-LSP	***0.50***	***0.62***	***0.82***	***0.76***	***0.83***	***0.87***
N97-MAP	0.78	0.78	1.05	0.87	1.10	1.10
F273-LDP	0.79	0.97	1.13	1.08	1.01	1.15
LTHP	0.86	0.85	0.91	0.99	0.90	1.09
F273-NSP	0.84	1.11	0.95	1.35	0.84	2.01
CSM-NSP	1.33	1.29	1.48	1.52	1.34	2.05

Bias Factors Using Calculated Fundamental Period

	3-story		9-story		20-story	
	2/50	**50/50**	**2/50**	**50/50**	**2/50**	**50/50**
N97-LSP	***0.90***	***0.87***	***1.14***	***1.06***	***1.35***	***1.02***
F273-LSP	***0.63***	***0.87***	***0.82***	***1.06***	***0.97***	***1.02***
N97-MAP	0.78	0.78	1.05	0.87	1.10	1.10
F273-LDP	0.79	0.97	1.13	1.08	1.01	1.15
LTHP	0.86	0.85	0.91	0.99	0.90	1.09
F273-NSP	0.84	1.11	0.95	1.35	0.84	2.01
CSM-NSP	1.33	1.29	1.48	1.52	1.34	2.05

(ii). Recommended Bias Factors

Bias Factors Using Empirical Equation for Fundamental Period

	3-story		9-story		20-story	
	2/50	**50/50**	**2/50**	**50/50**	**2/50**	**50/50**
N97-LSP	***0.75***	***0.65***	***0.80***	***0.75***	***1.15***	***0.90***
F273-LSP	***0.50***	***0.65***	***0.85***	***0.75***	***0.85***	***0.90***
N97-MAP	0.80	0.80	1.05	0.90	1.10	1.10
F273-LDP	0.80	1.00	1.15	1.10	1.00	1.15
LTHP	0.85	0.85	0.90	1.00	0.90	1.00
F273-NSP	0.85		0.95		0.85	
CSM-NSP	1.30		1.50		1.35	

Bias Factors Using Calculated Fundamental Period

	3-story		9-story		20-story	
	2/50	**50/50**	**2/50**	**50/50**	**2/50**	**50/50**
N97-LSP	***0.90***	***0.90***	***1.15***	***1.10***	***1.35***	***1.05***
F273-LSP	***0.65***	***0.90***	***0.85***	***1.10***	***1.00***	***1.05***
N97-MAP	0.80	0.80	1.05	0.90	1.10	1.10
F273-LDP	0.80	1.00	1.15	1.10	1.00	1.15
LTHP	0.85	0.85	0.90	1.00	0.90	1.00
F273-NSP	0.85		0.95		0.85	
CSM-NSP	1.30		1.50		1.35	

B.2.2 Pre-Northridge Bias Factors

(i). Calculated Bias Factors

Bias Factors Using Empirical Equation for Fundamental Period

	3-story		9-story		20-story	
	2/50	**50/50**	**2/50**	**50/50**	**2/50**	**50/50**
N97-LSP	***0.84***	***0.42***	***0.95***	***0.55***	***0.88***	***0.65***
F273-LSP	***0.58***	***0.42***	***0.65***	***0.55***	***0.61***	***0.65***
N97-MAP	0.86	0.66	0.99	0.59	1.09	0.79
F273-LDP	1.19	0.98	1.29	1.05	1.22	1.28
LTHP	1.35	0.92	1.17	1.03	0.98	1.13
F273-NSP	1.25	0.90	1.33	1.08	1.31	1.31

Bias Factors Using Calculated Fundamental Period

	3-story		9-story		20-story	
	2/50	**50/50**	**2/50**	**50/50**	**2/50**	**50/50**
N97-LSP	***1.26***	***0.73***	***1.40***	***0.81***	***1.02***	***0.76***
F273-LSP	***0.87***	***0.73***	***0.96***	***0.81***	***0.70***	***0.76***
N97-MAP	0.86	0.66	0.99	0.59	1.09	0.79
F273-LDP	1.19	0.98	1.29	1.05	1.22	1.28
LTHP	1.35	0.92	1.17	1.03	0.98	1.13
F273-NSP	1.25	0.90	1.33	1.08	1.31	1.31

(ii). Recommended Bias Factors

Bias Factors Using Empirical Equation for Fundamental Period

	3-story		9-story		20-story	
	2/50	**50/50**	**2/50**	**50/50**	**2/50**	**50/50**
N97-LSP	***0.85***	***0.45***	***0.95***	***0.55***	***0.90***	***0.65***
F273-LSP	***0.60***	***0.45***	***0.65***	***0.55***	***0.60***	***0.65***
N97-MAP	0.90	0.70	1.00	0.60	1.10	0.80
F273-LDP	1.20	1.00	1.30	1.05	1.20	1.30
LTHP	1.35	0.95	1.20	1.05	1.00	1.15
F273-NSP	1.25		1.35		1.30	

Bias Factors Using Calculated Fundamental Period

	3-story		9-story		20-story	
	2/50	**50/50**	**2/50**	**50/50**	**2/50**	**50/50**
N97-LSP	***1.25***	***0.75***	***1.40***	***0.80***	***1.00***	***0.75***
F273-LSP	***0.90***	***0.75***	***1.00***	***0.80***	***0.70***	***0.75***
N97-MAP	0.90	0.70	1.00	0.60	1.10	0.80
F273-LDP	1.20	1.00	1.30	1.05	1.20	1.30
LTHP	1.35	0.95	1.20	1.05	1.00	1.15
F273-NSP	1.25		1.35		1.30	

REFERENCES, FEMA REPORTS, SAC REPORTS, ACRONYMS, AND LIST OF SYMBOLS

References.

AISC, 1994, *Manual of Steel Construction: Load & Resistance Factor Design*, Vol. 1 and 2., American Institute of Steel Construction, Chicago, Illinois.

AISC, 1997, *Seismic Provisions for Structural Steel Buildings*, American Institute of Steel Construction, Chicago, Illinois.

Allahabadi, R., and Powell, G.H., 1988, *DRAIN-2DX User Guide*, UCB/EERC 88/06, University of California, Berkeley.

Anderson, J., Duan, J., Maranian, P., and Xiao Y., 2000, *Improvement of Welded Connections Using Fracture Tough Overlays*, SAC/BD-00/20.

Anderson, J.C., and Bertero, V., 1991, *Seismic Performance of an Instrumented 6-Story Steel Buildings*, EERC-91/11, University of California, Berkeley.

Anderson, J.C., and Bertero, V.V., 1987, "Uncertainties in Establishing Design Earthquakes," *Journal of Structural Engineering*, ASCE, Vol. 113, No. 8.

Anderson, J.C., Johnston, R.G, and Partridge, J.G., 1995, *Post Earthquake Studies of a Damaged Low Rise Office Building* (CE95-07), Department of Civil Engineering, University of Southern California, pp. 3-1/3-146.

ATC, 1974, *An Evaluation of a Response Spectrum Approach to Seismic Design of Buildings*," ATC-2, Applied Technology Council, Redwood City, California.

ATC, 1978, *Tentative Provisions for the Development of Seismic Regulations for Buildings*, ATC 3-06, Applied Technology Council, Redwood City, California.

ATC, 1982, *An Investigation of the Correlation Between Earthquake Ground Motion and Building Performance*, ATC-10, Applied Technology Council , Redwood City, California.

ATC, 1984, *Comparison of Seismic Design Practices in the United States and Japan*, ATC-15, Applied Technology Council, Redwood City, California.

ATC, 1995, *Structural Response Modification Factors*, ATC-19, Applied Technology Council, Redwood City, California.

ATC, 1995, *A Critical Review of Current Approaches to Earthquake Resistant Design*, ATC-34, Applied Technology Council, Redwood City, California.

ATC, 1996, *Seismic Evaluation and Retrofit of Concrete Buildings*, ATC-40, Applied Technology Council, Redwood City, California.

ATC, 1997a, *NEHRP Guidelines for the Seismic Rehabilitation of Buildings*, FEMA-273, prepared by the Applied Technology Council, Redwood City, California, for the Building Seismic Safety Council, published by the Federal Emergency Management Agency, Washington, DC.

ATC, 1997b, NEHRP *Commentary on the Guidelines for the Seismic Rehabilitation of Buildings*, FEMA-274, prepared by the Applied Technology Council, Redwood City, California, for the Building Seismic Safety Council, published by the Federal Emergency Management Agency, Washington, DC.

Astaneh-Asl, A., Nader, M.N., and Harriott, J.D., 1991, "Seismic Behavior and Design Considerations in Semi-Rigid Frames," *Proceedings of the 1991 National Steel Construction Conference*, American Institute of Steel Construction, Chicago, Illinois.

Barsom, J.M., 1999, *Failure Analysis of Welded Beam to Column Connections*, SAC/BD-99/23.

Bertero, V.V., and Kamil, H., 1974, "Nonlinear Seismic Design of Multistory Frames," *Canadian Journal of Civil Engineering*, Vol. 2, No. 4, pp. 494-516.

Bertero, V.V., et al., 1976, "Establishment of Design Earthquakes-Evaluation of Present Methods," *Proceedings*, International Symposium on Earthquake Structural Methods, St. Louis, Missouri, pp. 551-580.

Bertero, V.V., and Bresler, B., 1977, "Design and Engineering Decisions: Failure Criteria (Limit State)," *Proceedings*, Sixth World Conference on Earthquake Engineering, New Delhi, India.

Bertero, V.V., 1986, "Evaluation of Response Reduction Factors Recommended by ATC and SEAOC," *Proceedings*, Third U.S. National Conference on Earthquake Engineering, Charleston, South Carolina, Earthquake Engineering Research Institute, El Cerrito, California, Vol. III, pp. 1663-1673.

Bertero, V.V., 1986, *Lessons Learned from Recent Earthquakes and Research Implications for Earthquake-Resistant Design of Building Structures in U.S.*, UCB/EERC-86/03, Earthquake Engineering Research Center, University of California, Berkeley.

Bertero, V.V., 1988, "Ductility-Based Structural Design," *Proceedings*, Ninth World Conference on Earthquake Engineering, Tokyo-Kyoto, Japan, Vol. VIII, pp. 673-685.

Bertero, V.V., and Miranda, E., 1990, *Analysis of the Implications of the Ground Motions Recorded During the Loma Prieta Earthquake*, In-House Report, Earthquake Engineering Research Center, University of California, Berkeley.

Bertero, V.V., Anderson, J.C., Krawinkler, H., and Miranda, E., 1991, "The CUREe and Kajima Research Teams," *Design Guidelines For Ductility and Drift Limits*, UBC/EERC-91/15, Earthquake Engineering Research Center, University of California, Berkeley.

Bertero, V.V., and Uang, C.M., 1992, "Issues and Future Directions in the Use of an Energy Approach for Seismic-Resistant Design of Structures," *Nonlinear Seismic Analysis and Design of Reinforced Concrete Buildings*, Edited by Fajfar, P., Krawinkler, H., and Elsevier H., Applied Science, London and New York.

Biddah, A., and Heidebrecht, A.C., 1998, "Seismic Performance of Moment-Resisting Steel Frame Structures Designed for Different Levels of Seismic Hazard," *Earthquake Spectra*, pp. 597-627.

Bonowitz, D., and Youssef, N., 1995, *Technical Report: Surveys and Assessment of Damage to Buildings Affected by the Northridge Earthquake of January 17, 1994*, SAC 95-06, pp. 2-1/2-169.

BOCA, 1999, *National Building Code*, Building Officials and Code Administrators, www.bocai.org.

BSSC, 1985, *NEHRP Recommended Provisions for Seismic Regulations for New Buildings*, prepared by the Building Seismic Safety Council for the Federal Emergency Management Agency, Washington, DC.

BSSC, 1997a, *NEHRP Recommended Provisions for Seismic Regulations for New Buildings and Other Structures, Part 1 – Provisions*, FEMA-302, prepared by the Building Seismic Safety Council for the Federal Emergency Management Agency, Washington, DC.

BSSC, 1997b, *NEHRP Recommended Provisions for Seismic Regulations for New Buildings and Other Structures, Part 2 – Provisions*, FEMA-303, prepared by the Building Seismic Safety Council for the Federal Emergency Management Agency, Washington, DC.

Chen, P-T, and Collins, K.R., 1999, *Investigation of Pushover Analysis Procedures for Reliability-Based and Performance-Based Seismic Design with Applications to Asymmetric Building Structures*, Department of Civil Engineering, University of Michigan, Ann Arbor.

Chen, C.C., Bonowitz, D., and Astaneh-Asl, A., 1992, *Studies of a 49-Story Instrumented Steel Structure Shaken During the Loma Prieta Earthquake*, EERC-92/01, University of California, Berkeley.

Collins, K.R., Wen, Y.K., and Foutch, D.A., 1996, "Dual-Level Seismic Design: A Reliability-Based Methodology," *Earthquake Engineering and Structural Dynamics*, 25, pp. 1433-1467.

Chen, W.F., and Yamaguchi, E., 1996, "Spotlight on Steel Moment Frames," *Civil Engineering*, March.

Chen, W.F., and Atsuta, T., 1976, *Theory of Beam-Columns*, Vols. 1 and 2, McGraw-Hill, New York.

Choi, J., Stojadinovic, B., and Goel, S.C., 1999, *Parametric Tests on the Free Flange Connections*, SAC/BD-00/02.

Chopra, A.K., 1995, *Dynamics of Structures: Theory and Applications to Earthquake Engineering*, Prentice Hall, New Jersey.

Clark, P., 2000, *Design of Steel Moment Frame Model Buildings in Los Angeles, Seattle and Boston*, SAC/BD-00/08.

Clark, P., 2000, *Development of Improved Post-Earthquake Inspection Procedures for Steel Moment Frame Buildings*, SAC/BD-00/11.

Cofie, N.G., and Krawinkler, H., 1985, "Uniaxial Cyclic Stress-Strain Behavior of Structural Steel," *Journal of Engineering Mechanics*, ASCE, Vol. III, No. 9.

Cornell, A.C., 1999, "Critical – SAC Uncertainties: Meeting on November 16, 1999," Personal Communication, Palo Alto, California.

Cornell, A.C., 1999, "SAC Uncertainties: Meeting on December 2, 1999," Personal Communication, Palo Alto, California.

Cornell, A.C., 2000, "SAC Uncertainties and Correlation of Uncertainties," Personal Communication, March 28-April 3.

Cosenza, E., Manfredi, G., and Ramasco, K., 1990, "An Evaluation of the Use of Damage Functionals in Earthquake Resistant Design," *Proceedings*, 9th European Conference on Earthquake Engineering, Moscow.

Court, A.B., and Kowalsky, M.J., 1998, "Performance-Based Engineering of Buildings – a Displacement Design Approach," *Proceedings*, 6th U.S. National Conference on Earthquake Engineering, Seattle, Washington, May 31-June 4, 1998, Earthquake Engineering Research Institute, Oakland, California.

Deierlein, G.G., 1998, "Summary of SAC Case Study Building Analyses," *Journal of Performance of Construction Facilities,"* ASCE, 12(4), 202-212.

Deierlein, G.G., and Chi, W., 1999, *Integrative Analytical Investigations on the Fracture Behavior of Welded Moment Resisting Connections*, SAC/BD-99/15.

Deirlein, G.C., and Hsieh, S.-H, 1990, "Seismic Response of Steel Frames with Semi-Rigid Connections Using the Capacity Spectrum Method," *Proceedings*, Fourth U.S. National Conference on Earthquake Engineering, May 20-24, Palm Springs, California, Vol. 2, pp. 863-872.

Department of the Army, the Navy and the Air Force, 1986, *Seismic Design Guidelines for Essential Buildings*.

DRAIN-2DX, 1993, *DRAIN-2DX: Basic Program Description and User* Guide, UCB/SEMM-93/17, by Prakash, V., Powell, G.H., and Campbell, S., University of California, Berkeley.

Duan, X., and Anderson, J.C., 1999, *Elastic Models for Predicting Building Performance*, SAC/BD-99/21.

Durkin, M.E., 1995, "Inspection, Damage, and Repair of Steel Frame Buildings following the Northridge Earthquake", *Technical Report: Surveys and Assessment of Damage to Buildings Affected by the Northridge Earthquake of January 17, 1994*, SAC 95-06, pp. 1-1/1-41.

Elghadanisi, F.E., and Mohraz, B., 1987, "Inelastic Earthquake Spectra," *Journal of Earthquake Engineering and Structural Dynamics*, 15, pp. 91-104.

Engelhardt, M., Fry, G., Johns, S., Venti, M., and Holliday, S., 2000, *Behavior and Design of Radius-Cut, Reduced Beam Section Connections*, SAC/BD-00/17.

FEMA-222A, 1995, *1994 Edition: NEHRP Recommended Provisions for Seismic Regulations for New Buildings*, Federal Emergency Management Agency, Washington, DC.

FEMA-223A, 1995, *1994 Edition: NEHRP Recommended Provisions for Seismic Regulations for New Buildings, Part 2 – Commentary*, Federal Emergency Management Agency, Washington, DC.

FEMA-267, 1995, *Interim Guidelines: Evaluation, Repair, Modification and Design of Welded Steel Moment Frame Structures*, Federal Emergency Management Agency, Washington, DC.

FEMA-273, 1997a, *NEHRP Guidelines for the Seismic Rehabilitation of Buildings*, prepared by the Applied Technology Council, Redwood City, California, for the Building Seismic Safety Council, published by the Federal Emergency Management Agency, Washington, DC.

FEMA-274, 1997b, *NEHRP Commentary on Guidelines for the Seismic Rehabilitation of Buildings*, prepared by the Applied Technology Council, Redwood City, California, for the Building Seismic Safety Council, published by the Federal Emergency Management Agency, Washington, DC.

FEMA-302 and FEMA 303, 1998, *NEHRP Recommended Provisions for Seismic Regulations for New Buildings and Other Structures (Part 1–Provisions) and (Part 2–Commentary)*, Federal Emergency Management Agency, Washington, DC.

Foutch, D.A, Yun, S., and Lee, K., 1998, "Comparative Reliability of Linear and Nonlinear Approaches to Demand Characterization in Steel Structures," *Proceedings*, 6th U.S. National Conference on Earthquake Engineering, Seattle, Washington, May 31-June 4, 1998, Earthquake Engineering Research Institute, Oakland, California.

Foutch, D.A., 1976, *A Study of the Vibration Characteristics of Two Multistory Buildings*, EERL 76-03, California University Institute of Technology.

Foutch, D.A., 2000, *State of the Art Report on Performance Prediction and Evaluation for Steel Moment-Frame Buildings*, 90% Draft, prepared by the SAC Joint Venture for the Federal Emergency Management Agency, Washington, DC.

Foutch, D.A., and Shi, S., 1997, *Connection Element (Type 10) for DRAIN-2DX*, Internal Report, University of Illinois, Urbana, Champaign.

Foutch, D.A., and Shi, S., 1998, "Effects of Hysteresis Types on the Seismic Effects of Buildings," *Proceedings*, 6th U.S. National Conference on Earthquake Engineering, Seattle, Washington, May 31 - June 4, 1998, Earthquake Engineering Research Institute, Oakland, California.

Foutch, D.A., Calabrese, F.A., and Yu, C-Y., 1990, "Vibration of Steel Buildings Shaken by The Whittier Earthquake," *Proceedings of 4th U.S. National Conference on Earthquake Engineering*, Palm Beach, California.

Foutch, D.A., Yun, S.Y., and Lee, K., 1998, "Comparative Reliability of Linear and Nonlinear Approaches to Demand Characterization in Steel," *Structural Engineers World Congress*, San Francisco, California.

Foutch, D.A., Yun, S.Y., and Lee, K., 1999, "Analysis and Behavior of Steel Buildings," *ASCE 1999 Structures Congress*, New Orleans, Louisiana.

Foutch, D.A., Yun, S.Y., and Lee, K., 2000, "Performance Prediction for Steel Moment Frames," *ASCE 2000 Structures Congress*, Philadelphia, Pennsylvania.

Foutch, D.A., Goel, S.C., and Roeder, C.W., 1987, "Seismic Testing of Full-scale Steel Building, Part 1," *Journal of Structural Engineering*, ASCE, 113(11), pp. 2111-2129.

Freeman, S.A., 1990, "On the Correlation of Code Forces to Earthquake Demands," *Proceedings of Fourth U.S.-Japan Workshop on Improvement of Building Structural Design and Construction Practices*, ATC-15-3, Redwood City, California.

Frye, M.J., and Morris, G.A., 1975, "Analysis of Flexibly Connected Steel Frames," *Canadian Journal of Civil Engineering*, 2(3).

Gates, W.E., 1995, "Interpretation of SAC Survey Data on Damaged Welded Steel Moment Frames following the Northridge Earthquake", *Technical Report: Surveys and Assessment of Damage to Buildings Affected by the Northridge Earthquake of January 17, 1994*, SAC 95-06, prepared by the SAC Joint Venture for the Federal Emergency Management Agency, pp. 4-1/4-10.

Gates, W.E., and Morden M., 1995, "Lessons from Inspection, Evaluation, Repair and Construction of Welded Steel Moment Frames following the Northridge Earthquake", *Technical Report: Surveys and Assessment of Damage to Buildings Affected by the Northridge Earthquake of January 17, 1994*, SAC 95-06, prepared by the SAC Joint Venture for the Federal Emergency Management Agency, pp. 3-1/3-79.

Ghobarah, A., Osman, A., and Korol, R.M., 1990, "Behavior of Extended End-Plate Connections under Cyclic Loading," *Engineering Structures*, Vol. 12, No. 1.

Gilton, C., Chi, B., and Uang, C.M., 2000, *Cyclic Response of RBS Moment Connections: Weak Axis Configuration and Deep Column Effects*, SAC/BD-00/23.

Goel, R.K., and Chopra, A.K., 1997, *Vibration Properties of Buildings Determined From Recorded Earthquake Motions*, UCB/EERC-97/14, University of California, Berkeley.

Gomez, R., and Garcia-Rang, F., 1988, "Complementary Technical Norms for Earthquake Resistant Design," *Earthquake Spectra*, EERI, 4 (3), pp. 441-460.

Graham, J.D., Sherbourne, A.N., Khabbaz, R.N., and Jensen, C.D., 1959, "Welded Interior Beam-to-Column Connections," *AISC Publication*, A.I.A. File No. 13-C.

Green, M., 1995, "Santa Clarita City Hall: Northridge Damage", *Technical Report: Case Studies of Steel-Moment Frame Building Performance in the Northridge Earthquake of January 17, 1994*, SAC 95-07, prepared by the SAC Joint Venture for the Federal Emergency Management Agency, Washington, DC, pp. 1-1/1-13.

Gupta, A., and Krawinkler, H., 2000, *Benchmarking of Analysis Programs for SMRF System Performance Studies*, SAC/BD-00/09.

Gupta, A., and Krawinkler, H., 1998, "Effect of Stiffness Degradation on Deformation Demands for SDOF and MDOF Structures" *Proceedings*, 6th U.S. National Conference on Earthquake Engineering, Seattle, Washington, May 31-June 4, 1998, Earthquake Engineering Research Institute, Oakland, California.

Gupta, A., and Krawinkler, H., 1998, "Influence of Design Parameters on Connection Demands," *Proceedings of the First International Congress of Structural Engineers*, July 19-23, 1998, San Francisco, California.

Gupta, A., and Krawinkler, H., 1998, "Influence of Design Parameters on Connection Demands," *Proceedings*, 6th U.S. National Conference on Earthquake Engineering, Seattle, Washington, May 31-June 4, 1998, Earthquake Engineering Research Institute, Oakland, California.

Hajjar, J.F., Gourley, B.C., O'Sullivan, D.P., and Leon, R.T., 1998, "Analysis of Mid-Rise Steel Frame Damaged in Northridge Earthquake," *Journal of Performance of Constructed Facilities*, ASCE, 12(4), pp. 221-231.

Hajjar, J.F., O'Sullivan, D.P., Leon R.T., and Gourley, B.C., 1995, "Evaluation of Damage to the Borax Corporate Headquarters Building as a Result of the Northridge Earthquake,"*Technical Report: Case Studies of Steel Moment-Frame Building Performance in the Northridge Earthquake of January 17, 1994*, SAC 95-07, prepared by the SAC Joint Venture for the Federal Emergency Management Agency, Washington, DC, pp. 2-1/2-76.

Hamburger, R.O., 1996, "Performance-Based Seismic Engineering: The Next Generation of Structural Engineering Practice," *EQE Summary Report.*

Hamburger, R.O., Foutch, D.A., and Cornell, C.A., 2000, "Performance Basis of Guidelines for Evaluation, Upgrade and Design of Moment-Resisting Steel Frames," *12th World Conference in Earthquake Engineering*, Auckland, New Zealand.

Han, S.W., Oh Y-H, Lee L-H, and D.A. Foutch, 1999, *Effect of Hysteretic Models on the Inelastic Response Spectra*, SRS-No. 628, Department of Civil Engineering, University of Illinois, Urbana, Champaign.

Housner, G.W., 1956, "Limit Design of Structures to Resist Earthquakes," *Proceedings*, World Conference on Earthquake Engineering, Berkeley, California, pp. 501-511.

ICBO, 1997, *Uniform Building Code*, International Conference of Building Officials, Whittier, California.

Jalayer, F., and Cornell, A., 1998, *Development of a Probability-Based Demand and Capacity Factor Design Seismic Format*, Draft 8/11/98, Publication as a SAC Background Document Pending.

Johnson, M.Q., 2000, *Evaluation of the Effect of Welding Procedure on the Mechanical Properties of FCAW-S and SMAW Weld Metal Used in the Construction of Seismic Moment Frames*, SAC/BD-00/12.

Johnson, M.Q., 2000, *Preliminary Evaluation of Heat Affected Zone Toughness in Structural Shapes Used in the Construction of Seismic Moment Frames*, SAC/BD-00/13.

Johnson, M.Q., Mohr, W., and Barsom, J., 2000, *Evaluation of Mechanical Properties in Full-Scale Connections and Recommended Minimum Weld Toughness for Moment Resisting Frames*, SAC/BD-00/14.

Kappos, A.J., 1990, "Sensitivity of Calculated Inelastic Seismic Response to Input Motion Characteristics," *Proceedings*, Fourth U.S. National Conference on Earthquake Engineering, May 20-24, Palm Springs, California, Vol. 2, pp. 25-34.

Kasai, K., and Maison, B.F., 1999, *Effects of Partially Restrained Connection Stiffness and Strength on Frame Seismic Performance*, Draft Report SAC002.

Kasai, K., Maison, B.F., and Mayangarum, A., 1999, *Effects of Partially-Restrained Connection Stiffness and Strength on Frame Seismic Performance*, SAC/BD-99/17.

Kato, B., Aoki, H., and Tagawa, Y., 1984, "Seismic Behavior of Steel Frames with Composite Girders," *Proceedings*, 8th World Conference on Earthquake Engineering, San Francisco, California, Vol. VI.

Kaufman, E.J., and Fisher, J.F., 1996, *A Study of the Effects of Material and Welding Factors on Moment Frame Weld Joint Performance Using Small-Scale Tension Specimen*, SAC Report.

Kim, K., 1995, "Development of Analytical Models for Earthquake Analysis of Steel Moment Frames," Ph.D. Dissertation, Department of Civil Engineering, University of Texas, Austin.

Kircher, C.A., 1999, *Earthquake Loss Estimation for WSMF Buildings*, SAC/BD-99/13.

Kishi, N., and Chen, W.F., 1990, "Moment-Rotation Relations of Semi-Rigid Connections with Angeles," *Journal of Structural Engineering*, ASCE, Vol. 116, No. 7.

Krawinkler, H., 1978, "Shear Design of Steel Frame Joints," *Engineering Journal*, AISC, Vol. 15, No. 3.

Krawinkler, H., 1994, "New Trends in Seismic Design Methodology," *Proceedings of the 10th European Conference in Earthquake Engineering*, Vienna, Austria.

Krawinkler, H., 1996, "Earthquake Design and Performance of Steel Structures," *EERI Regional Seminar Series*, Chicago, Illinois.

Krawinkler, H., 1996, "Earthquake Design and Structural Performance of Steel Structures," *Bulletin of the New Zealand National Society for Earthquake Engineering*, Vol. 29, No. 4, December 1996, pp. 229-241.

Krawinkler, H., 1996, "Pushover Analysis: Why, How, When, and When Not to Use It," *Proceedings of the 1996 Convention of the Structural Engineers Association of California*, Maui, Hawaii, October 2-4, 1996, pp. 17-36.

Krawinkler, H., 1997, *System Behavior of Structural Steel Frames Subjected to Earthquake Ground Motion*, FEMA-288, Program to Reduce the Earthquake Hazards of Steel Moment Frame Structures-Background Reports, March 1997, pp. 6-1 to 6-42.

Krawinkler, H., 2000, *State of the Art Report on System Performance of Steel Moment Frames Subject to Earthquake Ground Motion*, FEMA-355C, prepared by the SAC Joint Venture for the Federal Emergency Management Agency, Washington, DC.

Krawinkler, H., and Zohrei, M., 1983, "Cumulative Damage in Steel Structures Subjected to Earthquake Ground Motions," *Journal on Computers and Structures*, Vol. 16, No. 1-4.

Krawinkler, H., and Al-Ali, A., 1996, "Seismic Demand Evaluation for a 4-Story Steel Frame Structure Damaged in the Northridge Earthquake," *The Structural Design of Tall Buildings*, Vol. 5, Number 1, March 1996, pp. 1-27, John Wiley & Sons.

Krawinkler, H., and Gupta, A., 1997-1, "Deformation and Ductility Demands in Steel Moment Frame Structures," *Proceedings of the 5th International Colloquium on Stability and Ductility of Steel Structures,* Nagoya, Japan, July 29-31, 1997, pp. 57-68.

Krawinkler, H., and Gupta, A., 1998, "Story Drift Demands for Steel Moment Frame Structures in Different Seismic Regions," *Proceedings,* 6th U.S. National Conference on Earthquake Engineering, Seattle, Washington, May 31-June 4, 1998, Earthquake Engineering Research Institute, Oakland, California.

Krawinkler, H., and Mohasseb, S., 1987, "Effects of Panel Zone Deformations on Seismic Response," *Journal of Constructional Steel Research,* Elsevier Applied Science Publishers, England, Vol. 8.

Krawinkler, H., and Mohasseb, S., 1987, "Effect of Panel Zone Deformations on Seismic Response," *Journal of Constructional Steel Research*, 8, pp, 233-250.

Krawinkler, H., and Popov, E.P., 1982, "Seismic Behavior of Moment Connections and Joints," *Journal of the Structural Division,* ASCE, 108(2), pp. 373-391.

Krawinkler, H., Bertero, V., and Popov, E.P., 1971, *Elastic Behavior of Steel Beam-to-Column Subassemblages*, EERC 71-7, University of California, Berkeley.

Krawinkler, H., Bertero, V.V. and Popov, E.P., 1971, *Inelastic Behavior of Steel Beam-to-column Subassemblages,* Report No. UCB/EERC-71/7, Earthquake Engineering Research Center (EERC), University of California, Berkeley.

Krawinkler, H., et al., 1983, *Recommendations for Experimental Studies on the Seismic Behavior of Steel Components and Materials*, John A. Blume Earthquake Engineering Center, Report No. 61, Department of Civil Engineering, Stanford University.

Krawinkler, H., Gupta, A., Medina, R., and Luco, N., 2000, *Loading Histories for Seismic Performance Testing of SMRF Components and Assemblies*, SAC/BD-00/10.

Kwasniewski, L., Stojadinovic, B., and Goel, S.C., 1999, *Local and Lateral-Torsion Buckling of Wide Flange Beams,* SAC/BD-99/20.

Lawson, R.S., Vance, V., and Krawinkler, H., 1994, "Nonlinear Static Push-over Analysis - Why, When, and How?," *Proceedings of the 5th U.S. Conference in Earthquake Engineering,* Vol. 1, Chicago, Illinois.

Lee, K., and Foutch, D.A., 2000, *Performance Prediction and Evaluation of Steel Special Moment Frames for Seismic Loads*, Report SAC/BD-00/25, SAC Joint Venture.

Lee, K.-H., Stojadinovic, B., Goel, S.C., Margarian, A.G., Choi, J., Wongkaew, A., Reyher, B.P. and Lee, D.Y., 2000, *Parametric Tests on Unreinforced Connections*, SAC/BD-00/01.

Leelataviwat, S., S.C. Goel, and Stojadinovic, B., 1998, *Drift and Yield Mechanism Based Seismic Design and Upgrading of Steel Moment Frames*, Department of Civil Engineering, University of Michigan, Ann Arbor.

Leon, R.T., Hoffman, J.J., and Staeger, T. , 1996, "Partially Restrained Composite Connections," *Steel Design Guide Series*, No. 8, AISC, Chicago, Illinois.

Leon, R.T., *Seismic Performance of Bolted and Riveted Connections*, to be published by SAC.

Leon, R.T., and Forcier, G.P., 1991, "Performance of Semi-Rigid Composite Frames," *Proceedings of the 1991 Annual Technical Session*, Structural Stability Research Council.

Liu, J., and Astaneh-Asl, A. 2000, *Cyclic Tests on Simple Connections Including Effects of the Slab*, SAC/BD-00/03.

Lu, L.W., Wang, S.J., and Lee, S.J., 1988, "Cyclic Behavior of Steel and Composite Joints with Panel Zone Deformation," *Proceedings of the 9th World Conference on Earthquake Engineering*, Vol. IV, Tokyo-Kyoto, Japan.

Luco, N., and Cornell, C.A., 1998, "Effects of Random Connection Fractures on the Demands and Reliability for a 3-Story Pre-Northridge SMRF Structure," *Proceedings*., 6th U.S. National Conference on Earthquake Engineering, Seattle, Washington, May 31-June 4, 1998, Earthquake Engineering Research Institute, Oakland, California.

Luco, N., and Cornell, C.A., 1998, "Seismic Drift Demands for Two SMRF Structures with Brittle Connections," *Proceedings*, 6th U.S. National Conference on Earthquake Engineering, Seattle, Washington, May 31-June 4, 1998, Earthquake Engineering Research Institute, Oakland, California.

Mahin, S.A., Hamburger, R.O., and Malley, J.O., 1998, "National Program to Improve Seismic Performance of Steel Frame Buildings," *Journal of Performance of Constructed Facilities*, ASCE, 12(4), pp. 172-179.

Mahin, S.A., and Bertero, V.V., 1976, "Problems in Establishing and Predicting Ductility in Aseismic Design," *Proceedings*, International Symposium on Earthquake Structural Engineering, St. Louis, Missouri.

Mahin, S.A., and Bertero, V.V., 1981, "An Evaluation of Inelastic Seismic Design Spectra," *Journal, Structural Division of the American Society of Civil Engineers*, 107, No. ST9, pp. 1177-1195.

MaIntosh, R.D., and Pezeshk, S., 1997, "Comparison of Recent U.S. Seismic Codes," *Journal of Structural Engineering*, ASCE, 123(8), pp. 993-1000.

Maison, B.F., and Bonowitz, D., 1999, "How Safe Are Pre-Northridge WSMFs? A Case Study of the SAC Los Angeles 9-Story Building," Opinion Paper *Manual of Steel Construction: Load and Resistant Factor Design*, 1997, American Institute of Steel Construction (AISC), Chicago, Illinois.

Maison, B.F., and D. Bonowitz, 1999, *Simplified Loss Estimation for Pre-Northridge WSMF Buildings*, SAC/BD-99/14.

Maison, B.F., and K. Kasai, 1999, *Seismic Performance of 3 and 9 Story Partially Restrained Moment Frame Buildings*," SAC/BD-99/16.

Mercado, L., and Ungermann, E., *Welded Steel Moment Frames Design in Los Angeles, California Using Pre- and Post Northridge Design Procedure*, to be published by SAC.

Midorikawa, M., Nishiyama, I., and Yamanouchi, H., 1989, "Analytical Evaluation of K-Braced Structure Seismic Test," *Journal of Structural Engineering*, ASCE, Vol.115, No.8.

Miranda, E., 1993, "Evaluation of Site-Dependent Inelastic Seismic Design Spectra," *Journal of Structural Engineering*, ASCE, Vol. 119, No. 5.

Miranda, E., and Bertero, V.V., 1994, "Evaluation of Strength Reduction Factors for Earthquake-Resistant Design," *Earthquake Spectra*, EERI, Vol. 10, No. 2, pp. 357-379.

Mohr, W., 1999, *Weld Acceptance Criteria for Seismically-Loaded Welded Connections*, SAC/BD-99/24.

Moses, F., 1974, "Reliability of Structural Systems," *Journal of the Structural Division*, ASCE, 100 (ST9), pp. 1813-1820.

Murphy, L.M., 1973, *San Fernando, California, Earthquake of Feb. 9, 1971*, U.S. Department of Commerce, National Oceanic and Atmospheric Administration, Environmental Research Laboratories.

Murray, T., and Sumner, E. 2000, *Cyclic Testing of Bolted Moment End-Plate Connections*, SAC/BD-00/21.

Murray, T.M., and Kukreti, A.R., 1988, "Design of 8-Bolt Stiffened Moment End Plate," *Engineering Journal*, AISC, Vol. 25, No. 2.

Naeim, K.S., Reinhorn, A.M., and Sivaselvan, M.V., 1999, *Effects of Hysteretic Deterioration Characteristics on Seismic Response of Moment Resisting Steel Structures*, SAC/BD-99/18.

Nakashima, M., 1994, "Variation of Ductility Capacity of Steel Beam-Columns," *Journal of Structural Engineering*, ASCE, Vol. 120, No. 7.

Nassar, A.A., and Krawinkler, H., 1991, "Seismic Demands for SDOF and MDOF Systems," John A. Blume Earthquake Engineering Center Report No. 95, Department of Civil Engineering, Stanford University, California.

NEHRP, 1988, *Recommended Provisions for the Development of Seismic Regulations for New Buildings*, Federal Emergency Management Agency (FEMA), Building Seismic Safety Council, Washington, D.C.

Newmark, N.M., and Hall, W.J., 1982, *Earthquake Spectra and Design*, EERI Monograph Series, EERI, Oakland, California.

Osteraas, J.D., and Krawinkler, H., 1990, "Strength and Ductility Considerations in Seismic Design," John A. Blume Earthquake Engineering Research Center Report No. 90, Department of Civil Engineering, Stanford University.

Popov, E.P., Blondet, M., Stepanov, L., and Stojadinovic, B., 1996, "Full Scale Steel Beam-Column Connection Tests," *Experimental Investigations of Beam-Column Subassemblages, Part 1 and 2*, SAC 96-01, Part II.

Popov, E.P., and Stephen, R.M., 1970, "Cyclic Loading of Full-Scale Steel Connections," CB/EERC-70/3, Earthquake Engineering Research Center (EERC), University of California, Berkeley.

Popov, E.P., and Stephen, R.M., 1976, "Tensile Capacity of Partial Penetration Welds," Report No. UCB/EERC-76/3, Earthquake Engineering Research Center (EERC), University of California, Berkeley.

Popov, E.P., and Pinkney, R.B., 1969, "Cyclic Yield Reversals on Steel Building Connections," *Journal of the Structural Division,* ASCE, Vol. 95, No. 3.

Prakash, V., Powell, G.H., and Campbell, S., 1993, *DRAIN-2DX, Element Description and User Guide*, University of California, Berkeley.

Prakash, V., Powell, G.H., and Campbell, S., 1993, *DRAIN-2DX, Base Program Description and User Guide*, University of California, Berkeley.

Rahnama, M., and Krawinkler, H., 1993, "Effects of Soft Soils and Hysteresis Models on Seismic Design Spectra," John A. Blume Earthquake Engineering Center Report No. 108, Department of Civil Engineering, Stanford University.

Rahnama, M., and Krawinkler, H., 1994-1, "Amplification of Seismic Demands in Linear and Nonlinear Soft Soils," *Proceedings of the 5th U.S. National Conference on Earthquake Engineering,* Vol. II, Chicago, Illinois.

Rahnama, M., and Krawinkler, H., 1994-2, "Effects of P-delta and Strength Deterioration on SDOF Strength Demands," *Proceedings of the 10th European Conference in Earthquake Engineering,* Vienna, Austria.

Rentschler, G.P., Chen, W.F., and Driscoll, G.C., 1980, "Tests of Beam-to-Column Web Moment Connections," *Journal of the Structural Division,* ASCE, Vol. 106, No. 5.

Ricles, J.M., Mao, C., Kaufmann, E.J., Lu, L.W., and Fisher, J.W., 2000, *Dynamic Tension Tests of Simulated Welded Beam Flange Connections*, SAC/BD-00/07.

Riddell, R., and Newmark, N.M., 1979, "Statistical Analysis of the Response of Nonlinear Systems Subject to Earthquakes," *Civil Engineering Studies, Structures Research Series 468,* University of Illinois, Urbana, Illinois.

Roeder, C.W., 1999, "*Connection Performance*," Draft Report, SAC Joint Venture.

Roeder, C.W., 1999, "*SAC Connection Performance Team Research Results and Prequalified Connection Recommendations*," SAC Joint Venture.

Roeder, C.W., Foutch, D.A., and Goel, S.C., 1987, "Seismic Testing of Full-Scale Building – Part II," *Journal of Structural Engineering*, ASCE, Vol.113, No.11.

Roeder, C.W., Schneider, S.P., and Carpenter, J.E., 1993, "Seismic Behavior of Moment-resisting Steel Frames: Analytical Study," *Journal of Structural Engineering*, ASCE, 119(6), pp. 1866-1884.

Roeder, C., 2000, *SAC Phase 2 Test Plan*, SAC/BD-00/16.

Roeder, C., Coons, R.G. and Hoit, M., 2000, *Simplified Design Models for Predicting the Seismic Performance of Steel Moment Frame Connections*, SAC/BD-00/15.

Roeder, C.W., Schneider, S.P., and Carpenter, J.E., 1993, "Seismic Behavior of Moment-Resisting Steel Frames: Analytical Study," *Journal of Structural Engineering*, ASCE, Vol. 119, No. 6.

Rojahn, C., Whittaker, A., and Hart, G., 1995, *Structural Response Modification Factors*, ATC-19, Applied Technology Council, Redwood City, California.

Rosenblueth, E., et al., 1989, "The Mexico Earthquake of September 19, 1985 - Design Spectra for Mexico's Federal District," *Earthquake Spectra*, Earthquake Engineering Research Institute, Vol. 5, No. 1, pp. 273-292.

SAC, 1995, *Interim Guidelines, Inspection, Evaluation, Repair, Upgrade and Design of Welded Moment Resisting Steel Structures*, FEMA-267, prepared by the SAC Joint Venture for the Federal Emergency Management Agency, Washington, DC. Superseded b FEMA 350.

SAC, 1995, *Steel Moment Frame Connection Advisory No. 3*, SAC 95-01, prepared by the SAC Joint Venture for the Federal Emergency Management Agency, Washington, DC.

SAC, 1995, *Analytical and Field Investigations of Buildings Affected by the Northridge Earthquake of January 17, 1994*, SAC 95-04, Part I and Part II, prepared by the SAC Joint Venture for the Federal Emergency Management Agency, Washington, DC.

SAC, 1997, *Protocol for Fabrication, Inspection, Testing, and Documentation of Beam-Column Connection Tests and Other Experimental Specimens*, SAC/BD-97/02 by Clark, P., Frank, K., Krawinkler, H., and Shaw, R.

Salmon, C.G., and Johnson, J.E., 1996, *Steel Structures: Design and Behavior, Emphasizing Load and Resistance Factor Design*, 4th Edition, Harper Collins College Publishers.

Saunders, C.M., 1998, "Design Criteria for Steel Moment Frame Buildings," *Proceedings, 6th U.S. National Conference on Earthquake Engineering*, Seattle, Washington, May 31-June 4, 1998, Earthquake Engineering Research Institute, Oakland, California.

SEAOC, 1997, *Recommended Lateral Force Requirements and Commentary*, Structural Engineers Association of California, Sacramento, California.

SEAOC Vision 2000 Committee, 1995, *A Framework for Performance Based Design*, Volumes I, II, and III, Structural Engineers Association of California (SEAOC), Sacramento, California.

SBCCI, 1999, *Standard Building Code*, Southern Building Code Congress International, Birmingham, Alabama.

Schneider, S.P., Roeder, C.W., and Carpenter, J.E., 1993, "Behavior of Moment Resisting Steel Frame: Experimental Investigation," *Journal of Structural Engineering*, ASCE, 119(6), pp.1885-1902.

Schneider, S.P., Roeder, C.W., and Carpenter, J.E., 1993, "Behavior of Moment Resisting Steel Frame: Analytical Study," *Journal of Structural Engineering*, ASCE, 119(6), pp. 1866-1884.

Schneider, S.P., Roeder, C.W., and Carpenter, J.E., 1991, "Seismic Performance of Weak-Column Strong-Beam Steel Moment Resisting Frames," *Final Report on Research Sponsored by the National Science Foundation*, Seattle, Washington.

Schneider, S.P., and Teeraparbwong, I., 2000, *Bolted Flange Plate Connections*, SAC/BD-00/05.

Schneider, S.P., and Amidi, A., 1998, "Seismic Behavior of Steel Frames with Deformable Panel Zones," *Journal of Structural Engineering*, ASCE, 124(1), pp. 35-42.

Seekins, L.C., Brady, A.G., and Carpenter, C., 1992, "Digitized Strong-Motion Accelerograms of North and Central American Earthquakes 1933-1986," *United States Geological Survey Digital Data Series DDS-7*.

Seneviratna, G.D.P.K., 1996, *Evaluation of Inelastic MDOF Effects for Seismic Design*, John A. Blume Earthquake Engineering Center Report, Department of Civil Engineering, Stanford University.

Seya, H., Talbot, M.E., and Hwang, H.M., 1993, "Probabilistic Seismic Analysis of a Steel Frame Structure," *Probabilistic Engineering Mechanics*, 8, 127-136.

Shaw, R.E., Jr., 2000, *Round Robin Testing of Ultrasonic Testing Technicians*, SAC/BD-00/06.

Shen, J.H., and Astaneh-Asl, A., 1990, *Seismic Response Evaluation of an Instrumented 6-Story Steel Building*, EERC-90/20, University of California, Berkeley.

Shi, S., 1997, "Evaluation of Connection Fracture and Hysteresis Type on the Seismic Response of Steel Buildings," Ph.D. Thesis, University of Illinois.

Shimazaki, K., 1988, "Strong Ground Motion Drift and Base Shear Coefficient for R/C Structures," *Proceedings*, Ninth World Conference on Earthquake Engineering, Tokyo-Kyoto, Japan, August 2-9, Vol. V, pp. 165-170.

Shimazaki, K., and Sozen, M.A., 1984, *Seismic Drift of Reinforced Concrete Structures*, Technical Research Report Hazama-Gumi Ltd., pp. 145-166.

Shome, N., and Cornell, C.A., 1998, "Normalization and Scaling Accelerograms for Nonlinear Structural Analysis," *Proceedings of the 6th U.S. National Conference on Earthquake Engineering*, May 31 - June 4, 1998, Seattle, Washington.

Shome, N., and Cornell, C.A., 1999, *Probabilistic Seismic Demand Analysis of Nonlinear Structures, Report No. RMS-35*, Department of Civil Engineering, Stanford University, California.

Singhal, A., and Kiremidjian, A.S., 1996, "Method for Probabilistic Evaluation of Seismic Structural Damage," *Journal of Structural Engineering*, ASCE, 122(12), pp. 1459-1467.

Sivakumaran, K.S., and Chen, S., 1994, "Seismic Behavior of Type PR Steel Frames," *Proceedings of the Structures Congress 1994*, ASCE.

Skokan, M.J., and Hart, G.C., 1999, *Reliability-Based Seismic Performance Evaluation of Steel Frame Buildings Using Nonlinear Static Analysis Methods*, SAC/BD-99/22.

Sohal, I.S., and Syed, N.A., 1992, "Inelastic Amplification Factor for Design of Steel Beam-columns," *Journal of Structural Engineering*, ASCE, Vol. 118, No. 7.

Somerville, P., Smith, N., Puntamurthula, S., and Sun, J., 1997, *Development of Ground Motion Time Histories for Phase 2 of the FEMA/SAC Steel Project*, SAC/BD-97/04.

Song, J., and Ellingwood, B., 1999, "Seismic Reliability of Special Moment Frames with Welded Connections: II," *Journal Structural Engineering*, ASCE, 125(4), pp. 372-384.

Song, J., and Ellingwood, B., 1999, "Seismic Reliability of Special Moment Frames with Welded Connections: I," *Journal of Structural Engineering*, ASCE, 125(4), 357-371.

SSPC, 1994, *Statistical Analysis of Tensile Data for Wide Flange Structural Shapes*, Steel Shape Producers Council.

Swanson, J., Leon, R., and Smallridge, J., 2000, *Tests on Bolted Connections*, SAC/BD-00/04.

Tabuchi, M., 1998, "Panel Zone Shear Behavior," *3rd U S – Japan Workshop on Steel Fracture Issues*, National Science Foundation and Building Research Institute/Japan Ministry of Construction.

Tsai, K.C., and Popov, E.P., 1988, "Steel Beam-Column Joints in Seismic Moment Resisting Frames," UCB/EERC-88/19, Earthquake Engineering Research Center (EERC). University of California, Berkeley.

Tsai, K.C., and Popov, E.P., 1990, "Cyclic Behavior of End-plate Moment Connections," *Journal of Structural Engineering*, ASCE, Vol. 116, No. 11.

Tsai, K.C., and Popov, E.P., 1990-1, "Seismic Panel Zone Design Effect on Seismic Story Drift in Steel Frames," *Journal of Structural Engineering*, ASCE, Vol. 116, No. 12.

U.S. Army, 1986, *Seismic Design Guidelines for Upgrading Existing Buildings*, Technical Manual: Army TM5-809-10-2.

Uang, C.M., and Bertero, V.V., 1991, "UBC Seismic Serviceability Regulations: Critical Review," *Journal of Structural Engineering*, ASCE, 117(7), pp. 2055-2068.

Uang, C.M., and Fan, C.C., 1999, *Cyclic Instability of Steel Moment Connections with Reduced Beam Section*, SAC/BD-99/19.

Uang, C.M., 1991, "Establishing R (or R_W) and C_d Factors for Building Seismic Provisions," *Journal of Structural Engineering*, ASCE, Vol. 117, No. 1.

Uang, C.M., and Bertero, V.V., 1988, *Implications of Recorded Earthquake Ground Motions on Seismic Design of Building Structures*, UCB/EERC-88/13, Earthquake Engineering Research Center, University of California, Berkeley.

Uang, C.M., and Bertero. V.V., 1988, *Use of Energy as a Design Criterion in Earthquake-Resistant Design*, UCB/EERC-88/18, Earthquake Engineering Research Center, University of California, Berkeley.

Uang, C.M., and Bertero, V.V., 1986, *Earthquake Simulation Tests and Associated Studies of a 0.3-Scale Model of a Six-Story Concentrically Braced Steel Structure*, UCB/EERC-86/10, Earthquake Engineering Research Center, University of California, Berkeley.

Uang, C.M., and Bondad, D., 1996, "Static Cyclic Testing of Pre-Northridge and Haunch Repaired Steel Moment Connections," SAC 96-01, Part I.

UBC, 1997, *Uniform Building Code*, International Conference of Building Officials, Whittier, California.

UBC, 1997, "Structural Engineering Design Provisions," *Uniform Building Code*, Vol. 2, International Conference of Building Officials.

Uniform Building Code, 1988, International Conference of Building Officials, Whittier, California.

Venti, M., and Engelhardt, M., 2000, *Test of a Free Flange Connection with a Composite Floor Slab*," SAC/BD-00/18.

Venti, M., and Engelhardt, M.D., 1999, "*Brief Report of Steel Moment Connection Test, Specimen DBBW (Dog Bone – Bolted Web)*." Internal SAC Phase 2 Report.

Wen, Y.K., and Foutch, D.A., 1997, *Proposed Statistical and Reliability Framework for Comparing and Evaluating Predictive Models for Evaluation and Design*, SAC/BD-97/03.

Y.K., and Foutch, D.A., 1997, "Proposed Statistical and Reliability Framework Comparing and Evaluating Predictive Models for Evaluation and Design and Critical Issues in Developing Such Framework," SAC-2 Task 5.4.0 Report.

Whittaker, A., Bertero, V., and Gilani, A., 1996, "Seismic Testing of Full-Scale Steel Beam-Column Assemblies," *Experimental Investigation of Beam-Column Subassemblages*, SAC 96-01, Part I, pp. 2.1-2-2.221.

Woodward Clyde Federal Services, 1995, *Characterization of Ground Motions During the Northridge Earthquake of January 17, 1994*, SAC 95-03.

Wu, J., and Hanson, R.D., 1989, "Study of Inelastic Spectra with High Damping," *ASCE Journal of Structural Engineering*, 115 (6), pp. 1412-1431.

Yu, Q.S., Gilton, C., and Uang, C.M., 2000, *Cyclic Response of RBS Moment Connections: Loading Sequence and Lateral Bracing Effects*, SAC/BD-00/22.

Yun, S.Y., Foutch, D.A., and Lee, K., 2000, *Reliability and Performance Based Design for Seismic Loads*, PMC2000-311, Notre Dame, Indiana.

Ziemian, R.D., McGuire, W., and Deierlein, G.G., 1992-1, "Inelastic Limit States Design. Part I: Planar Frame Studies," *Journal of Structural Engineering*, ASCE, Vol. 118, No. 9.

Ziemian, R.D., McGuire, W., and Deierlein, G.G., 1992-2, "Inelastic Limit States Design. Part II: Three-Dimensional Frame Study," *Journal of Structural Engineering*, ASCE, Vol. 118, No. 9.

FEMA Reports.

FEMA reports are listed by report number.

FEMA-178, 1992, *NEHRP Handbook for the Seismic Evaluation of Existing Buildings*, developed by the Building Seismic Safety Council for the Federal Emergency Management Agency, Washington, DC.

FEMA-267, 1995, *Interim Guidelines, Inspection, Evaluation, Repair, Upgrade and Design of Welded Moment Resisting Steel Structures*, prepared by the SAC Joint Venture for the

Federal Emergency Management Agency, Washington, DC. Superseded by FEMA 350 to 353.

FEMA-267A, 1996, *Interim Guidelines Advisory No. 1*, prepared by the SAC Joint Venture for the Federal Emergency Management Agency, Washington, DC. Superseded by FEMA 350 to 353.

FEMA-267B, 1999, *Interim Guidelines Advisory No. 2*, prepared by the SAC Joint Venture for the Federal Emergency Management Agency, Washington, DC. Superseded by FEMA 350 to 353.

FEMA-273, 1997, *NEHRP Guidelines for the Seismic Rehabilitation of Buildings*, prepared by the Applied Technology Council for the Building Seismic Safety Council, published by the Federal Emergency Management Agency, Washington, DC.

FEMA-274, 1997, *NEHRP Commentary on the Guidelines for the Seismic Rehabilitation of Buildings*, prepared by the Applied Technology Council for the Building Seismic Safety Council, published by the Federal Emergency Management Agency, Washington, DC.

FEMA-302, 1997, *NEHRP Recommended Provisions for Seismic Regulations for New Buildings and Other Structures, Part 1 – Provisions*, prepared by the Building Seismic Safety Council for the Federal Emergency Management Agency, Washington, DC.

FEMA-303, 1997, *NEHRP Recommended Provisions for Seismic Regulations for New Buildings and Other Structures, Part 2 – Commentary*, prepared by the Building Seismic Safety Council for the Federal Emergency Management Agency, Washington, DC.

FEMA-310, 1998, *Handbook for the Seismic Evaluation of Buildings – A Prestandard*, prepared by the American Society of Civil Engineers for the Federal Emergency Management Agency, Washington, DC.

FEMA-350, 2000, *Recommended Seismic Design Criteria for New Steel Moment-Frame Buildings*, prepared by the SAC Joint Venture for the Federal Emergency Management Agency, Washington, DC.

FEMA-351, 2000, *Recommended Seismic Evaluation and Upgrade Criteria for Existing Welded Steel Moment-Frame Buildings*, prepared by the SAC Joint Venture for the Federal Emergency Management Agency, Washington, DC.

FEMA-352, 2000, *Recommended Postearthquake Evaluation and Repair Criteria for Welded Steel Moment-Frame Buildings*, prepared by the SAC Joint Venture for the Federal Emergency Management Agency, Washington, DC.

FEMA-353, 2000, *Recommended Specifications and Quality Assurance Guidelines for Steel Moment-Frame Construction for Seismic Applications*, prepared by the SAC Joint Venture for the Federal Emergency Management Agency, Washington, DC.

FEMA-354, 2000, *A Policy Guide to Steel Moment-Frame Construction*, prepared by the SAC Joint Venture for the Federal Emergency Management Agency, Washington, DC.

FEMA-355A, 2000, *State of the Art Report on Base Metals and Fracture*, prepared by the SAC Joint Venture for the Federal Emergency Management Agency, Washington, DC.

FEMA-355B, 2000, *State of the Art Report on Welding and Inspection*, prepared by the SAC Joint Venture for the Federal Emergency Management Agency, Washington, DC.

FEMA-355C, 2000, *State of the Art Report on Systems Performance of Steel Moment Frames Subject to Earthquake Ground Shaking*, prepared by the SAC Joint Venture for the Federal Emergency Management Agency, Washington, DC.

FEMA-355D, 2000, *State of the Art Report on Connection Performance*, prepared by the SAC Joint Venture for the Federal Emergency Management Agency, Washington, DC.

FEMA-355E, 2000, *State of the Art Report on Past Performance of Steel Moment-Frame Buildings in Earthquakes*, prepared by the SAC Joint Venture for the Federal Emergency Management Agency, Washington, DC.

FEMA-355F, 2000, *State of the Art Report on Performance Prediction and Evaluation of Steel Moment-Frame Buildings*, prepared by the SAC Joint Venture for the Federal Emergency Management Agency, Washington, DC.

SAC Joint Venture Reports.

SAC Joint Venture reports are listed by report number, except for SAC 2000a through 2000k; those entries that do not include a FEMA report number are published by the SAC Joint Venture.

SAC 94-01, 1994, *Proceedings of the Invitational Workshop on Steel Seismic Issues, Los Angeles*, September 1994, prepared by the SAC Joint Venture for the Federal Emergency Management Agency, Washington, DC.

SAC 94-01, 1994b, *Proceedings of the International Workshop on Steel Moment Frames, Sacramento*, December, 1994, prepared by the SAC Joint Venture for the Federal Emergency Management Agency, Washington, DC.

SAC 95-01, 1995, *Steel Moment Frame Connection Advisory No. 3*, prepared by the SAC Joint Venture for the Federal Emergency Management Agency, Washington, DC.

SAC 95-02, 1995, *Interim Guidelines: Evaluation, Repair, Modification and Design of Welded Steel Moment Frame Structures*, prepared by the SAC Joint Venture for the Federal Emergency Management Agency, Report No. FEMA-267, Washington, DC.

SAC 95-03, 1995, *Characterization of Ground Motions During the Northridge Earthquake of January 17, 1994*, prepared by the SAC Joint Venture for the Federal Emergency Management Agency, Washington, DC.

SAC 95-04, 1995, *Analytical and Field Investigations of Buildings Affected by the Northridge Earthquake of January 17, 1994*, prepared by the SAC Joint Venture for the Federal Emergency Management Agency, Washington, DC.

SAC 95-05, 1995, *Parametric Analytic Investigations of Ground Motion and Structural Response, Northridge Earthquake of January 17, 1994*, prepared by the SAC Joint Venture for the Federal Emergency Management Agency, Washington, DC.

SAC 95-06, 1995, *Technical Report: Surveys and Assessment of Damage to Buildings Affected by the Northridge Earthquake of January 17, 1994*, prepared by the SAC Joint Venture for the Federal Emergency Management Agency, Washington, DC.

SAC 95-07, 1995, *Technical Report: Case Studies of Steel Moment-Frame Building Performance in the Northridge Earthquake of January 17, 1994*, prepared by the SAC Joint Venture for the Federal Emergency Management Agency, Washington, DC.

SAC 95-08, 1995, *Experimental Investigations of Materials, Weldments and Nondestructive Examination Techniques*, prepared by the SAC Joint Venture for the Federal Emergency Management Agency, Washington, DC.

SAC 95-09, 1995, *Background Reports: Metallurgy, Fracture Mechanics, Welding, Moment Connections and Frame Systems Behavior*, prepared by the SAC Joint Venture for the Federal Emergency Management Agency, Report No. FEMA-288, Washington, DC.

SAC 96-01, 1996, *Experimental Investigations of Beam-Column Subassemblages, Part 1 and 2*, prepared by the SAC Joint Venture for the Federal Emergency Management Agency, Washington, DC.

SAC 96-02, 1996, *Connection Test Summaries*, prepared by the SAC Joint Venture for the Federal Emergency Management Agency, Report No. FEMA-289, Washington, DC.

SAC 96-03, 1997, *Interim Guidelines Advisory No. 1 Supplement to FEMA-267 Interim Guidelines*, prepared by the SAC Joint Venture for the Federal Emergency Management Agency, Report No. FEMA-267A, Washington, DC.

SAC 98-PG, *Update on the Seismic Safety of Steel Buildings – A Guide for Policy Makers*, prepared by the SAC Joint Venture for the Federal Emergency Management Agency, Washington, DC.

SAC 99-01, 1999, *Interim Guidelines Advisory No. 2 Supplement to FEMA-267 Interim Guidelines*, prepared by the SAC Joint Venture, for the Federal Emergency Management Agency, Report No. FEMA-267B, Washington, DC.

SAC, 2000a, *Recommended Seismic Design Criteria for New Steel Moment-Frame Buildings*, prepared by the SAC Joint Venture for the Federal Emergency Management Agency, Report No. FEMA-350, Washington, DC.

SAC, 2000b, *Recommended Seismic Evaluation and Upgrade Criteria for Existing Welded Steel Moment-Frame Buildings*, prepared by the SAC Joint Venture for the Federal Emergency Management Agency, Report No. FEMA-351, Washington, DC.

SAC, 2000c, *Recommended Postearthquake Evaluation and Repair Criteria for Welded Steel Moment-Frame Buildings*, prepared by the SAC Joint Venture for the Federal Emergency Management Agency, Report No. FEMA-352, Washington, DC.

SAC, 2000d, *Recommended Specifications and Quality Assurance Guidelines for Steel Moment-Frame Construction for Seismic Applications*, prepared by the SAC Joint Venture for the Federal Emergency Management Agency, Report No. FEMA-353, Washington, DC.

SAC, 2000e, *A Policy Guide to Steel Moment-Frame Construction*, prepared by the SAC Joint Venture for the Federal Emergency Management Agency, Report No. FEMA-354, Washington, DC.

SAC, 2000f, *State of the Art Report on Base Metals and Fracture*, prepared by the SAC Joint Venture for the Federal Emergency Management Agency, Report No. FEMA-355A, Washington, DC.

SAC, 2000g, *State of the Art Report on Welding and Inspection*, prepared by the SAC Joint Venture for the Federal Emergency Management Agency, Report No. FEMA-355B, Washington, DC.

SAC, 2000h, *State of the Art Report on Systems Performance*, prepared by the SAC Joint Venture for the Federal Emergency Management Agency, Report No. FEMA-355C, Washington, DC.

SAC, 2000i, *State of the Art Report on Connection Performance*, prepared by the SAC Joint Venture for the Federal Emergency Management Agency, Report No. FEMA-355D, Washington, DC.

SAC, 2000j, *State of the Art Report on Past Performance of Steel Moment-Frame Buildings in Earthquakes*, prepared by the SAC Joint Venture for the Federal Emergency Management Agency, Report No. FEMA-355E, Washington, DC.

SAC, 2000k, *State of the Art Report on Performance Prediction and Evaluation*, prepared by the SAC Joint Venture for the Federal Emergency Management Agency, Report No. FEMA-355F, Washington, DC.

SAC/BD-96/01, *Selected Results from the SAC Phase 1 Beam-Column Connection Pre-Test Analyses*, submissions from B. Maison, K. Kasai, and R. Dexter; and A. Ingraffea and G. Deierlein.

SAC/BD-96/02, *Summary Report on SAC Phase 1 - Task 7 Experimental Studies*, by C. Roeder (a revised version of this document is published in Report No. SAC 96-01; the original is no longer available).

SAC/BD-96/03, *Selected Documents from the U.S.-Japan Workshop on Steel Fracture Issues*.

SAC/BD-96/04, *Survey of Computer Programs for the Nonlinear Analysis of Steel Moment Frame Structures*.

SAC/BD-97/01, *Through-Thickness Properties of Structural Steels*, by J. Barsom and S. Korvink.

SAC/BD-97/02, *Protocol for Fabrication, Inspection, Testing, and Documentation of Beam-Column Connection Tests and Other Experimental Specimens*, by P. Clark, K. Frank, H. Krawinkler, and R. Shaw.

SAC/BD-97/03, *Proposed Statistical and Reliability Framework for Comparing and Evaluating Predictive Models for Evaluation and Design*, by Y.-K. Wen.

SAC/BD-97/04, *Development of Ground Motion Time Histories for Phase 2 of the FEMA/SAC Steel Project*, by. P. Somerville, N. Smith, S. Punyamurthula, and J. Sun.

SAC/BD-97/05, *Finite Element Fracture Mechanics Investigation of Welded Beam-Column Connections*, by W.-M. Chi, G. Deierlein, and A. Ingraffea.

SAC/BD-98/01, *Strength and Ductility of FR Welded-Bolted Connections*, by S. El-Tawil, T. Mikesell, E. Vidarsson, and S. K. Kunnath.

SAC/BD-98/02, *Effects of Strain Hardening and Strain Aging on the K-Region of Structural Shapes*, by J. Barsom and S. Korvink

SAC/BD-98/03, *Implementation Issues for Improved Seismic Design Criteria: Report on the Social, Economic, Policy and Political Issues Workshop* by L. T. Tobin.

SAC/BD-99/01, *Parametric Study on the Effect of Ground Motion Intensity and Dynamic Characteristics on Seismic Demands in Steel Moment Resisting Frames* by G. A. MacRae.

SAC/BD-99/01A, *Appendix to: Parametric Study on the Effect of Ground Motion Intensity and Dynamic Characteristics on Seismic Demands in Steel Moment Resisting Frames* by G. A. MacRae.

SAC/BD-99/02, *Through-Thickness Strength and Ductility of Column Flange in Moment Connections*, by R. Dexter and M. Melendrez.

SAC/BD-99/03, *The Effects of Connection Fractures on Steel Moment Resisting Frame Seismic Demands and Safety*, by C. A. Cornell and N. Luco.

SAC/BD-99/04, *Effects of Strength/Toughness Mismatch on Structural and Fracture Behaviors in Weldments*, by P. Dong, T. Kilinski, J. Zhang, and F.W. Brust.

SAC/BD-99/05, *Assessment of the Reliability of Available NDE Methods for Welded Joint and the Development of Improved UT Procedures*, by G. Gruber and G. Light.

SAC/BD-99/06, *Prediction of Seismic Demands for SMRFs with Ductile Connections and Elements*, by A. Gupta and H. Krawinkler.

SAC/BD-99/07, *Characterization of the Material Properties of Rolled Sections*, by T. K. Jaquess and K. Frank.

SAC/BD-99/08, *Study of the Material Properties of the Web-Flange Intersection of Rolled Shapes*, by K. R. Miller and K. Frank.

SAC/BD-99/09, *Investigation of Damage to WSMF Earthquakes other than Northridge*, by M. Phipps.

SAC/BD-99/10, *Clarifying the Extent of Northridge Induced Weld Fracturing and Examining the Related Issue of UT Reliability*, by T. Paret.

SAC/BD-99/11, *The Impact of Earthquakes on Welded Steel Moment Frame Buildings: Experience in Past Earthquakes*, by P. Weinburg and J. Goltz.

SAC/BD-99/12, *Assessment of the Benefits of Implementing the New Seismic Design Criteria and Inspection Procedures*, by H. A. Seligson and R. Eguchi.

SAC/BD-99/13, *Earthquake Loss Estimation for WSMF Buildings*, by C. A. Kircher.

SAC/BD-99/14, *Simplified Loss Estimation for Pre-Northridge WSMF Buildings*, by B. F. Maison and D. Bonowitz.

SAC/BD-99/15, *Integrative Analytical Investigations on the Fracture Behavior of Welded Moment Resisting Connections*, by G. G. Deierlein and W.-M. Chi.

SAC/BD-99/16, *Seismic Performance of 3- and 9- Story Partially Restrained Moment Frame Buildings*, by B. F. Maison and K. Kasai.

SAC/BD-99/17, *Effects of Partially-Restrained Connection Stiffness and Strength on Frame Seismic Performance*, by K. Kasai, B. F. Maison, and A. Mayangarum.

SAC/BD-99/18, *Effects of Hysteretic Deterioration Characteristics on Seismic Response of Moment Resisting Steel Structures*, by F. Naeim, K. Skliros, A. M. Reinhorn, and M. V. Sivaselvan.

SAC/BD-99/19, *Cyclic Instability of Steel Moment Connections with Reduced Beam Section*, by C.-M. Uang and C.-C. Fan.

SAC/BD-99/20, *Local and Lateral-Torsion Buckling of Wide Flange Beams*, by L. Kwasniewski, B. Stojadinovic, and S. C. Goel.

SAC/BD-99/21, *Elastic Models for Predicting Building Performance*, by X. Duan and J. C. Anderson.

SAC/BD-99/22, *Reliability-Based Seismic Performance Evaluation of Steel Frame Buildings Using Nonlinear Static Analysis Methods*, by G. C. Hart and M. J. Skokan.

SAC/BD-99/23, *Failure Analysis of Welded Beam to Column Connections*, by J. M. Barsom and J. V. Pellegrino.

SAC/BD-99/24, *Weld Acceptance Criteria for Seismically-Loaded Welded Connections*, by W. Mohr.

SAC/BD-00/01, *Parametric Tests on Unreinforced Connections, Volume I – Final Report*, by K.-H. Lee, B. Stojadinovic, S. C. Goel, A. G. Margarian, J. Choi, A. Wongkaew, B. P. Reyher, and D.-Y, Lee.

SAC/BD-00/01A, *Parametric Tests on Unreinforced Connections, Volume II – Appendices*, by K.-H. Lee, B. Stojadinovic, S. C. Goel, A. G. Margarian, J. Choi, A. Wongkaew, B. P. Reyher, and D.-Y, Lee.

SAC/BD-00/02, *Parametric Tests on the Free Flange Connections*, by J. Choi, B. Stojadinovic, and S. C. Goel.

SAC/BD-00/03, *Cyclic Tests on Simple Connections Including Effects of the Slab*, by J. Liu and A. Astaneh-Asl.

SAC/BD-00/04, *Tests on Bolted Connections, Part I: Technical Report*, by J. Swanson, R. Leon, and J. Smallridge.

SAC/BD-00/04A, *Tests on Bolted Connections, Part II: Appendices*, by J. Swanson, R. Leon, and J. Smallridge.

SAC/BD-00/05, *Bolted Flange Plate Connections*, by S. P. Schneider and I. Teeraparbwong.

SAC/BD-00/06, *Round Robin Testing of Ultrasonic Testing Technicians*, by R. E. Shaw, Jr.

SAC/BD-00/07, *Dynamic Tension Tests of Simulated Welded Beam Flange Connections*, by J. M. Ricles, C. Mao, E. J. Kaufmann, L.-W. Lu, and J. W. Fisher.

SAC/BD-00/08, *Design of Steel Moment Frame Model Buildings in Los Angeles, Seattle and Boston*, by P. Clark.

SAC/BD-00/09, *Benchmarking of Analysis Programs for SMRF System Performance Studies*, by A. Gupta and H. Krawinkler.

SAC/BD-00/10, *Loading Histories for Seismic Performance Testing of SMRF Components and Assemblies*, by H. Krawinkler, A. Gupta, R. Medina, and N. Luco.

SAC/BD-00/11, *Development of Improved Post-Earthquake Inspection Procedures for Steel Moment Frame Buildings*, by P. Clark.

SAC/BD-00/12, *Evaluation of the Effect of Welding Procedure on the Mechanical Properties of FCAW-S and SMAW Weld Metal Used in the Construction of Seismic Moment Frames*, by M. Q. Johnson.

SAC/BD-00/13, *Preliminary Evaluation of Heat Affected Zone Toughness in Structural Shapes Used in the Construction of Seismic Moment Frames*, by M. Q. Johnson and J. E. Ramirez.

SAC/BD-00/14, *Evaluation of Mechanical Properties in Full-Scale Connections and Recommended Minimum Weld Toughness for Moment Resisting Frames*, by M. Q. Johnson, W. Mohr, and J. Barsom.

SAC/BD-00/15, *Simplified Design Models for Predicting the Seismic Performance of Steel Moment Frame Connections*, by C. Roeder, R. G. Coons, and M. Hoit.

SAC/BD-00/16, *SAC Phase 2 Test Plan*, by C. Roeder.

SAC/ BD-00/17, *Behavior and Design of Radius-Cut, Reduced Beam Section Connections*, by M. Engelhardt, G. Fry, S. Jones, M. Venti, and S. Holliday.

SAC/BD-00/18, *Test of a Free Flange Connection with a Composite Floor Slab*, by M. Venti and M. Engelhardt.

SAC/BD-00/19, *Cyclic Testing of a Free Flange Moment Connection*, by C. Gilton, B. Chi, and C. M. Uang.

SAC/BD-00/20, *Improvement of Welded Connections Using Fracture Tough Overlays*, by James Anderson, J. Duan, P. Maranian, and Y. Xiao.

SAC/BD-00/21, *Cyclic Testing of Bolted Moment End-Plate Connections*, by T. Murray, E. Sumner, and T. Mays.

SAC/BD-00/22, *Cyclic Response of RBS Moment Connections: Loading Sequence and Lateral Bracing Effects*, by Q. S. Yu, C. Gilton, and C. M. Uang.

SAC/BD-00/23, *Cyclic Response of RBS Moment Connections: Weak Axis Configuration and Deep Column Effects*, by C. Gilton, B. Chi, and C. M. Uang.

SAC/BD-00/24, *Development and Evaluation of Improved Details for Ductile Welded Unreinforced Flange Connections*, by J. M. Ricles, C. Mao, L.-W. Lu, and J. Fisher.

SAC/BD-00/25, *Performance Prediction and Evaluation of Steel Special Moment Frames for Seismic Loads*, by K. Lee and D. A. Foutch.

SAC/BD-00/26, *Performance Prediction and Evaluation of Low Ductility Steel Moment Frames for Seismic Loads*, by S. Yun and D. A. Foutch.

SAC/BD-00/27, *Steel Moment Resisting Connections Reinforced with Cover and Flange Plates*, by T. Kim, A. S. Whittaker, V. V. Bertero, A. S. J. Gilani, and S. M. Takhirov.

SAC/BD-00/28, *Failure of a Column K-Area Fracture*, by J. M. Barsom and J. V. Pellegrino.

SAC/BD-00/29, *Inspection Technology Workshop*, by R. E. Shaw, Jr.

SAC/BD-00/30, *Preliminary Assessment of the Impact of the Northridge Earthquake on Construction Costs of Steel Moment Frame Buildings*, by Davis Langdon Adamson.

Acronyms.

2-D, two-dimensional
3-D, three-dimensional
A, acceleration response, amps
A2LA, American Association for Laboratory Accreditation
ACAG, air carbon arc gouging
ACIL, American Council of Independent Laboratories
AE, acoustic emission (testing)
AISC, American Institute for Steel Construction
AISI, American Iron and Steel Institute
AL, aluminum
ANSI, American National Standards Institute
API, American Petroleum Institute
ARCO, Atlantic-Richfield Company
As, arsenic
ASD, allowable stress design
ASME, American Society of Mechanical Engineers
ASNT, American Society for Nondestructive Testing
ASTM, American Society for Testing and Materials
ATC, Applied Technology Council
AWS, American Welding Society
B, boron
BB, Bolted Bracket (connection)
BD, background document
BF, bias factor
BFO, bottom flange only (fracture)
BFP, Bolted Flange Plates (connection)
BM, base metal
BO, Boston, Massachusetts
BOCA, Building Officials and Code Administrators
BOF, basic oxygen furnace
BSEP, Bolted Stiffened End Plate (connection)
BSSC, Building Seismic Safety Council
BUEP, Bolted Unstiffened End Plate (connection)
C, carbon
CA, California
CAC-A, air carbon arc cutting
CAWI, Certified Associate Welding Inspector
CGHAZ, coarse-grained HAZ
CJP, complete joint penetration (weld)
CMU, concrete masonry unit, concrete block
COD, crack opening displacement
"COV," modified coefficient of variation, or dispersion
CP, Collapse Prevention (performance level)
Connection Performance (team)
Cr, chromium
CSM, Capacity Spectrum Method
CTOD, crack tip opening dimension or displacement
CTS, controlled thermal severity (test)
Cu, copper
CUREe, California Universities for Research in Earthquake Engineering
CVN, Charpy V-notch
CWI, Certified Welding Inspector
D, displacement response, dead load
DMRSF, ductile, moment-resisting, space frame
DNV, Det Norske Veritas
DRAIN-2DX, analysis program
DRAIN-3DX, analysis program
DRI, direct reduced iron
DST, Double Split Tee (connection)
DTI, Direct Tension Indicator
EAF, electric-arc furnace
EBT, eccentric bottom tapping
EE, electrode extension
EERC, Earthquake Engineering Research Center, UC Berkeley
EGW, electrogas welding
ELF, equivalent lateral force
EMS, electromagnetic stirring
ENR, Engineering News Record
ESW, electroslag welding

EWI, Edison Welding Institute
FATT, fracture appearance transition temperature
fb, fusion boundary
FCAW-G, flux-cored arc welding – gas-shielded
FCAW-S or FCAW-SS, flux-cored arc welding – self-shielded
FEMA, Federal Emergency Management Agency
FF, Free Flange (connection)
FGHAZ, fine-grained HAZ
FL, fusion line
FR, fully restrained (connection)
GBOP, gapped bead on plate (test)
gl, gage length
GMAW, gas metal arc welding
GTAW, gas tungsten arc welding
HAC, hydrogen-assisted cracking
HAZ, heat-affected zone
HBI, hot briquetted iron
HSLA, high strength, low alloy
IBC, *International Building Code*
ICBO, International Conference of Building Officials
ICC, International Code Council
ICCGHAZ, intercritically reheated CGHAZ
ICHAZ, intercritical HAZ
ID, identification
IDA, Incremental Dynamic Analysis
IMF, Intermediate Moment Frame
IO, Immediate Occupancy (performance level)
IOA, Incremental Dynamic Analysis
ISO, International Standardization Organization
IWURF, Improved Welded Unreinforced Flange (connection)
L, longitudinal, live load
LA, Los Angeles, California
LACOTAP, Los Angeles County Technical Advisory Panel
LAX, Los Angeles International Airport
LB, lower bound (building)
LBZ, local brittlezone
LDP, Linear Dynamic Procedure
LEC, Lincoln Electric Company
LMF, ladle metallurgy furnace
LRFD, load and resistance-factor design
LS, Life Safety (performance level)
LSP, Linear Static Procedure
LTH, linear time history (analysis)
LU, Lehigh University
M, moment
MAP, modal analysis procedure
MAR, microalloyed rutile (consumables)
MCE, Maximum Considered Earthquake
MDOF, multidegree of freedom
MMI, Modified Mercalli Intensity
Mn, manganese
Mo, molybdenum
MRF, steel moment frame
MRS, modal response spectrum
MRSF, steel moment frame
MT, magnetic particle testing
N, nitrogen
Nb, niobium
NBC, *National Building Code*
NDE, nondestructive examination
NDP, Nonlinear Dynamic Procedure
NDT, nondestructive testing
NEHRP, National Earthquake Hazards Reduction Program
NES, National Evaluation Services
NF, near-fault, near-field
Ni, nickel
NLP, nonlinear procedure
NLTH, nonlinear time history (analysis)
NS, north-south (direction)
NSP, Nonlinear Static Procedure
NTH, nonlinear time history (analysis)
NVLAP, National Volunteer Laboratory Accreditation Program
O, oxygen
OHF, open hearth furnace
OMF, Ordinary Moment Frame
OTM, overturning moment
P, axial load
P, axial load, phosphorus
Pb, lead

PGA, peak ground acceleration
PGV, peak ground velocity
PIDR, pseudo interstory drift ratio
PJP, partial joint penetration (weld)
PPE, Performance, Prediction, and Evaluation (team)
PQR, Performance Qualification Record
PR, partially restrained (connection)
PR-CC, partially restrained, composite connection
PT, liquid dye penetrant testing
PWHT, postweld heat treatment
PZ, panel zone
QA, quality assurance
QC, quality control
QCP, Quality Control Plan, Quality Certification Program
QST, Quenching and Self-Tempering (process)
RB, Rockwell B scale (of hardness)
RBS, Reduced Beam Section (connection)
RCSC, Research Council for Structural Connections
RT, radiographic testing
S, sulphur, shearwave (probe)
SAC, the SAC Joint Venture; a partnership of SEAOC, ATC, and CUREe
SAV, sum of absolute values
SAW, submerged arc welding
SBC, *Standard Building Code*
SBCCI, Southern Building Code Congress International
SCCGHAZ, subcritically reheated CGHAZ
SCHAZ, subcritical HAZ
SCWB, strong column, weak beam
SCWI, Senior Certified Welding Inspector
SDC, Seismic Design Category
SDOF, single degree of freedom
SE, Seattle, Washington
SEAOC, Structural Engineers Association of California
SFRS, seismic-force-resisting system
Si, silicon
SMAW, shielded metal arc welding
SMF, Special Moment Frame
SMRF, special moment-resisting frame (in 1991 UBC)
SMRF, Steel Moment Frame
SMRSF, special moment-resisting space frame (in 1988 UBC)
SN, strike-normal, fault-normal
Sn, tin
SP, Side Plate (connection)
SP, strike-parallel, fault-parallel
SP, Systems Performance (team)
SPC, Seismic Performance Category
SRSS, square root of the sum of the squares
SSPC, Steel Shape Producers Council
SSRC, Structural Stability Research Council
SUG, Seismic Use Group
SW, Slotted Web (connection)
SwRI, Southwest Research Institute
T, transverse
TBF, top and bottom flange (fracture)
Ti, titanium
TIGW, tungsten inert gas welding
TMCP, Thermo-Mechanical Processing
TN, Tennessee
TT, through-thickness
TWI, The Welding Institute
UB, upper bound (building)
UBC, *Uniform Building Code*
UCLA, University of California, Los Angeles
UM, University of Michigan
URM, unreinforced masonry
US, United States of America
USC, University of Southern California
USGS, US Geological Survey
UT, ultrasonic testing
UTA, University of Texas at Austin
UTAM, Texas A & M University
V, vanadium
VI, visual inspection
w/o, without
WBH, Welded Bottom Haunch (connection)
WCPF, Welded Cover Plate Flange (connection)
WCSB, weak column, strong beam
WF, wide flange

WFP, Welded Flange Plate (connection)
WFS, wire feed speed
WPQR, Welding Performance Qualification Record
WPS, Welding Procedure Specification
WSMF, welded steel moment frame
WT, Welded Top Haunch (connection)
WTBH, Welded Top and Bottom Haunch (connection)
WUF-B, Welded Unreinforced Flanges – Bolted Web (connection)
WUF-W, Welded Unreinforced Flanges – Welded Web (connection)

List of Symbols.

$\hat{C}$ = estimate of median drift capacity – Equation 5-1

C_0 = modification factor to relate spectral displacement to roof displacement

C_1 = modification factor to relate expected maximum inelastic displacements to displacements calculated for linear elastic response.

C_2 = modification factor to represent the effect of hysteresis shape on the maximum displacement response. Values for C_2 may be as 1.0 for steel moment frames.

C_3 = modification factor to account for P-delta effects

C_4 = modification factor to account for effects of overstrength

C_B = bias factor

C_d = deflection amplification factor in Table 4-1

C_s = the seismic response coefficient determined by Equation 4-2

C_{sm} = the modal seismic response coefficient determined below,

C_{vsm} = the vertical distribution factor in the m^{th} mode,

C_{vx} = Vertical distribution factor

$\hat{D}$ = estimate of median drift demand

F_{xm} = the portion of the seismic base shear in the m^{th} mode, induced at Level x,

F_y = the yielding strength of the panel zone

G = the shear modulus = $\dfrac{E}{2 \cdot (1+\nu)}$

$H_{Sa}(Sa_{10\%})$ = probability of exceedance for 10% in 50 years = 1/474 = 0.0021

$H_{Sa}(Sa_{2\%})$ = probability of exceedance for 2% in 50 years = 1/2475 = 0.00040

I = the occupancy importance factor determined in accordance with Sec. 1.4

I_b = moment of inertia of beam, in^4

I_c = moment of inertia of column, in^4

K_e = effective lateral stiffness of the building in the direction under consideration

K_θ = the rotational stiffness of the connection

K_i = elastic lateral stiffness of the building in the direction under consideration

K_x = standard Gausian variate associated with probability x of not being exceeded. (found in standard probability tables)

M_{fail} = minimum of the failure mechanisms specified in Table 7-8

$M_{fail\text{-}TStem}$ = failure moment of T-section flanges and net section fracture of the stem of the T-section

$M_{fail\text{-}TFlngFlex}$ = failure moment of T-section in local plastic flexure of the T-section flanges

M_{PE} = the moment capacity of the connection

$\overline{N}$ = blow count

P_{uc} = column axial compression force, kips

R = the response modification factor given

R_v = required shear strength of the panel zone

S_1 = the mapped maximum considered earthquake spectral acceleration at a one-second period

S_a = spectral acceleration at the natural period of the structure

S_a = response spectrum acceleration at the fundamental period and damping

$Sa_{10\%}$ = spectral amplitude for 10/50 hazard level

$Sa_{2\%}$ = spectral amplitude for 2/50 hazard level

S_{am} = the design spectral response acceleration at period T_m

S_{D1} = the design spectral acceleration at a period of 1.0 seconds

S_{DS} = the design spectral acceleration in the short period range as determined

T = fundamental period of the building

T_0 = characteristic period of the design response spectrum

T_i = elastic fundamental period in the direction under consideration

T_m = the modal period of vibration (in seconds) of the m^{th} mode of the structure

V = a design base shear

V = Pseudo lateral load

V_m = the total design lateral force or shear at the *base* in the m^{th} mode,

V_y = yield strength calculated using the FEMA-NLP

W = the total dead load and applicable portions of other loads

$\overline{W_m}$ = the effective modal gravity load including portions of the live load

b = slope of the curve

d_b = depth of beam

d_c = depth of column

f_i = applied force at floor level *i*

g = the acceleration due to gravity (ft/s^2 or m/s^2)

h = story height, in

h_i = Height (in ft) from the base to floor level i

h_x = Height (in ft) from the base to floor level x

h_x = height of story x

k = slope of the hazard curve

l_b = beam length, in

t = thickness of panel zone which is the thickness of the web of the column plus the

thickness of the doubler plates if they are utilized.

$\overline{v_s}$ = measured shear wave velocity

w_i, w_x = the portion of the total gravity load, *W*, located or assigned to Level *i* or *x*

α = ratio of post yield stiffness to effective elastic

$\beta_{BF.}$ = associated with uncertainty in the bias factor

β_{RC} = Standard deviation of the natural logs of the drift capacities

β_{UC} = Standard deviation of the natural logs of the drift capacities derived from testing.

β_{UT}^2 = $\Sigma\sigma_i^2$ where σ_i is for uncertainties in the demand and capacity

β_{Ud} = dependent part of uncertainty

β_{Ui} = independent part of uncertainty

β_{cd} = dependent part of capacity

β_{dd} = dependent part of demand

β_{NTH} = associated with uncertainties in the nonlinear time history analysis procedure

$\beta_{damping}$ = associated with uncertainty in the estimating the damping value

$\beta_{live\ load}$ = associated with uncertainty in live load applied

$\beta_{material\ property}$ = associated with uncertainty in material property which is quite small

γ = demand factor

γ_a = analysis demand factor – Table 5-4

Δ_x = the drift angle of story x

Δ_{xm} = drift angle for level x for mode m

δ_i = displacement at floor level i

δ_x, δ_{x-1} = deflection at floors x and x-1

δ_{xem} = the deflection of level *x* in the m^{th}

θ_m = the maximum story drift angle, Δ_x, for all stories

λ_{con} = The ratio of the factored capacity and factored demand

λ_{con} = confidence factor

λ_0^o = median drift for the 0^0 rotated (fault parallel) ground motions

λ_{90}^o = median drift for the 90^0 rotated (fault normal) ground motions

ν = Poisson's ratio = 0.30

σ_{ori} = standard deviation of uniform distribution from 0^o to 90^o = 26^0

ϕ = Resistance factor

ϕ_{RC} = Contribution to ϕ from randomness of the earthquake accelerograms

ϕ_{UC} = Contribution to ϕ from uncertainties in measured connection capacity

ϕ_{im} = the displacement amplitude at the i^{th} level of the structure when vibrating in its m^{th} mode

ϕ_{xm} = the displacement amplitude at the x^{th} level of the structure when vibrating in its m^{th} mode

SAC PHASE II PROJECT PARTICIPANTS

FEMA Project Officer

Michael Mahoney
Federal Emergency Management Agency
500 C St. SW, Room 404
Washington, DC 20472

FEMA Technical Advisor

Robert D. Hanson
Federal Emergency Management Agency
DFO Room 353
P.O. Box 6020
Pasadena, CA 91102-6020

Joint Venture Management Committee (JVMC)

William T. Holmes, Chair
Rutherford and Chekene
427 Thirteenth Street
Oakland, CA 94612

Christopher Rojahn
Applied Technology Council
555 Twin Dolphin Dr., Suite 550
Redwood City, CA 94065

Edwin T. Huston
Smith & Huston, Inc.
8618 Roosevelt Way NE
Seattle, WA 98115

Arthur E. Ross
Cole/Yee/Shubert & Associates
2500 Venture Oaks Way, Suite 100
Sacramento, CA 95833

Robert Reitherman
California Universities for Research in Earthquake Engineering
1301 South 46th St.
Richmond, CA 94804

Robin Shepherd
Earthquake Damage Analysis Corporation
40585 Lakeview Drive, Suite 1B
P.O. Box 1967
Big Bear Lake, CA 92315

Project Management Committee (PMC)

Stephen A. Mahin, Project Manager
Pacific Earthquake Engr. Research Center
University of California
Berkeley, CA 94720

William T. Holmes, JVMC
Rutherford and Chekene
427 Thirteenth Street
Oakland, CA 94612

Ronald O. Hamburger, Project Director for Project Development
EQE International
1111 Broadway, 10th Floor
Oakland, CA 94607-5500

Christopher Rojahn, JVMC
Applied Technology Council
555 Twin Dolphin Dr., Suite 550
Redwood City, CA 94065

James O. Malley, Project Director for Topical Investigations
Degenkolb Engineers
225 Bush St., Suite 1000
San Francisco, CA 94104-1737

Robin Shepherd, JVMC
Earthquake Damage Analysis Corporation
40585 Lakeview Drive, Suite 1B
P.O. Box 1967
Big Bear Lake, CA 92315

Peter W. Clark, Technical Assistant to PMC
SAC Steel Project Technical Office
1301 South 46th St.
Richmond, CA 94804

Project Administration

Allen Paul Goldstein, Project Administrator
Allen Paul Goldstein and Associates
1621B 13th Street
Sacramento, CA 95814

Lori Campbell, Assistant to the Project Administrator
4804 Polo Court
Fair Oaks, CA 95628

Project Oversight Committee (POC)

William J. Hall, Chair
3105 Valley Brook Dr.
Champaign, IL 61821

Shirin Ader
International Conference of Building Officials
5360 Workman Mill Rd.
Whittier, CA 90601-2298

John M. Barsom
Barsom Consulting, Ltd.
1316 Murray Ave, Suite 300
Pittsburgh, PA 15217

Roger Ferch
Herrick Corporation
7021 Koll Center Parkway
P.O Box 9125
Pleasanton, CA 94566-9125

Theodore V. Galambos
University of Minnesota
122 CE Building, 500 Pillsbury Dr. SE
Minnneapolis, MN 55455

John L. Gross
National Institute of Stds. & Technology
Building and Fire Research Lab,
Building 226, Room B158
Gaithersburg, MD 20899

James R. Harris
J.R. Harris and Co.
1580 Lincoln St., Suite 550
Denver, CO 80203-1509

Richard Holguin
520 Kathryn Ct.
Nipomo, CA 93444

Nestor Iwankiw
American Institute of Steel Construction
One East Wacker Dr., Suite 3100
Chicago, IL 60601-2001

Roy Johnston
Brandow & Johnston Associates
1600 West 3rd St.
Los Angeles, CA 90017

Leonard Joseph
Thornton-Tomassetti Engineers
641 6th Ave., 7th Floor
New York, NY 10011

Duane K. Miller
The Lincoln Electric Company
22801 St. Clair Ave.
Cleveland, OH 44117-1194

John Theiss
EQE/Theiss Engineers
1848 Lackland Hills Parkway
St. Louis, MO 63146-3572

John H. Wiggins
J.H. Wiggins Company
1650 South Pacific Coast Hwy, Suite 311
Redondo Beach, CA 90277

Team Leaders for Topical Investigations

Douglas A. Foutch
University of Illinois
MC-250, 205 N. Mathews Ave.
3129 Newmark Civil Engineering Lab
Urbana, IL 61801

Karl H. Frank
University of Texas at Austin
10100 Bornet Rd.
Ferguson Lab, P.R.C. #177
Austin, TX 78758

Matthew Johnson
Edison Welding Institute
1250 Arthur E. Adams Drive
Columbus, OH 43221

Helmut Krawinkler
Department of Civil Engineering
Stanford University
Stanford, CA 94305

Charles W. Roeder
University of Washington
233-B More Hall FX-10
Dept. of Building and Safety
Seattle, WA 98195-2700

L. Thomas Tobin
Tobin and Associates
134 California Ave.
Mill Valley, CA 94941

Lead Guideline Writers

John D. Hooper
Skilling Ward Magnusson Barkshire, Inc.
1301 Fifth Avenue, Suite 3200
Seattle, WA 98101-2699

Lawrence D. Reaveley
University of Utah
Civil Engineering Dept.
3220 Merrill Engineering Building
Salt Lake City, UT 84112

Thomas A. Sabol
Englekirk & Sabol Consulting Engineers
P.O. Box 77-D
Los Angeles, CA 90007

C. Mark Saunders
Rutherford & Chekene
303 Second St., Suite 800 North
San Francisco, CA 94107

Robert E. Shaw
Steel Structures Technology Center, Inc.
42400 W Nine Mile Road
Novi, MI 48375-4132

Raymond H. R. Tide
Wiss, Janney, Elstner Associates, Inc.
330 Pfingsten Road
Northbrook, IL 60062-2095

C. Allin Cornell, Associate Guideline Writer
Stanford University
Terman Engineering Center
Stanford, CA 94305-4020

Technical Advisory Panel (TAP) for Materials and Fracture

John M. Barsom, POC
Barsom Consulting, Ltd.
1316 Murray Ave, Suite 300
Pittsburgh, PA 15217

Serge Bouchard*
TradeARBED
825 Third Avenue, 35th Floor
New York, NY 10022

Michael F. Engestrom*
Nucor-Yamato Steel
P.O. Box 678
Frederick, MD 21705-0678

Karl H. Frank, Team Leader
University of Texas at Austin
10100 Bornet Rd.
Ferguson Lab, P.R.C. #177
Austin, TX 78758

Nestor Iwankiw, POC*
American Institute of Steel Construction
One East Wacker Dr., Suite 3100
Chicago, IL 60601-2001

Dean C. Krouse*
705 Pine Top Drive
Bethelem, PA 18017

Frederick V. Lawrence
University of Illinois at Urbana-Champaign
205 N. Mathews Ave.
Room 2129 Newmark Lab
Urbana, IL 61801

Robert F. Preece
Preece, Goudie & Associates
100 Bush St., Suite 410
San Francisco, CA 94104

Raymond H. R. Tide, Guideline Writer
Wiss, Janney, Elstner Associates, Inc.
330 Pfingsten Road
Northbrook, IL 60062-2095

TAP for Welding and Inspection

John M. Barsom, POC
Barsom Consulting, Ltd.
1316 Murray Ave, Suite 300
Pittsburgh, PA 15217

John W. Fisher
Lehigh University
117 ATLSS Drive
Bethlehem, PA 18015-4729

J. Ernesto Indacochea
University of Illinois at Chicago
Civil and Materials Engineering (mc 246)
842 West Taylor Street
Chicago, IL 60607

Matthew Johnson, Team Leader
Edison Welding Institute
1250 Arthur E. Adams Drive
Columbus, OH 43221

David Long
PDM Strocal, Inc.
2324 Navy Drive
Stockton, CA 95206

Duane K. Miller, POC
The Lincoln Electric Company
22801 St. Clair Ave.
Cleveland, OH 44117-1194

Robert Pyle*
AISC Marketing
10101 South State Street
Sandy, Utah 84070

Douglas Rees-Evans*
Steel Dynamics, Inc.
Structural Mill Division
2601 County Road 700 East
Columbia City, IN 46725

Richard I. Seals
P.O. Box 11327
Berkeley, CA 94712-2327

Robert E. Shaw, Guideline Writer
Steel Structures Technology Center, Inc.
42400 W Nine Mile Road
Novi, MI 48375-4132

TAP for Connection Performance

Charlie Carter*
American Institute of Steel Construction
One East Wacker Drive, Suite 3100
Chicago, IL 60601-2001

Robert H. Dodds
University of Illinois at Urbana-Champaign
205 N. Mathews Ave.
2129 Newmark Lab
Urbana, IL 61801

Roger Ferch, POC
Herrick Corporation
7021 Koll Center Parkway
P.O Box 9125
Pleasanton, CA 94566-9125

John D. Hooper, Guideline Writer
Skilling Ward Magnusson Barkshire, Inc.
1301 Fifth Avenue, Suite 3200
Seattle, WA 98101-2699

Egor Popov
University of California at Berkeley
Department of Civil and Environmental
Engineering, Davis Hall
Berkeley, CA 94720

Steve Powell*
SME Steel Contractors
5955 W. Wells Park Rd.
West Jordan, UT 84088

Charles W. Roeder, Team Leader
University of Washington
233-B More Hall FX-10
Dept. of Building and Safety
Seattle, WA 98195-2700

Stanley T. Rolfe
University of Kansas
Civil Engineering Department
2006 Learned Hall
Lawrence, KS 66045-2225

Rick Wilkinson*
Gayle Manufacturing Company
1455 East Kentucky
Woodland, CA 95695

TAP for System Performance

Jacques Cattan*
American Institute of Steel Construction
One East Wacker Drive, Suite 3100
Chicago, IL 60601-2001

Gary C. Hart
Hart Consultant Group
The Water Garden, Ste. 670E
2425 Olympic Blvd.
Santa Monica, CA 90404-4030

Y. Henry Huang*
Los Angeles County Dept. of Public Works
900 S. Fremont Avenue, 8th Floor
Alhambra, CA 91803

Helmut Krawinkler, Team Leader
Department of Civil Engineering
Stanford University
Stanford, CA 94305

Dennis Randall*
SME Steel Contractors
5955 West Wells Park Road
West Jordan, UT 84088

Andrei M. Reinhorn
State University of New York at Buffalo
Civil Engineering Department
231 Ketter Hall
Buffalo, NY 14260

Arthur E. Ross, JVMC
Cole/Yee/Shubert & Associates
2500 Venture Oaks Way, Suite 100
Sacramento, CA 95833

C. Mark Saunders, Guideline Writer
Rutherford & Chekene
303 Second St., Suite 800 North
San Francisco, CA 94107

W. Lee Shoemaker*
Metal Building Manufacturers Association
1300 Summer Avenue
Cleveland, OH 44115

John Theiss, POC
EQE/Theiss Engineers
1848 Lackland Hills Parkway
St. Louis, MO 63146-3572

TAP for Performance Prediction and Evaluation

Vitelmo V. Bertero
University of California at Berkeley
Pacific Earthquake Engr. Research Center
1301 S. 46th St.
Richmond, CA 94804

Bruce R. Ellingwood
Johns Hopkins University
Department of Civil Engineering
3400 N. Charles St.
Baltimore, MD 21218

Douglas A. Foutch, Team Leader
University of Illinois
MC-250, 205 N. Mathews Ave.
3129 Newmark Civil Engineering Lab
Urbana, IL 61801

Theodore V. Galambos, POC
University of Minnesota
122 CE Building, 500 Pillsbury Dr. SE
Minnneapolis, MN 55455

Lawrence G. Griffis
Walter P. Moore & Associates
3131 Eastside, Second Floor
Houston, TX 77098

Edwin T. Huston, JVMC
Smith & Huston, Inc.
8618 Roosevelt Way NE
Seattle, WA 98115

Harry Martin*
American Iron and Steel Institute
11899 Edgewood Road, Suite G
Auburn, CA 95603

Thomas A. Sabol, Guideline Writer
Englekirk & Sabol Consulting Engineers
P.O. Box 77-D
Los Angeles, CA 90007

Tom Schlafly*
American Institute of Steel Construction
One East Wacker Drive, Suite 3100
Chicago, IL 60601-2001

Technical Advisors

NormAbrahamson
Pacific Gas & Electric
P.O. Box 770000, MC N4C
San Francisco, CA 94177

C.B. Crouse
URS – Dames and Moore
2025 First Avenue, Suite 500
Seattle, WA 98121

Robert Kennedy
RPK Structural Mechanics Consultants
18971 Villa Terr
Yorba Linda, CA 92886

Social Economic and Policy Panel

Martha Cox-Nitikman
Building and Owners and Managers Association, Los Angeles
700 South Flower, Suite 2325
Los Angeles, CA 90017

Karl Deppe
27502 Fawnskin Dr.
Rancho Palos Verdes, CA 90275

Eugene Lecomte
Institute for Business and Home Safety
6 Sheffield Drive
Billerica, MA 01821

James Madison
Attorney at Law, Mediator and Arbitrator
750 Menlo Avenue, Suite 250
Menlo Park, CA 94025

Alan Merson
Morley Builders
2901 28th Street, Suite 100
Santa Monica, CA 90405

Joanne Nigg
University of Delaware
Disaster Research Center
Newark, DE 19716

William Petak
University of Southern California
Lewis Hall, Room 201
650 Childs Way
Los Angeles, CA 90089

Francine Rabinovitz
Hamilton, Rabinovitz and Alschuler
1990 South Bundy Drive, Suite 777
Los Angeles, CA 90025

Dennis Randall
SME Steel Contractors
5955 West Wells Park Road
West Jordan, UT 84088

David Ratterman
Stites and Harbison
400 West Market St., Suite 1800
Louisville, KY 40202-3352

L. Thomas Tobin, Panel Coordinator
134 California Ave.
Mill Valley, CA 94941

Stephen Toth
TIAA-CREF
730 Third Avenue
New York, NY 10017-3206

John H. Wiggins, POC
J.H. Wiggins Company
1650 South Pacific Coast Hwy, Suite 311
Redondo Beach, CA 90277

Performance of Steel Buildings in Past Earthquakes Subcontractors

David Bonowitz
887 Bush, No. 610
San Francisco, CA 94108

Peter Clark
SAC Steel Project Technical Office
1301 South 46th St.
Richmond, CA 94804

Michael Durkin
Michael Durkin & Associates
22955 Leanora Dr.
Woodland Hills, CA 91367

James Goltz
California Institute of Technology
Office of Earthquake Programs
Mail Code 252-21
Pasadena, CA 91125

Bruce Maison
7309 Lynn Ave
Elcerrito, CA 94530

Peter Maranian
Brandow & Johnston Associates
1660 West Third Street
Los Angeles, CA 90017

Terrence Paret
Wiss Janney Elstner Associates, Inc.
2200 Powell St. Suite 925
Emeryville, CA 94602

Maryann Phipps
Degenkolb Engineers
225 Bush Street, Suite 1000
San Francisco, CA 94104

Allan Porush
Dames & Moore
911 Wilshire Blvd., Suite 700
Los Angeles, CA 90017

Access Current Knowledge Subcontractors

David Bonowitz
887 Bush , No. 610
San Francisco, CA 94108

Stephen Liu
Colorado School of Mines
Mathematics and Computer Science
Department
Golden, CO 80401

Materials and Fracture Subcontractors

Robert Dexter
University of Minnesota
122 Civil Engineering Building
500 Pillsbury Drive SE
Minneapolis, MN 55455-0116

Karl H. Frank
University of Texas at Austin
10100 Bornet Rd.
Ferguson Lab, P.R.C. #177
Austin, TX 78758

Welding and Inspection Subcontractors

Pingsha Dong / Tom Kilinski
Center for Welded Structures Research
Battelle Memorial Institute
501 King Avenue
Columbus, OH 43201-2693

Matthew Johnson
Edison Welding Institute
1250 Arthur E. Adams Drive
Columbus, OH 43221

Glenn M. Light / George Gruber
Southwest Research Institute
6220 Culebra Road, P. O. Drawer 28510
San Antonio, TX 78228-0510

William C. Mohr
Edison Welding Institute
1250 Arthur E. Adams Drive
Columbus, OH 43221

Connection Performance Subcontractors

Gregory Deierlein
Stanford University
Terman Engineering Center
Department of Civil and Enviromental Engr.
Stanford, CA 94305-4020

Charles W. Roeder
University of Washington
233-B More Hall FX-10
Seattle, WA 98195-2700

Sherif El-Tawil / Sashi Kunnath
University of Central Florida
Civil and Environmental Engr. Department
Orlando, FL. 32816-2450

Anthony Ingraffea
Cornell University
School of Civil Engineering
363 Hollister Hall
Ithaca, NY 14853

System Performance Subcontractors

Paul Somerville
Woodward-Clyde Federal Services
566 El Dorado St., Suite 100
Pasadena, CA 91101-2560

Farzad Naeim
John A. Martin & Associates
1212 S. Flower Ave.
Los Angeles, CA 90015

Andrei M. Reinhorn
State University of New York at Buffalo
Civil Engineering Department
231 Ketter Hall
Buffalo, NY 14260

C. Allin Cornell
Stanford University
Terman Engineering Center
Stanford, CA 94305-4020

Helmut Krawinkler
Dept. of Civil Engineering
Stanford University
Stanford, CA 94305

Gregory MacRae
University of Washington
Civil Engineering Department
Seattle, WA 98195-2700

Kazuhiko Kasai
Tokyo Institute of Technology
Structural Engineering Research Center
Nagatsuta, Midori-Ku
Yokohama 226-8503, JAPAN

Bruce F. Maison
7309 Lynn Avenue
El Cerrito, CA 94530

Performance Prediction and Evaluation Subcontractors

James Anderson
University of Southern California
Civil Engineering Department
Los Angeles, CA 90089-2531

Douglas A. Foutch
University of Illinois
MC-250, 205 N. Mathews Ave.
3129 Newmark Civil Engineering Lab
Urbana, IL 61801

Gary C. Hart
Department of Civil and Environmental Engineering
University of California
Los Angeles, CA 90095

Y.K. Wen
University of Illinois
3129 Newmark Civil Engineering Lab
205 N. Mathews Ave.
Urbana, IL 61801

Testing Subcontractors

Subhash Goel / Bozidar Stojadinovic
University of Michigan
Civil Engineering Department
Ann Arbor, MI 48109

Roberto Leon
Georgia Institute of Technology
School of Civil & Environmental Engr.
790 Atlantic Ave.
Atlanta, GA 30332-0355

Vitelmo V. Bertero / Andrew Whittaker
UC Berkeley
Pacific Earthquake Engr. Research Center
1301 S. 46th St.
Richmond, CA 94804

Thomas Murray
Virginia Tech, Dept. of Civil Engineering
200 Patton Hall
Blacksburg, VA 24061

James M. Ricles / Le-Wu Lu
Lehigh University
c/o ATLSS Center
117 ATLSS Drive, H Building
Bethlehem, PA 18015-4729

John M. Barsom
Barsom Consulting, Ltd.
1316 Murray Ave, Suite 300
Pittsburgh, PA 15217

Hassan Astaneh
University of California at Berkeley
Dept. of Civil and Environmental Engr.
781 Davis Hall
Berkeley, CA 94720

Michael Engelhardt
University of Texas at Austin
Ferguson Laboratory
10100 Burnet Road, Building 177
Austin, TX 78712-1076

Gary T. Fry
Texas A&M University
Department of Civil Engineering
Constructed Facilities Division, CE/TTI
Building, Room 710D
College Station, TX 77843-3136

Chia-Ming Uang
University of California at San Diego
Dept. of AMES, Division of Structural Engr.
409 University Center
La Jolla, California 92093-0085

Stephen Schneider
University of Ilinois at Urbana-Champaign
3106 Newmark Civil Engr. Lab, MC-250
205 N. Mathews Avenue
Urbana, IL 61801

Matthew Johnson
Edison Welding Institute
1250 Arthur E. Adams Drive
Columbus, OH 43221

James Anderson
University of Southern California
Civil Engineering Department
Los Angeles, CA 90089-2531

Bozidar Stojadinovic
Dept. of Civil & Environmental Engr.
University of California
Berkeley, CA 94720

Inspection Procedure Consultants

Thomas Albert
Digiray Corporation
2235 Omega Road, No. 3
San Ramon, CA 94583

Randal Fong
Automated Inspection Systems, Inc.
4861 Sunrise Drive, Suite 101
Martinez, CA 94553

Andre Lamarre
R.D Tech, Inc.
1200 St. Jean Baptiste, Suite 120
Quebec City, Quebec, Canada G2ZE 5E8

Glenn Light
Southwest Research Institute
6220 Culebra Road
San Antonio, TX 78228

Andrey Mishin
AS & E High Energy Systems
330 Keller Street, Building 101
Santa Clara, CA 95054

Robert Shaw
Steel Structures Technology Center, Inc.
42400 W. Nine Mile Road
Novi, MI 48375-4132

Carlos Ventura
Dept of Civil Engineering
University of British Columbia
2324 Main Hall
Vancouver, BC, Canada V6T 1Z4

Guideline Trial Applications Subcontractors

John Hopper
Skilling Ward Magnusson Barkshire, Inc.
1301 Fifth Avenue, Suite 320
Seattle WA 98101-2699

Lawrence Novak
Skidmore, Owings, and Merrill
224 S. Michigan Ave, Suite 1000
Chicago, IL 60604

Leonard Joseph
Thornton-Tomassetti Engineers
641 6th Avenue, 7th Floor
New York, NY 10011

Maryann Phipps
Degenkolb Engineers
225 Bush Street, Suite 1000
San Francisco, CA 94104

Economic and Social Impact Study Subcontractors

Ronald Eguchi
EQE Engineering and Design
300 Commerce Dr., Ste. 200
Irvine, CA 92602

Charles Kircher
Charles Kircher & Associates
1121 San Antonio Road, Suite D-202
Palo Alto, CA 94303

Martin Gordon / Peter Morris
Adamson Associates
170 Columbus Avenue
San Francisco, CA 94133

Lizandro Mercado
Brandow & Johnston Associates
1600 West 3rd St.
Los Angeles, CA 90017

Richard Henige
Lemessurier Consultants Inc.
675 Massachusetts Ave.
Cambridge, MA 02139-3309

Greg Schindler
KPFF Consulting Engineers
1201 3rd Ave.
Seattle, WA 98101-3000

Report Production and Administrative Services

A. Gerald Brady, Technical Editor
Patricia A. Mork, Administrative Asst.
Peter N. Mork, Computer Specialist
Bernadette A. Mosby, Operations Admin.
Michelle S. Schwartzbach, Pub. Specialist
Applied Technology Council
555 Twin Dolphin Drive, Suite 550
Redwood City, CA 94065

Carol Cameron, Publications Coordinator
Ericka Holmon, Admin. Assistant
California Universities for Research in
Earthquake Engineering
1301 S. 46th Street
Richmond, CA 94804

*indicates industrial or organizational contact representative